Forensic Engineering Fundamentals

Harold Franck
Darren Franck

CRC Press
Taylor & Francis Group

Forensic Engineering Fundamentals

Harold Franck
Darren Franck

CRC Press
Taylor & Francis Group
Boca Raton London New York

CRC Press is an imprint of the
Taylor & Francis Group, an **informa** business

CRC Press
Taylor & Francis Group
6000 Broken Sound Parkway NW, Suite 300
Boca Raton, FL 33487-2742

© 2013 by Taylor & Francis Group, LLC
CRC Press is an imprint of Taylor & Francis Group, an Informa business

No claim to original U.S. Government works
Version Date: 20120608

International Standard Book Number-13: 978-1-4398-7840-8 (eBook - PDF)

This book contains information obtained from authentic and highly regarded sources. Reasonable efforts have been made to publish reliable data and information, but the author and publisher cannot assume responsibility for the validity of all materials or the consequences of their use. The authors and publishers have attempted to trace the copyright holders of all material reproduced in this publication and apologize to copyright holders if permission to publish in this form has not been obtained. If any copyright material has not been acknowledged please write and let us know so we may rectify in any future reprint.

Except as permitted under U.S. Copyright Law, no part of this book may be reprinted, reproduced, transmitted, or utilized in any form by any electronic, mechanical, or other means, now known or hereafter invented, including photocopying, microfilming, and recording, or in any information storage or retrieval system, without written permission from the publishers.

For permission to photocopy or use material electronically from this work, please access www.copyright.com (http://www.copyright.com/) or contact the Copyright Clearance Center, Inc. (CCC), 222 Rosewood Drive, Danvers, MA 01923, 978-750-8400. CCC is a not-for-profit organization that provides licenses and registration for a variety of users. For organizations that have been granted a photocopy license by the CCC, a separate system of payment has been arranged.

Trademark Notice: Product or corporate names may be trademarks or registered trademarks, and are used only for identification and explanation without intent to infringe.

Visit the Taylor & Francis Web site at
http://www.taylorandfrancis.com

and the CRC Press Web site at
http://www.crcpress.com

Dedicated to

Vincent, Alexander, Evan, Dominic, and Isaac

Contents

Preface

This book has been written with the forensic engineering practitioner in mind. It may also be used as a textbook in the curriculum of a forensic engineering program. The use of numerous examples and end-of-chapter problems is designed to introduce the student or reader into the diverse environment that encompasses forensic engineering. The book also includes a solutions manual for all the end-of-chapter problems to be utilized by the course instructor. As the book title implies, this textbook is an introduction to the many facets of forensic engineering. As such, most of the material is somewhat introductory in nature. The breadth of the forensic engineering field makes it impossible to provide an in-depth coverage in one text of all the various subjects. It is assumed that the reader has a grasp of the fundamental topics as covered in the various areas of study. However, some areas of study deal with fairly complex subjects such as the current flow in conductors. The various references at the end of the book are designed to guide the student toward further study. The reader will notice that simple plug-and-chug type of problems have generally not been included because it is assumed that the reader has a fairly advanced level of proficiency with mathematical equations. If the book is used as a textbook, there is ample material for a two-semester course of study. The topics that may be covered in a semester course are left up to the instructor or the reader. The forensic practitioner may also only be interested in some topics and not others.

Forensic engineering may be divided into four major categories: structures, the environment, accidents/incidents, and failures. In many instances, these four major categories may be intertwined. A component failure may cause an accident involving vehicles or fires. Similarly, the structural components of the environment may cause a pedestrian to fall or cause water infiltration to induce mold growth and pose serious health problems. The environment may also affect the stability of structures.

The first of these categories involves structures. When we think of structures, what first comes to mind is a building, small or large, a bridge, a roadway, or maybe a crane or derrick. However, structures may, in fact, be smaller subcomponents of a large structure or they may include the rolling mill process of a factory that produces sheet aluminum. The structure may involve the drivetrain of an automobile or a recreational vehicle that has experienced a fire. The environment is generally regarded as the climatic conditions that affect the structure, the failure, or the accident/incident. Environmental factors such as rain can significantly affect a structure or component. For example, if a house has been built in a low-lying area that is subject to flooding, it is often necessary to determine whether the structure was built in the 10-year or 100-year flood plain. Flood plains are determined by the Authority Having Jurisdiction (AHJ), which may be a city, county, state, or federal agency such as the State Fire Marshal. When significant property damage occurs or when there is loss of life resulting from a fire, fire marshals are often involved, and in those cases, the forensic engineer must coordinate his or her activities accordingly.

In many instances, the forensic engineer works in concert with a regulatory agency such as the Occupational Safety and Health Administration (OSHA) in a case involving a workplace accident, or the Mining Safety and Health Administration (MSHA) in the case of a mining accident or failure.

When accidents/incidents come to mind, we think of car crashes, slips, trips, falls, electrocutions, or maybe a crane failure. An accident is defined as a happening that is not expected, foreseen, or intended. It is an unpleasant or unintended happening, sometimes resulting from negligence that results in injury, loss, or damage. According to this definition by Webster's Dictionary, the term "accident" does not apply to most events that are investigated by forensic engineers. A better term to be used is "incident" rather than "accident." We will attempt to use incident rather than accident throughout this book. The reasoning for this change in terminology is shown in the following examples. In the case of a vehicular collision, it is clear that the parties involved did not intend for the crash to occur. The exception is when deception is involved, when car crashes are staged. However, in most instances, the crash could be expected or foreseen because such events are generally due to a combination of human errors or influences such as road conditions, the environment, or failure of a particular component of the vehicle such as excessive tire wear. Car crashes, as with most events classified by the general public as accidents, are actually due to a combination of many factors leading to the incident. A driver may be changing lanes without properly signaling or looking for other vehicles, a driver may run a red light, or another driver may be speeding. As another example, consider a crane failure that may occur because the bolts supporting the outriggers became loose and were subject to cyclic fatigue to the point that they sheared and caused the crane to topple over. This condition may have been exacerbated by operator error and poor maintenance. Certainly, in these cases, the events leading to the failure would not be properly characterized as accidents because there may be significant expected and foreseen circumstances surrounding and affecting the incident. A better characterization is then to refer to the accident as an incident. The definition of an incident is an event that is likely to happen, an occurrence as a result of or in connection with something else. In this context, as a third example, bald tires on a vehicle being driven at 90 miles per hour on a wet road caused the right front tire to delaminate, the vehicle to hydroplane and roll over, ejecting the unbelted driver. This event would not be an accident but rather an incident caused by a complex combination of factors.

When discussing failures in a forensic engineering context, the other factors affecting the outcome need to be considered. Did the delamination of the tire in the example above cause the event or was it a combination of the factors that led to the "accident"? As another example, consider the case of an electrician at a steel mill who is asked to troubleshoot some electrical cabling. The electrical cabling is at a potential of 2300 V. This fact is unknown to the electrician or his supervisor. What is known is that the load supplied by the electrical cables is not receiving electrical energy. Conditions demand that in order to test the circuitry, the test must be conducted live, that is, while the circuitry is energized. The only test equipment available to the electrician is a volt-ohm meter rated at 1000 V. The electrician is not supplied with protective gear necessary to conduct a live test as required by codes. The meter to be used is not rated for the voltage to be measured. The electrician climbs a ladder in order to measure the voltage at a particular location.

When the test probes of the meter touch the 2300 V lines, the meter explodes, causing severe facial injuries to the electrician. The failures associated with this example are numerous but do not include the failure of the meter. The meter was not intended to be used at 2300 V. Rather the failures in this incident are improper use of a meter, disregard for codified safety concerns, lack of electrical diagrams outlining the voltages involved, and the lack of protective equipment to name a few.

We see from these examples that the structures, environment, incident, and the failures are inextricably intertwined. These forensic incidents are very rarely an accident. More generally, a combination of factors leads to the incident. A recent incident that has affected the environment, equipment, lives, and the livelihood of the region is the Deepwater Horizon oil spill catastrophe associated with the drilling rig for British Petroleum in the Gulf of Mexico. A brief summary of the parties involved and the events leading to the explosion are as follows.

British Petroleum (BP) contracted with Transocean and their Deepwater Horizon drilling rig to conduct an exploratory well at a depth of approximately 5000 ft in the Macondo Prospect in the Gulf of Mexico. Halliburton Energy Services was installing and cementing the production casing for the well. In the March and April 2010 time frame, platform workers and supervisors were concerned with certain aspects of well control. On April 20, 2010, at 9:45 p.m. high-pressure methane gas escaped the drill column, expanding throughout the drilling platform and igniting. The platform burned for approximately one and one half days before sinking irrespective of all efforts to combat the inferno and save it. This catastrophe caused significant loss of life and serious injuries to a multitude of platform workers. Several efforts were considered and employed to cap the well. On August 4, 2010, the well was sealed, and it was declared that the static kill on the well was working. Throughout the process of the flow of oil into the Gulf, a massive cleanup effort ensued and will likely continue for a very long period of time. Accordingly, the ecological damage will continue to be assessed and expanded.

The United States Coast Guard (USCG) and the Minerals Management Service (MMS) began their investigation on April 22, 2010. On May 11, the president of the United States requested an independent investigation by the National Academy of Engineering. On May 22, a bipartisan National Commission was established to determine the root causes of the disaster. On June 1, the U.S. Attorney General opened an investigation into the oil spill. On April 30, the United States House Committee on Energy and Commerce queried Halliburton on their cementing procedures with respect to the problems associated with the blowout preventer. According to testimony, the underwater control panel was disconnected from the pipe ram and instead connected to a test ram. There was a leak in the hydraulic system that provided power to the shear rams. The schematic diagrams for the underwater structure did not correspond to the in situ structure at the bottom of the ocean. The design of the shear rams would not allow for their application on screwed joints or on tools passed through the blowout preventer. Communication lines may have been severed so that the blowout preventer may not have received a signal to engage. The control pods for the dead man switch had a dead battery. Weeks before the explosion, a leak was detected on a crucial piece of equipment for the blowout preventer. BP overruled Transocean and insisted that seawater be used instead of drilling mud hours before the explosion. It is also apparent that the Minerals Management Service approved drilling

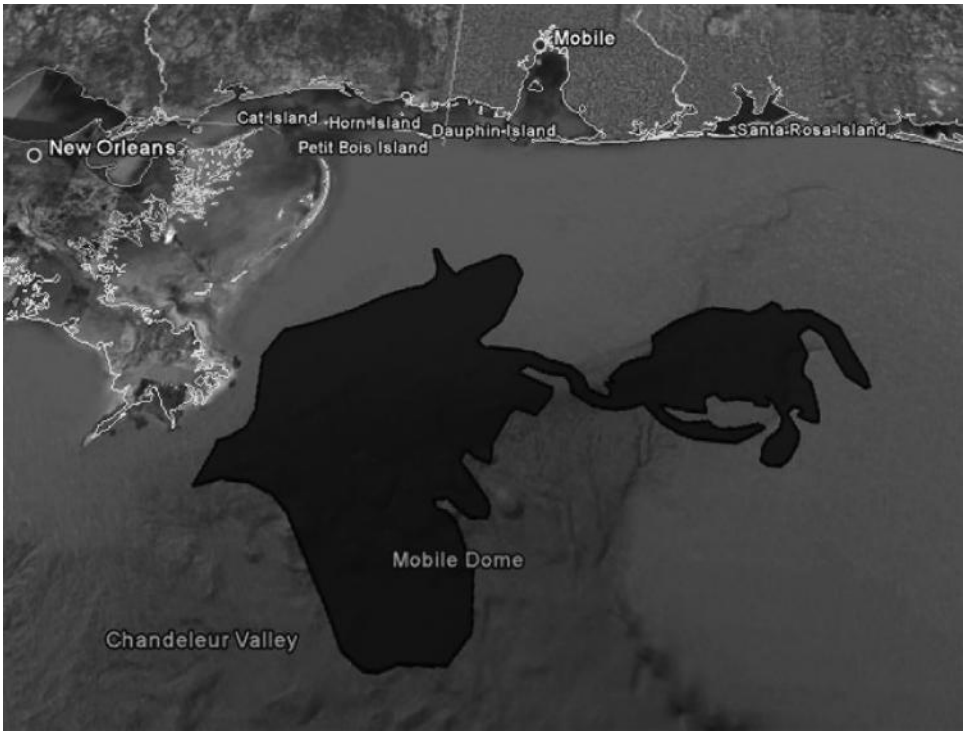

Figure P.1 The BP oil spill in the Gulf of Mexico.

and disaster plans without proper diligence and following proper standard of care. This incident is a classic case of how a combination of events can lead to a major disaster. What is known as of this writing is that a combination of complex factors produced the incident. The satellite view in Figure P.1 shows the extent of the oil in the Gulf of Mexico on July 13, 2010.

Acknowledgments

The authors wish to express their gratitude for all the technical help in the preparation of this manuscript to Janice Franck, Amanda Morris, and the staff of Taylor & Francis Group.

Symbols and Units

$\boldsymbol{F}$	Force (lb)
$\boldsymbol{M}$	Moment (ft-lb)
$\boldsymbol{r}$	Distance (ft)
W	Work (ft-lb)
E_p	Potential energy (ft-lb)
E_k	Kinetic energy (ft-lb)
mv	Momentum (lb-s)
m	Mass (slug)
w	Weight (lb)
g	Gravitational acceleration (ft/s^2)
$\boldsymbol{v}$	Velocity (ft/s)
V	Speed (ft/s)
D, d	Distance (ft)
t	Time (s)
$P_{\max}$	Stress force (lb)
σ_x, σ_y, σ_z	Stress (lb/ft^2)
ε_x, ε_y, ε_z	Strain
δ	Deflection (ft)
η	Variable
h	Height (ft)
h	Enthalpy (Btu/lb)
f	Frictional force (lb)
μ	Coefficient of friction
P, p	Pressure (lb/ft^2)
q_s	Wind stagnation pressure (lb/ft^2)
γ	Lateral soil load (lb)
$\boldsymbol{u}$	Strain energy per unit volume (in.-lb/in.^{3})
$\boldsymbol{I}$	Moment of inertia (in.^{4})
τ	Torsional shearing stress (lb/ft^2)
$\boldsymbol{T}$, Γ	Torque (ft-lb)
$\boldsymbol{J}$	Polar moment of inertia (in.^{4})
ρ	Density (lb/ft^3)
c	Wave velocity (ft/s^2)
I	Wave intensity
v_p	Particle velocity (ft/s)
k	Scaling factor
k	Spring constant (lb/ft)
$\boldsymbol{a}$	Acceleration (ft/s^2)
$\boldsymbol{x}$	Displacement (ft)

$\boldsymbol{w}$	Angular velocity (rad/s)
α	Angular acceleration (rad/s^2)
P, $p(t)$	Power (ft-lb/s)
$v(t)$	Voltage (V)
$i(t)$	Current (A)
E	Energy (J)
$\boldsymbol{E}$	Electric field intensity (V/m)
$\boldsymbol{H}$	Magnetic field intensity (A/m)
$\boldsymbol{B}$	Magnetic flux density (W/m^2)
$\boldsymbol{D}$	Electric flux density (C/m^2)
$\boldsymbol{M}$	Impressed magnetic current density (V/m^2)
$\boldsymbol{J}$	Electric current density (A/m^2)
I	Current (A)
R	Resistance (ohms)
q_e	Electric charge density (C/m^3)
q_m	Magnetic charge density (W/m^3)
ε	Permittivity (F/m)
μ	Permeability (H/m)
σ	Conductivity (mhos/m)
$\boldsymbol{P}$	Poynting vector (W/m^2)
$q(t)$	Time-dependent charge density (C/m^2)
t_r	Relaxation time
HRR	Heat release rate (kW)
Q	Heat (Btu)
Q	Water flow (ft^3/day)
S	Entropy (Btu/°R)
H	Heat current (Btu/s)
k	Thermal conductivity (Btu/(ft-h°F))
UEL	Upper explosive limit
LEL	Lower explosive limit
B_e	Breaking load (lb)
S_x^P	Sensitivity of parameter P to variable x
T	Temperature (°F)

Synopsis

This book incorporates some of the most common forensic engineering disciplines encountered by the practicing forensic engineer. Many forensic engineers throughout the United States specialize in a particular area such as in structures, fires, accident reconstruction, and many others. However, the nature of the cases encountered by forensic engineers requires broad knowledge in diverse and sometimes interrelated areas of physics, chemistry, and engineering. For example, in the area of structures, it is often necessary for the investigating engineer to have knowledge of soils, hydrology, building materials, as well as structural elements. In the area of fire dynamics, the engineer should have a mastery of chemistry, thermodynamics, and fire patterns. Similarly, accident reconstructions and slip, trip, and fall cases incorporate the same basic physical fundamentals and may also necessitate a knowledge of biomechanical systems and behavior.

This book has been organized into 15 chapters. Chapter 1 discusses the role of the forensic engineer and outlines some of the generalities of the field. Chapters 2 through 5 are in the civil, structural, and environmental areas. They deal mainly with structures and the problems encountered therein. Structural distress is commonly related to natural phenomena or substandard construction techniques. Strong emphasis is placed on standards and codes in this portion of the book. Chapter 6 is devoted to the failure of appliances. These failures can cause water or fire-related losses.

Chapters 7 through 9 deal with the common types of accidents referred to as incidents. Chapter 7 deals with slips, trips, and falls of pedestrians. Standards such as the accessibility of walking surfaces and international and countrywide standards are discussed. Industrial incidents in Chapter 8 involve both the loss of equipment as well as injury and loss of life of people. Strong emphasis is placed on OSHA and MSHA regulations. Chapter 9 deals with the basic theory of standard accident reconstruction involving vehicles.

Chapter 10 covers electrical incidents and lightning and discusses some theoretical calculations and data related to those events. Chapter 11 expands on Chapter 10 to evaluate the effect of electrical energy on the human body.

Chapter 12 is a different approach to the analysis of fires from the standard one found in most fire-related publications. The emphasis is on thermodynamics, testing, and simulation. Chapter 13 deals with some miscellaneous losses such as carbon monoxide incidents and discusses some of the more common fire suppression and warning systems. As expected, this chapter outlines the various NFPA codes.

Chapter 14 covers probability and uncertainty, detailing some basic calculations available to the forensic engineer.

Finally, Chapter 15 describes applicable standards. Pertinent problems are included at the end of each chapter. A separate solutions manual is provided.

Introduction 1

Twenty-five years ago when the authors began practicing forensic engineering, the term forensic was not widely known. Today, when we are asked what we do for a living and we respond saying we are forensic engineers, it often confuses people because they have a misconception about the work we do. This misconception is partly due to the forensic programs that are shown on television and partly due to the misunderstanding of the term forensic. Most of the television programs where the term forensic is introduced deal with DNA and deaths of individuals. Thus, most people correlate the term forensic with the work that laboratory analysts or coroners perform. Television portrays these forensic experts as wearing a clean lab coat, inspecting, and solving cases with a small flashlight. The truth is that forensic engineering is far from what is depicted in these programs.

The term forensic must be first defined. Webster, defines forensic as "the characteristic of, or suitable for a court of law, public debate, or formal argumentation, specializing in or having to do with the application of scientific knowledge to legal matters, debate or formal argumentation and the use of knowledge and techniques derived from various sciences." Of course, forensics relates to the investigation of crime and medicine. These two areas are generally recognized by most people and often confused with the work of forensic engineers. The definition of engineering is the science of putting scientific knowledge to practical uses. Thus, a forensic engineer is one who applies scientific knowledge to an event that may lead to a debate, formal argument, or a court of law.

There are four main areas in engineering: civil, electrical, mechanical, and chemical. Within these main areas there are a myriad of specialties. For example, civil engineers may specialize in structures, foundations, soils, hydraulics, road construction, sanitation, or the environment. Electrical engineers may specialize in power, electronics, computers, communications, or process control. Mechanical engineers may be involved in vibrations, metallurgy, thermodynamics, engines, or heat transfer. Chemical engineers deal with processes, biotechnology, nanotechnology, minerals, and reactions. This list is not exhaustive and some of these subspecialties may be further divided. For example, the engineer may specialize in computer software or computer hardware. As a general rule, forensic engineers are generalists rather than specialists. Since the core of all engineering is common to all specialties, forensic engineers are well versed in the fundamentals. Furthermore, the practice is so diverse that practicing in only one very limited specialty would decrease the number of assignments.

Forensic engineers apply science to some form of potential argument that may arise. The nature of the argument may be in different forms. For example, two cars collide and the respective insurance companies or attorneys wish to determine who was at fault. This type of assignment may come soon after the collision when the insurance company needs to determine the liability of their insured. The assignment may also come years after the fact when a law suit has been filed, and attorneys wish to determine the strength or weakness in the case they represent. Another form of an assignment may

come after a natural disaster such as a snow storm that collapses various roof structures. In such a case, the insurance company may need to determine the extent of the damage and if extenuating circumstances, such as the failure to adhere to recognized construction standards, contributed to the roof failure. Extent of damage analysis is important to the insurance industry because repairs can only be determined based on what was damaged. Failure of the builder of the structure to follow recognized standards is important because the insurance company may wish to subrogate against the builder if it can be proven that the structure would not collapse had recognized standards of construction been employed. Subrogation is the substitution of one creditor for another, along with the transference of the claims and rights of the old creditor. In simple terms, the insurance company has the right to cause the negligent builder to pay for the repairs of the structure if it was improperly constructed. Most states have limits on such recovery by the party seeking restitution. These limits are commonly referred to as the statute of repose, limits of liability, or subrogation limits. A third form of an assignment may come from a fire that destroyed a residence. It may be suspected that an appliance such as a clothes dryer caused the fire. If the dryer was relatively new, and it can be shown through the application of scientific principles, that a failure of the dryer caused the fire, then the potential for subrogation against the manufacturer is greatly enhanced. It should be pointed out and emphasized that the forensic engineer is never the advocate and should never hold himself or herself as a subrogation specialist. Subrogation is the purview of the insurance company. Advocacy is restricted to attorneys. Engineers are simply the detailers of the evidence or as Detective Joe Friday stated in the 1950s and 1960s television show Dragnet, "just the facts ma'am."

These examples of the involvement of forensic engineers are some of the most common types. Another example involves coverage issues. Insurance companies always include exclusions to their policies. For example, surface and subsurface water associated with a structure is seldom a covered loss. A policy owner may have preexisting water problems associated with his home. The owner may wait for a convenient extreme rainfall to put in a claim resulting from this natural event, which may be covered under the policy. In such a case the forensic engineer may be employed to determine if the problems associated with the house are due to the storm or due to preexisting subsurface and surface water conditions. Sometimes forensic engineers are asked not only to determine the cause of the failure but also to design the repair. An example of such a case might involve a landslide that was caused by a contractor cutting a portion of a hillside. In such a case, the forensic engineer may have been hired by the insurance company representing the contractor. As part of the subrogation agreement, the insurance company may agree to repair the hillside by designing a suitable retaining structure through their forensic engineer. As is evident from the limited examples mentioned earlier and as will be further shown in the many cases throughout the book, the role of a forensic engineer is quite varied and requires broad knowledge for most investigations. In its broadest sense, forensic engineering may be broken down into four main categories of structures, fires, the environment, and accidents or, more properly stated, incidents. Accordingly, one might wonder what the qualifications of a forensic engineer are.

Most forensic engineers are either civil, mechanical, or electrical engineers simply because these disciplines are the ones that are represented the most in terms of forensic investigations. Many forensic engineers have a combination of degrees. For example, one may have a bachelor's degree in civil and a master's degree in mechanical engineering. The type of degree is not necessarily the most important. What is more important are experience

and professional registration. Experience is gained through the type of work performed by the engineer and by subsequent training in specialized courses. Professional registration is obtained by taking a battery of tests for engineering internship and professional licensure. Professional licensure is followed by registration as a professional engineer in a particular state or states. Professional registration as a licensed engineer generally requires graduation from an accredited institution. Higher education degrees such as Masters and PhD only add to the credentialism of the practitioner. Involvement in professional organizations helps with the qualification of the forensic engineer. Some of the more common professional organizations include the American Society of Civil Engineers (ASCE), the American Society of Mechanical Engineers (ASME), the Institute of Electrical and Electronic Engineers (IEEE), and the American Society of Chemical Engineers (ASChE). Membership in these professional societies requires degrees from accredited institutions in engineering fields. These professional societies promulgate an exhaustive list of standards that are very valuable to the practicing forensic engineer.

There are many other professional societies that are pertinent to the forensic engineer but generally do not require a degree in a field of engineering for membership. These include the National Fire Protection Association (NFPA), the American Society of Testing and Materials (ASTM), the American National Standards Institute (ANSI), the Society of Automotive Engineers (SAE), the American Society of Metals (ASM), and Underwriters Laboratories (UL). Additionally there are government standards included in the Code of Federal Regulations (CFR) and the National Institute of Standards and Technology (NIST).

The client of the forensic engineer, usually the insurance company or an attorney, dictates the scope of the work to be performed in a particular investigation. However, the practitioner has to take care that due diligence is followed in the investigation. The client may want the engineer to cut corners and only perform certain tasks. For example, the insurance company may only want to know if a particular footer failed but may not be concerned why the failure occurred. In order to determine the mode of failure, laboratory tests may need to be performed as well as calculations made based on the physical evidence. The client may wish to exclude one or the other in an effort to keep costs down. Such restrictions can put the practicing engineer in a predicament because under the rules of conduct in a particular state, the engineer may have failed to meet minimum engineering standards and could be subject to a fine, reprimand, suspension, or revocation of his license. Thus, authors support and encourage the use and development of standards in the field.

The role of the forensic engineer is first to protect life and property and secondly to be the purveyor of the facts. Engineers investigate losses in order to determine the mode of failure so that future losses may be prevented. By gathering data and performing tests engineers can greatly enhance the safety of products and further the development of safety practices. Engineers can never be advocates but instead report their findings so that future losses may be mitigated or prevented. It is within this context that the chapters in the book are outlined. Engineering and sciences have a variety of goals, which are readily understood by the general public. Some of the most important goals, such as the protection of life and property, are not so well known or understood. In engineering and in science there are ethical standards to which practitioners adhere. In the context of forensic science, investigations are carried out to determine the events that led to the incident and in many instances, to develop methods of avoidance. At the present time there are two standards that are used by the courts to determine the validity of the expert's testimony.

The Frye Standard stems from a 1923 case that established the minimum standard required for the admission of expert testimony in federal cases. This standard requires the expert to use data and methodology "generally accepted" by other experts. In the Daubert case in 1993 the evidence that was presented by the plaintiff was considered to be novel scientific evidence or junk science. Therefore, this novel scientific evidence did not qualify under the Frye Standard as admissible expert testimony. In the U.S. Supreme Court appeal, the lower court rulings were overturned and a new standard was developed where the reliability of the evidence must meet a nonexclusive four part test:

1. Can the theory or technique be tested?
2. Has it been subjected to peer review and publication?
3. Is there a known or potential rate of error?
4. Is there general acceptance in the scientific community similar to the Frye Standard?

On November 22, 2005, the Science, State, Justice, Commerce, and Related Agencies Appropriations Act of 2006 became law. The U.S. Congress authorized the National Academy of Sciences (NAS) to conduct a study on forensic sciences. The U.S. Senate Report set forth many charges to the forensic sciences community including the dissemination of best practices and guidelines concerning the collection and analysis of forensic evidence to help insure quality and consistency in the use of forensic technologies and techniques to solve crimes, investigate deaths, and protect the public. One of the issues covered during the committee's hearings was the fundamental of the scientific method as applied to forensic practice—hypothesis generation and testing, falsifiability and replication, and peer review of scientific publications. Another observation was the lack of mandatory standardization, certification, and accreditation. The committee stated that the fragmentation problem is compounded because operational principles and procedures for many forensic science disciplines are not standardized or embraced. Often there are no standard protocols governing forensic practice in a given discipline. One recommendation is to establish a national code of ethics for all forensic science disciplines.

It is clear that standards and protocols must be developed for the forensic sciences. In the engineering sciences there are many recognized standards in certain fields, but they are utterly lacking in others. For example, the fire sciences have a multitude of standards, guides, and protocols that were developed by ASTM and NFPA. In the engineering sciences there are but a handful of standards. Some were developed 25 years ago and a few others were developed 5 years ago when a major push was made in ASTM to develop such standards. Since then, their development has actually been curtailed. The American Academy of Forensic Sciences (AAFS), through its long and close association with ASTM, has an opportunity to develop standards, guides, and protocols in forensic engineering sciences. Additionally, the National Academy of Forensic Engineering (NAFE), a subsidiary of the National Society of Professional Engineers (NSPE), can aid in the development of forensic engineering standards.

An issue that has arisen over the past 15 years is that of *spoilation of evidence*. Spoilation of evidence simply means that in the process of an investigation, one party may alter or make the evidence inaccessible to an investigation by another party. Spoilage can happen in a variety of ways. The evidence is somehow lost or discarded. Clearly, in such a case, the evidence is not available for inspection and analysis by the second party. It is also clear that destructive testing of an item may alter the characteristics.

Such an event can occur when laboratory testing consumes the evidence to the point where further testing or confirmation of the results by a second party is not possible. Many times spoilation issues arise when a piece of equipment that is suspected to have caused a loss is removed from in situ. It is possible in such cases that all the evidence is not collected or that the second party does not have the opportunity to analyze the surrounding circumstances to properly assess the events of the loss. This type of spoilation issue most often arises in fire losses or mechanical loss events.

A more egregious form of spoilation occurs when one party physically changes the characteristics of the evidence either through a wanton and willful act or through carelessness. Although this type of calculated spoilation seldom occurs, it is known to happen especially when large sums of money are involved. More often, carelessness by the investigator can lead to incomplete recovery or an alteration of the evidence such that some or all of the evidence is compromised. One example of such an event is when the *black box*, the event recorder, of a vehicle is retrieved from a crash vehicle by cutting the data link cables and removing the air bag module for testing at a laboratory. The action of cutting the cabling using a pair of cutters may produce a short circuit condition between conductors that would alter the recording of the event. This type of spoilation often occurs when untrained investigators retrieve the Crash Data Recorder (CDR) from the vehicle by cutting the data cables instead of interrogating the unit in situ. Interrogation of the CDR in a vehicle requires that either the electrical system of the vehicle is still operational and/or that the proper equipment is available to perform the tests on site.

One way of avoiding spoilation issues is to notify all parties that may be involved in order to conduct a joint inspection. Such inspections are cumbersome simply because many parties are involved. In such cases, problems can be averted by following a set of protocols for the inspection as designated by the lead investigator. The lead investigator is usually the expert representing the equipment, structure, or facility that is involved in the loss. It is noteworthy that the protocol agreed upon at the initiation of the inspection may be modified as the investigation progresses depending on the circumstances that are found. Generally, changes in the protocol are determined through mutual consent.

When joint inspections are not carried out and the investigator decides, based on the circumstances, that a piece of evidence needs to be retrieved in order to preserve it, then it is acceptable to do so by properly documenting the evidence. This proper documentation is carried out by systematically photographing or video recording the removal process. ASTM has such a procedure in place and should be reviewed by all forensic engineers.

As stated in this introduction, there are some standards available in forensic engineering. However, there is a glaring lack of standards in many areas. The advantages of standards based forensic engineering investigations include conformity, repeatability, standardization, diminishment of errors, recognition by the scientific community, and adherence to the recommendations set forth by the NAS Report of 2005 and the subsequent Science, State, Justice, Commerce, and Related Agencies Appropriations Act of 2006.

Structural Distress 2

Introduction

Structures have a propensity for failure for a variety of reasons. Consequently structural distress, in its many forms, is one of the four major categories that a forensic engineer investigates. Structural distress can be produced by many factors such as improper design, improper construction, component failures, manufacturing defects, failure to meet applicable codes, natural events, or unforeseen or unexpected events. The forensic engineer is often employed by an attorney, an insurance company, or an owner to investigate the nature of the failure and to determine culpability. A note of caution is necessary at this point, and it needs to be explained.

As outlined in the introduction, the primary charge of an engineer is to protect life and property. This charge necessitates that the design, manufacture, and construction of structures adhere to recognized standards that conform to this charge. When structural distress can be shown to be a result of the failure to meet recognized standards, it is the duty of the engineer to point to the root cause of the failure. However, this charge does not involve the engineer as a proponent for a cause but rather as a finder of the facts. As such, forensic engineers must not be subrogation specialists. Subrogation is the purview of the attorneys and the interests they represent. Insurance coverage issues are similarly not a consideration for the forensic engineer. Whether a loss is covered or not is of no consequence to the engineer. Based on the facts of the investigation and the conclusions reached, the insurance company or their representatives make coverage decisions.

This chapter, then, deals with some of the most common modes of structural failure that the forensic engineer encounters. Since residential homes make up most of the structures in the world, the most prevalent issues deal with the structural distress experienced by residences. The same principles apply to commercial and residential structures. However, the applicable codes and standards differ somewhat for these other structures. It should be pointed out that building codes and standards are regionally specific. While most of the codes are universally applicable, weather and soil conditions vary according to specific regions. As a classic example, California is subject to earthquakes so that building design standards for that part of the country take into account the nature of the inherent distress that may be produced. Most people are not aware that there are other seismic fault lines in other parts of the United States as is detailed in a subsequent chapter in the book.

A knowledge of building codes and design standards is imperative for the forensic engineer. Normally, in analyzing losses, the forensic engineer must essentially perform the design computations in reverse. In design, initial conditions are considered to determine how a component will respond. In forensic analysis, the failure of a component will be used to determine the conditions that induced failure. Furthermore, codes and standards

promote a universal statement of the purpose of an engineer, especially with respect to structures and construction activity. That is, the primary goal of an engineer is to protect life, safety, and health of the general public. Loss of property is a secondary concern to life, safety, and health. This statement is not meant to downplay the importance of property, as economic considerations will always play a part in design or forensics. Codes and standards place minimum limits to ensure that economic factors do not take precedence over the general welfare of the public.

In this chapter, basic laws and principles will be presented, which form the foundation for analysis performed by a forensic engineer. Knowledge of these basics is essential. As in school, engineers must "show their work," or at least be ready to demonstrate their abilities when challenged. It is not enough to simply state an opinion and present it as fact. Forensic engineers are expected to perform computations, reference standards, and present verifiable evidence to bolster their case. The basis of an expert's conclusion may be presented to a property owner, injured worker, insurance adjuster, deposing attorney, judge, and jury. While these parties would be considered "lay people," they may have a greater-than-expected knowledge of math and science. Given this possibility, an ability to "show your work" is of greater importance.

Too often, engineers and experts working in this field get by with possessing a long resume, public speaking skills, and a convincing demeanor. Certainly these qualities are important and present obstacles if any are lacking. However, if experts are unable or unwilling to "show their work," they should be classified as a subset of this profession: the "hand-waving" experts. "Hand-wavers" never "show their work," never put "pen to paper," and never "crunch the numbers." Idioms aside, this book is not intended to reinforce the verbosity of a nonanalytical expert. Moreover, a nonanalytical expert will eventually be exposed through Daubert challenges in court and everyday challenges by any number of lay persons. The book is intended to reinforce or introduce basic principles used in forensic engineering. This chapter on structural distress presents a subset of forensic engineering that is specific to civil and structural engineers. Specific examples and cases that a forensic engineer may encounter will be presented later in this chapter.

Substandard Design and Construction

Except in some rural areas of the United States, most cities, counties, states, and government structures must adhere to codes that pertain to the design and the construction of these structures. These codes apply to residential, commercial, and industrial facilities as well as the appurtenances, sidewalks, parking spaces, paths, and roads leading to these structures. The codes also apply to the basic systems that service the structures including water, sewage, gas, electrical, lighting, and communications systems. Additionally, utility companies have a separate but interrelated set of standards that must be followed. The sum total of the applicable standards pertaining to these structures is referred by the authors as "standard design and construction." These standards set the baseline for any forensic investigation. Thus, a primary goal of a forensic engineer who is investigating the structural distress or failure of a structure is to research the applicable codes and to see if they were adhered to when the structure was designed and constructed. If a structure does not meet the recognized standards and has failed, then it is a prima facie case for the failure, and it is almost impossible to overcome. Of course, the standards that may have been violated have

to pertain to the loss. If standards unrelated to the loss have been violated, according to the scientific method, they play no part in the investigation and determination of the events and mode of failure.

Codes and standards are living documents, that is, they evolve with time. As knowledge grows and experience is gained, many recognized standards need to be updated to conform to the new knowledge. All codes and standards are subject to periodic review. It is, therefore, necessary for the forensic engineer to apply the appropriate code to the situation. For example, if a structure was built in 1960 according to the recognized standards of that date and a subsequent investigation in 2000 showed that the construction of the home did not meet the 2000 standards, that does not mean that the home was improperly constructed. In most instances, new codes are not retroactive. It is not necessary to bring a 1960 structure to 2010 standards. There is, of course, one exception—the American Disabilities Act that requires all commercial structures to retrofit their facilities to comply with handicap accessibility.

The hierarchy of standards begins with the Life and Safety Code known as NFPA 101. The National Fire Protection Association (NFPA) promulgates a multitude of codes primarily for the protection from the dangers of fires. These codes deal with fire protection, gas systems, electrical systems, to name a few. They promulgate hundreds of codes that fall under NFPA 101. These codes are a part of a set of codes and standards known as American National Standards Institute or ANSI. ANSI codes include more particular codes for mechanicals, electricals, machinery, safety, plumbing, and buildings. Most of these codes cross-reference other codes. However, all codes are under the influence of the Life and Safety Code. Since all jurisdictions in the United States have adopted NFPA 101, all other codes are applicable.

Structural distress to structures may be associated with foundations, walls, floors, ceilings, or roof structures. Many times the failure is due to ground movement or water infiltration. Sometimes damage can be produced by external activities such as nearby blasting or the use of heavy vibratory equipment. In such cases, preblast surveys or preconstruction surveys are critical in order to assess the amount of damage produced by these activities. Sometimes the damage may be attributed to natural weather events such as wind, hail, snow, ice, or earthquakes. This chapter outlines some of the more common types of structural distress that the forensic engineer encounters. Sometimes systems in a structure fail as in the case of frozen water pipes or leaking faucets or toilets. These types of failures may be due to improper construction or a failed component. A component may fail simply because its life expectancy has expired or there may be no recourse for recovery if the statute of limitations has passed. The engineer must keep these concerns in mind when a report is issued concerning the loss.

Some Structural Basics

Before we begin a discussion of some of the more typical failures that plague structures, we need to discuss some of the basics of statics, dynamics, and strength of materials. As has been stressed throughout the book, the emphasis on the analysis of failures from a forensic engineering standpoint is to perform calculations to support or refute the hypothesis of the failure. This portion of the chapter should be used as the basis of the principles that are employed. The reader is encouraged to review appropriate textbooks on these subjects.

It is assumed that the reader has a firm grasp of coordinate systems, vectors, friction, forces, moments, impulse, momentum, and Newton's Laws. Most of these concepts are covered in the chapter on accident reconstruction so that this section simply covers the fundamental principles that are applied when we analyze structural distress. The equations that govern these principles are summarized below and are further expanded in the next sections.

Forces

When bodies or systems are at rest or are not being accelerated the summation of all forces is zero.

$$\sum \boldsymbol{F} = \boldsymbol{0} \tag{2.1}$$

The vector product of two forces is given by

$$\boldsymbol{F} = \boldsymbol{F}_1 \bullet \boldsymbol{F}_2 \tag{2.2}$$

Moments

The moment of a force about a point is the vector product of a force and its moment arm:

$$\boldsymbol{M} = \boldsymbol{r} \bullet \boldsymbol{F} \tag{2.3}$$

Systems or bodies in equilibrium dictate that the summation of moments be zero.

$$\sum \boldsymbol{M} = 0 \tag{2.4}$$

Work

Work of a force thought a displacement is given by

$$W = \int \boldsymbol{F} \cdot d\boldsymbol{r} \tag{2.5}$$

Energy

Potential energy is a function of position relative to a datum reference,

$$E_p = mgy \tag{2.6}$$

Kinetic energy is a function of motion,

$$E_k = \frac{1}{2} m v^2 \tag{2.7}$$

Momentum

Momentum is conserved, so that initial momentum equals final momentum:

$$\sum mv_i = \sum mv_f \tag{2.8}$$

where

m is the mass
g is gravity
y is vertical displacement

Structures: Mechanics and Force Systems

Mechanics describes and predicts the motion of bodies when subjected to forces. Mechanics is generally divided into three categories: rigid bodies, deformable bodies, and fluids. In this chapter, we will only deal with mechanics of rigid bodies as it applies to structures that undergo distress. Mechanics of rigid bodies is further broken down into statics and dynamics. Again, in this chapter the emphasis is on statics.

In order to properly describe the concepts of mechanics, we must deal with space, time, mass, and force. In statics we disregard the effects of time and simply analyze the structures with respect to their potential for distress or failure. The concept of space allows for the determination of the position of a point P with respect to some reference point, which usually is characterized as the origin. The concept of mass allows for the comparison of bodies relative to each other. The concept of force represents the action of one body on another.

Mechanics is based on six fundamental principles based on observation and experiment. These are as follows:

1. The parallelogram law for the addition of forces
2. The principle of transmissibility
3, 4, 5. Newton's three fundamental laws
6. Newton's law of gravitation

Force systems are broken down and exemplified by the first two basic principles. In this discussion, it is assumed that the reader has an understanding of the concept and manipulation of vectors.

The parallelogram law states that two forces acting on a particle may be replaced by a single force. This resultant force is obtained by drawing the diagonal of the parallelogram, which has as its sides the two individual forces and is depicted in Figure 2.1.

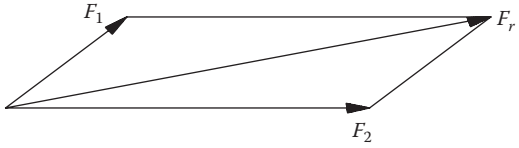

Figure 2.1 Parallelogram law.

Transmissibility requires that the conditions for equilibrium or motion of a rigid body will remain unchanged if a force acting at a given point is replaced by a force of the same magnitude and direction but acting at a different point, provided that both forces have the same line of action. This concept is extensively used in the analysis of structural elements such as trusses.

Newton's first law states that a particle will remain at rest as long as no force acts upon it or will move at a constant velocity if originally in motion.

Newton's second law states that if the resultant force acting on a particle is not zero, the particle will have an acceleration proportional to the magnitude and in the same direction as the resultant force. This force is given by the relationship,

$$\boldsymbol{F} = m\boldsymbol{a} \tag{2.9}$$

where

$\boldsymbol{F}$ is the force (lb)
m is the mass (slugs)
$\boldsymbol{a}$ is the acceleration (ft/s^2)

Newton's third law states that for every action there is an equal and opposite reaction or

$$\boldsymbol{F} = \boldsymbol{F}' \tag{2.10}$$

so that Equation 2.1 is satisfied and one condition for equilibrium is satisfied. The second condition for equilibrium is determined from Equation 2.4.

Newton's law of gravitation relates the force of attraction between two masses and is given by

$$\boldsymbol{F} = \frac{gm_1m_2}{r^2}\boldsymbol{a}_r \tag{2.11}$$

where

g is the gravitational constant = 32.2 ft/s^2
r is the distance between the two bodies
m_1 is the mass of the first body
m_2 is the mass of the second body
$\boldsymbol{a}_r$ is the unit vector in the radial direction

Newton's Laws and Equilibrium

A rigid body is considered to be in equilibrium if the external forces acting on it form a system of forces and moments equal to zero. The system is then considered to be stable. In equation form we summarize equilibrium by

$$\sum \boldsymbol{F} = 0; \quad \sum \boldsymbol{M} = \sum(\boldsymbol{r} \times \boldsymbol{F}) = 0 \tag{2.12}$$

These are necessary and sufficient conditions for equilibrium. Resolving the equations in (2.12) into their rectangular components yields six scalar equations for equilibrium.

Depending on the geometry of the problem, the analysis may be simplified from three to two or even one dimension. This is generally achieved by considering all the forces affecting the structure in a free body diagram. Omitting forces or adding extraneous forces destroys the conditions for equilibrium. In solving problems dealing with the equilibrium of a rigid body, the first step involves drawing the free-body diagram. The steps in drawing the free-body diagram involve the following: The portion of the structure to be analyzed is detached from the ground and separated from any other body. All external forces are indicated. These external forces represent the action on the body by the ground and the detached bodies. Their appropriate points of action are noted. The weight of the body is noted and applied at the center of gravity. Internal forces within the free-body diagram are not considered. Unknown external forces are considered reactions. Reactions are exerted at the points where the free body is supported or connected to the other bodies.

Work and Energy: Conservation Principles

The preceding section involved the equilibrium of rigid bodies utilizing the concept of the balance of the external forces, that is, the summation of forces and moments were zero. Certain types of equilibrium problems are more effectively solved by the principle of the work of a force. In mechanics, we may express a particle moving from point A to point B as shown in Figure 2.2.

The work of the force $\boldsymbol{F}$ corresponding to the displacement $d\boldsymbol{r}$ is defined as the dot product or

$$W = \boldsymbol{F} \circ d\boldsymbol{r} = F\,dr\cos\theta \tag{2.13}$$

where F and dr are the magnitudes of the force and the displacement.

The principle of virtual work is based on an imaginary displacement that does not actually take place. This principle states that if a particle is in equilibrium, the total virtual work of the forces acting on the particle, or a rigid body, is zero for any virtual displacement of the particle. To apply the principle of virtual work we consider the virtual work of all the reactions in a system that undergoes a virtual displacement and then sets the virtual work equal to zero. This method allows for the solution of the reactions.

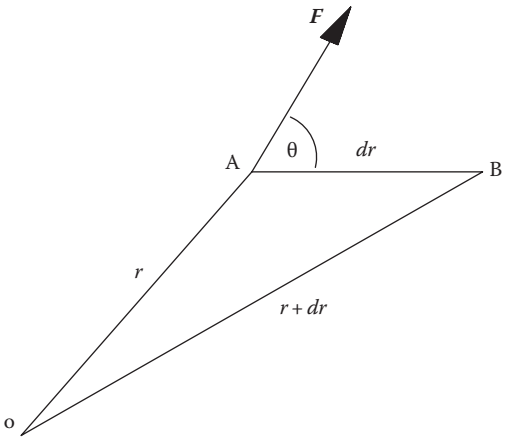

Figure 2.2 Work of a force.

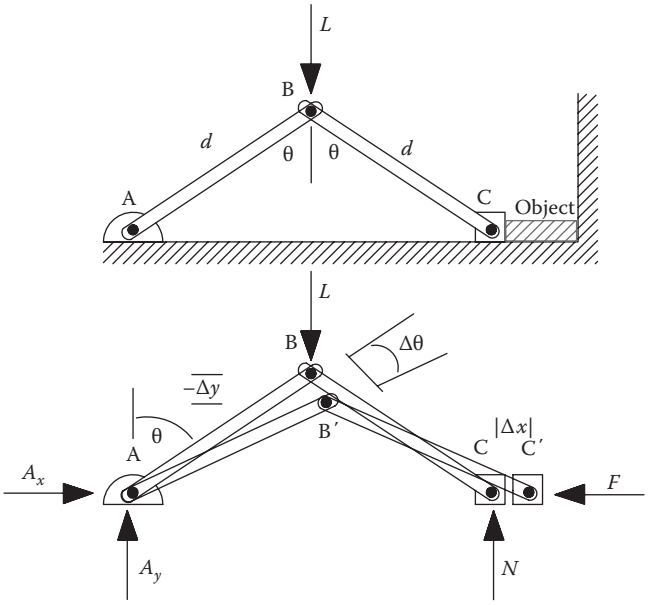

Figure 2.3 Mechanical press.

As an example, consider the structure shown in Figure 2.3, which is used to compress an object. Here we wish to compute the relationship between the applied load L and the force of compression F.

The free body diagram shows the reactions and the virtual work principles due to the virtual displacements Δx, Δy, and $\Delta\theta$. The reactions A_x, A_y, and N will do no work during the virtual displacement. Only the virtual work of L and F needs to be considered. From the geometry we get

$$x = 2d\sin\theta; \quad y = d\cos\theta \tag{2.14}$$

Differentiating,

$$\Delta x = 2d\cos\theta\,\Delta\theta; \quad \Delta y = -d\sin\theta\,\Delta\theta \tag{2.15}$$

The total virtual work is then

$$\Delta W = 0 = \Delta W_F + \Delta W_L = -2Fd\cos\theta\,\Delta\theta + Ld\sin\theta\,\Delta\theta \tag{2.16}$$

$$F = \frac{1}{2}L\tan\theta \tag{2.17}$$

Let us now turn our attention to a force $\boldsymbol{F}$ that produces a finite displacement as shown in Figure 2.4.

The work produced by the force through the displacement is given by

$$W = \int_a^b \boldsymbol{F}\circ d\boldsymbol{r} = \int_a^b F\cos\theta\,dr \tag{2.18}$$

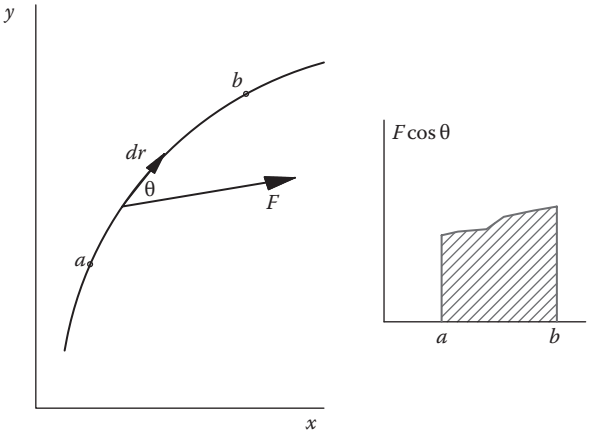

Figure 2.4 Force producing a displacement.

Similarly, the work of a couple $\boldsymbol{M}$ during a finite rotation is

$$W = \int_{\theta_1}^{\theta_2} \boldsymbol{M}\, d\theta \tag{2.19}$$

while the work of a weight $\boldsymbol{T}$ is only a function of its vertical displacement y so that

$$W = \pm \boldsymbol{T} \Delta y \tag{2.20}$$

The work is positive when the weight moves down and negative when the weight moves up. In contrast when we deal with a spring, we know from experimental data that the magnitude of the force $\boldsymbol{F}$ exerted by the spring is proportional to the deflection and the spring constant k, or

$$\boldsymbol{F} = kx \tag{2.21}$$

The work produced in pulling the spring is then

$$W = -\int_{x_1}^{x_2} \boldsymbol{F}\, dx = -\int_{x_1}^{x_2} kx\, dx = \frac{1}{2} k\left(x_1^2 - x_2^2\right) \tag{2.22}$$

We note that the work of the force $\boldsymbol{F}$ exerted by the spring on the body is positive when the spring is returned to its undeformed position.

Properties of Areas

In this section we wish to define the center of gravity for two- and three-dimensional bodies. The center of gravity is generally referred to as the first moment of inertia. Additionally we define the second moment or moment of inertia of an area and the mass moment of inertia.

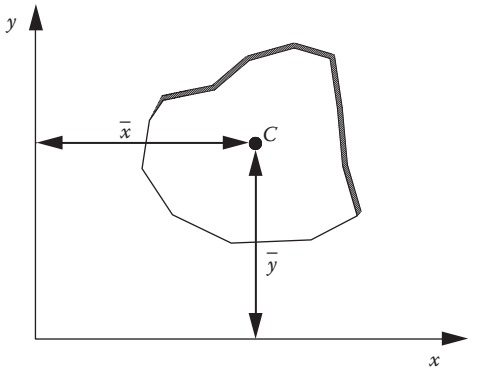

Figure 2.5 Centroid of a two-dimensional plate.

This analysis is required when investigating the properties of structures because we usually use the weight of the object as a single force located at the centroid. First let us consider a two dimensional plate as shown in Figure 2.5.

The centroid of the area is found from

$$\bar{x}A = \int x\,dA; \quad \bar{y}A = \int y\,dA \tag{2.23}$$

For a volume we simply add the term in the z-direction.

This analysis lends itself to find the location of the weight of a distributed load on a beam as shown in Figure 2.6.

The preceding discussion is used to analyze systems of forces distributed over an area. These distributed forces are proportional to the areas associated with them. The resultant of these forces can be obtained by summing the corresponding areas, and the moment of the resultant about any axis can be determined by computing the first moment of the area about the axis. It is also necessary for computational purposes to consider distributed forces whose magnitude depends on the element of the area and the distance to the axis. Consider the I-beam section shown in Figure 2.7.

This beam of uniform cross-section is subjected to bending so that equal and opposite couples affect the beam. The neutral axis is the x-axis so that the forces above the neutral axis are in compression and those below are in tension. The forces on the neutral axis are zero. The magnitude of the resultant $\boldsymbol{R}$ of the elementary forces $\Delta\boldsymbol{F}$ over the entire section is,

$$\boldsymbol{R} = \int ky\,dA \tag{2.24}$$

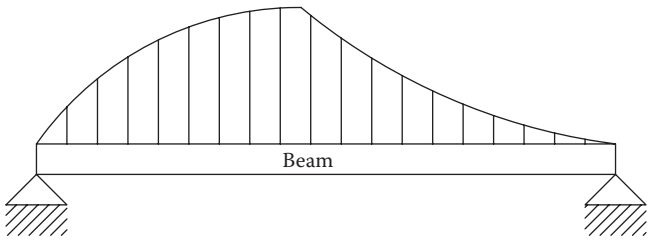

Figure 2.6 Distributed load on a beam.

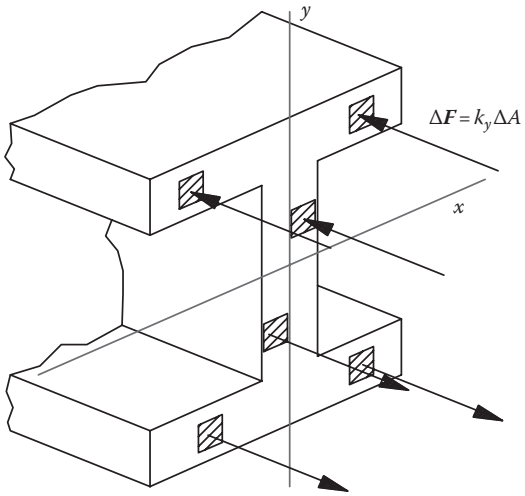

Figure 2.7 Section of an I-beam.

This integral is recognized as the first moment of the section about the x-axis and is equal to $\bar{y}\boldsymbol{A}$ and to zero about the centroid located on the x-axis. These forces are thus represented as a couple with a bending moment $\boldsymbol{M}$ so that if we integrate over the entire section we obtain

$$\boldsymbol{M} = \int k y^2 d\boldsymbol{A} = k \int y^2 d\boldsymbol{A} \tag{2.25}$$

This integral is the second moment or moment of inertia with respect to the x-axis and is denoted as $\boldsymbol{I_x}$. So with respect to both axes we define the moments of inertia as

$$\boldsymbol{I_x} = \int y^2 d\boldsymbol{A}; \quad \boldsymbol{I_y} = \int x^2 d\boldsymbol{A} \tag{2.26}$$

We may also define the polar moment of inertia as

$$\boldsymbol{J_o} = \int r^2 d\boldsymbol{A} \tag{2.27}$$

It can easily be shown that

$$\boldsymbol{J_o} = \boldsymbol{I_x} + \boldsymbol{I_y} \tag{2.28}$$

These concepts are summarized in Figure 2.8.

The radius of gyration of an area can be determined by the following equations:

$$k_x = \sqrt{\frac{I_x}{A}}; \quad k_y = \sqrt{\frac{I_y}{A}}; \quad k_o = \sqrt{\frac{J_o}{A}} \tag{2.29}$$

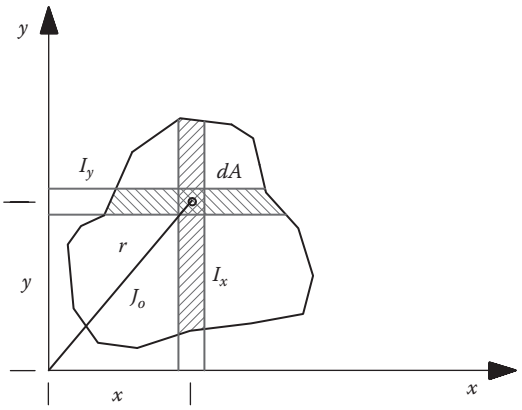

Figure 2.8 Moments of inertia.

Finally, the moment of inertia of a three dimensional body is obtained in a similar manner so that

$$I_v = \int r^2 dm = \rho \int r^2 dV \tag{2.30}$$

where

ρ is the density of the body
m is the mass
V is the volume
r is the radial distance to the center of mass

Structures

The preceding sections in this chapter dealt with the analysis mainly of single rigid bodies where all the forces were external to the bodies. Structures are collections of the connections of several parts. Structural analysis requires the determination of the external forces and those forces that hold the structure together. These forces that hold the structure together are considered internal forces of the structure.

Structures are generally constructed of columns, beams, and tension members. Consider the diagram in Figure 2.9.

In the diagram of Figure 2.9 we recognize all three types of members. T_1 and T_2 are tension members where T_1 is a cable and T_2 is a structural beam. C is a column and B is a beam with a weight W acting upon it. The external forces acting on the structure of Figure 2.9 are shown in the free-body diagram of Figure 2.10.

The free body diagram does not contain the internal forces holding the structure together. In order to visualize the internal forces, we must dismantle the frame members of the structure and represent the component parts and the forces acting upon them. Figure 2.11 shows the internal and external forces on the structure.

It should be noted that the diagram of Figure 2.11 is in conformity with Newton's third law.

The truss is the most recognized structure in the design of bridges and buildings. Trusses consist of straight members connected at the joints. Portions of a truss are columns, beams, and tension members. Truss members are connected at their ends so that

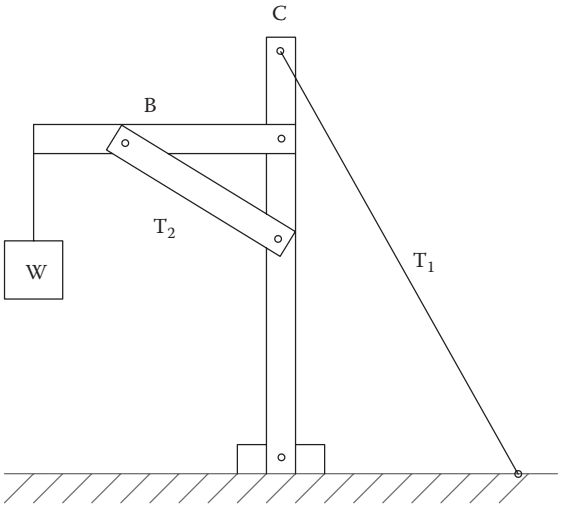

Figure 2.9 Structure.

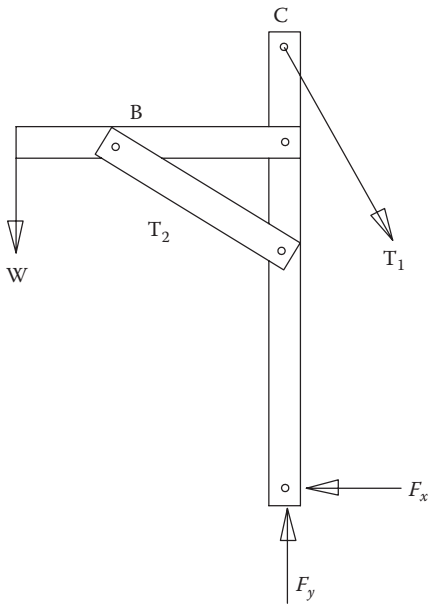

Figure 2.10 Free-body diagram.

no member is continuous through a joint. The members of a truss are generally slender and can support light loads individually. However, the various loads applied through the various joints form a robust structure that can handle significant loading. The various members of a truss are joined together in a variety of ways, including rivets, welds, and bolts. Sometimes pins are used if the design calls for the allowable movement of a joint. However, for the purposes of analysis, it is assumed that the joints are pins so that the forces acting on each end of a member are a single force. The section of trusses in this chapter further explains the analysis of trusses and the calculations of a truss failure. Figure 2.12 shows some typical truss designs found on roofs and bridges.

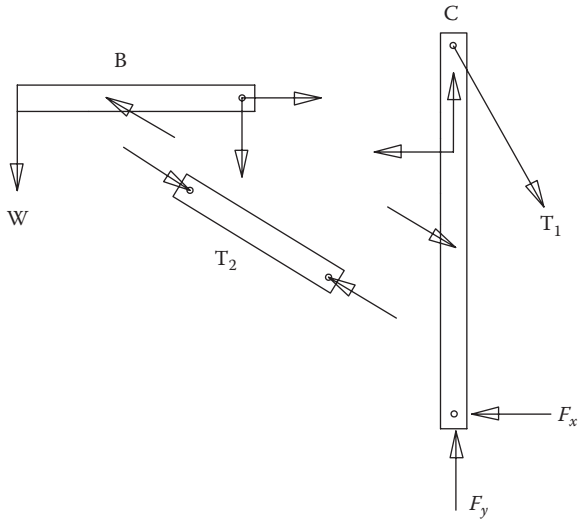

Figure 2.11 Internal and external forces.

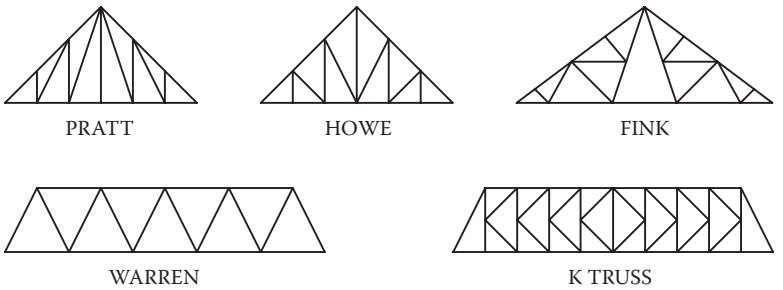

Figure 2.12 Typical trusses.

Mechanics or Strength of Materials

The strength or mechanics of materials deals with the development of the relationships between the loads that are applied to nonrigid bodies and the resulting internal forces and deformations that may occur within the body. In statics we simply assume that the bodies are perfectly rigid whereas in mechanics of materials we analyze how the external forces affect the internal structures of the bodies and the deformations they cause.

As a general rule, we assume that the materials that compose the structural elements, i.e., the bodies, are homogeneous and isotropic. A homogeneous material has the same elastic properties throughout the body. An isotropic material has the same elastic properties independent of the direction of the applied forces at any given point within the body.

The type of load that affects a material determines to a great extent the behavior of the body in question. What follows is a general description of the types of loads that materials may be subjected to.

1. Static loads are generally applied in a short time span until equilibrium is reached.
2. Sustained loads are constantly applied over long time spans.

3. Impact loads are very short duration and generally produce vibrations of the material.
4. Repeated loads are generally cyclic over time and can cause fatigue of the material.
5. Dynamic loads vary in intensity over time and may be cyclic.

All of these loads may be concentrated, distributed, centric, torsional, bending, producing tension or compression, or a combination of these over the material. Loading on a material gives rise to the concepts of stress and strain. Consequently, depending on the loading type, stress and strain may be normal, shearing, torsional, or a combination of the three. Consider the material in Figure 2.13 undergoing combined loading.

The usual method of analysis is to break down the stress and strain into a corresponding place. Three-dimensional stress and strain involve the use of tensor analysis, which is beyond the scope of the book. Note that in Figure 2.13 the hollow tube is being deflected, twisted, and pulled. So that realistically the analysis is in three dimensions. We formally define stress and strain as follows: *Normal stress* is defined as the normal force per unit area under centric loading, or

$$\sigma = \frac{N}{A} \ (\text{lb/in.}^2) \tag{2.31}$$

Shearing stress is defined in terms of the tangential moment per unit area again under centric loading. Thus, in equation form we have

$$\tau = \frac{M}{A} \ (\text{lb/in.}^2) \tag{2.32}$$

Normal strain is defined as the elongation per unit length under centric loading, or

$$\varepsilon = \frac{\Delta l}{L} \tag{2.33}$$

Shearing strain is defined for small deformations as

$$\gamma = \tan\gamma = \frac{\delta_s}{L} \tag{2.34}$$

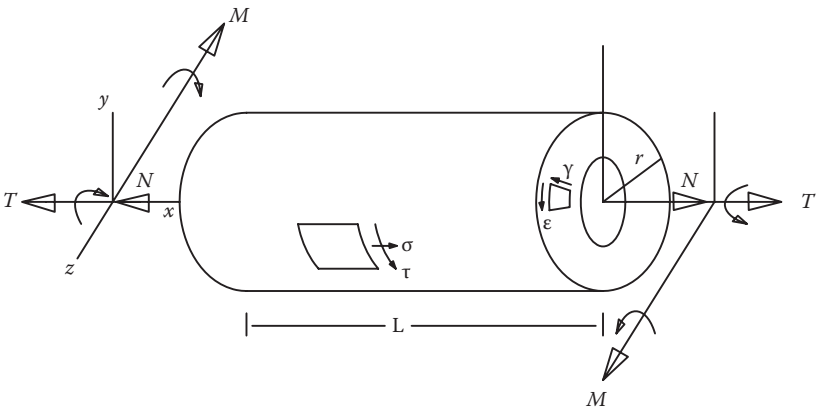

Figure 2.13 Combined loading.

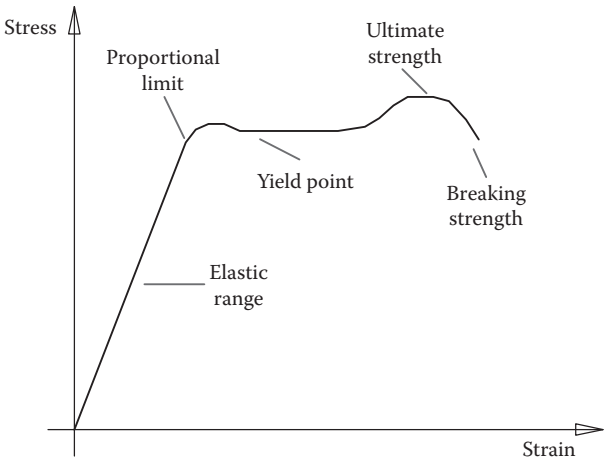

Figure 2.14 Stress–strain curve.

Figure 2.14 represents a typical stress–strain curve. The shape and consequently the behavior of the material will vary according to the material characteristics. Over the linear portion of the curve, Hooke's law or Young's modulus, is given by

$$E = \frac{\sigma}{\varepsilon}; \quad G = \frac{\tau}{\gamma} \tag{2.35}$$

where

E is used for normal stress and strain
G is used for shearing stress and strain

Young's modulus is also known as the modulus of elasticity.

The stress–strain curve can be used to characterize the strength characteristics of the material. Engineering materials made of metals are generally classified as either ductile or brittle. Ductile materials have relatively large tensile strain up to the point of rupture or failure. Steel and aluminum are two common ductile materials. In contrast, brittle materials such as cast iron or brick have small strain values up to the point of failure. Generally, a value of 0.05 is used as a dividing line for strain to delineate the two classes. Additionally, the following definitions are found throughout the literature:

Elastic range: Region of the stress strain curve from origin to the proportional limit.

Elastic limit: The uppermost point on the stress-strain curve where the linear portion of the curve ends.

Plastic range: The region of the curve from the proportional limit to the point of rupture.

Proportional limit: The limiting point on the linear portion of the curve.

Yield point: The point where an increase in strain with no increase in stress.

Tensile or ultimate strength: The point of failure of the material.

Breaking strength: The point where the material ruptures.

Modulus of toughness: The area under the curve to the point of rupture.

Modulus of resilience: The area under the curve to the proportional limit.

Percent elongation: The ratio of the increased elongation to the point of rupture per initial length.

Percent reduction in area: The ratio of decrease in area to the point of rupture per initial area.

Yield strength: The portion of the curve to the point of permanent deformation.

Working stress: Stresses within the elastic range of the material.

Tangent modulus: The slope of the tangent to the stress–strain curve at the origin.

Coefficient of linear expansion: The change in length per unit length due to a temperature change.

Poisson's ratio: The ratio of the strain in the lateral direction to that in the axial direction.

When design loads are determined, the working stresses and a factor of safety need to be incorporated into the design. The design should select materials and proportions of the material so that the functional properties are met without failure. The definitions above give some indication of failure. We may better define failure as a condition of the structure where the functional characteristics of the structure are no longer met. The failure may be *elastic*. In such cases, the structure should have been designed to incorporate any elastic properties of the materials or structures. Here, the stiffness of the material characterized by Young's modulus is the dominant and significant property. Another form of failure is *slip* failure where there is excessive plastic deformation due to slip. For members subjected to static loads, yield strength, yield point, and proportional limit are indicators of strength with respect to slip failure. Another form of failure is due to *creep*. This type of failure incorporates excessive plastic deformation under constant stress and over extended periods of time. Machines subjected to high stress and high temperature for extended periods of time should be designed with creep failure as a consideration. Finally, *fracture* failure is characterized by a complete separation of the structure or component. Indicators of these types of failure are the ultimate strength and the modulus of toughness.

All of these failure design methods, such as working or allowable stresses that are computed, should include a factor of safety. The factor of safety is a nebulous term that may differ depending on the application. There are many ways to define the factor of safety. It may be defined as the ratio of the failure load to the estimated load or as the ratio of the strength of the material to the maximum computed stress. It may also be defined as the ratio of the strain energy required for failure to the maximum computed strain energy under dynamic loading. It is apparent that the term factor of safety is meaningless without defining the criterion. In its simplest form, factor of safety is generally thought of as the ratio of the strength of the material to the maximum computed stress. It should be noted that the strength of the material may be the ultimate strength, proportional limit, yield point, or yield strength. These concepts tie into the next section.

Allowable Stress and Strength Design Methods

In analyzing a failed structure, it is often useful to assess the quality of its design. For structural elements made of steel or wood, various standards have been promulgated that outline proper design methods.

In some instances, there has been a shift to a factored design approach in the past few decades. For example, the design of steel structures, where once an allowable stress design

(ASD) method was the norm, load and resistance factored design (LRFD) has become established. The primary goal of LRFD type of design is to provide clarity and reliability for steel and wood structures under a variety of loading conditions. The uniformity of design is not reachable under ASD, but it is an integral part of LRFD.

Since many older structures were designed according to ASD, the forensic investigator must be aware of the fact and have a basic understanding of the method. The following equation details the method:

$$\sum Q_i \leq \frac{R_n}{FS} \tag{2.36}$$

The left side of the inequality represents the summation of the load effects, the forces and moments. The right side is the nominal strength resistance R_n divided by a factor of safety *FS*. If we divide by the appropriate section property such as the area or section modulus, the two sides of the inequality become the calculated stress and allowable stress, respectively. The left side is expanded as the absolute value of the loading combinations that may be represented as

$$D + L_t$$

$$(D + L_t + W) \times 0.75$$

$$(D + L_t + E) \times 0.75$$

$$D - W$$

$$D - E$$

where

D is the dead load
L_t is the total live load
W is the wind load
E is the earthquake load

The total live load is further broken down as

$$L_t = L + (L_r \text{ or } S \text{ or } R)$$

where

L is the live load due to occupancy
L_r is the roof live load
S is the snow load
R is the nominal load due to initial rainwater or ice exclusive of ponding

It is apparent from the discussion above that unfactored service loads and a single safety factor are applied to the resistance. However, due to the grater variance and unpredictability of the loads, a uniform reliability is not possible. When the design of a failed structure comes into question and the forensic engineer is asked to investigate for proper design, care must be taken in order to make the determination. Failed structures that were designed under ASD criteria should be assessed accordingly. Newer structures designed

under LRFD should be assessed under those criteria. It is not proper to evaluate a structure under LRFD if it was designed under ASD criteria and form an opinion of improper design. Essentially, the standards that applied at the time of the design must be followed.

The distinction between ASD and LRFD is that separate factors are used for each load and for the corresponding resistances. These factors are a result of extensive experience and research. Through these research and experience efforts, a more reliable method of analysis was developed and is characterized by Equation 2.37:

$$\sum \gamma_i Q_i \leq \varphi R_n \tag{2.37}$$

The left side of the inequality contains the load effects Q_i and the load factors γ_i. The design strength on the right side is R_n multiplied by the resistance factor φ. The values of φ and R_n are given through LRFD specifications. The strength reduction factor, φ, normally varies between 0.70 and 0.90. This value will depend on the material used and manner of loading (e.g., flexure, tension, compression, etc.) According to these specifications, the maximum absolute value of the left side of Equation 2.37 can be determined from the following combinations:

1.4D

1.2D + 1.6L + 0.5 (L or S or R)

1.2D + 1.6 (L_r or S or R) + (0.5L or 0.8W)

1.2D + 1.3W + 0.5L + 0.5 (L_r or S or R)

1.2D ± 1.0E + 0.5L + 0.2S

0.9D ± (1.3W or 1.0E)

There is an exception on the load factor L for garages, public assemblies, and areas where the live load is greater than 100 psf. In those areas the load factor is 1.0. The loads for the calculations are taken from the applicable codes or from *ASCE 7, Minimum Design Loads in Buildings and Other Structures*. For earthquake loads *AISC Seismic Provisions for Structural Steel Buildings* is used.

The American Wood Council promulgates general requirements for structural design. The specifications outline the method to be used with a variety of wood products that include visually graded lumber, mechanically graded lumber, structural glued laminated lumber, timber piles, and wood structures that are fastened. Wood structures and buildings are designed and constructed so that they may safely support all the loads that may be anticipated. These anticipated loads may include snow, wind, earthquake, flooding, as well as dead and live loads. Generally wind and earthquake loads would not be considered simultaneously but rather separately. In the design, the greatest load would be used of either the wind or the earthquake load. The design of wood structures is predicated on the principle that the lading assumed in the design represents actual conditions. This design methodology, as outlined in the National Design Specifications, does not involve load factors in computing the aggregate effect of combined loads. However, strength reduction factors are involved in the determination of allowable loads.

When combining loads utilizing strength design, the load factors and load combinations apply to limit states or strength design criteria known as load and resistance factor design (LRFD) as with steel structures. Standard design actually does not take into account extraordinary load combinations. Extraordinary load combinations are those events such as fires, explosions, sabotage, vehicular impact, misuse, subsidence, and tornadoes. The design requires that buildings and structures be robust, continuous, ductile, and provided with alternate paths for individual member failures so as to mitigate a total failure of the structure. These extraordinary loading conditions have a small likelihood of occurrence. All of these design schemes are to follow the local codes as promulgated by the Authority Having Jurisdiction (AHJ). The design schemes are outlined in the various codes such as the International building code and *ASCE Standard 7 Minimum Design Loads for Buildings and Other Structures*.

Most structures have some elements that are constructed with concrete. Portland cement is the binding agent in concrete and today represents the type of cement that is widely used in concrete mixtures. Most concrete mixtures include cement, and aggregate such as sand or stone. Portland cement is classified as a hydraulic cement because it is hardened by water. Portland cement was first made in England in 1824 and was so named because it resembled hardened mortar from the limestone on Portland Island. In 1878 Portland cement was first made in the United States in Coplay, Pennsylvania. The basic ingredients of cement are calcium carbonate ($CaCO_3$), silica (SiO_2), and alumina (Al_2O_3). Some other constituents may include magnesium oxide, ferric oxide, sulfur trioxide, and oxides of sodium and potassium.

Once the cement has set, the development of its strength is just at the beginning stages. The strength characteristics are determined by the hydration process of the concrete constituents. Various techniques are utilized to continue the hydration process depending on the alumina content of the cement. The period of curing may vary from as little as 24 h to at least 7 days. When high strengths are desired, it is imperative to maintain the curing conditions in a rigid manner because the high strengths are obtained from maintaining the moist state. Mortar mixtures are different from concrete in that the aggregate is simply sand with no large aggregates. The basic properties of mortar and concrete are the same as with any other building material. That is, terms such as modulus of elasticity, proportional limit, Poisson's ratio, stress, and others are utilized when describing these building materials.

Reinforced concrete construction is very common due to the availability of steel and concrete, its economy compared to other forms of construction, and relative ease and quickness of construction. Concrete structures have various advantages compared to wood or steel structures, such as fire resistance, stiffness, and low maintenance. The low tensile strength of concrete and time-dependent volume changes represent significant disadvantages to these structures. The use of steel reinforcement in concrete alleviates one of these concerns. However, reinforcement can only limit cracks, which will allow water penetration and subsequent degradation of the structure.

Concrete may be nonreinforced, nonprestressed reinforced, pretensioned or posttensioned, or prestressed. These concrete elements behave differently under loading. Nonreinforced, or plain, concrete beams will develop an internal couple involving tension that resists moments produced by loading. Failure of nonreinforced elements will occur suddenly and completely upon the first crack. Steel bars in a reinforced concrete beam will develop tension forces that provide moment equilibrium upon cracking of the concrete. Prestressed concrete involves reinforcement placed in tension and concrete placed in compression so as to delay cracking.

The minimum requirements for the design and construction of structural concrete elements under the building codes are governed by the *American Concrete Institute Building*

Code Requirements for Structural Concrete (ACI 318): As with steel or wood structures, concrete structures are designed with a margin of safety that includes a load factor on the service load and a strength reduction factor on the nominal strength. For a design example involving live and dead loading, the design strength must be equal to or greater than the required strength, or

$$\varphi M_n \geq 1.4M_d + 1.7M_l \geq \gamma_1 M_1 + \gamma_2 M_2 + \cdots \tag{2.38}$$

where

φ is the strength reduction factor
M_n is the nominal design moment
M_d is the dead load moment
M_l is the live load moment

The right side of this equation reflects problems where other loading combinations are considered and multiplied by the appropriate load factors (γ_i).

A structural element is deemed to be inadequate when it has reached its limit state. The above equation describes an ultimate limit state, wherein the design moment is not to exceed the strength of the reinforced concrete member. Ultimate limit states may be reached due to a loss of equilibrium, rupture, progressive collapse, or fatigue. A progressive collapse may be caused by a local failure, which can occur during construction. As such, construction loads and procedures must be considered.

Serviceability limit states, which involve the functional use of a structure, must also be considered. Serviceability normally refers to limits on deflection, crack width, and vibrations. These considerations disrupt the use of a structure but do not typically involve collapse or a threat to life, safety, and health. Some serviceability limits, such as mitigating crack width and deflection, can have long-term implications. Excessive cracking can lead to leakage through the cracks, subsequent corrosion of the reinforcing steal, and spalling of the concrete. A roof frame that experiences excessive deflections under normal loading conditions can result in ponding from rainwater. This ponding will increase as the roof deflections increase, which can ultimately lead to a collapse.

Chimney Damage

Most chimneys constructed today meet rigorous safety standards. A properly constructed chimney has several key elements that make the chimney a safe and useful device. The most common uses of a chimney are for aesthetic purposes and for heating. Whether the chimney is used as a flue mechanism for a free standing stove or insert or whether it is used by itself in the traditional log burning manner, chimneys have distinct characteristics in their mode of failure. The elements of the failure mechanism of a chimney can be broadly classified as follows.

First, since chimneys are very heavy structures, they must be properly supported and must rest on substantial footings. Typically, the footings are constructed of concrete, reinforced with steel bars (rebar), and placed on sound soils at appropriate depths for the climate. Care must be taken to ensure that the chimney footings are integrally tied to the house footings so that there is no differential or rotational settlement of the

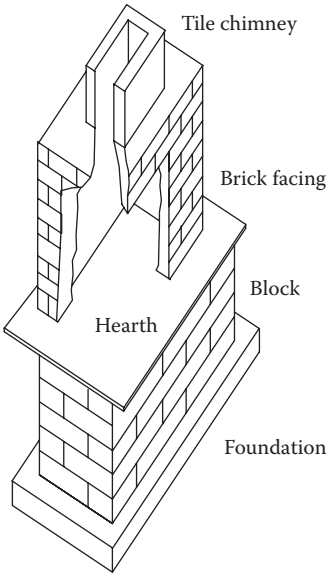

Figure 2.15 Fireplace.

two foundations. Differential settlement of the chimney foundation will often cause the chimney to lean away from the house and cause rotation. Additionally, water must be channeled away from all the footings so that erosion or hydraulic forces do not affect the structure. As with any footings, the foundation for a chimney must be below the frost line in order to avoid the destructive power of freezing water. The frost action can cause upheaval of the footings. The effect of the water content in the soils can have deleterious effects on the footings. If the footings were placed under damp conditions and not properly reinforced, then under arid conditions, the soils shrink and may cause footer failures. From the concrete footings, the chimney rises to the hearth level via a concrete block foundation as shown in Figure 2.15.

The second element of a properly constructed fireplace and chimney includes the elements of the hearth. The hearth rests on a slab atop the foundation. This slab must be constructed of fire retardant and fire proof materials. The hearth is typically constructed of concrete and lined with fire rated bricks. The hearth includes the recessed element that is commonly referred to as the fire box. The fire box is the volume in which the combustion process takes place. This fire box may contain a fireplace insert or may provide access to the flue from a free standing stove. With a traditional fireplace, the fire box is the place where logs are burned. The fire box may also contain a set of gas logs that may or may not need to be vented. Some fire boxes contain a rack for the wood logs and an additional set of burners to provide natural gas or propane in order to light the logs. These factors need to be considered in sooting incidents when a stove is suspected of causing sooting throughout the home. The front of the fire box is usually decorated with brick, stone, marble, or even wood. The top of the decorative front is called the mantle. All of these elements comprise the hearth. Improper foundations can cause the hearth to develop cracks that pose a fire danger. Additionally, the fire brick must be substantial enough to dissipate the heat properly without causing combustible materials to ignite. The chapter on fires covers some of these issues.

Emanating from the top of the hearth is the actual chimney or flue, the third element of a fireplace. The inside of the flue must be lined with fire-resistant materials. These materials may be fire brick, stainless steel liners, or more commonly flue liner material made of clay. This flue tile is recognized by its red color. Flue tile should never be mortared together because most mortars are not fire-resistant. Mortar joints in the flue tile disintegrate and allow fire to pass through the tile and attack other structural elements of a house. Many chimney fires are attributed to mortared flue joints. The flue tile by itself is not sufficient to dissipate the heat generated by the fire box. In order to protect other structural elements, the flue tile must be encased in either flue block or brick with an air or sand gap in between. In the case of a stainless flue liner, the piping must be double or triple lined piping and should not abut ignitable materials. The best chimneys consist of a proper flue liner encased in a flue block with sand in between the two and the entire structure faced with decorative brick or stone. The chimney should generally be 3 ft above the roof level. The top of the chimney consists of a cap. Often, the flue, itself, has a metal hat to prevent rain and moisture from entering the hearth. On large chimneys the cross-section may be 2-by-6 ft. If this large area is not properly capped, cracks will develop and allow moisture to enter the top of the structure. As water enters the brick facing, it freezes in cold weather and spalls the face of the brick. A white residue then forms from the infiltration of the water and its reaction with various salts and chemicals in the brick mortar mix. This white residue is known as calcination. This process is aided by heat from the chimney.

Each of the three major elements may experience failures. The foundation may fail and cause the chimney structure to lean, the hearth may crack and cause a fire, soot, and creosote in the liner may ignite and cause a fire, or the top of the chimney cap may develop cracks and deteriorate the chimney structure from the top down. The most common problems associated with chimneys are improperly constructed caps that allow water to enter and spall the brick facing. The key to analyzing this type of failure is to locate the cracks on the cap and find the white residue on the brick facing. These calcium salts that produce the white residue do not form rapidly as in the case of a chimney fire. The calcination and spalling of the brick are slow processes that normally take years to develop. Keep this in mind when investigating this type of a loss, which is attributed to a sudden event such as a snow or ice storm. Other problems associated with chimneys include water leaks into the hearth and leaks between the chimney and roof. Leaks at the roof chimney interface may result from improperly installed or deteriorated flashing or from settlement problems that cause the chimney to lean and rotate.

Truss Analysis

Many wood and steel framed structures include truss elements in their construction. Trusses and frames are composed of pin-connected members loaded axially. The connection points are referred to as joints. The axial loads can be in compression (pushing toward the joints) or in tension (pulling away from the joints). These loads are derived from forces acting on the truss, which are usually considered in the two-dimensional plane. Considering trusses as two-dimensional structures greatly simplifies the analysis.

Trusses are composed of chords (top and bottom), web members, and panel connections at the joints. Of importance are the composition and strength of the truss members, withdrawal strength of the connection joints, member lengths and cross sectional

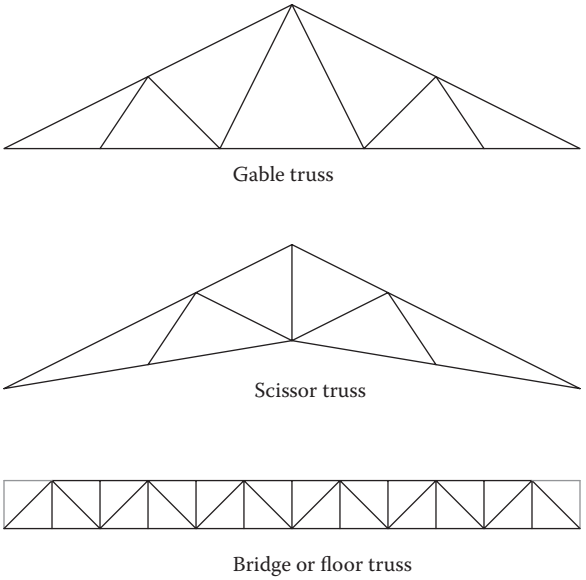

Figure 2.16 Trusses.

dimensions, and angle of the truss members. Shown in Figure 2.16 are common types of trusses used in house and bridge construction.

Analysis of a truss is performed along a two-dimensional plane. Free-body diagrams are produced for individual pins or sections of the truss. The method of joints permits the internal forces to be computed in a step-wise manner across the truss. The method of sections and the cut-and-sum method provide direct approaches for analyzing an individual truss member.

A truss will be statically determinate when the equations are independents. Thus, all unknowns can be computed if the following is achieved:

$$No.\,of\ members = 2(No.\,of\ joints) - 3 \tag{2.39}$$

If the left side of the equation is greater than the right side, there are redundant members, and the truss is therefore statically indeterminate. Conversely, if the right side of the equation exceeds the number of members, the truss is unstable and may collapse.

Thus, reviewing the composition of a truss prior to analyzing its forces will assist in a design

$$\sum M_{pt} = 0: \quad \sum F_x = 0: \quad \sum F_y = 0 \tag{2.40}$$

or analysis. Similarly, identification of zero-force members may simplify an analysis. A zero-force member is one that connects to an unloaded joint that already connects two collinear members. Two members joining at an apex are also zero-force members if there is no load applied to this point. A final factor that greatly simplifies a truss analysis is symmetry. For a symmetrical truss under uniform loading condition, the analysis can stop once the joints are considered for one-half of the truss.

Method of Joints

This method utilizes principles of equilibrium. Namely, the sum of forces in each direction, as well as the sum of moments about any point, will be equal to zero.

Consider the following diagram of a gable roof truss in two-dimensional Cartesian coordinates (Figure 2.17). The truss is being loaded by a combined live and dead load "L." Due to symmetrical loading, the total load is applied uniformly across the bottom chord panel points.

As shown, there are 7 joints and 11 members. From the determinancy equation, the number of members is equal to the number of joints multiplied by two and subtracting three. Thus, this truss is statically determinate. Taking the entire truss, the reaction forces can be easily determined. Since the load is applied uniformly across the symmetrical truss, the reaction forces are equal to half the total load. Given the known reaction force at point A (R_A), the following free-body diagram of Figure 2.18 for this joint is produced.

Summing in the y-direction yields

$$\sum F_y = 0: \quad R_A - F_{AB} \sin\theta = 0 \tag{2.41}$$

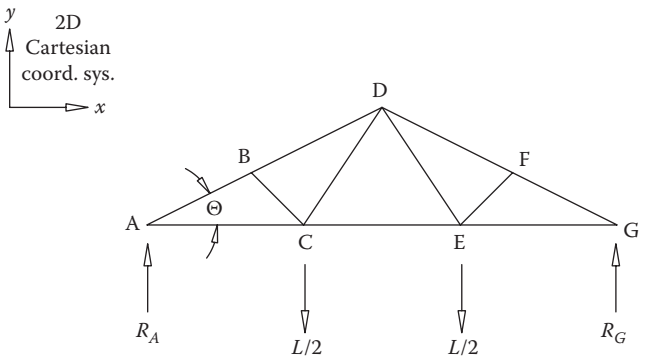

Figure 2.17 Method of joints.

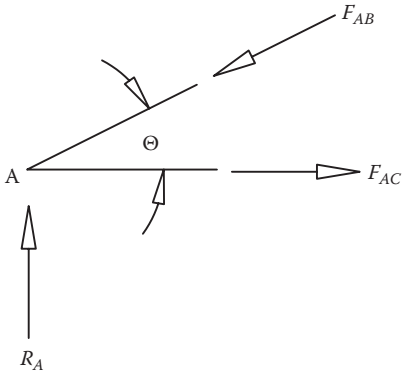

Figure 2.18 Free-body diagram.

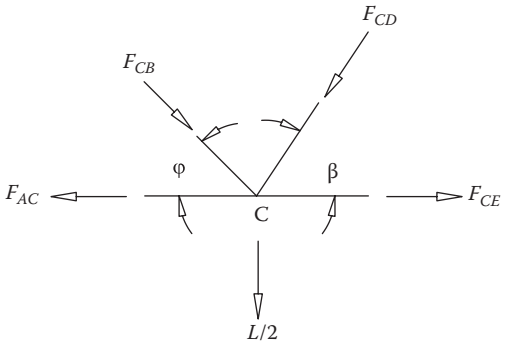

Figure 2.19 Free-body diagram.

Thus, since the reaction at point A is known, the force in member AB can be computed. Summing forces in the *x*-direction provides the force in member AC:

$$\sum F_x = 0: \quad F_{AC} - F_{AB}\cos\theta = 0 \tag{2.42}$$

As shown, member AB is in compression and member AC is in tension. Moving to joint C, the following free-body diagram can be drawn as in Figure 2.19.

Summing forces in the *x*- and *y*-directions yields the following relationships:

$$\sum F_x = 0: \quad F_{CE} - F_{CD}\cos\beta - F_{AC} + F_{CB}\cos\varphi = 0 \tag{2.43}$$

$$\sum F_y = 0: \quad -F_{CB}\sin\varphi - F_{CD}\sin\beta - L/2 = 0 \tag{2.44}$$

The initial diagram shows the forces in members CB and CD directed down. Given the equation for summing forces in the *y*-direction, the results for F_{CB} and F_{CD} will likely be negative. As such, the true forces will be directed away from joint C, and the members will therefore be in tension. Here, we have three unknowns for the two equations. As such, continuation to joints B and D will be necessary to determine all of the forces.

Method of Sections

As with the method of joints, it is first necessary to find the reactions before performing the method of sections on an individual member. If, for instance, it is desired to compute the force on member CD of the example truss, a virtual "cut" can be made across the truss as shown in Figure 2.20.

In addition to the end point reaction, the forces acting through BD and CD all pass through this point. Thus, the moments about point A produced by these forces will be zero. By summing moments about point A, we may consider only the force in member CD:

$$\sum M_A = 0: F_{CD}\sin\beta \cdot l_{AC} - L/2 \cdot l_{AC} = 0 \tag{2.45}$$

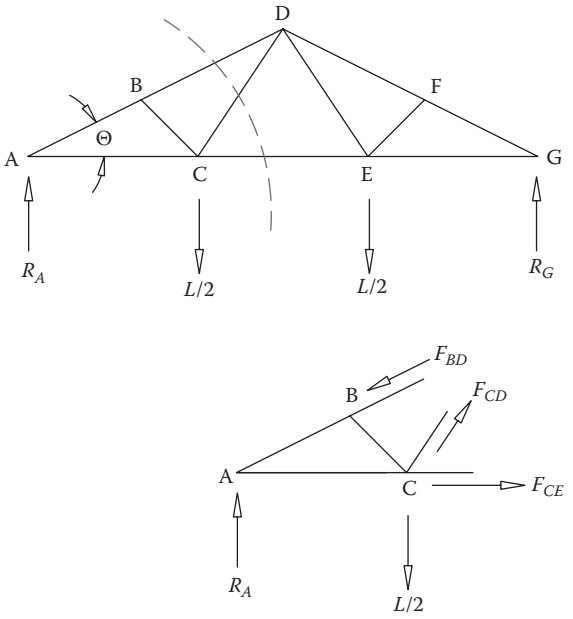

Figure 2.20 Method of sections.

Here, the moment arm is the length of member AC (l_{AC}). This moment arm cancels out, revealing that the force on member CD is equal to the panel point load divided by the sine of the member's angle.

Example: Truss Failure

Whenever roofs fail, the supporting capacity of the underlying structure is usually a truss system of some form. In this example we consider a failure of a mono-truss by the method of joints.

The loading conditions of the truss must first be determined. Figure 2.21 represents the truss and its physical dimensions. The trusses were spaced 3 ft apart and spanned 22 ft. The area covered by each truss is then 66 ft². A minimum value of 25 lb/ft² of horizontal covered surface should be used for snow load conditions for roof slopes up to 20°. The snow load per truss is then

$$W_S = (25\,\text{lb/ft}^2)(66\,\text{ft}^2) = 1650\,\text{lb} \tag{2.46}$$

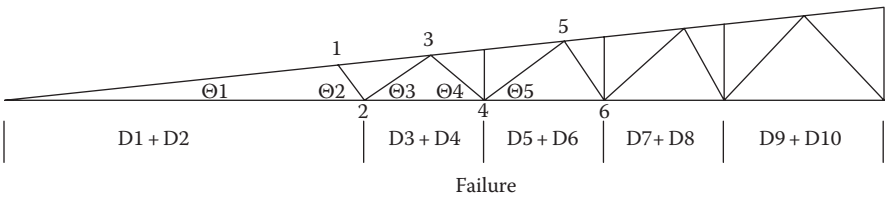

Figure 2.21 Truss failure.

The truss weight per square foot of covered horizontal area is computed from

$$W_a = \frac{1}{2}(1+0.1\ell) \tag{2.47}$$

where $\ell = 22$ ft (the length of the truss).

The total truss weight is then

$$W_T = W_a A_T = \frac{1}{2}(1+2.2)(66) = 106\,\text{lb} \tag{2.48}$$

The corrugated metal roof sheathing weighs approximately 1–2 lb/ft^2.

Therefore, the metal roof weight is

$$W_M = 2A_T = 132\,\text{lb} \tag{2.49}$$

The suspended ceiling weighs approximately 3 lb/ft^2, which produces a weight of

$$W_C = 3A_T = 198\,\text{lb} \tag{2.50}$$

The total load on each truss is then the sum of the live and dead loads, namely

$$W = W_S + W_T + W_M + W_C = 2086\,\text{lb} \tag{2.51}$$

This distributed load will be centered at joint 4. From the free-body diagram of the entire truss, we sum moments and forces, thus

$$\sum F_y = 0: \quad W = R_1 + R_{12} \tag{2.52}$$

$$\sum M_1 = 0: \quad W(D_1 + D_2 + D_3) = D_T R_{12} \tag{2.53}$$

$$R_1 = 1076\,\text{lb} \quad R_{12} = 1010\,\text{lb} \tag{2.54}$$

At joint 1

$$\sum F_x = 0: \quad A = .994B \tag{2.55}$$

$$\sum F_y = 0: \quad .105B = 1076\,\text{lb} \tag{2.56}$$

$$B = 10{,}248\,\text{lb} \quad A = 10{,}186\,\text{lb} \tag{2.57}$$

At joint 2

$$\sum F_x = 0: \quad (.994)(10{,}248) = -.598C + 994D \tag{2.58}$$

$$\sum F_x = 0: \quad 10{,}186 = 0.825E + F \tag{2.59}$$

$$\sum F_y = 0: \quad (.105)(10{,}248) = .8C + .105D \tag{2.60}$$

$$C \approx 0\,\text{lb} \quad D = 10{,}247\,\text{lb} \tag{2.61}$$

At joint 3

$$\sum F_y = 0: \quad E \approx 0 \tag{2.62}$$

$$E \approx 0\,\text{lb} \quad F = 10{,}186\,\text{lb} \tag{2.63}$$

At joint 4

$$\sum F_y = 0: \quad +(.105)(10{,}247) - 2{,}086 = .105G + .647H \tag{2.64}$$

$$\sum F_x = 0: \quad (.994)(10{,}247) = .994G + .762H \tag{2.65}$$

$$H = -3{,}683\,\text{lb} \quad G = 13{,}073\,\text{lb} \tag{2.66}$$

At joint 6

$$\sum F_x = 0: \quad G = I = 13{,}073 \tag{2.67}$$

$$\sum F_y 0: \quad .105I + .105G = J \tag{2.68}$$

$$I = 13{,}073\,\text{lb} \quad J = 2{,}745\,\text{lb} \tag{2.69}$$

At joint 5

$$\sum F_x = 0: \quad 10{,}186 + L = (.762)(3{,}683) - .512K \tag{2.70}$$

$$\sum F_y = 0: \quad 2745 - (.647)(3683) = .853K \tag{2.71}$$

$$K = 425\,\text{lb} \quad L = -7598\,\text{lb} \tag{2.72}$$

The free-body diagram at the failure is shown in Figure 2.22.

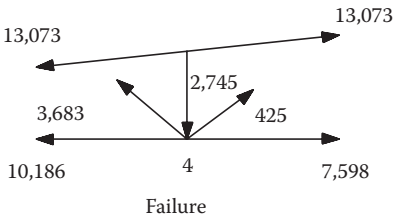

Figure 2.22 Free-body diagram.

The dimensions of this example truss are given below.

$D_1 = 8.33$	$h_1 = (D_1)(S) = 0.883$
$D_2 = 0.66$	$h_2 = (D_1 + D_2 + D_3)(S) = 1.13$
$D_3 = 1.66$	$h_3 = (D_1 + D_2 + D_3 + D_4)(S) = 1.27$
$D_4 = 1.33$	$h_4 = (D_1 + D_2 + D_3 + D_4 + D_5)(S) = 1.48$
$D_5 = 2.0$	$\sin \theta 1 = 0.105 \cos \theta 1 = 0.994$
$D_6 = 1.0$	$\sin \theta 2 = 0.800 \cos \theta 2 = 0.598$
$D_7 = 1.66$	$\sin \theta 3 = 0.564 \cos \theta 3 = 0.825$
$D_8 = 1.33$	$\sin \theta 4 = 0.647 \cos \theta 4 = 0.762$
$D_9 = 2.0$	$\sin \theta 5 = 0.853 \cos \theta 5 = 0.521$
$D_{10} = 2.0$	$\theta 1 = \tan^{-1} [h_8/D_T] = 6.05°$
$D_T = 22.0$	$\theta 2 = \tan^{-1} [h_1/D_2] = 53.22°$
$h_8 = 2.33$	$\theta 3 = \tan^{-1} [h_2/D_3] = 34.34°$
$S = h_8/D_t = 0.106$	$\theta 4 = \tan^{-1} [h_2/D_4] = 40.35°$
	$\theta 5 = \tan^{-1} [h_4/D_5] = 58.55°$

Dynamic Loading

Consider a case where a chute is installed on a parapet wall and roofing material is being released into the chute. If the material continues to build up inside the chute without being released into a container, significant forces can be created that will cause the parapet wall to fail. This type of analysis is dynamic loading or the equivalent static load.

When a body at rest is accelerated, the force necessary to produce the acceleration is called a dynamic force. In our case, the chute system was in equilibrium (at rest) until the alumabeam was dislodged. At that point in time, the support brackets on the outside of the parapet wall were accelerated downward and toward the exterior of the wall by the moments that were produced by the failure. The suddenly applied load produced by the bracket upon the wall exterior is referred to as an impact load. Since virtually no elastic action exists on the masonry parapet wall, the dynamic load may be expressed in terms of the acceleration and mass at the center, the rate of change of the momentum, or the change in kinetic energy of the body.

The energy approach is often the most effective when dealing with mechanics of materials. In this approach, the magnitude of the dynamic load is expressed in terms of kinetic energy delivered to the system. When a body of mass "m" moving at a speed "v" is stopped by another body, the energy absorbed is a fraction of the kinetic energy. The remainder of the energy is dissipated in the form of sound, heat, and permanent deformations. For low-velocity impacts, the velocity of the strain waves through the materials need not be considered. Essentially, at low velocities, the loading time permits the materials to behave in the same manner as under static loading conditions. Under these conditions, we can assume that the strain energy is equal to the effective applied energy (work done on the parapet wall). The effective energy in this case is that portion of the applied energy which produces the parapet wall failure.

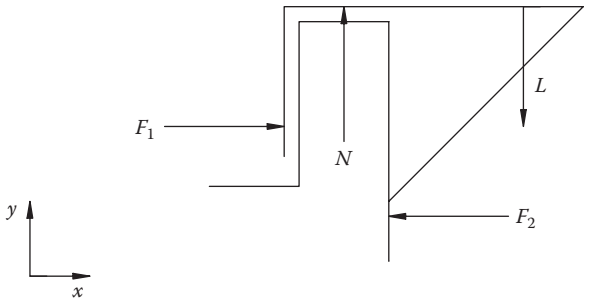

Figure 2.23 Static loading.

Consider the following free body diagram of the static loading on the parapet wall (Figure 2.23).

Summing forces we obtain

$$\sum F_x = 0: \quad F_1 = F_2$$
$$\sum F_y = 0: \quad N = L \tag{2.73}$$

When the alumabeam falls and the coupling moment is produced, the static force $F1$ must remain the same and produce the failure of the parapet wall. So summing moments about N,

$$\sum M_N = 0: \quad L(45-6.5) + F_2(31) + F_1(14) = 0$$
$$L(38.5) + F_2(17) = 0 \tag{2.74}$$
$$F_2 = 2.26L$$

The velocity at impact can be calculated through basic equations for the geometry of Figure 2.24:

$$d = \frac{1}{2}gt^2 \Rightarrow t = \sqrt{\frac{2d}{g}} = 0.22\,\text{s}$$
$$v = \frac{d}{t} = \frac{0.77\,\text{ft}}{0.22\,\text{s}} = 3.5\frac{\text{ft}}{\text{s}} \tag{2.75}$$

where

d is the distance to impact
t is the time to impact
v is the velocity at impact
g is the acceleration due to gravity = 32.2 ft/s^2

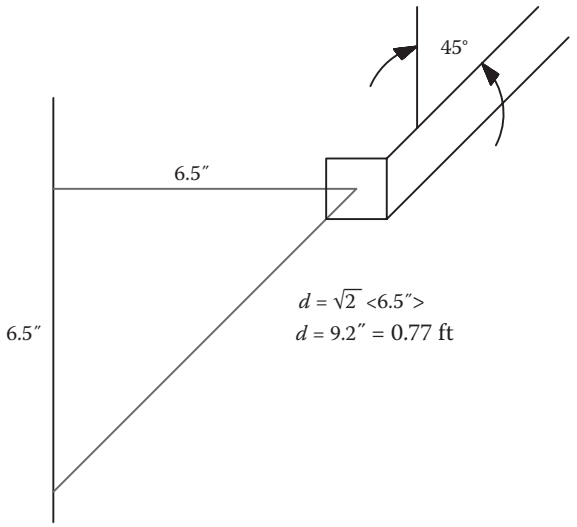

Figure 2.24 Impact velocity.

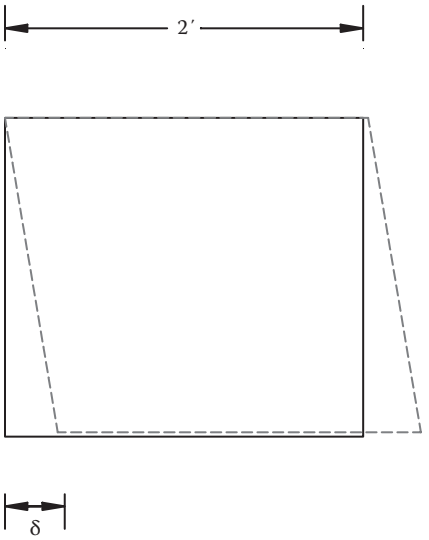

Figure 2.25 Square tubing deflection.

Consider the following diagram in Figure 2.25, which illustrates the deflection caused by impact on square steel tubing.

From measurements and photographs, the deflection of the tubing is known to be approximately ¼ in. (0.021 ft) to ½ in. (0.042 ft).

The dynamic loading of the bracket striking the parapet wall is best described by the energy applied to the wall. As described before, some of this energy is lost in the form of heat and sound. The effective energy applied is a fraction of the total energy and is related by the following equation. This principle only holds true for impacts at low velocities and where the load–deflection relationship is linear. The tubing is steel, which

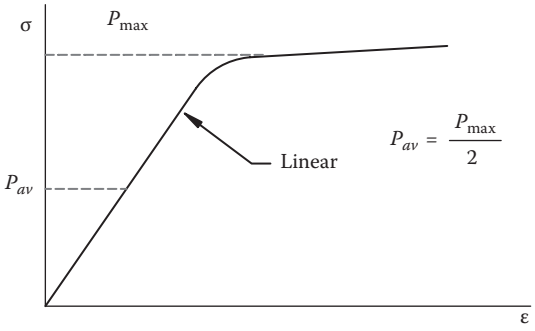

Figure 2.26 Stress–strain.

is an elastic material when enduring stresses below its characteristic yield stress. Elastic materials posses a linear stress-strain relationship below the yield stress as shown in Figure 2.26.

$$[\textit{Effective energy applied}] = [\textit{Work done by equivalent load}] \tag{2.76}$$

For steel, $P_{max} = \sigma_y A$

where

σ_y is the yield stress for steel = 36 ksi
A is the cross-sectional area = 1.27 in.^{2} for 2 × 2 × 3/8 steel tubing

Therefore, P_{max} = 45,720 lb. The work done by the equivalent static load to cause the deflection is the right side of equation P_{max}, which is

$$\begin{aligned} P_{av}\delta &= \frac{1}{2}P_{max}\delta \\ P_{av}\delta_{min} &= 476\,\text{ft-lb} \\ P_{av}\delta_{max} &= 952\,\text{ft-lb} \end{aligned} \tag{2.77}$$

The effective energy applied is given by the left side of the equation. For a moving body at a low velocity, it is a fraction of the kinetic energy, or

$$\frac{\eta}{2}mv^2 \tag{2.78}$$

The variable, η, describes the fraction of the total energy that is applied to the wall. The total mass, m, must be a function of the force F_2 into the wall, which is a function of L:

$$m = \frac{F_2}{g} = \frac{2.26L}{g} \tag{2.79}$$

From data provided by the manufacturer, we know that the empty chute weighs approximately 900 lb. Based on the volume of the chute sections that are loaded, we can calculate a range for the total load L. The volume of a truncated cone is known as a fustrum and is given by

$$V = \frac{\pi}{3} h\left[r_1^2 + r_1 r_2 + r_2^2\right] \tag{2.80}$$

For h = 4 ft, r_1 = 1.25 ft, and r_2 = 1 ft, the volume V equals 16 ft^3. Loose roofing material weighs between 15 and 25 lb/ft^3. Given that eight chutes were full, the total load of the chutes and roofing material weighs

$$2900\,\text{lb} < L < 4100\,\text{lb}$$

Then, the effective energy is

$$\frac{\eta}{2}\left(\frac{2.26L}{32.2}\right)(3.5)^2 = 0.43\eta L \tag{2.81}$$

Given the range of the total load,

$$\begin{aligned} \frac{\eta}{2} m v_{\min} &= 1247\eta \\ \frac{\eta}{2} m v_{\max} &= 1743\eta \end{aligned} \tag{2.82}$$

The values of η range between 0.27 and 0.76. The average η value is 0.48.

The above analysis considered $P_{\max}$ to be based on a yield stress of 36 ksi. The yield stress is in fact the maximum stress that the steel tubing can endure without deflection. Given the fact that the tubing did deform, the stress endured as a result of the impact must be greater that the yield stress of 36 ksi. Consider the equation in its mathematical form:

$$\frac{n}{2}\left(\frac{2.26L}{g}\right)v^2 = \frac{P_{\max}}{2}\delta_{\max} = \frac{\sigma_{\max}}{2A}\delta_{\max} \tag{2.83}$$

Solving for $\sigma_{\max}$ gives the following:

$$\sigma_{\max} = \frac{\eta 2.26 L A v^2}{g\delta_{\max}} \quad for \quad \eta > \eta_{\max}: \quad \sigma_{\max} > 36\,\text{ksi} \tag{2.84}$$

which satisfies the condition for failure.

Wind Damage

According to various weather reports and witness accounts, tornadoes were spotted in and around Lesage, West Virginia, on the evening of August 9, 2000. Wind and debris associated with the tornadoes caused extensive damage to several homes including the insured one. It has been alleged that the wind caused the left side wall of the insured's home to shift out from the foundation block at the base of the wall. This damage is indicative of suction pressure created by wind. Wind acting directly on a windward wall of the home also affects the leeward wall on the opposite end of the home. The wind blowing over the home creates a vacuum and corresponding suction pressure on the leeward wall. Consider Figure 2.27.

The loads created by the suction pressure are proportional to wind speeds. Given a certain wind speed, the force on the base of the wall will be sufficient to cause movement. Before determining the wind loads, it is necessary to calculate the force required to move the wall. This force is dependent on the load acting on the wall.

The hip roof is constructed such that there is no gabled end on the home. The rafters perpendicular to the left side are supported by the left side wall and by the angled hip rafters shown as dashed lines in Figure 2.28. The hatched region represents the area of the roof that is supported by the left side wall. The distributed load from the roof is based on the unit weights of the roof material and the hatched area. This load must be added to the weight of the wall to determine the distributed load on the foundation. Given a roof weight of 8 lb/ft^2 and a wall weight of 4 lb/ft^2, there are approximately 58 pounds per foot (plf) supported by the foundation wall.

In order to move the wall laterally at the base, a force F is required that is dependent on the load transferred through the wall (W) and the coefficient of friction (μ). As shown in Figure 2.28, a 1 ft section of the wall is considered. Therefore, the distributed 58 plf load is converted to a point load (W) of 58 lb.

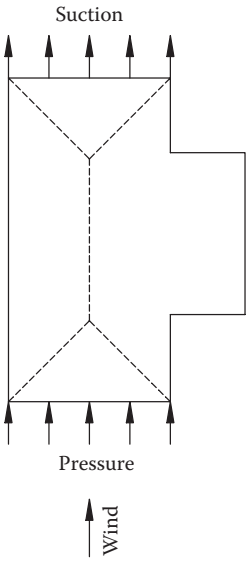

Figure 2.27 Roof view.

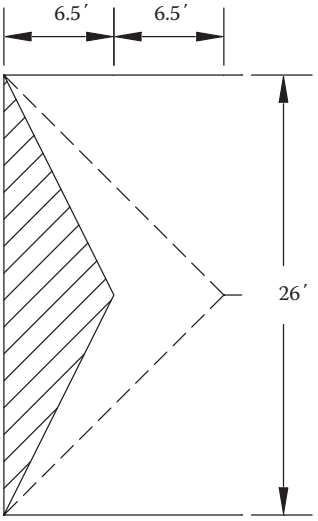

Figure 2.28 Hip roof deflection.

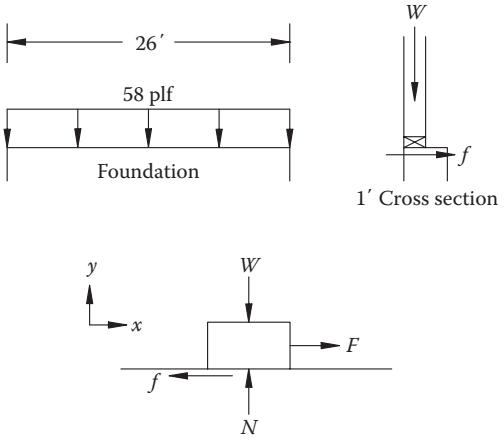

Figure 2.29 Wall cross-section. Where W is the load (lb), N is the normal load (lb), F is the applied force (lb), f is the frictional force (lb).

The cross-sectional diagrams in Figure 2.29 show only a friction force preventing the wall from moving at the base. During the inspection, no anchor bolts or other methods of attachment to the foundation block were observed. Although there may be a wall attachment to the foundation elsewhere around the home, none were found in the area of damage.

Summing forces according to the coordinate system in Figure 2.29: From the principles of static friction

$$f = \mu N \Rightarrow F = \mu W \tag{2.85}$$

$$\sum F_x = 0: \quad F - f = 0; \quad \sum F_y = 0; \quad N - W = 0 \tag{2.86}$$

Testing was performed to determine the coefficient of friction between standard lumber and cinder block. The tests provided an average μ value of 0.55:

$$F = \mu W = (0.55)(58\,\text{lb}) = 31.9\,\text{lb}$$

For each 1 ft section of the left side wall, 31.9 lb of force is required to move the base of the wall. This value can be compared to the force created by the wind suction.

The design wind pressure (p) is given by

$$p = C_e C_q q_s I \tag{2.87}$$

where

C_e is the Height, exposure, and gust factor = 0.62 for 0–15 ft height
C_q is the Pressure coefficient = −0.5 for suction on leeward wall
I is the Importance factor = 1.0
q_s is the Wind stagnation pressure (psf)

The wind stagnation pressure is dependent on the wind speed as shown in the following empirical equation:

$$q_s = 0.00256\ V^2 I \quad (\text{psf}) \tag{2.88}$$

where V is the wind speed (mph).

The actual wind speeds encountered at the home during the storm are unknown. However, since tornadoes were spotted and the extent of damage in the area is known, an approximate wind speed can be determined based on the Fujita–Pearson tornado intensity scale. This scale was developed in 1971 by Dr. T. Theodore Fujita and Allen Pearson. It is based on six categories and converts the degree and type of damage caused by a tornado into an estimation of the wind speeds inside the funnel. The classifications range from light (F0) to incredible (F5). Based on the extent of damage in Lesage, West Virginia, the damage could only be considered moderate, which classifies the tornadoes as an F1. Wind speeds inside F1 tornadoes range from 73 to 112 miles per hour.

Considering a median speed of 100 miles per hour within the F1 range, the wind stagnation pressure calculated in Equation 2.88 would be 25.6 psf. The actual pressure determined in Equation 2.87, which is based on design considerations, would be −8.0 psf acting on the entire left side wall. This pressure is given as a negative value as it is suction. Given a 1 ft section of the wall, the distributed load from the suction is 8.0 plf. The reaction forces are illustrated in Figure 2.30.

Since the summation of forces in one direction equal zero,

$$\sum F_x = 0: \quad P - 2R = 0 \Rightarrow R = \frac{P}{2} = \frac{64\,\text{lb}}{2} = 32\,\text{lb}$$

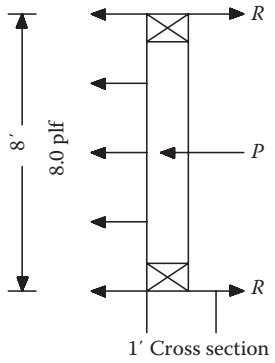

Figure 2.30 Reaction forces. Where P is the Resultant force from suction, P = (8.0 plf)(8 ft) = 64 lb, R is the Reaction force.

It has been determined that the force required to move the wall (F) is 31.9 lb. The reaction "R" is the force required to prevent the wind suction from moving the wall. This reaction created by the wind is greater than the force of friction preventing the movement. Therefore, the suction forces are sufficient to cause the base of the wall to shift outward.

Snow, Hail, and Rain

Hail Damage to Asphalt Shingles

The severity of hail damage to roofs depends on the kinetic energy of the hailstone and the amount of energy that is transferred to the roof in the impact. Generally, hailstones are spherical, and it is known from experimentation that when a hailstone strikes a flat surface, it contacts an area about half the diameter of the stone. The measure of hailstone impact is the amount of kinetic energy imparted to the impact area. Hailstones usually strike an area at an angle and for roof damage to occur, there must be a transfer of energy that can be quantified by a coefficient of restitution. Thus, from first principles, we may develop the equation for the amount of energy per contact area transferred during an impact as

$$K = \frac{4}{3} pdv^2 (i-e)^2 \cos^2 \theta \tag{2.89}$$

where

K is the energy transferred
p is the density of ice
d is the diameter of hailstone
e is the coefficient of restitution
θ is the angle of impact from the perpendicular
v is the hailstone velocity

Asphalt shingles have a hard coating of small stones to protect them from hail. As the shingles age, this coating is lost and the shingles lose their ability to withstand hail damage. When asphalt shingled roofs are past their useful life, they may be damaged by even trivial hailstones because they are essentially bare asphalt. Studies by the U.S. National Bureau of Standards have shown that damage to a roof in reasonably good condition will not occur if the impact energy is less 90 than 4000 g-m^2/cm^2-s^2. Since asphalt will become more brittle upon exposure to ultraviolet rays in sunlight, small impacts can cause damage to older roofs. Therefore, it is necessary to compare various areas of the damaged and undamaged shingles in order to evaluate the condition of the roof prior to the hailstorm whenever possible.

Stresses on Cylindrical Pressure Vessels

Thin-walled pressure vessels provide an important application of the analysis of plane stress. The internal forces exerted on a given portion of wall are tangent to the surface of the vessel. The resulting forces on an element of wall will thus be contained in a plane tangent to the surface of the vessel. The following analysis will concentrate on the thin-walled pressure vessel most frequently encountered: cylindrical pressure vessels.

Consider Figure 2.31 which illustrates a cylindrical vessel of inside radius r and wall thickness *t* containing a fluid under pressure. The internal pressure results in stresses exerted on the wall with sides parallel and perpendicular to the axis of the cylinder.

The σ_1 stress is known as the hoop stress because it is the type of stress found in hoops used to hold together slats of a wooden barrel. The stress σ_2 is called the longitudinal stress as it is parallel to the axis of the cylinder. In order to determine the hoop stress, an element of the vessel along the *x*-axis and bounded by the *y*- and *z*-axes is considered. Figure 2.32 shows the forces acting on the cylinder.

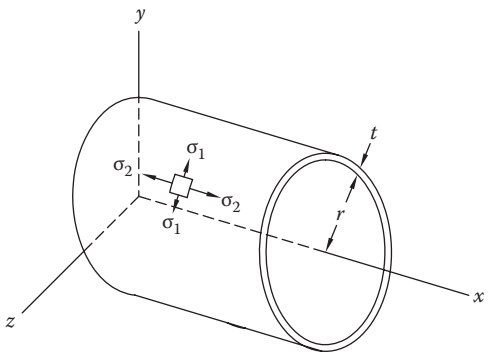

Figure 2.31 Cylindrical vessel. Where σ_1 is the hoop stress, σ_2 is the longitudinal stress.

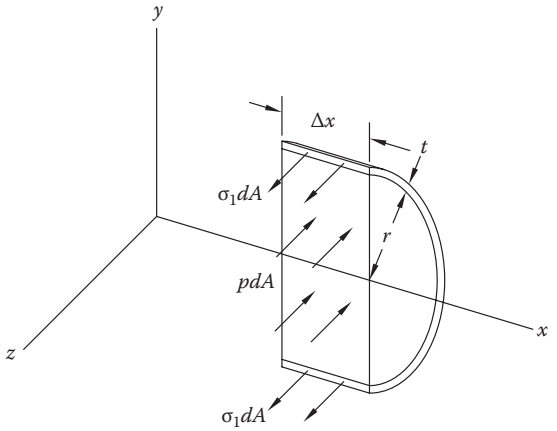

Figure 2.32 Forces on a cylinder. Where p is the internal pressure, Δx is the elemental width, dA is the elemental area.

Summing forces along the z-axis provides the following analysis:

$$\begin{aligned} \sigma_1 dA - pdA &= 0 \\ \sigma_1(2t\Delta x) - p(2r\Delta x) &= 0 \\ \sigma_1 &= \frac{pr}{t} \end{aligned} \tag{2.90}$$

The longitudinal stress can be analyzed by considering the free body consisting of the portion of the vessel and its contents located to the left of the section. Figure 2.33 represents the longitudinal stresses.

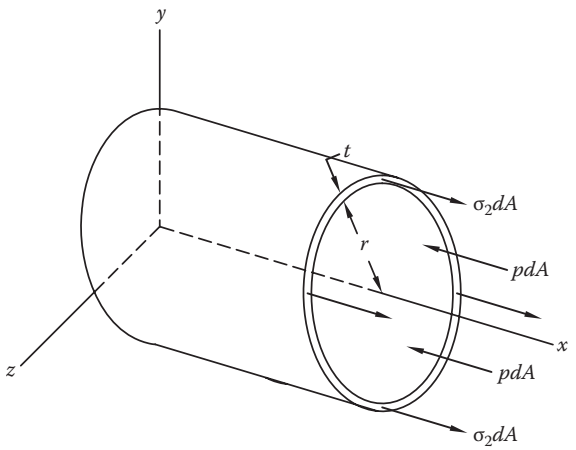

Figure 2.33 Longitudinal stresses.

Summing forces along the *x*-axis provides the following:

$$\sigma_2 dA - pdA = 0$$

$$\sigma_2(2\pi rt) - p(\pi r^2) = 0 \tag{2.91}$$

$$\sigma_2 = \frac{pr}{2t}$$

Relating the results from Equations 2.90 and 2.91,

$$\sigma_1 = 2\sigma_2 \tag{2.92}$$

In other words, given an internal pressure acting on the walls of a cylindrical vessel, the hoop stress will be twice as large as the longitudinal stress.

Modes of Failure

As shown in Equations 2.91 and 2.92, increased pressure inside a vessel will increase the stresses tangent to the surface. These stresses can increase to the point of failure. A common type of failure to thin-walled pipes is caused by freezing water. Water expands volumetrically as it freezes, which produces an increase in pressure on the walls of the pipe. Pipes damaged by freezing water are characterized by two kinds of failure, which are illustrated in Figure 2.34.

The pipe at the left side of Figure 2.34 represents failure due to excessive hoop stresses (σ_1). A split forms parallel to the cylinder axis from hoop stresses acting perpendicular to this axis. Thin-walled copper supply pipes most commonly incur this kind of failure from freezing water.

The right side of Figure 2.34 shows a pipe section that failed due to excessive longitudinal stresses (σ_2). Pipes break or loosen due to longitudinal stresses acting parallel to the cylinder axis. This kind of failure can occur at fittings of PVC compression, soldered copper, or threaded cast iron pipe, whether the fitting is a tee, elbow, or couple.

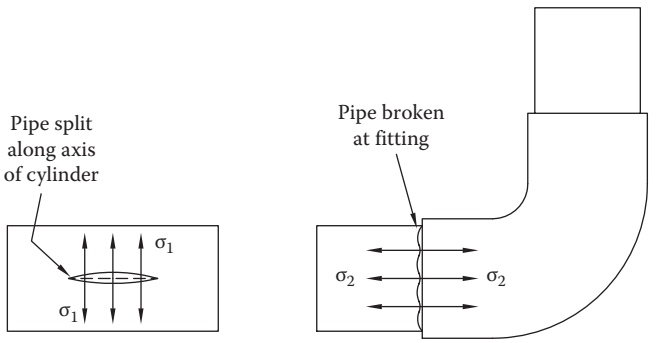

Figure 2.34 Modes of failure.

As stated previously, the hoop stresses are twice as large as the longitudinal stresses. Therefore, hoop stresses are more likely to cause failure along a continuous section of pipe. However, longitudinal stresses can cause failure at fittings, which may comprise a weak-point in the plumbing system.

Load Analysis on Pilings

An effective method of supporting unstable hillsides or embankments is to construct a retaining structure composed of piles and lagging. Piles are typically steel I-beams that are embedded into the earth. The I-beams are situated so that the strong-axis is in the direction of loading. This orientation also benefits the lagging, which are positioned within the flanges of the I-beam pile. Lagging may consist of precast concrete slabs with reinforcing steel or wooden timbers. Loads from the backfill and retained earth are supported by the lagging, which transfer these loads to the pilings. The pilings derive support from the soil and embedment into bedrock. Figure 2.35 details a cross section of a pile.

The forces acting on the wall are derived from the weight of soil retained by the wall. Dry soil typically weighs 90 pounds per cubic foot (pcf), whereas saturated soils can weigh in excess of 130 pcf. Thus, proper drainage is essential in order to prevent hydrostatic (water) pressures from affecting the wall. Given a soil's weight and natural angle of repose, a lateral soil pressure can be determined. According to the 1996 BOCA National Code, the design lateral soil load (γ) may vary between 30 and 55 pounds per square foot per foot of depth (psf/ft). These values depend on the grading and nature of the backfill behind the wall.

Figure 2.36 displays the pressure distribution on each side of the piling.

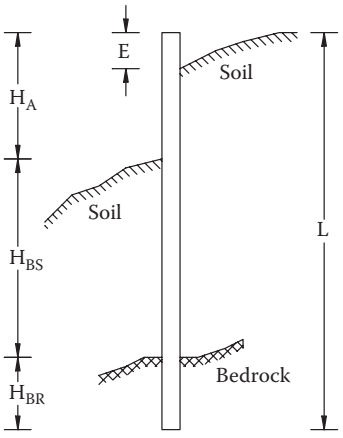

Figure 2.35 Pilings. Where H_A is the height above ground, H_{BS} is the height in soil, H_{BR} is the height in bedrock, L is the total length of pile = $H_A + H_{BS} + H_{BR}$, E is the extension of pile above retained soil.

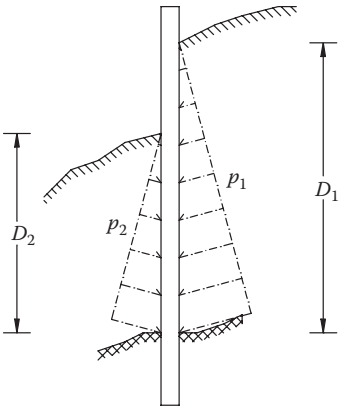

Figure 2.36 Pressure distribution. Where D_1 is the depth of soil behind wall = L – H_{BR} – E, D_2 is the depth of soil in front of wall = H_{BS}, p_1 is the pressure behind wall (psf), p_2 is the pressure in front of wall (psf).

The maximum pressures behind and in front of the wall are determined by the following relation:

$$p_1 = \gamma D_1; \quad p_2 = \gamma D_2 \tag{2.93}$$

The forces are determined by the product of their respective pressures acting on the effective areas. The pressure behind the wall (p_1) acts on the lagging and piling and is thus dependant on the piling spacing. The pressure in front of the wall (p_2) acts solely on the piling flange. The equation for the forces acting behind the wall (F_1) and in front of the wall (F_2) are as follows:

$$\begin{aligned} F_1 &= \frac{1}{2} s\gamma (D_1 - D_2)^2 + \frac{1}{2} b_f \gamma D_1 D_2 \\ F_2 &= \frac{1}{2} b_f \gamma D_2^2 \end{aligned} \tag{2.94}$$

where

s is the pile spacing
b_f is the flange width of pile I-beam

Referring back to Figure 2.16, the pressure increases linearly with depth. In other words, the pressure distribution is triangular. The forces derived from pressure act through the centroid of the pressure distribution. As a result, the forces act through a point located at one-third of the distance from bedrock to the top of the ground. The distance

between bedrock and the application of forces creates moment arms (r_1 and r_2), which are determined by the following:

$$r_1 = \frac{D_1}{3}; \quad r_2 = \frac{D_2}{3} \tag{2.95}$$

The moments created behind the wall (M_1) and in front of the wall (M_2) are given by

$$M_1 = F_1 \times r_1; \quad M_2 = F_2 \times r_2 \tag{2.96}$$

The figures indicate that the forces and moments created behind the wall will exceed that which is

$$F_R = F_1 - F_2; \quad M_R = M_1 - M_2 \tag{2.97}$$

formed in front of the wall. The resultant force (F_R) and moment (M_R) demonstrate the difference between the loads that push on the wall and the loads that resist movement.

The resultant forces and moments clearly serve to push and rotate the wall from a stable, vertical position. Thus, the embedment of the piling into bedrock is a critical element in the design of such a retaining structure. Specifications for piling walls from the West Virginia Division of Highways require that "a minimum of 1/3 the total pile length or 10 ft, whichever is greater, is to be placed in bedrock/shale." These specifications are rigorous in order to ensure that the embedment into bedrock is sufficient to resist the resultant moment.

Strain

Strain energy per unit volume

E is the Young's modulus

$$E = \frac{\sigma}{\in} = \frac{\text{stress}}{\text{strain}} = \text{Young's Module} \tag{2.98}$$

$$u = \frac{\sigma^2}{2E} = \frac{\sigma \in}{2} \tag{2.99}$$

u is the strain energy per unit volume
σ is the stress
ε is the strain

If an element is subject to triaxial loading, the stresses and strains can be resolved into their components. The total stain energy is the sum of the strain energies produced by each

stress (energy is a scalar quantity and can be added algebraically regardless of the directions of the individual stresses); thus,

$$u = \left(\frac{1}{2}\right)(\sigma_x \in_x + \sigma_y \in_y + \sigma_z \in_z) \tag{2.100}$$

Modulus of resilience {without deformation}

$$u_r = (35{,}000)(0.001{,}17)/2 = 22 \text{ in. lb/in.}^3$$

For steel E = 30 ksi modules of elasticity, specific weight .284 lb/in.^{3}

T1 Steel 100 ksi

$$\sigma_x^2 = \sigma_x \sigma_y + \sigma_y^2 = \sigma_f^2 \tag{2.101}$$

$$\sigma_{P1} = \frac{22.6R}{\pi} \quad \sigma_{P2} = \frac{1.6r}{\pi} \tag{2.102}$$

For a pipe, as shown in Figure 2.37

$$I = \frac{\pi(D_2^2 - D_1^2)}{4} \tag{2.103}$$

$$\sigma_1 = \frac{M}{I} = \frac{36R(2)}{I} \tag{2.104}$$

$$I = \frac{\pi}{64}(d_1^4 - d_2^4) = \frac{\pi}{64}[(2.875)^2 - (2.323)^4] = 0.04908[68.3206 - 29.120] = 1.924$$

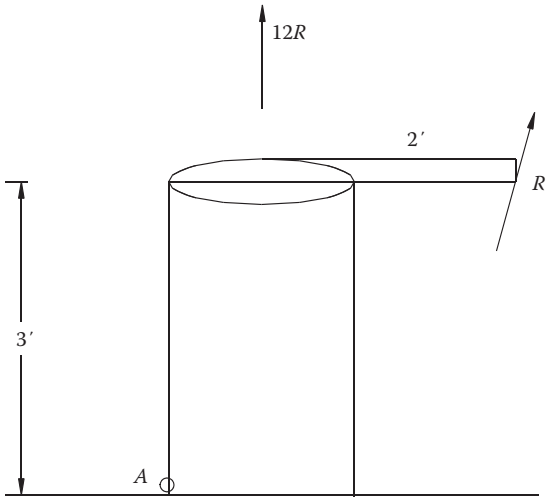

Figure 2.37 Pipe.

$$\sigma_1 = \frac{72R}{1.924} = 37.42R \quad \textit{Flexural Stress} \tag{2.105}$$

$$\sigma_2 = \frac{P}{A} = \frac{12R}{2.252} = 5.33R \quad \textit{Direct Stress} \tag{2.106}$$

Sum of two tensile stresses

$$\sigma = \sigma_1 + \sigma_2 = 42.75R \tag{2.107}$$

The torsional shearing stress at A is

$$\tau = \frac{T}{J} = \frac{24R(2)}{2(1.924)} = 12.47R \tag{2.108}$$

J = polar moment = 2I.

Maximum stresses at A are

$$\tau_{max} = \sqrt{(21.375R)^2 + (12.47R)^2} = [4.5689 \times 10^2 + 1.55 \times 10^2]R = 24.75R \tag{2.109}$$

$$\sigma_{P1} = 21.375R + 24.75R = 46.125R \tag{2.110}$$

$$\sigma_{P2} = 21.375R - 24.75R = -3.375R \tag{2.111}$$

According to the maximum normal stress theory using 64 ksi steel at max

$$64 = \tau_f = \tau_{P1} = 46.125R \tag{2.112}$$

$$R = 1.39\,\text{kip}$$

According to the maximum shear stress theory

$$64/2 = \tau_f = \tau_{max} = 24.75R \tag{2.113}$$

$$R = 1.29\,\text{kip}$$

According to the maximum distortion energy theory

$$64^2 = (46.125R)^2 + (-3.375R)^2 - (46.125R)(-3.375R) = 2127.52R + 11.39R + 155.67R$$

$$64^2 = 2294.58R$$

$$R = 1.78\,\text{kip}$$

This analysis shows that a reaction of between 1.3 kips < R < 1.8 kips will fail the supports at the base.

Foundations

Foundations are the basis for all structures. Foundations are not only necessary for buildings and houses, but for retaining structures, bridges, piers, railroads, and highways, to name a few. Foundations must meet three criteria. They must be able to support the load, they must be on solid earthen footings, and they must withstand the effect of moisture and temperature. Depending on the application, foundations may be relatively simple structures or they may be complex. Foundations that are required to support large weights may need to be anchored to bedrock. The usual foundation consists of two basic materials, concrete and steel. However, foundations may be constructed from a variety of materials such as stone or wood.

Common types of foundations include isolated spread footings, combined footings, and mat or raft footings. These types of foundations may rest on the bearing soil or rock formation or they may rest on pilings that may or may not rest on bedrock. The latter type of foundation is commonly referred to as pier or caisson foundation. As practical as possible, all foundations must be continuous. For example, the foundation of a house that is on the perimeter must be integrally continuous even though it may have a number of differential steps to fit the topography of the land. This is especially true in hilly terrains. If these footings are discontinuous at the steps, they provide a great propensity to differentially settle. Additionally, footings should be reinforced with steel and concentrically loaded with the column load so that a moment due to the eccentric load of the column does not produce uneven pressure on the spread portion of the footing. In this manner a critical shear section of the footing is not produced.

Builders in residential home construction rarely use forms to build their footings. They simply excavate the soil making the footings irregular and weak. They use the soil as the form for the foundation, a very bad practice that leads to a variety of foundation problems. In industrial construction, forms are always utilized for a variety of reasons. First, accurate volumes can be determined in this manner. Second, the sides of the footings become regular and smooth and have a lesser tendency to form cracks thereby repelling the infusion of water into the footing. Third, the footings can then be equipped with foundation drains located in the appropriate locations. Fourth, the concrete mixture can be vibrated to ensure homogeneity making the footings stronger, and allowed to cure properly. Fifth, reinforcement steel can then be located at the appropriate design location within the footing. Finally, it is easier to provide the reinforcement within the footings in a form than on the ground with crumbling sides, and the top of the footing can then be made level and smooth.

Foundations must be below the frost line for the particular section of the country, which is imperative because frost upheaval creates significant structural foundation distress. Foundations also require proper drains and sealing of the walls to eliminate the infusion of water. Maintaining a dry soil environment around the foundation minimizes the shrinkage and swelling of the soils, which also causes structural distress especially in clayed soils.

Retaining walls are built to sustain the lateral pressures of the earth or other materials. Generally, retaining walls are constructed when a slope has been excavated, a process referred to as cutting the toe of the slope. This activity can often lead to a slope that is unstable. Sometimes naturally occurring slopes are unstable. As a general rule, a

hillside with a slope of 1:1 is considered to be stable and one with a slope of 2:1 is considered unstable. Retaining walls depend on stability based on either their own weight or on their weight plus the weight of the material that is being supported.

As with any hillside, whether it is supported by a retaining wall or not, a slip plane forms in a curved path downward and across the weak areas of the soil. If the hillside slides downward, a scarp is formed. The scarp is associated with layers of the soil where friction between the interstitial particles is the least and generally the wettest. The curved direction of the rupture surface varies according to the moisture content of the soils. Thus, when retaining structures are designed, the control of the drainage behind the structure is of utmost importance. A very common mode of failure of retaining walls is that of inadequate control of the water from the hillside.

Blasting and Earth Movement 3

Introduction to Soil Behavior

The stability of soils is derived from the shearing strength. The ability of soils to support spread footings is directly proportional to their shearing strength. In a general manner, soils may be classified as granular or cohesive. Granular soils have internal friction resistance so that their shearing strength increases in relation to the normal pressure to which they are subjected. Purely granular soils have no cohesion. Clays found in the Appalachian basin are highly cohesive and have no angle of internal friction. They have a resistance to shearing due to their cohesive or molecular strength. Therefore, clays show that their shearing strength is the same regardless of the normal pressure to which they are subjected. Soil mixtures of clay and sand partake of both cohesive and internal friction resistance. Thus, most sands have some cohesion and most clays have some internal friction.

In order to judge the strength of the soils, they must first be properly classified. The classification is determined by grain size such as clay, silt, sand, or gravel. It is usually used with empirical tables to give the strength for building foundations. The identification of the principal types of soils is performed visually, by texture, by mechanical grain size analysis, by Horjous, by the Casagrande classification, or by performing Atterberg limit tests. A moisture determination of the soil must always be performed because soil performance is directly related to moisture content.

Granular soils do not hold water readily. In contrast, clays tend to hold free water in addition to their adhered water. They do not drain nor do they dry out rapidly. Clays are subject to a large amount of shrinkage, but the loss of water that causes this shrinkage is slow. Clays may shrink as much as 20%. Granular soils do not shrink appreciably when drying and do so more rapidly.

When granular soils are saturated with water and the water is trapped, the footings may be supported on hydraulic pressure. This is called pore water pressure. Soils under pore water pressure are without shearing strength; consequently the seepage out of pore water under pressure will cause settlement. Under these conditions, it is imperative to release the water.

Clay settlement varies directly with water content and inversely with cohesive strength. For a given unit pressure on a given clay, a definite amount of settlement may be expected. In contrast, settlement on sands and silts varies with density. For most soils there is a percentage of moisture at which the soil will compact to its greatest density and therefore its greatest supporting capacity for footings. This optimum moisture content may range from 8% for sands, 15% for silts, and 15%–20% for clays.

Blasting activities near construction or mine sites are often suspected to have influenced the strength and supporting capacity of a structure. Foundation failures, often associated with ground settlement, excessive water, hydrostatic pressure, inadequate design, substandard construction, or a combination of these factors are blamed on the activities of industry.

Whether the mine is an open surface or a deep underground facility, significant activity takes place including the detonation of charges to move soils and rock, as well as the use of heavy equipment that produces vibrations. Sometimes construction activities may change the characteristics of the water table and the water discharge from an area that affects an adjoining area.

Blasting activities cause two main types of wavefronts: one that is carried through the underlying strata and the other through the air. The wavefront carried through the air can cause structural damage to vertical weak surfaces such as windows. The air wavefront is generally incapable of producing structural damage to walls, floors, ceilings, roofs, and foundations. The ground wavefront may cause foundation and structural distress if the blast is strong enough and near enough to the structure.

Landscaping activities including the modification of embankments, the inclusion of ditches, and the defoliation of the soils can cause significant changes in the flow of water on the surface and in the ground. These activities are known to cause landslides, retaining wall collapses, flooding of structures and soils, and general mayhem. Often, the forensic engineer is called upon to investigate these concerns as well as the effect of the construction or mining activity. As a general rule, one of the first considerations for the investigation is the soil type and its effect on the loss in question. The following sections outline these investigations and the makeup of the strata associated with the particular claim.

Techniques of Subsurface Investigations

Before an engineer can design a foundation or determine if a structure is in danger of collapsing, he must have a reasonably accurate conception of the physical properties and the arrangement of the underlying materials. The field and laboratory examinations required to obtain this essential information are called the *exploratory program*. Because of the complexity of natural deposits, no one method of exploration is best suited for all situations. The method most suitable for a wide variety of conditions consists of drilling holes into the ground and extracting samples for identification and for testing.

Sampling

The kind of samples that should be obtained from an exploratory drill hole depends upon the purpose for which the exploration is made. For proper identification and classification of a soil or rock, representative samples are required. They should contain all their constituents in their proper proportions. Such samples are adequate for visual classification, for the performance of mechanical analyses, and for determining the Atterberg limits, the unit weight of the solid constituents, the carbonate content, and the quantity of organic matter. The mechanical properties of the soil, however, may be appreciably altered by the sampling process.

Most samples are obtained by driving an open ended cylindrical tube known as a *sampling spoon*. The degree of disturbance of spoon samples depends upon the way in which the force is applied to the spoon, whether by pushing or driving, on the rate of penetration, and on the dimensions of the sampler. If other conditions are equal, the degree of disturbance is roughly proportional to the area ratio

$$A_r\ (\%) = \frac{De^2 - Di^2}{Di^2} \times 100\% \tag{3.1}$$

Table 3.1 Correlation of Standard Penetration Test

Sands		Clays	
No. of Blows per ft, *N*	Relative Density	No. of Blows per ft, *N*	Consistency
0–4	Very loose	Below 2	Very soft
4–10	Loose	2–4	Soft
10–30	Medium	4–8	Medium
30–50	Dense	8–15	Stiff
Over 50	Very dense	15–30	Very stiff
		Over 30	Hard

If the area ratio is not greater than about 10%, the distortion of the sample is small in almost any type of soil. The degree of disturbance is also less if the sample is advanced with a rapid steady motion.

Direct Measurements of Consistency and Relative Density

In the United States, the most widespread penetration test is made by driving a sampling spoon into the ground and counting the number of blows of a drop hammer required to produce a given penetration. This procedure may be combined with boring and sampling operations to provide additional information concerning the characteristics of the subsoil. This *standard penetration test* is made by dropping a hammer weighing 140 lb onto the drill rods from a height of 30 in. The number of blows *N* necessary to produce a penetration of one foot is regarded as the penetration resistance.

The results of the standard penetration test can be correlated with the pertinent physical properties of the soil. Table 3.1 shows such a correlation.

Although the standard penetration test cannot be regarded as a highly reliable and completely refined method of investigation, the *N* value gives a useful indication of the consistency or relative density of soil deposits.

Interpretation of Water Content of Soils

The presence of water in soils can be broken down into three ranges. Dry to damp soils contain up to approximately 10% water, wet earth up to about 20%, and saturated earth up to about 35%. The combination of water content and the type of soils can make for conditions where the layer between the soils becomes very fluid and is subject to movement. This situation occurs most often when saturated clays lie atop limestone or bedrock, which is impervious to moisture.

Landslides

Landslides and avalanches are massive downward and outward movements of slope-forming materials; these masses may range from the size of cars to entire mountainsides. The term landslide is restricted to movement of rock and soil and includes a broad range of velocities, even slow movements that, although rarely a direct hazard to life, can destroy buildings or break buried utility lines. Landslides are generally naturally occurring but may be precipitated by human activity such as construction. The term avalanche includes movement of snow and ice as well as rock and soil materials and applies only to movements rapid enough to threaten life.

A landslide occurs when a portion of hillslope becomes too weak to support its own weight. The weakness is generally initiated when rainfall or some other source of water increases the water content of the slope, reducing the shear strength of the materials. Other causes of landslides include earthquakes and loud sounds. Landslides are abundant where erosion is most actively wearing away the terrain, as along some streams and seacoasts, but they also occur well away from areas of active downcutting. Many types of landslides move seasonally or sporadically and may lie dormant for years. Slow-moving landslides are distinguished from creep by having distinct boundaries with adjacent stable ground.

Ground that is stable in its natural state may slide after human alteration. Grading for roads or buildings on hillsides facilitates landsliding, both by cutting into the slope—removing support from materials higher up the slope—and by overloading the slope below with the excavated materials. Many damaging landslides occur where development alters natural slopes or groundwater conditions, especially within dormant landslide masses that are barely stable in their natural state.

Landslides are generally classified into slides, falls, and flows. Slides move as largely coherent bodies by slippage along one or more failure surfaces. Slumps are those slides which move largely by rotation along cylindrical slip surfaces. The resulting backward rotation of the slide mass commonly produces hillside flats in otherwise sloping terrain. Block glides, in contrast, slide along inclined planar slip surfaces. Slumps and block glides move up to 2 m/day (7 ft/day), though commonly much slower, and may involve the movement of enormous volumes of material. Debris slides and rockslides move slowly to rapidly down steep slopes. Falls of rock or soil originate on cliffs or steep slopes. Large rockfalls can be catastrophic events. An earthquake off the coast of Peru in 1970 started a rockfall from the northwest peak of Huascaran. The descending mass, which incorporated material as it accelerated to more than 280 km/h (170 mph), buried more than 18,000 people.

Flows are landslides that behave like fluids. Many varieties are recognized. Mudflows involve wet mud and debris. Earthflows involve wet clay-like material. Slow earthflows are tongues of material up to hundreds of meters long that commonly move less than several meters a year. They are abundant on clay-like hillslopes such as those in the California Coast Ranges. Rapid earthflows, in contrast, occur on very gentle slopes in sensitive silts and clays, as along Riviere Blanche, Quebec. Solifluction is the slow downslope flow of soil that occurs on arctic and alpine hillsides when thawed ice or snow saturates the soil cover. Dry flows occur where great kinetic energy, as from earthquake or fall from steep slopes, permits dry materials to flow unexpectedly long distances very rapidly. A large, rapid flow of dry loess (wind-deposited silt) accompanying an earthquake (1920) in Gansu Province, China, killed 100,000 people. A rockfall avalanche is a form of dry flow in which enormous rockfalls flow rapidly for kilometers across gentle slopes. Rockfall avalanche deposits are also recognized on the Moon.

Avalanches

Snow avalanches are caused by the added weight of fresh snow or by gradual weakening of older snow. They are often triggered by the weight of a skier or the impact of small masses of snow or ice falling from above. Snow avalanches are a major danger in high mountain areas. In the Dolomites of Italy during World War I, 6000 troops were killed in a single day by snow avalanches.

Two principal types of snow avalanches are distinguished. A loose snow avalanche gathers more and more snow as it descends a mountainside. A slab avalanche consists of more compact, cohesive snow and ice that breaks away from the slope in a discrete mass, much like block-glide landslide; this type is responsible for the great majority of accidents.

Prevention and Damage Limitation

A number of methods are employed to prevent landslides, such as the capture and drainage of water before it reaches the potential slide areas; the pumping of water from wells in the slide area; and the filling in of cracks that could be pervaded by precipitation or surface water. Damage to buildings and other structures is limited through geologic exploration of construction sites and through the design and construction of earthworks.

The avalanche danger of unstable slope accumulations is reduced or prevented through detonation, from either the tossing of grenade-like explosives or the shooting of basooka-like shells into the slope. Structural damage is limited by the construction of various types of fencing and of splitting wedges, V-shaped masonry walls that split an avalanche around a structure located behind the walls.

Mudflow

A mudflow is a sudden and destructive variety of landslide in which predominantly fine-grained earth material, mobilized by saturation of loose materials on steep slopes, flows down a channel or canyon. The term debris flow is used if more than half of the solid fraction is larger than sand size. The water content of mudflows may range up to 10%–60% by volume. Their high specific gravity permits transport of huge boulders for great distances down gentle slopes. Mudflows generally move faster than walking speed but slower than running water, often advancing in surges followed by a flow of muddy water.

Three types of mudflows are recognized. Desert mudflows occur when infrequent thunderstorms saturate surficial materials on sparsely vegetated slopes. The mass mixes as it moves downslope and then flows downcanyon, commonly onto alluvial fans. Most desert mudflows are thinner than 2 m (7 ft), but they have destroyed much life and property in such areas as Los Angeles. Alpine mudflows, which gain water from thaw or snowmelt, can be enormous, and they have demolished whole villages in the Alps and Himalayas. Volcanic mudflows, or lahars, occur on the flanks of volcanoes during or shortly after explosive eruptions; volcanic ash and debris are saturated by rains condensed from steam or other sources related to eruption. These flows can be particularly destructive. Mudflows from Mount Vesuvius buried the town of Herculaneum in AD 79. The 1980 eruption of Mount St. Helens in southwestern Washington state created a destructive lahar that moved as fast as 80 km/h (50 mph).

Erosion and Sedimentation

Erosion and sedimentation in geology are complementary processes that wear away rock materials, removing them from one area of the Earth's surface and depositing them in another. Before being deposited, the eroded material is usually transported for some time

and distance, often by the same agent. Human practices have caused massive soil erosion over historical time.

Modes of Erosion

Subaerail erosion includes all erosion that occurs on land exposed to the atmosphere. Exposed rock materials are often altered by chemical or mechanical processes (weathering) and then transported by various means. The main agents of subaerial erosion are gravity, running water, ice (mainly in glaciers), wind, and near-shore ocean waves.

Gravity erosion is often called mass wasting. It occurs where land-surface irregularities such as hillslopes allow gravity to transport the rock debris produced by weathering. Slopes originate in many ways, the most common being crustal movements, or diastrophism, and valley cutting by streams. Unless accelerated by the lubricating effect of running water, the downhill movement (creep) of rock debris ordinarily occurs so slow as to be imperceptible.

Running water, or fluvial, erosion includes erosion performed by the solvent action of water, by the force of moving water, and by the abrasive effects of rock particles in moving water. In humid, vegetated lands, the solvent action occurs beneath the mat of vegetal cover and along water courses that develop to drain surplus water. The force of running water in humid lands is greatest along stream channels where flow is rapid and perennial. Some sediment is acquired by direct corrosion of channel bottoms and sides, but more is supplied by mass wasting on hillslopes that extend to channel margins. In established stream systems, most erosion occurs during periods of especially high water discharge. Stream banks are undercut by the moving water, particularly along the outsides of bends, and channel floors are scoured and abraded by fragments moving along in the bouncing and rolling mode known as saltation. The solid sediment fragments themselves tend to change in shape from angular to rounded.

In deserts, where vegetation is sparse, fluvial erosion is virtually unrestricted. Water is rapidly lost by evaporation and infiltration, so there is less solvent action, but there is an almost limitless supply of rock debris. Water in sheetwash and flash floods quickly picks up large amounts of solid sediment. Later, runoff volume losses may convert stream runoff into mudflows, which eventually solidify and cease to move. Mudflows do not seem to be significant agents of erosion.

Glacial meltwater erodes rock debris and carries it away from the margins of moving ice masses, or glaciers. Meltwater streams, which are usually heavily loaded with rock debris, are not powerful enough to perform significant erosion in downstream reaches.

Ice erosion, or glaciation, is mainly accomplished by the movement of glaciers. Glacial ice freezes to rock fragments and literally plucks them loose. The fragments entrained by a glacier become erosive agents, rubbings and scraping against bedrock in a rasping action that abrades and polishes. In mountainous areas, where glacial ice is confined to elongate depressions, the erosive plucking action combines with abrasion to excavate U-shaped valleys. These valleys often extend upslope to ice-eroded bowls called cirques. Glacial erosion by continental ice sheets tends to be more broadly expressed on the land and produces plains of glacial scour, dotted in many places by lakes, drumlins, and moraines. The Great Lakes of North America seem to be productions of deep glacial scour of relatively soft rocks beneath continental ice sheets.

Erosion by wind action occurs mostly on beaches and in deserts, where there is no continuous groundcover of vegetation. Except for rare high-velocity tornadic winds, air currents can readily move only rock particles less than 2 mm in diameter. Most sand in desert dunes and on beaches is smaller than this, as are the finer silt and clay that blow out of deserts during dust storms. Most desert sand originates in dry watercourses, although some is freed each time fine-grained fractions of soils blow away following climatic changes from humid to arid. Wind can pick up rock particles by the process known as deflation and may thereby create depressions on the land surface. Where winds are strong, particles bounced and rolled along the surface may abrade and erode rock surfaces as well as polish them. On the dry surfaces of planets such as Mars, and in a few places on Earth, extremely strong winds have carved entire landscapes of elongate, streamlined hills and depressions.

Wave erosion, which occurs along beaches and coasts, is caused by the impact of breaking waves and the abrasion of wave-transport sediment. It is responsible for shaping the bedrock in headlands along ocean shores to form sea cliffs.

Subaqueous erosion results from the action of water currents on the bottoms of bodies of standing water. It can occur where strong currents develop because of lunar tides and of differences in water density. In the deep oceans, strong currents may develop in narrow constrictions between land areas or where masses of sediment slump from elevated plateaus or continental margins and move into the abyssal depths. The latter movements, called turbidity currents, may have been responsible for the erosion of some of the deep notches in continental margins called submarine canyons.

Processes of Sedimentation

Sedimentation, the process of sediment accumulation, occurs when a transporting agent is forced to deposit its load of sediment. Deposition may occur for physical reasons, as when a sediment mass moving downhill by gravity reaches the base of the slope, when a current of air or water slows down, or when the ice of a glacier melts; it may occur for chemical reasons, as when materials dissolved in water are precipitated; or it may occur for biological or biochemical reasons, as when organisms act to entrap or induce sediment accumulation.

Gravity deposition of sediment almost always occurs at the bases of hills or cliffs where slopes are too low to permit further downward movement. Deposits include soil and rock mixed by downslope creep (colluvium), fragmental rock (talus), and chaotic mixtures of soil, rock debris, and plant material (landslide deposits).

Running water, or fluvial, deposition of solid sediment occurs when currents slacken. In humid areas this occurs in deep, quiet pools, on the inner margins of stream bends, in slack water areas after overflow, and at stream mouths, where flow enters the standing water of seas, lakes, or swamps. In swamps, some sedimentation occurs by vegetal entrapment. Desiccation causes sedimentation in deserts.

Chemical and biochemical depositions occur when water containing dissolved solids becomes subject to conditions that reduce solubility. Cooling reduces the solubility of water flowing from hot springs, causing deposition of sinter. Agitation at falls and stream rapids may drive off dissolved carbon dioxide gas and cause calcium carbonate to precipitate, forming limestone. Similar processes may occur in bodies of standing water. Evaporation in caves may induce deposition of limestone; in seas it may cause deposition of salt and gypsum. Many organisms extract dissolved material from water

to use in building their skeletons. Fragments of these skeletons may in turn accumulate to form a special type of clastic rock called bioclastic.

Glacial deposition of sediment mainly results from the melting and other forms of wastage of immobilized ice masses. Rock debris accumulated in this way is unsorted (drift, till) and not layered, in contrast to sediment deposited by air or water, which tends to be divided into fractions of distinct sizes (sorted) and is also often layered. Sediment deposited by glacier meltwater closely resembles other streams and rivers.

Wind deposits particles of different sizes in different ways. Sand (1/16–2 mm in diameter) forms sand dunes in deserts and on beaches. Silt (1/256–1/16 mm) blows out of deserts and is trapped by vegetation in humid lands or bodies of water immediately downwind. Clay-sized sediment (less than 1/256 mm) moves readily and settles out of quiet air, often over distant lands and seas.

Standing-water deposition occurs in oceans, lakes, and seas when gravity causes particles of solid sediment to settle out and form layers on the bottom. In oceans, some causes include microorganisms that live near the surface (plankton); airborne dust from deserts, burning meteors, and volcanic eruptions; and fine-grained sediment introduced by rivers and turbidity currents.

Identification of Rocks

The rock materials encountered at the surface of the earth or beneath the surface soil are commonly classified into three groups according to their mode of origin. *Igneous* rocks are considered to be the primary rocks formed by the cooling of molten magmas, or by the recrystallization of older rocks under heat and pressure great enough to render them fluid. *Sedimentary* rocks are the products of deposition of plant and animal remains and of materials formed by the chemical decomposition and physical disintegration of igneous, sedimentary, or metamorphic rocks. *Metamorphic* rocks are those produced by internal processes acting on preexisting rocks of any kind, with the limitation that the rocks concerned remain essentially solid during their transformations.

It is usually possible to assign a given rock to one of these three groups after visual inspection, provided one is familiar with the typical characteristics of each. The most important properties used in identification are texture, structure, and mineralogical composition. The texture of rock refers to the size, shape, and manner of aggregation of the fragments, particles, or crystals of which the rock is composed. The structure refers to the gross features usually seen in large rock masses such as systems of cracks and joints, or planes of stratification. Since a relatively small number of rock minerals make up a very large portion of the common rocks, it requires little practice to learn to distinguish and classify rocks.

Igneous Rocks

Igneous rocks are classified primarily on the basis of texture and color. Since they were formed by solidification from the liquid state, they are very hard and have textures that vary from coarsely crystalline to glassy depending upon the rate of cooling. The principal mineral constituents are light-colored quartz and feldspar and dark-colored hornblende, biotite, angite, and olivine. Table 3.2 is a simple guide to field classification of the more common types of igneous rocks.

Table 3.2 Field Classification of Igneous Rocks

Color	Light		Intermediate	Dark	
Principal minerals texture	Quartz and feldspar, other minerals Minor	Feldspar, little or no quartz	Feldspar and hornblende	Augite and feldspar	Augite, hornblende, olivine
Very coarse, irregular crystalline	Pegmatite	Syenite Pegmatite	Diorite Pegmatite	Gabbro Pegmatite	
Coarse and medium crystalline	Granite	Syenite	Deorite Dolerite	Gabbro Dolerite	Peridotite
Fine crystalline	Aplite			Diabase	
Dense	Felsite			Basalt	
Glassy	Volcanic glass				
Porous	Pumice		Scoria or vesicular basalt		
Fragmental	Tuff (fine), breccia (coarse), cinders (variable)				

The structure of igneous rocks is usually described as massive. This term indicates a lack of structural features, but in reality joints and cracks may be found in all igneous rocks. If the rock masses were deformed at the same time that crystallization was taking place, they may have acquired a banded flow structure commonly called gneissic. Most of the igneous materials that cooled very rapidly either contain gas bubbles or else have a fragmental structure.

Sedimentary Rocks

The sedimentary rocks may be divided into three general groups in accordance with the origin of the sediment. Those consisting of rock or mineral fragments derived from preexisting material belong to the clastic group; those deposited from organisms living in water are called organic; and those precipitated by chemical activity or left by evaporation are chemical. The texture of the clastic and organic sediments may vary from coarse grained to microscopic, but the chemical sediments are usually microscopic. Only in classifying the clastic sediments is grain size of any importance. Table 3.3 illustrates the classification of sedimentary rocks.

The predominant minerals found in most sediments are quartz, calcite, and clay minerals. Consequently, about 99% of all sedimentary rocks may be classified as sandstone, limestone, or shale. Sandstone and shale can usually be differentiated by visual inspection on the basis of particle size. An estimate of the amount of lime in a given rock can be made by treating the rock with dilute hydrochloric acid and noting the vigor of the effervescence. The most important minor constituents are iron oxides, feldspar, and carbonaceous material. The most important structural characteristic of sedimentary rocks from the geological point of view is their bedding or stratification. A knowledge of the thickness, mineralogical character, and position of the beds is also of great importance. Of equal or greater significance may be information regarding structural defects such as joints, cracks, fault zones, and solution channels or cavities.

Table 3.3 Classification of Sedimentary Rocks

Group	Grain Size	Composition		Name
	Appreciable quantity of grains more than 2 mm diameter	Rounded pebbles in medium-grained matrix		Conglomerate
		Angular coarse rock fragments often quite variable		Breccia
			Less than 10% of other minerals	Siliceous sandstone
			Appreciable quantity of clay minerals	Argillaceous sandstone
	More than 50% of grains pall in range of 0.062.00 mm diameter	Medium quartz grains	Appreciable quantity of calcite	Calcareous sandstone
			Appreciable amount of iron oxide cement	Ferrugineous sandstone
Clastic			Over 25% feldspar	Arkose
			25%–50% feldspar and darker minerals	Graywacke
	More than 50% of grains pall in range of 0.002–0.06 mm diameter	Fine to very fine quartz grains with clay minerals		Siltstone (if laminated, shale)
			Less than 10% other minerals	Shale
			Appreciable calcite	Calcerous shale
	Predominately grains less than 0.002 mm diameter	Microscopic clay minerals	Appreciable carbonaceous material	Carbonaceous shale
			Appreciable iron oxide cement	Ferrugineous shale
	Variable	Calcite and fossils		Fossilferous limestone
Organic	Medium to microscopic	Calcite and appreciable dolomite		Dolomitic limestone or dolomite
	Variable	Carbonaceous material		Bituminous coal
		Calcite		Limestone
		Dolomite		Dolomite
Chemical	Microscopic	Quartz		Chert, flint, etc.
		Iron compounds in quartz		Iron formation
		Halite		Rock salt
		Gypsum		Rock gypsum

Metamorphic Rocks

The metamorphic rocks are differentiated from igneous and sedimentary rocks primarily on the basis of structure and mineralogical composition. The agents of metamorphism such as heat, pressure, and hydrothermal solutions lead to the crystallization and orientation of minerals not found in the parent rock. The most obvious characteristic of

Table 3.4 Classification of Metamorphic Rocks

Texture		Structure	
Coarse crystalline		Foliated	Massive
		Gneiss	Conglomerite granite gneiss
Medium crystalline	Schist	Sericite, mica, talc, chlorite, hematite, etc.	Marble, quartzite, serpentine, soapstone
Fine to microscopic crystalline	Phyllite slate		Hornfels, anthracite coal

metamorphic rock is the foliated structure that refers to the nearly parallel arrangement of platy or needlelike minerals. Some of the typical metamorphic minerals found in foliated rocks are chlorite, sericite, talc, hornblende, and biotite. Depending upon the grain size of the crystals, the structure may be described as gneissic (coarse), schistose (medium), or slaty (microscopic).

A large group of metamorphic rocks, most of which are derived from sediments, possesses a massive rather than a foliated structure. These may be distinguished from the parent sediment by their greater density, hardness, and crystallinity. Most rocks in this group are composed primarily of calcite, dolomite, or quartz. Table 3.4 is a simplified classification of metamorphic rocks showing the most frequently encountered. Although metamorphic rocks show such structural defects as cracks and joints, the most important characteristics are their softness or schist and the high susceptibility of all foliated rocks to weathering.

Supporting Capacity of Earth Formations

The supporting capacity of various earth formations varies from several hundred tons per square foot for solid rock in deep beds to practically nothing for saturated silts, and it depends upon (a) the character of the formation, (b) the bedding and stratification of this particular formation, and (c) the degree of saturation of this formation with water. The general character of the earth formation has to be considered when foundations are designed. Flood plains and alluvial deposits generally are nonhomogeneous in their composition. Their bearing capacity will generally be determined by the most porous material contained in their makeup. Thin strata of rock, especially when badly fissured, afford very little better foundation bed than does the stratum beneath the rock. Solid rock means a solid unfissured stratum not less than 10–15 ft thick. Not only should the present condition of the soil be taken into consideration, but its probable behavior when exposed to the weather, if it is to be exposed, should be investigated, for many formations, such as some shales and clays, disintegrate and change their properties when so exposed.

One factor that affects the bearing behavior of soils is the colloidal content, or ultrafine material, particularly the clay and humus. Its chief influence lies in the increased impermeability or capacity for holding water and the great shrinkage upon drying. Humus is the product of the 125 decomposition of vegetable matter and may vary from nothing to 100% as in peat. Humus has a tendency to lubricate or diminish internal friction between large grains of the soil. The proportion of colloidal material present in a soil may vary from a trace to almost 100%.

Clay beds may be residual (i.e., the result of the decomposition of a clay forming rock in place) or they may be sedimentary, which means they were transported and deposited under water. Swamp and lake clays have been formed in basins occupied by swamps and lakes and frequently comprise alternate layers of clay and sand. Clay beds of this type abound in glaciated areas.

The supporting capacity of clay depends upon its density, that is, upon the weight per cubic foot. Clay varies in specific weight from about 100 lb. for ordinary dry residual clays to 140 lb. for dense consolidated clays. The specific gravity of the minerals in clay is about 2.6. If solid, 1 ft^3 of clay would weigh about 162 lb. The difference between this figure and the actual weight represents voids and hence, compressibility. The ease and rapidity with which clay may be compressed depend upon the resistance to expelling the air and water that occupy this void space. Therefore, the rate of settlement of a load on a clay foundation depends upon the impermeability of the soil. The supporting capacity of clay may be taken roughly as 1–5.0 ton/ft^2, varying proportionally with the weight—100–140 lb./ft^3 in undisturbed conditions.

When water is present in soils to such a degree that it occupies all interstitial space, the soil is said to be saturated. Dry earth contains about 5% water, damp earth about 10%, wet earth about 20%, and saturated earth 25%–35%. When rain saturates the surface, a portion is evaporated, a portion runs off, and a third portion is drawn by gravity down into the water table. Whether moisture is being surrendered from the soil to the air or is being absorbed from the air depends on the relative humidity. The water below the plane of saturation has a natural hydraulic slope because of the losses of streams, wells, and springs and is constantly in slow motion, the velocity depending upon the gradient and the character of the soil. Foundations below this level will always be subject to water infiltration except where waterproofed. Moreover, in all but very dense soils, this water will exert an upward buoyancy, equal to the head of the ground water. The buoyancy effect of water under a foundation is effective up to 99% of the area depending on the soil conditions on which the structure rests.

Not only may water fill interstitial space, but because of a large adjacent supply at a higher level, it may be under head so as to flow whenever released at such velocities as to disturb the soil particles and to force them upward. The effect of moisture on the plasticity of soils depends primarily on the amount of clay present—the higher the percentage of clay, the more moisture required to produce plasticity. Saturated clays are very plastic and tend to move under loading conditions.

Soils under foundations may be classed roughly as granular, plastic, and solid. Plastic soils are compressible clay, silt, and mixtures of sand, gravel, and clay. In this type of soil, the deformation varies roughly with the pressure until a yield or fluid point is reached, and when the bearing surface settles rapidly without any proportionate increase in the superimposed load.

While the structural properties of soils vary, the range of variation for given conditions is not so wide as is frequently assumed. Foundation troubles arise from a lack of knowledge concerning the strata and water occurrence rather than from the variability of the soil behavior under known conditions.

In the settlement of foundation, three types are recognizable:

1. Uniform over the bearing area
2. Rotational, caused by a progressively greater settlement toward one side
3. Local, caused by an overloading of the soil

Uniform settlement results from loading a uniform compressible soil evenly over the bearing area. In general, this type of settlement does little harm. Rotational settlement usually results from one or more of three conditions:

1. The thickness of a compressible layer of soil under the foundation shows a variation.
2. The center of gravity of the foundation bearing area does not lie directly under the center of gravity of the superimposed loads.
3. Soil at one side flows out into an excavation or void in an adjacent area.

As previously outlined, soil may more readily flow from a foundation when it is plastic, saturated with water under hydraulic forces, and has been exposed due to excavations.

Local settlement is the most objectionable and may result from faulty proportioning of the foundation areas for the loads to be carried. This type of settling can best be prevented by designing the footing continuously either as slabs or as a mat over the entire area. Settlement at exterior walls of a structure may be greater than at interior columns under certain conditions, where uniform bearing obtains, because of a failure to reduce the live load to an equivalent dead load. On the other hand, under equal loadings the interior of a building usually settles more than the periphery because the close spacing of columns produces overlapping or interference of soil pressure under the footings. Most house designs support the loads at the exterior walls creating a shear supporting capacity of the footers. Settlement may be expected to amount between 0.01 and 0.1 ft for each ton per square foot of load depending on the density of the clay. Settlement on sand or gravel occurs immediately after loading; whereas on plastic soils, it may continue over a period of months and years.

Unequal settlement may cause a structure to lean considerably out of plumb as well as to be displaced vertically. When a structure settles unevenly, it rotates about an instantaneous axis. Within the range of well chosen soil loads, the settlement for homogenous soils will be essentially proportional to the pressure intensity, which is especially true of granular and of stiff clay soils.

In the case of wall footings typically found in residential construction, the footings act merely as a cantilever beam with the load acting upward and the support at the middle. It is commonly assumed that the bearing is uniformly distributed over the bearing area although the bearing may be somewhat greater at the middle than at the edges. Consequently, when the supporting capacity of the soil under the footings is eroded and especially if no reinforcement is present in the footers, the footings will shear, be local, and may rotate. This type of foundation failure typically exhibits itself on exterior walls as stair step cracks.

Stability of Natural Slopes

The stability of natural slopes can be quantified by asking two questions, each of which has two subdivisions as follows:

1. To what extent can we assess the stability of an existing natural slope
   a. If we do nothing to it but let the natural forces and agents act?
   b. If we alter the slope, for instance, by making a cut?

The second question is a corollary of the first in that a satisfactory answer to the first depends on a satisfactory answer to the second; that is,

2. To what extent do we understand the failures that have occurred in the existing natural slopes
   a. If only natural forces and agents have been acting?
   b. If the slopes have been altered, for instance, by making cuts?

It is the general opinion that the stability of slopes cannot be reliably assessed without extensive subsurface exploration. This is true because few natural slopes exist above homogeneous materials or above simple materials of which the shearing strength can be stated in terms of one or two parameters. Indeed, natural slopes above homogeneous soft clays are so rare that such a slope would be considered a geological anomaly. Almost always, soft clays are associated with stiffer material having some sort of secondary structure.

Generally, as shown in Figure 3.1, failure of a natural slope requires the simultaneous satisfactions of three criteria:

1. There must be large internal stresses in the clay mass.
2. The material must have a stress–strain curve exhibiting a substantial peak; that is, the material must be of a strain-softening variety.
3. There must be enough strain energy to produce sufficient strain to carry the material over the peak of the stress–strain curve.

The three criteria listed earlier can be greatly exacerbated by the infusion of large quantities of water from heavy rainfall, the disturbance of the top soils by the removal of vegetation, and the disturbance of the subsoils by cutting the slope. Part of the uncertainty in a stability analysis is caused by the wide variation of soil properties and groundwater conditions. When the nature and rate of stress changes due to the water content of the soils, it will also change the stress–strain characteristic that may be used to predict failure of the slope. Overconsolidated clays tend to expand during shear after the peak strength has been reached. The increased water content caused by this expansion, together with particle reorientation, local overstressing, and time effects, result in a reduced strength and large

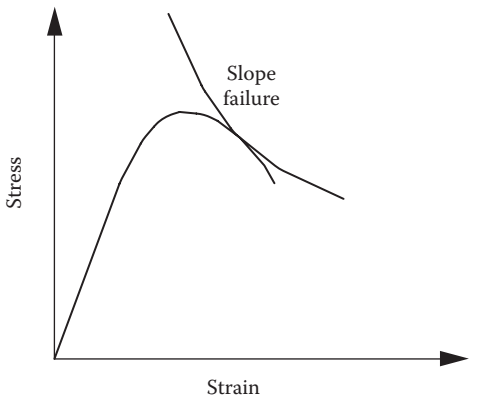

Figure 3.1 Failure of a natural slope.

strain, which is called the residual strength. The strength required for long-term stability of slopes in these clays approaches the residual strength.

Sensitive clays, unlike the soils just described, can exist in nature at rather high void ratios as a result of their bonded structure, even when they are substantially overconsolidated. Under increasing or sustained shearing stresses, the bonds are broken and the structure collapses causing a decrease in volume. If the drainage of pore water is too slow, pressures will build up in the water phase until the effective stress on the failure plane approaches zero, which is the state that exists on the failure plane of a flow slide.

Atterberg Limits

The purpose of the Atterberg limit tests is to classify soils into PRA, Casagrande, or CAA groups. These methods allow the assignment of an approximate value for the soils in terms of foundation design. It is a well-known fact that high values of liquid limit and plastic index indicate high compressibility and low bearing capacity.

Normally, the water content or moisture content is expressed as a percentage of the oven dried weight of the soil sample. These soil constants are determined from the soil fraction passing the No. 4 (420 μm) sieve. The liquid limit (LL) of a soil is the water content at which the groove formed in a soil sample with a standard grooving tool will just meet when the dish is held in one hand and tapped lightly 10 times with the heel of the other hand. By hand, the sample size is 30 g. Several trials are made, the moisture content being gradually increased. Blows are plotted against water content and the liquid limit picked off from the curve in Figure 3.2.

The liquid limit (LL) according to ASTM 423 is

$$\text{LL} = \frac{\text{weight of water}}{\text{weight of oven dried soild}} \times 100 \tag{3.2}$$

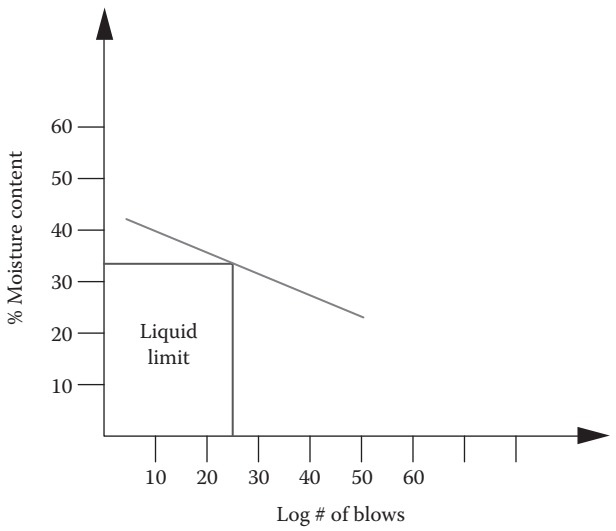

Figure 3.2 Determination of liquid limit.

The plastic limit (PL) is the lowest water content at which a thread of the soil can be just rolled to a diameter of 1/8 in. without cracking, crumbling, or breaking into pieces. According to ASTM 424,

$$\text{PL} = \frac{\text{weight of water}}{\text{weight of oven dried soild}} \times 100 \tag{3.3}$$

The plastic index (PI) AASHO T-91 is the numerical difference between the LL and the PL or

$$\text{PI} = \text{LL} - \text{PL} \tag{3.4}$$

For our example soil samples, we find

$$\text{LL} = 32 \quad \text{and} \quad \text{PL} = 16$$

so that the PI is

$$\text{PI} = 32 - 16 = 16$$

For bearing soils the P.I. should not exceed 6, and the L.L. should not exceed 25. This soil is not capable of supporting footings.

Subsidence

Natural subsidence rarely occurs. The word subsidence comes from subside, which, according to Webster's Dictionary, means to sink or fall to the bottom; settle as sediment or to sink to a lower level. From a forensic engineering standpoint, subsidence deals with the causes of the downward shift of the earth's surface. Most subsidence can be attributed to human activity in a variety of forms. The most common forms of subsidence created by humans are outlined in the following.

Mining

Mining activities where large portions of the earth have been removed underground can cause severe subsidence, which is especially true in coal mining when a method of mining, referred to a longwall or pillar extraction, is utilized. In longwall mining, a horizontal shaft is excavated, and as the machinery is retracted, the coal is removed letting the voids collapse as the operation continues outward to the face of the shaft. In pillar extraction, large areas of coal are mined utilizing blocks of coal as supporting structures for the roof of the mine. Once most of the material has been excavated, the remaining pillars are systematically removed in order to accumulate the most product. As these pillars are removed, the supporting capacity of the roof of the mine is compromised, causing subsidence. Mining for other substances such as metals may also cause subsidence. Mining activities generally cause relatively sudden subsidence to ground structures. When investigating mining subsidence on structures, particular attention should be paid to new or old structural distress.

The effects of surface and subsurface water should also be investigated to determine its relevance to the failure. Topographic maps, mine maps, and global positioning systems (GPS) are invaluable in these types of investigations. Additionally subsurface investigations involving core samples are most helpful.

Water

Water and subsidence can be related in two ways. The first way that water and human activities can cause subsidence is by leaking water mains or sewers or the disruption of the natural drainage of an area. Building activities normally require some modification to the flow of surface and subsurface water. These modifications are most pronounced in regions of the earth where differences in elevation exist. Mountainous regions are most susceptible because the pull of gravity on water is the most intense.

The second way that water affects subsidence is in the carbonate dissolution of certain topographies. These underlying soils consisting of carbonate rocks, such as limestone, are composed mainly of calcite, a mineral that is highly susceptible to dissolution by ground water. This dissolution of the limestone can produce a series of caves, sinkholes, and produce what is referred to as karst topography. Karst topography, as defined by Webster's dictionary, is a region made up of porous limestone containing deep fissures and sinkholes characterized by underground caves and streams.

The atmosphere contains a certain amount of carbon dioxide, CO_2. Rain water then produces carbonic acid, H_2CO_3 which infiltrates into the groundwater system and affects the carbonate rocks and dissolves the calcite in the limestone. The chemical reaction for this process is given by

$$CaCO_3 + H_2CO_3 \rightarrow Ca^{+2} + 2HCO_3^{-2} \tag{3.5}$$

Dissolution of karst topography can cause sudden or slow collapse of the underlying strata. The methods of investigation include topographic examinations and subsurface exploration.

Oil and Gas

Oil and gas reserves are normally under pressure beneath the surface of the earth. The fluid pressure produces a natural countering force that supports the overlaying soil structures. Exploration and the resulting production of oil and gas can then remove these fluids and result in subsidence. It is also possible that natural phenomena can release these fluids and result in a natural subsidence not caused by human activity.

Earthquakes

Earthquakes are natural events that the forensic engineer may be asked to investigate relative to the strength, susceptibility, and performance of a particular structure under the forces that affected the structure. Structural code requirements in different parts of the United States vary according to the region where earth faults may occur. The most noted

fault line is in California and is known as the San Andreas fault. Numerous earthquakes and tremors have occurred along this crust line that is part of the North American plate and the Pacific Plate. The San Andreas fault is by no means the only fault line in the earth's crust in the United States. Several others include the Ramapo Fault in New York and the New Madrid fault at the confluence of the Mississippi and Ohio Rivers. In 1811 the New Madrid fault experienced a 7.3 strength earthquake and in 1884 the Ramapo fault produced a magnitude 5.2 earthquake. Forensic engineers investigating damage caused by earthquakes are referred to the 2009 AASHTO Guide Specifications for LRFD Seismic Bridge Design.

The general public has been introduced to the Richter magnitude scale as a measure of the intensity of earthquakes. This scale measures the seismic energy released during an earthquake. In particular it calculates the base ten logarithm of the horizontal amplitude of the displacement on a Wood-Anderson torsion seismometer. In equation form the Richter magnitude is given by

$$M_R = \log(A) - \log(A_0)\delta \tag{3.6}$$

where

M_R is the Richter magnitude
A is the maximum value obtained from the seismograph
A_0 is the empirical value dependent on the station distance from the epicenter
δ is the station distance

An inherent problem with the Richter scale and modifications of that scale known as body wave magnitude and surface wave magnitude is that they may saturate the seismographs. These older scales have been superseded by the moment magnitude scale, which alleviates the saturation problem experienced by the seismographs for higher order earthquakes. The magnitude moment scale was developed in the 1970s and is given by

$$M_M = \frac{2}{3}\log M_0 - 10.7 \tag{3.7}$$

where

M_0 is the seismic moment magnitude measured in dyne centimeters
M_M is the moment magnitude

The Richter and moment scales are similar in value and do not vary significantly. Generally, news reports refer to the Richter scale when discussing earthquakes.

In the 1960s the theory of plate techtonics was developed based on observational, empirical, and computational dynamics. Plate techtonics helped to understand the motion of the continents and the similarity in the flora, fauna of separate continents. This theory is by now part of established science and explains in very elegant terms the actions of the movement of continents, the eruption of volcanoes, the rise of mountain ranges, the creation of rift valleys, and earthquakes.

The plates of the earth can move in a variety of ways. The plates can separate so that a rift between the plates occurs. At the bottom of the ocean molten lava fills the gap and is known as magma. The plates can push against each other. In this case one plate may slide under the other in a process called subduction. If one plate cannot slide under, the

other the plates push upward creating mountains. Finally, the plates may slide laterally past each other. Knowledge of the type of fault associated with a particular earthquake and the observed structural damage to a structure can assist the forensic engineer in damage assessment and repair.

Foundations

The term foundation can take several meanings. For construction or engineering purposes, keywords associated with a foundation are establishment and the supporting material. Establishment relates to the actual element that is the basis for the particular structure and supporting material relates to the type of soil on which the foundation rests. These two elements are intertwined because the structural foundation can only support a load that can safely be transferred to the underlying soils. The performance of a foundation is subject to the engineering characteristics of the underlying clays, sands, rocks, and silts. At this point it should be quite evident to the reader why we covered the variety of topics on soils in the preceding sections of this chapter.

The forensic engineer is called upon to investigate the cause of the failure of a foundation. This failure may be due to a variety of effects. Some of these effects may include nearby construction activities, subsidence, water-related problems, improper design of the foundation, or a combination of these effects. The foundation element may fail in bending, shear, or rotation. Rotational settlement of the foundation element is the most egregious and costly in terms of repair. Foundation failures will affect the structures above and cause floor, wall, and roof settlement. Foundation failures also allow for the intrusion of water through the development of cracks in foundation walls.

The underlying supporting capacity of the soils upon which the foundation rests should be carried out by borings and laboratory testing. However, as a general rule, the supporting capacity of soils as determined by the New York City Code of 1950 is given in Table 3.5.

When a failure occurs and the forensic engineer is called out to investigate, there may be limitations placed on the extent of activities that take place. These limitations are generally placed by the insurance company, the attorney, or the client who may be

Table 3.5 Supporting Capacity of Soils

Material	Tons per Square Feet
Hard rock	60
Medium hard rock	40
Hard pan over rock	12
Compact gravel and sand	10
Soft rock	8
Loose and sandy gravel	6
Hard dry consolidated clay	5
Loose coarse sand	4
Compact sandy clay soils	3
Loose fine sand	2
Stiff clays	1.5
Medium clays	1

the structure's owner. Whenever possible, subsurface investigations should be carried out in terms of core samples, water content, nature of the underlying soils, etc. Sampling and laboratory testing is relatively expensive and the nature of the loss may not warrant such a detailed examination. In such cases there are alternative methods of identifying the nature of the soils. These are obtained from geologic surveys, maps, and engineering books. Although these methods are not as reliable as the information that is available through sampling, they are sufficient for a significant portion of investigations. If the forensic engineer deems it necessary to do subsurface investigations before a reliable opinion can be rendered, then these views should be made known.

Ideally, all foundations would be to bedrock. Such a scenario is simply not possible for most applications, which is true for residential and most commercial structures because bedrock is often very deep. It is even true for many skyscrapers that have been built. There are alternate methods of providing proper foundations for even the largest structures without reaching bedrock. Foundations are constructed of square and rectangular shapes on the plain. They may be trapezoidal or cantilevered. Other foundation designs involve piles and pile footings of various shapes. These piles may reach bedrock and be grouted to the bedrock or they may extend to an engineered footing. Some foundations are designed to hold back earthen formations. In this case they are referred to as cantilever and gravity type retaining walls. The most common type of foundation and retaining structure involves the basement of a house. These foundations are the ones that most often are investigated forensically.

Building codes in the United States require that footers, that is, foundations, be below the frost line. This is important because if the footer is above the frost line, it will be subjected to frost upheaval. If footers above the frost line, especially in damp soil conditions, the surrounding soils will freeze, expand, and cause movement and possibly footer failure. Additionally footers need to be kept at relatively dry levels through the use of footer drains. This requirement is especially true if the footers are located in expansive soils. As the soils dry out, the expansive clayed soils will shrink, crack, and affect the bearing capacity by creating voids under the foundation elements. Footings must then be monolithic and be reinforced and constructed of sufficiently strong concrete. Again, code requirements dictate the amount of reinforcement necessary, the strength of the concrete, and the depth of the footings.

In a typical basement foundation, the engineer may be asked to investigate the cause of structural distress. This distress may be characterized by the inward bowing of the block foundation walls, stair step cracks, vertical cracks, horizontal cracks, and/or water infiltration. In such a scenario, subsurface investigations generally do not take place. In some cases, however, an excavation may be performed in order to expose the foundation and its walls to determine the extent and the cause of the failure. Without excavating and performing subsurface investigations, much information can be gleaned from the inspection of the basement walls. First, the nature of the cracks should be investigated. Are the cracks only at the mortar joints or do they permeate through the block work? Are the cracks vertical, horizontal or stair step? The propagation of the crack in each plane indicates the relative movement of the wall. Are drainage deficiencies evident along the wall? Do the cracks have dirt and cob webs inside of them? Have the cracks been previously patched? Oxidation of the crack is indicative of the relative age of the crack. Measurements with a tape and a level greatly aid in these types of investigations. The evidence, of course, should be documented photographically. Most footers investigated by the forensic engineer are limited so that

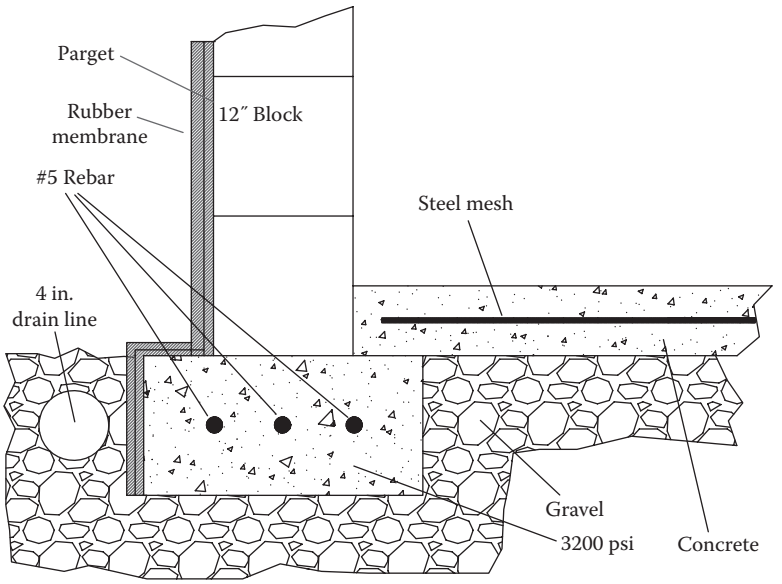

Figure 3.3 Foundation diagram.

the amount of reinforcement in the footers and the strength of the concrete is not known. However, in these investigations, the engineer does a worst-case analysis utilizing presumptive soil capacities, assumed dimensions, and reinforcement of the footings. In this manner the analysis of the failure can be determined. In some cases design drawings may be available for the investigation. Figure 3.3 shows a typical basement foundation footing.

Blasting Damage

Vibrations from nearby blasting are typically transmitted by air or by ground. Damage caused by air vibrations, usually referred to as the blast concussion or the airborne shock wave, occurs when the blast is relatively close to the structure. If the effect of topography or intervening structures are not present when a blast occurs, the blast creates a concussion or airborne shock wave that radiates in all directions. The effect is similar to the waves that radiate out of the point where a stone drops into a pool of water. Like the water waves, the shock wave will arrive and contact the side of the structure that faces the point of origin of the blast. The weakest structural element of a building is typically the windows. Loosely set glass will often break when subjected to a pressure difference of only 1 lb/in.^{2} Windows will often break when the pressure difference is 2 lb/in.^{2} As a comparison, it takes a wind speed of over 200 miles/h to produce a pressure of 2 lb/in.^{2} At the pressure thresholds necessary to break glass, the associated sound wave level exceeds 90 dB, which is comparable to the noise of a heavy diesel truck. The normal noise level of a business office is about 65 dB or a wave pressure of 0.107 lb/in.^{2} Thus, in order for an air blast to damage a building, the associated noise level must be very very high. Simply being able to hear an air blast at moderate sound levels is not evidence that the air blast was sufficient to cause damage. If the air blast was not sufficient to break glass on the side of the building facing the point of origin of the explosion, then it is not possible that it could have caused any structural damage to the building.

When an explosive is detonated, it is generally intended that most of the explosive energy be directed into the surrounding ground, rather than into the air. The general purpose of using an explosive is to shatter rock or other impediments to construction. Two kinds of vibrations are created when a blast is set off, surface or shear vibrations and longitudinal vibration. Roughly 95% of the blast energy that reaches a structure through the ground does so in the form of surface vibrations. There are three common ways by which vibration levels can be measured: displacement, velocity, and acceleration. In a 10-year study, the U.S. Bureau of Mines found that there was little chance of structural damage as the shock wave passing through a given area had a peak particle velocity of less than 2 in./s. Minor damage could be expected at levels of 7.6 in./s or more. The threshold for human perception of blast ground vibrations in this study was found to be several times less than that for "safe" vibration levels for structures. In other words, a person will sense ground vibrations at much lower levels than are needed for damage to occur in a structure. In certain blast frequencies, the levels that a person may consider intolerable were found to be still less than levels that would cause actual damage to a structure.

Blasting damage to structures is produced by two separate and distinct wavefronts. The detonation of an explosive device produces a high-intensity and short-duration pulse of energy that is dissipated over two distinct mediums, thereby producing the two distinct wavefronts. One of the mediums, the earth/rock strata, in which the explosive charge is set, produces the most significant damage to property. The other medium, the air surrounding the volume of space about the detonation site, produces much less intense damage. Figure 3.4 shows topographic and cross-sectional views of the detonation of a charge.

Longitudinal wavefronts are produced by the pressure variations in a sound wave. The reception of a sound wave by the ear gives rise to a vibration of the air particles at the eardrum with a definite frequency and a definite amplitude. This vibration may also be described in terms of the variation of air pressure at the same point. The air pressure rises above atmospheric pressure and then sinks below atmospheric pressure with simple harmonic motion.

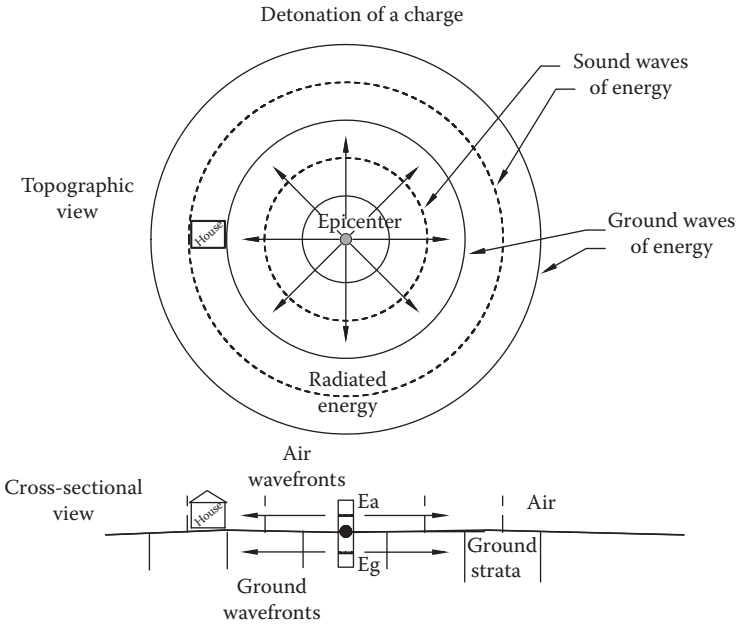

Figure 3.4 Propagation of blast wavefronts.

Measurements of sound waves show that the maximum pressure variations in the loudest sounds that the ear can tolerate are of the order of magnitude of 280 dyn/cm^2 (above and below atmospheric pressure, which is about 1,000,000 dyn/cm^2). The corresponding maximum displacement for a frequency of 1000 Hz is about a thousandth of a centimeter. Therefore, the displacement amplitudes, even in the loudest sounds, are extremely small.

From a purely geometrical point of view, that which is propagated by a traveling wave is the *waveform*. From a physical viewpoint, however, something else is propagated by a wave, namely, *energy*. The intensity I of a traveling wave is defined as the time average rate at which energy is transported by the wave per unit area across a surface perpendicular to the direction of propagation. More briefly, the intensity is the average power transported per unit area. Since the power developed by a force equals the product of force and velocity of the wavefront, it can be shown that the intensity over one cycle is given by

$$I = \frac{P^2}{2\rho c} \tag{3.8}$$

where

I is the intensity of the traveling wave
P is the pressure amplitude of the wave
ρ is the average density of the medium (for air, $\rho = 1.22 \times 10^{-3}$ g/cm^3)
c is the velocity of the wave (for air, $c = 3.46 \times 10^4$ cm/s)

Since the energy transported by the waves spreads out over spheres of radius r and area $4\pi r^2$, the intensity of the waves (energy per unit time per unit area) must vary as the square of the distance from the epicenter. Since the intensity varies as the square of the amplitude, it follows that the amplitude of the wave varies inversely as the first power of the distance. At sufficiently large distances from the source (epicenter), however, the waves can be considered plane, with pressure variations in phase with the particle velocity, so that there is always a flow of energy outward from the epicenter. Explosives produce wavefronts through the air that may travel as fast as 30,000 mph.

This discussion reveals that the object which is to be damaged by the air wavefronts from an explosion must be very close to the epicenter, and the wavefronts must normally be traveling at supersonic speeds. Although explosions produce supersonic wavefronts, they dissipate rapidly over distance and only produce damage to flat, thin surfaces such as windows and glass doors. The wavefronts produced by the pressure distributed over the earth/rock strata from an explosion may also be analyzed as a plane wave so that the previous analysis applies to them as well. These wavefronts, however, are generally subsonic, of greater amplitude, and of much longer wavelength. Figure 3.5 represents a typical pulse of energy produced by the detonation of an explosive.

This pulsed function of large amplitude can be approximated as an impulse function of the form

$$\delta_e = \lim_{\varepsilon \to 0} KA\varepsilon = K \tag{3.9}$$

Therefore, the impulse response of rock strata corresponds to the natural frequency of the earthen formation, which explains the long wavelength associated with the ground effects produced by blasting. Blasting damage to structures is similar to damage produced by

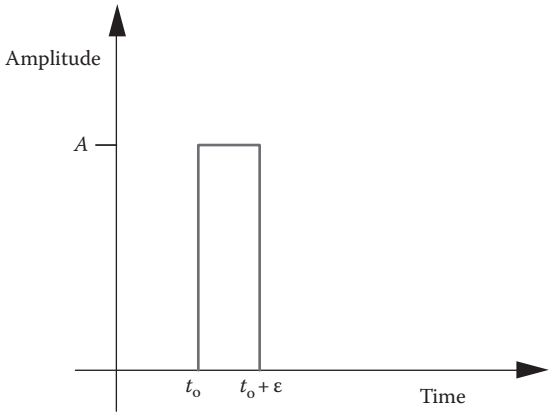

Figure 3.5 Pulse of energy.

earthquakes but is of significantly less intensity. Blasting damage to a structure displaces foundations, walls, etc., in one direction—the direction of the wavefront.

The pressure produced by the ground wave actually displaces the earth/rock strata so that damage to structures may occur. These long wavelength ground wavefronts also dissipate rapidly over distance. Normally no damage occurs from ground waves at distances approaching a mile. At short distances from the epicenter, a wavefront traveling along the same rock strata can produce significant damage to structures. However, if the structure is on a different rock stratum, separated by clayed soils, bodies of water, and a mile or more away, there is normally no measurable or observable damage to structures. Figure 3.6 shows the human response to vibrations.

Extensive tests and measurements by various governmental agencies have determined the safe blasting criterion for damage to structures and the response to humans. Figure 3.6 illustrates the Human Response and Damage Criterion. Figure 3.7 indicates the safe blasting limit for vibrations in terms of the distance to the nearest structure and the weight of the explosive charge.

A standard measurement for blasting activities uses a seismograph that measures the particle velocity of the blast wavefront. Testing by the U.S. Bureau of Mines has shown that safe blasting occurs when the peak particle velocity is not greater than 2.0 in./s. This limit insures that the probability of damage from blasting is less than 5%. Seismograph readings indicate that minor damage to structures occurs at a particle velocity of 5.4 in./s while major damage is experienced at particle velocities in excess of 7.6 in./s. Modifications have set the safe blasting criterion to a range between 0.5 and 2.0 in./s. At these particle velocities or lower, it is impossible to create damage to structures. The particle velocity is given by

$$v_p = 160\left[\frac{R}{W^{1/2}}\right]^{-1.6} \tag{3.10}$$

where

v_p is the particle velocity (in./s)
R is the radial distance from blast epicenter (ft)
W is the maximum weight per delay or instantaneous shot (lb)

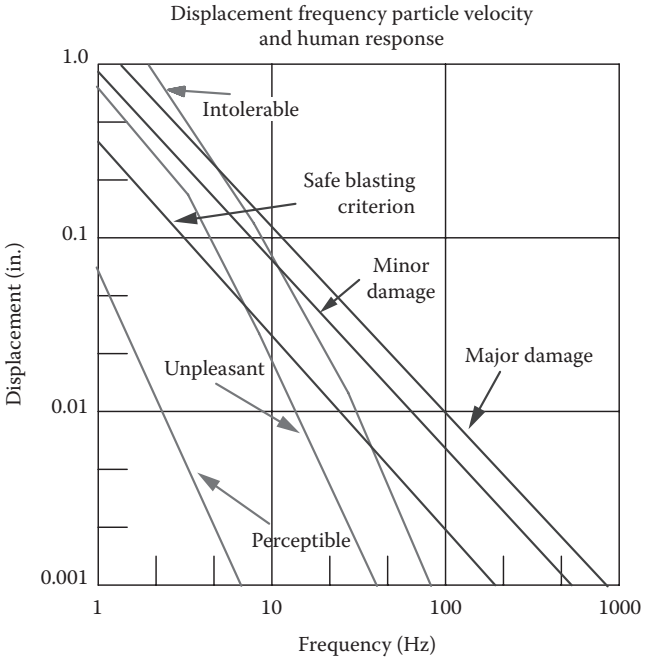

Figure 3.6 Human response and damage criterion.

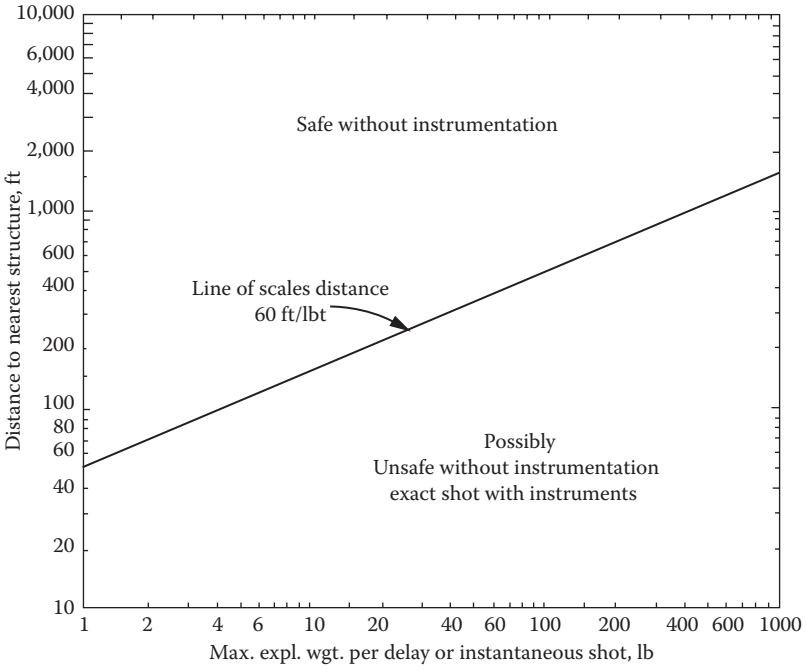

Figure 3.7 Safe blasting limit for vibrations.

When seismographs are not used to monitor vibrations, a safe blasting formula is used:

$$D = K(W^{1/2}) \tag{3.11}$$

where

D is the safe blasting distance from structure to blast hole
K is the scaling factor = 55 ft/lb$^{1/2}$ for structures between 301 and 5000 ft from the blast
W is the charge weight per delay

The scaling factor varies depending on the distance to the blast. At a distance less than 301 ft, the scaling factor reduces to 50 ft/lb$^{1/2}$. The scaling factor corresponding to a distance greater than 5000 ft is 65 ft/lb$^{1/2}$.

Heavy Equipment Vibrations

Heavy equipment, such as jack hammers, large trucks, and roller compactors can cause vibrations similar to those of blasts. Such activities produce waves of energy that are directed into the surrounding ground. The energy waves propagate radially from the source and can cause damage to structures that are relatively close. Most of the energy that reaches a structure through the ground does so in the form of surface vibrations.

Vibration levels that are considered safe range from 0.5 to 2 in./s. Safe levels are those that will not cause damage to the most delicate of structures. According to the United States Bureau of Mines, the threshold for human perception of ground vibrations was found to be several times less than that for safe vibration levels for structures. Vibration levels that may be considered intolerable by a person were found to be still less than levels that would actually cause damage to a structure. It is often useful to monitor construction equipment vibration levels with a seismograph, as is done during blast monitoring. The data from the seismograph testing would provide reasonable estimates of the vibration levels encountered in and around the construction site.

One concern is settlement of structures due to vibrations. Vibrations can greatly increase the relative density of cohesionless soils, thereby increasing the amount of stress in the soil mass. The change in stress is inevitably accompanied by deformation, or settlement, of the soil. However, vibrations have very little effect upon cohesive soils, such as clay. The moisture content in clay soils and sands above the water table provide sufficient cohesion to prevent rearrangement of the grain structure. Furthermore, ground waves on fill or separately stratified soil deposits do not transfer considerable energy to soils of some different strata. In other words, vibrations are not likely to affect structures lying on different soil strata than the source of the vibrations.

Effect of Compaction Effort

The compaction energy per unit volume (E) used for a Standard Proctor Test is given by

$$E = \frac{(\text{Blows per layer})\,(\text{Layers})\,(\text{Weight of hammer})\,(\text{Height of drop})}{\text{Volume of mold}} \tag{3.12}$$

In most specifications for earthwork in construction sites, the contractor is instructed to achieve a compacted field dry unit weight of 90%–95% of the maximum dry unit weight as determined by the Standard or Modified Proctor Test. The compaction energy per unit volume of soil according to the Modified Proctor Test is given by

$$E = \frac{(5\,\text{layers})\,(25\,\text{blows})\,(10\text{ lb hammer})\,(1.5\text{ ft drop})}{\left[\frac{1}{30}\,\text{ft}^3\right]} \tag{3.13}$$

$$E = 56{,}250\,\frac{\text{ft-lb}}{\text{ft}^3} = 56{,}250\,\frac{\text{lb}}{\text{ft}^2} \tag{3.14}$$

These ASTM and AASHTO specifications have been adopted for fine grain sands that pass through a U.S. No. 4 sieve.

Field Compaction Equipment

Most of the compaction in the field is done with rollers. Smooth wheeled rollers provide pressures between 45 and 55 lb/in.^{2} Pneumatic rubber tired rollers produce contact pressures between 85 and 100 lb/in.^{2} Sheepsfoot rollers are capable of producing pressures between 200 and 1000 lb/in.^{2} Like sheepsfoot rollers, vibratory rollers are extremely efficient in compacting granular soils and achieve similar pressures.

Excavation of concrete and rock commonly requires the use of a hydraulic breaker or jack hammer. The hammer may be individually operated or attached to an excavator. The size and weight of the hammer depend on the amount of material to be excavated. For excavation of unfractured granite or heavily reinforced concrete, a heavy-duty breaker is necessary. Once excavation is completed, compaction is often necessary to prevent backfill settlement. Compaction can be achieved by static, impact, and vibration methods. Some equipment, such as jumping jack rammers, uses impact and vibration in compacting soils. In this case, the impact force is achieved by a ramming shoe alternatively leaving the surface at a high speed.

Particle Velocity Calculation

First Example

The particle velocity of hammering or compacting activities which are produced in a construction zone can be determined by Equation 3.10 duplicated in the following:

$$v_P = 160\left[\frac{R}{\sqrt{W_T}}\right]^{-1.6}$$

where

v_P is the particle velocity measured in inches per second
R is the radial distance measured in feet
W_T is the equivalent energy measured in pounds of dynamite (TNT)

The energy rating of a breaker quantifies the amount of energy transferred from the tool to the striking surface. The tool energy rating of the hammer depends on the size of the equipment. Breakers weighing 3300 lb produce a 1976 ft-lb. rating, while breakers in excess of 4700 lb can produce an energy rating of 3141 ft-lb. These data were provided by Tramac (www.tramac.com), which is a supplier of hydraulic breakers and other excavation equipment.

The impact force of a jumping jack rammer is determined by the weight of the machine, the stroke, and the percussion rate. The impact force varies between 2590 and 4410 lb, depending on the make of the rammer. Assuming the largest impact force, which corresponds with a 13 × 13 in. shoe, the equivalent impact pressure is approximately 3758 lb/ft^2, or 3758 ft-lb of energy in a unit volume. These specifications were provided by Sunbelt Rentals, which provides rammers manufactured by Wacker and Multiquip.

One pound of dynamite produces 1.566×10^6 ft-lb of energy. Thus, the ratio equivalence for energy produced by breaking hardened rock:

$$\frac{3{,}141\,\text{ft-lb}}{1{,}566{,}000\,\text{ft-lb}} = 0.002$$

Employing the 3758 ft-lb of energy produced by compacting soil provides a 0.0024 ratio equivalence for energy. In other words, the energy produced by 0.002–0.0024 lb of TNT is equivalent to the energy produced by a heavy-duty jack hammer or ramming compactor. Therefore, the particle velocity can be computed as it depends on the distance from the source of vibrations. Considering a structure 15 ft from the construction activity, the particle velocity computes as follows:

$$v_P = 160\left[\frac{15\,\text{ft}}{\sqrt{0.0024\,\text{lb}}}\right]^{-1.6} = 0.017\,\text{in./s}$$

The particle velocity at 5 ft from the source of vibrations computes as 0.098 in./s. As explained in the introduction, safe vibration levels are considered to range from 0.5 to 2 in./s. Therefore, it is physically impossible that excavation with heavy breakers or ramming compactors will damage a structure that is five to 15 ft from the source of vibrations.

Second Example

The particle velocity of a compaction activity which is produced in a construction zone can be again determined by

$$v_P = 160\left[\frac{R}{\sqrt{W_T}}\right]^{-1.6}$$

where

v_P is the particle velocity measured in inches per second
R is the radial distance measured in feet
W_T is the equivalent energy measured in pounds of dynamite (TNT)

Roller pressures, depending on the type of equipment, vary as shown in the following:

Smooth wheeled roller	50 lb/in.^{2}	7,200 lb/ft^2
Pneumatic tire roller	100 lb/in.^{2}	14,400 lb/ft^2
Sheepsfoot roller	200–1000 lb/in.^{2}	28,800–144,000 lb/ft^2

Note that the Modified Proctor Test specifications for field compaction require the compaction energy to be 56,250 lb/ft^2 of equivalent pressure and lie within the range of pressures provided by a sheepsfoot compactor roller.

One pound of dynamite produces 1.566×10^6 ft-lb of energy, or 1.566×10^6 lb/ft^2 of pressure per cubic foot. Thus, the ratio equivalence for roller energy meeting the Modified Proctor Test is

$$\frac{56{,}250\,\text{lb/ft}^2}{1{,}566{,}000\,\text{lb/ft}^2} = 0.036$$

In other words, the energy produced by 0.036 lb of TNT is equivalent to the energy of compaction by a roller. Therefore, the particle velocity can be computed as it depends on the distance from the source of vibrations. Considering a structure 50 ft from a roller that is actively compacting soil, the particle velocity computes as follows:

$$v_p = 160\left[\frac{50\,\text{ft}}{\sqrt{0.036\,\text{lb}}}\right]^{-1.6} = 0.021\,\text{in./s}$$

The particle velocity at 25 ft from the source of vibrations is computed as 0.065 in./s. The particle velocity at 15 ft from the source of vibrations is computed as 0.147 in./s. As explained in the introduction, safe vibration levels are considered to range from 0.5 to 2 in./s. Therefore, it is unlikely that compaction efforts will damage a structure that is 15–25 ft from the source of vibrations.

Wave Pressure

Plane Wave Transmission at an Interface

When a sound wave strikes a surface, or an interface between two substances, a reflected wave results whose nature depends on the characteristics of the surface and of the adjoining substances. If the struck surface is not rigid, an acoustic disturbance is produced on the other side of the surface. This disturbance is referred to as a refracted, or transmitted, wave.

Figure 3.8 displays an incident wave (P_I) approaching a planar surface at an angle θ_1. The reflected wave is described as the product of the incident wave and a reflection coefficient R. Phase matching indicates that the angle of reflection is equal to the angle of incident (θ_1). The transmission coefficient (T) describes the refracted wave in the second

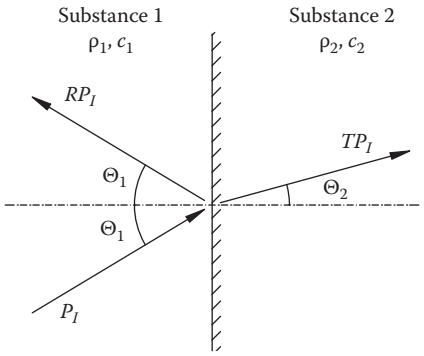

Figure 3.8 Wave transmission.

substance. The transmitted wave propagates at an angle θ_2. The density (ρ) and speed of sound c are unique to each substance.

The pressure field (p) and velocity (v) of a traveling wave may be defined by the following equation:

$$p(x,t) = \mathrm{Re}[P(x)e^{i\omega t}]$$
$$v(x,t) = \mathrm{Re}[V(x)e^{i\omega t}] \tag{3.15}$$

where

$P(x)$ is the complex pressure amplitude
$V(x)$ is the complex velocity amplitude
ω is the frequency of the wave
i = imaginary number = $(-1)^{1/2}$

The variables "x" and "t" refer to space and time, respectively. The derivation in Equation 3.15 satisfies continuity, momentum, and thermodynamic conditions for an ideal fluid. The derivation may be considered for nonideal fluids or solids by ignoring shear forces in the mediums.

At the boundary, or interface, the pressure amplitude may be described in terms of the incident wave (P_I):

$$P_I e^{ik_1 x \sin\theta_1} + RP_I e^{ik_1 x \sin\theta_1} = TP_I e^{ik_2 x \sin\theta_2} \tag{3.16}$$

where

k_1 = wave number in substance 1 = ω/c_1
k_2 = wave number in substance 2 = ω/c_2

By considering continuity of pressure and velocity at the interface, the reflection and transmission coefficients can be given by the following:

$$R = \frac{Z_2 - Z_1}{Z_2 + Z_1}; \quad T = \frac{2Z_2}{Z_2 + Z_1} \tag{3.17}$$

The "Z" terms depend on the properties of the material containing the wave

$$Z_1 = \frac{\rho_1 c_1}{\cos\theta_1}; \quad Z_2 = \frac{\rho_2 c_2}{\cos\theta_2} \tag{3.18}$$

Finally, the angle of refraction can be determined by Snell's law, which results in the following:

$$\theta_2 = \sin^{-1}\left[\frac{c_2}{c_1}\sin\theta_1\right] \tag{3.19}$$

Determination of the reflection and transmission coefficients allows energy to be quantified. The potential energy (PE) per unit volume stored in the traveling waves is given by the following equation:

$$\mathrm{PE}_{IN} = \frac{|P_I|^2}{2\rho_1 c_1}; \quad \mathrm{PE}_R = \frac{|R|^2 |P_I|^2}{2\rho_1 c_1}; \quad \mathrm{PE}_T = \frac{|T|^2 |P_I|^2}{2\rho_2 c_2} \tag{3.20}$$

Mold and Environmental Problems

4

Introduction

Buildings can be affected by a variety of environmental problems and maladies. These problems are not restricted to residential structures, office buildings, commercial buildings, or industrial facilities. They tend to affect all structures to some degree. Certain types of problems affect some types of structures more than others. These environmental problems could be produced by inadequate design or construction, improper materials, building age, infiltration of hazardous materials, or naturally occurring phenomenon, health issues, and improper use of the facility. The quality of indoor air has been a concern for several hundred years with a dramatic increase in the 1970s as a result of the energy crisis that developed in that decade. During that decade, building occupants increased the reporting of a multitude of maladies arising from the occupation of indoor environments. A common term used to describe the variety of environmental problems that may arise is the "sick building syndrome." Another term often used is "building-related illness." It should be noted that there is no widespread agreement on the definition of these terms. Before we cover some of the more common environmental problems that may arise we need to first discuss the administration and the classification of buildings because the requirements for different structures differ considerably in detail although they share most of the common elements.

From an administrative standpoint, there are two principal codes. These are the *International Building Code* and the *International Residential Code*. Both of these codes apply to the construction, alteration, movement, enlargement, replacement, repair, equipment, use and occupancy, location, maintenance, removal, and demolition of these structures. These international codes have supplanted earlier codes such as BOCA, ICBO, and SBCCI and have been in effect for approximately 10 years. Buildings older than 10 years or in localities where these international codes have not yet been adopted should be referenced to the appropriate codes. The intent of these codes is to establish minimum requirements to safeguard public health, safety, and welfare. This is accomplished by ensuring structural strength, means of egress, sanitation, lighting, ventilation energy conservation, and safety to life and property. Of course, fire prevention is a major issue. The enforcement agency responsible is the department of safety for a particular city or state that has adopted the codes. These codes are generally administered through the local building official known as the Authority Having Jurisdiction (AHJ).

For new construction and for most older buildings, the building official is or was responsible for reviewing construction documents, keeping records, issuing permits, collecting fees, performing inspections, issuing certificates of occupancy, noting violations, and issuing stop work orders when applicable. In some instances, the forensic engineer may need to review the records of the construction documents and the permitting that

took place. The records from the building official may include a record of any unsafe condition that arose during construction.

All structures or portions of structures are classified with respect to occupancy according to Table 4.1. The classification may include one or more of the groups because room or spaces may be utilized for different purposes at different times.

In order to maintain a healthy environment within a building, key elements must be maintained. These elements include ventilation, temperature control, lighting, yards and courts, sound transmission, room dimensions, surrounding materials, rodent proofing, and waterproofing. The basic requirements are as follows according to the International Building Code.

Table 4.1 Use and Occupancy Classification

Group		Description
A	Subgroup	Gathering of persons
	A1	Fixed seating
	A2	Consumption of food or drink
	A3	Worship, recreation, amusement
	A4	Indoor sporting events
	A5	Outdoor activities
B		Business group
E		Educational group and day care
F	Subgroup	Factory industrial group
	F1	Factory industrial moderate hazard
	F2	Factory industrial low hazard
H	Subgroup	High-hazard group
	H1	Detonation hazard
	H2	Deflagration and accelerated burning hazard
	H3	Readily supporting combustion hazard
	H4	Health hazard
	H5	Semiconductor bulk materials hazard
I	Subgroup	Institutional group
	I1	Supervised residential environment
	I2	Medical, surgical, hospital environment
	I3	Restraint, security, prison environment
	I4	Day care facilities
M		Mercantile group
R	Subgroup	Residential group
	R1	Hotel, motel, boarding house, transient
	R2	Apartments, dormitories, not transient
	R3	Not R1, R2, R4, or I
	R4	Assisted living 5–16 occupants
S	Subgroup	Storage group
	S1	Moderate hazard
	S2	Low hazard
U		Utility and miscellaneous group

Ventilation

Natural or mechanical ventilation will be provided. In attics a minimum of 1 in. of air space shall be provided between the insulation and the roof sheathing. The net free ventilating area is to be at least 1/150 of the area being ventilated; 50% if the area being ventilated by ventilators is at least 3 ft above the eaves with the balance of the ventilation provided by vents in the eaves. All ventilators are to be screened so that birds, rodents, snakes, etc. cannot gain access to the area being ventilated.

Underfloor ventilators, between the floor joist and the earth, not in basements, shall not be less than 1 ft^2 for each 150 ft^2 of crawl space area and shall be covered to prevent infestation and provide cross ventilation.

Natural ventilation for occupied spaces shall be provided by windows, doors, and other openings and shall comprise at least 4% of the area being ventilated. For adjoining rooms without ventilation, they may be ventilated into ventilated rooms provided that the opening is at least 8% of the floor area being ventilated but not less than 25 ft^2.

Contaminants from naturally ventilated spaces such as bathrooms shall be mechanically ventilated according to the International Mechanical code and the International Fire Code.

Temperature Control

Interior spaces shall be provided with active or passive heating in order to maintain an indoor temperature of 68°F 3 ft above the floor level.

Lighting

Every interior space shall be provided by natural or artificial lighting. Natural lighting area shall be at least 8% of the floor area of the room. For adjoining rooms lighted naturally, the opening between the rooms shall be not less than one-tenth of the floor area of the interior room or 25 ft^2.

Artificial lighting shall provide an average illumination of 10 fc 30 in. above the floor. Stairways shall have an illumination of at least 1 fc.

Emergency egress lighting shall be provided where required.

Yards and Courts

Yards and courts shall not be less than 3 ft in width for one- and two-story buildings. Yards shall be increased by one additional foot per story up to 14 stories. Buildings taller than 14 stories shall be computed at the 14-story level. Courts for buildings taller than two stories shall have the width increased by 1 ft and the length by 2 ft per additional story up to 14 stories.

Sound Transmission

Airborne and structural-borne should have a sound transmission class of not less than 50 according to ASTM E 90 and ASTM E 492.

Interior Space Dimensions

Rooms shall be at least 7 ft wide in one dimension. Kitchens shall have a clear passageway of 3 ft. Minimum ceiling heights shall be at least 7 ft 6 in. Bathrooms, kitchens, and storage and laundry rooms may have ceilings of 7 ft. Every dwelling shall have at least one room of 120 ft^2 with other rooms no smaller than 70 ft^2. Kitchens shall be at least 50 ft^2. Efficiency dwelling units shall have a living room of at least 220 ft^2 with an additional 100 ft^2 for each occupant in excess of two.

Access to Unoccupied Spaces

Crawl spaces shall have an opening of at least 18 × 24 in. Attic spaces shall have an opening of at least 20 × 30 in. Mechanical appliances shall have access in accordance to the International Mechanical Code.

Surrounding Materials

Toilet and bathing room floors shall have smooth, hard, and nonabsorbent surfaces extending upward on the walls at least 6 in. Showers and bathtubs shall be furnished with smooth nonabsorbent surfaces extending at least 70 in. above the drain.

Damp and Waterproofing

Walls that retain earth and enclosed interior spaces and floors below grade shall be waterproofed and damp proofed. Crawl spaces shall be waterproofed and damp proofed. The top of the soil in a crawl space shall be covered with a 6 mile waterproofed fabric.

All of these elements are minimal requirements to maintain habitability of living spaces. The earlier list is simply an introduction into the topics that make a building habitable. The appropriate codes must be examined in order to properly assess a structure and the underlying problems that may exist.

The investigation of the health environment in a particular building can be quite complex and may involve a variety of health sciences. These sciences may include biology, genetics, industrial hygiene, and toxicology. The recognition of the problems associated with a building includes a proper evaluation of the hazard and a method of control. The hazard may be classified as chemical, biological, physical, or ergonomic. Chemical hazards may be airborne or direct contact type exposures. Biological hazards may be airborne, contact, or ingestion produced. Physical hazards include radiation whether ionizing or not, noise, vibration, temperature, and illumination. An additional physical hazard involves forces produced by machinery or equipment. Ergonomic hazards generally refer to repetitive motions or positions that are injurious to human health as a result of the work environment. The most common methods of control of the hazards include removal, isolation, ventilation, and cleaning of the air.

Airborne Particles

Airborne particles affect virtually all indoor environments whether the environment is the home, the office, or an industrial setting. The types of particles that affect these various places may vary or may be the same or similar. These particles may have a biological

origin, a nonbiological origin, smoke by-products, combustion by-products, aerosols, and chemical by-products. The particles may simply be dust and dirt. In an industrial setting, these dusts may include silica or coal. Nonbiological particles may result from the release of fibers such as asbestos or synthetics. The biological particles are generally viruses, mold, bacteria, pollens, or detritus. These airborne contaminants may originate within the building or they may be carried in from the outside environment. Combustion by-products may originate from smog outside or from improper or inefficient combustion of furnaces or water heaters. Generally, when airborne contaminants are suspected, air sampling will determine the cause and source.

Airborne particles may be solid or liquid and vary greatly in size. They are generally measured in terms of mass per volume or particle count per volume. A typical mass measurement may be in milligrams or micrograms per cubic meter or cubic foot. Dust particles are those that are smaller than 100 μm include minerals, grains, pollens, and organism detritus. Fumes may arise from oxidation, sublimation, distillation, or other chemical reactions and agglomerate into particles of 1–2 μm. Biological aerosols include viruses of between 0.003 and 0.006 μm, bacteria ranging in size between 0.4 and 0.5 μm. Fungal and bacterial spores range in size between 2 and 10 μm. Pollens vary greatly in size and range between 10 and 100 μm. Liquid particles may be classified as mists or fogs. Mists are produced by mixing and spraying activities or by chemical or physical processes. Fogs are produced by the condensation of vapors and are microscopic in size and are transitions between mists and vapors.

Other solid particles include smoke and smog. Smoke is produced by the incomplete combustion of organic materials such as wood, coal, oil, and tobacco. These particles are generally in the range of 0.1–0.3 μm. One of the products produced by the burning of tobacco is carbon monoxide. Smog particles generally include what is known as air pollution and consist of a variety of industrial compounds, exhaust from vehicles, fog, and a variety of other materials surrounding larger cities. Smog production is exacerbated by sunlight, which produces photochemical reactions, and by weather-produced inversions in the atmosphere. The Environmental Protection Agency (EPA) classifies airborne particles as either coarse or fine. Coarse mode particles have a minimum size of 1–3 μm and are generally naturally and chemically inert and include mold and pollen. Fine mode particles are generally formed by condensing gases or chemical reaction and have a maximum size of 1–3 μm.

The size of the airborne particles will determine where they will be deposited in the human system. As a general rule, most particles are deposited in the nasal cavities, some will pass through the bronchial and tracheal passages, and a portion will be deposited in the regions of the lungs where gas exchange occurs. According to the EPA, particles that can penetrate into the pulmonary passages are 10 μm in size and those that pass into the gas exchange region of the lungs are 2.5 μm in size. Equipment used in the measurement of airborne particles must be calibrated accordingly to meet EPA requirements. Figure 4.1 shows the distribution of particle size according to the EPA. Figure 4.2 shows the infiltration efficiency regions of the human respiratory system according to particle size and the aerodynamic properties of airborne particles.

There are three methods commonly employed to measure airborne particles. Direct gravimetric measurements are those where a dusty air sample is drawn through a filter that is preweighted. Filter sizes may be 2.5, 10, or other sizes in terms of the sieve size in microns. These methods are employed in industrial settings. Optical particle counters

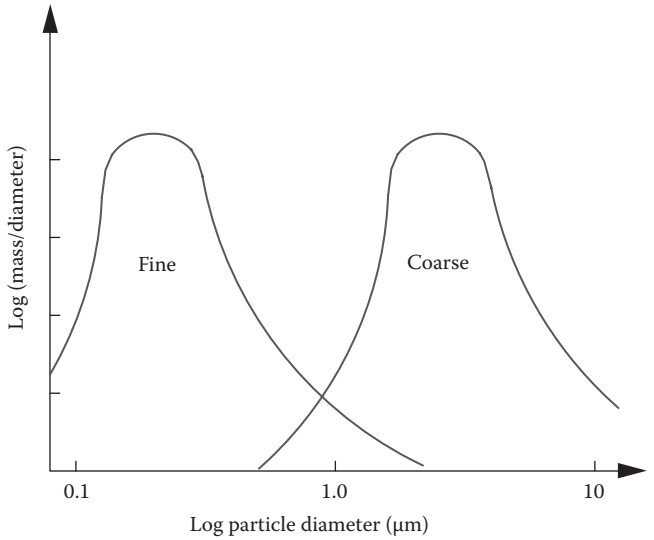

Figure 4.1 EPA particle size distribution.

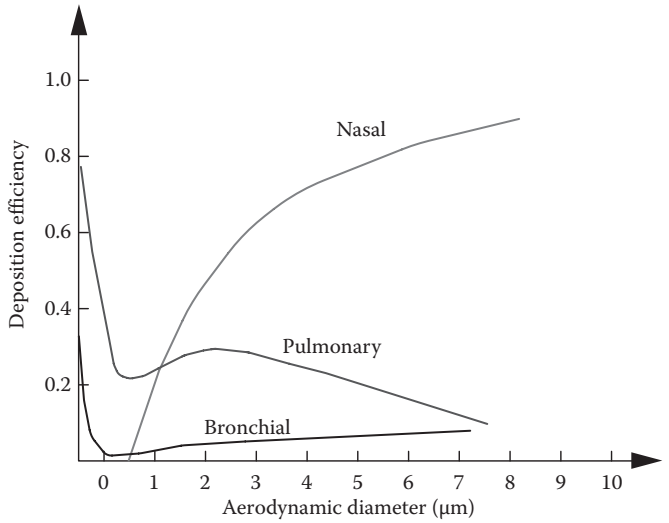

Figure 4.2 Human respiratory infiltration.

provide sampling in real time where gravimetric measurements do not. These optical devices make use of the scattering of light that interacts with a sensor that produces a voltage pulse when so excited. There are a variety of standards both from ASTM and ASHRAE that pertain to this technology. The third commonly utilized method is a condensation nucleus counter that can discern particles as small as 0.01 μm. A clean room may appear to have very little airborne particulate matter. Typically clean rooms can have as many as 10^6 particles per ft^3. A smoky room may have 10 times the amount of airborne particles.

Mold

Bioaerosols refer to airborne particles that are biological. These particles are generally microscopic and include pollens, viruses, bacteria, fungi, hair, dander, dust mites, fecal matter, and mold to name a few. These agents are found indoors as well as outdoors and are generally alive. However, non living bioaerosols can also be toxic, allergic, and inflammatory. The most common of the living airborne agents is, of course, mold and is probably the most widely studied and certainly investigated by the forensic practitioner. A common problem encountered is that a home owner complains to the insurance company that a storm or a flood has caused mold to grow in a certain location in their home. Although a natural event as described may have happened, the investigation may uncover that the source of the mold is a long duration leak of a water line. Alternatively, the mold may have been produced by a leaking roof that has allowed an interior wall to be saturated with water, consequently producing the mold. Figure 4.3 shows an interior wall in a house that is suspected of harboring mold in the interior cavity. Figure 4.4 shows the infrared image

Figure 4.3 Wall in house.

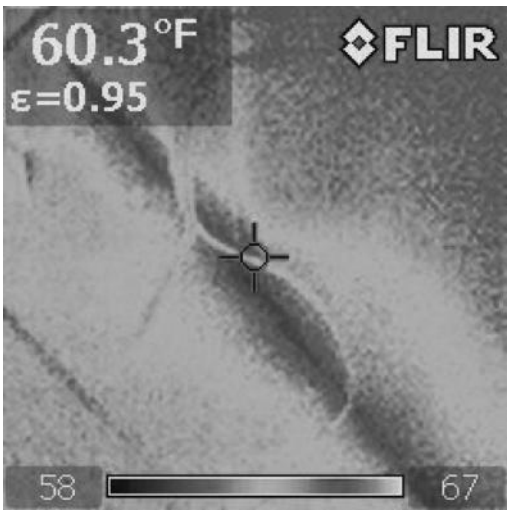

Figure 4.4 **(See color insert.)** Infrared image.

Figure 4.5 Moisture readings.

Figure 4.6 **(See color insert.)** Infrared camera.

of the wall and reveals the color variance indicating the presence of moisture. To verify the moisture content in the wall moisture readings were taken as displayed in Figure 4.5. The infrared camera used in the analysis is shown in Figure 4.6.

Mold is a fungi that has a structure that is filamentous. Mold reproduces by spores. These spores are quite small between 2 and 10 μm in size. The mold spores can be dispersed by water and air and can remain suspended in air for long periods of time. Humans are susceptible to infection by some molds. One of the most common infections is aspergillosis, which affects the lungs. The general health effect of fungal spores is to cause respiratory ailments and allergies.

Ventilation, temperature control, and lighting have the greatest effect on the quality of the indoor environment. These three parameters have the greatest influence on the growth and control of mold. Mold is known to thrive in damp, dark, stale air environments. Psychometrics deals with the moisture content of the environment, which is a key ingredient in the development of mold. Generally, atmospheric air contains many gaseous components along with water vapor. Dry air has a gas constant R_d = 53.352 ft-lb/lb$_d$°R and the gas constant for water vapor is R_w = 85.778 ft-lb/lb$_w$°R. Since the temperature and barometric pressure of atmospheric air vary with altitude and weather conditions, the standard atmosphere gives a reference for

Figure 4.7 Relative humidity meter.

estimating the properties of the air at a particular location. At sea level the standard temperature is 59°F and the pressure is 14.696 psia or 29.921 in. Hg.

One of the most important parameters in the identification of mold in the environment is the determination of the relative humidity. Relative humidity is the ratio of the mole fraction of water vapor *WP* in a given moist air sample to the mole fraction *WS* in a saturated air sample at the same temperature and pressure and is given as

$$RH = \frac{WP}{WS} \tag{4.1}$$

Figure 4.7 shows a meter that measures the relative humidity.

The ideal gas equation is

$$pV = nRT \tag{4.2}$$

Since both dry air and water vapor obey the ideal gas equation, we may express

$$p_d V = n_d R_d T \tag{4.3}$$

$$p_w V = n_w R_w T \tag{4.4}$$

The relative humidity can then also be expressed as

$$RH = \frac{p_w}{p_{ws}} \tag{4.5}$$

where

p_w is the partial pressure of water vapor

p_{ws} is the saturation pressure of water vapor in the absence of air

The dew point temperature at a given pressure is that where water vapor condenses to liquid water and is given by the empirical power series equation for temperatures between 32°F and 200°F:

$$t_d = 100.45 + 33.193\alpha + 2.319\alpha^2 + 0.17074\alpha^3 + 1.2063(p_w)^{0.1984} \tag{4.6}$$

where

t_d is the dew point temperature
$\alpha = \ln p_w$

The saturation pressure can be determined by the empirical power series equation

$$\ln p_{ws} = -\frac{1.0440397 \times 10^4}{T} - 11.29465 - 2.7022355 \times 10^{-2} T + 1.289036 \times 10^{-5} T^2 - 2.47868 \times 10^{-9} T^3 + 6.5459673 \ln T \tag{4.7}$$

where T is the absolute temperature,°R = °F + 459.67.

As an example for a temperature of 40.33°F or 500°R, Equation 4.7 yields a value of p_{ws} of 0.123. At a relative humidity of 100%, the dew point temperature from Equation 4.6 yields a temperature value of 40.389°F. The error in the calculations is

$$\text{Error} = \frac{40.389 - 40.33}{40.33} \times 100\% = 0.146\%$$

If the investigator chooses not to perform these calculations, tables of the thermodynamic properties of water should be consulted as found in the ASHRAE Handbook—Fundamentals found in the references. Resistance to mold growth on surfaces can be determined in accordance with standard test methods as outlined in UL 181 or ASTM C 1384.

Radon

Most developed countries have established maximum levels of the exposure to radon. These levels vary from 200 to 400 Bq/m^3 or 5.4 to 10.8 pCi/L. In the United States, the standard is 148 Bq/m^3 or 4.0 pCi/L. Approximately 6% of the homes in the United States have annual average concentrations of radon that exceed the maximum level of concentration as determined by the EPA. Six percent of the homes in this country amounts to approximately 6 million homes. These levels of maximum exposure to radon were established from studies of uranium workers and other underground mine workers.

Radon is a naturally occurring decay product of uranium found in the soil. The radioactive decay of radon produces radioactive isotopes of lead, bismuth, and polonium. The progeny or descendants of radon are chemically active unlike the chemically

inert radon parent. The active progeny can become airborne by attachment to other airborne particles and can be deposited in the lung. The adverse health effects are a result of the decay products of radon so that when assessing the dangers imposed, the measure is the level of radon rather than the measure of the other by-products.

Radon is chemically inert, colorless, odorless, and a tasteless radioactive gas that enters a house or a structure through leakage paths in the foundation. These paths are produced by pressure-driven flow from the ground to crawl spaces, to cracks in the foundation, through porous block work, and through leaks in heating, ventilation, and air-conditioning (HVAC) systems. The pressure differences are produced by wind, HVAC equipment, and thermal effects of the structure in question. Radon can also enter a structure through the water supply. When measurements are taken for the radon concentration, these measurements can vary significantly daily and seasonally. Kits available to homeowners measure the radon concentrations over a 1-week period and can yield inaccurate results. Long-term measurements from a 3-month period to 1 year produce the most accurate measurements.

Typically the outdoor concentration of radon is 0.4 pCi/L, which is one-tenth of the level as set by the EPA. The annual average concentration in homes in the United States is 1.25 pCi/L. The allowable concentration for miners is an average of 4 pCi/L per year. The units are the pico curie per liter. One pico curie equals 3.7×10^{-2} radioactive disintegrations per second. Figure 4.8 shows a map of the United States and the radon concentration zones.

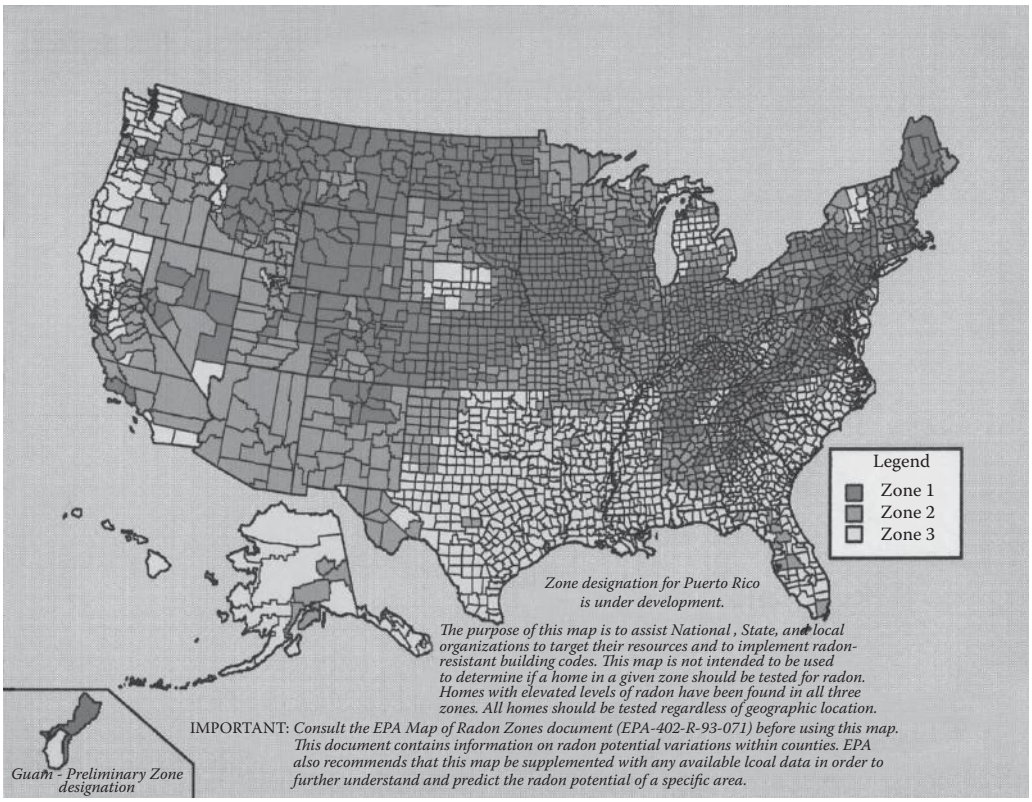

Figure 4.8 Map of radon zones.

Gases

Radon is not the only gas that comes from the ground but is the most widely known and feared. Another common gas is methane which can produce explosive events. Other toxic gases include chlorinated hydrocarbons and pesticides emanating from spills, leaks, and improper disposal. In this section we wish to discuss ambient gases which do not emanate from the soil but may be distributed by other means.

Gases that may affect structures may be organic or inorganic in nature. These gases may have a boiling point lower than room temperature or they may be vapors from liquids with boiling points above normal room temperatures. A great preponderance of these gases is from organic compounds that are volatile at room temperature. Volatile organic compounds include the wide variety of carbon compounds including gasoline, diesel fuel, oils, aromatics ethers, terpentine, and refrigerant gases. Some of the common inorganic gases include carbon monoxide ammonia, and carbon dioxide. Gases are measured by parts per million or parts per billion.

Gaseous contamination is much more likely in an industrial setting rather than in a home, office, or mercantile establishment. The health effects of these gases have not been extensively studied and are not very well understood. At the present time there are no standards for volatile organic compounds in nonindustrial settings. The Occupational Safety and Health Administration (OSHA) and the National Institute for Occupational Safety and Health (NIOSH) have set regulatory standards for industrial environments. These standards are published in the Code of Federal Regulations CFR Part 1910, Subpart Z. These regulatory standards were developed from recommendations of the American National Standards Institute (ANSI) and the American Conference of Governmental Industrial Hygienists (ACGIH). Table 4.2 summarizes some common acceptable levels for gasses.

Note that there is some agreement on the acceptable levels between the different agencies but there is also some disagreement. The difference in the values between the different agencies is due to the sampling and analytical methods employed in the testing protocols of the various agencies. Elevated levels of refrigerants such as R-11, R-12, and R-32 can also have a deleterious effect on humans. ASHRAE Standard 34, Designation and Safety Classification of Refrigerants and ASHRAE Standard 15, Safety Standard for Refrigeration Systems deal with these fluorocarbon refrigerants.

Table 4.2 Acceptable Levels of Gases

Compound	ACGIH (ppm)	NIOSH (ppm)	OSHA (ppm)
Carbon monoxide	25	35	50
Carbon dioxide	5000	5000	5000
Formaldehyde	0.3	0.16	0.75
Nitrogen dioxide	3	1	5
Ozone	0.05–0.2	0.1	0.1
Sulfur dioxide	2	2	5

Ventilation

Air quality in indoor environments is of critical importance. Up until the 1973 oil embargo, the standards for air quality required 15 ft^3/min of outside air for each building occupant. These air changes were considered essential to remove body odors. After this date, energy conservation became a top priority so that a reduction in air quality was required to a new level of 5 ft^3/min for each building occupant. In addition, HVAC systems may be inefficient and ineffectively distribute air throughout the building. Today, we recognize that 5 ft^3/min of fresh air is not sufficient to maintain a clean indoor air environment so that the minimum has been raised to 15 for residential and to 20 for office spaces. This standard is ASHRAE 62.1 Ventilation for Acceptable Indoor Air Quality. For residential structures the standard is ASHRAE 62.2 Ventilation and Acceptable Indoor Air Quality in Low-Rise Residential Buildings.

The more common causes of sick building syndrome are inadequate ventilation and chemical or biological contaminants from indoor or outdoor sources. Common indoor chemical contaminants are from manufactured building materials, cleaners, pesticides, and smoking. Unvented combustion products from furnaces, heaters, and fireplaces produce carbon monoxide, which is extremely lethal in minute quantities. Please refer to Chapter 13 for levels of carbon monoxide that are harmful to humans. Common outdoor chemical contaminants include vehicle exhausts, sewer gases, and chemicals from plants or factories. Biological contaminants from indoor and outdoor sources include water infiltration, insects, birds, rodents, and bacteria. Many of these contaminants fester in temperature, lighting, and humid conditions.

The procedure to determine the source of the problem is to do a preliminary walk-through of the building. Proper sampling of the environment should then take place, which may include testing for combustion gases, measuring air flow, measuring temperatures, measuring illumination levels, and measuring moisture contents. Hidden spaces may require opening wall cavities or utilizing boroscopes. Thermal imaging equipment and photographs or videos will aid in the analysis. Figures 4.9 through 4.11 display some of the

Figure 4.9 Boroscope.

Figure 4.10 Anemometer.

Figure 4.11 Light meter.

common equipment utilized in the sampling process. Laboratory air sampling may also be required to determine certain pollutants such as asbestos and radon.

The outdoor airflow that is required in a breathing zone is determined from the following equation:

$$V_{af} = R_p P_z + R_a A_z \tag{4.8}$$

where

V_{af} is the outdoor air flow in cfm
R_p is the outdoor air flow rate per person in cfm/person
P_z is the population—number of people in the zone
R_a is the outdoor air flow rate per unit area in cfm/ft^2
A_z is the zone floor area in ft^2

A summarized version of minimum ventilation rates in various breathing zones is shown in Table 4.3. A detailed compilation is found in ASHRAE 62.1.

In particular, for residential occupancies, a mechanical exhaust ventilation system or a supply system for each dwelling unit must supply ventilation with outdoor air each hour according to Equation 4.9 and Table 4.4 according to ASHRAE Standard 62.2. These requirements vary according to floor area and number of bedrooms:

$$Q_f = 0.01A_f + 7.5(N_b + 1) \tag{4.9}$$

where

Q_f is the flow rate in cfm
A_f is the floor area in ft^2
N_b is the number of bedrooms

Table 4.3 Ventilation Rates

Category	R_p (cfm/Person)	R_a (cfm/ft^2)
Correctional	5–7.5	0.06–0.12
Educational	7.5–10	0.06–0.18
Food	7.5	0.12–0.18
General	5	0.06–0.12
Hotel	5–7.5	0.06–0.12
Office	5	0.06–0.12
Miscellaneous	5–10	0.06–0.18
Public	5–7.5	0.06–0.12
Residential	5	0.06
Retail	7.5–20	0.06–0.18
Sports	7.5–20	0.06–0.48

Table 4.4 Ventilation Requirements

Floor Area (ft^2)	Bedrooms 0–1	Bedrooms 2–3	Bedrooms 4–5	Bedrooms 6–7	Bedrooms ≥7
≤1500	30	45	60	75	90
1501–3000	45	60	75	90	105
3001–4500	60	75	90	105	120
4501–6000	75	90	105	120	135
6001–7500	90	105	120	135	150
≥7501	105	120	135	150	165

Ventilation rates in kitchens of residential buildings shall be 100 cfm and in bathrooms they shall be 50 cfm. Air inlets that are part of the ventilation system design must be located a minimum of 10 ft away from stacks, vents, exhaust hoods, or vehicle exhausts. Ventilation openings may be as close as 3 ft from roof vents or dryer exhausts. Garages adjacent to occupied spaces must be air sealed to prevent unwanted exhaust gases from vehicles entering the living areas.

Building Materials

Building materials have a great influence and effect on the indoor environment. Typical materials in the interior of a building provide a variety of purposes including coverings for walls, floors, and ceilings, insulation, thermal barriers, lighting, and sound transmission properties, as well as fire protection. They provide physical barriers and means of egress. In some instances, building materials can pose a hazard to the occupants. The most highly publicized building material in recent history is Chinese drywall.

Drywall or gypsum board is commonly used to line the interior of walls in a building. Drywall is made by placing a plaster made mainly of gypsum between two layers of paper. Gypsum is a monoclinic mineral found in sedimentary rock. Sometimes gypsum is mixed with fly ash to make the plaster mix. Fly ash is a by-product of the burning of coal and is generally used as an additive to a variety of products. One of the by-products of drywall is hydrogen sulfide, which is lethal in concentrations of 1 part in 50,000. Fortunately, at concentrations far below this level, the odor prevents sufficient exposure. At reduced levels, people have complained of breathing difficulties, coughing, sinus, and respiratory problems. Additionally, the hydrogen sulfide reacts with copper and produces a black colored corrosion on air conditioning coils and copper electrical wiring. This corrosion may produce a significant risk to electrical wiring and junctions.

It should be noted that drywall manufactured in the United States also contains some of the same compounds as Chinese drywall but generally in lesser quantities. Laboratory comparisons of Chinese- and U.S.-made drywall revealed that the Chinese drywall contained significantly more pyrite. It appears that the oxidation of the pyrite may be the source of the sulfur compounds. The first order of business from a forensic standpoint is to identify where the drywall was manufactured. Second, components in the home containing copper should be investigated, and the color of the corrosion noted. Copper components, when oxidized, will turn either a dark red color or a green blue color. The presence of hydrogen sulfide corrodes the copper to a black color. If such conditions are found in a structure, the drywall should be removed and the copper components removed and replaced.

Asbestos

Asbestos is a naturally occurring mineral. It is distinguished from other minerals by the fact that its crystals form into long, thin fibers. This mineral has been extensively used in construction and building materials because of its excellent thermal properties. The health

effects of asbestos have been extensively studied, and it is now recognized that the deleterious effects are significant. Consequently, the use of this product is severely restricted and its removal and disposal highly regulated. Asbestos minerals are divided into two groups: serpentine and amphibole. Serpentine minerals have a sheet or layered structure while amphiboles have a chain-like crystal structure.

Chysotile is the only mineral in the serpentine group and accounts for approximately 95% of the asbestos found in buildings in the United States. The amphibole group has five types of asbestos with amosite as the second most likely type to be found in buildings. High-temperature insulation applications normally used crocidolite. The remaining three amphibole asbestos minerals are anthophyllite, tremolite, and actinolite and are occasionally found as contaminants in other asbestos-containing materials (ACMs).

Asbestos has been used in hundreds of products. Collectively these products are referred to as asbestos-containing material. The characteristics of asbestos proved well suited for many uses in the construction trades and can be found in large quantities especially in older buildings. One of the most common uses for asbestos was as a fireproofing material. It was sprayed on steel beams used in construction of multistoried buildings. This application prevented these structural members from warping or collapsing in the event of a fire. Chrysolite was the commonly used asbestos constituent in sprayed-on fireproofing. Asbestos comprised between 5% and 95% of the mixture and was used in conjunction with materials such as vermiculite, sand, cellulose fibers, gypsum, and a builder such as calcium carbonate. These materials are soft and may be fluffy in appearance and to the touch. They vary in color from white to dark gray. Occasionally, they have been painted or encapsulated with a clear or colored sealant. The material may be exposed or concealed behind a suspended ceiling. The application to structural members (beams and columns) often resulted in some overspray on walls and ceilings.

Asbestos is added to a variety of building materials such as concrete to enhance strength. Asbestos cement products generally contain Portland cement, aggregate, and chrysotile fibers. The asbestos content may vary up to 50%. Asbestos cement products are used as siding and roofing shingles, as wallboard, as corrugated and flat sheets of roofing, cladding, partitions, and as pipes. Asbestos has been added to asphalt, vinyl and other materials to make products like roofing felts, exterior siding, floor tile, joist compounds and adhesives.

Fibers in asbestos cement, asphalt, and vinyl are firmly bound to the product and will be released only if the material is mechanically damaged by drilling, cutting, or sanding. Roofing shingles and siding may also show slow deterioration due to weathering. As an insulator, asbestos has been widely used for thermal insulation and condensation control. It was normally sprayed, troweled, or manually applied after prefabrication. Asbestos is widely found in acoustical plaster. The material was generally sprayed or troweled on ceilings and walls. It was sometimes mixed with other products and applied to walls and ceilings to produce a soft decorative textured appearance.

The U.S. EPA and others distinguish between friable and nonfriable forms of ACM. Friable ACM can be crumbled or reduced to powder by hand pressure. Other things being equal, friable ACM is thought to release fibers into the air more readily. However, many types of nonfriable ACM can also release fibers if disturbed.

The EPA identifies three categories of ACM used in buildings:

1. *Surfacing material*: ACM sprayed or troweled on surfaces (walls, ceilings, structural members) for acoustical, decorative, or fireproofing purposes, including plaster and fireproofing insulation
2. *Thermal system insulation*: Insulation used to inhibit heat transfer or prevent condensation on pipes, boilers, tanks, ducts, and various other components of hot and cold water systems and HVAC systems, which includes pipe lagging, pipe wrap, block, bath and blanket insulation, cements, muds, gaskets, and ropes
3. *Miscellaneous materials*: Other largely nonfriable products and materials such as floor tile, ceiling tile, roofing felt, concrete pipe, outdoor siding, and fabrics

While it is often possible to suspect that a material or product is or contains asbestos by visual determination, actual determinations can only be made by instrument analysis. The EPA requires that the asbestos content of suspect materials be determined by collecting bulk samples and analyzing them by polarized light microscopy (PLM). The PLM technique determines both the percent and type of asbestos in the bulk material. However, some of these materials do not have to be inspected and inventoried under the Asbestos Hazard Emergency Response Act (AHERA) Rule. Asbestos-containing building materials (ACBM) as defined by the rule exclude materials installed outside a building such as roofing felt, siding, and all fabric materials.

Electromagnetics

Electromagnetic radiation consists of two components: the electric field and the magnetic field. The electric field is associated with voltage and the magnetic field is associated with current. The radiation is actually the combination of the two fields and is generally described by its power content in the Poynting vector, which is the cross product of the electric and magnetic fields. For sinusoidal variations in the fields, the resultant energy is a function of frequency and corresponding wavelength. In free space the wavelength is given by

$$\lambda = \frac{v_p}{f} \tag{4.10}$$

where

λ is the wavelength (m)
v_p is the velocity of propagation = 3×10^8 m/s in free space
f is the frequency (Hz)

In a medium such as water, the velocity of propagation slows accordingly. Electromagnetic radiation in terms of its effects on biological systems may be classified as either ionizing or nonionizing. Ionizing radiation is at the lower wavelengths, or correspondingly higher frequencies in the ultraviolet range and into the x-ray and cosmic ray ranges. Nonionizing radiation is at the lower ultraviolet, infrared, microwave, and radio wave ranges. These are the lower frequencies, or corresponding higher wavelengths of the electromagnetic spectrum. Please refer to the electromagnetic spectrum in Chapter 12. Ionization of biological tissues refers to the change in the neutral charge status of the material. Ionization of biological matter can

Table 4.5 Ionizing Radiation Exposure Limits

Occupational dose limits based on stochastic effects	50 mSv annual effective dose limit and 10 mSv times age in years cumulative effective effect dose limit
Occupational dose limits based on deterministic effects	150 mSv annual equivalent dose limit to lens of the eye and 500 mSv annual equivalent dose limit to skin, hands, and feet
Public dose limits based on stochastic effects	1 mSv annual effective dose limit for continuous exposure and 5 mSv annual effective dose limit for infrequent exposure
Public dose limits based on deterministic effects	

be very destructive and is regulated by the Code of Federal Regulations, Title 10, Part 20. Generally the boundary between ionizing and nonionizing radiation is considered as 100 nm.

According to 10 CFR 20.1004 the units of ionizing radiation are as follows. The old units were measured in RADS, REMS, or ROENTGENS. These units have the following conversions to the new units:

1RAD = absorbed dose of 100 ergs/g = 0.01 J/kg = 0.01 Gy
1 Gy is the absorbed dose of 1 J/kg = 100 RADS
100 REMS = 1 seivert = 1 Sv
100 REMS = 8.38 R

Table 4.5 shows the recommended exposure limit to ionizing radiation according to the National Council on Radiation Protection and Measurement, NCRP Report No. 116.

Nonionizing radiation is not as benign as it would seem. Visible light from the ultraviolet to the infrared is part of sunlight that can cause significant damage to humans. This optical radiation from 1 mm to 100 nm interacts with human tissues in a variety of ways through reflection, absorption and transmission. The skin and the eyes are most at risk as any person who has experienced a severe sunburn knows. The higher the frequency of the radiation, the more penetration into the human tissue. At the lower frequencies in the radio wave range especially in the X and K band ranges this effect is less pronounced. The permissible level of exposure of radio frequency waves is regulated by ANSI/IEEE C95.1-2005 and is shown in Figure 4.12. Note the difference between the two standards. The electric field intensity is measured in volts per meter, the magnetic field intensity in amperes per meter, and the power density in milliwatts per squared centimeter.

The Federal Communications Commission essentially follows these standards and includes the average time for exposure. For the general population, the average exposure time is 30 min and for occupational exposure it is 6 min. There are two documents that may be obtained for further study free of charge from the Internet. These are the International Commission on Non-Ionizing Radiation Protection, Guidelines for Limiting Exposure, 1998 and The Federal Communication Commission OET Bulletin 56, 1999.

Vibrations and Sound

Humans and inanimate structures are influenced by mechanical vibrations. In this chapter we are not concerned with the effects of mechanical vibrations on structures but rather on the effect that they may have on the human population. Humans respond to mechanical vibrations through a combination of sensory stimuli that includes sight, sound, and touch.

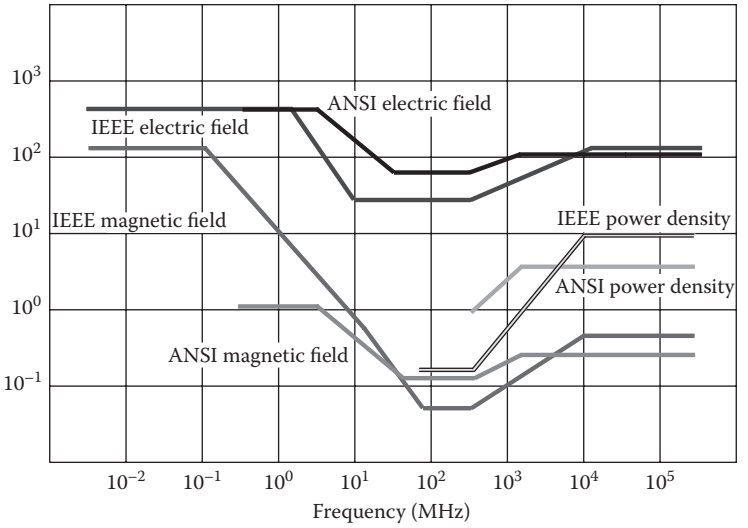

Figure 4.12 Permissible levels of radio waves.

Building vibrations are generally divided into two categories, low-frequency vibrations less than 1 Hz and high-frequency vibrations between 1 and 80 Hz.

For low-frequency building vibrations, the physical dimensions of the building are the critical factors. Taller buildings have a greater tendency to sway. The perception threshold for low-frequency vibrations of buildings by humans is between 0.06 and 1.0 Hz or a period of 1 to about 17 s. For example, the natural frequency of the Empire State Building has been measured to be 0.1205 Hz or a period of about 8.3 s. These thresholds are measured in terms of the relative accelerations, or

$$\mu_r = \frac{a}{g} \tag{4.11}$$

where

μ_r is the relative acceleration
a is the actual acceleration
g is the acceleration due to gravity = 32.2 ft/s^2

Higher frequency vibrations in buildings are produced by a combination of factors that include foot traffic, elevators, machinery, and HVAC systems. The average perception threshold for these higher frequency vibrations in buildings is between 0.03 and 0.3 ft/s^2.

An additional source of vibrations comes from the sounds that are produced. Sound that is transmitted consists of oscillations above and below atmospheric pressure. The greatest health effect of excessive sound is hearing loss. The generally acceptable maximum level of noise is 75 dBA for an 8 h working day over a working lifetime. The human ear is susceptible to longitudinal waves in frequency between 20 and 20,000 Hz. Atmospheric pressure is approximately 10^6 dyn/cm^2. Measurement of sound waves reveals that the human ear can withstand maximum pressure variations of approximately 280 dyn/cm^2 above and below atmospheric pressure. The minimum pressure variations, or faintest sounds, detectable by the human ear at a frequency of 10^3 Hz is approximately 3×10^{-4} dyn/cm^2.

Table 4.6 Common Sound Levels

Source	Level in dBA
Pain threshold	120
Traffic	70
Conversation	60
Quiet conversation	40
Hearing threshold	0

The energy propagated by a sound wave is a function of its intensity. Conversely, the intensity of the wave is the average power per unit area. The power per unit area of a sound wave equals the excess pressure times the particle velocity. The intensity over one cycle is given by

$$I = \frac{P^2}{2\rho v} \tag{4.12}$$

where

I is the intensity
P is the pressure amplitude
ρ is the average density of air
v is the velocity of the sound wave

Since the human ear has a large range of intensities over which it responds, a logarithmic scale is used instead of a linear scale. The intensity levels are then expressed in decibels or dBA where

$$\text{dBA} = 10 \log_{10} \frac{I}{I_0} \tag{4.13}$$

We can calculate the intensity of the loudest tolerable sound from Equation 4.12 as follows:

$$I = \frac{(280\,\text{dyn/cm}^2)^2}{2(1.22\times10^{-3}\,\text{g/cm}^3)(3.46\times10^4\,\text{cm/s})} = 94\times10^{-6}\,\text{W/cm}^2$$

In Equation 4.13, I_0 is the arbitrary reference intensity equal to 10^{-16} W/cm^2, which corresponds to the faintest sound which can be heard by humans. So from the earlier calculation, we can safely say that the maximum tolerable sound is approximately 10^{-4} W/cm^2. This intensity level corresponds to approximately 120 dBA. Table 4.6 summarizes some common sound levels.

Temperature

Along with the other physical factors that influence the indoor environment, moisture, air movement, radiant energy, mechanical energy, and electromagnetic energy, temperature ranks as a very primary factor because the thermal environment determines how humans

are able to regulate their body temperature. Healthy humans have core temperatures that normally vary by less than 1° F at an average of 98.6°F. Core temperature is different than skin temperature that can vary between 88°F and 98.6°F depending on the location where it is being measured.

As a standard, 75°F is considered a mean temperature for human comfort for a resting person that is normally clothed. The range of temperatures is from 72°F to 78°F. In this range of temperatures normal healthy humans are quite capable of adjusting their internal temperature controls to remain comfortable. The body regulates temperature by two basic means; increased blood flow when cold and increased perspiration when hot. Older individuals have metabolic temperature controls that may be about 80% of that of younger individuals so that they may feel more comfortable at greater temperature ranges than listed here. Extreme temperature ranges experienced by humans can lead to hypothermia and hyperthermia.

When the core body temperature of a human falls below 95°F, hypothermia sets in. In an occupational environment, hypothermia may be produced by a combination of factors that include age, drug use, environmental temperature, decrease in work activity, and metabolic disorders. Hyperthermia occurs when the core temperature of a human increases 4°F above normal and not resulting from strenuous exercise. This condition is referred to as heat stroke and is very dangerous to human life unless cooling of the body takes place. Occupations where the extreme effects of temperature may affect workers include mining, smelting, and outdoor construction.

Ergonomics and Illumination

Ergonomics deals with the relationship between the work environment and humans. Ergonomically designed environments optimize efficiency and ease of the work environment. Although ergonomics deals with the entire work environment such as walking surfaces, chairs, tables, work benches, and tools, one of the most important aspects is illumination. Too much or too little illumination can be detrimental to the work environment. Illumination can be a detriment to a means of egress, which is a vital component of safety. Safety concerns arise in outdoor environments, especially in high crime areas.

The quantity of light intensity is not the only measure that should be considered. Other factors such a glare, flicker, shadows, and contrast play a significant role in the quality of the available light. The color of the light is also an important factor. High light levels

Table 4.7 Minimum Illumination Levels

Area or Activity	OSHA (fc)	ANSI/IESNA (fc)
General construction	3–5	
Tunnels underground	5–10	
Construction plantsshops	10	
First aid	30	
Low-hazard environment		0.5–1
High-hazard environment		2–5
Public spaces		3
Working spaces		9–90

Table 4.8 Japanese Illumination Standards

Category	Subcategory	(fc)	(lx)
Offices			
	Food, bath, entrance, warehouse	7–15	75–150
	Bath, stairs, hallway	10–20	100–200
	Library, machinery, elevator	15–20	150–200
	Meeting, reception, kitchen, dining	20–50	200–500
	Office, printing, computer	30–70	300–700
Work			
	Outdoor	1–3	10–30
	Emergency, stairs	3–7	30–75
	Entrances, warehouses, lavatory	7–15	75–150
	Machinery rooms	15–30	150–300
	Control rooms	30–75	300–750
	Design rooms	75–150	750–1500
	Instrumentation	150–300	1500–3000
Schools			
	Auditoriums, stairs, locker/rest rooms	7–30	75–300
	School rooms, laboratory, faculty	20–75	200–750
	Drawing, computer, classrooms	30–150	300–1500
Stores			
	Suburban shops	30–75	300–750
	Midtown shops	75–100	750–1000
	Special displays	100–300	1000–3000
Restaurant			
	Passages	7–15	75–150
	Entrances, bathrooms	15–30	150–300
	Dining, services	30–75	300–750
Apartments		3–7	30–75
	Stairs, garages	7–15	75–150
	Entrances, bathrooms	10–20	100–200
	Offices	15–50	150–500

affect what we see. Under these conditions, the human eye responds by switching to conic vision. All of these factors affect the recognition of an object. Unfortunately, these other parameters are very difficult to quantify. In fact, in the United States, the quantity of light necessary for proper performance is somewhat, from a standard stand point, inadequate. A measure of the illuminance is the foot-candle. A foot-candle is the amount of light from one candle at a distance of 1 ft and equal to one lumen per square foot. Sunny days can illuminate between 5,000 and 10,000 fc. Normal illumination in a room is about 30 fc.

A full moon produces an illumination of approximately 0.2 fc. A lux is a measure of lumens per square meter where 1 fc is equal to about 10.7 lx, or more precisely

$$1 \text{ fc} = 10.764 \text{ lx} \tag{4.14}$$

Needless to say, when a forensic engineer is asked to determine the illumination levels of a particular site and form an opinion on what an involved party could see, the opinion could be quite subjective. All of the factors mentioned earlier come into play as well as the attentiveness of the subject, the condition of his or her vision, and reaction performance. We find it extremely nonscientific to state with any certainty what another person could or could not see. The forensic engineer can only state with certainty the amount of illumination that is present at a site and whether the illumination meets minimum criteria. This is determined by measuring the light intensity with a light meter as shown in Figure 4.11.

The U.S. Department of Labor OSHA provides under Part 1926.56 some minimum illumination levels for construction areas. Table 4.7 summarizes some of these minimum illumination levels. Included are values from ANSI/IESNA RP-7. IESNA is the Illuminating Engineering Society of North America.

In contrast to the standard illuminations earlier, the Japanese have promulgated much more comprehensive standards. These are JIS Z 9110 published by the Japanese Standards Association, some of which are summarized in Table 4.8. Note that the values in footcandles have been rounded.

Water-Related Losses 5

Introduction

One of the most common types of loss or investigation that is undertaken by the forensic engineer is that which is related to water. These losses take a variety of forms including the effects of ground water, open channel flow, flow in pipes, flow under pressure, the effects of rain water on structures, and the related components that are used to divert water in its many forms. These losses may be produced by naturally occurring water or by the diversion or restriction of water from effluent systems, sanitary systems, or naturally occurring surface or subsurface water flow. Water is a naturally occurring compound consisting of two atoms of hydrogen and one atom of oxygen (H_2O). Water in its chemically pure state is not found in nature. Normally water will contain a variety of chemical elements and compounds depending on the soil conditions over which it flows and the extent of purification that it undergoes by man-made structures and systems.

Water has certain properties, which are in many respects, ideal. Recall that water is a standard in science and engineering. Water is *fluid*, which means that it offers very little resistance to a change in form. Water has a definite volume but no definite shape and takes the shape of the containment. Water has a definite *density* at 39.3°F and as a standard has a specific gravity of unity. The weight of fresh water is taken as 62.4 lb/ft^3. The relative density and weight of fresh water varies according to temperature. At 32°F water has a relative density of 0.99987 and weighs 62.416 lb. At 212°F the relative density is 0.95865 at a weight of 59.843 lb. For most hydraulic computations water is assumed to be incompressible, although like most liquids it is slightly *compressible*. For most computations the density of water can be assumed to be unity. Water is perfectly elastic so that after the release of pressure it regains its original volume. The modulus of elasticity is constant for constant temperature and pressures below 1000 psi. Table 5.1 gives the modulus of elasticity for temperatures over the liquid range of water.

Viscosity is the propensity of a liquid to resist movement between its particles. As temperature increases, the viscosity of the liquid decreases. In more technical terms, viscosity is the property of the liquid to resist shear stress. It is proportional to the force required to produce shearing deformation at a given time rate. Table 5.2 shows the variation in the viscosity and density of water as the temperature rises. The units of viscosity are the dyne-s/cm^2, which is the poise. In the English system the value of the poise is multiplied by 0.002088.

Cohesion and adhesion help to explain the behavior of water under certain conditions. The cohesive forces between the molecules of water are the same in all directions. On the surface of the water, the top surface molecules are attracted downward with no attraction from above so that a film is developed across the surface of the water, which is commonly

Table 5.1 Modulus of Elasticity for Water

Temperature (°F)	Modulus of Elasticity (psi)
32	282,000
50	308,000
100	335,000
150	348,000
212	360,000

Table 5.2 Viscosity and Density versus Temperature

Temperature (°F)	Viscosity (η, lb/ft-s)	Density ρ (lb/ft^3)
32	0.001206	62.42
50	0.000880	62.41
60	0.000759	62.37
70	0.000660	62.3
90	0.000513	62.12
150	0.000291	61.2
200	0.000205	60.14
212	0.000141	59.84

known as surface tension. In an open channel, the surface tension tends to retard the flow so that the velocity at the surface is less than the velocity below the surface. This effect explains why you can swim faster below the surface or why submarines travel faster than surface ships of the same physical characteristics. When solids come into contact with liquids, the cohesive forces may be stronger than the adhesive forces or vice versa. Inserting a thin glass tube into water produces adhesion forces greater than cohesive forces so that the water will rise in the tube, a phenomenon known as capillary action. The water surface inside the tube will be concave upward. When a thin tube is inserted into mercury, the cohesive forces are greater than the adhesive forces so that the mercury inside the tube will be lower than the surface. The surface of the mercury inside the tube will be concave downward. As the diameter of the capillary tube increases, the effect decreases. These concepts allow us to introduce the principles of hydrostatics and hydrodynamics. Figure 5.1 represents a typical hydrologic cycle model.

The hydrologic cycle in this simple representation assumes that water would be in its chemically pure state. We know that chemically pure water is not found in nature. The water in inland rivers, lakes, and aquifers contains a variety of minerals. The oceans are heavily infused with a variety of chemicals including sodium chloride. Water vapor resulting from condensation is an important element in the earth's atmosphere. The amount of water vapor in the atmosphere varies with temperature, pressure, and a variety of other factors. The accumulation of condensation and circulation of the atmosphere causes precipitation, which is the source of all inland water.

Forensically speaking, the investigating engineer may be asked to analyze a variety of water related losses. These losses may be due to the movement of water through the soils that may affect retaining structures, culverts, dams, weirs, and foundations.

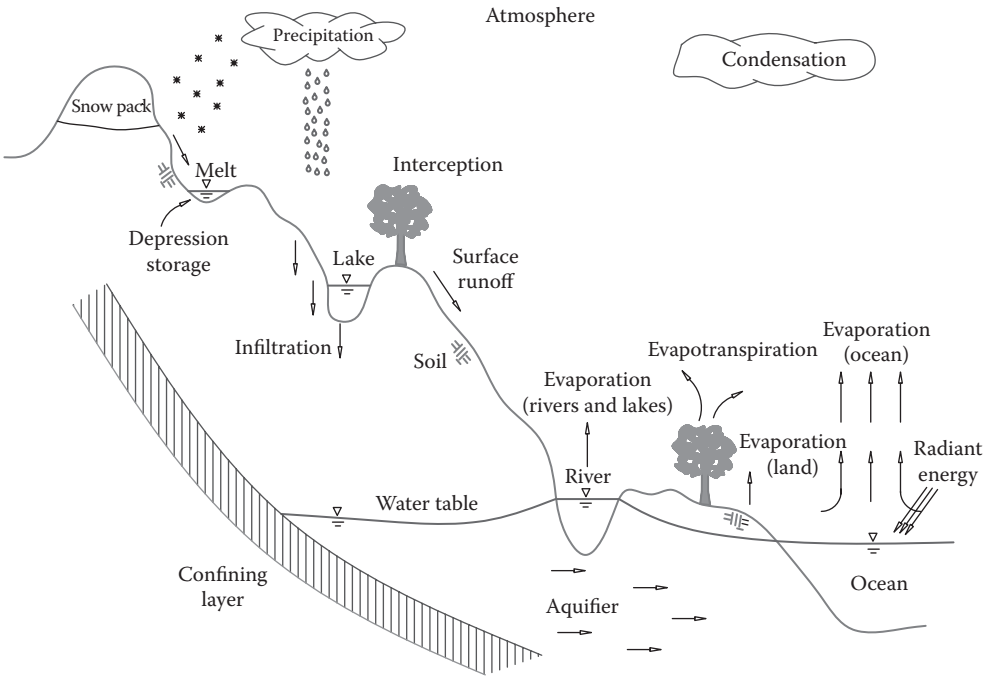

Figure 5.1 Hydrologic cycle model.

The water-related losses may also be due to the flow of water through pipes, conduits, orifices, and gates. These systems may be under- or overpressurized. The loss may be due to a malfunction in a boiler or hot water system in a building or a home. The water related loss may be due to a fire suppression system either through the standpipe or the fire suppression distribution system. The loss may be due to flooding by natural occurrences or due to a failure of a component such as a commode, or a frozen water pipe. The diverse nature of the uses of water requires the investigator to have a broad knowledge of weather, soil behavior, metrology, and hydrology.

Fluid Statics and Dynamics

Hydraulics is the science associated with fluids. The most common fluid is water although these principles apply to all fluids encountered in engineering. More formally, we may classify hydraulics as *hydrostatics*, water at rest, *hydrokinetics*, water in motion, and *hydrodynamics* as the forces associated with the motion of water. Simply, we refer to two classifications incorporating hydrokinetics into hydrodynamics and refer to the two subjects as *fluid statics* and *fluid dynamics*.

The most common units in hydraulics involve volume measured in cubic feet and the acre-foot, which covers an area of an acre at a depth of 1 ft and is therefore equal to 43,560 ft^3. The gallon is also used and is equal to 0.1337 ft^3. The standard units of flow are the cubic foot per second, or the cubic foot per minute, or the gallon per minute. Sometimes these flows are expressed in terms of hours or even days depending on the application and the volumes in question.

Fluid Statics

This section of hydraulics mainly deals with problems involving the intensity of the pressure, the total pressure, and the center of the pressure that is applied to a given surface. To begin the discussion of pressure, we must first introduce atmospheric pressure, which is due to the weight of the air on the earth's surface. Meteorological conditions can affect atmospheric pressure. At sea level the mean pressure is 14.7 psi or 2116 lb/ft^2. This pressure is designated as one atmosphere. As the altitude increases, the pressure and the density of air decrease. For most engineering problems, we assume that atmospheric pressure is at sea level, and we do not attempt to correct for elevation although at an altitude of 10,000 ft, atmospheric pressure has dropped to approximately 10 psi. The main reason for ignoring atmospheric pressure is that we are dealing with liquids where atmospheric pressure is constant over the surface of the liquid or the liquid is completely contained within a vessel such as a pipe, a boiler, a pump, a valve, or some other contraption where atmospheric pressure may be neglected.

Hydrostatic pressure is the pressure that the fluid exerts on an object that is immersed or on the surfaces of the containment vessel. The characteristics of hydrostatic pressure are the following:

1. Pressure is a function of depth and density and varies linearly.
2. Pressure is independent of the area, size, and weight of the immersed object.
3. Pressure obeys Pascal's law and is equal in all directions.
4. Pressure is normal to the surface and cannot support shear stress.
5. The pressure distribution on the object acts through the center of pressure.

Hydrostatic pressure is the pressure that a fluid exerts on an immersed object or on the walls of the container. Simply defined, pressure if the force per unit area, or

$$p = \frac{F}{A} \left(\text{lb/in.}^2\right) \tag{5.1}$$

For an incompressible fluid, the relationship between pressure and depth is given by

$$p = \rho g h + p_a = wh + p_a \tag{5.2}$$

where

p_a is the atmospheric pressure
ρ is the density of the fluid
g is the gravity
h is the depth
w is the weight

Pascal's law states that the pressure at any point within a fluid at rest is transmitted equally in all directions and acts in a normal direction to the surface to which it is in contact with. The magnitude of the resultant of all the components of the total pressure in any direction can be expressed as

$$P = \int wh \cos\varphi dA \tag{5.3}$$

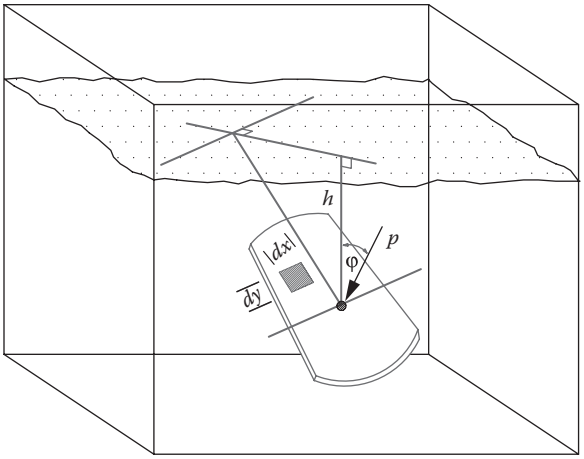

Figure 5.2 Submerged body.

Figure 5.2 represents a body submerged in water.

We can now visualize the pressure on this submerged body. The distance to the center of pressure of the submerged body in the plane of the body from and normal to the axis of the body extending to the surface is

$$y = \frac{I_y}{S_y} \tag{5.4}$$

where

I_y is the moment of inertia
S_y is the gravity moment

The distance x to the center of pressure from an axis in the plane of the submerged body is

$$x = \frac{\int xydA}{\int ydA} \tag{5.5}$$

When the surface of the submerged body is nonplanar, the vertical distance from the surface of the water to the center of pressure can be found from

$$h = \frac{\int h^2 dA}{\int hdA} \tag{5.6}$$

As an example, consider a wall with two different levels of water as shown in Figure 5.3.

In Figure 5.3 water is acting on both sides of the wall. On the left side the depth of the water is D_1 and on the right side it is D_2. The water pressure on both sides of the wall is represented by the corresponding triangles. At the surface, the pressure is zero and at the bottom

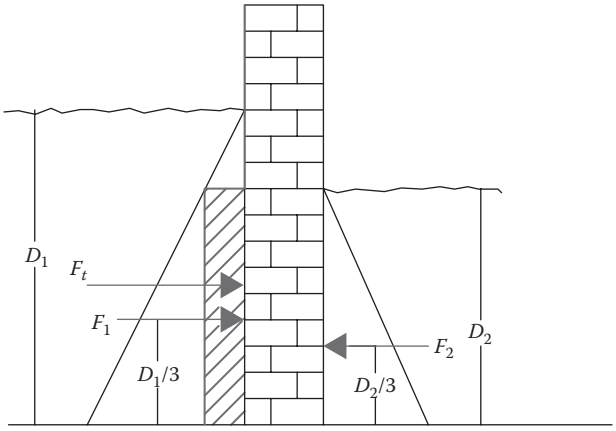

Figure 5.3 Wall.

the pressures are D_1w and D_2w. The weight of the water w is taken to be 62.4 lb. The corresponding pressures are then

$$F_1 = \frac{D_1^2 w}{2}; \quad F_2 = \frac{D_2^2 w}{2} \tag{5.7}$$

The total effective pressure is then

$$F_t = (D_1^2 - D_2^2)\frac{w}{2} \tag{5.8}$$

The total effective pressure passes through the center of the trapezoid shown in red and is given by

$$D_t = \frac{1}{3}\left(D_1 + \frac{D_2^2}{D_1 + D_2}\right) \tag{5.9}$$

For $D_1 = 12$ and $D_2 = 9$, $D_t = 5.28$.

As another example that is commonly encountered consider a dam structure that is constructed to retain the water in a pond. The pond experiences a large accumulation of water runoff so that the dam has an overflow condition as shown in Figure 5.4.

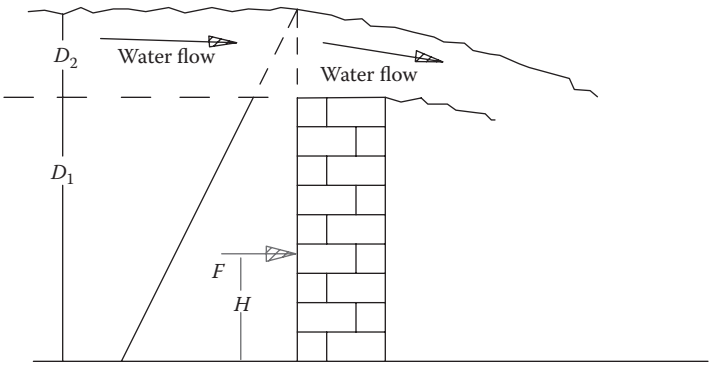

Figure 5.4 Dam overflow.

The triangle of pressure is reduced by the small triangle at the top of the dam structure because there is no surface to oppose the pressure at a depth D_2. At the depth D_2 the pressure is wD_2 and at a depth $D_1 + D_2$ the pressure is $(D_1 + D_2)w$. The dam is then subjected to a total pressure per unit length represented by the trapezoid. The total pressure per unit length is equal to the area of the trapezoid of pressure which is given by

$$F = D_1(2D_2 + D_1)\frac{w}{2} \tag{5.10}$$

The height H above the base of the dam is where the resultant force acts. Thus, for the trapezoidal area the height is

$$H = \frac{D_1}{3}\left(1 + \frac{D_2}{2D_2 + D_1}\right) \tag{5.11}$$

Fluid Dynamics

This section deals with the movement of fluids. As with any body, a fluid requires energy in order to produce movement. This movement of the fluid can be produced by kinetic, potential, and pressure energy. The kinetic energy of a fluid flow per unit weight with uniform velocity is given by

$$E_k = \frac{v^2}{2g} \tag{5.12}$$

The per unit weight or per unit mass potential energy is given by

$$E_p = z \tag{5.13}$$

The pressure energy in consistent units per unit mass is

$$E_p = \frac{p}{w} \tag{5.14}$$

Keep in mind that the liquid in this chapter is water so the density of water is unity and the unit weight is 62.4 lb/ft^3. We are now ready to introduce Bernoulli's equation as an energy conservation equation based on reasonable assumptions. We assume that water is incompressible and that changes in thermal energy are negligible. We neglect fluid friction. Consider the flow of water in the tube of Figure 5.5.

Bernoulli's Theorem states that a mass of liquid flowing possesses kinetic, potential, and pressure energy, and if we neglect friction, it is the same at every position in the mass. In equation form we say

$$\frac{v_1^2}{2g} + \frac{p_1}{w} + z_1 = \frac{v_2^2}{2g} + \frac{p_2}{w} + z_2 \tag{5.15}$$

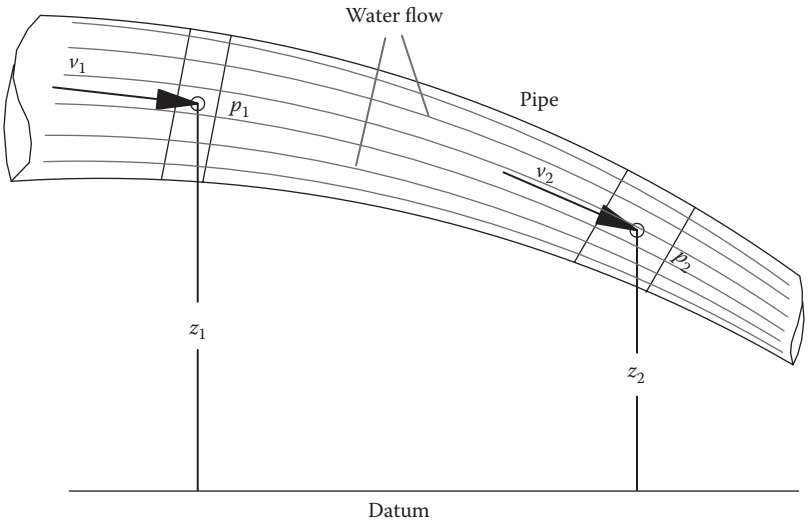

Figure 5.5 Water flow in a tube.

The three terms on either side of Equation 5.15 are referred to as the velocity head, the pressure head, and the potential head, respectively. When we apply the earlier equation to actual conditions, we may include the losses between the two heads as h_l or

$$\frac{v_1^2}{2g} + \frac{p_i}{w} + z_1 = \frac{v_2^2}{2g} + \frac{p_2}{w} + z_2 + h_l \tag{5.16}$$

From Equation 5.15, it is evident that if the velocities are zero, we have

$$(p_1 - p_2) = w(z_2 - z_1) \tag{5.17}$$

Equation 5.17 is the same as Equation 5.2 so that we see that the hydrostatic equations are special cases of Bernoulli's equation.

Let us now consider a tank full of water as seen in Figure 5.6, which includes an orifice.

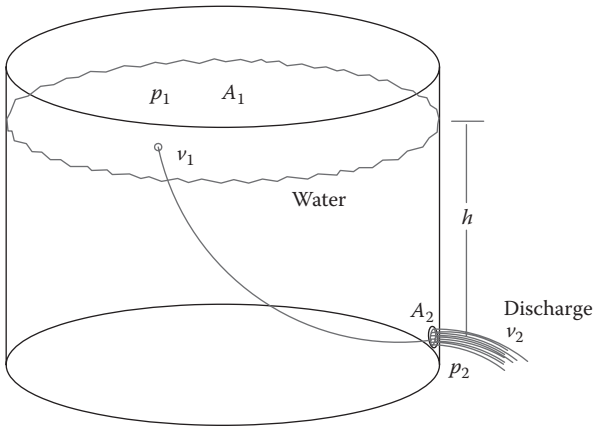

Figure 5.6 Tank and orifice.

We choose to have the reference datum at the orifice so if we apply Bernoulli's equation, we have

$$h + \frac{p_1}{w} + \frac{v_1^2}{2g} = \frac{p_2}{w} + \frac{v_2^2}{2g} \tag{5.18}$$

Rearranging Equation 5.18, we obtain

$$v_2^2 = v_1^2 + \frac{2g}{w}(p_1 - p_2) + 2gh \tag{5.19}$$

As the water flows out of the orifice, there is continuity of flow so *that* $A_1\ v_1 = A_2\ v_2$. If $A_1 >> A_2$, then we see that $v_2 >> v_1$. If the tank is open to the atmosphere then $p_1 = p_2$ so that Equation 5.19 becomes

$$v_2 = \sqrt{2gh} \tag{5.20}$$

Equation 5.20 is known as the *speed of efflux* or *Torricelli's theorem*. It is surprising how basic equations appear in so many diverse fields. Obviously the size and shape of the orifice will make a difference in the flow rate. The actual velocity of the jet of water will be affected by a coefficient of velocity C_v so that Equation 5.20 is modified as follows:

$$v_o = C_v\sqrt{2gh} \tag{5.21}$$

Experimentation with orifices has determined that the rate of flow is due not only to the coefficient of velocity but also to the contraction of the jet passing through the orifice. Momentum effects continue to contract the jet at it passes through the orifice. The velocity calculated from Equation 5.21 is assumed to be the velocity of the vena contracta. The coefficient of contraction C_c is defined as the ratio of the area of vena contracta to the orifice area. The rate of flow through the orifice can then be expressed as

$$Q = C_v C_c A\sqrt{2gh} = C_d A\sqrt{2gh} \tag{5.22}$$

where

Q is the rate of flow
A is the area of orifice opening
C_v is the coefficient of velocity
C_c is the coefficient of contraction
C_d is the coefficient of discharge
g is the acceleration due to gravity
h is the head on center of orifice

The coefficients for the flow through an orifice depending the shape of the orifice are given in Figure 5.7.

For an orifice with very smooth and well tapered nozzle, the coefficient of discharge is approximately 0.98. If the tank is pressurized, the earlier equations are still the same except that the value of the head h changes accordingly.

Orifice flow	Description	C_d	C_c	C_v
	Sharp edge	0.62	0.63	0.98
	Rounded edge	0.98	1.00	0.98
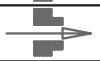	Short tube	0.61	1.00	0.61
	Long tube	0.82	1.00	0.82
	Short rounded tube	0.97	0.99	0.98
	Short reentrant tube	0.54	0.55	0.99
	Long reentrant tube	0.72	1.00	0.72
	Borda	0.51	0.52	0.99

Figure 5.7 Orifice coefficients.

The flow of water through a pipe can vary considerably depending on several factors, including the velocity of the stream. In other words, the flow can be laminar or turbulent. When the velocity of a fluid in a tube exceeds a critical value, the nature of the flow becomes turbulent. Adjacent to the inner walls of the tube, the flow may still be laminar, but as the flow is measured toward the center of the tube, it becomes more and more turbulent. Empirical data have shown that four factors influence the flow of the liquid through the tube. This combination of factors is known as the *Reynolds* number and is defined as

$$N_R = \frac{\rho v D}{\eta} \tag{5.23}$$

where

ρ is the density of the fluid
v is the velocity of the fluid
D is the diameter of the tube
η is the viscosity of the fluid

The *Reynolds* number is a dimensionless quantity. Experimentation shows that for a Reynolds number less than 2000, the flow is laminar. For values above 4000 the flow is turbulent. Some authors make the distinction between 2300 and 4000. These are general guides, and exact values are difficult to determine because turbulence is chaotic and highly dependent on initial conditions. In the transition the flow is unstable and may vary in degrees from laminar to turbulent. As an example, we may compute the Reynolds number for water at a tank temperature discharge of 150°F where the velocity is 1 ft/s and the diameter of the orifice is 1 in. The density and the viscosity can be obtained from Table 5.2, then

$$N_R = \frac{(61.2\,\text{lb/ft}^3)(1.0\,\text{ft/s})(0.0833\,\text{ft})}{(2.91\times10^{-4}\,\text{lb/(ft}-\text{s))}} = 17{,}519 \tag{5.24}$$

Therefore, the flow would be turbulent. This finding is consistent with what we experience. Consider a water heater tank that normally has a discharge valve at the bottom. When we choose to drain the tank and open the valve, we see that the water gushing out is, in fact, turbulent.

Suppose we wish to determine the time that a tank takes to discharge its water. For example, a pin hole leak develops at the base of a 40 gal water heater. The shell of the tank has corroded due to age. The home owners have gone on vacation and have turned the main water valve off so that additional water will not enter the tank. The pin hole is measured to be 1/8 of an inch in diameter. Since the tank is full of hot water, the tank is pressurized to 5 psi. To solve this problem we can make use of Equation 5.22, the flow through an orifice. Assume that for a sharp edged orifice C_d is 0.62 from Figure 5.7. Now

$$Q = vA = A\frac{dz}{dt} \tag{5.25}$$

As the water level of the tank z drops as time t increases, we say

$$Qdt = -A_t dz \tag{5.26}$$

where A_t is the cross section of the tank. A 40 gal tank has the following dimensions: height 58 in., outside diameter 18 in., and inside diameter 16 in. Now we calculate the cross sections of the tank and the orifice as

$$l_z = \frac{\pi}{4}\left(\frac{16}{12}\right)^2 = 1.396\,\text{ft}^2; \quad A_0 = \frac{\pi}{4}\left(\frac{1/8}{12}\right)^2 = 8.522\times10^{-5}\ \text{fi} \tag{5.27}$$

We may now rearrange Equation 5.26 and solve for time:

$$t = \int_{z_1}^{z_2} \frac{-A_t dz}{C_d A_0\sqrt{2gz}} = \frac{2A_t\left(\sqrt{z_1}-\sqrt{z_2}\right)}{C_d A_0\sqrt{2g}} \tag{5.28}$$

Since the tank is full and the temperature of the water is at 120°F, the density of the water is 61.73 lb/ft^3. The heads z_1 and z_2 are determined as follows:

$$\begin{aligned} z_1 &= \text{h (assumed that tank is full)} + \text{pressure head } (h_p) \\ &= 58/12 + (5\,\text{psi}(144\ \text{in.}^2/\text{ft}^2))/(61.73\,\text{lb/ft}^3) \\ &= 4.833 + 11.664 = 16.5\,\text{ft} \end{aligned}$$

so z_2 = 11.664 ft (elevation head = 0, pressurization remains)

Then, substituting into Equation 5.28, we obtain

$$t = 4258.7\ \text{s} = 71\ \text{min} = 1.18\ \text{h}$$

If we assume that the pressure drops to zero, $z_2 = 0$ and $z_1 = 4.833$. For this case t = 4.02 h.

Another type of computation that may be undertaken is the case of a leaking water pipe. Let us say that a pin hole develops in a pipe made of plastic supplying water to an ice maker in a refrigerator. If the leak develops over a 12 h period while the occupants of the home are away and the line is pressurized to 5 psi, we wish to estimate the volume of water leaking into the house. Note that we again, in this example, have assumed a pressure of 5 psi because that value is a customary pressure that water companies supply to homes. From the development of the equations in this section we know that the volume is governed by the rate of flow through the orifice. The pressurization can be assumed to be constant as the pressure head produced by the municipal supply. We will consider two cases. In one the pin hole is rather sharp, and in the other the pin hole is rounded. In this manner we look at minimum and maximum amounts of water infused into the home.

The analysis is undertaken utilizing Equation 5.22. Recall that

$$Q = C_d A_0 \sqrt{2gz}; \quad Vol = Qt \tag{5.29}$$

The density of water at 70°F is 62.3 lb/ft^3, so the head is

$$z = \frac{P}{\rho} = \frac{5\,\text{lb/in.}^2 (144\,\text{in.}^2/\text{ft}^2)}{62.3\,\text{lb/ft}^3} = 11.55\,\text{ft} \tag{5.30}$$

For a sharp edge C_d is 0.62 and for a rounded edge it is 0.98. If the pin hole diameter is 1/8 in., then A_0 is 8.522×10^{-5} ft^2. The value of Q then varies between

$$0.00144 \le Q \le 0.00228\,\text{ft}^3/\text{s} \tag{5.31}$$

For a 12-h period, the volume then varies between 62.2 and 98.5 ft^3, or

$$465 \le Vol \le 737\,\text{gal} \tag{5.32}$$

This problem exemplifies how a relatively small breach in a line can have dire consequences over the course of a normal day in a home.

In the previous discussion we quantified laminar and turbulent flow with respect to the *Reynolds* number. In this section we wish to more explicitly discuss laminar flow in a pipe. Figure 5.8 shows the distribution of laminar flow inside a pipe.

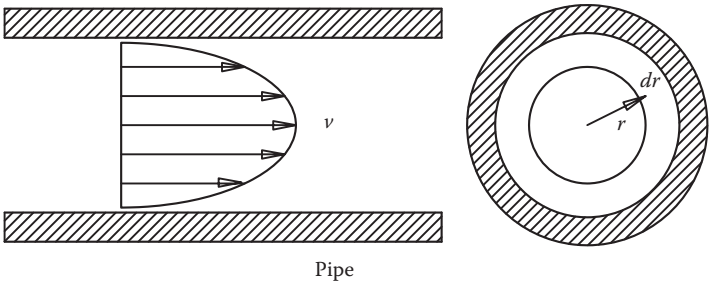

Figure 5.8 Pipe laminar flow.

A viscous fluid flowing through a pipe will not be the same through the cross section because adjacent to the walls the fluid will tend to adhere to the walls where the velocity will be zero. This laminar flow will increase toward the center of the pipe where it will be a maximum and then decrease accordingly. The force due to a difference in the pressure for laminar flow is given by

$$F = (p_1 - p_2)\pi r^2 \tag{5.33}$$

The viscous force is

$$F_v = -\eta A \frac{dv}{dr} = -\eta 2\pi r L \frac{dv}{dr} \tag{5.34}$$

In Equations 5.33 and 5.34 we have

p_1 is the pressure on the left side
p_2 is the pressure on the right side
r is the radius
L is the length of pipe
η is the viscosity of the fluid
A is the area of the pipe
v is the velocity

Equating the two forces and integrating, we obtain

$$-\int_v^0 dv = \frac{p_1 - p_2}{2\eta L}\int_r^R r dr \tag{5.35}$$

or

$$v = \frac{p_1 - p_2}{4\eta L}(R^2 - r^2) \tag{5.36}$$

Equation 5.36 is of a parabola and the velocity distribution in shown in Figure 5.8. The element of volume of fluid is

$$dV = \frac{p_1 - p_2}{4\eta L}(R^2 - r^2)(2\pi r dr)(dt) \tag{5.37}$$

The rate of flow is determined by integrating Equation 5.37 and dividing by dt:

$$Q = \frac{1}{dt}\frac{\pi(p_1 - p_2)}{2\eta L}\int_0^R (R^2 - r^2) r dr = \frac{\pi R^4 (p_1 - p_2)}{8\eta L} \tag{5.38}$$

Equation 5.38 shows that the rate of flow in a tube is inversely proportional to the viscosity and proportional to the fourth power of the tube radius. Equation 5.38 only holds for laminar flow. The difference in the pressures divided by the length is the pressure gradient. This equation was developed by Poiseuille which bears the units of viscosity.

Let us now turn our attention to turbulent flow in pipes. Turbulent flow is generally agreed upon when the *Reynolds* number is above 4000. Turbulent flow is characterized by three dimensional movement of the fluid particles. At values below 2000 the flow is considered laminar. In the region between laminar and turbulent flow, the flow is considered to be critical. In turbulent flow all the fluid particles are assumed to have the same bulk velocity. The velocities of the particles in turbulent flow are all assumed to be approximately the same. As with laminar flow, in turbulent flow, the maximum velocity of the stream will tend to be at the center of the pipe. An empirical formula for turbulent flow is

$$v = v_{\max}\left(\frac{r_0 - r}{r_0}\right)^n \tag{5.39}$$

For smooth tubes the exponent n is 1/7 for *Reynolds* numbers up to 100,000 or 1/8 for numbers between 100,000 and 400,000. It is obvious by comparing Equation 5.36 with Equation 5.39 that a similar expression for laminar flow may be determined where the exponent of Equation 5.39 would be 2 for laminar flow.

Equation 5.16 is the Bernoulli equation including losses, and the term h_l is the head loss due to friction. The Darcy friction factor is a parameter used to calculate friction loss. For laminar flow, the friction factor decreases as the *Reynolds* number increases and is given by

$$f = \frac{64}{N_R} \tag{5.40}$$

For turbulent flow there is a plethora of equations that may be employed. One equation attributed to Blasius is

$$f = \frac{0.316}{N_R^{0.25}} \tag{5.41}$$

Probably the most widely used equation for the friction factor is attributed to Colebrook and applies to any pipe roughness and *Reynolds* number. This equation, as with many others, is an implicit formula that must be solved iteratively:

$$\frac{1}{\sqrt{f}} = -2\log_{10}\left(\frac{\dfrac{\varepsilon}{D}}{3.7} + \frac{2.51}{N_R\sqrt{f}}\right) \tag{5.42}$$

where

f is the friction factor
N_R is the Reynolds number
ε/D is the relative roughness

The friction factor can be obtained from a Moody chart and the iterative solution applied from Equation 5.42. Figure 5.9 shows what a Moody chart looks like.

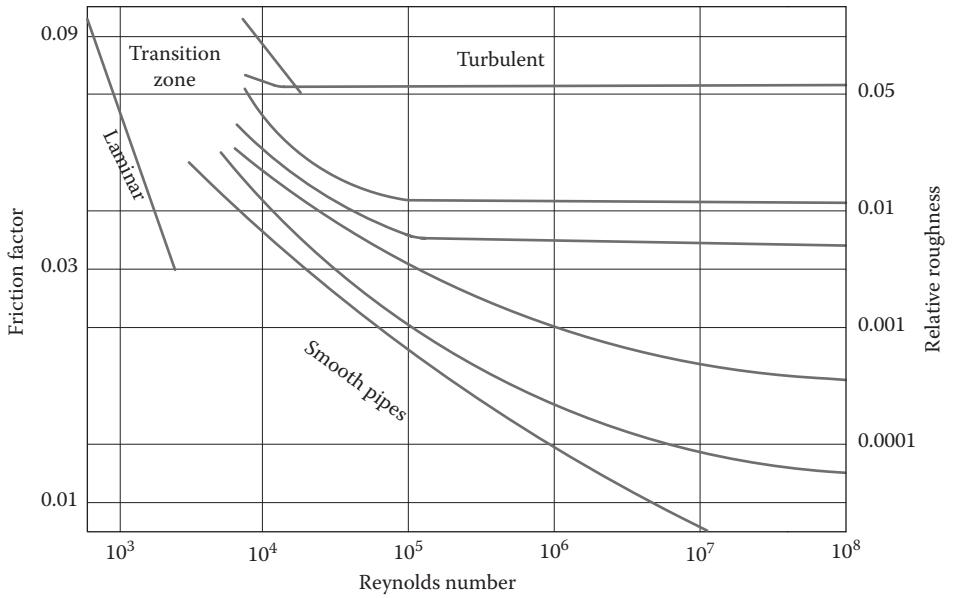

Figure 5.9 Moody chart.

Once the frictional coefficient is known, the Darcy equation can be used to find the frictional loss between the two heads for both laminar and turbulent flow as

$$h_l = \frac{fLv^2}{2gD} \tag{5.43}$$

where

h_l is the loss of head (ft)
L is the length of pipe (ft)
v is the velocity (ft/s)
D is the diameter of the pipe (ft)
f is the friction factor
g is the gravity (ft/s^2)

As an example, consider a 12 in. diameter pipe that is 100 ft long. We wish to calculate the loss of head due to friction at 70°F when the flow velocity is 10 ft/s. From Table 5.2 $\eta = 0.00066$, $\rho = 62.3$. The *Reynolds* number is

$$N_R = \frac{(62.3\,\text{lb/ft}^3)(10\,\text{ft/s})(1\,\text{ft})}{(0.00066\,\text{lb/ft-s})} = 943,939$$

For this turbulent flow, we may apply Equation 5.41 to find the frictional factor:

$$f = \frac{0.316}{(943,939)^{0.25}} = 0.01014$$

The loss of head can now be determined from Equation 5.43, or

$$h_l = \frac{(0.01014)(100\text{ ft})(10\text{ ft/s})^2}{2(32.2\text{ ft/s}^2)(1\text{ ft})} = 1.6\text{ ft}$$

Open Channel Flow

As the name implies, open channel flow is partially open to the atmosphere. This type of flow includes rivers, streams canals, culverts, flumes, and pipes flowing under the influence of gravity. This type of flow is not under pressure as with a piping system in a house that always flows full. Generally, we refer to a canal as an open conduit either covered or uncovered and utilized to carry water. If the canal is supported on or above the ground surface it is referred to as a flume. If the canal is underground, it is called a tunnel. The most economical shape for the cross section of a canal is the semicircle from a hydraulic standpoint because it gives the most hydraulic radius for a given cross section. A trapezoidal canal is easier to construct and to maintain, so that if we consider the trapezoid circumscribing a circle with its center at the surface, we maximize the hydraulic characteristics of the channel.

The steepness of the sides of the slope depends on the angle of repose of the material that forms the banks for unlined channels. For earth channels the slopes vary from 1 to about 2.5. For stiff clays the slopes may be as low as 1.25, and if rock is used to line the banks, the sides may be near vertical. The advantage of lining the canal is to increase flow velocities, thereby reducing the cross-sectional area.

There are significant problems associated with the evaluation of open channel flow because of the variety of cross-sectional areas and lack of scientific observations. Consequently, the open channel flow analysis is more empirical than exact. However, the variability in the runoff calculations offset the errors in the channel flow. Thus, in these types of problems, a wide range is given to the flow calculations. A further complication arises because channel flow is most always turbulent. In other words, the flow is generally neither steady nor uniform. The minimum permissible flow is one that prevents sedimentation and plant growth. This flow is in the range of 2–3 ft/s.

The cross section of a canal that has the greatest hydraulic efficiency is one that has the shortest wetted perimeter. The channel for the stream may take many forms. However, for this analysis we will only consider three cross sections: the circle, the rectangle, and the trapezoid. The wetted perimeter is the length of the line of the cross-sectional area of the channel that is wet. Figure 5.10 shows a hypothetical canal with an irregular cross section as may be encountered in a stream.

For any conduit, the hydraulic radius is the cross-sectional area divided by the wetted perimeter. Figure 5.11 shows the hydraulic parameters for the three cross sections most commonly encountered in these types of calculations.

In a channel flow, the velocity of flow will not be uniform because of the adhesion between the wetted surface and the water. Consequently when performing flow quantities, the

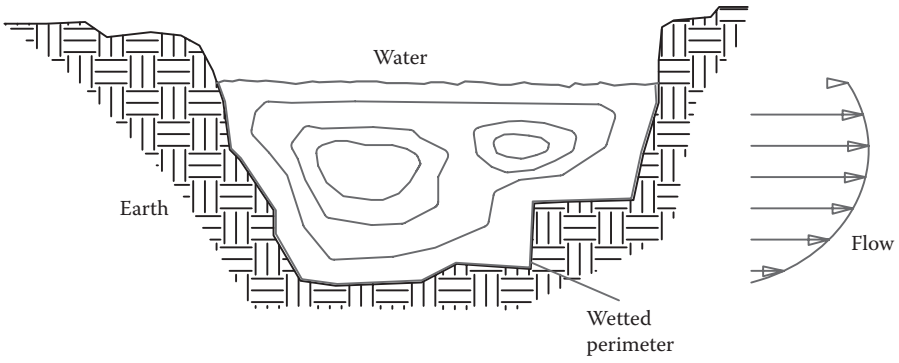

Figure 5.10 Wetted perimeter.

Section	Area	Perimeter	Hydraulic radius
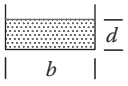	bd	$2d + b$	$\frac{db}{b + 2d}$
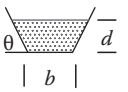	$\left[b + \frac{d}{\tan\theta}\right] d$	$b + \frac{2d}{\text{Sin}\,\theta}$	$\frac{bd \sin\theta + d^2 \cos\theta}{b \sin\theta + 2d}$
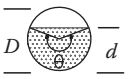	$\frac{1}{8}\left[\theta - \sin\theta\right] D^2$	$\frac{1}{2}\,\theta D$	$\frac{1}{4}\left[1 - \frac{\sin\theta}{\theta}\right] D$

Figure 5.11 Hydraulic parameters.

mean velocity is used. The location of this mean velocity is dependent on the distribution of all the velocities in the channel. The flow quantity is given by

$$Q = Av \tag{5.44}$$

where

Q is the flow quantity
A is the flow area
v is the mean velocity

As defined, the hydraulic radius is given by

$$R = \frac{A}{P} \tag{5.45}$$

where

R is the hydraulic radius
P is the wetted perimeter

Water is incompressible so that by the continuity equation we have

$$A_1 v_1 = A_2 v_2 \tag{5.46}$$

There are multitude of equations that may be used to calculate the flow of water in open channels. However only two equations will be discussed in this section as they are the most common. The Chezy formula is given by a modification of Equation 5.21 or

$$v = C\sqrt{RS} \tag{5.47}$$

The coefficient C can be determined from the Moody diagram according to the equation

$$C = \sqrt{\frac{8g}{f}} \tag{5.48}$$

The Moody diagram from the Engineer's Tool Box is shown in Figure 5.12.

The Chezy formula is often combined with the Manning formula to find the coefficient C from

$$C = \left(\frac{1.49}{n}\right) R^{\frac{1}{6}} \tag{5.49}$$

so that

$$v = \frac{1.49}{n} R^{\frac{2}{3}} S^{\frac{1}{2}} \tag{5.50}$$

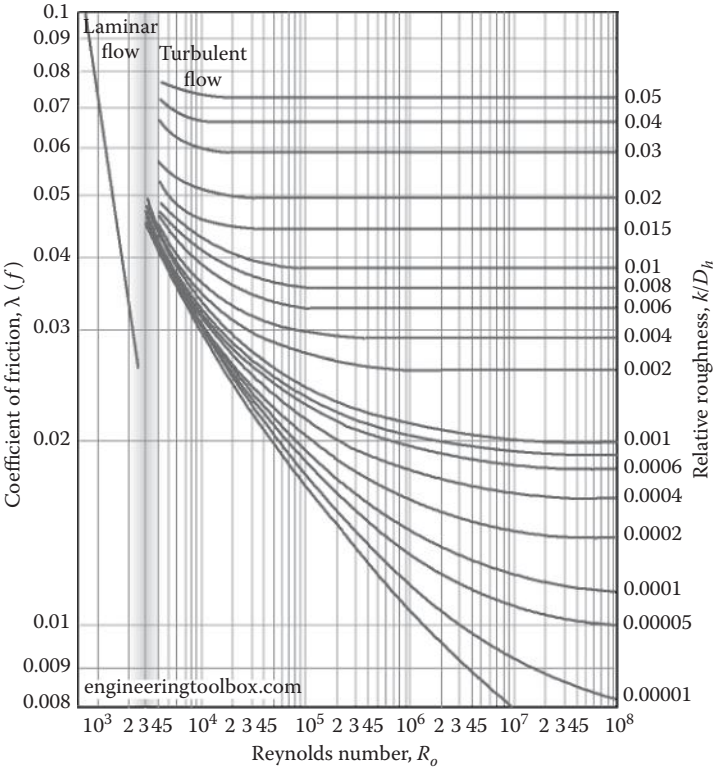

Figure 5.12 Moody diagram.

The flow is then given by

$$Q = Av = \frac{1.49}{n} AR^{\frac{2}{3}} S^{\frac{1}{2}} \tag{5.51}$$

where

A is the area of cross section of stream in ft^2
$R = A/P$ is the hydraulic radius in ft
P is the wetted perimeter in ft
$S = H/l$ is the loss of head due to friction per foot
H is the loss of head due to friction in ft in length l
l is the length of reach of channel in ft
v is the mean velocity of water in ft/s
Q is the discharge in ft^3/s
C is the coefficient of discharge
n is the Manning roughness coefficient
f is the friction factor dependent on *Reynolds* number

The value of the Manning roughness coefficient can be found from a variety of tables. Many of these values can vary greatly as much as 30%. Table 5.3 gives a wide range of values for the Manning roughness coefficient for a variety of pipes and channels.

As an example, we may compute the coefficient of discharge with Equations 5.48 and 5.49 for a corrugated rectangular flume with the following dimensions: width 2 ft, height 1 ft, $n = 0.025$, and $N_R = 10^6$. From the Moody chart we determine $f = 0.055$. Substituting into Equation 5.48,

$$C = \sqrt{\frac{(8)(32.2)}{0.055}} = 68.43$$

The area is $A = (1\text{ ft})(2\text{ ft}) = 2\text{ ft}^2$, the wetted perimeter is $P = 2(1\text{ ft}) + 2\text{ ft} = 4\text{ ft}$. The hydraulic radius is $R = (2\text{ ft})(1\text{ ft})/P = 0.5\text{ ft}$. Substituting into Equation 5.49,

$$C = \frac{1.49}{0.025}(0.5)^{0.166} = 53.122$$

Table 5.3 Manning Roughness Coefficient

Pipe or Surface of Channel	n
Cast iron pipe	0.01–0.015
Brass or copper pipe	0.009–0.013
Concrete pipe	0.01–0.017
Clay drainage pipe or channel	0.011–0.017
Concrete lined channels	0.012–0.018
Semicircular smooth metal flumes	0.011–0.015
Semicircular corrugated flumes	0.0225–0.03
Canals and ditches	0.017–0.033
Natural channels and streams	0.025–0.08

These two methods of analysis point out the discrepancy in the discharge calculations depending on the method of attack. Depending on which value of *C* is used to measure the discrepancy in the calculations, the error is between 22% and 28%.

These channels or flumes are often used to divert the flow of water. Often the flumes are guided under a road. When that happens, a culvert is inserted to carry the water under the road. Culverts are designed in a variety of manners, but they generally have a pipe that, at the inlet side, has a variety of features. One of the features is the diameter and nature of the pipe itself. The other prominent feature is the design of the inlet. It is of course prudent to design the inlet for maximum efficiency for the water to be channeled into the pipe. Some inlets can have much greater capacity than a conventional culvert design with square edges. In inlet control only the entrance configuration and the depth of the headwater determine the hydraulic capacity of the culvert. The characteristics of the barrel and the tail water depth play no role. There are a variety of equations that are a modification of the basic flow equation depending on the type of flow that pertains to the application. Equation 5.22 determines the flow where the *h* term in the radical varies depending on the geometry of the culvert.

Sometimes the case arises where the forensic engineer is asked to evaluate a culvert that has eroded or failed in any number of manners. This type of loss occurs when neighboring properties will be blamed for causing a flood loss. In these cases the offending culvert needs to be analyzed for its flow characteristics based on 10-, 20-, 50-, or 100-year flood rainfalls. The next section covers rainfall calculations and flooding events.

Hydrology and Water Runoff

Water is a constant in nature. The amount of water on the earth is also a constant. However, the cyclic nature of water on the earth can cause great local variations in the water content in a particular region of the earth. These variations are exemplified by storms that produce rainfall or snowfall. As such, the sciences that deal with water are meteorology, hydrology, and hydrography. Hydrography, as the name implies, deals with graphs of the amount of precipitation. As precipitation falls, part of the water is evaporated and part falls onto the soil. The soil consequently absorbs the water to the point where it becomes saturated. Then the excess water begins to pool. As the capacities of the pools are exceeded, they begin to overflow and drain so that water runoff occurs. This water runoff can cause havoc on the surrounding landscape.

Flooding, or the excessive runoff, is attributed to excess water that cannot be drained into the watershed. This excess water can overflow creeks and rivers. The severity of the flooding can vary greatly depending on the consistency of the soils, the amount of vegetation, and the saturation capacity of the soils from previous rainfall. Another consideration is the deflection of runoff by man-made structures such as culverts. Within regions of the United States, designations have been made for the probability of maximum floods to occur. Generally a 100-year flooding event is used in the design although local municipalities may allow for designs for less than 100-year events. It should be noted that 100-year floods are not generally caused by 100-year storms.

Obviously, the forensic engineer has no control of the forces of nature, that is, the amount of rainfall that may occur. The forensic engineer, however, is often called upon to determine is a particular culvert or similar structure in an adjoining property contributed to a flooding event. In simple terms, often, one is asked whether the size of the culvert pipe was sized properly to allow the water to flow freely and not accumulate forming a partial dam that resulted

in a flooded basement in the upstream side basement of a house. For those types of cases, the watershed upstream needs to be determined along with the design of the culvert.

The probability that a flooding event will occur in a particular year is given by

$$P = \frac{1}{I} \tag{5.52}$$

The probability of an event occurring in n years is

$$P = 1 - \left(1 - \frac{1}{I}\right)^n \tag{5.53}$$

where

P is the probability of the event
I is the event

For example, the probability of a 100-year flood occurring in 1 year is, from Equation 5.52, 1%. The probability that a 100-year flood will occur in 20 years can be calculated from the following equation:

$$P = 1 - \left(1 - \frac{1}{100}\right)^{20} = 18.2\%$$

Precipitation records are performed by the Weather Bureau in the United States. A plot of the amount of water discharge from a stream versus time is a hydrograph. The amount of water flow may be determined from hydrographic data or it may be determined from the watershed area. Figure 5.13 shows a stream hydrograph.

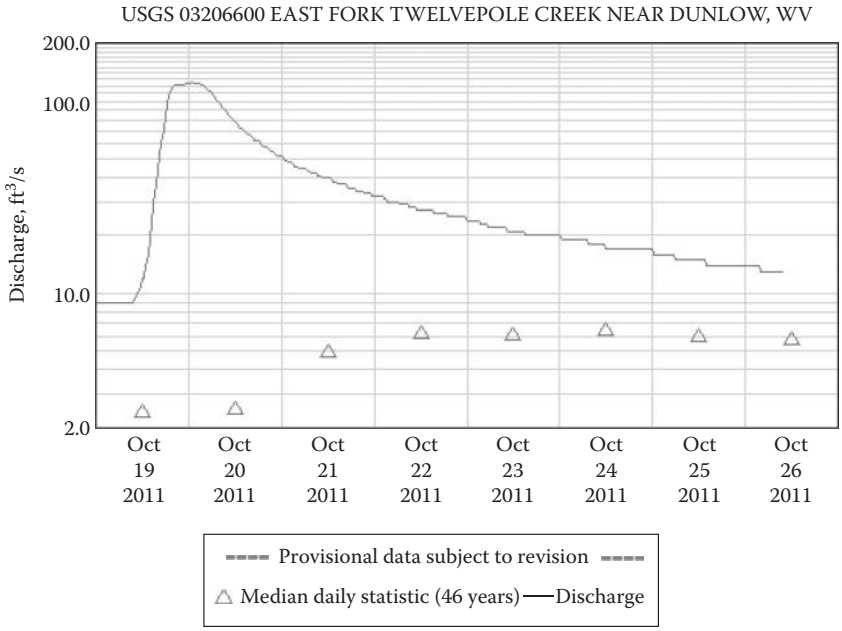

Figure 5.13 Stream hydrograph.

The most widely utilized method for over the past century has been the Rational Method. Peak flows from the watershed can be obtained from the National Weather Service for the particular creek or stream and the particular period from http://waterdata.usgs.gov. as displayed in Figure 5.13. The rational method is applicable for small areas less than several hundred acres. The maximum runoff is given by

$$Q_R = AIR \tag{5.54}$$

where

Q_R is the maximum runoff in ft³/s
A is the area of the watershed in acres
I is the coefficient due to losses
R is the rainfall intensity in in./h

Note that the units on the right side of Equation 5.54 are in acre-inches per hour while in the left side of the equation the units are in ft³/s. Since the conversion factor between the two is 1.008, it can be disregarded. Table 5.4 shows typical values for the coefficient due to losses for differing watershed areas.

For example, a field of approximately 5 acres consisting of loam and clay is subjected to the rainfall as represented in the stream hydrograph of Figure 5.13. We wish to determine the size of the culvert to install on a road crossing the creek. The stream hydrograph shows that the maximum flow was approximately 120 ft³/s. We can assume that the loam and clay are evenly distributed, and we will use the average values from Table 5.4. Calculating the value of I

$$I = \frac{1}{2}\left(\frac{(0.1+0.65)}{2} + \frac{(0.15+0.75)}{2}\right) = 0.4125$$

The peak flow is then

$$Q_R \approx (0.4125)(5)(120) \approx 247.5\,\text{ft}^3/\text{s}$$

In order to determine the size of concrete pipe, we need to know certain parameters. The length of the pipe is to be 10 ft with n = 0.15. The slope of the pipe is 10%, so S = 0.1.

Table 5.4 Coefficient of Runoff

Coefficient for various surfaces	Value of I
Roofs	0.9–1.0
Concrete	0.9–1.0
Gravel	0.25–0.7
Sand	0.1–0.5
Loam	0.1–0.65
Clay	0.15–0.75

We wish to fill the pipe only to the halfway point in order to allow debris to pass through, so θ = 180°. We also round the flow to 250 ft³/s. From Figure 5.11, we obtain

$$A = \frac{2\pi D^2}{8} = \frac{\pi D^2}{4}$$

Substituting into Equation 5.51

$$250 = \frac{1.49}{0.15}\frac{(\pi D^2)}{4}\left(\frac{D}{4}\right)^{\frac{2}{3}}(0.1)^{\frac{1}{2}}; \quad D = 7.97 \text{ ft}$$

Therefore, the diameter of the concrete pipe should be 8 ft.

Groundwater

As the hydrologic cycle model of Figure 5.1 implies, when rain water saturates the soil, a portion of the water is evaporated, a portion is run off, and a portion enters the water table as a result of gravity. The behavior of water in the soils can have a marked influence on the stability of the soils and any structures that are located in the soil. Saturated soils have water occupying all the interstitial spaces. When the amount of water is less than the saturated conditions, the term used is capillary water. The relative humidity determines whether water is being released into the atmosphere or whether it is being absorbed into the soils. Since gravity produces a constant gradient, water in the soils is in constant motion. The velocity of the water flow in the ground is dependent on the gradient and the nature of the soils.

Groundwater or subsurface water may be contained in saturated geological formations known as aquifers. When the water is at atmospheric pressure and is not confined within the stratum, it is referred to as a free aquifer. Water in free aquifers varies, and this variation is the water table. Foundations below the water table will always be subjected to pressures from the water and the soils. The water will produce a buoyancy effect of approximately 97%–99% of the area of the foundation. The water affecting a foundation may fill the interstitial spaces of the soil and may be under head if the stratum adjacent to the structure has the water table above this level.

The moisture content of the soil can simply be determined by measuring the weight of the wet soil and comparing it to the weight of the soil after drying. The porosity of the soil is determined as the percentage of the void volume to the total volume. These parameters are obtained from field measurements and laboratory analysis. Another important parameter is the hydraulic gradient, which is the change in head over a specified distance. At a particular point, the hydraulic head is determined from an instrument called a piezometer and is given by

$$h_g = \frac{\Delta H}{L} \tag{5.55}$$

where

h_g is the hydraulic gradient (ft/ft or ft/mile depending on the units of area)
ΔH is the change in the head at a distance L (ft or miles)

Table 5.5 Typical Permeabilities

Soil	Permeability K (gal/day-ft^2)	Permeability K (ft^3/day-ft^2)
Gravel	10^4–10^6	0.1337×10^5
Gravel sand mixture	10^4	0.1337×10^4
Sand	10^3	0.1337×10^3
Sandstone	10^2	0.1337×10^2
Limestone or shale	1	0.1337
Quartzite or granite	10^{-2}	0.1337×10^{-2}
Clay	10^{-2}	0.1337×10^{-2}

The flow of water through the permeable soil is a function of both the water and the nature of the soil. When conducting studies involving the flow of subsurface water through an aquifer, it is important to determine the permeability of the soil. Some typical permeabilities are given in Table 5.5.

Darcy's law determines the flow of the water through the aquifer and is given by

$$Q = -KAh_g \tag{5.56}$$

where

Q is the flow of water through the soil (in gallons or ft^3 per day)
K is the permeability of the soil
A is the area of the cross section under consideration
h_g is the hydraulic gradient

Equation 5.56 is only applicable for flows with a *Reynolds* number less than 1.

Plumbing and Fittings

Water-related losses in homes and structures include naturally occurring water that affects the structure and water from the potable supply. In rural areas the potable water supply may be derived from wells or springs or cisterns. The water is then distributed throughout the structure. In urban areas, the potable water supply is delivered through the water mains to a meter that measures the usage in the home or building. From the meter, the water is distributed through various plumbing and fittings to sinks, commodes, water heaters, showers, tubs and spigots.

The plumbing may be made of copper, iron, or various plastics. Local codes require a variety of safety features to be installed throughout the system. These may include valves, pressure relief, pressure reduction, and freeze protection. The plumbing system takes a variety of routes, which require a variety of elbows and connections throughout the system. Depending on the complexity of the system, the water lines also need to be sized properly. Some of the water lines are also connected to appliances such as refrigerators, washing machines, and dishwashers. The entire potable water system is subject to failure by any of the components or appliances. Careful inspection of the water system in a particular structure will reveal the nature and the cause of the failure.

Another component of the water system is the drainage of the water after use. This brown or black water is carried away from the home through the sewage system. This system also

utilizes plumbing and fittings that are generally constricted of plastic, iron, or clay pipes in a variety of combinations. The sewage system is also subject to failure. Typical sewage system failures include plugged lines, degraded lines, damaged lines resulting from construction activities, and separated lines resulting from age and misuse. The previous sections in this chapter exemplify the types of analysis that can be made for these water related losses.

Water Hammer

Water hammer is a pulsation of pressures above and below the operating pressure, resulting in a rapid deceleration or acceleration of the velocity of flow of water in a closed conduit. The forces required to decelerate and to accelerate the confined column of water must be absorbed by or supplied by the elastic properties of the pipe and of the water.

Water hammer may be caused by the quick opening or closing of valves or gates, the sudden starting, stopping, or variation in speed of pumps, breakage of pipe lines, and other conditions. Design values for pipes and proper connections take into account appropriate safety factors to allow for water hammer. Some devices and methods for the control and prevention of water hammer include

1. Relief valves
2. Air valves
3. Air chambers
4. Surge tanks or towers
5. Surge suppressors
6. Slow closing valves
7. Mechanically or spring controlled valves or cushions

Relief valves may be actuated by a slight change in pressure, as little as 10 psi, to open wide in a few seconds to discharge water to waste if an increase in pressure is to be relieved.

Pressure Measurements

In practice, pressures above and below atmospheric are determined by means of a pressure gauge. The dial of a pressure gauge is marked to read the *gauge pressure*, usually in pounds per square inch (psi). The pressure gauge reads the difference in pressures between that inside the threaded connection and the region in which the dial is, as between the pressure inside of a vessel and the atmospheric pressure outside. Thus, to find the *absolute pressure*, when this pressure is above atmospheric, we must add the atmospheric pressure to the gauge reading. For example, a gauge has a Bourdon movement instrument with a single elliptical metal tube that, as the pressure entering the threaded connection increases, tends to straighten the tube. As the tube is straightened, the linkage movement mounted to a small pinion gear activates the index bands. The particular gauge has a minimum and maximum adjustment and a mercury switch that deactivates the system through electrical contacts when pressures are exceeded. In essence then, the gauge is a pressure control gauge, which is designed to operate within the pressure ranges established by the index hands and this device may be used to control water hammer.

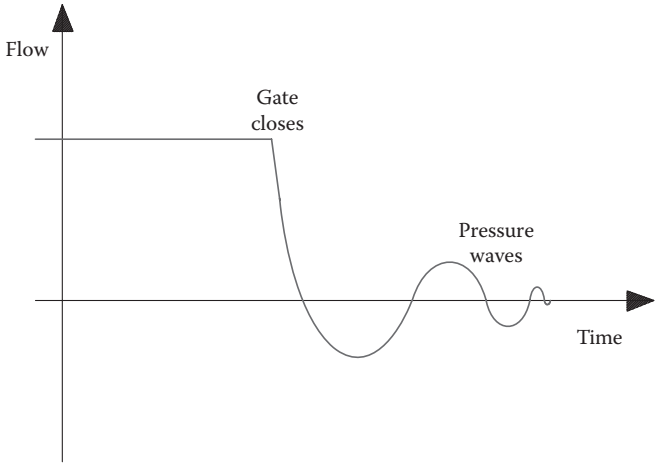

Figure 5.14 Water hammer pressure waves.

Pressure Relief

Pressure relief valves are intended to release excessive pressure that may build up in a closed container or system. For example, the pressure relief valve connected to a system may be a simple spring loaded valve in which the spring tension is adjusted to compress at a given pressure. Pressure relief valves are often used to eliminate water hammer.

Let us assume that the valve at the outlet of a pipe is closed suddenly so that the kinetic energy is transformed into dynamic pressure which is the water hammer. Since the pipe and the water are essentially inelastic, the pressure due to the water hammer will be given by

$$P = M\frac{dv}{dt} \tag{5.57}$$

In actuality, the water and the piping are somewhat elastic. Consequently, a series of pressure waves are produced. These pressure waves decrease as the pressure cycles develop until they finally die out. The closest analogy to the water hammer is an input of a square wave to the water flow that decrease from the maximum flow rate to zero. Figure 5.14 is a graphical representation of the waves that flow when water hammer is produced.

Water hammer can be very destructive, especially when large water mains are involved, as with stand pipes for fire protection. As the water main enters a building underground, it makes a turn vertically upward. At this transition point a 90° coupling is used. Fire codes require that a thrust block be installed at the transition in order to prevent the coupling from coming loose as a result of water hammer. Whenever possible, pipes should have slow-closing gates. Air chambers, surge tanks, and pressure abating devices are often used to quell the effects of water hammer.

Soils and the Water Table

Effects on Soil from the Lowering of the Water Table

Whenever a lake or reservoir is drained, the water table in the surrounding area also lowers. Subsequently, a higher amount of stress arises in the soil. This increase in pressure results from an increase in the effective weight of the soil. The soil under the water

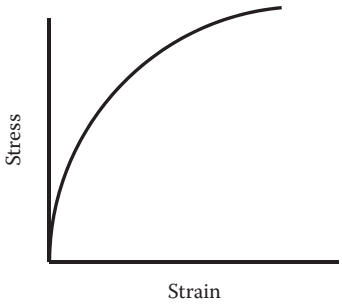

Figure 5.15 Stress–strain diagram of elastic materials.

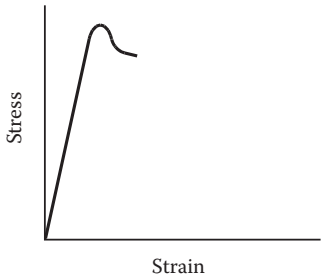

Figure 5.16 Stress–strain diagram of inelastic materials.

table is almost completely submerged. However, as the water table is lowered, the soil becomes saturated or moist, resulting in a higher effective weight. The corresponding increase in stress can result in soil failure, depending on the stress–strain relationship of that particular soil. If failure occurs, the slippage proves to be proportional to the descent of the water table.

The amount of damage incurred from a drop in the water table is directly related to the composition of the soil. If the soil consists of mostly clay, settlements can be excessive but will vary depending on time. Impervious clays, while highly compressible, may provide for less excessive damage. Highly permeable clays, including silt or peat material, normally produce rapid settlement and in amounts upwards of several feet. Moreover, silty or organic clays tend to be more sensitive and have linear stress–strain relationships. Materials possessing these characteristics behave inelastically to increasing stress, and upon reaching a certain level of pressure, fail. Unlike elastic materials, inelastic materials cannot remold after reaching their ultimate stresses. Lastly, noticeable damage may occur in distances up to 2000 ft from construction sites where the water table has been lowered by 20 ft. Figures 5.15 and 5.16 show the difference in the stress strain curves for elastic and inelastic materials.

Appliances and Equipment Failures

6

Introduction

The failure of appliances or equipment should not be investigated by the forensic engineer unless there are substantive reasons to do so. Simply because an appliance or a piece of equipment fails, it may not be investigated. For example, if a refrigerator stops working after 20 years of service, it probably would not be analyzed for the cause of the failure because its warranty would have run its course and because its life expectancy of the refrigerator may be over. The warranty period for equipment varies from state to state and may be related to the statutes of repose for a particular state in this country or to a particular country.

As a general rule, the timeframe for the statute of repose for a particular region may vary from 5 to 10 years. At this point it is necessary to explain what is meant by the statute of repose. *Webster's New World Law Dictionary* defines the statute of repose as a statute barring a suit a fixed number of years after the defendant had acted, usually by designing or manufacturing an item, even if an injury suffered by the plaintiff occurred after the period had lapsed. The statute of repose cuts off legal rights if not acted upon in a certain period of time. Let us use 10 years after the manufacture of a refrigerator as an example. A refrigerator fails and causes a fire. If the fire occurs after 15 years from the date of manufacture, the plaintiff, generally the homeowner's insurance company, is barred from subrogating against the manufacturer of the refrigerator. The insurance company would generally cover the loss of the homeowner and then attempt to mitigate its expenses by subrogating against the manufacturer of the refrigerator. If the statute of repose had run out, then there would be no action. If, however, the fire occurred 2 years after the date of the manufacture of the refrigerator, and it could be shown that the improperly designed or manufactured refrigerator caused the fire, the homeowner's insurance company may be able to recover some or part of its losses.

Sometimes statutes of repose and statutes of limitations are confused because they are similar but not strictly the same. The statute of limitations is set in motion by an injury, such as when a refrigerator failed and caused the fire. In contrast, the statute of repose is set in motion by the completion of an act, such as the date of manufacture of the refrigerator. If the statute of repose is 10 years and the fire occurs 5 years after the manufacture of the refrigerator, there may be cause for action. However, if the statute of limitations is two years and no action is brought about for two and a half years, the statute of limitations would have run out and there would be no cause for action.

Forensic engineers are the purveyors of facts and would, in the course of their investigation, determine the manufacturer of the refrigerator and the mode of failure. However, forensic engineers are not advocates and should not make recommendations as to the possibility for a course of action. If action in subrogation is warranted, that decision is made by the insurance company and/or the lawyers involved in the case.

Figure 6.1 Microscope and camera.

The analysis of failures is necessary in order to determine the root cause of the failure. The most common technique employed in failure determination is root cause analysis (RCA). The role of failure analysis is as an engineering tool for the enhancement and development of products, for quality control, and for the prevention of failures in concert with the engineering charge to protect life and property. Failure analysis is important because of its relation to the development of products and systems that are safe, reliable, economic, and perform as designed. Consequently, the products and systems that are designed lead to the expectation of the performance of the product by the user.

In analyzing the root causes of the failure, not only is the actual failure examined but contributing circumstances are also analyzed. These circumstances may include deficiencies in the design of the product, deficiencies in the materials used in the product, installation or manufacturing defects, and the life expectancy of the product. Often, the forensic engineer is called upon to determine the root cause of the failure. In that capacity, the lead investigator may need the assistance of several experts. The sections that follow provide a glimpse into some common failures that may be encountered.

Some equipment failures lend themselves to mathematical analysis such as a structural component for a piece of equipment. However, very often mathematical analysis cannot be made or is not necessary. In those cases visual inspection is generally all that is needed. The visual inspection may be aided by the use of a microscope or a macro lens on a camera system. Most of the appliance failures that are shown in the pages that follow are of this type. Figure 6.1 shows a typical microscope and camera arrangement.

Kitchen and Household Appliances

Stoves

Cooking stoves seldom fail. Most fires that are attributed to cooking stoves are actually cooking fires that occur as a result of the spillage of food onto the burners. A very common food spillage is cooking oil. The patterns that are produced in cooking fires are all external to the unit and on the surface of the burners or inside of the oven cavity.

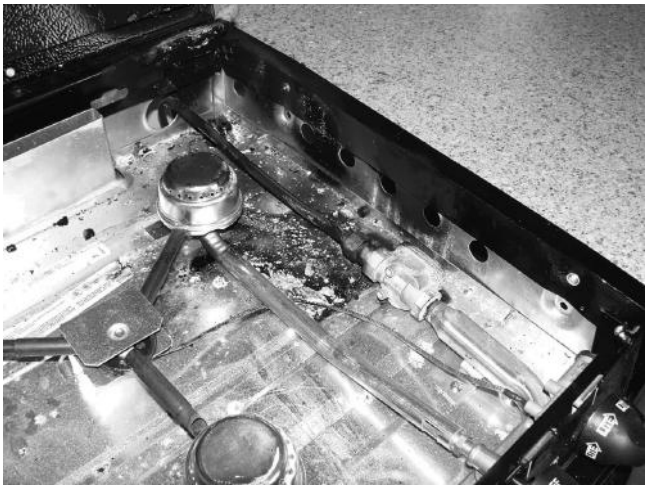

Figure 6.2 **(See color insert.)** Gas appliance.

For electrical stoves, the failures occur in the wiring or in the controls. For gas-fired stoves, the failures occur in the gas lines or controls. Sometimes stoves are set up to look like they failed to create a fire. Figure 6.2 shows the gas line to a cooking stove that was tampered with to make it look like it failed. In fact the compression fitting on the copper tubing had been loosened and papers were placed to start a small fire. Luckily, the arsonist was not very adept, and the fire did not progress significantly because the propane cylinder was almost empty.

Figure 6.3 shows an electric cooking stove where the wiring to one of the controls short circuited and caused a small fire.

Figure 6.4 shows a commercial oven that experienced a fire when the contents ignited.

Figure 6.3 **(See color insert.)** Electric stove.

Figure 6.4 Commercial oven.

Refrigerators

In more than 25 years of forensic engineering practice, we have never investigated a failure of a vapor compression refrigerator with respect to a fire or a failure of the refrigeration system. However, household refrigerators that have ice makers may leak and cause flooding. We commonly refer to these refrigerators as electric refrigerators. The water line for the water dispenser or ice maker may be damaged and cause the leak. Additionally, the solenoid valve that is electrically controlled may malfunction and cause a leak. These types of failures are very easy to detect and find the root cause. These refrigerators have an electrically driven compressor that turns the vapor refrigerant into a liquid to produce the reverse Carnot cycle. That is not to say that these refrigerators cannot fail with respect to the refrigeration cycle or that an electrical failure may cause a fire. Certainly, the power cord to the refrigerator can be damaged, be short circuited, and produce a fire. However, these types of refrigerators are so safe and well designed that failures are rare. Nevertheless, we have investigated numerous absorption refrigerator fires. We should explain the difference in the two types of refrigerators by reverting to a little basic thermodynamics.

A reversed thermodynamic cycle essentially pumps heat from one temperature to a higher temperature. A reversed thermodynamic cycle may be used for heating or for cooling. The most efficient of these cycles is the Carnot cycle. Figure 6.5 shows the characteristics of a reversed cycle that may be used for refrigeration or for heating. The cycle is represented in the temperature–entropy diagram.

In the refrigeration cycle, the refrigerant is isentropically compressed 1–2 from a cold temperature T_1 to a temperature T_2 available above a sink t0. An isentropic process is a reversible adiabatic process, and an adiabatic process is one in which no heat is transferred. The system then discharges heat at a constant temperature T_2 along 3–4 to a point where an isentropic expansion 4–1 lowers the temperature to T_1 lower than T_r (the room temperature) The heat from the room flows to the refrigerant cooling the room. The refrigerant receives the heat along the path and the cycle repeats. For the heating cycle, the sequence is the same as for refrigeration except for the relative temperatures. For this cycle, the temperature T_2 must be above T_r so that the heat can flow from the refrigerant to the room. Both of these

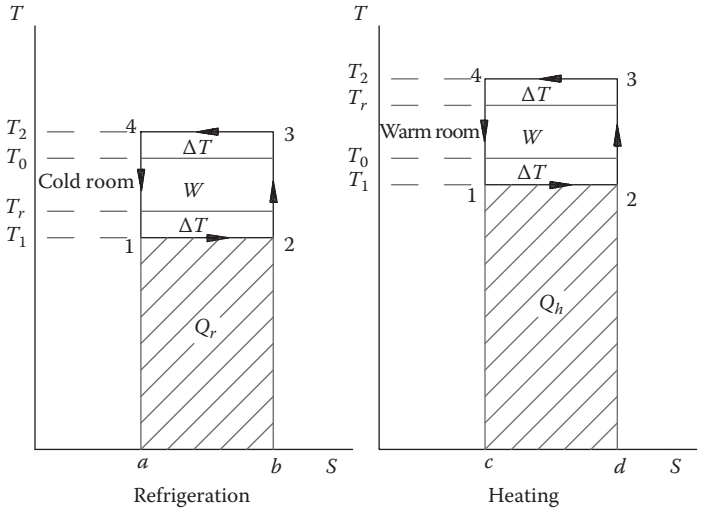

Figure 6.5 Reversed cycle.

reversible systems approach external reversibility as ΔT approaches zero. In both cases, the work is given by

$$W = (T_2 - T_1)\Delta S \text{ Btu} \tag{6.1}$$

The output of the refrigeration cycle is given by

$$Q_r = T_1 \Delta S \text{ Btu} \tag{6.2}$$

Similarly, the output of the heating cycle is

$$Q_h = T_2 \Delta S \text{ Btu} \tag{6.3}$$

The performance of these cycles can be measured in terms of the output and the input or

$$\gamma_r = \frac{Q_r}{W} = \frac{T_1}{T_2 - T_1} \tag{6.4}$$

for refrigeration and for heating

$$\gamma_h = \frac{Q_h}{W} = \frac{T_2}{T_2 - T_1} \tag{6.5}$$

For refrigeration the unit commonly used is the ton. This unit is derived from the number of Btu required to freeze 1 ton of water. Since the heat of fusion of ice is approximately 144 Btu/lb, then 288,000 Btu are required to freeze 2,000 lb of water. This is the standard definition of a commercial ton of refrigeration at a uniform rate during a 24 h period.

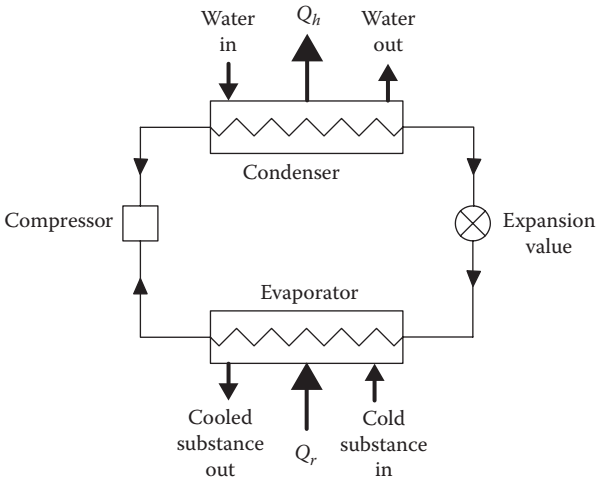

Figure 6.6 Compression refrigerator.

This capacity is also the same as 12,000 Btu/h or 200 Btu/min. The efficiency of a vapor compression system is given by the horsepower used per ton of refrigeration. If the refrigeration is N tons, or 200 N Btu/min, and since 1 hp = 42.44 Btu/min, then

$$\frac{hp}{N} = \frac{200}{42.44\,\gamma} = \frac{4.72}{\gamma} \tag{6.6}$$

Equation 6.6 represents the horsepower per ton of refrigeration required for the cycle. Figure 6.6 represents a compression refrigeration cycle. The main components include a compressor, a condenser, an expansion valve, and an evaporator.

The refrigeration takes place on either side of the evaporator where

$$Q_r = \Delta h_E \text{ Btu/lb} \tag{6.7}$$

In the heating mode, the heat rejected is carried away by the cooling water in the condenser, or

$$Q_h = \Delta h_C \text{ Btu/lb} \tag{6.8}$$

h represents the enthalpies so that the total work is

$$W = Q_C - Q_E \text{ Btu/lb} \tag{6.9}$$

The refrigerant in absorption refrigerators is absorbed on the low-pressure side of the system, which is then given up on the high-pressure side. The advantage of these systems is that the work supplied to the system only needs to be enough to pump the liquid from the low-pressure side to the high-pressure side. The work required to pump a fluid is less than the work required to pump a gas. The common refrigerant used in these

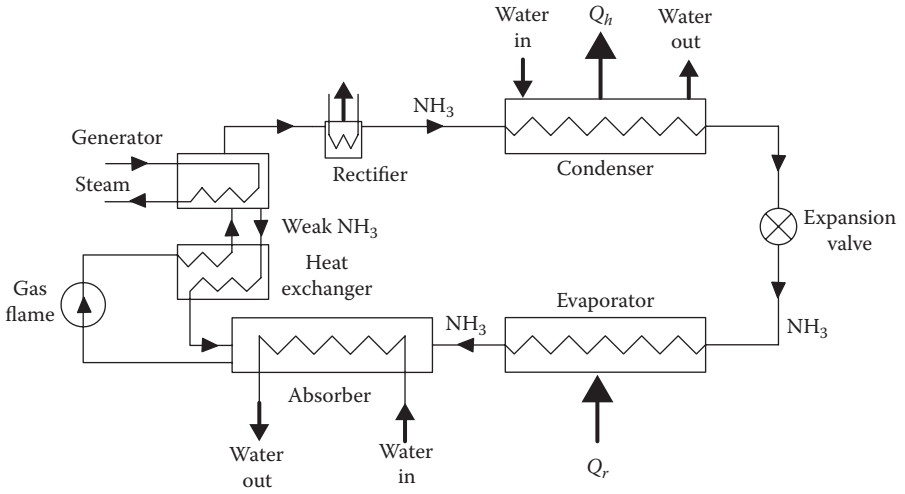

Figure 6.7 Absorption refrigerator.

systems is a water–ammonia (absorbent–refrigerant) mixture. Instead of the compressor, these systems have a more complicated set of devices, and instead of using a pump, there are liquid seals between the high-pressure (condenser) and low-pressure (evaporator) sides. A gas flame is used in the generator that has the potential of producing a fire. The fire danger is heightened because the ammonia is flammable. If a leak of the refrigerant develops and the gas flame is on, a fire is most likely to develop, which is the common mode of failure of absorption refrigerators. Figure 6.7 shows the basic schematic diagram of an absorption refrigerator.

Figure 6.8 shows an absorption refrigerator that caused a fire. The leak of the refrigerant occurred at the boiler tubes that exchange the refrigerant at the base where the gas flame is located. Figure 6.9 shows the leaking boiler tubes when pressure tested.

Figure 6.8 **(See color insert.)** Absorption refrigerator fire.

Figure 6.9 **(See color insert.)** Pressure testing.

Washers/Dryers

Washing machines have two modes of failure. The first mode is an electrical failure. Either an electrical short circuit occurs at the electrical cord or plug or some of the internal wiring that drives the motor. A motor failure may occur making the unit nonfunctional. Internal failures of the motors very seldom cause a fire. Simply, the wiring in the armature or rotor fails as a result of heat and the motor quits working. The timer and cycle controls may fail electrically. Electrical fire failures of washing machines are rare because they do not utilize copious amounts of electrical energy. The systems run on 120 V AC. The second mode of failure is one involving water. Either the control relay valve that allows for water to enter the machine or the high water disconnect switch fails and produces a flooding type of loss. The control relay is electrical, and tests on it will determine if the relay is open or not. The high water limit switch is pressure activated and is also easy to test. Figure 6.10 shows a typical solenoid valve in a washing machine. Figure 6.11 shows a power cord that has short circuited in a washing machine.

Dryers are much more susceptible to failures mainly because of the higher power requirements. Most commercial dryers are gas fired, but most residential dryers are electrically driven and heated. The standard voltage for a residential electric dryer is 220 V. Electrical residential dryers have at least two modes of failure. Either the wiring in the dryer short circuits or lint builds up around the heating element and catches on fire. Some fire experts have opined that the lint in the exhaust tubing can catch on fire. This assertion is simply not true because the temperature of the exhaust air is simply too low. You can actually place your hand at the exhaust elbow and feel nothing but warm air. Tests conducted at our laboratories have never measured a temperature above 110°F at the exhaust. This temperature decreases along the vent tube because of simple thermodynamics. In these cases what actually happens is that the lint builds up and

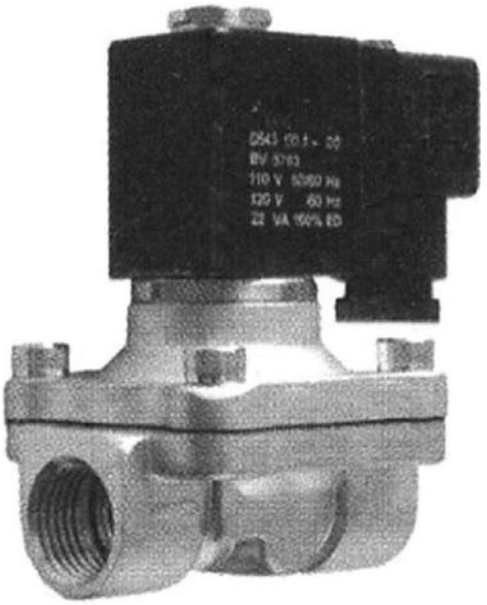

Figure 6.10 Solenoid valve.

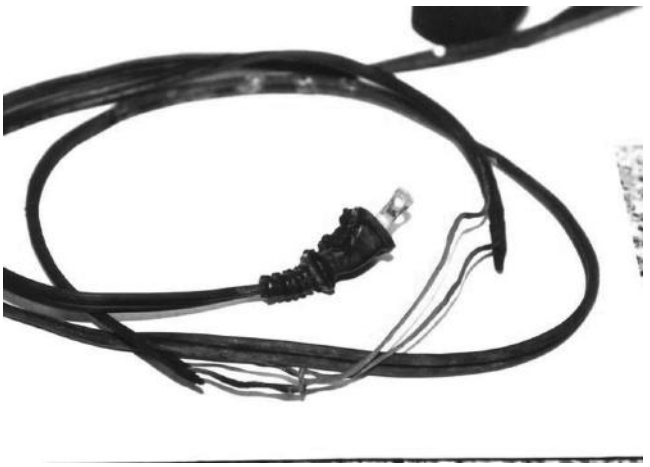

Figure 6.11 Electrical cord.

backs up into the heating element at the rear of the drum where it ignites because the heating element glows red hot producing temperatures in excess of 1000°F. Lint will ignite in the range of approximately 400°F. Figures 6.12 and 6.13 show typical dryer failures that produced fires.

Coffee Makers

The typical drip coffee maker has a steam pump. Over the years, these appliances have caused a multitude of fires. The power cord is subject to misuse and failure. Most of these units are constructed of plastic in close proximity to the heating and warming elements, which is never a good thing.

Figure 6.12 Lint fire.

Figure 6.13 Electrical short fire.

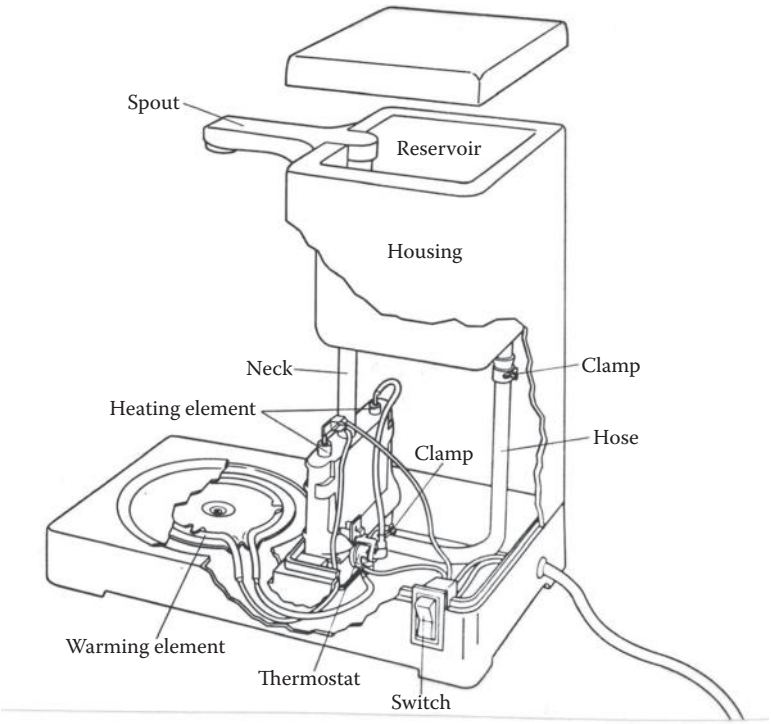

Figure 6.14 Coffee maker.

Figure 6.14 illustrates the basic components of the standard coffee maker available through a variety of manufacturers.

This type of coffee maker has a water reservoir usually located on top of the unit, which allows water to flow down a hose to a steam pump. The heating element in the pump turns some of the water into steam, which pushes the heated water up the neck, through the spout, and down into the ground coffee. After the water has passed through, the thermostat turns the heating element off, but the warming element stays on. These devices may fail because the heating element is in close proximity to the surrounding plastic housing or the power cord may short circuit. The thermal overload switches for the unit and the power cord should be analyzed, inspected, and tested. A common mode of failure can be produced by a failure of the overload switch. This problem has generally been corrected by the manufacturers, but many old designs of these coffee makers are still in use.

Fans and Heaters

Area fans and heaters can fail and cause fires. If the units simply fail and produce no damage, they are repaired or simply discarded. The relative low cost of these appliances makes them disposable. Let us look at how these appliances can fail and cause a fire, which is generally what they are suspected of having produced, especially if they are near the area of origin.

Both of these appliances have a power cord and plug that attach to a wall receptacle. The power cord normally has two conductors with no grounding wire. The size of the conductors is normally AWG 18. Normal house wiring will have three conductors that include a grounding wire. The size of the house wiring is generally AWG 12 although some is AWG 14. The larger the wire size, the smaller the diameter. The normal current capacity of AWG 12

Figure 6.15 **(See color insert.)** Arced conductors.

wire is 30 A and is protected with a 20 A circuit breaker. The smaller wire, AWG 14, is supposed to be protected by a 15 A circuit breaker. Actually, the current carrying capability of these wires depends on several factors, such as the number of wires in a bundle, the ambient temperature and the type of insulation on the wires. These wires can carry more current than what is stated here but not by a significant amount. The values are according to NFPA 70, the National Electrical Code. AWG 18 wire is generally rated at 15 A and is extensively used in power cords for small appliances such as fans and area heaters as well as extension cords for general use. These appliances are normally rated at 1000 W or less so that they carry 10 A of current or less. Consequently, the use of AWG 18 power cords is sufficient under normal conditions. The failure of these power cords is produced by damage to the insulation in most instances. Figure 6.15 shows a close-up of two solid wire conductors that arced as a result of a failure in the insulation. This type of saddle arcing is classic and is not produced by melting of the conductors from an external fire source.

Area heaters may fail as a result of the heating element igniting the plastic casing around the unit. If the casing is made of metal, this type of failure is not possible simply because the heating element separates when it comes into contact with a metal object. Once the circuit is broken, current ceases to flow, and the ignition source is removed unless there are ignitable materials in close proximity. The most likely scenario is that the heating element comes into contact with a material such as a curtain or some other material which may ignite. Close examination of the unit will very often reveal the mode of failure.

Televisions and VCRs

Small electrical appliances of this type also include radios, clocks, and computers. These appliances are powered by 120 V and are simply not designed to operate at 240 V. One mode of

Figure 6.16 Circuit board short.

failure can occur when the power into the home or office has a ground fault so that 240 V is applied to 120 V circuits. The electrical distribution system in the home is capable of handling the excess in the voltage. The wiring, switches, and outlets are not damaged by the doubling of the voltage. This is not true for small appliances because of the nature of the circuitry within these appliances. Internal failures of these appliances can also be produced under normal 120 V operation or they may be produced by voltage surges due to switching transients or lightning. Figure 6.16 shows a shorted circuit board while Figure 6.17 shows an arced transformer.

In the earlier examples, the failures did not produce any significant damage outside of the particular units. However, the cause of these failures needs to be determined in order to find the root cause. The cause may be due to lightning, in which case mother nature does not take responsibility. Alternatively, the cause of the failure may be due to switching transients produced by the local power company when electrical service was interrupted. In that case, there may be some liability on the part of the power company. If the failure resulted from a 20-year-old unit, the cause of the loss is simply age and life expectancy of the particular unit.

HVAC Systems

Furnace Humidifiers and Furnaces

Central humidifier systems pass the heated air from the furnace through a wet pad or disk before the air is distributed throughout the house. These wetted-element humidifiers are designed to fit on the warm air plenum connecting the furnace to the duct work. Some models call for a bypass pipe between the plenum and the cold air return duct. The humidistat control is to be mounted on the return air duct. If the unit contains an air conditioner, the wetted element is to be installed on the side of the plenum parallel to the length of the A-frame coil and above the condensate pan. Figure 6.18 illustrates the proper mounting procedure for

Figure 6.17 Arced transformer.

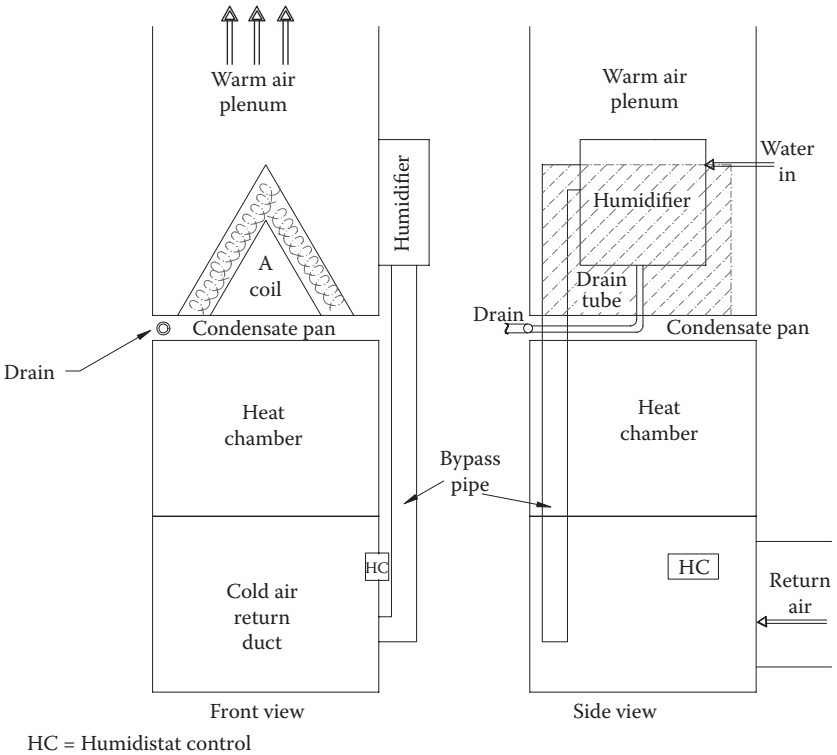

Figure 6.18 Humidifier with AC furnace.

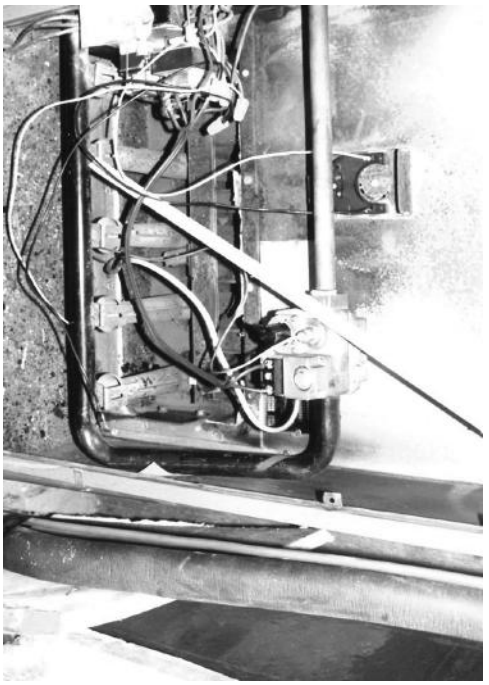

Figure 6.19 Furnace fire.

an updraft forced air furnace with air conditioning. If these units are not mounted properly or if the condensate pan becomes clogged, water can overflow and cause water damage.

Figure 6.19 shows a small fire that developed at the gas burners of a furnace as described by Figure 6.18. The fire was caused by lint that collected in the area of the burners and was attributed to improper maintenance of the unit.

Air Conditioners

Residential air conditioners are commonly a part of the HVAC system for the home. These types of systems are also found in small office complexes. The furnace and the A-coil are located inside the home or building and the compressor and evaporator coil are located outside. A common mode of failure of these units is that the compressor fails due to age. Simple resistance tests on the compressor can be conducted to see if that is the case absent of other physical evidence. The windings of the compressor can short circuit internally or they may short circuit to ground. Normally each winding of the coils of the compressor motor should have 2–4 Ω of resistance and each of the coils should be open circuited to case ground. In many instances when these units fail, the cause may be blamed on overvoltages produced by either lightning or electrical line transients. Power surges leave a definite trace that can be investigated by inspection of the electrical controls of the unit and checks on lightning discharges and power outages. Figure 6.20 shows a fire in an air conditioner where lightning produced a short circuit igniting the insulation.

When air conditioner losses are investigated, care must be taken to examine the electrical panel, the disconnect switch, and the wiring to the unit. In the case of a power surge produced by the power company, excessive heating or arcing may be apparent in these components. In the case of suspected lightning, the loss date and the proximity of lightning strikes must be

Figure 6.20 **(See color insert.)** Air conditioner fire.

correlated. Additionally, lightning will produce arcing either from a positive conductor to ground or arcing from ground to frame elements on the unit. Internal evidence may be found in the air conditioner as exemplified in Figure 6.20, and a failure of the compressor may exist.

Fireplaces and Water Heaters

In some instances a fireplace may cause sooting of the home. There are many causes for these sooting events. Some of the causes are improper construction of the fireplace, improper use, closed draft gates, or failures of installed fireplace inserts. Keep in mind that for proper combustion to take place, there has to be sufficient air to mix with the fuel. If there is insufficient air within the home, then the air–fuel mixture will not burn optimally and sooting can take place.

Gas-fired vented or ventless fireplace inserts are common. These units may be attached to natural gas or to propane. If a natural gas appliance is connected to a fireplace that has propane for a fuel source, or vice versa, it is assured of producing sooting because the gas orifice for these units is not the same size, and complete combustion does not take place. Either the fire produced in the appliance is fuel rich or oxygen rich so that the flame does not burn cleanly. It may be possible that the unit was installed according to manufacturers' instructions, or some of the packaging material was left on the logs. Figure 6.21 shows the sooting of a natural gas fireplace insert that was connected to propane gas.

Water heaters are also prone to failure. Most of these failures are caused by corrosion of the inner tank at the bottom. Sometimes the water fittings fail because they were improperly installed. The electrical or the gas service to the unit may cause a fire. In a relatively few cases, a manufacturing defect may cause a failure and produce a leak. Figure 6.22 shows an internal seam failure of a water heater.

Figure 6.21 Sooted fireplace.

Figure 6.22 **(See color insert.)** Failed water heater.

Pumps, Generators, and Motors

These appliances or components are found in a variety of applications. These applications include hot tubs, sump pumps, emergency power service, water wells, furnaces, and many others. They are found in the home, the office, the factory, and the industrial plant. They may be relatively small or massive, such as a motor or generator in a power plant or a steel mill. One common component of these types of devices is that they must have bearings. The bearings will have a variety of design components depending on the application and the size of the dynamo. A dynamo is a general term for a rotating device whether it is a motor or a generator. A generator will convert mechanical energy to electrical energy and a motor will convert electrical energy to mechanical energy. The bearings are needed because the dynamo rotates, and produces friction. Friction is an underestimated force. At high revolutions, friction is very capable of producing sparks that can cause a fire.

Bearing failures are easy to spot because they leave conclusive evidence. When a bearing fails, the lubrication is lost, or there is a misalignment of the shaft and the

bearing causing abnormal wear. In the case of a loss of lubrication, the bearing produces high temperatures that cause the rotating components to exceed the melting temperature of the metal surfaces. The sparks produced by the metal on metal contact are more than capable of producing a fire. These sparks have a temperature in excess of 3500°F, which is far and above the melting temperature of steel which is approximately 1000°F less than that.

As with electrical failures where we look for evidence of metal transfer, when mechanical friction type failures are investigated, we also look for metal transfer. This metal transfer is called galling. We look for metal transfer on the bearing raceways or on the rollers or balls of the bearings. In a case where a pump motor to a hot tub lost lubrication, ignited the fiberglass tub and burned a house down, the bearing was found to have galled. The motor and bearings were retrieved. The bearing was frozen on the motor shaft. The failure of the bearing was consistent with the fire origin. The failed bearing was blamed for the cause of the fire. The opposing expert stated that there was no evidence of galling on the bearing balls. He stated that upon examination, the balls should look like the surface of the moon. Apparently he did not look at the balls closely enough. To disprove the other expert's assertion, an identical exemplar bearing was obtained and heated with a torch to a temperature in excess of 2000°F. This temperature was selected because live fire tests reveal that most fires do not exceed this temperature. The heated balls of the exemplar bearing were then photographed to compare to the balls from the ceased bearing. The difference in the two is remarkable and accurately described the effect from the opposing expert. When the opposing side was shown the evidence, the case was quickly settled. Even though the opposing expert was given the evidence to examine, he obviously did not look or assumed that we would not. Figure 6.23 shows that exemplar bearing that was heated. Note the smooth surface. Figure 6.24 shows the failed bearing with the cratered effect produced by galling.

Figure 6.23 Heated bearing ball.

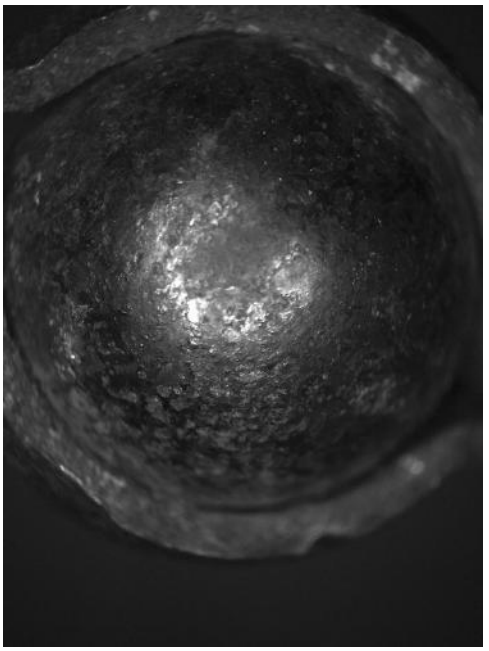

Figure 6.24 Galled bearing ball.

Boilers

Boilers may be classified into two basic types: fire tube (tubular) boilers allow hot gases from the fire to pass through the tubes and water tube (tubulous) boilers allow the hot gases to pass outside the tubes. Common accessories include Bourdon tube-type steam gauges, gauge glass tubes, safety valves, and blow-off cocks. This boiler is a water tube unit, which includes most of the safety devices available to boilers except for a filtration system for the raw water entering the boiler.

New high-volume boilers must be given special consideration in terms of the purity of the feed water. Most natural waters contain impurities that can cause problems within the boiler. Raw water from surface or subsurface sources usually contains in solution some degree of scale forming materials, such as free oxygen and certain acids. Dissolved oxygen will attack steel, and the rate of attack increases sharply with rising temperature. High chemical concentrations in the boiler water can cause furnace tube deposits. As boiler temperatures increase, water treatment systems become more critical. Another consideration that must be considered in such systems is feed water temperature so that condensation and acid attack on the gas side of the tubes is diminished. Dew point and rate of corrosion vary with the sulfur content of the fuel and the type of fuel firing equipment.

Raw water can cause one or more of the following events:

1. Deposits of scale
2. Foaming
3. Priming
4. Corrosion
5. Embrittlement

Table 6.1 Classification of Impurities, Effect, and Some Methods of Relief

Difficulty Resulting from Presence of	Nature of Difficulty	Ordinary Method of Overcoming or Relieving
Sediment, mud, etc.	Incrustation	Settling tanks, filtrating, blowing down
Readily soluble salts	Incrustation and priming	Blowing down
Bicarbonates of lime, magnesia, etc.	Incrustation	Heating feed. Treatment of magnesia, etc. by addition of lime or lime and soda. Caustic soda barium hydrate
Sulfate of lime	Incrustation	Treatment by addition of soda. Barium carbonate
Chloride and sulfate of magnesium	Corrosion	Treatment by addition of soda
Acid	Corrosion	Alkali
Dissolved carbonic acid and oxygen	Corrosion	Heating feed, keeping air from feed, addition of caustic soda or slacked lime
Grease	Corrosion	Filter, iron alum as coagulant, neutralization by carbonate of soda, use of best hydrocarbon oils
Organic matter	Corrosion	Filter, use of coagulant
Organic matter (sewage)	Foaming	Settling tanks, filter in connection with coagulant

Deposits of scale result from solids in solution or in suspension, and they reduce the rate of heat transfer, sometimes being responsible for burned-out tubes. Foaming, caused by a scum of oil and vegetable matter on the surface of the water in the boiler shell or by excessive alkalinity of the boiler feed, occurs when a mass of bubbles forms on the surface of the water, and particles of water are projected into the steam space. Foaming is one, but not the sole cause, of priming. A boiler is priming when relatively large quantities of water are passing out with the steam. This water is a hazard to pipe lines and apparatus. Corrosion is a transformation of the metal, as by oxidation. Embrittlement, which occurs when certain impurities are present, is a phenomenon that manifests itself by cracks in and failure of riveted boiler joints. Since impurities that are responsible for the foregoing ills are of varying kinds and amounts, all boiler water should be analyzed so that a suitable treatment may be prescribed. Table 6.1 shows the approximate classification of impurities found in feed waters, their effect, and some methods of relief.

Swimming Pool Failures

Hydrostatic Pressure and in-Ground Pools

The standard requirement of a pool is that its walls should be able to withstand pressures produced by water. This fact is the same whether the pool is an aboveground aluminum pool or an in-ground fiberglass pool. However, aboveground pool walls need only withstand the weight of the water. In-ground pools must contain the water and withstand the weight of the earth acting around the perimeter. The water inside the pool does provide resistance to the earthen pressures. However, these pressures can increase and cause failure of the liner or walls of the pool. Figure 6.25 illustrates a configuration of an in-ground pool.

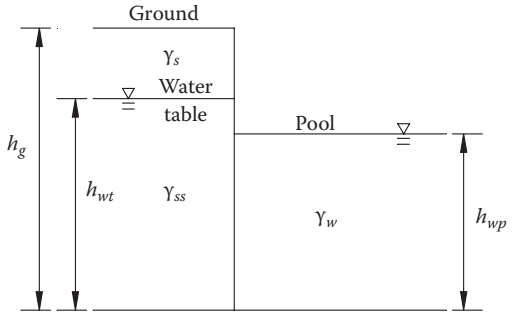

Figure 6.25 Configuration of in-ground pool. Where h_g is the height of ground earlier datum, h_{wt} is the height of water table earlier datum, h_{wp} is the height of pool earlier datum, γ_s is the weight of unsaturated soil = 90–120 pcf, γ_{ss} is the weight of saturated soil (below water table) = 120–132 pcf, γ_w is the weight of water = 62.4 pcf.

The pressures acting on the wall of the pool are directly proportional to the height and weight of material denoted in Figure 6.25. The pressure (p) is given by the following linear relationship:

$$p = \gamma h \tag{6.10}$$

Figure 6.26 displays the pressures acting on the wall.

The following equations describe the lateral pressures according to Equation 6.10:

$$\begin{aligned} p_s &= k\gamma_s(h_g - h_{wt}) \\ p_{ss} &= k\gamma_{ss}h_{wt} \\ p_s + p_{ss} &= k\gamma_s h_g + (\gamma_s - \gamma_{ss})h_{wt} \\ p_w &= \gamma_w h_{wp} \end{aligned} \tag{6.11}$$

where k is the coefficient of earth pressure (accounts for soil friction angle).

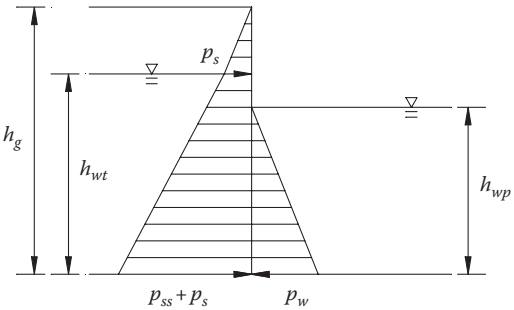

Figure 6.26 Pressures acting on pool wall.

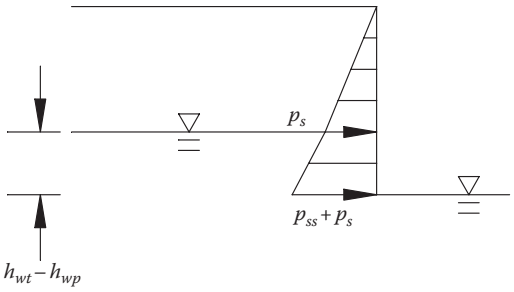

Figure 6.27 Pressure acting on wall above pool level.

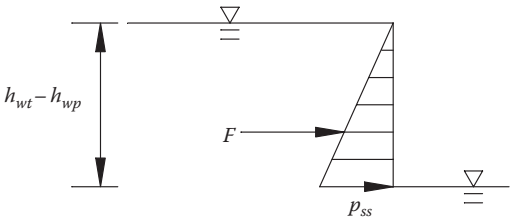

Figure 6.28 Pressure and force.

When lateral soil pressures exceed the water pressure in the pool, the resultant pressures act to push the pool walls inward. Furthermore, the pool level is often dropped in winter months in order to prevent freezing damage to the pool plumbing. This lowering of the pool level reduces the supportive pressure provided by the weight of the water. Due to this disparity in pressure, the wall must be structurally sufficient to withstand the lateral forces produced from the earth. Even if the walls are adequate to support the loads, the pore pressures within the soil can be greater than the pressures in the pool even when the pool is at its highest level. This disparity in pressure can result in a direct failure of the pool liner and an influx of ground water. Consider Figure 6.27, which shows the pressure acting on the wall above pool level.

With no resistance to lateral pressures above the pool level, the walls may fail if not properly constructed. This problem is intensified during periods of heavy rainfall. The water table, and corresponding height of saturated soil, can rise to ground level with long duration rains. This rise in the water table results in greater weight of the soil and higher pore pressures acting on the pool walls. Figure 6.28 displays the pressure and equivalent force that affect the wall above pool level.

The equivalent force per unit width (F) is equal to the area of the pressure triangle. The equivalent force also acts through the centroid of the pressure triangle. This dimension is known to be two thirds of the difference in ground height to pool level.

Dissolution of Aluminum

The liquid resulting from passing chlorine (Cl) into water (H_2O) is often regarded simply as a solution of chlorine in water and is called chlorine water. The chlorine, however, reacts slowly with the water to form a mixture of hydrochloric acid (HCl)

and hypochlorous acid (*HClO*), until the equilibrium expressed in the following equation results:

$$Cl_2 + H_2O \leftrightarrows HCl + HClO \tag{6.12}$$

Hypochlorous acid is unstable, however, and decomposes (slowly in the dark but rapidly in sunlight) into hydrochloric acid and oxygen:

$$2HClO \rightarrow 2HCl + O_2 \tag{6.13}$$

This removal of the hypochlorous acid through decomposition disturbs the equilibrium expressed in Equation 6.12 so that the interaction of the chlorine and water continues as long as any free chlorine is left. There finally results a dilute solution of hydrochloric acid, as is shown by combining Equations 6.12 and 6.13:

$$2Cl_2 + 2H_2O \rightarrow 4HCl + O_2 \tag{6.14}$$

The decomposition of water through the action of chlorine is greatly increased in the presence of a substance that combines with oxygen as fast as it is set free. Consequently, a solution of chlorine in water is a good oxidizing agent.

Aluminum is but slightly acted upon by pure water. Moist air merely dims its luster. Further action is prevented in each case by the formation of a very thin film of oxide upon the surface of the metal. However, chlorine water through the action of sunlight produces hydrochloric acid as expressed in Equation 6.14. Hydrochloric acid is aluminum's best solvent, and the reaction is governed by

$$2Al + 6HCl \rightarrow 2AlCl_3 + 3H_2 \tag{6.15}$$

where $AlCl_3$ is aluminum chloride and is a salt.

Table 6.2 shows the physical data on the elements that constitute the chemical equations for a swimming pool failure and Figure 6.29 shows the diagram of the failure.

Table 6.2 Physical Data

Element	Symbol	Atomic Number	Atomic Weight	Valence
Aluminum	Al	13	26.97	Tervalent
Chlorine	Cl	17	35.456	Univalent
Oxygen	O	8	16.00	Bivalent
Hydrogen	H	1	1.008	Univalent

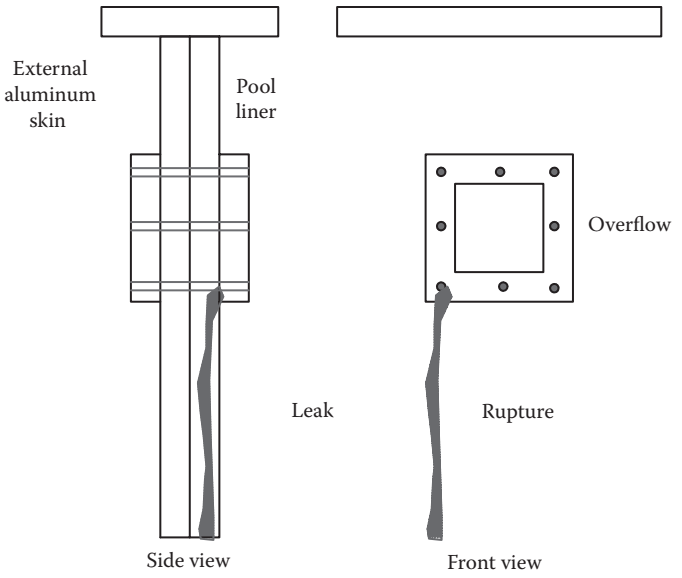

Figure 6.29 Diagram of failure.

Welding Failures

The integrity of welded materials is dependent on the quality of the weld. The structural life and in many instances, the safety of the welded product are dependent on welding integrity. Radiography and ultrasonic inspection can be used to confirm weld integrity. However, deficient welds can be identified through a visual inspection especially after a failure occurs. Substandard welds can exhibit themselves in a variety of manners as outline below.

Dimensional Discrepancies

These types of weld problems include misalignment, weld size, warping, incorrect joint preparation, and cross-sectional or profile discrepancies. For example, centerline mismatch can create stress risers that could exceed the design strength.

Weld Undercut

This weld discrepancy is characterized by a notch in the base metal. Commonly, the notch is in a stress sensitive portion of the weld so that the mechanical properties of the metal are altered because they are in the heat-affected zone.

Surface Porosity

Porosity is caused by gas bubbles that are trapped in the weld material. Surface porosity indicates porosity throughout the weld. The most common source of porosity is improper surface preparation leaving oils or rust on the weld surface. Since almost all fatigue fractures begin at the surface of the metal, anything that interrupts the surface is a crack nucleation point. Excessive porosity can hinder the detection of weld defects such as undercut and lack of penetration.

Weld Cracks

Weld cracks are characterized as hot cracking or cold cracking. Hot cracking occurs just after the weld has solidified while cold cracking occurs at ambient temperature after the weld has cooled. Most weld cracks are hot cracking and occur as the weld is pulled apart during cool down. If the weld configuration does not allow the weld area to contract as it cools, then hot cracking is likely to occur. If the width to depth ratio of the weld is too high, edge cooling can pull the bead apart and cause centerline cracking. Unlike hot cracking, cold cracking can occur hours or days after welding. The most damaging form of cold cracking is hydrogen embrittlement that occurs when hydrogen is absorbed into the metal. Hydrogen embrittlement is normally associated with rust and dirt that has accumulated on the weld surface or from using a damp electrode. Structures suffering from hydrogen embrittlement often fail.

Insufficient Throat or Leg

These welding deficiencies reduce the mechanical strength of the weld causing failure under either static or dynamic loading.

Excessive Convexity and Overlap

The opposite of insufficient throat is excessive convexity, which is distinguished by a thick, rounded fillet. Often this convexity has a sharp approach into the toe of the weld with an angle of 45° or greater. These steep edges create stress risers that can initiate fatigue failure. Like convexity, overlap extends the weld metal beyond acceptable limits. Overlap is often a symptom of lack of penetration and lack of fusion that creates a crevice. This crevice is subject to stress risers and crack initiation.

Cars

Torque Converters

Automatic transmissions provide somewhat different performance than standard transmissions. Automatic transmission performance more closely matches the ideal characteristics because of the torque converter on the input. Torque converters are fluid couplings that use hydrodynamic principles to amplify the torque input to the transmission at the expense of speed. Figure 6.30 shows the torque ratio and efficiency characteristics of a typical torque converter as a function of speed ratio (output/input speed). At zero output speed (speed ratio of zero) the output torque will be several times that of the input.

Thus, the torque input to the transmission will be twice the torque coming out of the engine when the transmission is stalled, providing for good "of the line" acceleration performance. As the speed builds up and the transmission input approaches engine speed, the torque ratio drops to unity.

The torque amplification provides for more favorable tractive effort–speed performance. Because of the slip possible with the fluid coupling, the torque curves in each gear can extend down to zero speed without stalling the engine. At low speed in first gear, the effect of the torque converter is especially evident as the tractive effort descends toward the zero speed condition. Typical torque converter failures are associated with loss of fluid.

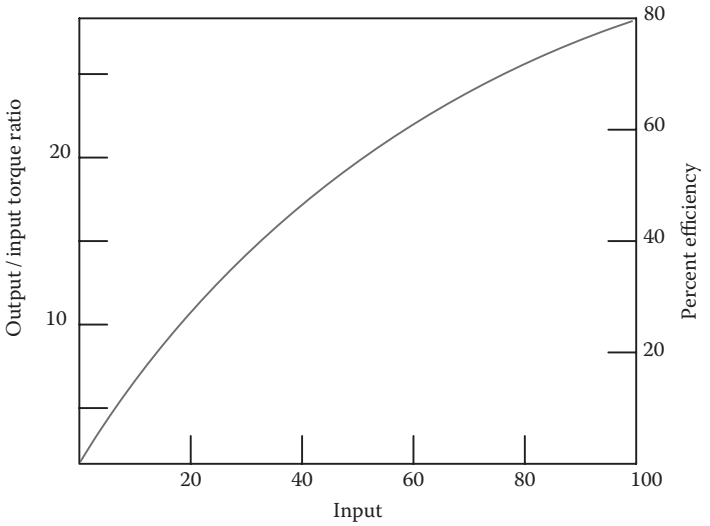

Figure 6.30 Characteristics of a typical torque converter.

Brake System Overview

The basic functions of a brake system are to slow a vehicle's speed, to maintain its speed during downhill operations, and to hold a vehicle stationary after it has come to a complete stop. These basic functions must be performed during normal operation of the brakes. Additionally, a certain amount of braking effectiveness is needed during a brake system failure. A typical automotive, small truck hydraulic brake system is illustrated in Figure 6.31.

All brake systems can be divided into four basic subsystems as follows: These four basic subsystems apply to all the braking systems in passenger, commercial, or specialty vehicles. The difference between brakes for tractor/trailers and passenger vehicles, for example, is in the design and execution of the various systems but not in the classification of the subsystems. The systems identified in this section relate to the common passenger vehicle and are not typical of braking systems for large commercial vehicles such as tractor/trailers, or industrial vehicles. Braking systems for specialty vehicles vary greatly in design and

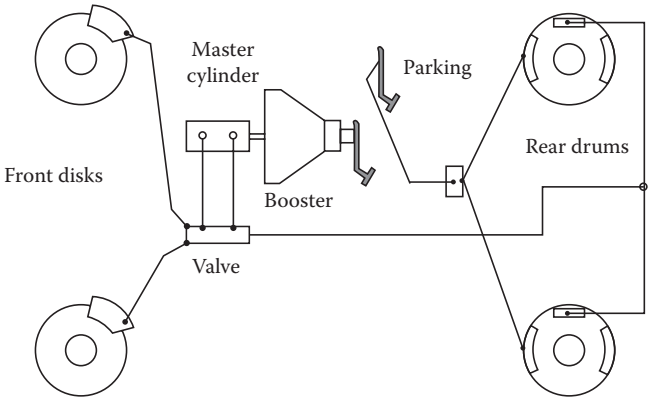

Figure 6.31 Typical automotive brakes.

complete coverage of these systems is beyond the scope of this book. According to Limpert, these systems are

1. Energy source system: includes the components that produce, store, and make available the energy required for braking
2. Activation system: the components that are used to modulate or regulate the level or intensity of braking
3. Transmission system: the components through which the braking energy travels from the activation system to the wheel brake systems
4. Wheel brake system: the components that apply the forces to the wheels that retard the vehicle through the force of friction

Vacuum-Assisted Brake Booster

Vacuum-assisted hydraulic brakes, also called power brakes, use a vacuum booster as illustrated in Figure 6.32 to assist the driver's effort in pressing the shoes against the drum.

For most passenger cars, the power brake system is oriented at the fire wall between the foot pedal and master cylinder. The master cylinder piston is activated by an assist force produced by the booster. A pressure difference across the booster piston or diaphragm may provide this force. This pressure differential may be derived from low pressure on the master cylinder side and (higher) atmospheric pressure on the input side. The low pressure is caused by the engine operation via a connection to the intake manifold of the engine. The intake manifold's low pressure is created as the engine draws air for the detonation of the fuel in the cylinders.

Brake Line Pressure Control Devices

There are two basic types of brake line pressure valves: the brake pressure limiter and the brake pressure reducer. Each of these devices can be activated either by brake line pressure or by vehicle deceleration. In many cases, two or three different functions are combined into one valve, commonly called a combination valve as shown in Figure 6.33.

The valve to the left is the metering valve, and the valve to the right is the reducer or proportioning valve discussed earlier. The switch in the center is the differential pressure

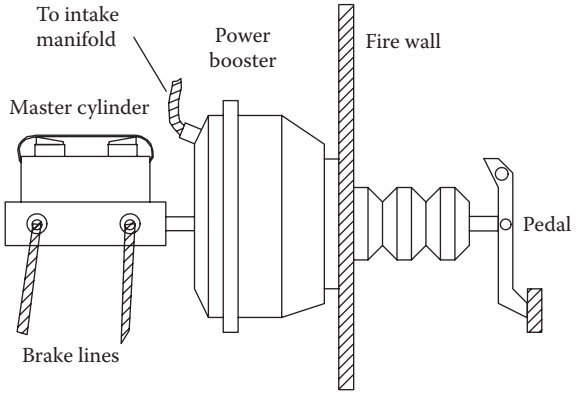

Figure 6.32 Power brakes.

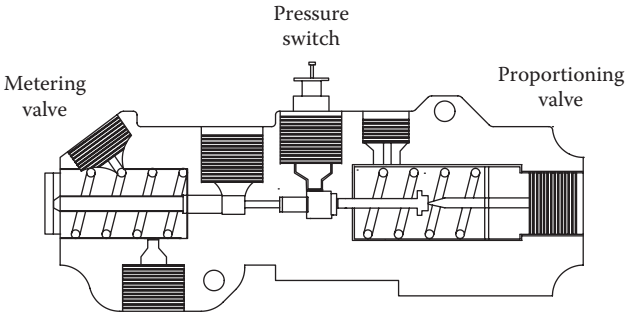

Figure 6.33 Combination valve.

switch, which is activated in the event of a hydraulic leak in one of the dual brake circuits. Metering valves are used primarily for rear wheel-driven vehicles, using the front disk/rear drum system.

Step Bore Master Cylinder

Brake line pressure valves are typically mounted between the outlet of the master cylinder and the rear brake wheel cylinders. As shown in Figure 6.34, both pistons will have the same diameter for a standard dual or tandem master cylinder design. The equivalent diameters yield the same pressure levels across each piston.

In a step or adjustable step bore master cylinder, the pistons are of different diameters and therefore produce varying pressure.

Brake Designs

Most passenger cars and trucks utilize drum (radial) or disk (axial) friction brakes. Types of drum brakes include external haul and internal shoe designs. Shoe brakes may have varying arrangements, such as leading/trailing, two leading or duo-servo brakes. Other variances in shoe brake design include shoe abutment, parallel or inclined sliding abutments, or pivoting shoes. Actuation of the brake shoe may be dependent on hydraulic wheel cylinders, wedges, cams, screws, and mechanical linkages. Disk brakes may be either a fixed or floating caliper design. Fixed caliper disk

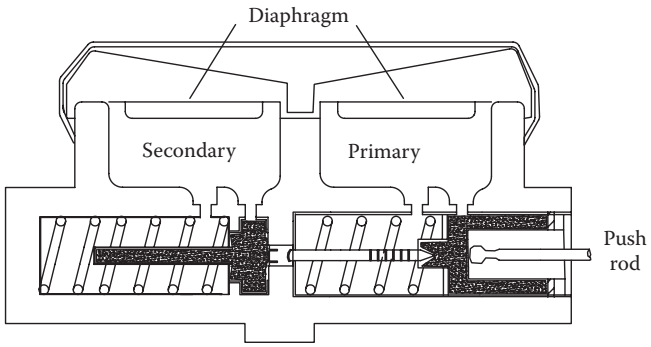

Figure 6.34 Master cylinder.

brakes have either two or four pistons that push the pads out on either side of the disk. In contrast, floating caliper disk brakes have one or two pistons on the inboard side only. The actual brake designs vary greatly in design and construction depending on the manufacturer or the application. However, in all the systems the braking action is produced by creating friction between the brake shoes or pads and the wheel attachment whether disk or drum.

In order to keep the clearance between brake lining and drum or pad and rotor at an optimum, manual or automatic adjustment becomes necessary as the linings wear. Since the return springs pull the shoes against a stop to their full retracted position, the clearance between shoe lining and drum increases as linings wear. By adjusting the brake shoes out, the stops are moved toward the drum, thus preventing excessive return movement of the shoes. Automatic adjusters are designed to keep the lining to drum clearance at an optimum value.

Drum parking brakes utilize the same drum and lining components as the service brakes. However, different components are employed for brake shoe application. In contrast to disk brakes, drum brakes are ideal for use as parking brakes due to their high torque output and relatively simple design.

Large Vehicles

The predominant large vehicle in the United States is the tractor/trailer combination. Vehicles with hydraulic brake systems, as with passenger motor vehicles, employ the components listed in the previous sections to control the braking performance. Those vehicles are subject to Federal Motor Vehicle Safety Standard (FMVSS) 105. Large vehicles are generally equipped with pneumatic (air brake) systems and are subject to FMVSS 121. Since March 1, 1997, all new tractor/trailers have been required to have antilock brake systems. Buses and other large vehicles were subject to this requirement effective March 1, 1998. The antilock brake systems on large vehicles behave just as they do for smaller vehicles. That is, they do not necessarily stop the vehicle any faster, but they allow for control of the vehicle as the brakes are applied because they do not lock the brakes.

The basic components of air brake systems include an air compressor that behaves as the energy source. The compressor is governed by controls that maintain a pressure between 100 and 125 pounds per square inch (psi). The air is stored in tanks that vary in number and size according to the design. However, the reserve capacity of these tanks is sufficient to allow the brakes to be used over several cycles even if a compressor failure occurs. A safety valve set at 150 psi is generally installed on the tanks, and the tanks have drains to rid them of water. Some systems have an alcohol evaporator that reduces the risk of ice forming in the brake valves during cold weather.

The brake pedal, which is often referred to as the foot valve or more accurately known as a treadle valve, activates the brakes and controls the air pressure in the system. Applying the brake pedal activates the foundation brakes, which may be of three basic designs: the S-cam, wedge, or disk brake designs. The most common is the S-cam design. The front brakes of tractor/trailers generally have a brake chamber with a single air chamber with no spring. The rear brakes of the tractor and the trailer have a brake chamber with two air chambers. Associated with these basic components are various valves, fittings, and lines. A typical single circuit air brake system is shown in Figure 6.35.

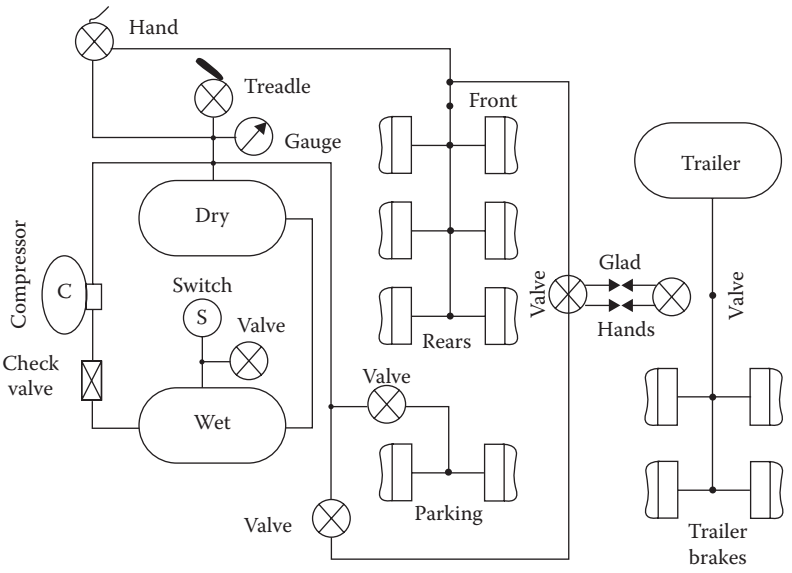

Figure 6.35 Air brake system.

Steering

All of us have driven a variety of vehicles and noted that the steering systems of those vehicles vary widely. The actual steer angles are a function of the type of steering mechanism employed, the suspension system, the linkages, and whether the vehicle is front wheel drive. The actual conversion of the steering wheel input to the steer angles imposed on the wheels is achieved by two basic mechanisms: the steering box or the rack and pinion steering system. Figure 6.36 shows a generalized diagram of the steering system employed in most passenger vehicles.

The steering wheel is connected to the steering box or the rack and pinion gears through the shaft, universal joints, and vibration dampers. The rack or steering box transfers the rotational motion of the steering wheel to lateral translational motion that affects the steer angles of the wheels. From the rack or the gear box, there are a variety of linkages and joints that tie the system together. According to Gillespie, if the steer linkages connect to the rear of the wheel centers, the configuration is called rear-steer and if connected to the front, it is forward-steer. For heavy trucks, the steering arrangement is similar, utilizing a gear box and a connection to the left wheel.

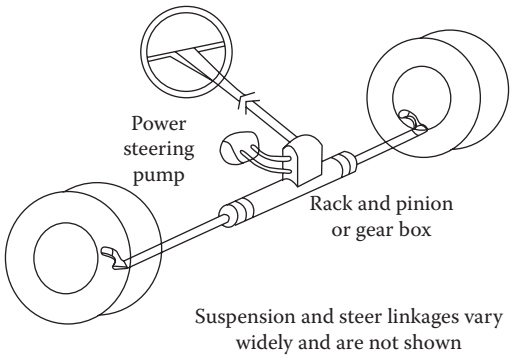

Figure 6.36 Steering system.

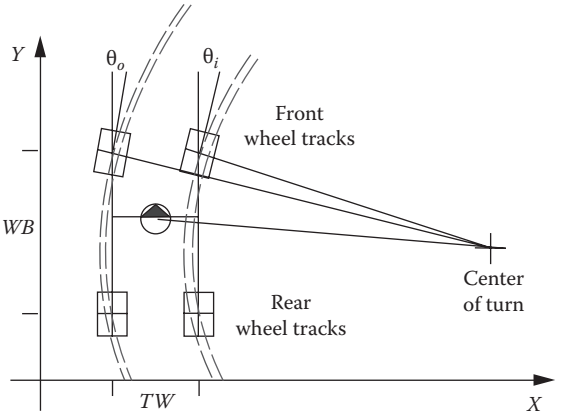

Figure 6.37 Ackerman geometry.

The left wheel is then connected to the right wheel through appropriate linkages. The output shaft of the gear box, whether for a truck or a passenger vehicle, is connected to a pitman arm that activates the linkages. The geometrical configuration of the linkages produces unequal steer angles between the inner and the outer turn wheels. This "Ackerman" geometry is shown in Figure 6.37.

Note from Figure 6.37 that the front track radiuses are greater than the rear track radiuses. The front outer and the front inner radiuses are also slightly greater than the rear outer and rear inner radiuses. Thus, the rear wheels of all vehicles off-track the front wheels to the inside of the turn. This effect is more pronounced the larger the vehicle. Tractor/trailers off-track to a much greater degree than solid frame uncoupled vehicles. The outer and inner steer angles are given by

$$\theta_o \cong \tan^{-1} \frac{WB}{R + TW/2} \tag{6.16}$$

$$\theta_i \cong \tan^{-1} \frac{WB}{R - TW/2} \tag{6.17}$$

In the earlier equations, R is the mean radius passing through the center of mass of the vehicle with respect to the center of the turn.

Coupled vehicles behave somewhat differently from what is presented earlier. Coupled vehicles must be analyzed by the earlier method for the tractor and by tractrix equations as described later for the trailer. Thus, the off-tracking is the summation of that produced by the Ackerman geometry and the tractrix displacement. The Ackerman offset relates to the front wheel of the tractor with respect to the tractor axle or tandem axles. The tractrix equations relate to the relative displacement between the king pin on the tractor and the axle or tandems on the trailer. Consider Figure 6.38, which represents the path followed by the trailer as it follows the tractor around a curve.

The paths of the front wheels of the tractor, the rear wheels of the tractor, and the wheels of the trailer will all follow different paths. As previously mentioned, the difference in the paths of the tractor can be analyzed by the Ackerman formula. The path difference

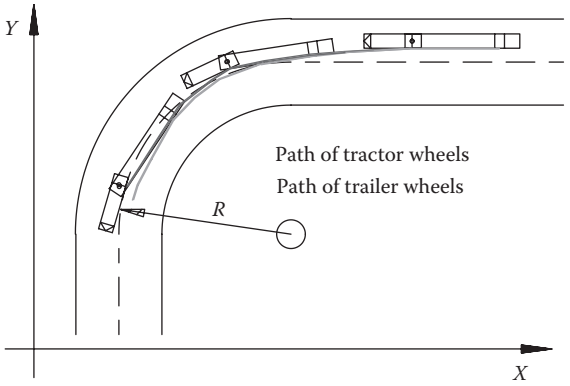

Figure 6.38 Trailer off-tracking.

between the rear wheels of the tractor and the wheels of the trailer follow a curve known as a catenary involute. The catenary is the tractrix evolute so that the tangent of the curve is described by the differential equation

$$\frac{dy}{dx} = -\frac{\sqrt{L^2 - x^2}}{x} \tag{6.18}$$

The solution to the equation is

$$y = -L\log\left(\frac{L + \sqrt{L^2 - x^2}}{x}\right) + \sqrt{L^2 - x^2} \tag{6.19}$$

L represents the distance from the kingpin to the rear wheels of the trailer. Figure 6.39 shows the relative displacement of the rear wheels for distances of 24, 30, and 36 ft at a given radius produced by the tractrix equation. These relative curves reveal, as would be expected, that the longer the trailer, the more severe the off-tracking that occurs as an articulated vehicle rounds a curve.

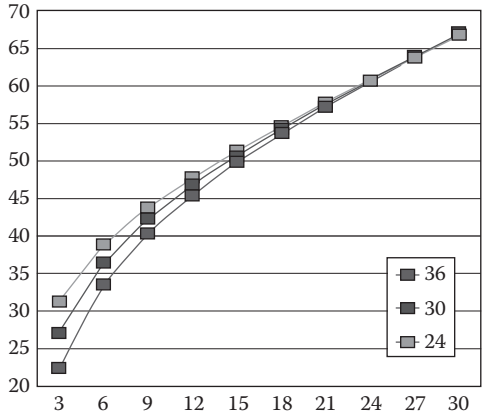

Figure 6.39 Relative off-tracking displacement.

Interpreting Electrical Activity

Interpreting Electrical Fire Evidence

It is often possible to properly interpret electrical activity after a fire in order to determine if the activity caused the fire or was produced by the fire. Many types of damage can occur from nonelectrical activity or from electrical activity during the fire. Many times the evidence is misinterpreted by investigators. NFPA 921 explains most of the common mistakes made in the interpretation of electrical fires. Below are pertinent sections of NFPA 921 that define the evidence in this case.

Appearance of Arced and Fire-Melted Conductors

When conductors are subjected to highly localized heating, such as from arcs, the ends of the individual conductors may become rounded or have bulbous globules of resolidified molten metal. These globules are called beads. Beads can be differentiated from globules created by nonlocalized heating, such as overload or fire melting, by the presence of a distinct and identifiable line of demarcation between the melted bead and the adjacent nonmelted portion of the conductor. Globules due to fire melting are irregular in shape and size, often tapered, and may be pointed. They have no distinct boundary lines of demarcation between the globule and the adjacent fire-heated conductor.

Short Circuit and Ground Fault Arcs

Whenever an energized conductor contacts a grounded conductor or a metal object that is grounded with nearly zero resistance in the circuit, there will be an arc discharge at the point of contact. The high current flow can melt the metals in small areas in the conductors or other metal objects involved producing a gap and an arc. The arcing faults melt the metals only at the point of initial contact. The adjacent surfaces will be unmelted unless fire or some other event causes subsequent melting. In the event of subsequent melting, it may be difficult to identify the site of the initial short circuit or ground fault. If the conductors were installed prior to the faulting, it will be necessary to determine how the insulation failed or was removed and the conductors came in contact with each other. If the conductor or other metal object was bare of insulation at the time of the faulting, there may be spatter of metal onto the otherwise unmelted adjacent surfaces. A stranded conductor may exhibit a notch with only some of the strands severed, or all of the strands may be severed with strands fused together or individual strands melted.

Arcing during Fires

Insulation on conductors when exposed to direct fire will likely be charred before being burned off in branch circuits; holes extending for several inches may be seen in the conduit or in metal panels to which the conductor arced. When stranded conductors are involved, a bead may be formed that fuses most of the strands together at the severed end or at the point of arcing.

Effects Not Electrically Caused

Conductors may be damaged before or during a fire by other than electrical means, and often these effects are distinguishable from electrical activity.

Melting by Fire

When exposed to fire, copper conductors can reach melting temperatures. Stranded conductors that just reach melting temperatures become stiffened by the fused copper and oxide mixture of the strands. Further heating can let copper flow among the strands so that the conductor becomes solid with an irregular surface that can show where the individual strands were. Continued heating can cause the flowing, thinning, and drop formation of solid conductors. Magnification is needed to see some of these effects.

Alloying

Metals such as aluminum and zinc can form alloys when melted in the presence of other metals. If aluminum drips into a bare copper conductor during a fire and cools, the aluminum will be just lightly stuck to the copper. If that spot is further heated by fire, the metals can penetrate the oxide interface and form an alloy that melts at a lower temperature than does either pure metal.

Misconceptions and Cautions

There are several ideas that have been common among fire investigators, which are either unproven, misconstrued, incorrect, or true under only limited circumstance. Some of the more common misconceptions are detailed in the sections that follow.

Undersized Conductors

Undersized conductors, such as a 14 AWG conductor in a 20 A circuit, are sometimes thought to overheat and cause fires. There is a large safety factor in the allowed ampacities. Although the current in a 14 AWG conductor is supposed to be limited to 15 A, the extra heating from increasing the current to 20 A would not necessarily indicate a fire cause. The higher operating temperature would deteriorate the insulation faster but would not melt it or cause it to fall off and bare the conductor without some additional factors to generate or retain heat. The presence of undersized conductors or overfused protection is not proof of a fire cause.

Nicked or Stretched Conductors

It is sometimes thought that pulling conductors through conduit can stretch them like taffy and reduce the cross section to a size too small for the ampacity of the protection. Whatever stretching can occur before the range of plastic deformation is exceeded would not cause either a significant reduction in cross section or excessive resistance heating.

Deteriorated Insulation

When thermoplastic insulation deteriorates with age and heating, it tends to become brittle and will crack if bent. Those cracks do not allow leakage current unless conductive

solutions get into the cracks. Arc tracking through the insulation can produce increasing current, which carbonizes the insulating material and further increases the current and may lead to an eventual arc of the conductors.

Short Circuit

It is often thought that a short circuit in wiring on a branch circuit would ignite insulation on the conductors and allow a fire to propagate. Normally, the quick flash of a parting arc prior to operation of the circuit protection cannot heat insulation enough to generate ignitible fumes even though the temperature of the core of the arc may be several thousand degrees. Continued arcing, however, may ignite the surrounding material and produce a fire.

The figures that follow show typical arced conductors in stranded and solid conductors. Figure 6.40 shows arced solid conductors with beading while Figure 6.41 shows arced

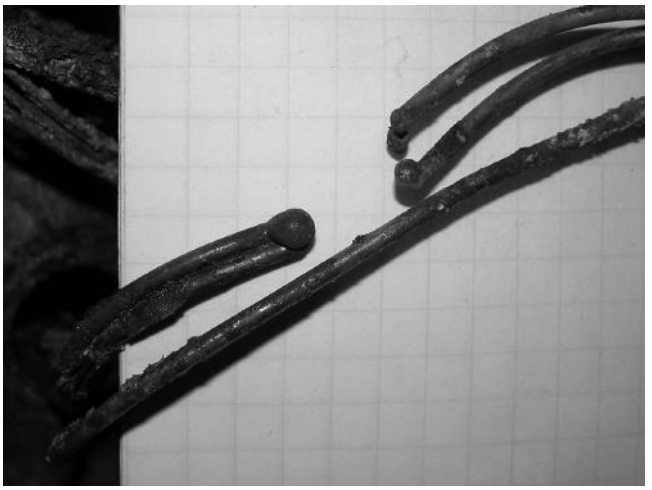

Figure 6.40 **(See color insert.)** Arced solid conductors—beads.

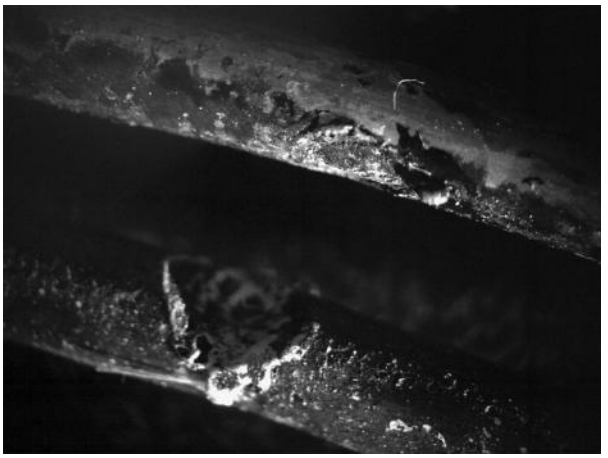

Figure 6.41 **(See color insert.)** Arced solid conductors—saddle.

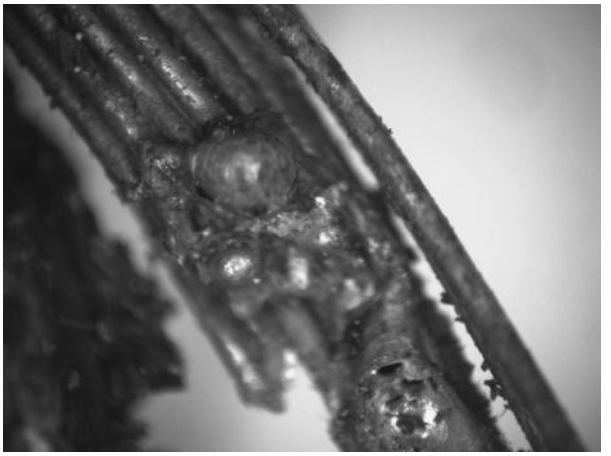

Figure 6.42 **(See color insert.)** Arced stranded conductors—beads.

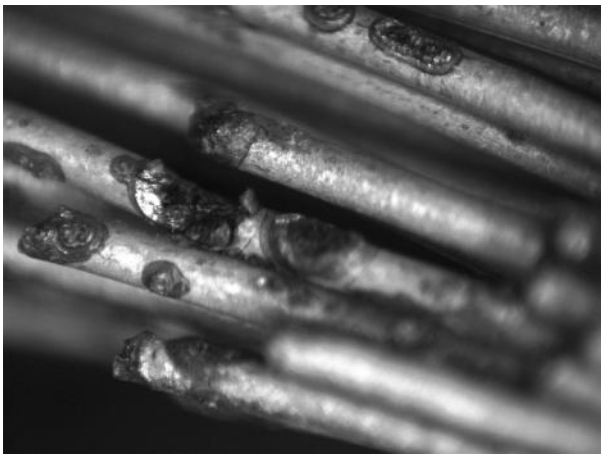

Figure 6.43 Arced stranded conductors—saddles.

solid conductors with a saddle mark. Figure 6.42 shows arced stranded conductors with beading and Figure 6.43 shows stranded conductors with saddles.

Component Fracture Mechanics

Load Analysis on Support Bracket

West Virginia coal is ranked as a bituminous coal whose bulk density varies between 42 and 57 lb/ft^3. The bulk density of broken coal varies according to the specific gravity, size, distribution, and moisture content of the coal. The amount of settling when the coal is piled also affects the bulk density. A support bracket for the hydraulic lift on a dump truck was made of mild steel angle with nominal dimensions of 4 × 4 in.

While this truck was dumping a load, the support bracket failed. From the truck dimensions, we can calculate the volume of the truck bed as

$$V = W \times L \times D = (8\text{ ft})(21\text{ ft})(8\text{ ft}) = 1344\,C.F. \tag{6.20}$$

The weight of the coal is therefore

$$W_c = V \times B_d = (1{,}344)(57) = 76{,}608\,\text{lb} \tag{6.21}$$

Assuming the weight of the truck bed to be $W_B = 7000$ lb, the total weight of the uniformly distributed load is approximately

$$W_T = W_B + W_c = 76{,}608 + 7{,}000 \approx 83{,}608\,\text{lb} \tag{6.22}$$

A kip is 1000 lb so that the total weight is 83.6 kips. The support pins at the rear of the truck and the hydraulic piston both carry the load equally so that the support bracket for the hydraulic piston must carry 40 kip. The support bracket dimensions are approximately 2 ft by 1 ft. Thus, the span length of the angle is from 1 to 2 ft.

The American Steel Institute reveals that for the angle dimensions of L4X4X½, the weight per foot is 12.8 lb (pp. 1–56). In their design criteria (pp. 2–59) they include L6X4X⅜ angle at a weight of 12.3 lb and L4X4X⅜ angle at a weight of 9.8 lb. Analyzing the data for both angles for span lengths between 1 and 2 ft reveals that the allowable load will vary between 20 and 40 kip depending on the span. Since the weight on the cylinder is 40 kip and the allowable load varies from 20 to 40 kip, it is evident why the bracket failed.

Analysis of Crane Failure

The point of failure occurred on the boom at approximately 150 ft from the pivot point at the base of the crane. The bottom chord of the boxed truss that comprises the boom frame buckled, causing the upper boom section and the jib to collapse onto the silo. The boom frame is composed of four pieces of steel angle welded into a 6 × 6 ft box. This boxed truss is further strengthened by steel pipes that serve as web members. The first 150 ft of the boom is constructed with 3½ × 3½ × ½″ angle, while 3 × 3 × ⅜″ angle composes the upper 70 ft of the boom. The bottom chords of the upper 30 ft of the boom are stiffened with a ½″ plate. The failure occurred along the unstiffened section, which possessed the weakest members of the boom.

The angle members along the unstiffened bottom chord of the boom buckled due to the combined axial and bending loads. These loads are a function of the load lifted by the crane and the orientation of the boom. The specifications called for the 220 ft boom to be angled at 80° with the 50 ft jib at a 20° offset angle. As seen in Figure 6.44, this orientation results in a bound and uncentered load line. Additionally, the specified 75 ft jib radius would have actually been 88 ft. Figure 6.44 also shows that the boom angled at 83.5° provides a vertical load orientation and a 75 ft jib radius. In order to determine the loads on the failed boom section, Figure 6.44 must be considered.

Free body diagrams at points 1, 2, and 3 must be made to determine the load carried by the boom. Figure 6.45 represents the free body diagram at point 1.

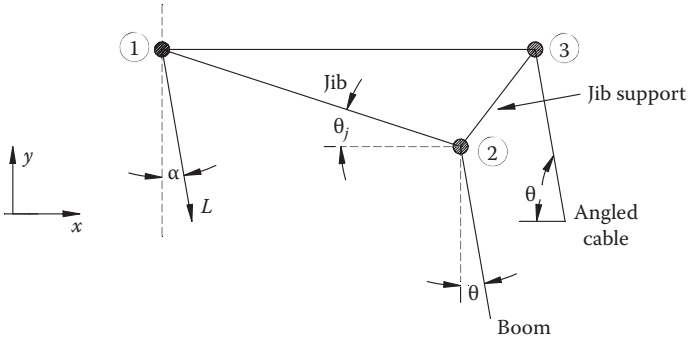

Figure 6.44 Crane diagram. Where L is the load lifted by crane = 15–17 kip, α is the angle of load from vertical, θ_j is the jib offset angle = 20°, θ is the angle of boom and load line.

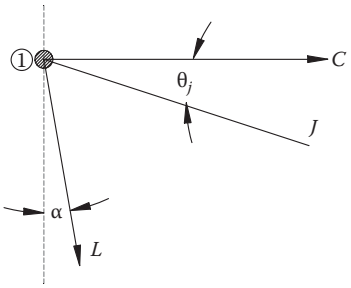

Figure 6.45 Free body diagram at point 1. Where J is the load carried by jib (kip), C is the load carried by horizontal cable (kip).

Summing forces in the x and y directions,

$$\begin{aligned} J_y &= L_y = L\cos\alpha \\ J_x &= L_x + C = L\sin\alpha + C \end{aligned} \tag{6.23}$$

The horizontal and vertical loads on the jib are related by the offset angle, θ_j:

$$J_x = \frac{J_y}{\tan\theta_j} = \frac{L\cos\alpha}{\tan\theta_j} \tag{6.24}$$

Therefore,

$$C = J_x - L_x = \frac{L\cos\alpha}{\tan\theta_j} - L\sin\alpha \tag{6.25}$$

The determination of the horizontal cable load, C, allows us to calculate the loads at point 3, as shown in Figure 6.46.

$$\begin{aligned} O_x + C_{tx} - C &= 0 \\ O_y - C_{ty} &= 0 \end{aligned} \tag{6.26}$$

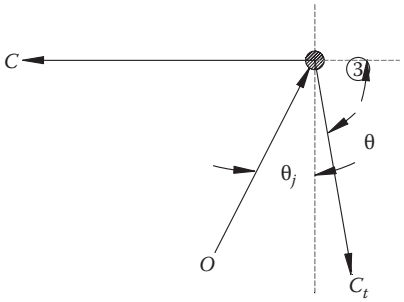

Figure 6.46 Free body diagram at point 3. Where C_t is the load carried by angled cable (kip), O is the load carried by jib support (kip).

Again, summing forces acting at point 3 and considering the angles of the cable and jib support,

$$\tan\theta = \frac{C_{ty}}{C_{tx}}$$
$$\tan\theta_j = \frac{O_x}{O_y} \tag{6.27}$$

The following loads are given:

$$O_x = C_{tx}\tan\theta\tan\theta_j$$
$$O_y = C_{tx}\tan\theta$$
$$C_{tx} = \frac{C}{1+\tan\theta\tan\theta_j}$$

The free body diagram at point 2 is represented in Figure 6.47.

$$J_x - B_x - O_x = 0$$
$$B_y - J_y - O_y = 0 \tag{6.28}$$

Summing Forces

Equations 6.23 and 6.28 provide the determination of the horizontal and vertical loads acting on the boom:

Finally, the Pythagorean theorem gives us B:

$$B = \sqrt{B_x^2 + B_y^2} \tag{6.29}$$

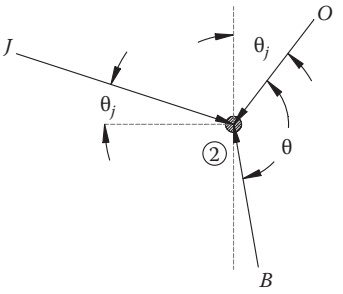

Figure 6.47 Free body diagram at point 2. Where *B* is the load carried by boom (kip).

$$B_x = J_x - O_x = \frac{L\cos\alpha}{\tan\theta_j} - C_{tx}\tan\theta\tan\theta_j$$
$$B_y = J_y + O_y = L\cos\alpha + C_{tx}\tan\theta \tag{6.30}$$

The determination of *B* quantifies the compressive load carried by the boom. Since the boom is a boxed truss, the load is separated and transferred through the support members. Since four steel angles enclose the box, the load through each angle, *P*, can be assumed to be one-quarter of the load:

$$P = \frac{1}{4}B \tag{6.31}$$

The failed section can be analyzed as a column since a compressive axial load is carried. However, the failure occurred because of a combined axial and flexural load. The bending is produced by a moment, which is caused by an eccentric load as represented in Figure 6.48.

Since the load is applied at the centroid, which lies outside of the cross section, a moment, *M*, is created:

$$M = P \times x \tag{6.32}$$

The actual stresses created by the loading are determined by the following:

$$\sigma_{cen} = \frac{P}{A}$$
$$\sigma_{bend} = \frac{M}{S} \tag{6.33}$$

where

σ_{cen} is the axial stress (ksi)
σ_{bend} is the bending stress (ksi)
A is the cross-sectional area (in.^{2})
S is the section modulus (in.^{3})

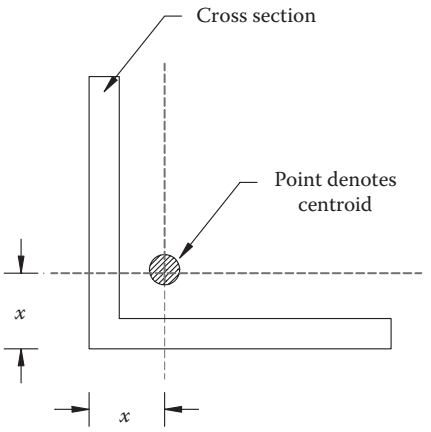

Figure 6.48 Eccentric load. Where *x* is the centroidal distance, (*x* is equal in both axes because angle legs are equal).

The actual loads must be compared to the design loads in order to determine the likelihood of failure. The interaction equation (I.E.) allows the conditions of failure to be determined:

$$\text{I.E.} = \frac{\sigma_{cen}}{\sigma_{all\_c}} + \frac{\sigma_{bend}}{\sigma_{all\_b}} \leq 1.0 \tag{6.34}$$

where

$\sigma_{all\text{-}c}$ is the allowable axial stress (ksi)
$\sigma_{all\text{-}b}$ is the allowable bending stress (ksi)

The value calculated for I.E. must be less than or equal to 1.0 for the member to be adequate. If the I.E. value is above 1.0, then the member will fail.

The allowable stresses are based on safety factors determined by the American Institute of Steel Construction (AISC):

$$\sigma_{all\_c} = \frac{\sigma_{CR}}{F.S.}$$
$$\sigma_{all\_b} = 0.66\sigma_y \tag{6.35}$$

where

σ_{CR} is the critical axial stress (ksi)
σ_y is the yield stress of steel = 36 ksi
F.S. is the factor of safety = 1.92

The critical axial load is dependent on the length of the failed member and the connections at each end:

$$\sigma_{CR} = \frac{n\Pi^2 Er^2}{l^2} \tag{6.36}$$

where

r is the radius of gyration (in.)
E is the modulus of elasticity = 29,000 ksi
l is the length of member (ft)
n is the effective length factor

The failure occurred at the end member of a 40 ft section. On one end, the angle is connected to a perpendicular 3 × 3 × ⅜″ angle and an adjoining 3½ × 3½ × ½″ angle. The other end is denoted by the web member attached to the failed member. These connections and the properties of the adjoining members provide a value for the effective length factor. Consider the diagram of the column connections as shown in Figure 6.49.

The effective length factor is determined by the K value for the column:

$$n = \frac{1}{K^2} \tag{6.37}$$

The K value is calculated from an alignment chart, which uses G values for each end connection. The G values are given by the summation of the column moments of inertia (I_c) divided by the column lengths (l_c), which is divided by the summation of the girder moments of inertia (I_g) divided by the girder lengths (l_g):

$$G = \frac{\sum(I_c / l_c)}{\sum(I_g / l_g)} \tag{6.38}$$

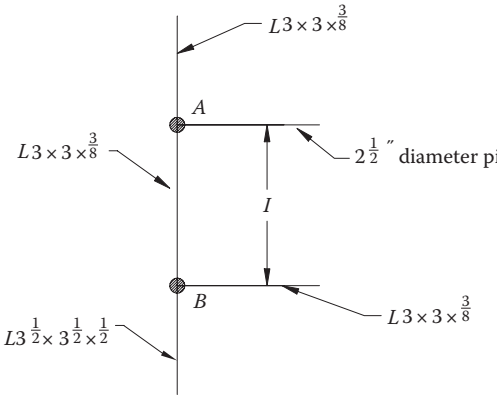

Figure 6.49 Column connections.

The G values calculated at each end are used in the appropriate alignment chart, which provides the values for K. From the known lengths and moments of inertia, a range for n can be determined:

$$1.50 \le n < 1.83$$
$$n_{avg} = 1.665$$

Gouge Spacing

Relative to Vehicle Motion and Wheel Lug Distribution

Large trucks have significant front wheel lugs that attach the front wheels to the axle assemblies. If those attachments protrude beyond the outer surface of the tire while the vehicle is rolling over, then gouges are produced on the road surface. The spacing of the gouges that are produced can be analyzed according to the lug distribution and the velocity of the vehicle. Consider the wheel shown in Figure 6.50 with an impending lug moving toward the creation of a gouge.

The angular velocity of the wheel is given by

$$\frac{S_A}{2\pi R_2} = \frac{\theta_A}{2\pi} \Rightarrow S_A = R_2\theta_A \tag{6.39}$$

Differentiating with respect to time yields

$$\bar{v}_A = R_2 \frac{d\bar{\theta}}{dt} = R_2 \bar{w} \tag{6.40}$$

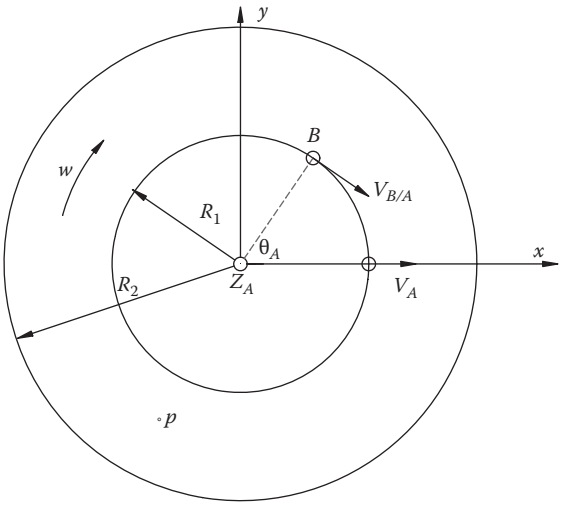

Figure 6.50 Wheel.

where

$$\overline{w} = \frac{\overline{v}_A}{R_2}\frac{(\text{in./s})}{(\text{in.})} = \frac{-v_A}{R_2}\overline{k}(\text{rad/s}) \tag{6.41}$$

where

$\overline{w}$ is the angular velocity
R_2 is the tire radius
R_1 is the lug radius
$\overline{ijk}$ is the Cartesian unit vectors

Velocities of rolling motion must be resolved into two components: translation with the center at "*A*" and rotation about the center at "A." In translation, all points of the wheel move with the same velocity $\overline{v}_A$. In rotation, each point of the wheel moves about "*A*" with a relative velocity

$$\overline{v}_{P/A} = \overline{w} \times \overline{R}_{P/A} \tag{6.42}$$

where $\overline{R}_{P/A}$ is the position vector of "*P*" relative to "*A*."

Accordingly, the velocity at a point "*P*" can be determined from the vector sum

$$\overline{v}_P = \overline{v}_A + \overline{v}_{P/A} = \overline{v}_A + \overline{w} \times \overline{v}_{P/A} \tag{6.43}$$

The velocity $\overline{v}_A$ of a moving vehicle whose wheel lugs create gouges on the pavement surface can therefore be analyzed in the following manner:

$$\overline{v}_B = \overline{v}_A + \overline{v}_{B/A} = \overline{v}_A + \overline{w} \times \overline{R}_{B/A} \tag{6.44}$$

Please refer to Figure 6.51 for the wheel vectors.

where

$$\overline{v}_{B/A} = R_1(\cos\theta\bar{i} + \sin\theta\bar{j}) \tag{6.45}$$

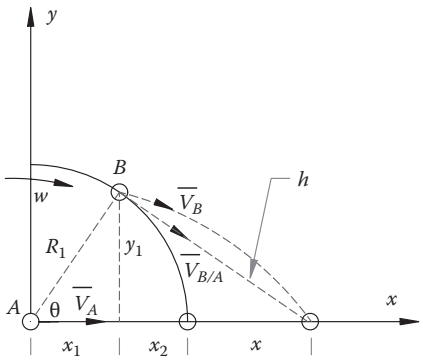

Figure 6.51 Wheel vectors.

or

$$\bar{v}_B = \bar{v}_A + \left(\frac{-v_A}{R_2}\bar{k}\right) \times \left[R_1(\cos\theta\bar{i} + \sin\theta\bar{j})\right] \tag{6.46}$$

where

$x_1 = R_1 \cos\theta$
x is the gouge spacing
$\theta = 2\pi/5$ for five lugs
$\theta = 2\pi/10$ for 10 lugs

For a wheel consisting of five lugs,

$$\bar{v}_B = v_A(1.38\bar{i} - 0.124\bar{j}) \tag{6.47}$$

or

$$|\bar{v}_B| = 1.385\,|\bar{v}_A| \tag{6.48}$$

for a wheel consisting of 10 lugs,

$$\bar{v}_B = v_A(1.324\bar{i} - 0.245\bar{j}) \tag{6.49}$$

$$|\bar{v}_B| = 1.35\,|\bar{v}_A| \tag{6.50}$$

From Figure 6.51, the hypotenuse can be determined as follows:

$$y_1 = R_1 \sin\theta \tag{6.51}$$

$$h = \sqrt{y_1^2 + (x + x_2)^2} \tag{6.52}$$

$$h = \sqrt{R_1^2 \sin^2\theta + (x + R_1(1 - \cos\theta))^2} \tag{6.53}$$

In Equation 6.45 we can approximate the hypotenuse as $h \approx v_B\theta/w$ so

$$x \approx \sqrt{(v_B\theta/w)^2 - R_1^2 \sin^2\theta} - R_1(1 - \cos\theta) \tag{6.54}$$

The lug spacing then becomes

$$(v_B\theta/w)^2 = R_1^2 \sin^2\theta + (x + R_1(1 - \cos\theta))^2 \tag{6.55}$$

Calculations on the gouge spacing for five lug and ten lug wheels at velocities ranging from 20 to 70 miles per hour can be made. Additionally, if the wheel rotation slips by 10% from its nominal value, that is,

$$\overline{w}_s = 1.1\overline{w} \tag{6.56}$$

The corresponding wheel spacings can be calculated. This analysis reveals that five lug wheels produce gouges 32 in. apart with no slip and 28.3 in. apart with 10% wheel slip. Similarly, ten lug wheels produce gouges varying between 16.6 and 14.8 in. apart. It should be noted that the gouges are irrespective of vehicle speed.

Broken Pole Analysis

When a vehicle impacts a telephone pole, a bridge railing, or any unmovable barrier, the work produced is irreversible. In general, the application of the energy method states that the total energy of the system prior to the accident is equal to the total energy of the system after the accident plus the irreversible work done during the accident interval. In equation form, the conservation of energy is stated as follows:

$$E_i = E_f + u \tag{6.57}$$

where

E_i is the total energy of the system prior to the collision
E_f is the total energy of the system after the collision
u is the total irreversible energy produced by the collision

It is noteworthy that irreversible work is done by the conversion of kinetic energy. Potential energy must first be converted into potential energy before it can be dissipated as irreversible work. In a conservative system, there is reversibility between the potential and kinetic energies, and there is not irreversible work.

In a nonconservative system, the total energy change due to the collision including kinetic and potential energy may be described as

$$\Delta E = E_i - E_f = u \tag{6.58}$$

Generally,

$$\Delta E = \Delta(E_k + E_p) \tag{6.59}$$

where

E_k is the kinetic energy
E_p is the potential energy

Table 6.3 Vehicle Speed (*v*, mph)

Dependence on Pole Diameter (D) and Ultimate Pole Strength (U_{shear})					
U_{shear}	2000	2250	2500	2750	3000
D					
10	40.9	43.4	45.7	47.9	50.0
11	44.9	47.6	50.3	52.7	55.0
12	48.7	52.0	54.8	57.5	60.0

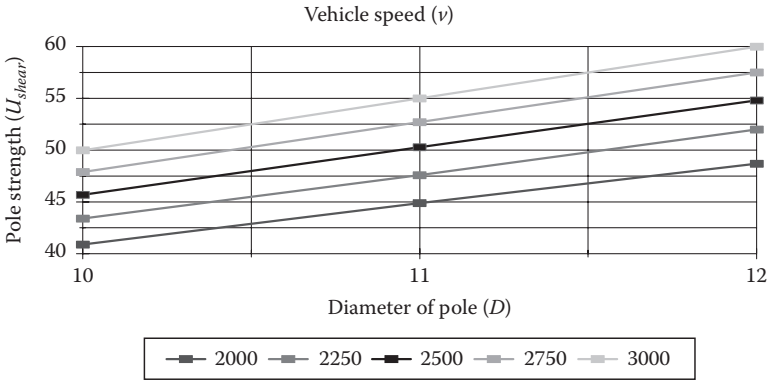

Figure 6.52 Graph of speeds.

When a vehicle collides with a pole on level ground, there is no change in potential energy, so that Equations 6.58 and 6.59 can be combined as

$$\Delta E = \Delta E_k = \frac{1}{2} mv^2 = U_{shear} \tag{6.60}$$

where U_{shear} is the shear strength of pole which broke as a result of the collision.

Most poles vary in diameter, D, from

$$10'' < D < 12''$$

and the shear strength of wooden poles varies according to

$$2000 \text{ lb/in.}^2 < U_{shear} < 3000 \text{ lb/in.}^2$$

From Equation 6.60, we can solve for the vehicle speed required to shear the pole according to the constraints listed earlier. We have assumed the weight of the vehicle to be 2800 lb. Table 6.3 lists the vehicle speeds depending on the pole diameter and the shear strength of the pole.

The pole in question had an approximate diameter of 10–11 in. and was quite old. Table 6.3 and Figure 6.52 indicate that the pole impact analysis due to crush as performed is within engineering accuracy with respect to the analysis.

Slips and Falls
Injuries to Humans

7

Introduction

In this chapter we attempt to quantify most of the ways in which humans are injured as a result of the environment, the workplace, their activities, their actions, or the actions of others. It is important to note that some activities or incidents are not generally injurious to humans. When small children fall, the distances and forces upon their bodies are considerably less than when adults fall. The biological structures of children are more pliable and less prone to injury. In contrast, adults, especially the elderly, have weakened biological structures and are more capable of being injured. In some instances, the elderly have preexisting conditions, such as fractures of their bones, that may contribute to an injury. In this respect, emphasis is placed on the strength of biological materials that comprise the human anatomy. Human evolution, as with evolution of all animal types, has placed a minimum requirement for injury to particular structures. Otherwise, humans and animals would have a difficult time in their environment and most likely would not survive the natural dangers that present themselves. Let us make it clear that we are not talking about long-term environmental and climatic events and changes that may affect the long-term survival of the particular human species. Rather we are concerned with incidents that are drastic and sudden such as car crashes, falls, and other incidents that have the capacity to maim or kill.

A couple of simple examples will explain a typical characteristic which may be injurious to some but not to others. To further explain let us look at human evolution from a perspective of our modern world. Before the world became industrialized and urban, the dangers posed by the environment were much less: roads and walkways were much softer (dirt as opposed to concrete), and travel was mainly by foot rather than by high-speed transportation. When people walked, they generally walked on slip-resistant surfaces, and if they fell, the ground was much softer. Today, walking surfaces have the capability of being very slick and not particularly slip resistant. The surfaces are much harder and may have the potential for injury. The modern shoe, some with leather or synthetic soles, might also be quite slippery on certain surfaces. Women's high-heeled shoes defy the ability to walk in a normal fashion. A particular walking surface may be perfectly safe for pedestrian traffic under most weather conditions. However, under wet or frozen conditions, the walking surface may become impossible to walk on. In such cases, standard of care must be considered. Standard of care falls upon the walking surface owners or keepers and on the person walking.

The next four sections in this chapter discuss walkway safety, standard of care, the American Disabilities Act, and testing of slip resistance or walking surfaces. These four topics are integrally tied together. Walkway safety is codified by certain standards. These standards were developed from scientific studies conducted by various organizations of private industry and government. Walkway safety is concerned with providing means of egress from buildings in case of emergencies such as fires. Standard of care

addresses the responsibility of the premises' owner or keeper. Again, there are standards that delineate the responsibilities of the owner of the premises. Codes do not address the responsibility of the person who is walking and may be subject to falling or being injured. However, in some instances, the actions of the pedestrian may be the primary cause of the fall or injury. These types of issues must always be considered when performing calculations and attempting to report on the root cause of the incident. The American Disabilities Act ensures that proper means of access is provided for people who have physical limitations on their means of propulsion. In such an analysis, the codified requirements are very clear and succinct. Taking these three topics together, the forensic engineer must make certain basic measurements in order to ensure that the walking surface was code compliant. These measurements include, lengths, widths, slopes, treads, risers, sight distances, and frictional slip resistance tests. The rest of the chapter is devoted to various types of human injuries and the tolerance of the human body to mechanical insult.

Walkway Safety

In order to put walkway safety into perspective, it is necessary to give some insight into its historical development. Prior to 2000 most states and municipalities in the United States had adopted the Building Officials and Code Administrators (BOCA) Code. The BOCA Code dated back approximately 50 years and was reissued every two or three years in order to keep up with modern changes. During that era there were two other important codes promulgated in the United States that included the International Conference of Building Officials (ICBO) and the Southern Building Code Congress International (SBCCI). Although these three codes were very similar, some discrepancies between the codes existed. The International Code Council (ICC) determined to draft a comprehensive set of regulations for building systems that were consistent and exclusive of the existing codes. This effort led to the first edition of the 2000 International Building Code (IBC). A new edition of this code is promulgated every three years and is designed to protect the public health, safety, and welfare.

Walkway safety includes protections for people with disabilities. The provisions for disabled persons are covered within the IBC and are further expanded in ICC/ANSI A 117.1 Accessible and Usable Buildings and Facilities. The acronym ANSI stands for American National Standards Institute. The scope of the IBC applies to the construction, alteration, movement, enlargement, replacement, repair, equipment, use and occupancy, location, maintenance, removal, and demolition of buildings and structures. Family dwellings are covered under the International Residential Code. The intent of these codes is to safeguard life and ensure safety through minimum requirements. In addition to these codes, the National Fire Protection Association has promulgated NFPA 101 Code for Safety to Life from Fire in Buildings and Structures. The Code of Federal Regulations (CFR) deals with public safety and the safety in the work place. The most common source for this information is contained within 16 CFR Commercial Practices, 29 CFR Labor, 30 CFR Mineral Resources, and 49 CFR Transportation. It should be emphasized that walkway safety deals with not only the surface that is being traversed but also all the other appurtenances required for the protection of the individual, which include fall protection devices, ladders, scaffolding, chutes, rollover protection, falling object protection, and associated components.

When the forensic engineer is examining or analyzing a case where an individual has been injured or killed, the applicable codes must be researched in order to determine if a code violation existed that contributed to the incident. In this respect it is also important to determine if the code sections studied are retroactive or not. Whenever possible, the applicable code year promulgation should be studied. Sometimes the code interpreted by the engineer may or not be retroactive. That is, for example, was the building retrofitted to comply with recognized standards such as the accessibility standard for handicapped persons? Some codes are not retroactive and should not be applied. When structures or buildings were erected, they may or may not have been in accordance with applicable codes. If they were not according to an applicable code, according to the situation of the case, then citing the code and its relationship to the incident is pertinent. However, if the structure was built according to the existing code and the code later changed so that the incident could be tied to the new code requirements, then the new code is only applicable if it is retroactive.

Standard of Care

Standard of care is a rather nebulous term. To an attorney it may mean completely a different thing than to a forensic engineer. As engineers, we deal with concrete facts whenever possible. We quantify, measure, calculate, and then describe. In explanatory terms let us analyze a slip and fall case outside a store in a city from two perspectives under two different climatic conditions. First consider that 20 in. of snow fell the previous night and the city was essentially shut down the next morning. The salt trucks were not yet operating. The store owner could not open up because he could not get to the store. Nothing was moving except for some youngsters who lived near the store who decided to play in the snow. While playing at the entrance of the store, one of the youngsters fell and broke his arm. Was the store responsible for not providing standard of care? Codes require that the means of egress, the walking surfaces, need to be kept clear of potential hazards. Was snow a hazard? Yes, but the circumstances surrounding the events were unusual and the store owner could not foresee the events that led to the incident. If he or his representatives could not get to the store to shovel the snow and since the mayor of the city closed all businesses, he could not proceed with his duties. Second, the store was open for business on a sunny, dry Saturday but the exit walkway had a 2 in. drop at an expansion joint. A lady carrying packages tripped on the walkway at the elevation differential in the expansion joint and broke her arm. This walkway had been in that condition for years and was not repaired by the owner although various complaints had been filed about the condition of the walking surfaces. Does the lady have a case? The walkway does not meet recognized standards. Standard of care by the store owner was not carried out.

Alternatively, an inebriated individual enters the store, falls, and breaks his teeth. The walking surface is measured at the point of the fall and is determined to have a difference of elevation at an expansion joint of one-quarter of an inch. The individual sues. Does he have a case? The standard for elevation transitions is one-half inch. The standard of care then falls on the impaired individual. Additionally, we as humans should always be aware of our environment and the actions that we take. Codes are designed to provide the minimum of safety under most conditions. Logic along with measurable quantities should dictate where the standard of care rests.

American Disabilities Act

The University of Illinois conducted research on the accessibility of buildings and walkways in the late 1950s. This work was a product of a grant from the Easter Seal Research Foundation and resulted in the 1961 edition of ANSI Standard 117.1, which outlined the first codified criteria for accessibility for persons with physical disabilities. Through the past 50 years ANSI 117.1 has undergone extensive modifications, reaffirmations, and additions. Large segments of the changes have taken place in 1971, 1974, 1980, and 1987. By the 1987 edition, elements of the Council of American Building Officials (CABO) were incorporated into the development of the standard and its adoption to the building code. It took another 10 years to achieve the melding of BOCA and ANSI 117.1. In 1998 CABO was consolidated with the ICC. At the time of this writing, the latest edition (2009) has improved the level of coordination between the Fair Housing Accessibility Guidelines, the American Disabilities Act, and the Architectural Barriers Act Accessibility Guidelines.

The purpose of ANSI 117.1 is to make sites, buildings, facilities, and elements accessible to people with physical disabilities. Physical disabilities are broadly defined to include hearing, impairment, visual impairment, and extremes of physical size among the more common ambulatory disabilities. At this point you might wonder that if you are investigating a slip and fall case where your client was not physically disabled, would ANSI 117.1 apply? The answer is generally yes because of the incorporation and coordination with the ICC. In essence, the requirements for walking surfaces and changes in elevation are identical for both codes. Additionally, the incorporation by reference of a variety of other codes in ANSI 117.1 allows for cross referencing.

Testing of Slip Resistance of Walking Surfaces

Over the years, various contraptions have been devised to measure the slip resistance of walking surfaces. The general term used for these devices is tribometer. The basic definition of a tribometer is that of a device that measures the slip resistance or friction between two surfaces. Some of these machines utilize a standard representative sole to simulate a shoe. Some of these machines are taken to the site where the slip and subsequent fall occurred and tests are conducted. Sometimes a representative sole is used on a representative walking surface and then tests are conducted.

Various technical papers have been presented over the years that attempt to duplicate the natural walking or running gate of humans. These valiant efforts place specific importance on various characteristics of walking, running, or slipping. So the questions to be asked are as follows: Do these machines represent the actual slip-resistant conditions at the time of the fall? Do the technical papers represent the gate and the nature of the fall in the particular case? We don't think so as we will explain.

First let us address the question of what machine to use. Any machine that uses some representative sole or surface yields irrelevant results. In order to determine the slip resistance of the particular shoe on the particular surface, any test performed must include the shoe and the surface. One tribometric machine uses a standard leather sole. Not only are leather soles generally different from one shoe to another but are distinctly different with rubber soles or synthetic materials used in the shoe industry. Furthermore, the amount of

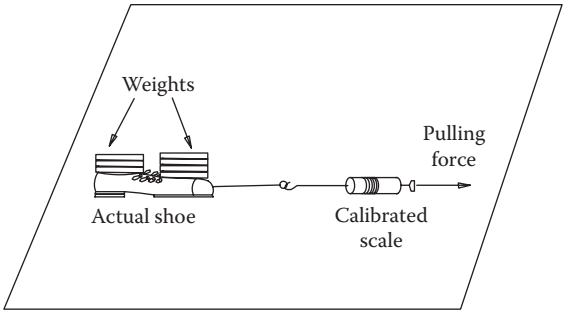

Figure 7.1 Testing for slip resistance.

wear on the shoe is a factor in its slip resistance, and the wear pattern on the show affects its slip resistance. The wear pattern on the shoes is significant to answer the second question that we posed. Testing for slip resistance is only meaningful if the particular shoe is used on the actual surface consistent with the conditions present at the time of the fall.

What machine does the forensic engineer use in order to more closely replicate the slip resistance of the surface? The forensic engineer reverts to what he learned in introductory physics when the issue of coefficient of friction was addressed. The actual shoe is obtained, and various weights are used along with a spring scale that is calibrated. Then a series of tests are performed on the actual surface with various weights and in various directions. These tests should validate the difference between the static and the dynamic coefficient of friction, the effect that contact area and weight are not functions of the frictional coefficient, and give an accurate representation of the slip resistance of the shoe–surface interaction. The data are analyzed and plotted and the results of the tests are then compared to what is considered a safe walking surface. Walking surfaces with a coefficient of friction above 0.5 are considered slip resistant. Safe walking surfaces under normal dry conditions are those with a coefficient of friction above 0.3.

It is truly amazing to see how different people walk. Some walks resemble a duck, a chicken, a penguin, a pigeon, etc.; some have a high step gait, others a shallow gait; some drag one or more of their feet; some bounce on their toes in an athletic manner; some lumber along. Some people have preexisting conditions that may contribute to the gait, some are thin, others obese, some are young, others are old. This discussion attempts to address the second question we posed. The manner in which people walk or ambulate is extremely diverse, impossible to quantify, and pertinent to the wear pattern on their shoes. The only factors that can be factually addressed are weight, age, health, and distinctive walking pattern. The diagram in Figure 7.1 represents the method used to determine the coefficient of friction on the walking surface.

Force Required to Pull a Dolly

A soda delivery person was unloading product on a dolly and carrying the load up a ramp at the rear of a store. The ramp was covered in ice and snow, and the store personnel had not made efforts to clear the ramp surface. In the process of carrying the load up the ramp, the person slipped, fell, and sustained injuries. Note the low values of frictional coefficient used in the Table 7.1 to represent the icy conditions.

Table 7.1 Force Required to Pull a Dolly and Load Up a Ramp

	$\mu_s = 0.05$		$\mu_s = 0.10$		$\mu_s = 0.15$	
A_i	F_h	F	F_h	F	F_h	F
0	12.82	17.27	25.65	32.96	38.47	47.30
2	21.76	29.30	34.58	44.44	47.39	58.26
4	30.67	41.30	43.57	55.86	56.26	69.16
6	39.55	53.25	52.30	67.22	65.05	79.98
8	48.37	65.53	61.07	78.49	73.77	90.69
10	57.14	76.94	69.77	89.67	82.40	101.30
12	65.84	88.65	78.38	100.74	90.93	111.78
14	74.46	100.25	86.9	111.69	99.34	122.13
16	82.99	111.73	95.31	122.50	107.64	132.33
18	91.41	123.07	103.61	133.16	115.80	142.37

Dependence on coefficient of friction μ_s, angle of incline a_i, and angle of pull.

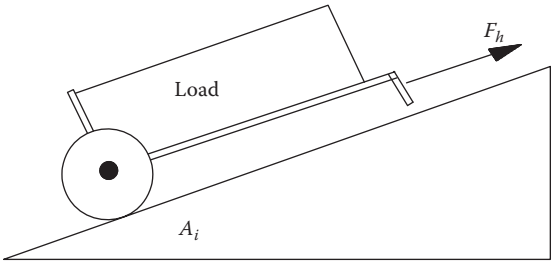

Figure 7.2 Dolly on a ramp.

The analysis used to compute the forces in Table 7.1 follows:

A free body diagram of the forces involved if the load is pulled horizontally F_h, and the ramp are shown in Figure 7.2.

Summing forces

$$\Sigma F_y = 0$$

$$N = W\cos\theta$$

$$\Sigma F = 0$$

$$F_h = f + W\sin\theta$$

$$\mu = \frac{f}{N} \rightarrow f = \mu N \tag{7.1}$$

$$F_h = \mu N + W\sin A_i \tag{7.2}$$

$$F_h = \mu W\cos A_i + W\sin A_i$$
$$F_h = W(\mu\cos A_i + \sin A_i) \tag{7.3}$$

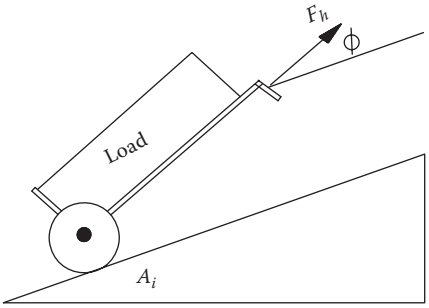

Figure 7.3 Dolly on a ramp on an angle.

If the force is applied at an angle φ, which is a more realistic scenario, then the free body diagram is shown in Figure 7.3.

Summing forces

$$\Sigma F_y = 0$$

$$F\sin\varphi + N = W\cos A_i$$

$$\Sigma F_x = 0$$

$$F\cos\varphi = f + W\sin A_i$$

But

$$f = \mu N$$

1. $F\sin\varphi + N = W\cos A_i$
2. $F\cos\varphi - \mu N = W\sin A_i$

$$F = \frac{\begin{vmatrix} W\cos A_i & 1 \\ W\sin A_i & -\mu \end{vmatrix}}{\begin{vmatrix} \sin\varphi & 1 \\ \cos\varphi & -\mu \end{vmatrix}} = \frac{-W(\mu\cos A_i + \sin A_i)}{-(\mu\sin\varphi + \cos\varphi)} \tag{7.4}$$

$$F = \frac{W(\mu\cos A_i + \sin A_i)}{(\mu\sin\varphi + \cos\varphi)} \tag{7.5}$$

F will be a minimum when the denominator is a maximum; therefore, differentiate and set to zero:

$$\frac{d}{d\varphi}(\mu\sin\varphi + \cos\varphi) = 0 \tag{7.6}$$

$$\mu\cos\varphi - \sin\varphi = 0 \tag{7.7}$$

$$\mu\cos\varphi = \sin\varphi$$

$$\mu = \tan\varphi \tag{7.8}$$

Biomechanics of Falls

According to Randall Noon, slip, trip, and fall pedestrian accidents account for approximately 12,000 deaths in the United States. The number of men dying from falls is relatively even when compared to women. However, 86% of these deaths occurred to people older than 45 years, indicating that age is a contributing factor to death from a fall. Arthur Damask states, "The act of walking involves the following sequence of motion: (1) The walker leans forward so that the center of mass of the body is forward of the support of the tibia against the talus. (2) In this position, the walker would fall, but the hip is raised slightly on one side so that the body weight is shifted to the down side while the up side frees its leg to swing forward. Note that at this point, if something catches and holds the foot, the center of mass will cause the body to fall face downward. We say that the walker has tripped…" Figure 7.4 represents Damask's description of a tripping incident.

In a hypothetical incident, Joan Falldown claimed to be walking out of a store and across the parking lot when she slipped and fell as a result of wet granular material on the parking lot surface. A case was brought for the failure of the store owners to help the walking surfaces of the parking lot free of debris, which might cause pedestrians to slip and fall. The physical evidence on the parking lot was found to be contrary to a slip and fall incident and consistent with a trip and fall incident. The location of the fall was reported to be at the location of a parking barrier.

A review of the medical records indicates that Mrs. Falldown received injuries to her nose, knees, and hands. These medical records are consistent with the statements and depositions of Catherine Sawitall and Mandy Meetoo, witnesses to the event. The injuries are consistent with a trip and fall incident and not with a slip and fall incident as we describe.

It was alleged that granular material on the pavement caused Mrs. Falldown to fall and become injured. Therefore, it was necessary to analyze the fall with respect to stepping on a surface (such as pebbles, rocks, etc.), which would act like ball bearings and cause a slip and a fall. Damask explains, "If the person unknowingly steps on a wet spot in which the coefficient of friction with the shoe is 0.3, there will not be sufficient friction force to prevent the shoe from sliding forward, and the result is a slip and fall accident." It should be noted that by all reports, the area of the parking lot at the time of the incident was not wet. However, the introduction of granular material would reduce the coefficient of friction so that the biomechanics of the fall would be similar to that on a wet floor. Figure 7.5 represents a slip and fall scenario. In this scenario, we would expect injuries to the buttocks and to the ligaments of the legs at the knees or hips. There may also be some injuries to the hands but not necessarily to both knees or the nose. One knee may be affected, but only in trip cases are both knees generally affected.

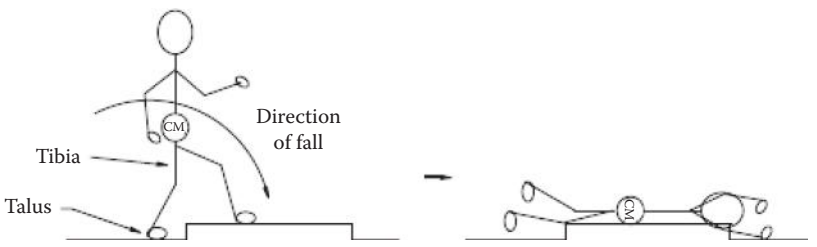

Figure 7.4 Tripping incident.

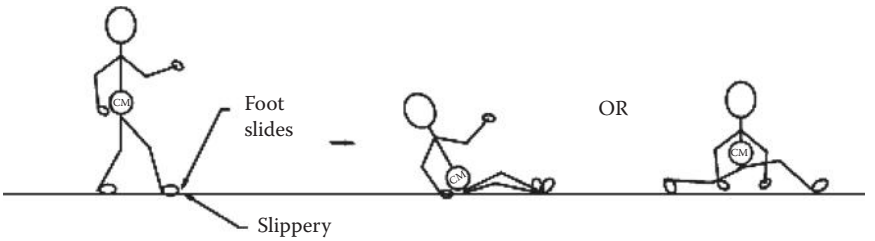

Figure 7.5 Slip and fall incident.

This analysis reveals that calculations are not always necessary and that impartial witnesses and medical records may be sufficient to dispute the claims that are made. In this case the lady was walking across the parking spaces carrying packages and stepping over the tire barriers. As she stepped over one barrier, she tripped and fell forward.

Sight Distance for Pedestrians

Sight distance is dependent on a variety of factors. The most obvious is the physical obstruction by an object. Pedestrian sight distance is also a function of the potential for injury with a moving object such as a car, truck, train, or motorcycle. All of these objects have a great potential for creating significant injury or death to pedestrians. When measuring sight distance, the Green Book, the Geometric Design of Highways and Streets, specifies definite criteria. It should be understood that the driver of a vehicle has an equal or greater responsibility for sight distance as a pedestrian. The sight distance is the distance along the road, street, or topology through which the object is continuously visible to each party. The distance depends on the height of the driver's eye and the height of the pedestrian relative to the road surface. The height of the driver's eye depends on the vehicle being driven and may vary from 3.5 to 7.9 ft. The height of the object, or in this case the pedestrian, is assumed to be at least 2 ft above the road surface. The area of approach, such as near an intersection, should be clear of obstructions that may block the view of the driver and the pedestrian. This area is known as the clear sight triangle and applies to an intersection where there is a crosswalk. A common type of an incident involving a vehicle and a pedestrian is at a crosswalk where several vehicles are stopped in some of the lanes and one lane is free. A pedestrian crossing in front of the stopped vehicles at the crosswalk may not be observed as the light changes, and a passing vehicle through the clear lane collides with the pedestrian. This type of collision is most prevalent when the view blocking stopped vehicle is a large tuck or van. These types of collisions require the calculation of the sight distance triangle relative to the speed of the vehicle. The following sections show some of the sight distance calculations for different scenarios.

Pedestrians and Trains

You would think that pedestrians and train collisions would be an oddity. Surely, this type of collision would rarely occur. Trains are loud, big, and sometimes fast. There are many signals such as whistles, gates, flashing lights, and crossing markers that warn vehicles and pedestrians when a train is approaching. The railroad tracks are clearly visible, flat, and generally free of visible obstructions. According to the 2010 Federal Railroad Administration statistics there has been a recent increase in pedestrian-train collisions. According to these

statistics, 451 pedestrians were killed and 382 injures in the United States in 2010. In 2009 there were 417 pedestrian deaths and 343 pedestrian injuries. The states with the most pedestrian train deaths and injuries were California, Texas, Illinois, Florida, and New York. We begin the calculation sections with the departure sight distance calculations for stopped vehicles or pedestrians for different train speeds.

Departure Sight Distance Calculations

The departure sight distance for stopped vehicles or pedestrians for a range of train speeds is given by

$$d_{\tau s} = 1.4667 V_t \left(\frac{V_G}{a_t} + \frac{L + 2D + W - d_a}{V_G} + J \right) \tag{7.9}$$

where

$d_{\tau s}$ is the sight distance along railroad tracks for a stopped vehicle or pedestrian (feet)
V_t is the velocity of train (mph) (34 mph by recording, for example)
V_G is the maximum speed of vehicle in first gear (8.8 ft/s), or 20 ft/s for running pedestrian
a_t is the acceleration of vehicle in first gear (1.47 ft/s^2)
L is the length of vehicle (65 ft)
D is the distance from stop line to nearest rail (15 ft)
J is the perception/reaction time (2 s)
W is the distance between outer rails (5 ft for single track) (18 ft measured)
$d_a = V_G^2/2a_t = (8.82)^2/2(1.47) = 26.4$ ft

Substituting the appropriate values for our case shown in parenthesis, we obtain

$$d_{\tau s} = (1.4667)(34)\left(\frac{8.8}{1.47} + \frac{65 + 30 + 18 - 26}{8.8} + 2 \right) \tag{7.10}$$

$$d_{\tau s} \approx 890\,\text{ft} \tag{7.11}$$

For a moving vehicle, the sight distance along the tracks is

$$d_\tau = \frac{V_t}{V_v}\left(1.47 V_v t_{pr} + \frac{V_v^2}{30f} + 2D + L + W \right) \tag{7.12}$$

while for a moving vehicle, the sight distance along the highway is

$$d_H = 1.47 V_v t_{pr} + \frac{V_v^2}{30f} + D + d_e \tag{7.13}$$

where

d_τ is the sight distance along the tracks for a moving vehicle or pedestrian (ft)
d_H is the sight distance along the highway for a moving vehicle or pedestrian (ft)
V_t is the velocity of train (mph) (34 mph)

V_v is the velocity of vehicle (mph) (25 mph)
t_{pr} is the perception reaction time (2.5 s)
f is the coefficient of friction (.375 for V_v = 30 mph)
D is the clearance distance from vehicle or pedestrian to nearest rail (15 ft)
L is the length of vehicle (65 ft)
W is the distance between outer rails (18 ft)
d_e is the distance from driver to front of vehicle (10 ft)

$$d_\tau \approx 350 \text{ ft} \tag{7.14}$$

$$d_H \approx 170 \text{ ft} \tag{7.15}$$

Moving Vehicle Sight Distance Calculations

For a moving vehicle or pedestrian, the distance along the highway is given by the following equation:

$$d_H = 1.47V_v + t_{pr} + \frac{V_v^2}{30_f} + D + d_e \tag{7.16}$$

where
V_v is the vehicle velocity
t_{pr} is the perception/reaction time (s), assumed a value of 2.5
f is the coefficient of friction from Table 7.2
D is the distance from front of vehicle to nearest rail (ft). Assumed 15 ft
d_e is the distance from driver to front wheel of vehicle. Assumed 10 ft
L is the length of vehicle
W is the distance between outer rails
V_T is the velocity of train
(from 15 to 65 ft)
(5 ft for single track)

$$d_{TM} = \frac{V_T}{V_v}\left(1.47V_v t_{pr} + \frac{V_v^2}{30_f} + 2D + L + W\right) \tag{7.17}$$

d_{TM} = distance along the tracks for a moving vehicle
d_H = distance along the highway
d_{TS} = distance along the tracks for a stopped vehicle

$$d_{TS} = 1.47V_T\left(\frac{V_G}{a_1} + \frac{L + 2D + W - d_a}{V_G} + J\right) \tag{7.18}$$

Table 7.2 Coefficient of Friction

Speed (mph)	f
10	0.4
20	0.4
30	0.35
40	0.32
50	0.3
60	0.29
70	0.28

For a stopped vehicle, the distance along the tracks is

where

V_G = maximum speed of vehicle in first gear. Assumed 8.8 fps
a_1 = acceleration of vehicle in first gear. Assumed 1.47 ft/s^2
J = sum of perception time and time to activate the clutch. Assumed 2 s
d_a = distance vehicle travels while accelerating to a maximum speed in first gear

or

$$d_a = \frac{V_G^2}{2a_1} = \frac{(8.8)^2}{2(1.47)} = 26.4 \text{ ft} \tag{7.19}$$

Substituting into Equation 7.1,

$$\begin{aligned} d_H &= (1.47)(V_v) + 2.5 + \frac{V_v^2}{(30)(.32)} + 15 + 10 \\ d_H &= 2.7.5 + (1.47)V_v + (0.104)V_v^2 \end{aligned} \tag{7.20}$$

This equation may be solved for various values of V_v to obtain Table 7.3.

Table 7.3 Distance vs. Speed

Vehicle Speed (V_v)	Distance along Highway (d_H)
0	27.5
5	37.5
10	52.5
20	98.4
30	165.1
40	237.9
50	360.9

Table 7.4 Distance vs. Speed

Vehicle Speed (V_v)	Distance along Tracks (d_{TM})
0	—
5	582
10	398.3
20	338.5
30	347
40	372.65
50	405.1

Substituting into Equation 7.2 for a train speed of 41 mph

$$d_{TM} = \frac{41}{V_v}\left((1.47)(2.5)V_v + \frac{V_v^2}{(30)(.32)} + 2(15) + 15 + 5\right)$$
$$d_{TM} = 150.6 + 4.27V_v + \frac{2050}{V_v} \tag{7.21}$$

For various vehicle speeds, we obtain Table 7.4.

Substituting, we obtain

$$d_{TS} = (1.47)(41)\left(\frac{8.8}{1.47} + \frac{15 + 2(15) + 5 - 26.4}{8.8} + 2\right) \tag{7.22}$$

$$d_{TS} = 642.6\,\text{ft}$$

Calculation of Train Speed

A train's speed may be determined from

$$V = \frac{21}{W}\left(-F_T t + \sqrt{F_T^2 t^2 + 0.065 L F_T W}\right) \tag{7.23}$$

where

W is the total weight of train in tons including locomotive
L is the train braking distance in ft
$t = T/1860 + 5.5$
T is the train length in ft
Locomotive weight 100–210 ton
Locomotive length 55–73 ft
Car length 55 ft
Car weight 30 ton

Train length

$$T = (9)(55) + 2(65) = 495 + 130 = 625 \text{ ft}$$

$$t = 625/1860 + 5.5 = \underline{5.8}$$

$$F_T = (\text{NC})(\text{NBR}_C)(W_C)(f_C) + (\text{BCP}_C/50) + (\text{NL})(\text{NBR}_L)(W_L)(f_L)(\text{BCP}_L/50) \pm F_g$$

$$F_g = gW = \text{force grade} = 0 \text{ in this case}$$

$$\text{NC} = \text{number of cars} = 9$$

$$\text{NL} = \text{number of locomotives} = 2$$

$$\text{NBR}_C = \text{empty car net braking ratio } \{19\% - 23\% \ (20\%) \text{ or } 38\% - 49\% \ (40\%)\}$$

$$W_C = \text{car weight in tons } (28 \square 35 \text{ ton})$$

$$f = \text{car coefficient of friction} = .1 \square 4 \approx .2$$

$$\text{BCP}_C = \text{car brake cylinder pressure} = 60 \square 90 \text{ psi}$$

$$F_T = (9)(.2)(30)(.2)(75/50) + (2)(.2)(130)(.2)(75/50)$$

$$F_T = 31.8$$

$$W = (2)(13) + (9)(30) = 260 + 27 - = 530$$

$$V = \frac{21}{530}(-31.8)(5.8) + \sqrt{(31.8)^2(5.8)^2 + (0.065)(1346)(31.8)(530)}$$

$$V = 41 \text{mph}$$

Human Injuries and the Strength of Human Tissue

Engineering students traditionally take a course on strength of materials. This topic is a follow-up to courses in statics and dynamics. The main thrust of a course in strength of materials is to study the behavior of materials under static and dynamic loading conditions. Strength of materials allows for the determination of the conditions necessary for the materials to fail. These computations are generally referred to as failure analysis, and they are an integral part of forensic engineering.

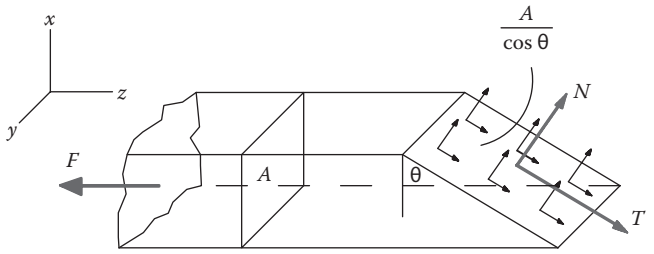

Figure 7.6 Stresses in an element.

The main topics studied in the mechanics or strength of materials are the concepts of stress, strain, elasticity, and loading both statically and dynamically. These concepts are analyzed under torsional, flexural, and shear loading. Loading may further be classified as static, sustained, impact, repeated, concentrated, or distributed. We can then summarize that the strength of materials is a study of the relationship between the loads that are applied to a non rigid body and the resulting deformations and internal forces that are induced in the body. In this case, the nonrigid body under study is the human body and most of its component parts. The human body is no different from any other body such as a beam or a column, for example, so that the same principles of the mechanics of materials apply. The values of the constitutive structures, the bones, ligaments, tendons, the soft tissues, etc., are simply a different value than for structural elements such as steel and wood. However, these biological materials have been widely studied, and their physical properties are very well understood. It is with this background that we introduce the basic components of the strength of materials concepts.

Simply defined, stress is the ratio of the force F per unit area A. Figure 7.6 shows an element that is subject to a force where a break may occur at a plane that is not normal to the axis. In fact, with actual structural elements such as bones, the breaks are usually ragged and angled as a result of the applied force. The applied force that produces the break may be due to tension, compression, flexion, or torsion, or a combination of these. For this analysis we are simply concerned with the maximum values of the stresses.

We define the stresses as follows:

σ = normal stress in tension or compression (psi)

τ = shearing stress (psi)

Summing forces in the normal and tangential directions,

$$\sum F_n = 0; \quad F\cos\theta = N = \frac{\sigma A}{\cos\theta} \tag{7.24}$$

$$\sigma = \frac{F}{2A}(1+\cos 2\theta) \tag{7.25}$$

$$\sum F_t = 0; \quad F\sin\theta = T = \frac{\tau A}{\cos\theta} \tag{7.26}$$

$$\tau = \frac{F}{2A}\sin 2\theta \tag{7.27}$$

The maximum values of the normal and shearing stresses are given by

$$\sigma_{max} = \frac{F}{A} \tau_{max} = \frac{F}{2A} \tag{7.28}$$

Note that the normal stress is either a maximum or minimum on planes where the shearing stress is zero. Shearing and normal stresses under axial loading will fail in tension on the transverse plane for brittle materials. In contrast ductile materials loaded in tension will fail in shear on the 45° plane. For calculations of bone fractures, it is sufficient to calculate the forces that break the bone assuming the maximum stresses. Then, some variability analysis can be introduced to take care of any uncertainties in the calculations.

Strain

Strain has to do with the elongation of an element. This elongation is exhibited by changes in the size or shape of the element. This change in the dimensions of the element is referred to as the deformation δ. As with stress, there are two types of strain.

ε = normal strain = deformation per unit length
γ = shearing strain = change in angle between the two planes

Figure 7.7 represents the characteristics of strain.

In equation form, the normal strain is given by

$$\varepsilon = \frac{\delta_n}{L}; \quad \varepsilon = \frac{d\delta_n}{dL} \tag{7.29}$$

For small deformations, the shearing strain is defined as

$$\gamma = \frac{\delta_s}{L}; \quad \gamma = \frac{d\delta_s}{dL} \tag{7.30}$$

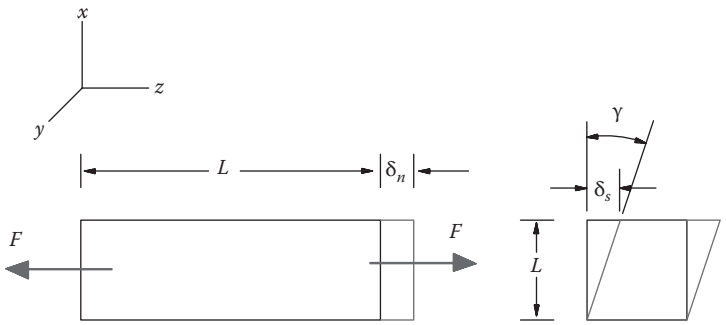

Figure 7.7 Normal and shearing strain.

Hooke's Law and Young's Modulus

Useful data for materials are the relationship between stress and strain. The data are referred to as stress–strain diagrams. These diagrams may be obtained for any material including biological structures such as bones, muscles, tendons, ligaments, organs, etc. The data are obtained by applying an axial load to a test specimen and measuring the load and deformation simultaneously. The stress is obtained by dividing the load by the initial cross-sectional area. Normal strain can be obtained by measuring the deformation δ in the length *L*. Shearing strains require the measurement of normal strains in several directions and then calculating the shearing strains by methods such as Mohr's Circle. A typical stress–strain curve looks like Figure 7.8.

Young's modulus or the modulus of elasticity is written as

$$E = \frac{\sigma}{\varepsilon}; \quad G = \frac{\tau}{\gamma} \tag{7.31}$$

where

E is used for normal stress and strain
G is used for shearing stress and strain

The modulus of elasticity is the slope of the straight line portion of the stress–strain diagram.

There are a variety of reference sources to obtain the values of the strength of biological materials. However, the most comprehensive source is by Yamada. This book has been out of print for several years so that we include some of the most pertinent data in the tables and graphs that follow. We strongly suggest referring to this invaluable source for a comprehensive and detailed listing of human strength properties.

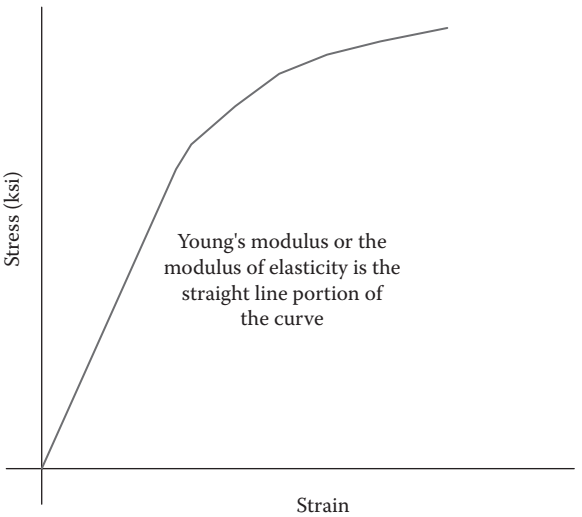

Figure 7.8 Stress–strain curve.

For this information we define the following acronyms:

UTS = ultimate tensile strength
UCS = ultimate compressive strength
UBS = ultimate bending strength
USS = ultimate shearing strength
UD = ultimate displacement
UTORS = ultimate torsional strength
MOE = modulus of elasticity

Table 7.5 gives the strength of human compact bone in kg/mm^2.

Table 7.6 gives the tensile properties of wet human bone for ages 20–39 in kg/mm^2.

Table 7.7 gives the shearing properties of wet human bone perpendicular to the long axis in kg/mm. The displacement is in mm.

Graphs in Figures 7.9 through 7.12 show the stress–strain curves for human bone under tension, compression, bending, and torsion.

The impact bending properties of human bone are 0.14 ± 0.018 kg cm/mm^2 and the impact snapping properties are 0.26 ± 0.029 kg cm/mm^2 in the radial direction and 0.19 ± 0.029 kg cm/mm^2 in the tangential direction.

Table 7.5 Strength of Bone

Age	10–19	20–29	30–39	40–49	50–59	60–69	70–79	80–89
UTS	11.6	12.5	12.2	11.4	9.5	8.8	8.8	
UCS		17	17	16.4	15.8	14.8		
UBS	15.4	17.7	17.7	16.5	15.7	14.2	14.2	
UTORS		5.82	5.82	5.37	5.37	4.96	4.96	4.96

Table 7.6 Tensile Properties of Bone

Bone	UTS	MOE
Femur	12.4 ± 0.11	1760
Tibia	14.3 ± 0.12	1840
Fibula	14.9 ± 0.15	1890
Humerus	12.5 ± 0.08	1750
Radius	15.2 ± 0.14	1890
Ulna	15.1 ± 0.15	1880
Average	14.0 ± 0.13	1830

Table 7.7 Shearing Properties of Bone

Bone	USS	UD
Femur	8.4 ± 0.18	0.60 ± 0.015
Tibia	8.2 ± 0.19	0.66 ± 0.014
Fibula	8.2 ± 0.59	0.69 ± 0.018
Humerus	7.5 ± 0.27	0.64 ± 0.012
Radius	7.2 ± 0.08	0.68 ± 0.040
Ulna	8.3 ± 0.18	0.71 ± 0.030
Average	7.97 ± 0.25	0.66 ± 0.022

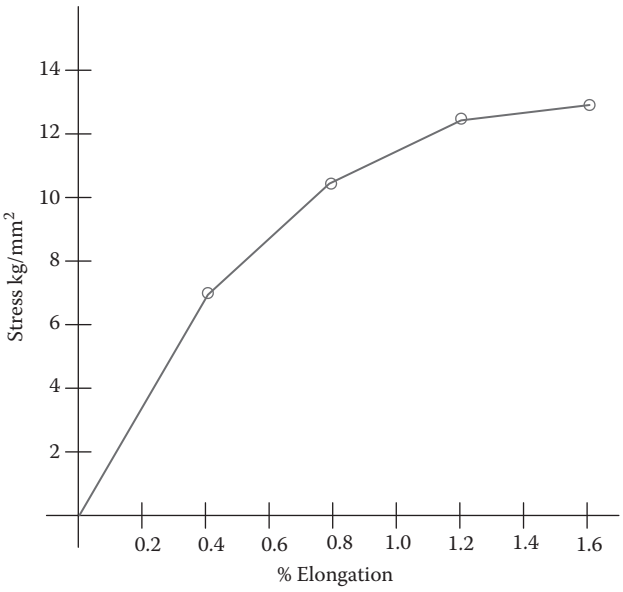

Figure 7.9 Human bone in tension (average of all bones).

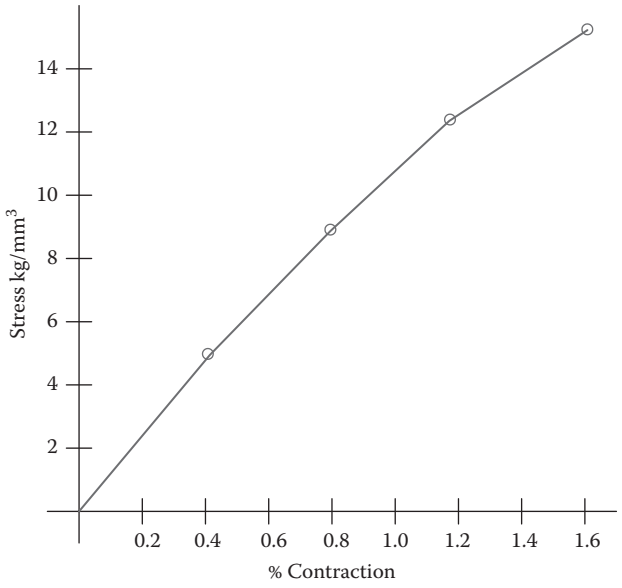

Figure 7.10 Human bone in compression (femur ages 20–39).

Human vertebrae for adult averages have the following tensile properties as shown in Table 7.8.

The adult average compressive properties of adult human vertebrae are given in Table 7.9.

The cross-sectional area and height of average adult vertebrae is given in Table 7.10.

The torsional properties of adult average vertebrae are given in Table 7.11.

Another human material that is subject to distress is cartilage. Hyaline cartilage usually covers the bony ends of joints and is somewhat transparent and glassy. Costal cartilage

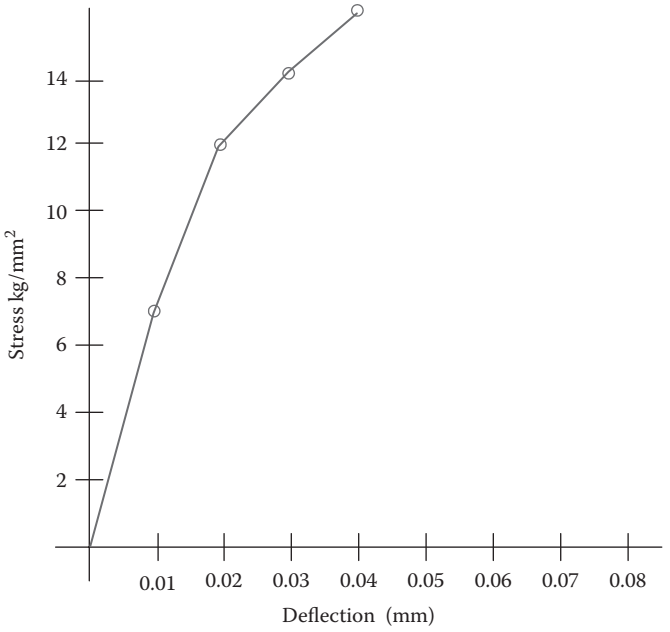

Figure 7.11 Human bone in bending.

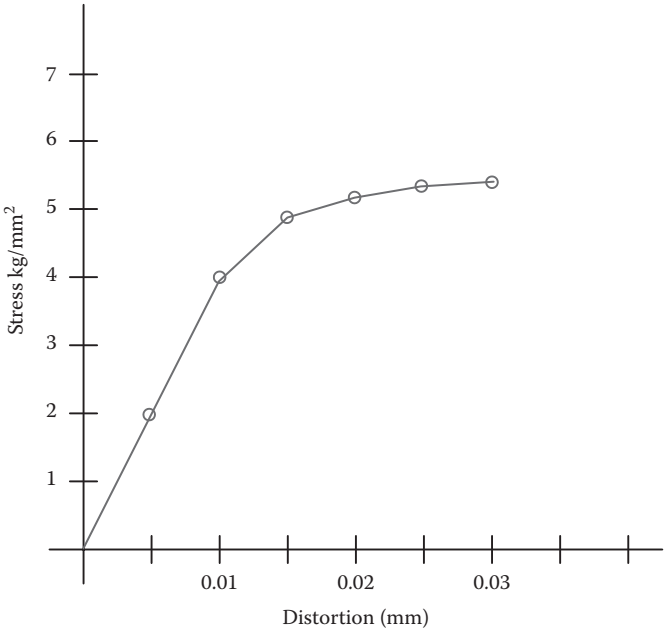

Figure 7.12 Human bone in torsion.

is associated with the ribs. Some cartilage is elastic and fibrous. Table 7.12 lists the properties of hyaline cartilage.

Human tendons have an average ultimate tensile strength of 5.4 kg/mm^2 at an ultimate average percent elongation of 9.4. The estimated breaking load on average is 192 kg. Skeletal muscle for an adult average is 11 g/mm^2 for its ultimate tensile strength at an ultimate percent elongation of 61.

Table 7.8 Tensile Properties of Vertebrae

Vertebrae	Tensile Breaking Load (kg)	Ultimate Tensile Strength (kg/mm²)	Ultimate Percent Elongation
Cervical	102	0.32	0.75
Upper thoracic	147	0.34	0.77
Lower thoracic	298	0.36	0.78
Lumbar	409	0.38	0.80

Table 7.9 Compressive Properties of Vertebrae

Vertebrae	Compressive Breaking Load (kg)	Ultimate Compressive Strength (kg/mm²)	Ultimate Percentage Contraction
Cervical	315	1.03	6.6
Upper thoracic	308	0.72	5.5
Middle thoracic	354	0.61	5.2
Lower thoracic	458	0.54	4.5
Lumbar	505	0.47	4.3

Table 7.10 Human Vertebral Dimensions

Vertebrae	Cross-Sectional Area (mm²)	Height (mm)
Cervical	305	14.1
16 Upper thoracic	415	16.6
Middle thoracic	546	19.4
Lower thoracic	830	22.5
Lumbar	1055	26.2

Table 7.11 Torsional Properties of Vertebrae

Vertebrae	Torsional Breaking Moment (kg cm)	Ultimate Torsional Strength (kg/mm²)	Ultimate Angle of Twist (°)
Upper thoracic	49	0.33	11
Middle thoracic	90	0.32	8
Lower thoracic	139	0.31	6
Lumbar	214	0.29	4

Table 7.12 Properties of Cartilage

Ultimate tensile strength = 0.29 kg/mm²	Ultimate percent elongation = 18.2
Ultimate compressive strength = 0.82 kg/mm²	Ultimate percent contraction = 13.6

Intervertebral disks are often associated with accidents and vehicular collisions. Normally, people older than 40 years have the beginnings of degenerative disk bulging. In many low-impact collisions, a common complaint is that the bulging was due to a collision involving some sort of whiplash-related injury. Tables 7.13 through 7.15 list the properties of the disks of the spine.

Table 7.13 Tensile Properties of Disks

Vertebrae	Tensile Breaking Load (kg)	Ultimate Tensile Strength (kg/mm^2)	Ultimate Percent Elongation
Cervical	88	0.3	77
Upper thoracic	118	0.21	46
Lower thoracic	244	0.23	46
Lumbar	325	0.26	59

Table 7.14 Compressive Properties of Disks

Vertebrae	Compressive Breaking Load (kg)	Ultimate Compressive Strength (kg/mm^2)	Ultimate Percent Contraction
Cervical	320	1.08	35.2
Upper thoracic	450	1.02	28.6
Lower thoracic	1150	1.08	31.4
Lumbar	1500	1.12	35.5

Table 7.15 Torsional Properties of Disks

Vertebrae	Torsional Breaking Moment (kg cm)	Ultimate Torsional Strength (kg/mm^2)	Ultimate Angle of Twist (°)
Cervical	51	0.48	34
Upper thoracic	84	0.41	26
Middle thoracic	167	0.44	22
Lower thoracic	265	0.45	17
Lumbar	440	0.48	14

Bone Fractures

In order to understand how bones may fracture or be damaged, a brief discussion of the makeup and function of bone is necessary. Bones are an integral part of the musculoskeletal tissues of human or animal bodies. The other components are cartilage, tendons, ligaments, and muscle. In many instances bone failure is associated with a failure of the other connective tissues of the musculoskeletal system. There are two major types of bone: cancellous bone and compact bone. Compact bone makes up approximately 80% of the human skeleton. Cancellous bone makes up the interior of most bones and is rather spongy. With respect to bone fractures only compact bone needs to be considered. Since most bone fractures result from complex loading in a multiaxial fashion, we often need to calculate the failure in tension, compression, and torsion.

Transverse Fracture of Long Bones

The fracture strength of long bones subject to transverse forces to their axis can be calculated in terms of the ultimate tensile strength of bone. Applying Young's modulus of elasticity of bone in conjunction with an approximation of a hollow cylinder for the long bone

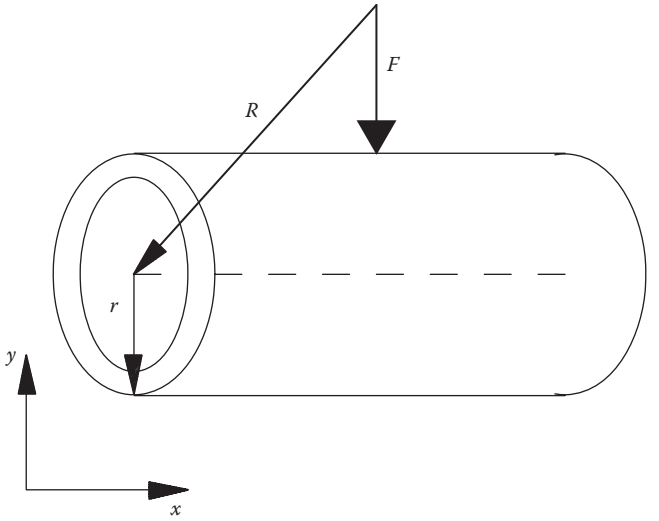

Figure 7.13 Transverse fracture of long bones.

determines the bending moment necessary to break the bone. Consider the bone under pressure as shown in Figure 7.13.

ε = strain
σ = stress

Young's modulus

$E = \sigma/\varepsilon$
F = force

The stress σ is related to the force F and the area A as

$$dF = \sigma dA \tag{7.32}$$

The torque τ exerted about the neutral axis

$$d\tau = \sigma dA$$

However,

$$\sigma = \frac{Ey}{R} \tag{7.33}$$

and

$$d\tau = \frac{Ey^2}{R} dA \tag{7.34}$$

The total torque about the neutral axis is called the bending moment M_b, so

$$M_b = \int d\tau = \frac{E}{R}\int y^2 dA \tag{7.35}$$

The integral is called the area moment of inertia I_a and we can then write

$$M_b = \frac{EI_a}{R} \tag{7.36}$$

The maximum stress, o_{max}, occurs at the radius r of the cylinder so that Equation 7.33 may be written as

$$\sigma_{max} = \frac{Er}{R} = Y_b \tag{7.37}$$

where Y_b is called the ultimate bending stress for human long bones. The external bending moment or torque M_b can then be expressed in terms of the ultimate bending stress, the area moment of inertia, and the radius as

$$M_b = \frac{Y_b I_a}{a} \tag{7.38}$$

For a child of 6 years, we determine

$$I_a \approx 0.017 \text{ in.}^4, \quad Y_b = 3.3\times10^4 \text{ lb/in.}^2, \quad a = .4 \text{ in.} \tag{7.39}$$

Therefore, the bending moment is

$$M_b = \frac{(3.3\times10^4)(0.017)}{0.4} \approx 1400 \text{ lb-in.} \tag{7.40}$$

The total leg of a human represents 15.7% of the total body weight. Of this, the thigh represents 63.7% of the leg weight. Assuming the break occurred about in the middle of the thigh (a distance of 7 in.), the force required was

$$F = M_b/7 \text{ in.} \approx 200 \text{ lb} \tag{7.41}$$

If the child weighs approximately 50 lb, then the thigh weighs approximately (50 lb)(.157)(.637) ≈ 5 lb. Using Newton's second law to determine the acceleration of the leg as it was struck by the vehicle,

$$a = \frac{F}{M} \quad \text{where } M = \frac{5 \text{ lb}}{32.2 \text{ ft/s}^2} = 0.155 \text{ slugs}, \quad \text{then } a = \frac{200}{0.155} = 1290 \text{ ft/s}^2 \tag{7.42}$$

The compression, s, of the muscle tissue around the bone is approximately 1 in, or 0.083 ft. Thus, the truck struck the child's femur at a speed given by

$$v = \sqrt{2as} = \sqrt{(2)(1290)(0.083)} \approx 14.6 \text{ ft/s}, \quad v \approx 10 \text{ mph} \tag{7.43}$$

This speed very closely matched the speed calculated in the analysis of the accident by conventional means.

Head Injury

Approximately 50% of all head injuries are caused by motor vehicle collisions. Falls account for 20%, physical violence for about 13%, and the remainder for sporting events and miscellaneous causes. The severity of the injuries results in fractures, contusions, and concussions. Skull fractures occur from failure loads ranging from about 1000 to 3100 lb loads. SAE J 885 further lists the fracture force of varying head bones as outlined in the Table 7.16. The range of the loads depends not only on the individual but also on the region of the skull that is affected.

The effects of the fracture are often exacerbated by the effects of the contusion and concussion that may follow. These effects to the underlying structures of the brain may produce intracranial hemorrhage and buildup of fluids leading to edema.

Brain or head injuries involve at least two and sometimes three separate and distinct collisions for which the forces need to be calculated. In a vehicular incident, the first collision occurs between the vehicles. The second collision involves the occupants with various structures of the interior of the vehicle. The third collision involves the collision of the intracranial structures with the bony interior of the skull. In cases where falls occur or when objects directly impact the head, only two collisions occur.

Head Injury Criterion

Data have been assembled through the years in concussion and other severe closed head injuries. These data have been arranged by scientists at Wayne State University and others (Lissner et al.) into the curve as shown in Figure 7.14.

It is seen that the time of application of an acceleration to the head as well as the peak acceleration plays a significant role in closed head injuries, which is called the head injury

Table 7.16 Fracture Forces for the Head

Bone	Mean (lb)	Range (lb)
Zygoma	283–516	138–780
Maxilla	258	140–445
Mandible	431–697	184–925
Frontal lobe	1000–1710	184–925
Tempo-parietal	702–1910	140–3360
Occipital	1440	1150–2150

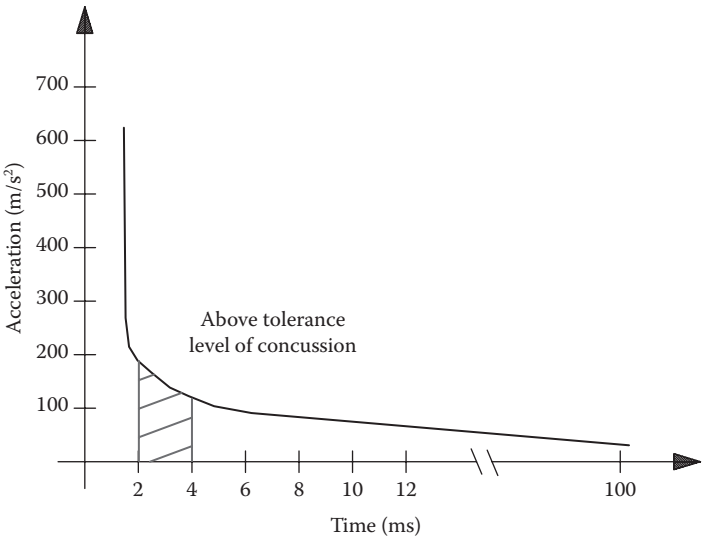

Figure 7.14 Closed head injury.

criterion (HIC). The curve in Figure 7.14 has been approximately fitted by the equation by Versace (1971):

$$\text{HIC} = (t_2 - t_1)\left[\frac{1}{(t_2 - t_1)}\int_{t_1}^{t_2} a(t)d(t)\right]^{2.5} \tag{7.44}$$

where $a(t)$ is the acceleration at each increment of time in g units (32.2 ft/s^2). The level of concussion is when the HIC number equals or exceeds 700. Evaluating the integral

$$\frac{1}{t_2 - t_1}\int_{t_1}^{t_2} a(t)d(t) = \frac{a}{2}(t_2 - t_1) \tag{7.45}$$

where a is now the maximum value. We may express the ratio of two HIC numbers given that

$$a = \frac{\Delta v}{(t_2 - t_1)} \tag{7.46}$$

as represented in Equation 7.47:

$$\frac{\text{HIC}_1}{\text{HIC}_2} = \left[\frac{\Delta v_1}{\Delta v_2}\right]^{2.5} \tag{7.47}$$

Nahum et al. (1977) in their experiments on cadavers obtained pressure versus acceleration data of the brain for frontal impacts to the skull. These linear data are reproduced in Figure 7.15.

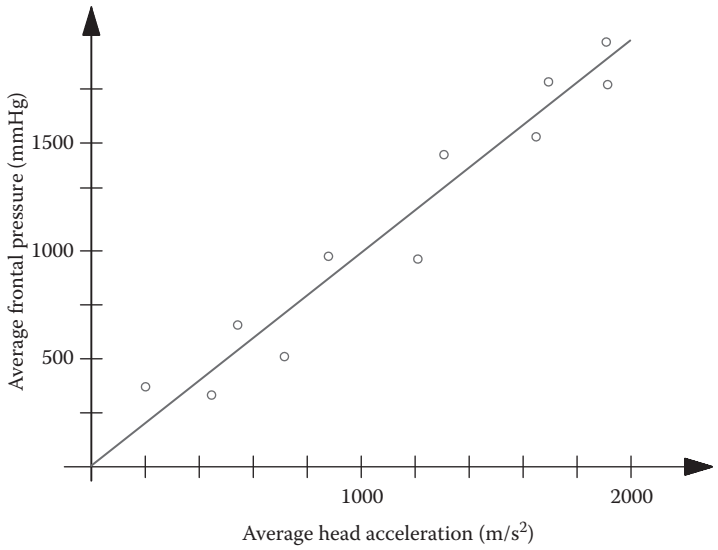

Figure 7.15 Frontal skull impacts.

Ward et al. (1980) have shown that the threshold intercranial pressure for brain injury is 24 lb/in.^{2} (1240 mmHg), and above 34 lb/in.^{2} (1758 mmHg) severe injury results. From Figure 7.15, the threshold of injury occurs at an acceleration of 1293 m/s^2, and the condition of serious injury occurs at an acceleration of 1758 m/s^2 or above. From these experiments, the HIC values were determined, and pressure vs. HIC values were plotted as shown in Figure 7.16. Originally, the HIC value was determined to be 1000 but has been lowered to 700.

The serious injury level of 34 lb/in.^{2} (1750 mmHg) corresponds to an HIC of about 1000, the accepted value for the threshold of brain injury. We may make a rough estimate of the velocity of impact of the frontal skull against a rigid surface that will give rise to an

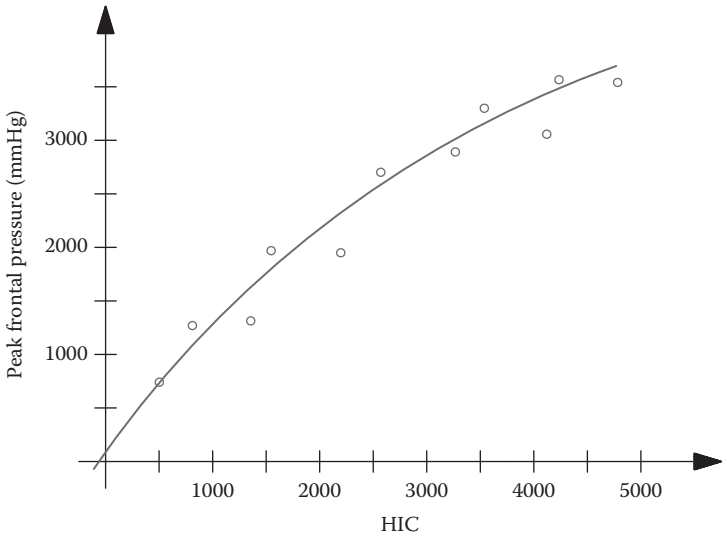

Figure 7.16 Pressure versus HIC.

HIC of 1000. The associated acceleration is 1293 m/s^2. Stalnaker et al. (1977) have used high-speed cineradiography to x-ray the motion of the brain in frontal impacts to cadaver skulls. It appears that the brain moves about 3 cm forward. We may calculate the associated velocity required to produce serious head injury as follows:

$$v = \sqrt{2ax} = \sqrt{(2)(1293)(0.03)} = 8.9 \text{ m/s} = 19.8 \text{ mph} \tag{7.48}$$

Compilation of Studies Involving Occupant Kinematics and Vehicle Impacts

In the absence of direct physical evidence of injury to occupants of motor vehicles, the question arises as to the occurrence of soft tissue injuries. Soft tissue injuries involve a variety of ailments including whiplash and sprained backs as well as more serious injuries to the internal organs, such as the liver, spleen, lungs, and heart. Many serious injuries to internal organs involve direct damage to the interior compartment of the vehicle, including head impacts on windshields, bent steering wheels, indentations on dash panels, and broken or bent seats.

Injuries to soft tissues occur when rapid decelerations cause the tensile strength of the particular tissue to be exceeded. Consequently, internal organs, muscles, tendons, and ligaments can tear, abrade, bruise, and lacerate. Newton's second law, $F = ma$, states that the force F exerted on a body of mass m is equal to the product of the mass and the acceleration a. This principle has been applied by various investigators to determine the acceleration necessary to produce injury to humans and animals. Damask states that there is a 5% probability of injury to humans at 12g (g = 32.2 ft/s^2 is the acceleration due to gravity on earth). For accelerations greater than 12g, the risk of injury increases proportionally. It is generally accepted that accelerations in the range of 100–150g produce severe injuries to soft tissues in humans and animals. One can therefore safely conclude that accelerations less than 10g will not produce significant injuries to humans while accelerations greater than 100g will almost always result in severe injuries of the soft tissue type. Injuries associated with accelerations in excess of 100g are always accompanied by significant physical damage to the vehicle interior, exterior, and outward direct physical evidence of injury to the occupants. Ogan et al. have shown that vehicle to curb impacts produce peak acceleration on humans less than 4g. The peak acceleration occurred at speeds of approximately 5 mph and decreased as speed increased. Ogan concluded that peak acceleration levels experienced by vehicle occupant when striking curbs are minimal.

Rear end collisions at low speeds using human subjects have been conducted by West et al. These tests revealed that at impact speeds of between 3 and 5 mph, the forces experienced by the vehicle occupants were sufficient to cause their heads to be displaced rearward and make contact with head supports at the rear top of the seats. The maximum levels of head acceleration for these tests were between 3g and 7.5g. "Neither the level of cervical bending nor the level of cervical torque measured in these tests reached the level at which injury to the vehicle occupant would be expected. Therefore, for an individual who does not have any predisposition to injury, a whiplash injury would

not be expected for impacts of this magnitude.... In our experiences, low back pain and injury to the temporal mandibular joint are often claimed as a result of minor low speed collisions. When seated normally within the vehicle seat, the thoracic and lumbar spines are fully supported by the seat back. Our testing has revealed that when exposed to a minor rear impact the seat back bends in response to the collision forces but maintains full support of the lower spine.

A model has been proposed to explain how Temporomandibular Joint (TMJ) injuries may result from an excessive opening of the mouth induced during a rear end collision event. Review of the videotape records of the collision tests which have been conducted failed to demonstrate any opening of the jaw as a result of the impact forces. This is as expected as there are no forces present during the collision phase which would articulate the jaw, as suggested by the model.... Even at the highest level of testing we performed, significant relative movement between the thoracic and lumbar spine did not occur.... Our tests indicate that singular low back strain is not expected as a consequence of low speed rear impacts."

Mertz and Patrick have established the noninjury level to the human neck and the kinematics of whiplash. The noninjury level for a 50th percentile male occurs when a human's head is subjected to a torque of 35 ft-lb. The torque level at which injuries to the neck ligaments occurred was 42 ft-lb. The torques can be converted to accelerations of 14*g* and 16.8*g*, respectively, assuming a 0.25 ft displacement and a head weight of 10 lb. It is important to note that the studies by Mertz and Patrick (injury threshold of 14*g*) when compared to Damask (injury to humans at 12*g*) are in excellent agreement.

We may correlate the accelerations produced by low-impact vehicular speeds to normal activities associated with everyday living. As human body structures evolved, structural resilience and strength of the soft tissues had to adapt to walking, running, and jumping. Man would not have survived if his structural components produced injury from simple activities. Allen et al. have measured the accelerations produced on the heads of eight volunteers performing 13 daily activities. The measured values ranged from less than 1*g* to as high as 8.5*g*. These activities included head movements in various directions, sneezing, coughing, kicking, standing, hopping off steps, and plopping in chairs. Certainly none of these activities producing in excess of 8*g* caused any injury to the test subjects. Man is certainly capable of greater physical feats than those experienced in daily activities without sustaining an injury.

When standard reconstruction techniques are coupled with occupant kinematics, the acceleration of the occupants can be calculated. Unless the occupants are subjected to accelerations greater than 10*g*, no soft tissue injury can occur. The 10*g* limit is very conservative because researchers have shown that the first indications of injury occur at between 12*g* and 14*g*.

Biomechanics of Injury

The human body is no different from any other structure that is analyzed by engineers. When vehicular accidents are reconstructed, basic principles of physics and strength of materials are utilized. These principles include forces, moments, energy, stress, strain, and acceleration, to name a few. Similarly, once the dynamic forces acting on the vehicles are determined, these forces impact the occupants so that the same principles apply

with respect to the biomechanics of injury, the only difference being the materials studied are human body parts such as bones, ligaments, muscles, tendons, and soft tissues. The properties of human tissue are well known through experimentation as outlined in the references.

A basic premise of science is that theoretical and experimental results must agree. In other words, what we observe must be explained by the theories and equations that are developed to explain the processes we experience. The basic dynamic laws of physics are Newton's laws, which cannot be broken by the reconstructionist. The biological data on human injury analysis are gathered from STAPP Car Crash Conferences and from *Strength of Biological Materials* by Yamada. These biological data obtained through experimentation place lower and upper limits on the forces, velocities, and accelerations necessary to injure the human body. One of the most violated principles of injury analysis is that of soft tissues. The U.S. Aerospace Medical Laboratory conducted numerous tests on monkeys and transposed that data to humans to determine the upper limit of human tissue to accelerations without the occurrence of injury. This upper limit has been placed at 12*g* where *g* is the acceleration due to gravity. Similarly, at accelerations in the range of 125–150*g*, there is a 99% probability of injury to human soft tissues.

Anteflex whiplash injuries have been extensively studied. Some of the most comprehensive studies were conducted by Clemens and Burrow in Berlin on 53 cadavers. These studies found three areas of the spine that are susceptible to injury. These areas are at the base of the cranium and C1, the region of C3 and C4, and the region of C6 and C7. These tests, in the range of 17 mph and decelerations in the range of 30*g*, correlated to serious injury involving 90% of ruptures of disks and 30% fractures. The exact limit of vulnerability was found to be at 13 mph and 13*g*. According to Damask there are four degrees of injuries associated with whiplash as shown in Table 7.17.

Note that in the earlier discussion there is excellent agreement on the accelerations required for the onset of injury as determined by the U.S. Aerospace Medical Laboratory and the studies conducted by Yamada and Clemens/Burrow. Therefore, at accelerations of 12*g* or less, corresponding to speed changes less than 10 mph, no soft tissue injuries occur to the human body.

SAE Technical Paper 930889 states, "For rear end collisions within the velocity range included in our test series, the classic 'whiplash' injury mechanism, seems unlikely since no hyperextension or hyperflexion was observed in any of our test subjects." SAE Technical Paper 940532 states, "The present study enhances the existing data base of volunteer studies

Table 7.17 Injury Degree

Degree	Comments	Speed and Acceleration
1	Isolated fissures of disks without injury to the ligaments or bones	13–16 mph 13–15*g*
2	Injury to disks, ruptures of interspinal ligaments, rupture of joint capsules, fractures of vertebral processes, but no rupture of the posterior longitudinal ligaments. Subluxation is possible and probable at the sixth vertebra as well as teardrop fractures	17 mph 16–30*g*
3	Rupture of posterior longitudinal ligament, luxation of all vertebral joints, injury centered at C6, but increased vulnerability of C1/C2, possible basal skull fracture	34*g*
4	Complete disconnection of the neck	42*g*

which support the premise that, for restrained occupants with a head restraint available, single exposure to a rear end collision with a Delta V of 8 KPH or less is within human tolerance levels, and extends the data base to include females and those with some degree of pre-existing spinal pathology."

To examine a case study where the Delta V's are minimal or negligible, we will assume a worst-case scenario of a Delta V of 5 mph (7.33 ft/s). The accelerations can be calculated to the occupants as follows: Since the differential distance between the lower spine and the rest of the spine is approximately 2.5 in. or approximately 0.2 ft, we may calculate the acceleration from

$$a = \frac{v^2}{2x} = \frac{(7.33)^2}{2(0.2)} = 134 \text{ ft/s}^2$$

This computed acceleration is approximately 4*g*. For the case of a 230 lb individual, the torso weighs approximately 115 lb and the upper part of the torso is 5/6 of the weight or approximately 96 lb. Therefore, the mass in slugs is

$$m = \frac{96}{32.2} \approx 2.98 \text{ slugs}$$

Thus, the total force exerted on the spinal column is

$$F = ma = (2.98)(134) = 399 \text{ lb}$$

If we assume that the shearing force will be evenly distributed over the 15 disks, we obtain

$$\frac{399}{15} \approx 26.6 \text{ lb} = 12 \text{ kg}$$

The ultimate tensile strength of disk cartilage is about 0.24 kg/mm^2. The cross section of a disk in a human is approximately 660 mm^2. Thus, the tensile stress for this application is

$$\frac{12 \text{ kg}}{660 \text{ mm}^2} = 0.018 \text{ kg/mm}^2$$

This value is approximately 7.6% of the ultimate strength. Therefore, some form of injury is not possible in the spinal column.

Vehicular Collisions with Pedestrians or Bicyclists

In collisions involving vehicles and pedestrians or bicyclists, vehicle speeds may be computed in a variety of manners. Important information, such as the exact point of impact, may not be available. Sometimes ancillary information, such as remains of shoes or hats,

helps to locate the approximate point of impact. Sometimes the exact distance the body slid after the collision is difficult to determine. In many cases, the vehicle does not leave skid marks prior to or after the collision takes place. This often happens when drivers are inattentive or when pedestrians or bicyclists dart in front of vehicles from obstructions to visibility such as between cars. Another consideration involves the perception or visibility of the pedestrian to the driver at night. This visibility depends on several factors such as the color of the clothing worn by the pedestrian, street lighting, and the intensity of the headlights. Pedestrian visibility at night for normal dark clothing is approximately 150 ft and low beam headlight conditions.

Four methods are commonly used in the analysis to estimate the vehicle velocity at impact. The first method involves the use of the vault equation. This equation is represented by

$$V_v = \sqrt{\frac{gD_1^2}{2\cos^2 A_v (D_1 \tan A_v + h)}} \tag{7.49}$$

A second method of analysis involves using the pedestrian sliding equation:

$$V_s = \sqrt{v_f^2 - 2aD_2} \tag{7.50}$$

The third method of analysis involves an empirical equation developed by Limpert:

$$V_e = 6.6\sqrt{8.4a^4 + aD} - 20a^2 \tag{7.51}$$

A fourth equation may sometimes be employed by solving for total stopping distance of the vehicle including reaction time. This equation is of the form

$$V_i = ga_2 t_r \left[\sqrt{1 + \frac{2D_T}{ga_2 t_r^2}} - 1 \right] \tag{7.52}$$

For Equations 7.49 through 7.52, the following parameters are defined:

V_v is the speed according to the vault equation (ft/s)
V_s is the speed according to the pedestrian sliding equation (ft/s)
V_e is the speed according to the empirical equation (ft/s) developed by Limpert
V_i is the speed according to total stopping distance (ft/s)
g is the acceleration due to gravity (ft/s^2)
D_1 is the vault distance (ft)
A_v is the vault angle (degrees)
h is the vault height (ft)
V_f is the final velocity (ft/s)
a is the acceleration of the body (ft/s^2)

D_2 is the distance the body slides (ft)
a_2 is the vehicle deceleration in g units
t_r is the driver reaction time (s)
D_T is the total stopping distance of vehicle

An average impact velocity (V_a) is used to give a median value for the velocities computed from Equations 7.49 through 7.52.

This analysis can only be used as an approximation when considering side impacts. Frontal impacts account for approximately 75% of all vehicle/pedestrian accidents.

Example

The pedestrian motion as a result of the collision is of utmost importance in order for a proper reconstruction and speed determination to take place. If the pedestrian is struck below his center of mass as shown in Figure 7.17, his body will rotate counterclockwise. This type of collision will cause the body to move upward over the hood and cause the pedestrian's head to strike the front windshield of the car. If the vehicle speed is high enough, the body may go over the roof of the vehicle. Head injury in vehicle pedestrian accidents is the highest cause of death. Serious head injuries occur at vehicle impact speeds above 30 mph.

Vehicle speed estimates may be conducted in a variety of manners. Important information, such as the exact point of impact, may not be available. Sometimes ancillary information, such as remains of shoes or hats, helps to locate the approximate point of impact. Sometimes the exact distance the body slid after the collision is difficult to determine.

The tabulated results, which are displayed in Tables 7.18 and 7.19, compare the three methods of analysis and yield a speed estimate of between 45 and 50 mph at impact. It should be pointed out that the vehicle stopping distance using a conservative coefficient of friction of 0.65 (indicative of some skid marks) is approximately 58 mph. This analysis does not include any braking action prior to impact so that the actual vehicle speed would normally be greater.

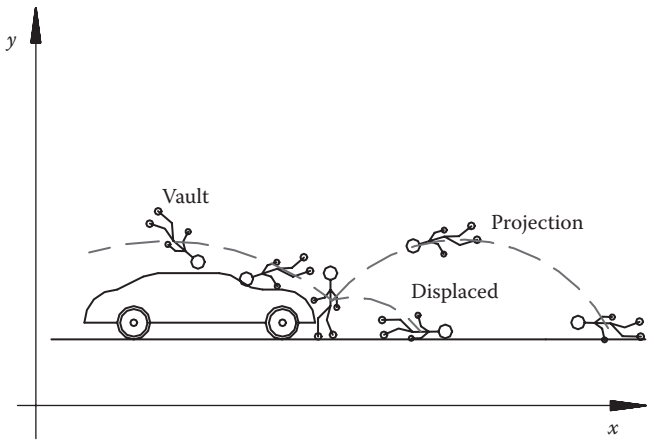

Figure 7.17 Pedestrian collision.

Table 7.18 Impact Velocity: Dependence on Horizontal Distance

D	V_0	V_s	V_e
86	46.5	48.3	44.1
87	46.8	48.6	44.4
88	47.1	48.9	44.7
89	47.4	49.2	45.0
90	47.7	49.5	45.4
91	48.0	49.7	45.7
92	48.3	50.0	46.0
93	48.5	50.3	46.3
94	48.8	50.5	46.6
95	49.1	50.8	46.9

Table 7.19 Impact Velocity: Dependence on Body Drag Factor and Horizontal Distance

	V_0			V_s			V_e		
f	$D = 86$	$D = 91$	$D = 95$	$D = 86$	$D = 91$	$D = 95$	$D = 86$	$D = 91$	$D = 95$
0.7	46.5	48.0	49.1	42.6	43.9	44.8	42.4	43.9	45.0
0.8	46.5	48.0	49.1	45.6	46.9	47.9	43.5	45.0	46.2
0.9	46.5	48.0	49.1	48.3	49.7	50.8	44.1	45.7	46.9
1.0	46.5	48.0	49.1	51.0	52.4	53.6	44.3	46.0	47.3
1.1	46.5	48.0	49.1	53.4	55.0	56.2	44.2	45.9	47.3
1.2	46.5	48.0	49.1	55.8	57.4	58.7	43.9	45.6	47.0

Internal Organ Injuries

Human organs and tissues are subjected to injury from secondary and tertiary collisions that occur in an event such as an accident, a fall, or an impact with a solid object. Table 7.20 summarizes some of the properties of various internal organs and tissues.

Knee Injuries

The meniscus distributes body weight across the knee joint. There are two menisci in the knee, the medial (on the inside) and the lateral (on the outside). These structures are C-shaped and have a wedge profile that keeps the rounded ends of the femur from sliding off the flat tibial surface. The meniscus is made of cartilage. Cartilage also covers the ends of the bones allowing for the smooth movement of the bones relative to each other. On the femoral condyle of the knee, the cartilage averages 2.21 mm. Under impact loads, cartilage behaves as a single-phase, incompressible, elastic solid. The aggregate modulus of cartilage varies between 0.5 and 0.9 MPa, and Young's modulus varies between 0.45 and 0.8 MPa. The tensile failure stress of human cartilage varies from 30 to 10 MPa

Table 7.20 Strength of Organs and Tissues

Organ	Ultimate Tensile Strength (kg/mm^2)	Average Ultimate Percent Elongation
Bone	10.9	1.4
Tendons	5.4	9
Fibrocartilage	1.3	12
Skin	1.1	47–111
Vertebra	0.35	0.8
Elastic cartilage	0.31	26
Venous/arterial tissue	0.17	66–89
Coronary artery	0.11	64
Large intestine	0.069	117
Esophagus	0.06	73–124
Stomach/small intestine	0.056	43–127

and is a function of age varying from 20 to 80 years. For a 55-year-old, the stress is approximately 17 MPa.

Meniscal injury is often caused by high rates of the application of force. Meniscal injury is either traumatic or degenerative. Traumatic injuries are usually seen in young active individuals. Degenerative tears are chronic injuries generally found in older persons. Damage usually occurs when the meniscus is subjected to a combination of flexion and rotation on extension and rotation during weight bearing and resultant shear between the tibial and femoral condyles. Sports related meniscal injury involves soccer, track and field, and skiing. Occupationally, jobs requiring repeated squatting, such as mining, carpet laying, or gardening, are associated with these injuries. For example, the lower leg of an individual weighing 200 lb weighs approximately 25 lb. The thickness of the meniscus is approximately 2.21 mm or 0.00725 ft. There are two menisci. If the vehicle experiences a speed change of 5 mph or 7.33 ft/s^2, the acceleration on the meniscus is

$$a = \frac{v^2}{2x} + \frac{(7.33)^2}{2(0.0015)} = 1790 \text{ ft/s}^2 \tag{7.53}$$

The mass of the lower leg pushing against the meniscus is

$$m = \frac{25 \text{ lb}}{32.2 \text{ ft/s}^2} = 0.77 \text{ slugs} \tag{7.54}$$

The force is

$$F = ma = (0.77)(1790) = 1389 \text{ lb} \tag{7.55}$$

The shearing force distributed over both menisci is then 1389/2 = 694 lb. The area of the meniscus is approximately 400 mm^2. The tensile stress on the meniscus is

$$\frac{694 \text{ lb}}{400 \text{ mm}^2} = \frac{3088 \text{ N}}{400 \text{ mm}^2} = 7.7 \text{ MPa} \tag{7.56}$$

Since the tensile failure stress is approximately 17 MPa, the force is approximately 45% of that required for failure.

Injuries of the Hand, Wrist, and Elbow

The upper part of the arm contains the humerus the biceps and the triceps. Tendons and ligaments help with the attachments at the shoulder and the elbow. Some of the more common types of injuries of the upper arm include fractures of the humerus, biceps tendon injuries, and distress of the structures of the elbow. The most common injuries to the elbow include tissue degeneration, dislocation, and fractures of the humerus, ulna, and radius. Many of these injuries are common to athletes and are produced by repeated loading. These repeated loading injuries are produced by overhead throwing, swinging of a racket or club, or by repeated actions by specific crafts such as carpentry. The most common form of elbow luxation (dislocation) is produced by axial forces applied when the elbow is extended. Elbow fractures are associated with falls when the elbow is extended and dislocated.

Many elbow injuries are commonly associated with injury to the wrist and hand. Most of these injuries are produced by falls or axial loading of the radius and ulna. The radius and ulna are the bones of the forearm and are surrounded by extensive muscles, tendons, and ligaments that allow for the complex articulation of the wrist and hand. One injury that is sometimes claimed in a fall or a vehicular collision is carpal tunnel syndrome. It should be pointed out that carpal fractures can occur to any of the eight carpal bones of the hand. These types of fractures result from compressive loads applied when the wrist is hyperextended. Carpal tunnel syndrome does not result in fractures but is rather an injury produced by repeated stresses on the tissues. Repeated loading compresses the neurovascular tissues causing inflammation and edema. Carpal tunnel syndrome is associated with repeated and extensive movements rather than with a single event. Finally, injuries can occur to the metacarpal and phalanges of the hand and these are associated with direct impacts, hyperextension, hyperflexion, twisting, or a combination of these.

Teeth Injuries

In this biomechanical calculation, it is necessary to determine if a candy stick held in the mouth can cause a broken tooth if the head moves forward as the candy stick strikes the hand or wrist. It is assumed that the hand and wrist are motionless. The compressive strength of the candy stick cannot be considered because there is insufficient information concerning the type and size of the candy. However, from the reconstruction of the collision, the speed change of the vehicle was determined based on the crush analysis as 8.1 mph or 11.87 ft/s. As a worst-case scenario, a speed change of 15 ft/s will be assumed.

In 1974 the *Journal of Dental Research* article "Breaking strength of fluoride-treated dentin" determined that the breaking stress varied from 28.62 ± 1.94 to 31.92 ± 2.44 kg/mm^2. Thus, the variability was from 26.68 to 34.36 kg/mm^2. According to the *Journal of Prosthetic Dentistry*, the breaking strength of ceramic crowns varies between 66.8 and 88.6 kg. The lowest value of 26 kg/mm^2 was used for this analysis.

The acceleration produced in the earlier described scenario is a function of the penetration of the candy stick into the tissue surrounding the hand or wrist. This penetration distance is at least ¼ of an inch or 0.02 ft so that

$$a = \frac{v^2}{2x} = \frac{(15)^2}{2(0.02)} = 5625 \text{ ft/s}^2 = 174 \text{ g/s} \tag{7.57}$$

The human head weighs approximately 10% of the total body weight. If an individual weighs 200 lb, the head would weigh approximately 20 lb. Its mass is

$$m = \frac{w}{g} = \frac{20}{32.2} = 0.62 \text{ slugs} \tag{7.58}$$

The force imparted by the acceleration is

$$F = ma = (.62)(174) = 108 \text{ lb} = 49 \text{ kg} \tag{7.59}$$

The standard tooth size of a human is approximately 5 mm × 3 mm = 15 mm^2. Thus, the stress on the tooth would be

$$S = \frac{F}{A} = \frac{49}{15} = 3.2 \text{ kg/mm}^2 \tag{7.60}$$

This stress is approximately 9%–12% of that required to break the tooth. Therefore, the forces imparted on a tooth by the scenario described are not sufficient to break or dislodge a tooth.

Lower Leg Injuries

Minimum Speed Required to Fracture the Tibia and Fibula

The mechanical insult to the lower leg stemming from a pedestrian–vehicle collision is classified as a high-energy injury that involves direct impact and high bending forces and results in transverse fractures of the tibia and fibula. The minimum speed required to fracture the long bones can be quantified as follows: the bending moment of a long bone is found from

$$M_b = \frac{Y_b I_a}{r} \tag{7.61}$$

where

M_b is the bending moment
Y_b is the ultimate tensile strength of bone
I_a is the area moment of inertia
r is the radius of the bone at the breaking point

The leg of a human is approximately 15% of the total weight. The lower leg is approximately one-third of the weight or approximately 5% of the weight of the pedestrian. The medical records indicate that his weight was 190 lb and his height was 6 ft 3 in. The ultimate strength of the fibula is 2.03×10^4 psi and that of the tibia is 2.12×10^4 psi, so that the ultimate strength of both bones would be approximately 4.15×10^4 psi. The bending moment for a combined radius of approximately 0.5 inches can then be computed as

$$Y_b = 4.15 \times 10^4 \text{ lb/in.}^2, \quad r = 0.5 \text{ in.}, \quad I_a = \frac{\pi}{4}(0.5)^4 = 0.049 \text{ in.}^4$$

$$M_b = \frac{(4.15 \times 10^4 \text{ lb/in.}^2)(0.049 \text{ in.}^4)}{(0.5 \text{ in.})} = 4072 \text{ in.-lb} \tag{7.62}$$

The mass of the leg is

$$m = \frac{w}{g} = \frac{10 \text{ lb}}{32.2 \text{ ft/s}^2} = 0.31 \text{ slugs} \tag{7.63}$$

The force required to break the bones that are approximately 12 in. long at midlength is

$$F = \frac{M_b}{6} = \frac{4072}{6} = 678 \text{ lb} \tag{7.64}$$

The acceleration is

$$a = \frac{678}{.31} = 2189 \text{ ft/s}^2 \tag{7.65}$$

The minimum vehicle speed compressing the leg approximately two inches is

$$v = \sqrt{(2)(2189)(.166)} = 26.96 \text{ ft/s} = 19 \text{ mph} \tag{7.66}$$

Shoulder Injuries

There are several main types of shoulder injury. These are acromioclavicular (AC) sprain, rotator cuff (RC) pathologies, glenohumeral instability and dislocation, bicep tendinitis, impingement syndrome, and labral pathologies. The more common types are AC sprain

and RC injuries. AC sprains result from forces that tend to displace the scapular acromion process from the distal end of the clavicle. Commonly, this type of injury is referred to as separated shoulder. A separated shoulder is not the same as a shoulder dislocation which is more serious. AC injuries may result from direct or indirect forces. The most common cause of AC injury is produced by a direct force applied to the point of the shoulder with the arm in an adducted (toward the median axis) position. Such injuries are produced in falls where the shoulder impacts the floor. Indirect forces that produce AC injuries occur in falls where the outstretched arm is laterally extended and the hand strikes the floor.

RC injuries are a common complaint of persons who use overhead movements. Glenohumeral impingement and RC lesions are the most common shoulder conditions because of their morphology. Impingement pathologies fall into two categories: for persons below and above 35 years of age. Younger individuals are susceptible to injuries resulting from sports- or work-related activities. Older individuals are more likely to suffer from the effects of degenerative processes that lead to bone spur formation, capsular thinning, decreased tissue perfusion, and atrophy of the muscles. The muscle action of the shoulder joint is designed to keep the reaction force in line with the glenoid. The joint becomes unstable as the line of action moves away from the geometric center of the glenoid. Individuals with lax shoulder muscles may experience glenohumeral dislocation resulting from minimal forces. The vast majority of dislocations occur anteriorly. Anterior luxation occurs most often from indirect forces when the axial loads are applied to the abducted, extended, and internally rotated arm. Anterior dislocation may also occur from direct forces applied to the posterior aspect of the humerus. Posterior glenohumeral dislocation (luxation) may occur from a direct force to the anterior aspect of the shoulder or from an indirect force through the arm if extended, flexed, adducted, and in an internally rotated position.

The shoulder contains two bones, the scapula and the clavicle. The clavicle attaches medially to the sternoclavical joint and laterally to the acromium process. The humerus articulates with the scapula at the glenohumeral joint commonly known as the shoulder joint. Figure 7.18 shows the shoulder joint, and Figure 7.19 shows the muscle attachments.

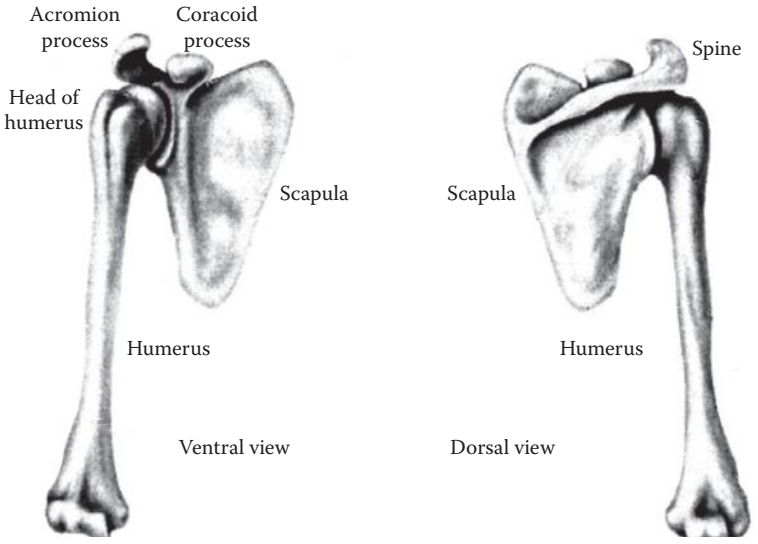

Figure 7.18 Shoulder joint.

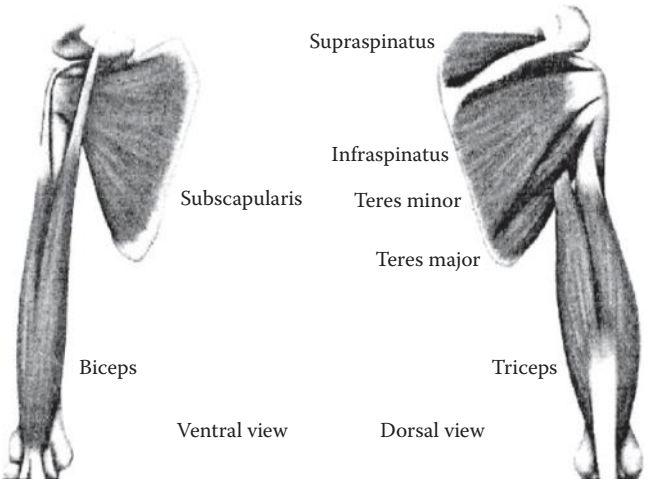

Figure 7.19 Shoulder muscles.

The most important muscles of the RC are the subscapularis, supraspinatus, infraspinatus, and teres minor. The muscles attach to the bony structures via tendons. These muscles stabilize the joint by forming a cuff around the humeral head. Several significant injuries to the shoulder occur including labral pathologies. The glenohumeral labrum is a fibrocartilage rim that encircles the articulalar surface of the scapular glenoid fossa. Labral injuries may be chronic or acute and are caused by a variety of mechanisms including compressive falls, traction (tension) from lifting, throwing, overhead movements, and dislocation.

The average and ultimate tensile stress of tendons and ligaments varies between 50 and 100 MPa or between 14,000 and 7,250 psi. Tendon cross sections vary between 125 and 150 cm^2 or 19.37 and 23.25 $in.^2$. The reconstruction of an alleged collision where shoulder injuries were claimed determined that the accelerations on the shoulder of an individual would vary between 4 and 8 *g*s. For a body weight of approximately 150 lb, the forces exerted on the shoulders varied between 260 and 511 lb. The tensile stresses on the shoulder tendons then varied between 13.7 and 22.2 psi. These stresses are between 0.19% and 0.31% of that required to produce injury.

Hip Injuries

The hip joint consists of the articulation of the femur (thigh bone) with the girdle of the pelvis (coxal bone). The articulating surfaces are those of the head of the femur and the acetabulum. The acetabulum is the cup-shaped socket of the hip bone. The two bones have an improved fit by the acetabular labrum. The labrum is a liplike structure made of fibrous cartilage attached to the coxal bone. The reinforcements of the hip include the iliofemoral ligament anteriorly and the ischiofemoral ligament posteriorly (see Figure 7.20).

A chondral lesion is a tear of the cartilage that helps to articulate the joint. In an alleged collision the claimant reported repair to the left hip as a result of a labral tear and chondral lesion of the acetabulum. This collision involved a passenger in the rear seat of the striking vehicle impacting the rear of another vehicle. The reconstruction of the collision revealed

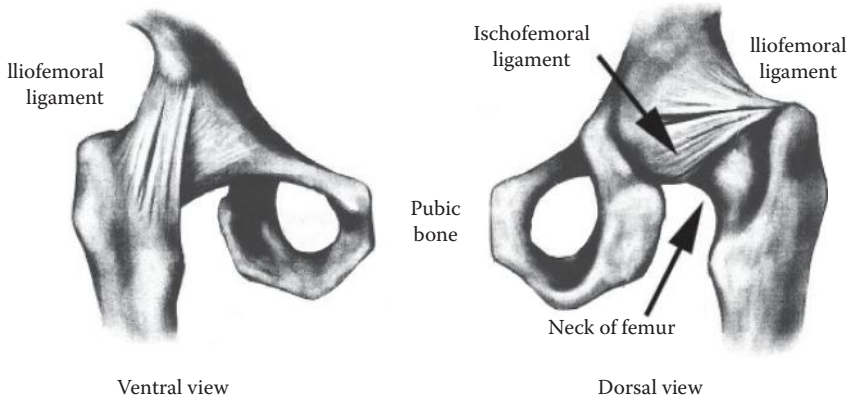

Figure 7.20 Hip joint.

that the impact produced a speed change of less than 5 mph. So that the forces produced in the collision were insufficient to cause the claimed injury. This type of injury requires significant forces due to the robust nature of the hip girdles. A predominant cause of this type of injury is luxation (dislocation) of the hip joint. Another cause of this type of injury results from significant wear resulting from heavy lifting or from contact sports. Age has an effect and may result in osteoarthritis. Generally high-energy trauma is required to produce these injuries.

In motor vehicle accidents, the direction of the force largely determines the type of injury that occurs. Hip injuries are much more prevalent in side impact collisions. Frontal collisions require significant speed changes at impact. There are two primary methods that the hip is injured in a frontal collision, first when the knee strikes the dashboard in unbelted occupants and second when a driver suddenly applies the brake and the force of the impact is transferred through the leg to the hip as the brake pedal is forcibly applied and the knee is locked. In the accident cited earlier, the collision involved the occupant seated in the rear seat. Consequently, an unbelted passenger in the rear seat would strike the rear of the front seat with his knees. The rear of the front seats is significantly softer and provides much more cushion that the front dashboard or the brake pedal with a locked knee. These types of collisions may involve both luxation and fracture of the hip joint. Dynamic modeling of hip injuries from falls has shown that the forces from such injury mechanisms may produce between 13,000 and 44,000 lb of force. This range of forces is certainly sufficient to cause luxation or fracture of the hip girdle.

Industrial and Construction Accidents

8

Introduction

Industrial accidents can take many forms in very diverse industries. These industries include mining, manufacturing, construction, farming, maritime, logging, and other specialties. In this chapter we are concerned with incidents involving humans and with losses involving the equipment. However, it is safe to say that the majority of industrial incidents involving injury or death to employees also involve some sort of mechanized equipment. A failure of the mechanized equipment may be responsible for creating the incident although that is not always the case. Consequently, the role of the equipment, its maintenance, and its safety design and usage are paramount in these types of incidents. As the nation has become ever increasingly industrialized, it has also become more mechanized. These types of incidents fall under the purview of the Occupational Safety and Health Administration under the U.S. Department of Labor. The Code of Federal Regulations (CFR) is the starting guide to use when investigating industrial incidents. Under the CFR there are a variety of codes that may be applicable to the incident.

In the Annual Survey of Occupational Injuries and Illnesses, the Bureau of Labor Statistics publishes estimates for occupational injuries for industries in the private sector. These estimates are based on a survey of approximately 280,000 private sector businesses. The employers are required to maintain records of such instances according to the Occupational Safety and Health Act of 1970. The U.S. Consumer Product Safety Commission also publishes estimates of product- or equipment-related injuries in the workplace. Additionally, the Department of Health and Human Services through the National Institute for Occupational Safety (NIOSH) began in 1985 a program to quantify the number of occupational deaths due to trauma in the United States. Additional governmental agencies that keep track of occupational injuries and death are the National Safety Council, the U.S. Department of Commerce, the U.S. Department of Agriculture, and the State Worker's Compensation Systems. It may be necessary to consult the various regulatory agencies listed in order to properly assess an industrial incident. We begin our discussion of industrial incidents by first looking at the equipment involved.

This chapter does not lend itself to analyzing problems by performing calculations, which does not mean that calculations are not performed when investigating industrial incidents. In fact, a variety of calculations are performed in these instances. The calculations may involve electrical load analysis in the case of an electrical failure. Motor generator calculations involving voltages, currents, and impedances are often performed in these cases. Mechanical industrial failures may involve tribometric computations, stresses, forces, and moments. Most often when an incident occurs, the investigator is to determine the root cause of the incident. This is particularly true in the event of injury or death.

We have outlined 10 actual cases in the examples that follow where a worker was injured or died. In these diverse cases, there are a multitude of violations of many standards. In an actual case where the investigator is performing the analysis, all pertinent standards are reviewed, including the CFR. We do not expect the student to do a literature search for the applicable codes since most of these codes are copyrighted and must be purchased. However, the CFR is available free of charge and can be accessed through the internet simply by typing CFR in your browser. From there you can navigate to the particular sections and if you desire, print those documents. So, for the problems at the end of the chapter, we have opted to introduce a case, and let you research the CFR so that you might gain insight into the process that is required to find any particular violations that may have taken place. On a final note, remember that we have stated in other portions of the book that all of these codes are incorporated by reference. Accordingly, sections of the CFR make reference to other codes such as ANSI, ASTM, NFPA, and many others. In industrial incidents, the beginning point is the CFR.

Equipment Losses

In this section we will deal with the types of equipment that may be involved in an industrial incident whether injury or death occurred. There are a variety of different types of equipment to consider from walkway safety to personal protection equipment to moving, rotating, or stationary equipment.

Walkway Safety

In an industrial environment, walkway safety includes climbing safety and fall protection. At a factory, the walkway environment may include passages around various types of stationary or moving equipment. As such, there are designated passages and aisle ways. Some walking surfaces may be elevated or require climbing stairs, ramps, or ladders. Walkway safety includes means of egress, and powered platforms and manlifts. The pertinent sections are found in CFR 29, Part 1910, subparts D, E, and F.

Personal Protection

Personal protection for workers includes control of the environment, hazardous materials, environmental controls, personal protective equipment, medical first aid, and fire protection. The pertinent sections are Part 1910, subparts G, H, I, J, K, and L.

Equipment

Under 29 CFR equipment includes compressed fluids, material handling, machinery and guarding, hand and power tools, welding, electrical, diving operations, and specialty industries. These sections are found in Part 1910, subparts M, N, O, P, Q, R, S, and T.

In addition to the requirements of 29 CFR, there are many other standards that may be incorporated by reference. Under section 1910.6, it is stated that the standards incorporated by reference have the same force and effect as other standards. The mandatory provisions containing the word shall be adopted as standards under the Occupational Safety

and Health Act. As in all standards, the word "shall" means that it is law. In contrast, if the word "shall" does not appear in a standard, the standard is deemed to be the general practice in the industry and does not carry the same weight. However, for all practical purposes, when performing forensic engineering investigations, the use of standards is sufficient to withstand challenges by the opposition, including Daubert challenges.

With respect to the equipment involved in an industrial incident, there are many standards incorporated by reference in sections 1910.5 and 1910.6. These include ANSI, API, ASME, ASTM, AWS, CGA, CMAA, GSA, IME, NEMA, NFPA, NIOSH, SAE, UL, and others. Note that reference is always made to NFPA Standards. The most important NFPA Standard is NFPA 101, the Life and Safety Code, which is always incorporated by reference.

The Life and Safety Code states that it shall be administered and enforced by the Authority Having Jurisdiction (AHJ) designated by the governing authority. The governing authority is usually a local, state, or federal agency, such as the code enforcement agency of a particular municipality. The purpose of the code is to provide minimum requirements of buildings and structures for safety to life from fire. Its provisions aid life safety in similar emergencies. The code addresses protective features and systems, building services, operating features, maintenance activities, and other provisions for the protection of life. Therefore, by reference, equipment losses can be tied to the life safety code because the malfunction of certain equipment can produce a danger to life. The code takes a broad interpretation of buildings and structures to include vessels and vehicles. NFPA 101 is the umbrella code under which all other required codes are covered.

Injuries and Death

These types of cases are different from those that simply involve the loss or failure of industrial equipment. Industrial equipment may fail as a result of inadequate design, improper use of the equipment, or a failure produced by improper maintenance or extension of the serviceable life of the equipment. Consider the case where a crane fails during use with no loss of life or injury to humans. Alternatively, a coal silo may fail as a result of improper welding after being recently constructed. Again, injuries to humans may not occur. In some cases equipment fails and workers are injured or die. Other times equipment does not fail, workers are injured, but safety procedures are not followed. In a preponderance of these cases, engineering calculations are not necessary but a thorough knowledge of applicable federal regulations will aid the forensic engineer in finding the root cause of the failure.

Industrial accidents with injuries and death are as diverse as the general field of construction. The best way to explain the process of investigation and the role that the forensic engineer may take is through a few examples.

Case #1: A young man with a wife and two small children begins working for his uncle's electrical construction company APEX Electric. APEX Electric has been doing residential and light commercial electrical service and installations for 30 years. The experience of APEX Electric is restricted to low voltages, that is, voltages less than 600 V as designated by the National Electrical Code NFPA 70. APEX Electric has never worked on systems above 600 V and does not have any employees with that type of training. The owner of APEX Electric, through his contacts in the area, is able to land a contract with the local electrical power plant to remove some unused electrical lines within the power plant that are being

taken out of service. These voltage lines are 2300 V distribution lines within the power plant. The power plant is aware that APEX Electric does not have the trained personnel to perform the job without supervision. Since the contractor, APEX, deems the removal of these lines to be simply manual labor, they place their most inexperienced worker, the young man, on the task under the supervision of an employee of the power plant. The young man has 2 weeks experience with APEX and has never performed any electrical work nor has he ever had any training in electricity.

The incident occurs when the power plant supervisor tells the young man to climb a ladder, stretch over a steel tank, take a pair of uninsulated dikes, and cut the lines. He is not given a protective blanket, insulated dikes, insulating gloves, and has no idea of lock-out–tag-out procedures. Since the steel tank is grounded and his torso rests upon the tank, he is sufficiently grounded. The line in the tray is live at a potential of 2300 V. When he cuts the line, the potential between his hands and his torso is energized to 2300 V and he expires.

The issues in this case are as follows: APEX Electric was not trained or experienced in medium voltage work. The power plant was aware of this deficiency. This fact is in violation of CFR 29, the National Electrical Safety Code, and NFPA 70E, the Standard for Electrical Safety in the Workplace, as well as NFPA 70B Recommended Practice for Electrical Equipment Maintenance. The power plant did not perform its duties in the supervision of the young man by not providing training and personal protective equipment. The power plant was negligent in its lock-out–tag-out procedures because the line was energized in violation of the codes mentioned earlier. At trial, the family of the young man prevailed. List the pertinent violations.

Case #2: A new transfer house was being built at a mine site owned by STEELCO. The transfer house redirects the mined coal from one direction to another direction. The coal enters the transfer house through a beltway to an opening on the second floor. From there, the coal dumps down to the lower level through a chute that is raised 6 ft above the floor level on the second floor. The difference in elevation between floors is 15 ft with the chute opening an additional 6 ft.

The incident involved the following scenario. A worker was installing a chain fall from the rafters of the second floor through the chute to the first floor in order to lift a drive motor from the first floor to the second floor. This motor was to be attached to the end of the belt at the top of the chute. In the process of installing the chain fall, the worker slipped and fell 21 ft through the chute to his death.

The issues are as follows: All floor openings must be protected so that workers cannot fall through. When workers are elevated, they must employ fall protection by the use of harnesses attached above to prevent an incident such as in this case. This case was settled before the deposition stage because a 3D animation based on measurements of the site pointed out the violations of CFR 29. What were the pertinent CFR violations?

Case #3: A local small community hospital, MEDFAC, had an in-house laundry facility where the sheets from the patient beds were laundered. Having the laundry in the hospital saved money and time. The laundry was serviced by hospital personnel. One of the functions of the laundry involved using a steam iron press for the sheets. This press was somewhat old and in need of repair. A reed switch by the rollers malfunctioned so that the attendant had to lift a cover in order to manually open the reed switch to operate the press.

This scenario poses some serious problems because placing hands near pinch points is dangerous. As a consequence of the malfunction of the press and the refusal of the hospital

to fix the problem, a worker's hand was caught between the rollers and was severely injured, losing a portion of his hand. It should be pointed out that the press had been operating for many months in this condition. Replacement of the reed switch by a qualified repair person was a matter of less than $200. The cost-saving measures of the hospital prevented the maintenance staff from correcting this machine.

The issues are as follows: The hospital was required to provide a safe working environment for its employees. Machine guarding is a very serious issue because machines can produce significant energy and are capable of maiming and killing individuals. As such, moving and rotating parts are to be guarded. At the beginning of the trial the case settled once the jury was sworn and testimony was to begin. What were the pertinent CFR violations?

Case#4: Underground mines have self-propelled personnel carriers to move employees and equipment inside of the mine shafts. Some of these personnel carriers ride on tracks inside the mine shafts and passageways. Since underground mines follow the contour and elevation of the coal seam, they are not necessarily level and have many dips or low points. During the day shift at COALCO, while production was taking place, a personnel carrier became disabled and got stuck at a dip in the track. The workers who were riding this carrier had to walk out of the mine and reported the problem to their supervisor. Since production was not to take place on the next shift, it was designated as a maintenance shift and an experienced mechanic was sent to the site of the stuck personnel carrier to diagnose the problem, correct the failure, and bring the carrier out.

The mechanic got into another carrier and proceeded to the site where he parked his vehicle at the top of the incline. He walked down the incline to the bottom of the dip where the disabled carrier was located and began his inspection. A few hours later, he was found pinned between the disabled carrier and the carrier he took to the site. He was deceased. Examination of the personnel carrier that he rode to the site revealed that the braking systems were ineffective. What went wrong? Can you site applicable sections of MSHA?

Case #5: An employee for POWERCO, a utility company, was to climb a pole in order to perform some electrical wiring erection. This pole was located in a rural mountainous area. The work involved installing electrical wires, insulators, and bracing for power distribution. The pole had been erected by a subcontractor of the utility company and now the employee of the utility company was to erect the wiring. Electrical power poles are to be installed according to regulations with respect to the depth of the pole in the ground, and the bracing cables that support the pole. This pole extended approximately 27 ft above the ground.

This subcontractor was known to be lax in its installation practices and the utility company had warned the subcontractor on various occasions that the work was not satisfactory. However, the subcontractor charged less than other subcontractors for work so that the utility company kept using their services.

As the utility company worker climbed the pole, the pole shifted and caused the worker to fall to the ground after he reached the desired elevation to begin the installation of the equipment. The worker sustained serious injuries including a broken leg and lower spinal injuries. The utility company refused to take responsibility for the incident citing a failure of the worker to adhere to due care. They unequivocally stated that the pole could not have shifted and caused the worker to fall. So, the question with respect to liability was whether the pole had shifted. A joint inspection was conducted with the utility company and forensic engineers hired to represent the utility worker. The pole was excavated on one

side making sure that it was not disturbed in the process. When the excavation was completed, it was evident that the pole was not buried to the required depth and the pole had shifted. At that point, the utility company settled with the worker. What were the pertinent CFR violations?

Case #6: A crane operator for LIFTALL was moving a load and a helper was helping guide the load with a guide cable. The guide cable was made of steel and the helper did not have insulated gloves or insulated boots. The crane operator did not adhere to the minimum distance required to be in the proximity of the energized power lines. The crane made contact with the energized lines and the helper died as a result of the medium voltage electrocution. The electrical lines were energized to 7200 V. Why did the crane operator survive?

Case #7: A utility company worker for a TELECO was in a bucket truck performing repair work on telephone and cable lines that had been damaged by a storm. In this case, as with many applications, the pole was owned by the local power company, and the electrical utility had leased a portion of the pole to the telecommunications company. This telecommunications worker was not trained in electrical work either with protective equipment or with live wire work. He had been on the job for less than a month and was just learning the trade. Because of the storm outage, the telecommunications company in an effort to repair service, placed this worker in a position where he was not fully trained. As he moved the bucket, he made contact with an energized conductor and was electrocuted. What are the pertinent CFR sections in this case? Who was responsible for his death?

Case #8: Construction operations by DIGDEEP required a large excavator to dig a trench in order to locate underground services. At this particular location, the service that was being located was a water line that was suspected of leaking. The water line was found at a depth of seven feet. Once the water line was partially exposed, the excavator could not be used to fully expose the line without causing further damage. Consequently, a worker was asked to get a shovel and start digging around the line where the leak occurred. Needless to say the soil around the leak was saturated.

The worker jumped into the trench and began to dig around the leaking water line. He made some progress by exposing the leak while digging on his knees when, suddenly, the walls of the trench caved in burying the worker. In the ensuing confusion, the excavator operator though he could dig most of the dirt around the buried worker. This attempt by the excavator operator only made matters worse because in his haste he caused a further collapse of the trench walls. At that point several workers jumped in with shovels and were able to locate the buried worker. This activity took approximately 30 min so that by the time they reached the buried worker he had expired as a result of suffocation. What went wrong?

Case #9: Coal-fired power plants require large amounts of water for cooling. As such, they are frequently located near rivers. The power plant at RIVELEC needed to have one of its intake grates repaired by a diver, so they contacted a local diving outfit to perform the repairs. This diving company was in the recreational diving business and had no experience with commercial or salvage diving operations. The repair work was to take place during the winter when the river temperature fell to approximately 37°F. In such cases, a dry diving suit is necessary with warm water heating. Such outfits are available but are quite expensive. Since the diving company had never performed this type of work, they decided to design their own warm water diving apparatus. They connected a gas powered boiler to a tank of water with circulation through the dry diving suit. As the diving operation began, all went well to the point where the boiler water temperature scalded the diver and

he suffered third degree burns over significant portions of his body. Their warm water suit design failed to incorporate a temperature sensor or a high temperature cutoff.

Case #10: Steel and metal mills require copious amounts of electrical energy. Consequently, the electrical supply equipment is very large and rated at high voltages and currents. The switches utilized to connect and disconnect power to various operations must be significantly more complex than a simple switch that is found in the electrical system of a home or a small office building. One of the safety features of a disconnect switch for large voltages and currents is a safety interlock. The safety interlock keeps the switch activated until the voltages and currents are sufficiently reduced to the point where an arc flash does not occur when the switch is attempted to be disconnected. There are various designs of safety interlocks. In this particular case, the safety interlock was mechanical. ALUMACORP, an aluminum processing plant, required one of its operations to be shut down for periodic maintenance. The shutdown required the electrical power to be disconnected so a trained electrician was sent to perform this duty. The electrician was familiar with this particular disconnect and knew that it was problematic. He opened the cabinet door and began the procedure for the disconnect. Unbeknownst to him, the interlock mechanical latch was bent so that its safety feature was ineffective. During his work he pulled on the switch to access a panel and the switch slid backward before the high currents and voltages were removed. The disconnection produced a severe arc flash, which burned portions of his face and chest. Inspection of the disconnect latch revealed that it was, in fact, bent and poorly designed so that normal wear would produce bending of the latch, which led to the failure and injuries.

Accident Reconstruction 9

Introduction

Mechanics, when applied to accident reconstructions, deals with the relationships between forces, bodies, and motion. The forces are produced by a combination of the relative motion of the vehicles, occupants, or systems. The method used to describe motion from a mathematical standpoint is called kinematics.

The motion of the particular body is defined as its continuous change in position relative to a coordinate system. For most applications in accident reconstruction, the preferred coordinate system is the Cartesian system. Some applications require cylindrical or spherical coordinate systems. In any of these coordinate systems, the position of the body is specified by its projection into the three axes of a rectangular coordinate system. As the bodies move along a path, the projections of the path to the respective axes move in straight lines. Thus, the motion of the bodies is reconstructed from the motions produced by the projections on the coordinate system. We begin this section with a discussion of the coordinate system adopted for vehicles.

The Society of Automotive Engineers (SAE) has adopted a coordinate system convention known as SAE J670e—Vehicle Dynamics Terminology. The SAE convention defines two individual coordinate systems: one that describes the dynamics of the vehicle with respect to its own coordinates and the other that describes the motion of the vehicle with respect to its location and dynamics with respect to the earth. These coordinate systems are simply modified forms of standard coordinate systems that are more aptly suited to the dynamics of a vehicle and the reconstruction of an accident. The first is the vehicle-fixed coordinate system, and the latter is referred to as the earth-fixed coordinate system. Figure 9.1 describes the vehicle-fixed coordinate system according to the SAE J670e convention.

For the vehicle-fixed coordinate system, the x-axis points straight ahead of the vehicle and originates at the center of mass of the vehicle. Accordingly, the y-axis points to the right or passenger's side of the vehicle, while the z-axis points downward toward the center of the earth. The vehicle-fixed coordinate system is attached to the vehicle's center of mass and moves along with the vehicle with respect to the earth-fixed coordinate system shown in Figure 9.2.

Note that in both the vehicle- and earth-fixed coordinate systems, the z-axis points toward the center of the earth and is therefore shifted by 180° from the conventional coordinate system. Care should be taken when converting data from standard coordinate systems to earth- or vehicle-fixed coordinate systems with respect to the orientation of the z-axis.

Basic Principles of Physics

Classical mechanics are based on three natural laws that are attributed to Sir Isaac Newton (1643–1727). Newton published in 1686 his *Philosophiae Naturalis Principia Mathematica* in which he described these laws. Engineers and scientists recognize these three basic

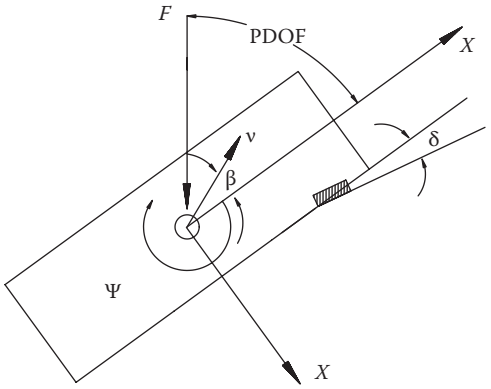

Figure 9.1 Vehicle-based coordinate system.

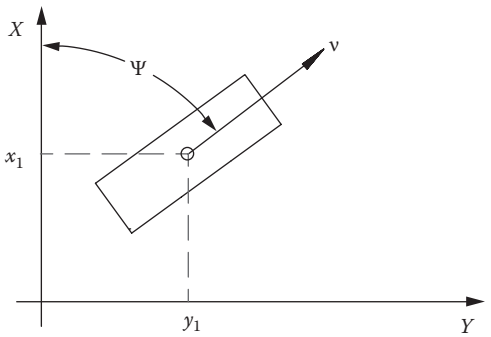

Figure 9.2 Earth-fixed coordinate system.

principles as laws because they have never been disproved. Keep in mind that Newton's laws do not take into account relativistic effects described by Albert Einstein. It suffices to say that relativistic effects are not encountered in accident reconstructions because the velocities are far below the speed of light and because Newton's first law is based on an inertial reference system. The basic equations are the following:

$$\boldsymbol{v} = \frac{d\boldsymbol{x}}{dt}; \quad \boldsymbol{a} = \frac{d\boldsymbol{v}}{dt} \tag{9.1}$$

where

$\boldsymbol{v}$ is the velocity
$\boldsymbol{a}$ is the acceleration
$\boldsymbol{x}$ is the displacement
t is time

Uniformly Accelerated Linear Motion

Many paths taken by vehicles involved in collisions take straight lines before and after the collision. Sometimes the paths are not quite straight but can be approximated by straight lines. The straight line approximations may be piecewise, that is, the curved path broken

down into linear pieces that closely approximate the actual path. Such piecewise approximations are common in engineering analyses and have a sound mathematical underpinning. This type of motion is then considered linear because it follows straight line paths. If the acceleration of the bodies in question is constant and linear, it is referred to as uniformly accelerated linear motion. For example, the acceleration or deceleration of an automobile is nearly constant when the brakes are applied or when the accelerator is activated. Generally, as a first approximation for most reconstructions, it is proper to assume constant acceleration. From Equation 9.1, we may write $\boldsymbol{a} = \boldsymbol{a}(t)$ = constant, or

$$\boldsymbol{v} = \int \boldsymbol{a}(t)dt + \boldsymbol{c}_1 = \boldsymbol{a}t + \boldsymbol{c}_1 \tag{9.2}$$

If we know the initial velocity of the vehicle or body, the constant $\boldsymbol{c}_1$ becomes $\boldsymbol{v}_0$, the initial velocity, thus

$$\boldsymbol{v} = \boldsymbol{v}_0 + \boldsymbol{a}t = \boldsymbol{v}(t) \tag{9.3}$$

Equation 9.2 yields the velocity as a function of time $\boldsymbol{v}(t)$. Thus, again from Equation 9.1 we say

$$\boldsymbol{x} = \int \boldsymbol{v}(t)dt + \boldsymbol{c}_2 = \boldsymbol{v}_0 + \tfrac{1}{2}\boldsymbol{a}t^2 + \boldsymbol{c}_2 \tag{9.4}$$

If we know the initial position x_0 at time $t = 0$, then $x_0 = c_2$ and

$$\boldsymbol{x} = \boldsymbol{x}_0 + \boldsymbol{v}_0 t + \tfrac{1}{2}\boldsymbol{a}t^2 \tag{9.5}$$

If we consider the acceleration as a function of the displacement or distance, we may write from Equation 9.1

$$\boldsymbol{a} = \frac{d\boldsymbol{v}}{dt} = \boldsymbol{v}\frac{d\boldsymbol{v}}{dx} \tag{9.6}$$

$$\int \boldsymbol{v}dv = \int \boldsymbol{a}dx + \boldsymbol{c}_3 \tag{9.7}$$

which yields

$$\frac{\boldsymbol{v}^2}{2} = \boldsymbol{a}x + \boldsymbol{c}_3 \tag{9.8}$$

If $\boldsymbol{v}_0$ is the velocity when the displacement is x_0, the constant of integration can be solved:

$$\boldsymbol{v}^2 = \boldsymbol{v}_0^2 + 2\boldsymbol{a}(x - x_0) \tag{9.9}$$

Thus, for uniformly accelerated linear motion, the equations may be summarized as follows:

$$\text{acceleration} \quad \boldsymbol{a} = \boldsymbol{a}(t) = \boldsymbol{a}(x) = \text{constant} \tag{9.10}$$

$$\text{velocity} \quad \boldsymbol{v} = \boldsymbol{v}(t) = \boldsymbol{v}_0 + \boldsymbol{a}t \tag{9.11}$$

$$\text{displacement} \quad \boldsymbol{x} = \boldsymbol{x}(t) = \boldsymbol{x}_0 + \boldsymbol{v}_0 t + \tfrac{1}{2}\boldsymbol{a}t^2 \tag{9.12}$$

$$\text{velocity} \quad \boldsymbol{v} = \boldsymbol{v}(x) = \sqrt{\boldsymbol{v}_0^2 + 2\boldsymbol{a}(x - x_0)} \tag{9.13}$$

Motion in a Plane

Up to this point, we have only considered motion along a straight line. The equations we have presented are used in accident reconstructions to describe the motions of vehicles as they are accelerating or decelerating (known as braking) or skidding. As we shall see at the end of the chapter in the sections of "Impulse" and "Momentum" and from our discussion of Newton's laws, vehicles skidding out of control tend to follow straight or slightly curved paths. Consider the vehicle in motion in Figure 9.3.

The velocity components are given by

$$v_x = \frac{dx}{dt}; \quad v_y = \frac{dy}{dt} \tag{9.14}$$

Similarly, the acceleration components become

$$a_x = \frac{dv_x}{dt} = \frac{d^2x}{dt^2}; \quad a_y = \frac{dv_y}{dt} = \frac{d^2y}{dt^2} \tag{9.15}$$

The velocity and acceleration vectors then become

$$\boldsymbol{v} = v_x\bar{\boldsymbol{a}}_x + v_y\bar{\boldsymbol{a}}_y \tag{9.16}$$

$$\boldsymbol{a} = a_x\bar{\boldsymbol{a}}_x + a_y\bar{\boldsymbol{a}}_y \tag{9.17}$$

Generally $\bar{\boldsymbol{a}}_x$; $\bar{\boldsymbol{a}}_y$; $\bar{\boldsymbol{a}}_z$ represent unit Cartesian coordinate vectors.

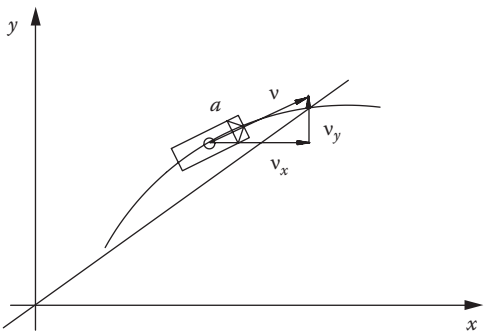

Figure 9.3 Motion in a plane.

Projectile Motion

A special case of uniformly accelerated linear motion occurs when a baseball is thrown, a gun is fired, a person jumps from a building, or a car drives off a cliff. In the absence of air resistance and near the surface of the earth, objects fall with almost constant acceleration. Figure 9.4 represents in a general manner the motion of a projectile. The x-y plane represents the surface of the earth or the reference plane and the *z*-axis represents the elevation relative to the reference plane.

The trajectory is the motion of the projectile. The projectile is the object with initial velocity that is acted upon by the acceleration due to gravity. In this analysis we neglect air resistance and the rotational motion of the earth. Strictly speaking, since the system is not inertial, it is not completely correct to use Newton's second law to relate the force on the projectile to its acceleration. Please refer to the section on "Newton's Second Law" for a more complete description. Based on the coordinates chosen, we may write

$$v_x = v_0 \cos\theta \tag{9.18}$$

$$v_z = v_0 \sin\theta - gt \tag{9.19}$$

Note that these components can be added vectorially as

$$\boldsymbol{v} = v_x \bar{\boldsymbol{a}}_{\boldsymbol{x}} + v_z \bar{\boldsymbol{a}}_{\boldsymbol{z}} \tag{9.20}$$

$$v = \sqrt{v_x^2 + v_z^2} \tag{9.21}$$

The coordinates of the projectile at any time can be found from the equations of uniformly accelerated linear motion. These are given by

$$x = v_0 \cos\theta t \tag{9.22}$$

$$z = v_0 \sin\theta t - \tfrac{1}{2} gt^2 \tag{9.23}$$

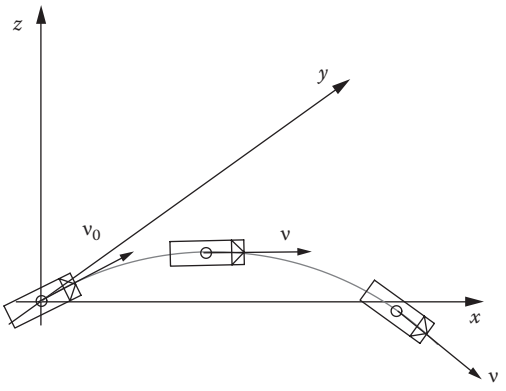

Figure 9.4 Projectile trajectory.

In the earlier equations, g is the acceleration due to gravity, t is the time, and θ is the angle of departure of the projectile relative to the reference plane. Equations 9.22 and 9.23 produce the trajectory in terms of time t. Eliminating t from the earlier equations, we obtain

$$z = \tan\theta x - \frac{gx^2}{2v_0^2 \cos^2\theta} \tag{9.24}$$

Equation 9.24 can be solved for the departure velocity given by

$$v_0 = \sqrt{\frac{gx^2}{2\cos^2\theta(x\tan\theta - z)}} \tag{9.25}$$

A special case of projectile motion occurs when an object falls freely. In terms of the coordinate system utilized in the previous discussion, Equation 9.12 may be written as

$$z = z_0 + v_0 t + \tfrac{1}{2} at^2 \tag{9.26}$$

but $z_0 = v_0 = 0$ and $a = g$, then

$$z = -\tfrac{1}{2} gt^2 \tag{9.27}$$

Uniformly Accelerated Curvilinear Motion

Curvilinear motion involves rotation and translation. Thus far we have only considered translational motion along a straight line or along a curve. Before we discuss the equations of curvilinear motion we will investigate rotation without translation. Figure 9.5 represents a rigid body, in this example, a vehicle that is undergoing rotation without translation about a fixed axis through point 0.

The instantaneous angular velocity $\boldsymbol{w}$ and the angular acceleration $\boldsymbol{\alpha}$ are given by

$$\boldsymbol{w} = \frac{d\theta}{dt}; \quad \mathbf{a} = \frac{d\boldsymbol{w}}{dt} \tag{9.28}$$

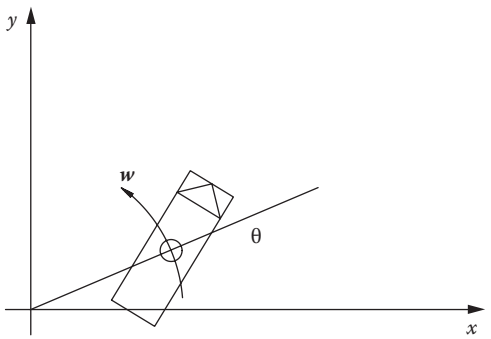

Figure 9.5 Vehicle rotation.

For rotation with constant angular acceleration

$$\alpha = \frac{d\omega}{dt} = \text{constant} \tag{9.29}$$

We may write

$$\omega = \int \alpha \, dt + c_1 \tag{9.30}$$

if ω_0 is the angular velocity when $t = 0$, the integration constant c_1 becomes the angular velocity:

$$\omega = \omega_0 + \alpha t \tag{9.31}$$

In a similar manner since $\omega = d\theta/dt$, we may write

$$\theta = \int \omega_0 dt + \int \alpha t dt + c_2 \tag{9.32}$$

Evaluating c_2 at θ_0 when $t = 0$, we obtain

$$\theta = \theta_0 + \omega_0 t + \tfrac{1}{2} \alpha t^2 \tag{9.33}$$

Since $\alpha = \omega d\omega/d\theta$ by the chain rule, then

$$\int \alpha d\theta = \int \omega d\omega + c_3 \tag{9.34}$$

If $\theta = \theta_0$ when $t = 0$ and $\omega = \omega_0$ is the initial angular velocity, then the constant of integration can be solved and

$$\omega^2 = \omega_0 = 2\alpha(\theta - \theta_0) \tag{9.35}$$

Relation between Angular and Linear Velocity and Acceleration

In many reconstructions of accidents, a vehicle loses control rounding a curve and deposits yaw marks on the read surface. The arc produced by the yaw marks can be used to determine to a first approximation the velocity of the vehicle when loss of control occurred. This method of analysis is the subject of much debate. In subsequent sections of the book we will pose our arguments for the accuracy and validity of this analysis. Consider Figure 9.6, which represents a vehicle losing control rounding a curve and producing a nearly circular path.

The radius of the circle and the arc length are given by

$$s = r\theta \tag{9.36}$$

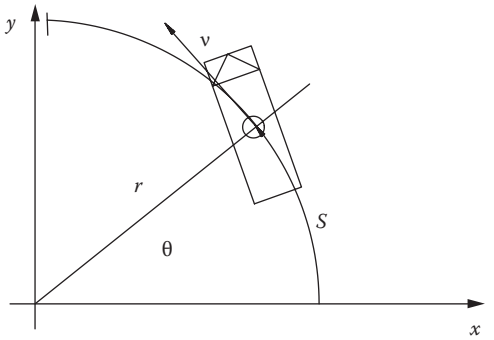

Figure 9.6 Vehicle loss of control.

If the radius is constant upon differentiation, we obtain

$$\frac{ds}{dt} = r\frac{d\theta}{dt} \tag{9.37}$$

In Equation 9.37, ds/dt represents the magnitude of the linear velocity v and $d\theta/dt$ is the angular velocity w, so

$$v = rw \tag{9.38}$$

If we differentiate again with respect to time,

$$\frac{dv}{dt} = r\frac{dw}{dt} \tag{9.39}$$

In Equation 9.39 the term dv/dt is the magnitude of the tangential component of the acceleration $\boldsymbol{a}_T$ and dw/dt is the angular acceleration $\boldsymbol{\alpha}$, so

$$\boldsymbol{a}_T = r\boldsymbol{a}_t \tag{9.40}$$

The radial component of the acceleration is then

$$\boldsymbol{a}_R = \frac{v^2}{r}\boldsymbol{a}_r = w^2 r\boldsymbol{a}_r = wv\boldsymbol{a}_r \tag{9.41}$$

In general, the acceleration can be expressed in terms of the tangential and radial, or normal, components:

$$\boldsymbol{a} = \boldsymbol{a}_T + \boldsymbol{a}_N \tag{9.42}$$

or for the case in question

$$\boldsymbol{a} = r\alpha\boldsymbol{a}_t + \frac{v^2}{r}\boldsymbol{a}_r \tag{9.43}$$

$\boldsymbol{a}_t$; $\boldsymbol{a}_r$ represent unit tangential, radial vectors.

Figure 9.7 represents the accelerations discussed earlier.

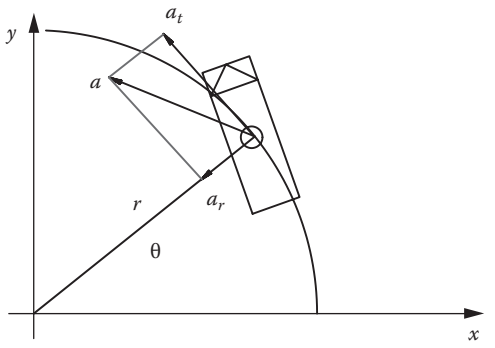

Figure 9.7 Angular acceleration.

Newton's First Law

At first glance, Newton's first law appears simple and self-evident. However, upon analysis, the first law has subtle points that need to be clarified. The first law deals with forces on bodies such as passenger vehicles. In an accident, forces alter the shape or dimensions of the vehicles and they change the state of motion of these vehicles. The motion of a vehicle consists of its translational motion and its rotational motion. When forces balance any translational and rotational motion, the vehicle is in equilibrium. A body or vehicle in equilibrium is therefore at rest or moves in a straight line with constant speed, and the body is either not rotating or rotating at a constant rate. In mathematical terms, we may refer to the vehicle representation of the vehicle-fixed coordinate system of Figure 9.2. We define the following for the earth-fixed system:

$\boldsymbol{V}$ = velocity of the vehicle relative to the earth
ψ_1 = vehicle heading relative to the earth
X_1 and Y_1 = coordinate positions at any instant of time t

Similarly, for the vehicle-fixed system, we define

$\boldsymbol{v}$ = velocity of the vehicle relative to its coordinates
β = sideslip angle of the vehicle
δ = steering angle of the vehicle
ψ = relative rotations of the vehicle
$\boldsymbol{F}$ = external force acting on the vehicle through a relative angle referred to as the Principal Direction of Force (PDOF)

Thus, the vehicle in equilibrium would meet the following criteria:

$$\boldsymbol{V} = \boldsymbol{v} = \psi = 0 \quad \text{or } a \text{ constant} \tag{9.44}$$

It is possible that the vehicle is in translational but not rotational equilibrium or vice versa. For the case of translational but not rotational equilibrium, the lines of action affecting the vehicle would not align and the vehicle would then form a couple. This motion is sometimes seen at the end of a skid mark when a vehicle tends to rotate about its center of mass. In other cases, the vehicle first rotates upon impact and then rolls

or slides to its rest position. In mathematical form, the resultant forces for a vehicle in equilibrium must cancel so that

$$\sum F_x = 0 \quad \text{and} \quad \sum F_y = 0 \tag{9.45}$$

Equation 9.45 in two dimensions is called the first condition of equilibrium. The second condition of equilibrium can be expressed in terms of the moments of the forces acting on the vehicle. Recall that the vector moment $\boldsymbol{\Gamma}$ of a force $\boldsymbol{F}$ about an arbitrary axis is defined as

$$\mathsf{G} = \boldsymbol{r} \times \boldsymbol{F} \tag{9.46}$$

where

$\boldsymbol{r}$ is the radial moment arm of the force $\boldsymbol{F}$
$|\boldsymbol{\Gamma}| = \Gamma = \boldsymbol{rF} \sin \theta$ = magnitude of the torque

In order to eliminate the condition of a couple, that is, the forces acting on the vehicle have the same line of action, the magnitude of the resultant moment about the perpendicular axis to the plane must be zero. Thus, for the equations described in 9.45, the condition must be

$$\sum T_z = 0 \tag{9.47}$$

Therefore, in order to meet both conditions of equilibrium, the resultant force $\boldsymbol{F}$ and the resultant vector moment $\boldsymbol{\Gamma}$ about any axis must be zero or

$$\boldsymbol{F} = 0; \quad \mathsf{G} = 0 \tag{9.48}$$

A statement of Newton's first law is generally expressed as "Every body continues in its state of rest or in uniform motion in a straight line unless acted upon by external forces." An inertial reference system is defined as one relative to which a body remains at rest or moves uniformly in a straight line when no external force acts on it. For the purpose of accident reconstruction, a reference system attached to the earth can be considered an inertial system if we disregard the earth's rotation. Thus, the earth-fixed coordinate systems of Figures 9.1 and 9.2 satisfy Newton's first law.

Newton's Second Law

The second law is a direct consequence of Newton's first law. The first law states that if the force on a body is zero, then the acceleration on the body must be zero. Recall from basic physics that acceleration is the time derivative of velocity. If velocity is a constant with respect to time, then the acceleration or time derivative of a constant must be zero. Newton's second law states that if the resultant force on a body is not zero, the body must move with accelerated motion. Furthermore, the acceleration produced by the force depends on the mass of the object. In equation form, Newton's second law is stated as

$$\sum \boldsymbol{F} = m\frac{d\boldsymbol{v}}{dt} = m\boldsymbol{a} \tag{9.49}$$

Newton's second law, as stated earlier, applies to rectilinear as well as curvilinear motion for a particle. In the context of a body such as a vehicle in an accident reconstruction, it is recognized that all the particles that comprise the vehicle are not rotating with the same acceleration if the vehicle is in curvilinear motion. It is sufficient, however, to consider the acceleration at the center of mass of the vehicle.

Accident reconstructions generally involve solutions to physical phenomena within the study of "mechanics." Mechanics includes the study of motion and the forces that produce the motion. More specifically, the study of motion is referred to as "dynamics" while in the special case where the acceleration is zero, it is known as "statics." Some authors use the term "kinematics" to describe systems in motion. It is again worthwhile to emphasize that the velocities encountered in accident reconstruction are very small compared to the velocity of light so that relativistic concepts need not be considered. All the velocities and accelerations are measured relative to an inertial reference system, namely, the earth. The earlier discussion reveals that Newton's first law is a special case of a more general phenomenon, which is recognized as Newton's second law.

Before we depart from Newton's second law, we need to include a final word about mass and its center. A discussion of finding the center of mass or gravity, as it is sometimes referred to, will follow in a later section. In accident reconstructions, it is sufficient to track the motion of the center of mass of the vehicle. Whether the motion is rectilinear, curvilinear, or a combination of both is immaterial. Newton's second law as expressed in Equation 9.49 is general. Knowing the acceleration vector $\boldsymbol{a}$ at any point in time and the corresponding force vectors $\Sigma \boldsymbol{F}$, a sufficient description of the accident event can be formulated.

Newton's Third Law

A single isolated force is physically impossible. Consider the case of an object resting on a table. If we only consider the force of gravity on the object, then the object should be accelerated toward the center of the earth. It is obvious that a resistive force, applied through the structure of the table, must be exerting a force equal in magnitude and opposite in direction. We see then that when a body exerts a force on another body, the second must always exert on the first an equal and opposite force through the same line of action in order to keep the object on the table. These two forces describing the interaction between two bodies are often called the action and reaction with no delineation as to which is the cause and which is the effect. Accident reconstruction analysis of crush energy deformation makes use of Newton's third law as a method of checks and balances for speed calculations. The general statement of Newton's third law is "for every action there is always an equal and opposite reaction." Mathematically, we represent Newton's third law for a force $\boldsymbol{F}$ and its reaction $\boldsymbol{F}'$ as

$$\boldsymbol{F} = -\boldsymbol{F}' \tag{9.50}$$

Newton's third law describes the equilibrium of a particle or an object. In nature, the forces acting on an object or vehicle do not all pass through one point such as the center of mass. Thus, the forces are noncurrent so that the vehicle, which is a relatively rigid body, undergoes rotational and translational motion. There are many accident scenarios where the rotation of the vehicle has a relatively small consequence on the accident reconstruction and can therefore be ignored. In these cases, translational linear motion suffices as accurate description of the accident scenario. In other instances, the effects of rotation cannot

be ignored and must be accounted for in the analysis. Several examples in the chapter will highlight the various techniques and appropriate assumptions employed by the authors.

Nature is deceptively complicated. Most processes are very complex. Take, for example, the motion of a pedestrian struck by an automobile. If the approximate point of impact and the approximate location of the pedestrian's landing are known, the speed of the vehicle at impact may be calculated. To do so, several simplifying assumptions may need to be made. First we consider the pedestrian to be an ideal object like a rigid smooth sphere. Second, we ignore the rotation of the body and the effects of air resistance including the buoyancy effects of air. The idealized problem is then quite different from the original problem. However, at relatively low velocities, the simplifying assumptions yield manageable calculations that solve the problem within engineering accuracy.

Center of Gravity or Mass

In a vehicle, every particle of that vehicle is attracted toward the center of the earth. Since the center of the earth is at a far distance, the forces attracting all the particles in the vehicle are essentially parallel. The sum of all the forces is the total weight of the vehicle or

$$\sum w_i = w_T \tag{9.51}$$

Since the resultant moment of the weight about any axis through the center of gravity is zero, the line of action of the weight of the vehicle passes through the center of mass. This concept allows the accident reconstructionist to track the path of the vehicles through their center of mass irrespective of the orientation of the vehicle when considering translational effects. Consequently, significant emphasis need not be placed on the relative shape of the skid marks deposited by the tires in a collision. The line of action of the weight of a vehicle in the respective rectangular coordinates can be expressed as

$$\overline{x} = \frac{\sum x_i w_i}{w_T} \tag{9.52}$$

$$\overline{y} = \frac{\sum y_i w_i}{w_T} \tag{9.53}$$

and

$$\overline{z} = \frac{\sum z_i w_i}{w_T} \tag{9.54}$$

Center of gravity calculations are sometimes necessary in accident reconstructions. Certain accident scenarios require the computations in order to determine the propensity for rollover or flip of the vehicle. Loading conditions on tractor trailers can significantly affect the center of mass, which sometimes causes these large vehicles to overturn. Similarly, hoists, manlifts, and cranes all operate on the premise that the center of gravity will dominate the loading conditions. Therefore, these devices have limits of operation that must be followed. Misapplication of loading conditions on cranes generally results in catastrophic failure.

Construction equipment, such as bulldozers, backhoes, and loaders, have safe ranges of operation all dealing with the center of mass. Sport utility vehicles and all terrain vehicles have relatively high centers of mass, making then more prone to overturning. These high centers of gravity for particular vehicles can influence the reconstruction and may lead to product liability considerations.

Impulse and Momentum

Newton's laws of motion give rise to the concepts of work and energy and the concepts of impulse and momentum. We will first consider impulse and momentum and then work and energy. Both concepts are similarly derived from Newton's second law:

$$\boldsymbol{F} = m\boldsymbol{a} = m\frac{d\boldsymbol{v}}{dt} \tag{9.55}$$

Figure 9.8 represents a vehicle moving along a roadway with coordinate axes x and y

Rearranging Equation 9.55 and providing limits of integration, we observe

$$\int_{t_1}^{t_2} \boldsymbol{F}dt = \int_{v_1}^{v_2} m d\boldsymbol{v} \tag{9.56}$$

The quantity on the left side of Equation 9.56 is called the impulse of the force $\boldsymbol{F}$ over the time interval $t_2 - t_1$. So by definition

$$\text{Impulse} = \int_{t_1}^{t_2} \boldsymbol{F}dt \tag{9.57}$$

The impulse is a vector quantity that can only be evaluated when the force $\boldsymbol{F}$ is known as a function of time t. In vehicular collisions or events, the force is simply not known as a function of time. In some instances the force may be calculated based on the results of the right side of Equation 9.56. The integral on the right side of Equation 9.56 yields the result

$$\mathrm{m}\,\boldsymbol{v}_2 - \mathrm{m}\,\boldsymbol{v}_1 \tag{9.58}$$

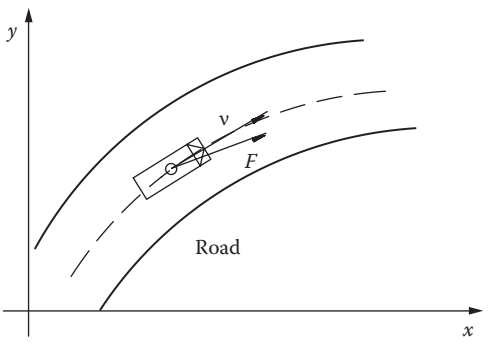

Figure 9.8 Vehicle in a curved path.

The product of the mass of the vehicle and its velocity is a vector quantity and is called the linear momentum:

$$\text{Linear momentum} = m\boldsymbol{v} \tag{9.59}$$

We may thus rewrite Equation 9.56 as

$$\int_{t_1}^{t_2} \boldsymbol{F}dt = mv_2 - mv_1 \tag{9.60}$$

Equation 9.60 expresses a subtle yet very important concept that applies to collisions between vehicles as will soon be discussed. First we wish to state the significant fact of Equation 9.60: The "vector impulse" of the resultant force on a vehicle or particle, over the time interval, is equal in magnitude and direction to the "vector change" in momentum of the vehicle or particle. This is the impulse momentum principle that is often violated in the reconstruction of vehicular collisions. The impulse momentum principle is chiefly applied to short duration forces arising from explosive events or collisions. These types of forces are often referred to as impulsive forces.

We will soon see that work and energy are scalar quantities where the development of impulse and momentum reveal that they are vector quantities. As such, the impulse and momentum may be broken down into component parts in the x–y plane of Figure 9.8 to yield

$$\int_{t_1}^{t_2} F_x dt = mv_{x2} - mv_{x1} \tag{9.61}$$

$$\int_{t_1}^{t_2} F_y dt = mv_{y2} - mv_{y1} \tag{9.62}$$

It follows that in a three-dimensional (3D) problem when the forces and velocities have a component in the z-direction,

$$\int_{t_1}^{t_2} F_z dt = mv_{z2} - mv_{z1} \tag{9.63}$$

Consider Figure 9.9 where the force produced in a collision decreases over time as shown.

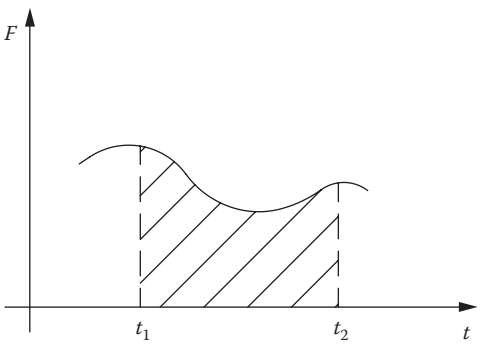

Figure 9.9 Force decreases over time.

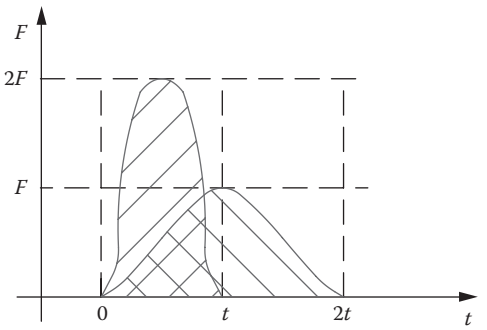

Figure 9.10 Equal areas.

The area under the curve between the times t_1 and t_2 is equal to the impulse of the force n the time interval. For vehicular collisions, the time interval is in the range of 100 ms. The force exerted on one vehicle may vary according to the stiffness of the vehicle. The stiffer the vehicle, the shorter the duration of the impulse. Accordingly, the more flexible the vehicle, the longer the duration of the pulse. Figure 9.10 shows the plot of the force on two vehicles with equal impulses but over different time elements.

The curves of Figure 9.10 represent the different designs exhibited by a stiff vehicle and a more crash worthy or flexible vehicle. The newer design in vehicles allows for the energy, or in particular the impulse pulse, to be spread out over a longer time span, which reduces the forces exerted on the occupants. In a collision, the change in momentum of the vehicle is dictated by the mass of the vehicle and the corresponding change in the velocity. The center of the mass of the vehicle is totally unimportant. Keep in mind that vehicles are relatively stiff structures even though the newer models contain crumple zones that help absorb the energy. Even in relatively violent collision, the center of mass of the vehicle does not move appreciably. We will come back to the concept of center of mass when discussing objections to the use of momentum techniques.

Conservation of Momentum

In a general sense, we now explain the concept of conservation of linear momentum. In later sections of the chapter, we will discuss the specific applications of various momentum methods. These include elastic, and plastic collisions, restitution, and rotational momentum techniques.

When two vehicles, bodies, or particles interact and produce forces, the momentum of each body is changed because of the forces that each exert on the other. Thus, by Newton's third law, the force that exerted on each body is equal in magnitude and opposite in direction to that which is exerted on the other. Notice that in this discussion we say that the vehicles, bodies, or particles are involved in the adherence to Newton's third law. A vehicle or body is simply a conglomeration of various particles or smaller bodies. Each portion of the vehicle is subject to the same law. Since these objects generally remain together as a result of the collision, it is useful to describe the behavior pre- and postcollision in terms of the center of mass of the object, machine, or vehicle. Even if a portion of a vehicle separates from the other portion, Newton's third law applies as does conservation of momentum. It is important to note that the impulses of the forces are equal in magnitude and opposite in direction.

This topic is very important and needs further clarification. Since the impulses of the forces are equal and opposite, the vector change in momentum of either vehicle, in any time interval, is also equal in magnitude and opposite in direction to the vector change in momentum of the other. Thus, the net change in momentum of the colliding bodies, the system, must be zero. Since the pair of action-reaction forces are internal forces of the system and since the total momentum of the system cannot be changed by internal forces, and since the only forces acting on the system are internal forces, the total momentum of the system must remain constant in magnitude and direction. Keep in mind that in such a collision there are no appreciable external forces acting on the system. Thus, when no external force acts on the system, the total momentum of the system must remain constant in magnitude and direction.

This is the principle of conservation of linear momentum. This principle is also misunderstood by some accident reconstructionists. Typical arguments against the use of conservation of linear momentum fall into four basic categories. One category involves collinear collisions. That is, both vehicles are traveling in the same or opposite directions. In such instances, many reconstructions fail at a solution because of their inability to understand the problem and their lack of mathematical sophistication. Another category involves low-velocity impacts. Some people state that momentum does not hold true for low-velocity impact. However, conservation of linear momentum places no restrictions on initial conditions and conservation of momentum can be used at any speed. A third category involves vehicles of significantly different masses such as a tractor trailer and a passenger vehicle. Again the development of conservation of linear momentum places no restrictions on masses, that is, initial conditions for the collision. In actuality, before the advent of sophisticated measurement techniques in the last century, the muzzle velocity of a bullet was measured using the concept of conservation of linear momentum. That is, a small mass, the bullet, traveling at a high velocity, was fired into a large block of wood and the deflection of the wood from the impact was measured. The block of wood was a large mass at rest. This standard test was used successfully to accurately determine the muzzle velocity of bullets. Note that this test setup involved greatly varying masses and velocities, two arguments used against the use of momentum. A final category of argument against the use of conservation of linear momentum is that it does not hold true for shallow angle collisions. Again there are no restrictions on initial conditions, that is, shallow angles, in the development of the theoretical arguments of momentum. It is true, however, that shallow angle collisions are very sensitive to the preimpact angles. These types of collisions lend themselves readily to computer solutions. It should be obvious that if two vehicles sideswipe and keep on going, it is not possible to utilize momentum to determine vehicle velocities. However, if they collide at shallow angles and skid to rest, there is no restriction on the use of momentum to determine the vehicle velocities. This is an example where engineering judgment, skill, and sophistication allow the problem to be solved.

In conclusion, it must be stated that the principle of conservation of momentum, whether linear or rotational, is extremely fundamental and powerful. Conservation of momentum is more fundamental and general than the principle of conservation of mechanical energy. Momentum methods have a wider application than energy methods. Conservation of momentum holds true no matter what the nature of the internal forces acting on the bodies, particles, or vehicles. In contrast, mechanical energy is conserved only when the internal forces are themselves conservative. We will discuss conservation of energy and work in the next section.

On a final note, often when other experts do use momentum, they generally apply it to T-bone type collisions because those are the easiest to solve and are not sensitive to pre- and postcollision angles.

Conservation of Energy and Work

In order to determine how energy and work affect a vehicle in motion, we consider the diagram shown in Figure 9.11.

The curved path represents the trajectory of the vehicle of mass m moving in the x–y plane and acted on by a force $\boldsymbol{F}$. This force may be produced by the driver's input or resulting from a collision and may vary from point to point along the path. We choose to resolve the force into its components F_s and F_n along and normal to the path. The normal component of the path, F_n, is the centripetal force and its effect is to change the direction of the velocity v. The effect of the component, F_s, is to change the magnitude of the velocity.

In general terms, the magnitude of F_s will be a function of the path s, where s is the distance that the vehicle has traveled from a fixed reference point D. Applying Newton's second law,

$$F_s = m\frac{dv}{dt} \tag{9.64}$$

Since F_s is a function of the path s, we may apply the chain rule, so

$$\frac{dv}{dt} = \frac{dv}{ds}\frac{ds}{dt} = v\frac{dv}{ds} \tag{9.65}$$

then

$$F_s = mv\frac{dv}{ds} \tag{9.66}$$

If v_1 is the velocity when $s = s_2$ and v_2 is the velocity when $s = s_2$, we may integrate Equation 9.66:

$$\int_{s_1}^{s_2} F_s d_s = \int_{v_1}^{v_2} mvdv \tag{9.67}$$

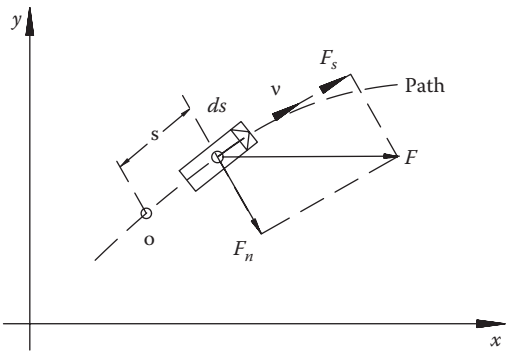

Figure 9.11 Vehicle in motion.

The integral on the left of Equation 9.67 is the work W of the force F and is defined as

$$W = \int_{s_1}^{s_2} F_s d_s \tag{9.68}$$

The integral given by Equation 9.68 can only be integrated when F_s is known as a function of s or when F_s and s are related by another variable. In accident reconstructions, this is seldom the case. However, the integral on the right side can always be evaluated:

$$\int_{v_1}^{v_2} mvdv = \frac{1}{2}mv_2^2 - \frac{1}{2}mv_1^2 \tag{9.69}$$

Equation 9.69 represents the kinetic energy of the vehicle and is represented as

$$E_k = \frac{1}{2}mv^2 \tag{9.70}$$

Equation 9.67 is generally written as

$$W = E_{k2} - E_{k1} \tag{9.71}$$

stating that the work of the resultant force exerted on the vehicle equals the change in the kinetic energy, and is known as the work–energy principle.

Some explanatory material is in order at this point so that work and energy are properly applied to vehicles and the resulting collisions. Work on a vehicle is only done when the forces are exerted while the components at the same time move along the line of motion:

$$W = \int_{s_1}^{s_2} \boldsymbol{F} \cdot d\boldsymbol{s} = \int_{s_1}^{s_2} F\cos\theta ds \tag{9.72}$$

If the component of the force is in the same direction as the displacement, the work is positive. If the force is opposite to the displacement, the work is negative. If the force is perpendicular to the displacement, the work is zero. If the car or a component of the car is lifted, the work of the lifting force is positive as when a spring is stretched or when the gas in a shock absorber is compressed. When the car skids on a road, the work of the frictional force exerted on the tires is negative along the path since the force is opposite the displacement of the vehicle. No work is done on the road by the frictional forces because there is no motion of the road.

In computing the work of a force, we multiply the magnitude of the vector $\boldsymbol{F}$ in the direction of the vector ds. This is the scalar product of the vectors. Thus, in general terms, care must be taken in computing the work as in the special case where $\cos\theta = \pm 1$.

$$W = \pm Fs \tag{9.73}$$

Only in this special case is work equal to force times distance. Figure 9.12 is a generalized diagram representing work according to Equation 9.72.

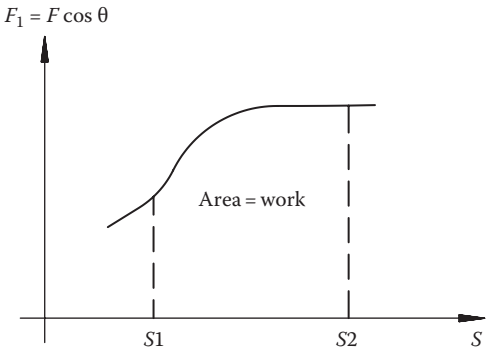

Figure 9.12 Work diagram.

The resultant force ***F*** acting on the vehicle may be made up of several forces acting such as the individual frictional forces on the tires as the vehicle skids out of control. Each of these may be computed from the basic definition of work. Since work is a scalar quantity, the total work is the algebraic sum of the individual works. These concepts are fully analyzed in "Friction and the Speed of a Vehicle" in the Energy Methods section of this chapter. Note that only the total work is equal to the change in kinetic energy of the vehicle.

Kinetic Energy

A review of Equation 9.71 reveals that kinetic energy and work are scalar quantities. The magnitude of the velocity of a moving vehicle is the only parameter that establishes the amount of kinetic energy. The process that produced the motion, not the direction of the motion, establishes the value of the kinetic energy. The work energy principle states that the change in the kinetic energy does not depend on the individual values of the force ***F*** and the path *s*. Kinetic energy increases if the work is positive and decreases if the work is negative. As a vehicle accelerates, the work is positive and as it decelerates, the work is negative. A vehicle traveling at a constant velocity does no work and the change in kinetic energy is zero.

Potential Energy due to Gravity

In accident reconstructions, the bodies in motion, whether vehicles, humans, or equipment, are near or on the surface of the earth so that variations in the gravitational force can be neglected. Figure 9.13 represents a body moving vertically along an arbitrary path.

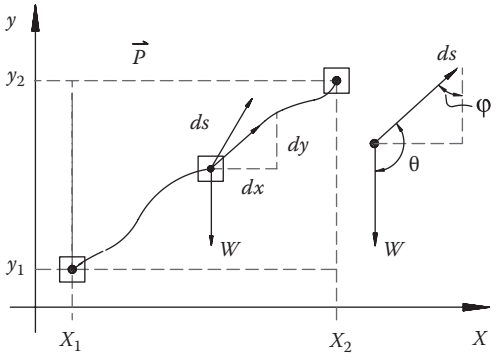

Figure 9.13 Gravitational potential energy.

The downward force on the body is produced by its weight w and P is the resultant of all the other forces acting on the body. The work of the gravitational force is

$$W_g = \int_{s_1}^{s_2} w \cos\theta ds \tag{9.74}$$

Since φ is the angle between ds and the vertical component dy, then $dy = ds \cos \varphi$ and $dy = -\cos \theta\ ds$, thus

$$W_g = -\int_{y_1}^{y_2} w dy = w(y_2 - y_1) = (mgy_2 - mgy_1) \tag{9.75}$$

Therefore, the work of the gravitational force depends only on the initial and final elevations and not on the path. Since the total work is equal to the change in kinetic energy,

$$W_T = W_P + W_g = E_{k2} - E_{k1} \tag{9.76}$$

where

W_T is the total work
W_P is the work of the force $\boldsymbol{P}$
W_g is the work due to gravitational effects
E_{k2} is the final kinetic energy
E_{k1} is the initial kinetic energy

Generally, it is convenient to express Equation 9.76 in terms of the work of the force $\boldsymbol{P}$ so that

$$W_{\boldsymbol{P}} = \left(\frac{1}{2}mv_2^2 - \frac{1}{2}mv_1^2\right) + (mgy_2 - mgy_1) \tag{9.77}$$

or

$$W_{\boldsymbol{P}} = \left(\frac{1}{2}mv_2^2 + mgy_2\right) - \left(\frac{1}{2}mv_1^2 + mgy_1\right) \tag{9.78}$$

where

$$E_{\boldsymbol{P}} = mgy \tag{9.79}$$

is the gravitational potential energy.

The sum of the kinetic and potential energy is called the total mechanical energy. The work of all the forces acting on the body, except for the gravitational force, equals the change in the mechanical energy. If the work $W_{\boldsymbol{P}}$ is positive, the mechanical energy

increases; if negative, it decreases. In the special case in which the only force on the body is the gravitational force, the work W_P is zero. Then

$$\frac{1}{2}mv_2^2 + mgy_2 = \frac{1}{2}mv_1^2 + mgy_1 \tag{9.80}$$

Elastic Potential Energy

Another concept that is utilized in accident reconstruction is that of elastic potential energy. This principle is introduced in the modeling of the crush deformation of a vehicle during a collision and is based on Hooke's law, which states that the elastic force is proportional to the displacement of the spring. Consider Figure 9.14.

When an external force ***P*** stretches or compresses the spring so as not to permanently deform it, the elastic force is given by

$$F = kx \tag{9.81}$$

where k is the stiffness constant of the spring and x is the displacement. The work of the elastic force is given by

$$W_e = \int \boldsymbol{F} \cdot d\boldsymbol{s} = \int_{x_1}^{x_2} F\cos\theta dx \tag{9.82}$$

since the force ***F*** is opposite the direction of dx, $\cos\theta = -1$ and

$$W_e = -\int_{x_1}^{x_2} Fdx = -\int_{x_1}^{x_2} kxdx \tag{9.83}$$

$$W_e = -\left(\frac{1}{2}kx_2^2 - \frac{1}{2}kx_1^2\right) \tag{9.84}$$

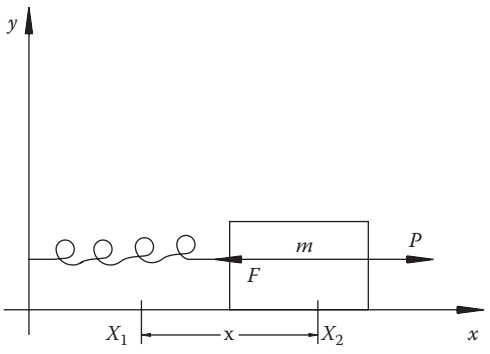

Figure 9.14 Hooke's law.

As in the previous section, we will let W_P be the work of the applied force $\boldsymbol{P}$ so that the total work is equal to the change in the kinetic energy, and

$$W_T = W_P + W_e = E_{k2} - E_{k1} \tag{9.85}$$

or

$$W_{\boldsymbol{P}} = \left(\frac{1}{2}mv_2^2 - \frac{1}{2}mv_1^2\right) + \left(\frac{1}{2}kx_2^2 - \frac{1}{2}kx_1^2\right) \tag{9.86}$$

where

$$E_{ep} = \frac{1}{2}kx^2 \tag{9.87}$$

is the elastic potential energy. Equation 9.86 may also be written similarly to Equation 9.78 as

$$W_P = \left(\frac{1}{2}mv_2^2 + \frac{1}{2}kx_2^2\right) - \left(\frac{1}{2}mv_1^2 + \frac{1}{2}kx_1^2\right) \tag{9.88}$$

In this case, the total mechanical energy is the sum of the kinetic and elastic potential energies. The work of all the forces acting on the body, except for the elastic force, equals the change in the mechanical energy. If W_P is positive, mechanical energy increases; if negative, it decreases. In the special case when W_P is zero, the mechanical energy is conserved and constant.

Dissipation and Conservation of Energy

The work of the gravitational force is independent of the path and purely dependent on the vertical displacement. Thus, when an object such as a vehicle or a person falls and is subject to the motion of a projectile, for the same initial speed, irrespective of the angle of departure, the speed is the same at all points at the same elevation. If the gravitational force acts alone on the object, the total mechanical energy is conserved. If the object first rises and then descends to its original position, the work is completely recovered.

Similarly, the extension and contraction of a spring to the original location, the elastic potential energies are conserved and the work is recovered. Thus, conservative forces as outlined earlier are characterized by independence of path, equality of the difference between initial and final energy functions, and are completely recoverable. In contrast, the force produced by friction depends on the path. When a vehicle skids for 50 ft or for 75 ft from one point to another, the energy expended differs. The skid of 50 ft may be a straight line between two points, whereas the skid of 75 ft may be a curved path between the two points. Much erroneous significance is often placed on which wheel produced which skid by many reconstructionists. Later sections of the book outline the fallacy in these arguments based on basic principles. If a vehicle skids to one location and then skids back to its original position, the work is not recovered and thus the total mechanical energy is not

conserved. Care must always be taken when applying conservation of energy principles. That is why in an earlier section, we stated that energy is not always conserved but momentum is always conserved and is therefore a more fundamental principle. Friction involves dissipative forces rather than conservative forces in classical Newtonian mechanics.

Internal Work, Energy, Power, and Velocity

Consider a vehicle undergoing acceleration as shown in Figure 9.15. The external forces on the automobile are the weight W and the normal forces N_1 and N_2. The work of these external forces is zero because they are perpendicular to the motion of the vehicle. The forces P_1 and P_2, depending on whether the vehicle is rear-, front-, or all-wheel drive are the unbalanced forces that produce the acceleration and velocity. The work of P_1 and P_2 is zero at the point of application and is not equal to the increase in kinetic energy of the system. Therefore, the internal work is responsible for the motion that is produced. In a more general sense, both internal and external forces produce the change in the total kinetic energy of the system. Thus

$$W_T = W_o + W_i = \Delta E_k \tag{9.89}$$

where

W_T is the total work
W_o is the external work
W_i is the internal work
ΔE_k is the kinetic energy change

A more general representation for the work produced by external and internal forces is then

$$W_P = W_T + \Delta E_{ep} + \Delta E_{ip} \tag{9.90}$$

where

W_T is the total kinetic energy change
ΔE_{ep} is the external potential energy
ΔE_{ip} is the internal potential energy

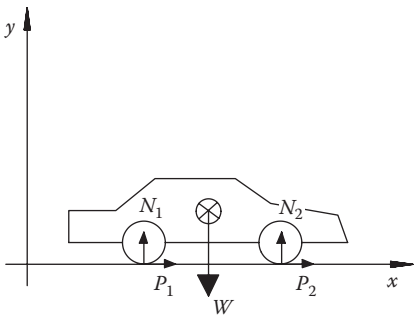

Figure 9.15 Accelerating vehicle.

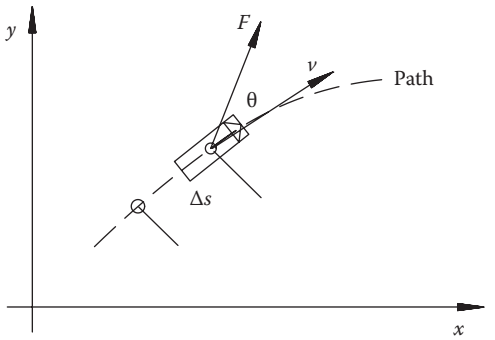

Figure 9.16 Forces on a vehicle.

In Equation 9.90 the total mechanical energy of the system includes the external and internal potential energies and the kinetic energy. The total mechanical energy is conserved only when W_P is zero.

The rate of doing work is defined as the power of the system so that the instantaneous power is given by

$$\boldsymbol{P} = \frac{dW}{dt} \tag{9.91}$$

and the average power is

$$P_{av} = \frac{\Delta W}{\Delta t} \tag{9.92}$$

Figure 9.16 represents a force on a vehicle causing a displacement Δs along a path.

The tangential component F_t of the force $\boldsymbol{F}$ is related to the power by the velocity $\boldsymbol{v}$ as

$$P_{av} = \frac{\Delta W}{\Delta t} = F_t \frac{\Delta s}{\Delta t} = F_t \boldsymbol{v} \tag{9.93}$$

In general we may write

$$P = \boldsymbol{F} \cdot \boldsymbol{v} \tag{9.94}$$

Equation 9.93 states that the instantaneous power is the product of the instantaneous velocity $\boldsymbol{v}$ and the tangential component of the force F_t. Equations 9.89 through 9.94 are used to compute the relationship between velocity and horsepower of a given vehicle if the gear ratio of the transmission is known.

Change in Velocity

When vehicles collide, they undergo a change in their velocities. The change in their velocities is a result of the conservation of energy and conservation of momentum, which we discussed in the previous sections. Change in velocity is a concept that is simple but often

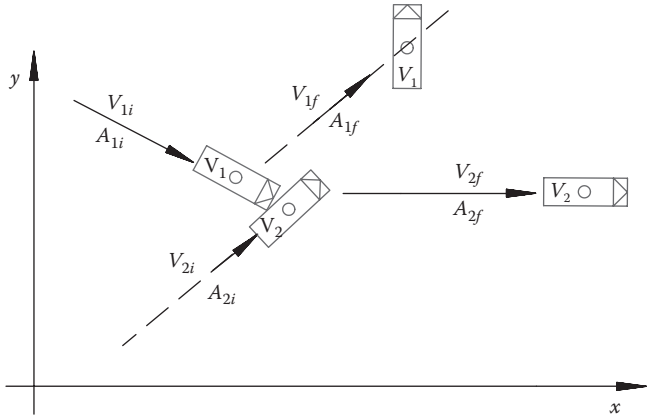

Figure 9.17 Change in velocity.

misunderstood. In order to properly define change in velocity, sometimes improperly referred to as change in speed, and commonly described as ΔV, we refer to Figure 9.17.

In a statement, change in velocity is defined as the change in the magnitude and the change in the direction of the velocity of a vehicle resulting from a collision. Thus, the change in velocity of a vehicle is a measure of the velocity vector preimpact and the velocity vector postimpact. In terms of equations we define

$$\Delta V = [(V_{ix} - V_{fx})^2 + (V_{iy} - V_{fy})^2]^{1/2} \tag{9.95}$$

Equation 9.95 represents the basic definition of the velocity change where

ΔV is the change in velocity
V_{ix} is the initial velocity in the x-direction
V_{fx} is the final velocity in the x-direction
V_{iy} is the initial velocity in the y-direction
V_{fy} is the final velocity in the y-direction

Thus, by definition, the velocity change is the vector from the tip of the initial velocity vector to the tip of the final velocity vector. This definition completely and accurately describes the velocity change. Furthermore when vehicles are instrumented for crash testing, the equipment that measures the velocity change does so in accordance with the equation described earlier. For two vehicles we can then define the velocity change equations as

$$\Delta V_1 = \sqrt{(V_{1i}\cos A_{1i} - V_{1f}\cos A_{1f})^2 + (V_{1i}\sin A_{1i} - V_{1f}\sin A_{1f})^2} \tag{9.96}$$

$$\Delta V_2 = \sqrt{(V_{2i}\cos A_{2i} - V_{2f}\cos A_{2f})^2 + (V_{2i}\sin A_{2i} - V_{2f}\sin A_{2f})^2} \tag{9.97}$$

In the earlier equations, V_{1i} and V_{2i} represent the initial velocities and V_{1f} and V_{2f} represent the final velocities of the vehicles. The initial and the final angles are represented by A_{1i} and A_{2i} and A_{1f} and A_{2f} respectively.

The astute observer will have noticed that depending on the direction of the initial and final angles of the vehicles, the change in velocity vector may lie in one of the four quadrants of a standard Cartesian set of coordinates in the x–y plane. The angle of the velocity change, ΔA, is therefore defined as follows:

First quadrant: $\Delta A = a \tan \theta$
Second quadrant: $\Delta A = 180 - a \tan \theta$
Third quadrant: $\Delta A = 180 + a \tan \theta$
Fourth quadrant: $\Delta A = 360 - a \tan \theta$
where θ is the angle of ΔV with respect to the x-axis

Introduction to Energy Methods

The path represented in Figure 9.18 is that of trajectory of a mass m moving arbitrarily in the x–y plane. The motion of the mass m is acted upon by a force $\boldsymbol{F}$ that can vary in magnitude and direction from point to point along the path. This force may represent the resultant velocity, acceleration, or any other measurement of a particular parameter of a vehicle in an accident reconstruction. The path of the mass may, in fact, represent the center of mass of a vehicle, the path of a pedestrian after being struck by an automobile, or the interval motions of a vehicle such as steering or braking inputs. Irrespective of the actual descriptions of the force $\boldsymbol{F}$, certain basic principles are derived as follows.

S is the path length or distance that the mass travels as it is measured along the path. $\boldsymbol{F}_s$ is the force along the path creating the motion. Associated with this force is the velocity vector $\boldsymbol{v}$. From Newton's second law we know

$$F_s = ma = m\frac{dv}{dt} \tag{9.98}$$

From the chain rule we express

$$\frac{dv}{dt} = \frac{dv}{ds}\frac{ds}{dt} = v\frac{dv}{ds} \tag{9.99}$$

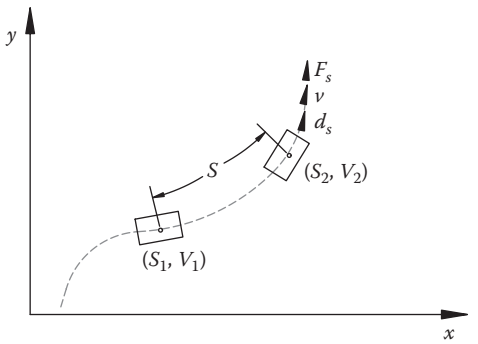

Figure 9.18 Trajectory of mass m.

then

$$F_s = mv\frac{dv}{ds} \tag{9.100}$$

or
over appropriate limits we may integrate Equation 9.101 to obtain

$$F_s ds = mvdv \tag{9.101}$$

$$\int_{s_1}^{s_2} F_s ds = \int_{v_1}^{v_2} mvdv \tag{9.102}$$

The integral on the left side is called the work $\boldsymbol{W}$ of the force $\boldsymbol{F}$ and can be integrated only when F_s is known as a function of s or when F_s and s are known as function of another variable such as friction. In other instances, when such relationships are not known, the left side of Equation 4.5 may not be classifiable. As we will see in the next section on friction, the work performed during braking or skidding can yield solutions to many reconstruction problems. However, the integral on the right side of equation 9.102 can always be evaluated as

$$\int_{v_1}^{v_2} mvdv = \frac{1}{2}mv_2^2 - \frac{1}{2}mv_1^2 \tag{9.103}$$

The kinetic energy of a mass is defined as

$$E_k = \frac{1}{2}mv^2 \tag{9.104}$$

We can now properly express the work energy principle in equation form as

$$W = \int_{s_1}^{s_2} F_s(s)d\boldsymbol{s} = \int_{v_1}^{v_2} mvdv = E_{k2} - E_{k1} \tag{9.105}$$

Equation 9.105 states that the work performed by the force that acts on a body equals the change in the kinetic energy. Equation 9.105 is known as the work energy principle. A more general form of Equation 9.105 presents itself when the force $\boldsymbol{F_s}(s)$ is not directed along the path ds. Consequently, the proper vector notation for the work energy principle is

$$W = \int_{s_1}^{s_2} \boldsymbol{F_s}(s) \cdot d\boldsymbol{s} = \Delta E_k \tag{9.106}$$

In this discussion the force ***F*** represents the resultant of all forces that externally may affect a body. Such a force may be produced by friction or the impact forces resulting from a vehicular collision. Often it is necessary to consider the work produced by separate forces. Each of these may be computed from the general definition as introduced by Equation 9.106. Since the work is a scalar quantity, the total work is the algebraic sum of all the individual components of work. In contrast, the individual forces are vectors and must be considered as such. As a consequence, the change in kinetic energy is equal to the total work. This subtle concept can be introduced when friction is considered on a nonlevel surface as will be seen in the various discussions of friction.

Friction

When two bodies slide over each other, they exert a frictional force on each other. The force is parallel to the surfaces and opposite in the direction of motion. Traditionally, friction is represented by drawing a free body diagram of a block sliding over a surface as shown in Figure 9.19.

Figure 9.19 represents a block resting on a horizontal surface. The block is in equilibrium as long as $N = W$ and $F = f$. The block will remain in equilibrium until the force F is greater than the frictional force f. A similar condition exists when the block rests on an incline as shown in Figure 9.20.

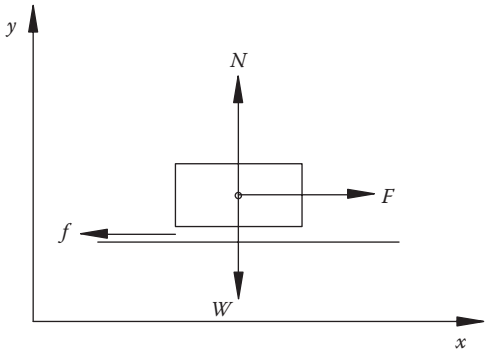

Figure 9.19 Frictional forces.

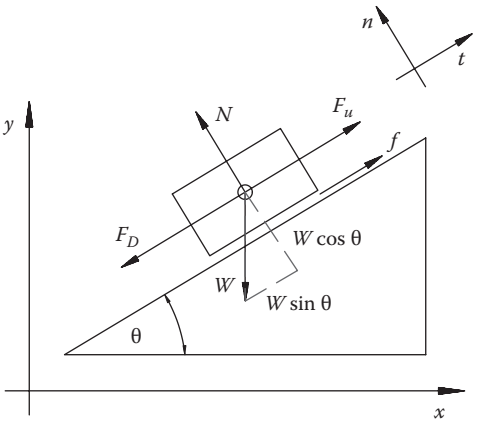

Figure 9.20 Frictional forces on an incline.

It is obvious that for the conditions represented in Figure 9.20, the block will remain at rest as long as $W \sin \theta < f$. Furthermore, an external force may be introduced to move the block down the slope (F_u) or to move it up the slope (F_d). Therefore, depending on the motion of the block, the total frictional force will be greater or lesser depending on the angle of incline and the relative motion of the block. The correction for friction on a slope follows from the free body diagram of Figure 9.20. Summing forces, we obtain for movement down the slope

$$\begin{aligned} \sum F_n = 0 &: N - W\cos\theta = 0 \\ \sum F_t = 0 &: F_d + W\sin\theta - f = 0 \end{aligned} \tag{9.107}$$

Summing forces for movement up the slope

$$\begin{aligned} \sum F_u = 0 &: N - W\cos\theta = 0 \\ \sum F_t = 0 &: -F_u + W\sin\theta - f = 0 \end{aligned} \tag{9.108}$$

The coefficient of friction is defined as the ratio of the tangential to the normal forces. On a horizontal surface as depicted in Figure 9.19, the coefficient of friction would be

$$\mu = \frac{F}{W} = \frac{f}{N} \tag{9.109}$$

Solving Equation 9.107 yields

$$\frac{F_d}{W\cos\theta} = \frac{f}{W\cos\theta} - \frac{W\sin\theta}{W\cos\theta} \tag{9.110}$$

or

$$\mu_{\text{CORR}} = \mu - S \tag{9.111}$$

where S = slope = tan θ and θ = angle of incline.

In general, a solution for Equation 9.111 yields a corrected value of the frictional coefficient on an incline as

$$\mu_{\text{CORR}} = \mu_{\text{NORMAL}} \pm S \tag{9.112}$$

where

μ_{NORMAL} is the coefficient of friction on a horizontal roadway
S is the slope of the road

The + sign is used if the vehicle travels up the slope and the − sign if it travels down the slope. At this point, it is warranted to derive two simple equations relating vehicle speeds

and skid marks. Generally, a vehicle may deposit skid marks on the road surface when the brakes are applied in a relatively straight trajectory or may deposit skid marks in a yaw while rounding a curve.

During the accident investigation, the skid marks may have been documented and measured. Let us consider the two cases separately.

Critical Speed: Straight Trajectory

Figure 9.21 represents a vehicle in which the brakes are suddenly applied. The forces acting on the vehicle are the force of gravity *W*, the normal force *N* (the component of the reaction force on the surface of the vehicle's tires perpendicular to the road surface), the applied force *F* (produced by the vehicle's speed), and the frictional force *f* (the component of the reaction force on the vehicle's wheels parallel to the road surface). At this point, we will assume that the entire weight of the vehicle is distributed evenly over the tires. The development, as represented by Figure 9.21, is based on the movement of the center of mass of the vehicle and is not dependent on the length or number of skid marks.

If we attempt to push a vehicle at rest with all wheels locked, we must overcome the static coefficient of friction. Once the vehicle is moving, again with locked wheels, the functional forces are dependent on the kinetic coefficient of friction. Let us discuss kinetic friction first since it is the simplest of the two forces. Kinetic friction has been found to have the following properties according to classical mechanics:

1. The force of kinetic friction is proportional to the normal force. The constant of proportionality is called the coefficient of kinetic friction and is denoted by μ_k. We write Equation 9.113.

$$f_k = \mu_k N \tag{9.113}$$

2. The coefficient of kinetic friction is independent of the surface area of contact.
3. The coefficient of kinetic friction is independent of the relative speed between the surfaces in contact.

The actual value of the coefficient of kinetic friction depends on the nature of the two surfaces in contact, for example wood on steel, rubber on concrete, etc. However, for a given pair of materials, the previous three rules are found to be valid to a reasonable

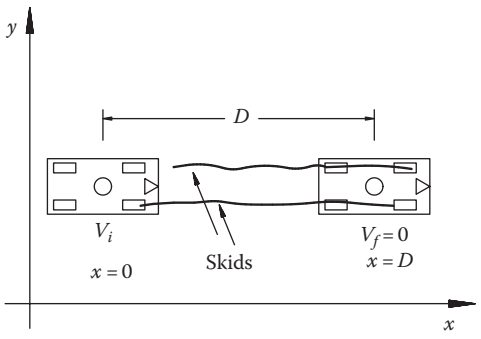

Figure 9.21 Straight skids.

Table 9.1 Coefficient of Friction

Solids	Static (μ_s)	Kinetic (μ_k)
Steel on steel	0.74	0.57
Brass on steel	0.51	0.44
Copper on cast iron	1.05	0.29
Glass on glass	0.94	0.40
Rubber on concrete	0.73	—
Rubber on carpet	0.66	—
Rubber on tile	0.39	—
Leather on concrete	0.60	—

degree of engineering certainty. In most cases we are dealing with automobile tire rubber on concrete or asphalt so that the kinetic coefficient of friction is about 0.8 on a good dry surface and as low as 0.3 on a slippery wet surface. On ice the kinetic coefficient of friction may drop to a dangerously slippery value of 0.1 or less. In some instances, when a vehicle overturns, the coefficient of friction of metal on the road surface may need to be considered. Table 9.1, which has been reproduced from a multitude of sources including the author's experiments, lists typical values of the frictional coefficient. Note that some of the values vary according to the speed of a vehicle. These adjustments to the values of μ are based on numerous skid tests performed by a variety of investigators and may seem to violate the third property of friction according to classical mechanics. However, the listed values of the coefficient of friction generally do not vary by more than 0.05 under or over 30 mph. From a realistic engineering standpoint, the percent error introduced into a speed equation by varying the kinetic coefficient of friction of 0.05 is insignificant as will be shown in the next section. The models that we use in engineering x design yield answers within engineering accuracy. Engineering accuracy is a measure of acceptable error in the computations. In most instances an error of 5% is quite acceptable when performing engineering calculations. Certain simplifying assumptions are always made when solving engineering problems. The assumptions should meet the following criteria: the methodology is proper and acceptable and the calculations reflect the accident scenario to within engineering accuracy.

After an appropriate selection for the coefficient of friction has been chosen, we can proceed with the development of the critical speed equation as follows. Suppose that the vehicle is given an initial velocity V_i in the x-direction. The force F is taken in this case to be zero. The only force acting on the vehicle in the x-direction is the force of kinetic friction. From Newton's second law and a modification of Equations 9.107 or 9.108 with $\theta = 0$, we obtain

$$\begin{aligned} F - f_k &= ma_x = 0 \\ N - W &= ma_y = 0 \end{aligned} \tag{9.114}$$

Thus, $N = W$ and $f_k = F$.

Static friction is more complicated because it does not have a fixed value. In fact, as long as the vehicle in Figure 4.4 does not move, a_x and a_y are zero, and Newton's

second law again gives Equation 9.114 with f_k replaced by f_s to indicate static friction. Now all we can say is

$$\mu_k = \frac{f_k}{N} = \frac{F}{W} \tag{9.115}$$

$$\begin{aligned} f_s &= F \\ N &= W \end{aligned} \tag{9.116}$$

We do not have a law for f_s like Equation 9.115 for f_k. Experiments show, however, that the force F can only grow so large before the vehicle breaks free and starts to slide, which shows that the force of static friction has a maximum value. The maximum force of state friction $f_{s\,\max}$ has the following two simple properties:

(a) The maximum force of static friction is proportional to the normal force. The constant of proportionality is called the coefficient of static friction and is denoted by μ_s. We write

$$\mu_s > \mu_k \tag{9.117}$$

(b) The coefficient of static friction is independent of the surface area of contact.

Again, as with kinetic friction, the coefficient of static friction depends on the nature of the two surfaces in contact. However, for a given pair of materials, the earlier two rules are found to be valid to a reasonable degree of engineering certainty. In typical cases of automobile rubber on concrete or asphalt, μ_s is about 0.9 on a good dry surface, about 0.4 on a wet slippery surface, and 0.2 or lower on ice. Experimentation has shown that the coefficient of static friction is always greater than the coefficient of kinetic friction, in mathematical terms. An important application of this principle is the antilock brake system.

Stopping Distances

Suppose the vehicle is given an initial velocity V_i in the x-direction. Again, the force F is taken in this case to be zero. The only force acting on the vehicle in the x-direction is the force of kinetic friction. A simple modification of the first part of Equation 9.114 yields

$$a_x = -\frac{f_x}{m} \tag{9.118}$$

The second part of Equation 9.114 gives $N = W = mg$. Then $f_k = \mu_k N = \mu_k mg$. Using the results in (9.118), we obtain

$$a_x = -\mu_k g \tag{9.119}$$

Applying the work energy principle as described in Equation 9.105, we may say

$$\int_{x=0}^{x=D} F dx = \frac{1}{2} m v_f^2 - \frac{1}{2} m v_i^2 \tag{9.120}$$

or when $v_f = 0$,

$$FD = -\frac{1}{2} m v_i^2 \tag{9.121}$$

Applying Equations 9.119 and 9.98 to Equation 9.121 yields

$$m(-\mu_k g) \quad D = -\frac{1}{2} m v_i^2 \tag{9.122}$$

or

$$v_i = \sqrt{2\mu_k g D} \tag{9.123}$$

An alternate form of Equation 9.123 is

$$D = \frac{v_i^2}{2\mu_k g} \tag{9.124}$$

In Equation 9.124, D represents the braking distance. The term stopping distance is usually reserved for the total distance traveled by the vehicle. Included in the stopping distance is the distance traveled during the driver's reaction time. Let t_r be the reaction time, which is required for the driver to recognize the problem, decide to apply the brakes, and perform the braking maneuver. A general range of reaction time is between 0.5 and 1.5 s. The total stopping distance can then be calculated from

$$D_s = D_r + D_b \tag{9.125}$$

or the total time may be computed from

$$t_T = t_r + t_b \tag{9.126}$$

Figure 9.22 summarizes the results of Equations 9.124 through 9.126.

Next, we introduce some refinements and expand on how friction affects the speed of a vehicle.

Friction and the Speed of a Vehicle

Accident reconstructionists sometimes manipulate the equations that govern the critical speed of a vehicle based on the coefficient of friction and the length of the skid. One would

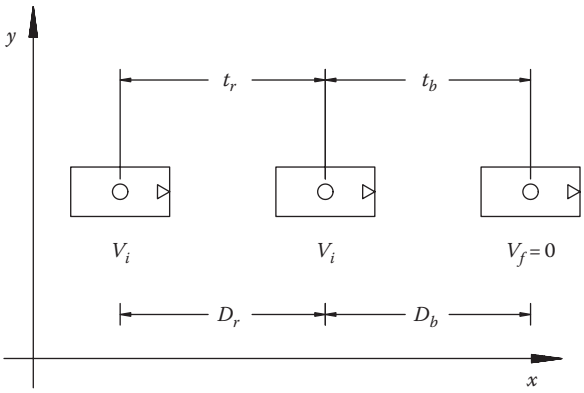

Figure 9.22 Reaction and stopping.

hope that this manipulation is due to ignorance rather than due to deception in order to skew results in a particular direction. Skid tests have been performed by numerous investigators to validate the critical speed equation. These tests have generated a plethora of well-documented data on the coefficient of friction under varying conditions. These data allow a reconstructionist to more precisely refine the coefficient of friction in a particular accident scenario. However, there is no scientific validity from an experimental or a theoretical viewpoint to manipulate the coefficient of friction based on the number of skid marks made by a vehicle under heavy braking conditions. Two theoretical arguments against the manipulation of the friction or "drag" coefficient based on the number of skid marks are provided.

The study of friction is referred to as "tribology" by physicists. Friction or tribology at the atomic scale is called nanotribology. Nanotribology can also be considered as friction at the microscopic level. In contrast, the friction encountered by accident reconstructionists is at the macroscopic level. In order to understand the frictional forces that affect the behavior of vehicles, some background and differences between friction at the microscopic and macroscopic levels should be explained.

Nanotribologists have found that friction at the atomic (microscopic) level differs significantly from the observations at the macroscopic (real-world) level. For example, surface roughness at the microscopic level has little correlation with friction, and sometimes wet surfaces are stickier than dry ones. Automotive engineers and other investigators have found that surface roughness could not explain real-world friction experienced in their designs. In some instances, friction between two surfaces decreased if one surface is smoother than the other. Two highly polished metals will adhere very firmly as in the case of "cold welding." Friction has been found to be proportional to true contact area in the microscopic level but independent of the macroscopic area as defined in classical physics. Over the past few years, researchers have found that "phonons" or sound waves are generated when two surfaces slide relative to each other. The mechanical energy needed to slide the surfaces is converted to sound energy and subsequently into heat. The amount of mechanical energy that must be added to keep the motion going depends on the nature of the sliding surfaces. The resonant frequencies excited during the sliding action are a direct consequence of the mechanical energy consumed. Clearly, accident reconstructionists cannot attempt to determine the true contact area between a vehicle's tires and the road or the true contact within the brakes of the vehicle. At best, they can

Table 9.2 Coefficient of Friction

	Dry		Wet	
Tires on Roads (μ_k)	<30 mph	>30 mph	<30 mph	>30 mph
New concrete	0.80–1.20	0.70–1.00	0.50–0.80	0.40–0.75
Old concrete	0.55–0.80	0.50–0.75	0.45–0.70	0.45–0.65
New asphalt	0.80–1.20	0.65–1.00	0.50–0.80	0.45–0.75
Old asphalt	0.50–0.80	0.35–0.70	0.30–0.80	0.25–0.75
Gravel	0.40–0.85	0.40–0.80	0.45–0.80	0.45–0.60
Cinders	0.50–0.70	0.50–0.70	0.65–0.75	0.65–0.75
Ice	0.10–0.25	0.07–0.20	0.05–0.10	0.05–0.10
Snow	0.10–0.55	0.10–0.55	0.30–0.60	0.30–0.60

perform a skid test with a sled or with an accelerometer. Another surprising discovery by nanotribologists is that the frictional force is related to how easily two surfaces become stuck relative to becoming unstuck. The discrepancy of friction at the microscopic and macroscopic levels diminishes when one realizes that the true contact area is proportional to the force that squeezes the objects together. At the macroscopic level, this force is produced by the mass of the vehicle and the subsequent forces that are imparted on the tire/road interface (Table 9.2).

These forces are often misunderstood by accident reconstructionists. When a vehicle is being decelerated by braking and before the tires lose traction, the forces of static friction are in effect between the tire/road interface. At the same time, the forces of kinetic friction are acting on the rotors, drums, and brake shoes. Many times during heavy braking, one or more of the brakes will lock. When the brakes of one wheel lock, the forces of static friction are acting upon those brakes while the forces of kinetic friction affect the tire/road interface. The tire/road friction utilization is concerned with the maximum deceleration when the wheels are unlocked relative to the lowest tire/road friction coefficient with which the deceleration can be achieved. When actual braking forces equal optimum braking forces, then tire/road friction is used for vehicle deceleration. The maximum wheels-unlocked deceleration yields the minimum stopping distance of a vehicle. The effect on the road/tire/brake system of that particular wheel is reversed from the effect of a wheel that is not losing traction. However, in all instances, except when defective brakes are present, the forces of friction are all working on all wheels to stop the vehicle.

One of the pieces of evidence that reconstructionists use is the length of skid marks to determine vehicle speeds. Skid marks are probably the most misunderstood and most abused evidence used by reconstructionists. There is no question that steering input, weight shift, torsion, and wheel lock up determine the shape, length, and number of skid marks deposited by vehicles under heavy braking. Similarly, in many collisions, the metal deformation will lock one or more wheels so that postcollision skid marks are deposited on the road surface. Simply because only one wheel deposits skid marks does not mean that frictional forces are not affecting the entire vehicle.

Let us consider a vehicle that deposits only one skid mark either under preimpact conditions or under postimpact conditions. Some reconstructionists use the number of skid marks deposited by a vehicle to adjust the coefficient of friction or "drag coefficient" used

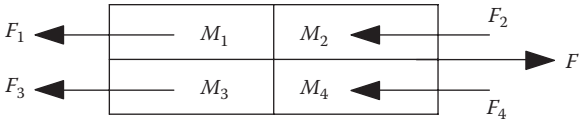

Figure 9.23 Vehicle masses.

in their calculations. For example, when μ = 0.8 with one wheel skidding, they will adjust the coefficient by dividing by four so that they use μ = 0.2. In other instances, when two skid marks are deposited, one longer than the other, they will average the length of the skid marks and use this value as the skid distance. In both cases they are affecting the equation used to calculate the minimum speed from skid marks, namely,

$$v_s = \sqrt{2g\mu D} \tag{9.127}$$

where

v_s is the minimum speed (ft/s)
g is the acceleration due to gravity (32.2 ft/s^2)
μ is the coefficient of friction or "drag coefficient"
D is the skid distance (ft)

The number 2 and g cannot be manipulated; however, μ and D can be, and many times are manipulated as in the earlier examples to affect speed calculations. Two mathematical arguments are presented later to show that manipulation of μ and D as explained earlier violates fundamental laws of physics. Consider Figure 9.23, which represents a vehicle divided into four masses and forces affecting each wheel.

The total force F is produced by the motion of the vehicle. The forces F_1, F_2, F_3, and F_4 are deceleration forces affecting each wheel. Summing forces, we obtain

$$F = F_1 + F_2 + F_3 + F_4 \tag{9.128}$$

Newton's Second Law Argument

By Newton's second law, we may say

$$F_1 = m_1 a_1, \quad F_2 = m_2 a_2, \quad F_3 = m_3 a_3, \quad F_4 = m_4 a_4 \tag{9.129}$$

Substituting, we obtain

$$F = m_1 a_1 + m_2 a_2 + m_3 a_3 + m_4 a_4 \tag{9.130}$$

If the vehicle remains together, the acceleration of each mass component must be the same:

$$a = a_1 = a_2 = a_3 = a_4 \tag{9.131}$$

Therefore,

$$F = (m_1 + m_2 + m_3 + m_4)a \tag{9.132}$$

Since weight W and mass m are related by gravity g,

$$W = mg \tag{9.133}$$

and the frictional force f is related to weight W by the coefficient of friction μ,

$$f = \mu W \tag{9.134}$$

we can find the total frictional force by summing the frictional forces on each wheel, namely,

$$f = f_1 + f_2 + f_3 + f_4 \tag{9.135}$$

By substituting we obtain

$$f = m_1\mu_1 g + m_2\mu_2 g + m_3\mu_3 g + m_4\mu_4 g \tag{9.136}$$

For simplicity's sake, let us assume that the coefficient of friction affecting each wheel is constant so that

$$\mu = \mu_1 = \mu_2 = \mu_3 = \mu_4 \tag{9.137}$$

Then

$$f = (m_1 + m_2 + m_3 + m_4)\mu g \tag{9.138}$$

From the basic definitions we see that

$$a = \mu g \tag{9.139}$$

Adjusting the masses in Equation 9.132 requires making the same adjustment in the masses of Equation 9.138. Even if a weight displacement during acceleration or deceleration causes a shift in the mass, the adjustment must be made to both sides of Equation 9.98. This effect is represented as follows:

$$(m_1 + m_2 + m_3 + m_4)\mu g = (m_1 + m_2 + m_3 + m_4)a \tag{9.140}$$

or

$$\Delta m\mu g = \Delta ma \tag{9.141}$$

where Δm is the mass shift or displacement.

Work–Energy Argument

This argument centers on the work done, or kinetic energy expended during acceleration or deceleration of a vehicle, namely,

where
K_e is the kinetic energy (ft-lb)
m is the mass (lb-s^2/ft)
v is the speed (ft/s)
f is the frictional force (lb)
D is the skid distance (ft)

In this argument, we use the same representation as in Figure 9.23 to find the total kinetic energy at each wheel, namely,

$$\text{Work} = K_e = \frac{1}{2}mv^2 = f \times D \tag{9.142}$$

$$K_e = K_{e1} + K_{e2} + K_{e3} + K_{e4} \tag{9.143}$$

or

$$K_e + \frac{1}{2}m_1v_1^2 + \frac{1}{2}m_2v_2^2 + \frac{1}{2}m_3v_3^2 + \frac{1}{2}m_4v_4^2 \tag{9.144}$$

Similarly, the total work done by the frictional forces is

$$\text{Work} = f_1D_1 + f_2D_2 + f_3D_3 + f_4D_4 \tag{9.145}$$

Substituting for the frictional forces, we obtain

$$\text{Work} = W_1\mu_1D_1 + W_2\mu_2D_2 + W_3\mu_3D_3 + W_4\mu_4D_4 \tag{9.146}$$

for a constant coefficient of friction and since each wheel of the vehicle travels the same distance,

$$D = D_1 = D_2 = D_3 = D_4 \tag{9.147}$$

then

$$\text{Work} = (W_1 + W_2 + W_3 + W_4)\mu D. \tag{9.148}$$

Substituting and realizing that $v = v_1 = v_2 = v_3 = v_4$ yield

$$\frac{1}{2g}(W_1 + W_2 + W_3 + W_4)v^2 = (W_1 + W_2 + W_3 + W_4)\mu D \tag{9.149}$$

Of course, the equations reduce as in Equation 9.150. We can again assume that a weight shift, torsion, steering input, or some other anomaly causes less than four equal length skid marks so that Equation 9.150 is represented as

$$\frac{1}{2g}(\Delta W)v^2 = (\Delta W)\mu D \tag{9.150}$$

The inescapable conclusions of the arguments summarized in Equations 9.141 and 9.150 are as follows:

1. The coefficient of friction or "drag factor" cannot be varied according to the number or length of the skid marks without violating fundamental laws of physics.
2. Simply because a tire does not leave a skid mark does not mean that frictional forces are not in effect. Actually, the braking efficiency of a wheel that does not skid is greater than the wheel that does skid across the pavement.
3. The longest skid mark is evidence that the vehicle was traveling at a minimum speed and that it was accelerating or decelerating. When calculating this minimum speed, it is improper to randomly vary the coefficient of friction based on the number or length of skid marks.
4. Adjustments to one side of the equations require adjustments to the other side. Analysis of equations explains this effect in greater detail.
5. Simple adjustments to the coefficient of friction and the length of skid marks require careful analysis of the equations. These analyses and data are seldom available in an accident reconstruction.
6. Calculating minimum speeds in pre- or postimpact phases of collisions by randomly varying the coefficient of friction or the skid distance often yields erroneous results. All calculations should be checked by independent second methods such as crush deformation analysis or various other techniques available to accident reconstructionists. The adage "garbage in equals garbage out" rings true.
7. It must be recognized that when brakes are applied, the vehicle decelerates before any skid marks are deposited so that the actual speed of the vehicle is greater than that calculated from the minimum speed formulas.
8. Modifying the coefficient of friction depending on how many tires deposit skid marks is equivalent to adjusting the apparent area of contact and is therefore in violation of the classic laws of physics relative to the frictional force.

Critical Speed: Curved Trajectory

Another consequence of a vehicle depositing skid marks on a road surface occurs when the vehicle loses traction while rounding a curve. The motion of such a vehicle is more complicated than realized at first glance. The trajectory of the vehicle may simply cause a yawing motion, or it could produce a spinning motion. The trajectory may be a combination of two paths and may include some rolling motion toward the end of the trajectory. Subtle differences are observed in the equations of motion under all these cases.

Let us describe some basic equations of motion. In order to describe the motion of a vehicle, a proper frame of reference must be established. Various coordinate systems uniquely

determine the position of the vehicle relative to its motion. Using a right-handed Cartesian coordinate system, which consists of three mutually perpendicular axes intersecting at some specified field point, 0 (origin), the distance from a point P to the origin is given by

$$D = \sqrt{x^2 + y^2 + z^2} \tag{9.151}$$

Similarly, the distance from point P_1 to point P_2 is described as

$$D_{12} = \sqrt{(x_1 - x_2)^2 + (y_1 - y_2)^2 + (z_1 - z_2)^2} \tag{9.152}$$

In general the quantity D_{12} is a vector so that a more generalized form of the vector equation would be

$$\boldsymbol{D}_{12} = D_x \boldsymbol{A}_x + D_y \boldsymbol{A}_y + D_z \boldsymbol{A}_z \tag{9.153}$$

Therefore, Equation 9.153 represents the magnitude of the vector distance D_{12}. Suppose in the earlier discussion that a vehicle travels from P_1 to P_2 in a straight line in two dimensions (x,y). The average velocity of the vehicle is defined as

$$\boldsymbol{v} = \frac{\Delta(x,y)}{\Delta t} = \left(\frac{\Delta x}{\Delta t}, \frac{\Delta y}{\Delta t}\right) = \left(\frac{dx}{dt}, \frac{dy}{dt}\right) = (\boldsymbol{v}_x, \boldsymbol{v}_y) \tag{9.154}$$

The extension of Equation 9.154 into three dimensions should be obvious to the reader. The average velocity is a vector. There are many instances when it makes sense to talk about the average velocity of the vehicle or for lack of a better term, the average speed. The average speed is a scalar quantity given by

$$s = \frac{D}{\Delta t} \tag{9.155}$$

where D is the total distance traveled by the vehicle between P_1 and P_2. In the simple case in which the vehicle travels in a straight line and does not stop and turn around or otherwise retrace its path, the average speed is simply the magnitude of the average velocity, that is,

$$s = \sqrt{v_x^2 + v_y^2} \tag{9.156}$$

If the vehicle stops and turns around, or if it moves with a variable speed in the same direction, or if it moves along a curved path, it is said to have acceleration. The description of the motion

$$\begin{aligned} x &= x(t), \quad v_x = \frac{dx}{dt} \\ v_x &= v_x(t), \quad a_x = \frac{dv_x}{dt} \end{aligned} \tag{9.157}$$

of such a vehicle requires the use of calculus. As a general rule in the case where acceleration is a constant, the velocity of the vehicle increases or decreases at a constant rate. With variable acceleration, the rate of change of the velocity would not be constant. Such a scenario might exhibit itself when a vehicle is performing complex maneuvers such as braking, acceleration, or turning. Most of these cases can be dealt with easily by analyzing each component separately. The total reconstruction can then be determined by a step-by-step analysis of the total scenario. For convenience, we list the general equations of motion in one dimension (x-direction) as derived from basic calculus.

In the case of constant acceleration, we obtain

$$v_x = v_{ox} + a_x t \tag{9.158}$$

$$x = x_o + v_{ox} t + \frac{1}{2} a_x t^2 \tag{9.159}$$

$$v_x^2 - v_{ox}^2 = 2a_x\,(x - x_o) \tag{9.160}$$

Equations 9.157 through 9.160 are used extensively to determine time, distance, velocity, and acceleration of vehicles in an accident reconstruction. The derivation of Equations 9.158, 9.159, and 9.160 from Equation 9.157 is left as exercise for the reader. The reader, as an engineering level accident reconstructist, should not have any trouble performing those derivations. In fact, during trial or deposition testimony, many attorneys ask that the expert derive the equations used in the reconstruction. Similar equations hold for the y and z directions.

Let us now return to our original development of the curved trajectory. The simplest curved trajectory is that of a circle. The acceleration of a vehicle moving in a circle can be resolved into components normal and tangential to the path. Figure 9.24a represents a vehicle moving in a circular path of a radius R with center at the origin. Vectors $\mathbf{v}_1$ and $\mathbf{v}_2$ represent the velocity of the vehicle at points P_1 and P_2, respectively. The vector change in velocity, Δv, is obtained in Figure 9.24b. Vectors Δv_N and Δv_t are the normal and tangential components of Δv.

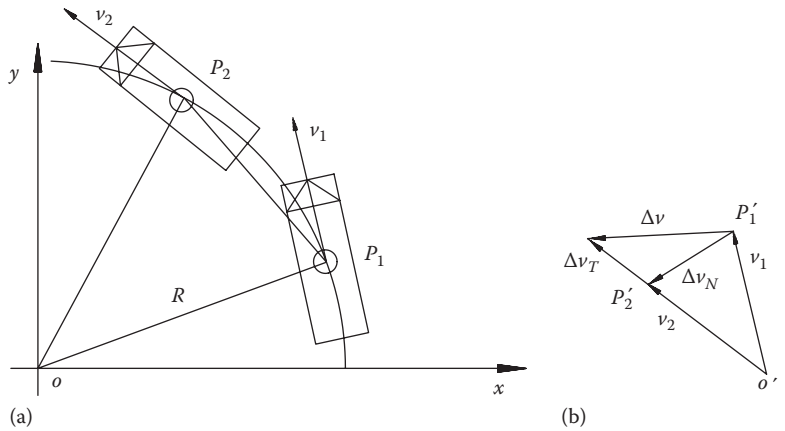

Figure 9.24 Vehicle in a circular path.

Triangles OP_1P_2 and $OP_1'P_2'$ in Figure 9.24 are similar triangles because both are isosceles and their long sides are mutually perpendicular. We may then say

$$\frac{\Delta s}{R} = \frac{\Delta v_N}{v_1} \tag{9.161}$$

By definition, the magnitude of the average normal acceleration $|\boldsymbol{a}_N|$ is

$$|\boldsymbol{a}_N| = \frac{\Delta v_N}{\Delta t} = \frac{v_1}{R}\frac{\Delta s}{\Delta t} \tag{9.162}$$

Taking the limit, we obtain

$$a_N = |\boldsymbol{a}_N| = \lim_{\Delta t \to 0} \frac{v_1}{R}\frac{\Delta s}{\Delta t} = \lim_{\Delta t \to 0} \frac{\Delta s}{\Delta t}\left(\frac{v_1}{R}\right) \tag{9.163}$$

In the earlier equation, we recognize the basic calculus definition of the speed v_1 to be the limit of $\Delta s/\Delta t$. Thus,

$$a_N = \frac{v^2}{R} \tag{9.164}$$

Thus, the magnitude of the instantaneous normal acceleration is inward and is referred to as the centripetal acceleration. Associated with the centripetal acceleration is the force according to Newton's second law. Since the magnitude of the centripetal acceleration equals v^2/R, and its direction is toward the center, the magnitude of the centripetal or radial force on a vehicle traveling in a circle is

$$F = \frac{mv^2}{R} \tag{9.165}$$

The term "centripetal" refers to the effect of the force on a body moving in a circular path. In other words, the effect of the force results in a change in the direction of the velocity of the vehicle upon which it acts. Note that the force does not change the magnitude of the velocity. The term centripetal means center-seeking. In fact, when a vehicle negotiates a circular path, it is accelerated toward the center as long as the frictional forces on the tires are not exceeded. Once the frictional forces are exceeded, the vehicle will lose control around the turn and may spin, yaw, or roll. Therefore, the critical speed at which this event occurs can be simply computed by analyzing the free body diagram in Figure 9.25.

While the vehicle remains under control, we may write

$$\boldsymbol{F} = m\boldsymbol{a}_N = \frac{w}{g}\frac{v^2}{R} \tag{9.166}$$

$$f = \mu w \quad \text{then}$$
$$\frac{w}{g}\frac{v^2}{R} - \mu w = 0 \tag{9.167}$$

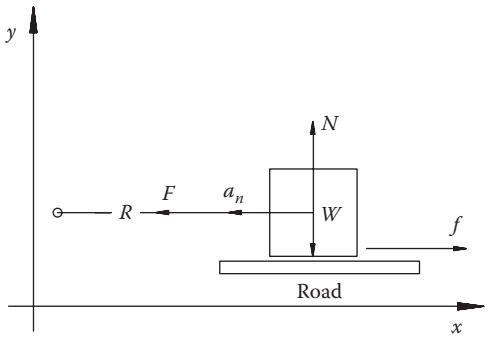

Figure 9.25 Critical speed in a turn.

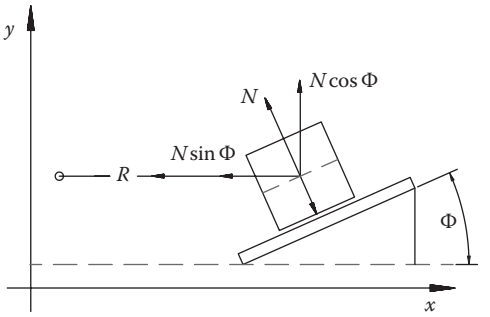

Figure 9.26 Superelevated turn.

Thus, the critical speed around a turn is

$$v = \sqrt{\mu g R} \tag{9.168}$$

The development of Equation 9.168 indicates that the forces acting on a vehicle that is rounding a curve are its weight *W*, the normal force *N*, and the centripetal force *F*. The centripetal force must be provided by friction. In order to minimize the effect that friction has to play on keeping a vehicle on track around a curve, many roads are banked. This banking is commonly known as "superelevation" of the roadway. Figure 9.26 shows a banked roadway and the forces affecting the vehicle.

In Figure 9.26 it is evident that the normal force *N* has a horizontal and a vertical component. The horizontal component $N \sin \Phi$ provides the centripetal force. Thus, applying Newton's second law, we obtain

$$N \sin \Phi = \frac{mv^2}{R}$$

while there is no vertical acceleration $W = N \cos \Phi$, then

$$\frac{N \sin \Phi}{N \cos \Phi} = \frac{mv^2}{WR}$$

or

$$\tan \Phi = \frac{v^2}{gR} \tag{9.169}$$

In Equation 9.169 for a given radius R there is no one speed that satisfies the angle criteria. Road designers have thus superelevated highways according to the average speed of the vehicles that traverse that particular section of roadway.

Critical Speed to Negotiate a Turn Including Superelevation

In some accident reconstructions, it is necessary to determine if the superelevation of a road surface is within design specifications for the radius of a curve that a vehicle is to maneuver safely. This section is devoted to the determination of the proper superelevation for varying a radii corresponding to varying speeds.

Normally curved road surfaces are designed as shown in Figures 9.27 and 9.28. Figure 9.27 represents a top view of a curved road surface, while Figure 9.28 shows a cross section of a superelevated road surface. Complex curves necessitate a transition region before and after the curve is negotiated. These transition regions involve spiral curves leading to or departing the main circular curve. We will restrict our analysis to the circular portion of the curve where the loss of control of a vehicle occurs in many accidents. The circular

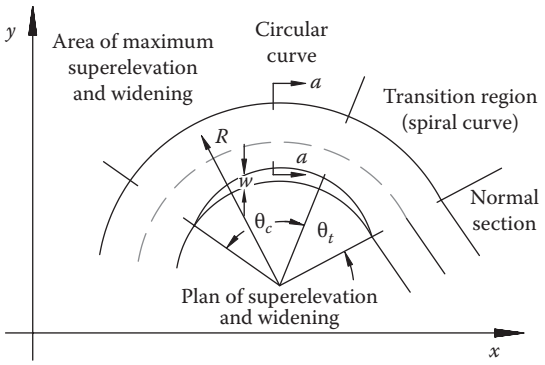

Figure 9.27 Typical road curve.

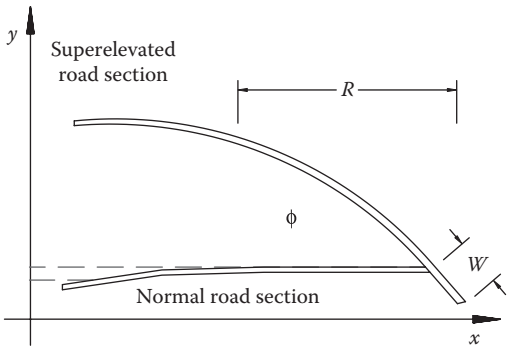

Figure 9.28 Road cross-section.

portion of the curve has a smaller radial distance than the transition spiral and thus yields a slower design speed.

Definition of terms:

Transition region = uniformly increasing or decreasing superelevation and widening
Curves of < 1° of arc require no superelevation
Curves of < 2° of arc require no transition region
θ_t = transition angle
θ_c = central angle of curve
w = widening
R = radius of curve in feet
C = crown (¼″ to ½″:1′)
Φ = angle of superelevation
F = force
a = acceleration in ft/s^2
W = weight
V = velocity in ft/s
g = gravity = 32.2 ft/s^2
f = side friction factor
S = superelevation
m = mass

Figure 9.29 shows a superelevated cross section of road with a vehicle negotiating a curve of radius R. We will proceed with a different derivation than previously presented. By Newton's second law,

$$\sum F = ma_r = \frac{W}{g}(a_r)$$

Centripetal acceleration is given by

$$a_r = \frac{v^2}{R}$$

The frictional force is

$$F = fW\cos\Phi$$

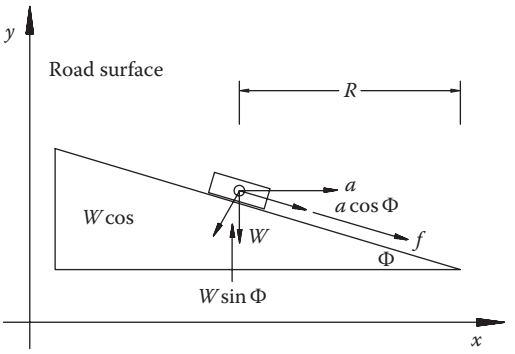

Figure 9.29 Superelevation section of road.

The component of the weight in the same direction as friction is

$$W \sin \Phi$$

The centripetal acceleration component of the superelevated road is

$$a_r = A \cos \Phi = \frac{V^2}{R} (\cos \Phi)$$

Summing forces

$$fW \cos \Phi + W \sin \Phi = M \frac{V^2}{R} \cos \Phi = \frac{W}{g} \frac{V^2}{R} \cos \Phi \tag{9.170}$$

$$f + \frac{\sin \Phi}{\cos \Phi} = \frac{V^2}{gR}$$

$$\tan \Phi = \frac{\sin \Phi}{\cos \Phi} = S = \text{Superelevation}$$

$$S + f = \frac{V^2}{gR}$$

$$S = \frac{V^2}{gR} - f \tag{9.171}$$

Standard road design handbooks specify f as the side friction factor with a value of 0.16 for speeds of 60 mph or less or 0.14 for 70 mph speeds. Additionally, the speed V earlier is to be 75% of the design speed. Equation 4.76 becomes negative for values of

$$f > \frac{V^2}{gR} \tag{9.172}$$

Since negative values of S mean that the superelevation is inclined in the wrong direction, making it easier for vehicles to slide while negotiating a curve, a design standard lower limit of superelevation for different radii has been established and is reproduced in Tables 9.3 and 9.4 from the earlier equations.

Conservation of Energy Analysis

Many vehicular accident reconstructions can be performed with the use of the principle of conservation of energy. The total energy of the system is comprised of potential and kinetic energy. Since most accidents occur on nearly level surfaces, potential energy can be disregarded. Alternatively, if the road surfaces are not significantly level, an adjustment can be

Table 9.3 Superelevation and Widening

Radius (*R*)	Degree of Curvature (D)	30 mph		50 mph		70 mph	
		S	*W*	*S*	*W*	*S*	*W*
5730	1	0.01	N/N	0.02	N/N	0.03	N/N
2865	2	0.01	N/N	0.03	N/N	0.06	N/N
1910	3	0.02	N/N	0.05	N/N	0.09	N/N
1432	4	0.02	N/N	0.06	N/N	0.10	2
1146	5	0.03	N/N	0.08	N/N		
955	6	0.03	N/N	0.10	2		
819	7	0.04	N/N	0.10	2		
716	8	0.05	2	0.10	2		
637	9	0.05	2	0.10	3		
573	10	0.06	2				
521	11	0.06	2				
477	12	0.07	3				
441	13	0.07	3				
409	14	0.08	3				
382	15	0.09	3				
358	16	0.09	3				
337	17	0.10	3				

Notes: *S*, superelevation in feet per foot; *W*, widening in feet for two lane roads; N/N, not necessary.

Table 9.4 Curve Radius and Speed

	30 mph	50 mph	70 mph	90 mph
Minimum safe radius "*R*" (ft)	232	644	1368	2714
Maximum degree of curve "*D*"	24.9	8.9	4.2	2.1

made to the frictional coefficient in order to incorporate any 3D effects. The basic premise states that the initial energy of the system must equal the final energy, or

$$\frac{1}{2}m(v_i)^2 = \frac{1}{2}m(v_f)^2 \tag{9.173}$$

For a system with two components such as two vehicles, Equation 9.1 becomes

$$w_1(v_{1i})^2 + w_2(v_{2i})^2 = w_1(v_{1f})^2 + w_2(v_{2f})^2 \tag{9.174}$$

Equation 9.174 can be broken down into its components in order to solve for the initial velocities of the system. The initial velocities are then given by

$$(v_{1i})^2 = \left(\frac{\left[\left(\sin A_{2i}\right)^2 - \left(\sin A_{1f}\right)^2\right](v_{1f})^2 + R_{21}\left[\left(\sin A_{2i}\right)^2 - \left(\sin A_{2f}\right)^2\right](v_{2f})^2}{\left[\left(\sin A_{2i}\right)^2 - \left(\sin A_{1i}\right)^2\right]} \right) \tag{9.175}$$

and

$$(v_{2i})^2 = \left(\frac{\left[\!\left[(\sin A_{2f})^2 - (\sin A_{1i})^2 \right]\!\right](v_{2f})^2 + (1/R_{21})\left[\!\left[(\sin A_{1f})^2 - (\sin A_{1i})^2 \right]\!\right](v_{1f})^2}{\left[\!\left[(\sin A_{2i})^2 - (\sin A_{1i})^2 \right]\!\right]} \right) \tag{9.176}$$

In the earlier equations we define the following:

w_1 = weight of vehicle 1
w_2 = weight of vehicle 2
m = mass
μ = coefficient friction
g = acceleration due to gravity
R_{21} = ratio of vehicle weights
v_{1i} = initial velocity of vehicle 1
v_{2i} = initial velocity of vehicle 2
v_{1f} = final velocity of vehicle 1; $v_{1f} = (2g\mu D_{1f})^{1/2}$
D_{1f} = vehicle 1 final distance
v_{2f} = final velocity of vehicle 2; $v_{2f} = (2g\mu D_{2f})^{1/2}$
D_{2f} = vehicle 2 final distance
A_{1i} = precollision angle of vehicle 1
A_{2i} = precollision angle of vehicle 2
A_{1f} = postcollision angle of vehicle 1
A_{2f} = postcollision angle of vehicle 2

Generalized Critical Speed Analysis

A study of the previous sections reveals that when a vehicle's path is known whether traveling down a straight road, on a level or inclined surface, whether negotiating a curve, whether the curve is banked or inclined, a speed calculation can be made. Various equations have been developed in this chapter to compute stopping distance, critical speed, coefficient of friction, and acceleration to name a few. An entire section was devoted to arguments concerning the manipulation of the coefficient of friction in critical stopping distance calculations. Recent arguments in the accident reconstruction field concerning the validity of the critical speed equation in a turn have emerged. These arguments state that the critical speed equation cannot be used. However, the arguments do not state what techniques can be used to calculate the critical speed in a turn. In this section we will present mathematically the validity of the critical speed equation. As with any analysis tool, the critical speed equation depends on the judicious use of the appropriate radial distance. Critical speed tests performed by the authors have validated the critical speed equation. The experienced investigator knows how to measure the yaw marks that yield the correct solution.

The argument against the use of Equation 9.168 usually goes like this: An automobile does not behave like a rock on a string. They reason that while a vehicle is negotiating a turn and going into a yaw, part of the available tire/road friction is drag and part keeps the vehicle from turning over. In contrast, they reason that a rock on a string uses all available force to keep moving in a circle. Furthermore, they state that since the critical speed method is

derived from a rock on a string, the critical speed derivation is improper. Another corollary argument deals with the coefficient of friction used. They reason that since the value of the coefficient of friction is derived from skid tests, these values are improperly applied in critical speed calculations. These erroneous arguments will be dispelled in this section and the next. In the previous sections we derived the critical speed-curved trajectory in terms of a circular path. In the last section it was pointed out that curves are complex, including sections of spirals and circles. However, the circular portion of a curve is the sharpest, and therefore, using the radius of the circular portion of the road will lead to the lowest solution of the critical speed in a turn equation. The derivations in the previous sections made no mention of rocks on a string. The equations that were developed arose from equilibrium or loss of equilibrium equations. The equations were derived from basic statics and their respective free body diagrams. Free body diagrams are acceptable analysis aids in engineering and physics. A proper free body diagram yields correct solutions and should not be construed as improper simply because it represents a static condition.

Figure 9.30 represents a vehicle on a curved trajectory. At any particular point in time *P*, the section of the trajectory has a radial distance *R*. Keep in mind that the development presented here is not static. We will develop a time varying equation for the critical speed in a curved path where control of the vehicle is lost.

From basic definitions we know that *R* is the radius at the point *P*, *S* is the arc length and ω is the angular velocity. The condition for loss of control can be gleaned from the vector accelerations, namely,

$$|\boldsymbol{a}| = |\boldsymbol{a}_n + \boldsymbol{a}_t| \geq \mu g \tag{9.177}$$

$$v = \frac{ds}{dt} = \frac{Rd\theta}{dt} = R\omega \tag{9.178}$$

In Equation 9.177 we consider the normal and tangential components of acceleration which cause the vehicle to leave its intended path. Note that there are no rocks or strings, only real forces that affect the vehicle. Since $S = R\theta$,
and

$$v^2 = R^2\left(\frac{d\theta}{dt}\right)^2 \tag{9.179}$$

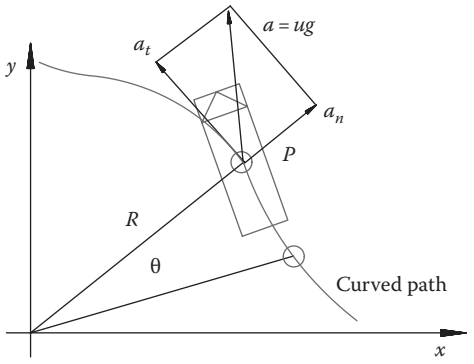

Figure 9.30 Critical speed: curved path.

By definition, the normal component of acceleration is

$$a_n = \frac{v^2}{R} = R\left(\frac{d\theta}{dt}\right)^2 \tag{9.180}$$

Again, by definition, the tangential component of acceleration is

$$a_t = \frac{dv}{dt} = \frac{d}{dt}\left(\frac{ds}{dt}\right) = \frac{d}{dt}\left(\frac{Rd\theta}{dt}\right) = \frac{Rd^2\theta}{dt^2} \tag{9.181}$$

At the inequality, from Equation 9.177, we may write

$$(a_n)^2 + (a_t)^2 = (\mu g)^2 \tag{9.182}$$

Substituting and separating the variables, we obtain

$$\frac{dv}{\sqrt{k^2 - v^4}} = \frac{dt}{R} \tag{9.183}$$

where $k = \mu gR$.

We are interested in the left side of the equation, which involves an elliptic integral of the first kind. The solution to this integral is given by

$$\frac{i\sqrt{-1/k}\,k\sqrt{1 - v^4/k^2}\,F[\varphi \mid m]}{\sqrt{k^2 - v^4}} \tag{9.184}$$

where

$F[\varphi|m]$ is the elliptic integral of the first kind

$$i = \sqrt{-1} \quad m = -1$$

$$\varphi = i\sinh^{-1}\left[\sqrt{-1/k}\,v\right]$$

We can simplify the left side of Equation 9.183 to

$$F[\varphi \mid -1] = -\sqrt{\frac{\mu g}{R}}\,t \tag{9.185}$$

Note that $v = \sqrt{\mu gR}$ is a solution to Equation 9.182. Let us now turn our attention to the value of the argument φ. We know that v will be a value in the neighborhood of $\sqrt{\mu gR}$ so the argument of φ is

$$\varphi \cong i\sinh^{-1}\left[\sqrt{-1}\right] \tag{9.186}$$

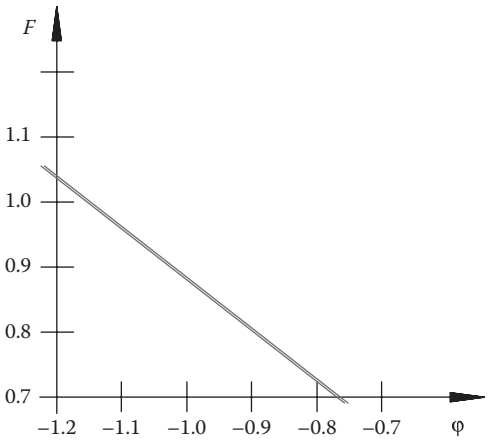

Figure 9.31 Plot of absolute value.

The plot of the absolute value of the function on the left side of Equation 9.184 is shown in Figure 9.31.

The earlier analysis illustrates that the solution for the critical speed equation is accurate to within 10% and is, therefore, within engineering accuracy. The variability in the actual coefficient of friction and the approximation of the radial distance play a more critical role in the solution for the loss of control around a curve. It should be pointed out that there is no unique solution to Equation 4.88. Instrumented tests performed by the authors validate the critical speed equation and reaffirm that the proper values of radial distance and coefficient of friction play a more critical role than the use of the critical speed equation. We can summarize the earlier generalized critical speed analysis as follows:

1. The analysis was based on a generalized curved path, irrespective of whether it was a circle, ellipse, parabola, hyperbola, or any number of spirals.
2. The analysis was dependant on the normal and tangential components of velocity and acceleration as their position changed with time.
3. The radius of the curve does not need to be constant over the entire path. The radius need only be determined at the point of loss of control.
4. The critical speed equation is valid for the design of highways because roads are constructed of circular and spiral sections.
5. Skid marks produced by yawing or spinning vehicles are in the shape of curves and at the point of loss of control the skid marks have a mean radius and a normal and tangential component.
6. The earlier development was based on a valid free body diagram at the point of loss of control about an arbitrary curved path and yields a general solution of motion where the loss of control occurs.

As previously mentioned, vehicles losing control around a turn may yaw, spin, roll, or flip over. Yaw marks are deposited when a rolling tire is also sliding sideways. For most passenger cars the darkest or heaviest yaw mark is made by the outside front tire. The outside rear tire runs outside the front tire and its mark is generally less heavy. In contrast, when a vehicle is spinning, the tire marks will cross at least at one point. For large angles of spin rotation the tire marks may cross over more than once.

Critical Speed from Yaw and Rollover

Many single-vehicle automobile accidents are characterized by the driver losing control over steering and over braking, causing the vehicle dynamics to yaw and then skid or roll to a stop. In a yaw, it is hard to tell which wheels are laying down the rubber. Many experts disagree on the actual tires that are producing one, two, three, or even four yaw marks. It is generally known, however, that the rear wheels track outside the front wheels. Many researchers pay too much attention to the radius of the individual yaw marks when, in fact, the important radial distance is that through which the center of mass of the vehicle traveled. The following speed calculations are in no way connected to which tires laid down the yaw marks. In fact, the center line through the yaw marks is a sufficiently accurate record of the path of the center of mass of the vehicle through the yaw and does not depend on which tires laid down the tracks. The yaw marks approximate sections of circles and the path drawn through the center of these yaw marks is also a section of a circle, which we take to be the path of the center of mass of the vehicle through the yaw. Since this type of accident occurs at high speeds, which corresponds to large radial distances, the arcs are relatively straight, making our assumptions valid.

Definition of terms:

V_a = average velocity through the yaw
V_c = critical speed of a vehicle in a yaw
V_i = speed entering the yaw
V_f = speed leaving the yaw
μ_a = average drag factor
μ_k = total vector coefficient of kinetic friction
μ_t = transverse drag factor in the yaw
μ_l = longitudinal drag factor in the yaw
D = distance of skid or roll after the yaw
R = radius of the yaw arc
S = arc length
L = length of the cord making up the yaw arc
h = rise of the arc above the cord
g = acceleration due to gravity

The radius R of the arc is related to the length L of the cord and the rise h of the arc above the cord by

$$R = \frac{4h^2 + L^2}{8h} \tag{9.187}$$

while the length of the arc S may be computed by

$$S = 2R\cos^{-1}\left(1 - \frac{h}{R}\right) \tag{9.188}$$

The critical speed of a vehicle in a flat turn of radius R is

$$V_c = \sqrt{\mu_t g R} \tag{9.189}$$

The speeds of the vehicle entering and leaving the yaw are related to the arc length S of the yaw by

$$V_i = \sqrt{V_f^2 + 2\mu_t gS} \tag{9.190}$$

The speed of the vehicle leaving the yaw and skidding or rolling to a stop through a distance D can be computed using the speed to stop formula:

$$V_f = \sqrt{2\mu_a gD} \tag{9.191}$$

Finally, the average velocity through the yaw is given by

$$V_a = \frac{V_i + V_f}{2} \tag{9.192}$$

Since the average speed through the yaw equals the critical speed,

$$V_a = V_c \tag{9.193}$$

substituting the earlier equation in accordance with Equation 9.191 yields

$$\sqrt{2\mu_t R} = \sqrt{\mu_a D} + \sqrt{\mu_a D + \mu_\ell S} \tag{9.194}$$

solving for μ_t yields

$$\mu_t = \frac{\mu_a D}{R} + \frac{\mu_\ell s}{2R} \pm \sqrt{\frac{(\mu_a D)^2}{R^2} + \frac{\mu_a D}{R}\frac{\mu_\ell S}{R}} \tag{9.195}$$

which is of the form

$$\mu_t = a + \frac{b}{2} \pm \sqrt{a^2 + ab} \tag{9.196}$$

Completing the square within the radical

$$\mu_t = a + \frac{b}{2} \pm \sqrt{\left(a + \frac{b}{2}\right)^2 - \frac{b^2}{4}} \tag{9.197}$$

Since $\mu_t < 1$ and $R > S$, then $b \ll 1$:

$$\frac{b^2}{4} \ll \left(a + \frac{b}{2}\right)^2 \tag{9.198}$$

Thus, the only reasonable solution is

$$\mu_t \approx 2a + b = \frac{2\mu_a D}{R} + \frac{\mu_\ell S}{R} \tag{9.199}$$

It is now easy to choose μ_a and μ_k. We must not choose the longitudinal and transverse drag factors independently of one another. The total kinetic vector frictional force is the vector sum of the longitudinal and transverse frictional forces. Therefore, μ_k is given by

$$\mu_k = \sqrt{\mu_\ell^2 + \mu_t^2} \tag{9.200}$$

Choosing different values of the coefficient of kinetic friction μ_k yields values of μ_t in terms of μ_t in Equations 9.199 and 9.200. Additionally, choosing values of μ_a and substituting into Equation 9.199 allow us to choose a suitable value of the transverse drag factor μ_t, which yields the critical speed of the vehicle in Equation 9.189.

Extension on Minimum Speed Calculations When Radius Cannot Be Determined Uniquely

In some reconstructions the yaw marks from a collision following loss of control have degraded to the point where they cannot be recognized. However, often, the beginning and end of the yaw was marked by the investigating officer. If these two points are known and the road geometry is known, then a minimum speed calculation can be made. In this analysis it is assumed that the vehicle did not leave the road surface. Figure 9.32 represents two points along a road where the points *A* and *B* are known as measured from the roadway. The separation of the points *L* along the road is also known. The arc is assumed to be tangent to the edge of the roadway on the *x*-axis.

Graphical or numerical solutions can be found that meet the requirements that have been specified. However, a general mathematical procedure will be outlined that lends itself to a variety of problems. To begin the analysis we construct a more general diagram as specified in Figure 9.33.

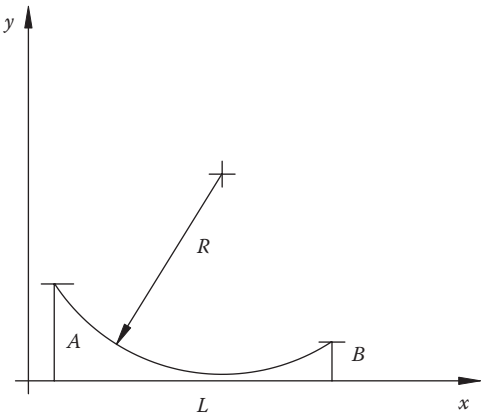

Figure 9.32 Unique radius.

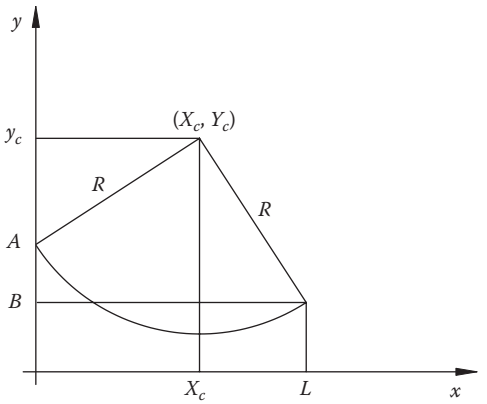

Figure 9.33 Unique radius general solution.

Figure 9.33 shows an arbitrary location for the center of the circle that produces the arc. We can write two equations for the radius in terms of the known quantities A, B, and L and the unknown center defined by x_c and y_c:

$$(y_c - B)^2 + (L - x_c)^2 = R^2 \tag{9.201}$$

$$(y_c - A)^2 + x_c^2 = R^2 \tag{9.202}$$

Solving for the coordinates of the center of the circle yields

$$x_c = ay_c + b \tag{9.203}$$

$$y_c = \frac{-(ab - A) \pm \sqrt{(ab - A)^2 - (1 + a^2)(A^2 + b^2 - R^2)}}{(1 + a^2)} \tag{9.204}$$

where

$$a = \frac{(A - B)}{L} \quad \text{and} \quad b = \frac{(L^2 + B^2 - A^2)}{2L}$$

The circle can be described as

$$(x - x_c)^2 + (y - y_c)^2 = R^2 \tag{9.205}$$

The condition that the arc AB lies entirely within the road is that R^2 be less than or equal to y_c^2. The radius of the circle that is tangent to the x-axis is

$$R_x = \frac{-(ab - A) \pm \sqrt{(ab - A)^2 - (A^2 + b^2)a^2}}{(a^2)} \tag{9.206}$$

This equation yields two real solutions and never a complex conjugate pair. The reason that the equation never yields a complex conjugate pair is that for real and positive values A, B, and L, the radicand is always greater than zero. It is obvious that the equation is not valid for L equal to zero, a nonphysical case. The physically acceptable solution is the smaller of the two real solutions because we are looking for the smaller radius that corresponds to a minimum speed from yaw marks. The arc with the corresponding smaller value of R is tangent to the x-axis within the distance L, while the larger value of R corresponds to an arc tangent to the x-axis outside of the range of L.

The general equation, as has been formulated, placed restrictions on the radius of the arc that may be tangent to the y-axis. Figure 9.34 shows a hypothetical road intersection with two vehicles approaching the intersection.

Vehicle 2 proceeds to run a stop sign forcing vehicle 1 to steer sharply to the left in order to avoid the collision. In doing so, the yaw marks deposited on the road may intersect the y-axis at one point or be tangent to the y-axis. These restrictions may yield a different solution for the minimum radius. It is possible that a circle of radius larger than the radius of the circle that is tangent to the x-axis will be tangent to the y-axis. This circle that is tangent to the x-axis may or may not cut the y-axis at two points with point A being the higher point as shown in Figure 9.35.

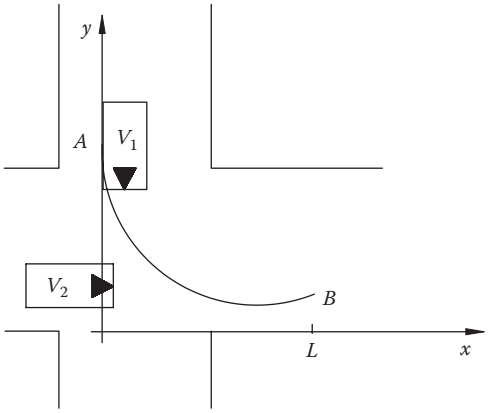

Figure 9.34 Intersection near collision.

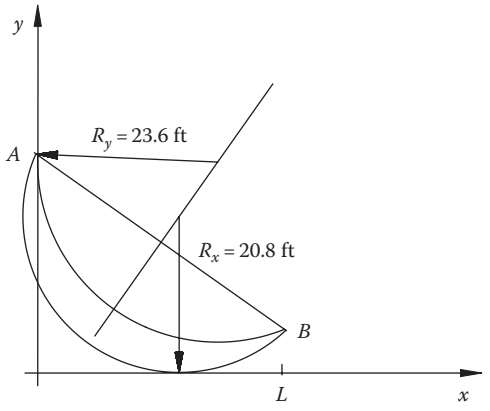

Figure 9.35 Possible solutions.

In this case, the minimum radius, determined by the conditions on the x-axis, should be rejected because a new radius tangent to the y-axis yields a larger value of minimum radius, which translates to a higher speed. Because the car is traveling parallel to the road and steering sharply to the left, it would not cut the y-axis in two places. It is also a more reasonable solution because as shown in Figure 9.16, vehicle 1 would not normally cross the y-axis at two points. The condition for a circle tangent to the y-axis is that $X_c = R$ and $Y_c = A$. Applying this condition to Equation 9.203 yields

$$R_y = \frac{(A-B)^2 + L^2}{2L} \tag{9.207}$$

As an example, if we assume $A = 28$ ft, $B = 8$ ft, and $L = 36$ ft, the radius of the circle tangent to the x-axis has two solutions: 20.8 and 131.8 ft. The radius of the circle tangent to the y-axis is 23.6 ft. The solution 20.8 ft is rejected because is cuts the y-axis in two places and is the smaller value. Please refer to Figure 9.17. Thus, the correct solution is the radius tangent to the y-axis.

Crush Analysis

Vehicle crush was first investigated in the 1970s by developing a correlation between damage to the vehicle and the related change in velocity, or ΔV. This analysis determined that there was a linear relationship between the impact speeds of vehicles into rigid barriers and the resulting crush from these collisions. From these data, mathematical models, known as algorithms, were developed to correlate vehicle damage measurements to accident reconstructions. The National Highway Traffic Safety Administration (NHTSA) developed the CRASH3 program. The crush behavior used in the CRASH3 program is modeled as a linear spring with characteristics as shown in Figure 9.36.

Based on this linear spring model, the crush coefficients A, B, and G are given by NHTSA from their crash tests. Generally, these crash tests are conducted against rigid barriers at 30–35 mph. The tests include frontal, offset frontal, angled frontal, rear, and side impact tests. Since the relationship between the impact force per width and the resulting crush on the vehicle is linear or nearly linear, it is possible to extrapolate the data to speeds lower and higher than the test speeds.

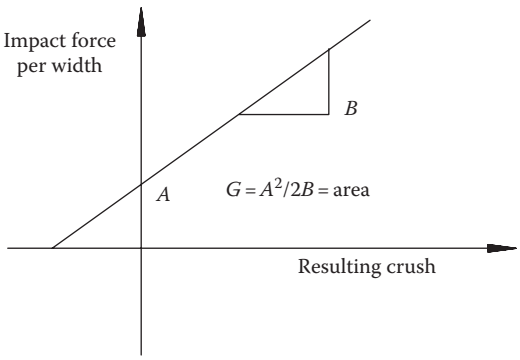

Figure 9.36 Crush model.

An argument made by some experts is that the NHTSA crash tests are not valid at lower and higher speeds. Thus, they argue that reconstructing accidents based on crush at lower speeds is not valid. This argument is simply not noteworthy for the following reasons: First, we must ask why the crash tests are conducted at around 35 mph. The answer is simple, because it is well documented through legitimate research, human tolerance, and experimentation that severe injuries begin to occur at those speeds. Second, the error published by developers of crash data state that it may vary from about 3% to 7% based on the amount of crush and, therefore, impact speed. For example, let us assume that very slight crush yields an impact speed of 7 mph. Let us further assume that the error is 15% so that the actual speed may vary between approximately 6 and 8 mph. For a higher collision speed, we may determine from crush that the impact speed is 63 mph. If we assume an error of 5%, the actual speed may vary from approximately 60 to 66 mph. Certainly, in both the lower and higher speed calculations, the range of speeds is acceptable and within the accuracy that is possible in a properly executed accident reconstruction. In a study conducted by Prasad, the energy dissipated in vehicle crush utilizing a repeated test technique essentially validated the linear relationship of crush deformation for modern cars and began the tests at speeds of 10–35 mph. The coefficients of crush, the "C" values, ranged from 1 to 46 in. for the various speeds and vehicles tested. The absorbed energies ranged from approximately 8,800 to 139,000 ft-lb.

The important point to make is that experts who attempt to discredit the relationship between vehicle crush and speed calculations cannot point to scientific or engineering studies that show the inappropriateness of the technique. The simple fact is that crush deformation is an acceptable method in accident reconstruction if properly utilized within the accuracy of the technique. Since crush deformation measurements are subjective to a certain extent, they have the potential for misuse. It is in the measurements of the crush values where the reconstructionist can distort and influence the outcome of the calculations. There are standards for crush measurements developed by the SAE. Please refer to Chapter 15 for the SAE Standards. These standards guide the investigator and help to reduce the potential of misuse of the technique. It should be pointed out that the authors have used crush deformation and validated the technique with a crush data retrieval (CDR) tool and standard energy and momentum methods. When used properly, crush deformation is an excellent method in accident reconstructions.

Since crush energy dissipation can be accurately correlated to vehicle speeds and change in velocity, the total energy dissipated in the collision between two vehicles can be computed as follows. The crush energy dissipation or CED goes mainly into the deformation of the vehicles. Some energy such as that translated to sound or heat cannot be determined. The CED can be computed by taking the difference between the total initial and final kinetic energies. Thus,

$$\text{CED} = \frac{W_1}{2g}\left[\left(V_{1i}^2 + R_{2v1}V_{2i}^2\right) - \left(V_{1f}^2 + R_{2v1}V_{2f}^2\right)\right] \tag{9.208}$$

The parameters in Equation 9.208 are detailed in the section on momentum methods.

One area of crush deformation that has produced considerable error from the published data from NHTSA is with pole impacts. Every year many injuries and deaths occur from collisions with poles and trees. In reconstructing these accidents it is desirable to determine the vehicle speed prior to impact. Originally two methods were employed to determine vehicle speed. One method employed observed crush geometry and the other utilized maximum crush. The method used commonly to estimate impact speed from

observed crush was developed by Campbell and has been incorporated into a variety of CRASH programs. In 1981, the National Transportation Safety Board (NTSB) released a report devoted to collisions with trees. The report recommended the method employing the *A* and *B* parameters as the most accurate method available to estimate impact speed from measured crush.

In 1983, Jones reported on an analysis of crush test data. That analysis found that using *A* and *B* stiffness parameters obtained from flat barrier tests underpredicted pole test speeds by approximately 67% of the actual test speed. In 1987, Smith et al. reported on tests with narrow object impacts. They found that the use of *A* and *B* parameters underestimated the speed by between 57% and 82%. In 1987 Morgan and Ivey developed an alternative formula that allows one to calculate the approximate impact speed given the maximum crush and vehicle weight. In 1992, Nystrom and Kost developed a formula based on regression analysis of actual staged tests and curve fitting techniques. The three methods outlined earlier are summarized in the following equations:

$$V_1 = \mathrm{BPO}_1 + \mathrm{BPI}_1 \cdot \mathrm{CRM} \tag{9.209}$$

$$V_2 = 395D_2 - 0.062W \tag{9.210}$$

$$V_3 = \mathrm{BPO}_3 + \mathrm{BPI}_3 \cdot \mathrm{CRM} \tag{9.211}$$

In the earlier equations, the following parameters are defined as

V_1 = preimpact speed according to NTSB (mph)
V_2 = preimpact speed according to Morgan and Ivey (mph)
V_3 = preimpact speed according to Nystrom and Kost (mph)
BPO_1 = speed at which no crush is expected (2.46 mph)
BPI_1 = slope of speed versus crush (0.648 mph/in.)
CRM = maximum crush on vehicle (in.)
D_2 = maximum residual deformation (ft)
W = weight of vehicle (lb)
BPO_3 = speed at which no crush is observed (5 mph)
BPI_3 = slope of speed versus crush (mph/in.)

where

$$\mathrm{BPI}_3 = 0.964 - (3.51 \times 10^{-5}) \times W \tag{9.212}$$

As an example, a vehicle weighing 2550 lb had a maximum crush of 36.4 in. with a residual deformation of 0.468 ft from an impact with a rigid pole. The maximum crush extended to the front axle. The analysis from crush gives a median speed of 23 mph. The NTSB and Morgan equations yield a speed between 18 and 28 mph The Nystrom and Kost equation produces a speed between 42 and 48 mph. Based on the severity of the impact it was deemed the speed was in the range calculated by the Nystrom and Kost equation was the most accurate. In this example we see that calculations performed by different investigators

can yield significantly different results when collisions with poles are analyzed. The crush analysis of 23 mph is near the center of the results from the NTSB and Morgan and Ivey equations between 18 and 28 mph. All three of these methods produce speeds significantly different than the median value of 45 mph from Nystrom and Kost.

Tree Impacts

In the previous section we saw how pole impacts can be analyzed through crush. In this section we offer an alternate solution when a vehicle impacts a tree. This type of collision can be treated as a strength of materials problem. We will assume that the tree is modeled as a cantilever beam of circular cross section. This type of analysis lends itself to problems where a small tree is broken by the impact with a car or where the crush on the car is in question as a result of an alleged collision with the tree. Figure 9.37 is relevant to the analysis.

For cylindrical shapes such as trees with diameter D, we define the following parameters. Moment of inertia,

$$I = \frac{\pi D^4}{64} \tag{9.213}$$

Section modulus,

$$S = \frac{\pi D^3}{32} \tag{9.214}$$

Area,

$$A = \frac{\pi D^2}{4} \tag{9.215}$$

The maximum shear is equal to the applied force F. If we know the modulus of elasticity E, we can compute the deflection at the load from Equation 9.216:

$$X = \frac{FY^3}{3EI} \tag{9.216}$$

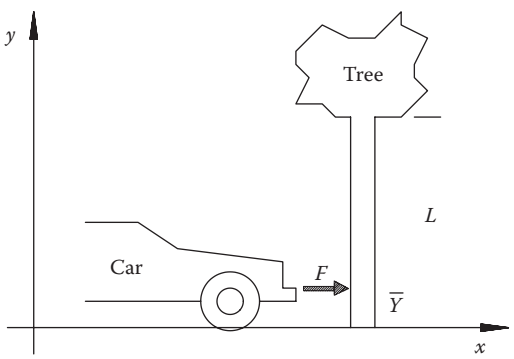

Figure 9.37 Tree impact.

The deflection end slope is then

$$\varphi = \frac{FY^2}{2EI} \tag{9.217}$$

The shear stress is

$$f_v = \frac{F}{A} \tag{9.218}$$

The maximum moment is

$$M = FY \tag{9.219}$$

The actual bending stress is then given by

$$f_b = \frac{M}{S} \tag{9.220}$$

For oak, the bending strength F_b is 800 psi, the shear strength F_v is 85 psi, and the modulus of elasticity is 900,000 psi. If f_v is greater than F_v, yield due to shear stress occurs. If f_b is greater than F_b, yield due to bending stress occurs.

Introduction to Momentum Methods

Probably the most powerful technique used in accident reconstruction is that of the conservation of momentum. Momentum may also be the most underused technique because of its subtleties and sensitivity. Previously we devoted an introduction into the conservation of momentum. In this chapter we will explore the techniques available in momentum solutions. Momentum can be subdivided into elastic and inelastic collisions and recoil. Conservation of momentum allows for the solution of velocities before or after a collision. Figure 9.38 represents a collision between two vehicles showing their pre- and postimpact paths for the solution based on momentum.

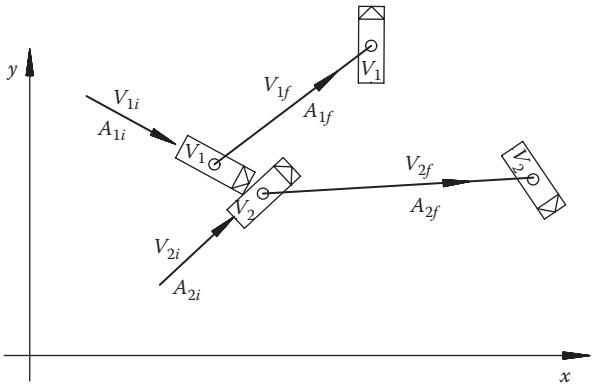

Figure 9.38 Conservation of momentum.

The basic equation of conservation of momentum is then

$$m_1\mathbf{V_{1i}} + m_2\mathbf{V_{2i}} = m_1\mathbf{V_{1f}} + m_2\mathbf{V_{2f}} \tag{9.221}$$

where

m_1 is the mass of vehicle 1
m_2 is the mass of vehicle 2
$\mathbf{V_{1i}}$ is the precollision velocity of vehicle 1
$\mathbf{V_{2i}}$ is the precollision velocity of vehicle 2
$\mathbf{V_{1f}}$ is the postcollision velocity of vehicle 1
$\mathbf{V_{2f}}$ is the postcollision velocity of vehicle 2

Elastic and Inelastic Collisions

A completely elastic collision is one in which the two vehicles come together, collide and separate. In the elastic collision, the forces of interaction between the vehicles are conserved, the total kinetic energy is the same before and after the collision. Completely elastic collisions never occur when two vehicles have an accident. However, for many collisions an elastic model is a sufficient solution of the event. At the opposite end of an elastic collision is one in which the two vehicles become coupled and move in unison after the collision. Such a collision is completely inelastic. Most vehicles collisions range from elastic to inelastic to some degree. In those cases, a coefficient of restitution is introduced into the conservation of momentum solutions. Before we develop specific equations, we wish to generalize conservation of momentum equations in terms of their elastic and inelastic qualities.

Elastic Collisions

In a perfectly elastic collision, the center of mass of the vehicles is central. After the collision, the vehicles separate at different velocities, and since kinetic energy and momentum are both conserved, we may write two equations. The first equation is given by (9.221) and the energy equation is

$$\frac{1}{2}m_1\mathbf{V_{1i}^2} + \frac{1}{2}m_2\mathbf{V_{2i}^2} = \frac{1}{2}m_1\mathbf{V_{1f}^2} + \frac{1}{2}m_2\mathbf{V_{2f}^2} \tag{9.222}$$

If the masses and the precollision velocities are known, the postcollision velocities are known. The postcollision velocities are given by

$$V_{1f} = \frac{2R_{2v1}V_{2i} + (1 - R_{2V1})V_{1i}}{(R_{2V1} + 1)} \tag{9.223a}$$

$$V_{2f} = \frac{2V_{1i} + (1 - R_{2v1})V_{2i}}{(R_{2V1} + 1)} \tag{9.223b}$$

If the masses and the postcollision velocities are given, the precollision velocities are given by

$$V_{1i} = \frac{2R_{2v1}V_{2f} + (1 - R_{2V1})V_{1f}}{(R_{2V1} + 1)} \tag{9.224a}$$

$$V_{2i} = \frac{2V_{1f} + (R_{2V1} - 1)V_{2f}}{(R_{2V1} + 1)} \tag{9.224b}$$

where

$$R_{2V1} = \frac{W_2}{W_1} \tag{9.225}$$

is the ratio of the masses.

In the case where one vehicle is at rest initially, say $V_{2i} = 0$, Equations 9.223 reduce to

$$V_{1f} = \frac{(1 - R_{2V1})V_{1i}}{(R_{2v1} + 1)} \tag{9.226a}$$

$$V_{2f} = \frac{2V_{1i}}{(R_{2v1} + 1)} \tag{9.226b}$$

If the weight of one vehicle is much more massive than the other, that is, $W_1 \gg W_2$ such as in a train–vehicle collision, Equations 9.226 reduce to

$$V_{1f} \approx V_{1i} \tag{9.227a}$$

$$V_{2f} \approx 2V_{1i} + V_{2i} \tag{9.227b}$$

It has been previously inferred that the energy may not always be conserved but that momentum is always conserved. Therefore, the equations developed earlier may not always hold true. In those cases, a more general solution of the conservation of linear momentum may be obtained by expanding Equation 9.221 into its appropriate components. This type of analysis is reserved for the next section. Before we leave this section, there are a couple of topics that need to be addressed. For the special case of the elastic collision in which one vehicle is at rest before the collision, $V_2 = 0$:

$$V_{1f} = \frac{(1 - R_{2V1})V_{1i}}{(R_{2v1} + 1)} \tag{9.228a}$$

$$V_{2f} = \frac{2V_{1i}}{(R_{2v1} + 1)} \tag{9.228b}$$

If the masses of the vehicles are equal and we know the final velocities of the vehicles, Equations 9.224 reduce to

$$V_{1i} = V_{2f} \tag{9.229a}$$

$$V_{2i} = V_{1f} \tag{9.229b}$$

Conservation of Linear Momentum

With reference to Figure 9.21 and given the pre- and postimpact angles of the vehicles as A_{1i}, A_{2i}, A_{1f}, and A_{2f}, we can again define the ratio of the masses in terms of the ratio of weights. Thus, in the collision between V_1 and V_2, the weight ratio is defined as follows where W_1 and

$$R_{2v1} = \frac{W_2}{W_1} \tag{9.230}$$

W_2 are the weights of vehicles V_1 and V_2, respectively. In a collision between two vehicles, conservation of momentum states that the total initial momentum is the same as the total final momentum. Momentum is an additive vector quantity defined as the product of mass and velocity. Since the mass of a vehicle is its weight divided by the acceleration due to gravity, weight may be used in place of mass in the momentum equation. Setting up an (x,y) coordinate system in the usual fashion and measuring angles positive counterclockwise from the x-axis allow the x and y components of the initial and final momentum to be expressed as

$$\begin{aligned} P_{ix} &= W_1 V_{1i} \cos A_{1i} + W_2 V_{2i} \cos A_{2i} \\ P_{iy} &= W_1 V_{1i} \sin A_{1i} + W_2 V_{2i} \sin A_{2i} \end{aligned} \tag{9.231}$$

$$\begin{aligned} P_{fx} &= W_1 V_{1f} \cos A_{1f} + W_2 V_{2f} \cos A_{2f} \\ P_{fy} &= W_1 V_{1f} \sin A_{1f} + W_2 V_{2f} \sin A_{2f} \end{aligned} \tag{9.232}$$

The equations of conservation of momentum

$$\begin{aligned} P_{ix} &= P_{fx} \\ P_{iy} &= P_{fy} \end{aligned} \tag{9.233}$$

may then be solved in a number of ways.

In this particular case, the angles and the final speeds will be taken as known quantities, and the initial speeds will be determined by the equations, producing the following results:

$$\begin{aligned} V_{1i} &= \frac{V_{1f} \sin(A_{2i} - A_{1f}) + R_{2v1} V_{2f} \sin(A_{2i} - A_{2f})}{\sin(A_{2i} - A_{1i})} \\ V_{2i} &= \frac{V_{1f} \sin(A_{1i} - A_{1f}) + R_{2v1} V_{2f} \sin(A_{1i} - A_{2f})}{R_{2v1} \sin(A_{1i} - A_{2i})} \end{aligned} \tag{9.234}$$

If the initial and final coordinates of the centers of mass of the two vehicles are known, the postcollision angles and distances may be computed using

$$A_{1f} = \tan^{-1}\left(\frac{Y_{1f} - Y_{1i}}{X_{1f} - X_{1i}}\right)$$
$$A_{2f} = \tan^{-1}\left(\frac{Y_{2f} - Y_{2i}}{X_{2f} - X_{2i}}\right) \tag{9.235}$$

and

$$D_{1f} = \sqrt{(X_{1f} - X_{1i})^2 + (Y_{1f} - Y_{1i})^2}$$
$$D_{2f} = \sqrt{(X_{2f} - X_{2i})^2 + (Y_{2f} - Y_{2i})^2} \tag{9.236}$$

The postcollision speeds are determined from the postcollision distances and the coefficient of kinetic friction using

$$V_{1f} = \sqrt{2\mu_k g D_{1f}}$$
$$V_{2f} = \sqrt{2\mu_k g D_{2f}} \tag{9.237}$$

Similarly, if the preskid and initial coordinates of the centers of mass of the two vehicles are known, the preskid angles and distances may be computed using

$$A_{1i} = \tan^{-1}\left(\frac{Y_{1i} - Y_{1o}}{X_{1i} - X_{1o}}\right)$$
$$A_{2i} = \tan^{-1}\left(\frac{Y_{2i} - Y_{2o}}{X_{2i} - X_{2o}}\right) \tag{9.238}$$

and

$$D_{1i} = \sqrt{(X_{1i} - X_{1o})^2 + (Y_{1i} - Y_{1o})^2}$$
$$D_{2i} = \sqrt{(X_{2i} - X_{2o})^2 + (Y_{2i} - Y_{2o})^2} \tag{9.239}$$

The preskid speeds may then be computed using

$$V_{1o} = \sqrt{V_{1i}^2 + 2\mu_k g D_{1i}}$$
$$V_{2o} = \sqrt{V_{2i}^2 + 2\mu_k g D_{2i}} \tag{9.240}$$

Finally, it is useful to compute the total energy dissipated in the collision. It is called the crush energy dissipation (CED) because most of the dissipated energy goes into the deformation of the vehicles. We may then compare the CED to the results of EDCRASH or other computer programs that calculate the energy based on crush. The computer program, EDCRASH, computes this quantity based on the class of the vehicles and the damage to the vehicles. Please refer to the EDCRASH program for more details. Here, the CED is computed by taking the difference between the total initial and final kinetic energies. Thus,

$$\text{CED} = \frac{W_1}{2g}\left[(V_{1i}^2 + R_{2v1}V_{2i}^2) - (V_{1f}^2 + R_{2v1}V_{2f}^2)\right]. \tag{9.241}$$

Conservation of Linear Momentum with Restitution

The beginning of this analysis is the same as the analysis of the conservation of linear momentum where W_1 and W_2 are the weights of V_1 and V_2, respectively.

The equations of conservation of momentum

$$\begin{aligned} P_{ix} &= P_{fx} \\ P_{iy} &= P_{fy} \end{aligned} \tag{9.242}$$

may then be solved in a number of ways.

In a standard momentum analysis, the angles and the final speeds are taken as known quantities. Energy methods are used to compute the postcollision velocities. These results are employed into the momentum equations to determine the impact speeds. The postcollision velocities are determined from the postcollision distances and the coefficient of kinetic friction using:

$$\begin{aligned} V_{1f} &= \sqrt{2\mu_k g D_{1f}} \\ V_{2f} &= \sqrt{2\mu_k g D_{2f}} \end{aligned}. \tag{9.243}$$

In some cases, the scene data are unreliable, which make determining the impact location difficult. Even small changes in the impact point will have significant effects on the postimpact distances and angles. As such, there will be a level of uncertainty with the final velocity calculations. Usually, an accurate determination of the postimpact phase of at least one vehicle can be made. However, the limited confidence in the scene data requires an analysis of the impact phase.

In an impact between two vehicles (V_1 and V_2), the impact phase can be separated into two periods. Following the initial contact, a short period of increasing deformation takes place until the contact area between the vehicles ceases to increase. During this instant, the vehicles are moving at the same velocity (V_o). During the remainder of contact, a period of restoration occurs during which the contact area is reduced to zero. The relationship between the restoration and deformation phases of impact is called the coefficient of restitution (e), which reflects the capacity of the contacting bodies to recover from the impact.

For each vehicle, e can be defined by the following ratios: where F_r and F_d are the contact forces during the restoration and deformation periods. Combining the two expressions in Equation 9.246 eliminates V_o and provides an equation for e.

The coefficient of restitution depends on the impact velocity, geometry of colliding objects, and given combination of contacting materials. The value of e will lie between 1.0 and 0. An e of 1.0 denotes a purely elastic impact where the energy loss through heat, deformation, and sound is negligible. The value $e = 0$ represents an inelastic, or plastic, impact where the vehicles cling together after colliding and the energy loss is maximum. In the purely plastic case ($e = 0$), the postimpact velocities (V_{1f} and V_{2f}) of the two vehicles will be equal:

$$e = \frac{V_o - V_{1f}}{V_{1i} - V_o} \quad \text{for} \quad V_1 \tag{9.244}$$

$$e = \frac{V_{2f} - V_o}{V_o - V_{2i}} \quad \text{for} \quad V_2 \tag{9.245}$$

$$e = \frac{V_{2f} - V_{1f}}{V_{1i} - V_{2i}} \tag{9.246}$$

For a given case, it may be found that V_{1f} can be more accurately determined from Equation 9.243. Then V_{2f} can be described as follows:

$$V_{2f} = V_{1f} + e(V_{1i} - V_{2i}) \tag{9.247}$$

Substituting yields

$$\begin{aligned} V_{1i} &= V_{1f} \frac{\sin(A_{2i} - A_{1f}) - R_{2v1}\sin(A_{2f} - A_{2i}) + e\sin(A_{2f} - A_{1f})}{\sin(A_{2i} - A_{1i}) + R_{2v1}\sin(A_{2f} - A_{2i}) + e\sin(A_{2f} - A_{1i})} \\ V_{2i} &= \frac{V_{1f}}{R_{2v1}} \frac{\sin(A_{1f} - A_{1i}) + R_{2v1}\sin(A_{2f} - A_{1i}) + R_{2v1}e\sin(A_{2f} - A_{1f})}{\sin(A_{2i} - A_{1i}) + R_{2v1}\sin(A_{2f} - A_{2i}) + e\sin(A_{2f} - A_{1i})} \end{aligned} \tag{9.248}$$

For the alternate case, V_{2f} may be more accurately determined. Then V_{1f} can be described as follows:

$$V_{1f} = V_{2f} - e(V_{1i} - V_{2i}) \tag{9.249}$$

Then substitution provides

$$\begin{aligned} V_{1i} &= R_{2v1}\ V_{2f} \frac{\sin(A_{2i} - A_{1f}) - R_{2v1}\sin(A_{2f} - A_{2i}) + e\sin(A_{2f} - A_{1f})}{R_{2v1}\sin(A_{2i} - A_{1i}) + e\sin(A_{1i} - A_{1f}) + R_{2v1}e\sin(A_{2i} - A_{1f})} \\ V_{2i} &= V_{2f} \frac{\sin(A_{1f} - A_{1i}) + R_{2v1}\sin(A_{2f} - A_{1i}) + R_{2v1}\ e\sin(A_{2f} - A_{1f})}{R_{2v1}\sin(A_{2i} - A_{1i}) + e\sin(A_{1i} - A_{1f}) + R_{2v1}e\sin(A_{2i} - A_{1f})} \end{aligned} \tag{9.250}$$

Comparison of results from Equations 9.248 and 9.250 will determine which postimpact speed (V_{1f} or V_{2f}) is more reliable. Finally, the preskid speeds may be computed using

$$V_{1o} = \sqrt{V_{1i}^2 + 2\mu_k g D_{1i}}$$
$$V_{2o} = \sqrt{V_{2i}^2 + 2\mu_k g D_{2i}} \tag{9.251}$$

Conservation of Rotational Momentum

Solutions using the conservation of linear momentum are sufficient for most kinds of collisions. However, errors are introduced when the impact load is directed at a considerable distance away from the vehicle's center of mass. Examples of such collisions are frontal-offset impacts or T-bone collisions centered at the front or rear of the target vehicle. In a collision between two vehicles, denoted as V_1 and V_2, the Figure 9.39 details the impact configuration.

In this diagram, the preimpact velocities are denoted V_{1i} and V_{2i} and the postimpact velocities are denoted V_{1f} and V_{2f}. These velocity vectors are directed at the respective angles denoted A_{1i}, A_{2i}, A_{1f}, and A_{2f} based on the Cartesian coordinate system. The rotational velocities are defined as ω_1 and ω_2. As the position and direction of the impact forces are located away from the center of mass, especially with vehicle 1 (V_1) in this example, moment arms l_1 and l_2 are defined. As shown in the figure, these moment arms can be broken down into their Cartesian components:

$$l_1 = \sqrt{l_{1x}^2 + l_{1y}^2}$$
$$l_2 = \sqrt{l_{2x}^2 + l_{2y}^2} \tag{9.252}$$

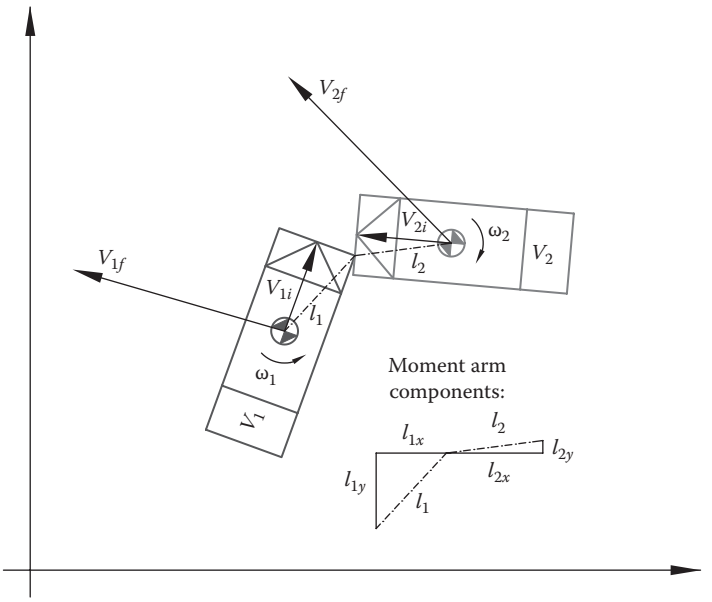

Figure 9.39 Rotational momentum.

Conservation of rotational momentum is given by the following equation, where "*I*" denotes the moment of inertia of the vehicles:

$$I_1\omega_{1i} + I_2\omega_{2i} = I_1\omega_{1f} + I_2\omega_{2f} \tag{9.253}$$

Solving this equation requires computing the angular velocities of the vehicles before and after the impact. Unless a vehicle is yawing at a significant rate prior to a collision, the left side of the equation can be considered as zero for most cases. Thus, we will only consider angular velocities resulting from impact. The postimpact rotational momentum of each vehicle is given by the following:

$$\begin{aligned} I_1\omega_{1f} &= m_1\Delta V_1 l_2 \\ I_2\omega_{2f} &= m_2\Delta V_2 l_1 \end{aligned} \tag{9.254}$$

Here, speed changes incurred by both vehicles as a result of the impact are defined as ΔV_1 and ΔV_2. The terms m_1 and m_2 refer to the masses of each vehicle. The ratio of the masses, or weights, is given by the following:

$$R_{2v1} = \frac{W_2}{W_1} = \frac{m_2}{m_1} \tag{9.255}$$

The speed changes are defined by the following relationships and Figure 9.40:

$$\Delta V_1 = \sqrt{\Delta V_{1x}^2 + \Delta V_{1y}^2} = \sqrt{(V_{1ix} - V_{1fx})^2 + (V_{1iy} - V_{1fy})^2} \tag{9.256}$$

$$\Delta V_2 = \sqrt{\Delta V_{2x}^2 + \Delta V_{2y}^2} = \sqrt{(V_{2ix} - V_{2fx})^2 + (V_{2iy} - V_{2fy})^2} \tag{9.257}$$

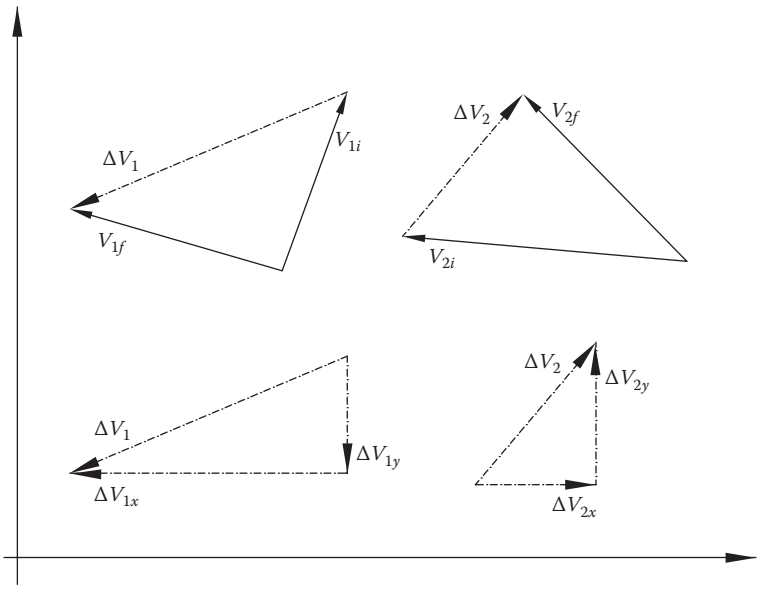

Figure 9.40 Speed change relationships.

Note that the x and y components of the pre- and postimpact velocities are based on the specified angles gathered by the accident site information. By implementing these definitions for speed change into the governing equation, the following equations are generated:

$$\begin{aligned} 0 &= R_{2v1}\Delta V_{2x} l_{1y} + \Delta V_{1x} l_{2y} \\ 0 &= R_{2v1}\Delta V_{2y} l_{1x} + \Delta V_{1y} l_{2x} \end{aligned} \tag{9.258}$$

Organization of this equation is performed to place the unknown variables (V_{1i} and V_{2i}) on the left side:

$$\begin{aligned} V_{2i} R_{2v1} l_{1y} \cos(A_{2i}) + V_{1i} l_{2y} \cos(A_{1i}) &= V_{2f} R_{2v1} l_{1y} \cos(A_{2f}) + V_{1f} l_{2y} \cos(A_{1f}) \\ V_{2i} R_{2v1} l_{1x} \sin(A_{2i}) + V_{1i} l_{2x} \sin(A_{1i}) &= V_{2f} R_{2v1} l_{1x} \sin(A_{2f}) + V_{1f} l_{2x} \sin(A_{1f}) \end{aligned} \tag{9.259}$$

Conservation of energy principles for the postimpact translational and rotational movement yields the following equations for postimpact speeds:

$$\begin{aligned} V_{1f} &= \sqrt{2\mu_{1f} g \left(\beta_1 WB_1 \frac{\pi}{360} D_{1f} \right)} \\ V_{2f} &= \sqrt{2\mu_{2f} g \left(\beta_2 WB_2 \frac{\pi}{360} D_{2f} \right)} \end{aligned} \tag{9.260}$$

where

μ is the coefficient of friction
g is the acceleration due to gravity
β is the magnitude of the postimpact rotation
WB is the vehicle's wheelbase
D_f is the postimpact skid distance

The postimpact rotation is taken as the absolute difference of the final heading angles (α_1 and α_2) to the initial heading angles (A_{1i} and A_{2i}). Note that it is assumed that the vehicle's preimpact heading corresponds with its direction, which is derived from the assumption that there is negligible rotational momentum prior to impact.

$$\begin{aligned} \beta_1 &= | A_{1i} - \alpha_1 | \\ \beta_2 &= | A_{2i} - \alpha_2 | \end{aligned} \tag{9.261}$$

Once the unknowns are reduced to the preimpact speeds (V_{1i} and V_{2i}), the governing equation can be solved by several methods. Solving the two governing equations simultaneously provides satisfactory answers but is not conducive to coding. These equations have been organized for implementation into direct or iterative solutions for linear algebraic equations ($Ax = b$). Cramer's rule can also be applied for implementation into spreadsheet programs.

Combined Linear and Rotational Momentum

Linear and rotational momentum may be combined in those reconstructions that combine both effects in the pre or post phases of the collision. Each section of the collision may be solved piecewise and then the two solutions may be then combined through superposition. Such solutions can be quite complex and can involve translation and rotation of the axes. In these types of reconstructions two sets of coordinates may need to be established to find the complete solution. For example, the linear momentum portion of the solution may utilize rectangular coordinates while the rotational portion of the solution may encompass cylindrical coordinates. These types of solutions also lend themselves to collisions involving more than one impact. For instance a first impact may occur between two vehicles where the solution to the velocities is found from linear momentum. A third vehicle may then strike one of the original vehicles causing the vehicle to spin from the second impact.

Rotational Momentum: Alternate Solution

Another method of analysis for the solution of rotational momentum problems may be obtained by considering the vector moment of torque produced by a force $\boldsymbol{F}$. Consider Figure 9.41.

Recall that the vector moment is given by

$$\Gamma = \boldsymbol{r} \times \boldsymbol{F} \tag{9.262}$$

The vector angular momentum is defined as

$$\boldsymbol{H} = \boldsymbol{r} \times m\boldsymbol{v} \tag{9.263}$$

The vector angular momentum is also defined as the momentum of momentum. The magnitude of angular momentum is given by

$$|\boldsymbol{H}| = H = I\omega \tag{9.264}$$

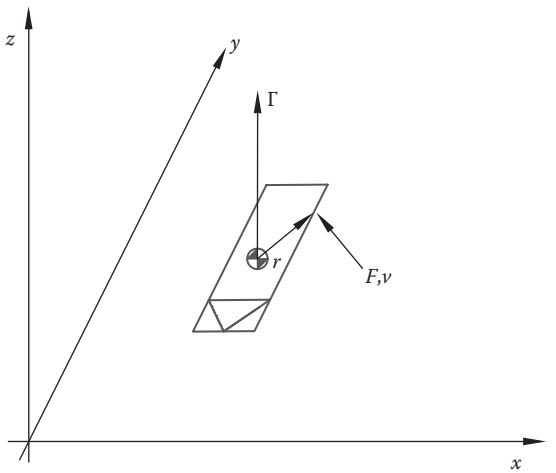

Figure 9.41 Rotational momentum.

where I = moment of inertia and ω is the angular velocity. For Figure 9.24 we may express the vectors as

$$\boldsymbol{r} = x\boldsymbol{a}_x + y\boldsymbol{a}_y \tag{9.265}$$

$$\boldsymbol{F} = F_x\boldsymbol{a}_x + F_y\boldsymbol{a}_y \tag{9.266}$$

$$\boldsymbol{v} = v_x\boldsymbol{a}_x + v_y\boldsymbol{a}_y \tag{9.267}$$

Then from Equation 9.262

$$\mathsf{G} = (xF_y - yF_x)\boldsymbol{a}_z \tag{9.268}$$

and from Equation 9.263, we obtain

$$\boldsymbol{H} = m(xv_y - yv_x)\boldsymbol{a}_z \tag{9.269}$$

where $\boldsymbol{a}_x$, $\boldsymbol{a}_y$, and $\boldsymbol{a}_z$ are unit vectors in the respective directions. Now consider the collision between two vehicles as shown in Figure 9.42.

The governing equations for vehicle 1 are

$$\mathsf{G}_1 = \boldsymbol{r}_1 \times \boldsymbol{F}_2 \tag{9.270}$$

$$\boldsymbol{H}_1 = \boldsymbol{r}_1 \times m_1\boldsymbol{v}_2 = I_1\mathsf{w}_1 \tag{9.271}$$

For vehicle 2,

$$\mathsf{G}_2 = \boldsymbol{r}_2 \times \boldsymbol{F}_1 \tag{9.272}$$

$$\boldsymbol{H}_2 = \boldsymbol{r}_2 \times m_2\boldsymbol{v}_1 = I_2\mathsf{w}_2 \tag{9.273}$$

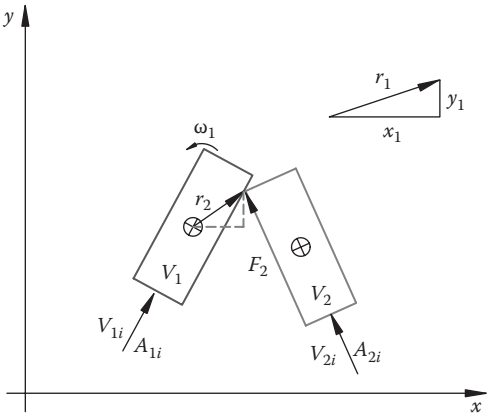

Figure 9.42 Collision between two vehicles.

The angular velocity of each vehicle's rotation may be determined from

$$\omega = \frac{2v_r}{WB} \tag{9.274}$$

where

WB is the wheelbase of the vehicle
v_r is the velocity of rotation

The velocity of rotation is dependent on the total angle of rotation so that

$$v_r = \sqrt{2g\mu s} = \sqrt{2g\mu\left(\frac{WB}{2}\right)\theta} = \sqrt{g\mu WB\theta} \tag{9.275}$$

Thus, the angular velocity of each vehicle becomes

$$\omega_1 = \frac{2v_{r1}}{WB_1} = \sqrt{\frac{4g\mu\theta_1}{WB_1}} \tag{9.276}$$

$$\omega_2 = \frac{2v_{r2}}{WB_2} = \sqrt{\frac{4g\mu\theta_2}{WB_2}} \tag{9.277}$$

where θ is the angle of rotation of the vehicle. As in the previous sections, we assume that there is negligible preimpact rotation. Applying Equation 9.264 to the conservation of rotational momentum equations developed earlier, we obtain

$$(|H|)_{\text{initial}} = (I\omega)_{\text{final}} \tag{9.278}$$

or

$$V_{1i} = \frac{2gI_2}{W_2(x_2 \sin A_{1i} - y_2 \cos A_{1i})}\sqrt{\frac{g\mu\theta_2}{WB_2}} \tag{9.279}$$

and

$$V_{2i} = \frac{2gI_1}{W_1(x_1 \sin A_{2i} - y_1 \cos A_{2i})}\sqrt{\frac{g\mu\theta_1}{WB_1}} \tag{9.280}$$

On a final note, it is sometimes useful to determine the kinetic energy of rotation, which is given by

$$E_{kr} = \frac{1}{2}I\omega^2 \tag{9.281}$$

The power is given by

$$P_r = \Gamma\omega \tag{9.282}$$

The torque vector moment is also related to the vector angular momentum as

$$\Gamma = \frac{d\boldsymbol{H}}{dt} \tag{9.283}$$

Parametric Analysis for Left of Center Collisions

Momentum methods can be used effectively to determine whether a particular vehicle was left of center in a collision where two vehicles approach each other from opposite directions. The following example shows how momentum equations are used by varying certain parameters, in particular, the preimpact angles to determine which vehicle was left of center. Figure 9.43 shows the geometry in a collision involving a dump truck and a Mustang. The Mustang is labeled vehicle 1 and the dump truck is labeled vehicle 2.

In this collision, the exact weight of the dump truck was not known. However, it was determined that it weighed between 22,000 and 24,000 lb. The dump truck was headed east, and the Mustang was headed west. The driver of the dump truck reported that the driver of the Mustang was passing another vehicle heading west and encroached into the eastbound lane. In order to prove that the Mustang was left of center at the point of impact, a parametric analysis was performed varying the weight of the dump truck and the precollision angle of the Mustang. Based on the variability of these parameters, the speeds of the Mustang and of the dump truck were calculated. Table 9.5 show the vehicle speeds as the preimpact angle of the Mustang is varied from 168° to 172°. Note that as the preimpact angle of the Mustang increases toward 180°, the speed of the Mustang becomes unreasonably fast. Since a reasonable speed for the Mustang would be less than approximately 90 mph, the preimpact angle of the Mustang would have to be less than 180° so that the Mustang was, in fact, left of center and attempting to reenter its lane of travel. This example,

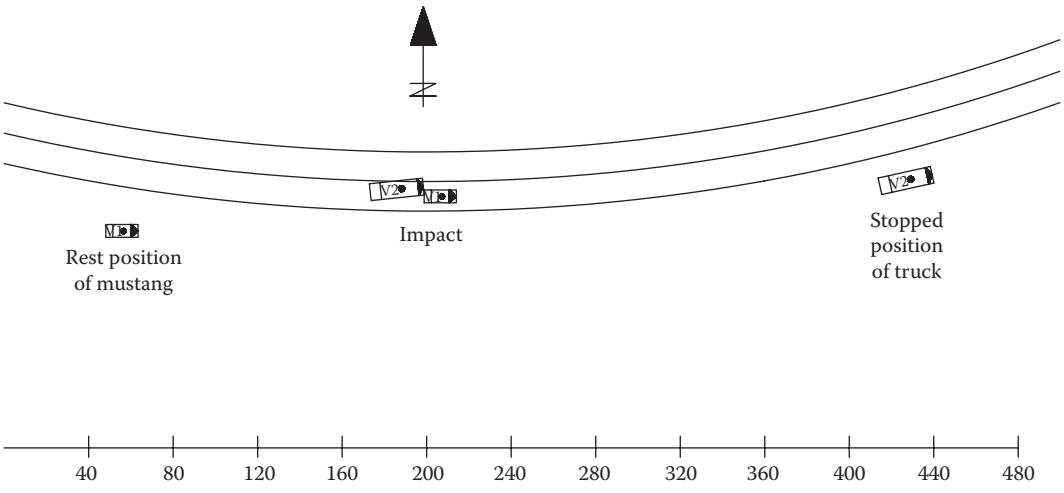

Figure 9.43 Left of center collision.

Table 9.5 Vehicle Speeds: Dependence on Weight of Dump Truck (W_2) and Preimpact Angle of Mustang (A_{1i})

W_2	22,000		23,000		24,000	
A_{1i}	V_{1o}	V_{2o}	V_{1o}	V_{2o}	V_{1o}	V_{2o}
168	59.4	55.8	63.1	56.3	66.8	56.8
169	64.3	56.6	68.2	57.1	72.2	57.6
170	70.0	57.5	74.3	58.0	78.6	58.6
171	76.8	58.6	81.6	59.2	86.3	59.7
172	85.2	60.0	90.5	60.6	95.7	61.1

from an actual case, shows the power of the conservation of momentum techniques. These solutions lend themselves to programming in spreadsheets where the parameters can be varied. By varying the parameters, unknowns can be ascertained through trial and error until a reasonable solution is obtained.

Plastic–Elastic Analysis

This example shows how a reconstruction can take place when the amount of vehicle coupling after the collision is not known. The development is in general terms with no actual values given. Two vehicles collided nearly head-on. A car (V_1) was traveling east and a pickup (V_2) was traveling west when they collided as shown in Figure 9.44. At the accident location, the road is slightly uphill going east at an angle θ.

The force of kinetic friction is given by

$$f = \mu N \tag{9.284}$$

Newton's second law perpendicular and parallel to the incline gives

$$N - Mg\cos\theta = 0 \tag{9.285}$$

$$Mg\sin\theta - f = Ma \tag{9.286}$$

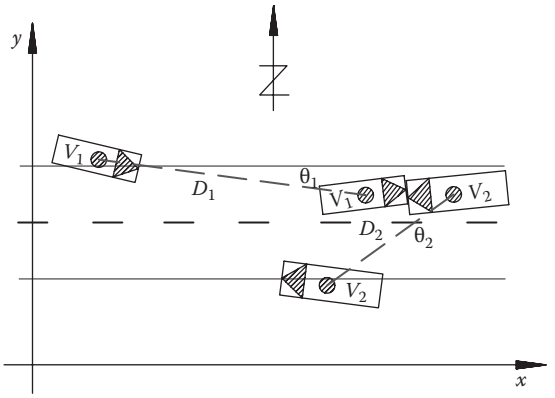

Figure 9.44 Plastic–elastic analysis.

Solving Equations 9.284 through 9.286 yields

$$a = -(\mu \cos\theta - \sin\theta)g \tag{9.287}$$

This shows that the effective coefficient of static friction is

$$\mu_e = \mu \cos\theta - \sin\theta \tag{9.288}$$

The velocities of the vehicles immediately after the collision can be obtained from the stopping distance and the effective coefficient of friction. From basic kinematics, one obtains

$$V_{1f} = \sqrt{2g\mu_{e1}D_1} \tag{9.289}$$

$$V_{2f} = \sqrt{2g\mu_{e2}D_2} \tag{9.290}$$

The inspection of the accident site revealed that the vehicles did not separate immediately. Upon impact the front wheels of the car were locked as a result of frame intrusion into the tires. Thus, the car slid to a stop under the full effect of kinetic friction. On, the other hand, the site inspection indicated that the truck was partially under control of the driver after the collision. Effectively, the full effect of kinetic friction was negated for the truck. Thus, it was considered that the effective coefficient of friction for V_2 was unknown. However, conservation of momentum perpendicular to the road allows us to express the velocity of the truck immediately after the collision in terms of the velocity of the car immediately after the collision. The component of momentum was zero before the collision, hence it must have been zero after the collision. Thus,

$$M_2 V_{2f} \sin\theta_2 = M_1 V_{1f} \sin\theta_1 \tag{9.291}$$

Defining the mass ratio

$$R = \frac{M_1}{M_2} \tag{9.292}$$

we get

$$V_{2f} = R\left(\frac{\sin\theta_1}{\sin\theta_2}\right)V_{1f} \tag{9.293}$$

Now

$$U_1 = V_{2f}\cos\theta_2 + RV_{1f}\cos\theta_1 \tag{9.294}$$

$$U_2 = \sqrt{V_{2f}^2 + RV_{1f}^2} \tag{9.295}$$

Conservation of momentum parallel to the road gives

$$V_{2i} = RV_{1i} + U_1 \tag{9.296}$$

while conservation of energy gives

$$V_{2i}^2 + RV_{1i}^2 = U_2^2 + \frac{2Q}{M_2} \tag{9.297}$$

where Q is the energy absorbed by the collision.

In order to obtain an expression for Q, consider the idealized case of a totally inelastic collision. In such a collision the vehicles move together as a single unit of mass $M_1 + M_2$ with velocity V after the collision. Then,

$$V_{2i} - RV_{1i} = (1+R)V \tag{9.298}$$

$$V_{2i}^2 + RV_{1i}^2 = (1+R)V^2 + \frac{2Q_0}{M_2} \tag{9.299}$$

Solving these equations for Q_0 gives

$$Q_0 = \frac{M_2}{2}\frac{R}{1+R}(V_{2i} + V_{1i})^2 \tag{9.300}$$

The amount of energy absorbed in a particular inelastic collision cannot exceed Q_0; thus,

$$Q = \frac{M_2}{2}\frac{RF}{1+R}(V_{2i} + V_{1i})^2 \tag{9.301}$$

where F is a number between 0 and 1. F represents the coefficient of inelasticity. For a perfectly elastic collision, $F = 0$. For a perfectly inelastic collision, $F = 1$. Substituting the appropriate equations gives

$$V_{1i}^2 + 2\frac{U_1}{1+R}V_{1i} - \frac{U_2^2 - \left(1 - \dfrac{RF}{1+R}\right)U_1^2}{R(1+R)(1-F)} = 0 \tag{9.302}$$

Solving Equation 9.301 for V_{1i} gives

$$V_{1i} = \frac{U_1}{1+R}\left[\sqrt{1 + \frac{(1+R)U_2^2 - (1+R-RF)U_1^2}{R(1-F)U_1^2}} - 1\right] \tag{9.303}$$

In Equation 9.303 the accident site determines the values of U_1 and U_2, so that a solution may be obtained by varying F.

Electrical Incidents and Lightning

10

Introduction

In 1897 various entities developed the original electrical code document. These entities included architects, electrical companies, and the insurance industry. In 1911 the National Fire Protection Association (NFPA) became the sponsor of the National Electrical Code. The code is updated approximately every 3 years to keep up with the state of the art in electrical systems and installations. The purpose of the code is to safeguard persons and property from hazards that may arise from the use of electricity. The national Electrical Code, NFPA 70, falls under the jurisdiction of NFPA 101, the Life and Safety Code, which has been adopted by most of the states in the United States.

The code covers the installation of the electrical conductors, equipment, signaling, and communications equipment and conductors including fiber optic systems for four distinctive areas. These areas are (1) public and private premises; (2) yards, lots, industrial substations; (3) conductors and equipment connected to the supply of electricity; and (4) installations used by the electrical utility. The code does not cover five areas. These are (1) ships, floating buildings, railroads, aircraft, and automobiles; (2) mines and mining machinery; (3) installations for the use of railroads; (4) installations exclusively under the control of communications utilities; and (5) installations under the exclusive use of electrical utilities.

The code distinguishes two groups of electrical voltages. These are voltages below 600 V and above 600 V. The 600 V distinction delineates systems between low voltages and what many consider medium voltages. The code simply does not delineate voltages any further. High voltages are considered those that are under the direct supervision of the electrical utilities and generally are considered above 35,000 V. Voltages below 50 V may be considered very low voltages because they do not pose a significant risk to humans. These classifications by the authors are not strictly set by any group. For example, the International Electrotechnical Commission defines high voltages as 1000 V for alternating current (AC) and 1500 V for direct current (DC). Electrical power transmission systems above 345,000 V is considered as extra high voltage (EHV). It is probably agreed to by most forensic engineering investigators that very low voltages are from 0 to 50 V, low voltages between 50 and 600 V, medium voltages between 600 and 35,000 V, and high voltages above 35,000 V. Additionally it is agreed that low, medium, and high voltages pose a threat to humans and that very low voltages do not. There is no recorded scientific instance of an electrocution below 50 V.

A word of caution is necessary at this point because the simple presence of a high voltage does not mean that there is a risk to humans. Consider the case of static electricity. In the winter under low humidity conditions, exiting an automobile can produce static discharges in the range of 20,000 V. As the occupant slides across the seat and then touches the door exterior, a static discharge is produced that stings but does no harm because the stored current is very low. The duration of the voltage pulse is also very short, in the range

of a microsecond, so that the energy is quite low. The danger to humans comes from the available energy in the source not necessarily the voltage.

Power is defined as the product of voltage and current or

$$p(t) = v(t)\, i(t) \text{ watts} \tag{10.1}$$

where

$i(t)$ is the current measured in amperes
$v(t)$ is the voltage measured in volts

From the work energy principle, the energy available is the area under the power curve or

$$E = \int p(t)dt \text{ joules} \tag{10.2}$$

We need some manner to quantify how much electrical energy is dangerous to humans, that is, what causes serious injury or death. We may use an analogy. Let us say that a human could enter a ring and do battle with a horse. This hypothetical would, of course, be the ultimate in mixed martial arts, and mixed species type of confrontation. The rules would be simple, no weapons or special armor of any type—just the man against the horse. Who would win? The odds would be on the horse for several reasons. The horse weighs about five times the human and has more potent legs with hoofs that can create serious damage. Horses' teeth and mouths are stronger too. Now recall that 1 hp is 745.7 W, for simplicity, 750 W. Now also assume that the horse is somewhat feeble while the man is quite virile, strong, and robust. In that scenario the comparison from horsepower to watts may only be 500 W. Surely, the odds would still be with the horse and that is the basis we may use to determine the amount of power necessary to seriously injure a human. Another analogy is to look at the conversion between horsepower and foot-pounds per second. That value is 550. Two thirds of 550 is 367 ft-lb/s. A moment of 367 lb at a distance of 1 ft can certainly cause serious injury to a human. Figure 10.1 exemplifies the amount of electrical

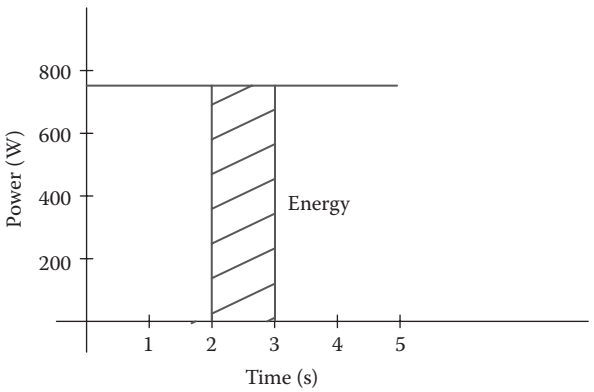

Figure 10.1 Quantity of electrical power that poses a hazard to humans.

energy that poses a distinct hazard to humans. This level of power and energy is not the minimum level required to damage equipment. Some equipment such as computer systems can be damaged by low power requirements while massive electrical systems require extreme energy to cause damage. The danger to humans by electrical energy will be more fully discussed in the next chapter.

Electrical Distribution Systems

Electrical energy is generated in a variety of ways. The power plant, or generating station may be powered by water flow as with a hydroelectric power plant. The primary source of power may be the thermonuclear process derived from the fission of radioactive materials. The other primary sources include the burning of fossil fuels such as coal and gas. Newer sources of energy are being developed and installed including solar and wind power. Whatever the source or type of generating system used, this power must then be distributed over high voltage lines to a substation where the voltages are reduced to distribution levels in a particular area. From there the power is distributed to the customers. Figure 10.2 shows a typical arrangement of the distribution system for AC in the United States. Other countries have systems that are similar but vary in the details. In the United States, AC systems operate at a frequency of 60 cycles per second. Other countries have 50 cycles per second systems. Some distribution systems operate with DC. EHV direct systems are more efficient than AC systems but are more expensive because the generating station voltage must be first converted to DC, transmitted, then reconverted to AC for distribution at the local level.

The electrical energy that is generated by the power plant is three phase. The three-phase voltage has each phase shifted by 120° from reference. This three-phase voltage is then stepped up through a series of transformers to a suitable voltage for the transmission over the high-voltage lines. The voltage of the transmission lines may be between 138 and 765 kV.

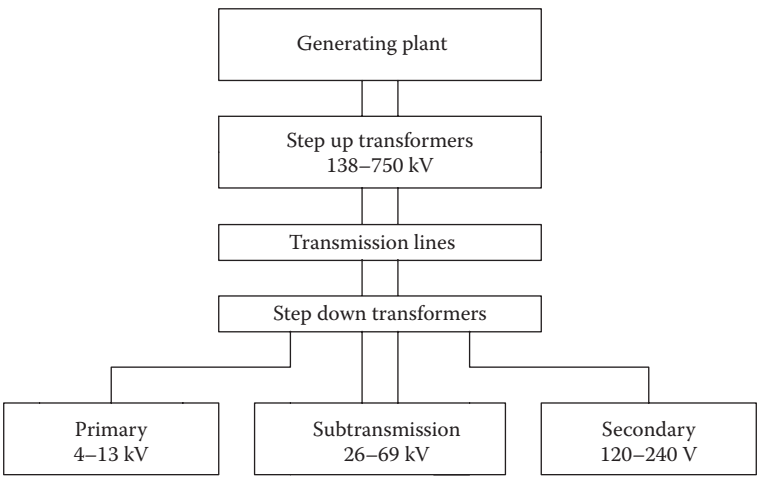

Figure 10.2 Typical arrangement of AC distribution from systems.

A transmission line customer may receive service between 138 and 230 kV. As the system distributes the service, the voltage needs to be stepped down at a substation. A series of transformers again is utilized to accomplish the step down of the voltage. The transformers linking the power plant to the transformers at the substation may be delta or wye connected. Delta transformers do not have a designated ground conductor whereas wye transformers have a common ground in which each phase connects to the others. Delta transformer connections are more economical because of the lack of the fourth conductor between connections. Delta-connected systems are three-wire systems, and wye-connected systems are four-wire systems.

From the substation, a subtransmission customer may receive service varying from 26 to 69 kV. This type of customer would generally be a large industrial complex that requires significant electrical service. The industrial customer would have its own set of transformers to further distribute electricity throughout the plant depending on the particular application. The transformers may be serviced by the electrical utility or they may be serviced by the industrial complex depending on the particular agreements that have been developed. Smaller industrial facilities of commercial establishments are generally referred to as the primary customers. These primary customers may receive service ranging between 4 and 13 kV. The service to primary customers is three phase where the voltages are subdivided by in-house transformers maintained by the customer. Residential customers are provided 120–240 V service from small transformers either mounted on poles or placed on the ground if the electrical lines are buried. One of these transformers may serve more than one home. From the transformer to the meter base, there are three lines. Two of the lines provide 120 V service that are 180° out of phase, and the third line is the grounded conductor. The electrical utility maintains the service up to the meter base. From the meter base to the electrical panel and the further distribution of the system within the home, the responsibility for maintaining the system falls to the customer.

Typically, the forensic electrical engineer may be contacted when a fault occurs from the substation level down. Perhaps a fault arises in one of the substation transformers. Perhaps the fault occurs in the transmission lines or equipment between the substation and the customer or at the transformers supplying the customer. The fault may be produced in the service drop to the customer or may be internal to the customer. The fault may occur during repair or installation activities of equipment or lines and may produce injury or death. In these type of cases, the codes that are of most importance are ANSI/NESC National Electrical Safety Code (C2), ANSI/IEEE C62 Surge Protection, NFPA 70 National Electrical Code, NFPA 70B Recommended Practice for Electrical Equipment Maintenance, NFPA 70E Standard for Electrical Safety Requirements for Employee Workplaces, NFPA 73 Residential Electrical Maintenance Code for One- and Two-Family Dwellings, NFPA 75 Standard for the Protection of Electronic/Data Processing Equipment, NFPA 78 Lightning Protection Code, NFPA 79 Electrical Standard for Electrical Machinery, NFPA 101 Life Safety Code, NFPA 780 Standard for the Installation of Lightning Protection Systems, IEEE 141-1986 Recommended Practice for Electrical Power Distribution for Industrial Plants (IEEE Red Book), IEEE 142-1991 Recommended Practice for Grounding Industrial and Commercial Power Systems (IEEE Green Book), and OSHA 29 CFR General Industry Safety and Heath Standards.

Some Basic Equations

All electrical phenomena can be described by the proper application of Maxwell's equations. These equations are fundamental principles of electricity and magnetism comparable to the equations of the motion of particles and bodies developed by Newton. This section includes the equations and defines all the terms associated with them. The equations are

$$\nabla \times \boldsymbol{E} = -\boldsymbol{M} - \frac{\partial \boldsymbol{B}}{\partial t} \tag{10.3}$$

$$\nabla \times \boldsymbol{H} = \boldsymbol{J} + \frac{\partial \boldsymbol{D}}{\partial t} \tag{10.4}$$

$$\nabla \cdot \boldsymbol{D} = q_e \tag{10.5}$$

$$\nabla \cdot \boldsymbol{B} = q_m \tag{10.6}$$

where

$\boldsymbol{E}$ is the electric field intensity (V/m)
$\boldsymbol{H}$ is the magnetic field intensity (A/m)
$\boldsymbol{D}$ is the electric flux density (C/m^2)
$\boldsymbol{B}$ is the magnetic flux density (Webers/m^2)
$\boldsymbol{M}$ is the impressed magnetic current density (V/m^2)
$\boldsymbol{J}$ is the electric current density (A/m^2)
q_e is the electric charge density (C/m^3)
q_m is the magnetic charge density (Webers/m^3)

The constitutive parameters and relations are given by

$$\boldsymbol{D} = \varepsilon \boldsymbol{E} \tag{10.7}$$

$$\boldsymbol{B} = \mu \boldsymbol{H} \tag{10.8}$$

$$\boldsymbol{J} = \sigma \boldsymbol{E} \tag{10.9}$$

where

ε is the permittivity of the medium (F/m)
ε_o is the free space permittivity = 8.854×10^{-12} (F/m)
μ is the permeability of the medium (H/m)
μ_o is the free space permeability $4\pi \times 10^{-7}$ (H/m)
σ is the conductivity of the medium (S/m)
σ_o is the free space conductivity = 0

By definition the Poynting vector is,

$$\boldsymbol{P} = \boldsymbol{E} \times \boldsymbol{H} \,(\mathrm{W/m^2}) \tag{10.10}$$

The total power exiting a volume V bounded by a surface S is

$$p = \oint_s (\boldsymbol{E} \times \boldsymbol{H}) \cdot ds \tag{10.11}$$

Since, in general, $\boldsymbol{P}$ is complex, the real part represents the real power density and the imaginary part represents the reactive power.

Most tables of permittivity and permeability are expressed in terms of the relative permeabilities and permittivities with respect to free space. These are expressed in equation form as follows:

$$\varepsilon_r = \frac{\varepsilon}{\varepsilon_0} \tag{10.12}$$

$$\mu_r = \frac{\mu}{\mu_0} \tag{10.13}$$

The constitutive parameters for common materials encountered in forensic electrical investigations are summarized in Tables 10.1 through 10.3. The relative permittivity of a material is often referred to as the dielectric constant.

The electrical properties of the materials with respect to their constitutive parameters determine how the field strength, position, orientation, or frequency of operation behaves in the material. If the material is linear, it is not a function of the field strength. The material is homogeneous if the parameters are not functions of position. If the material is isotropic, then the parameters are not functions of orientation of the field. In nondispersive materials, the constitutive parameters are not functions of frequency.

Most of the faults encountered when a piece of equipment fails as a result of an electrical malfunction can be analyzed through the relatively simple application of field theory. Generally what occurs is that excessive current flows as a result of an induced transient such as a switching action or lightning. Alternatively, an insulating material may break down as a result of its degradation in the aging process or through the introduction of a contaminant. Excessive heat can also degrade the properties of a material and thereby cause a fault. Vegetation or humans can come into contact with energized conductors and produce mayhem. Dry wood can have a conductivity of approximately 10^{-15} Seimeus/m but

Table 10.1 Relative Permittivities

Material	Dielectric Constant (ε_r)
Air	1.0006
Paraffin	2.1
Teflon	2.1–2.6
Polystyrene	2.56
Rubber	3.0
Bakelite	4.8
Lead glass	6.0
Flint glass	10.0
Silicon	12.0
Water	81.0

Table 10.2 Conductivities

Material	Conductivity (σ)	Classification
Wax	10^{-17}	Insulator
Paraffin	10^{-15}	Insulator
Rubber	10^{-15}	Insulator
Porcelain	10^{-14}	Insulator
Glass	10^{-12}	Insulator
Bakelite	10^{-9}	Insulator
Silicon	4.4×10^{-4}	Semiconductor
Gallium arsenide	8×10^{-3}	Semiconductor
Animal tissue	0.2–0.7	Semiconductor
Germanium	4	Semiconductor
Carbon	3×10^{4}	Conductor
Iron	10^{6}	Conductor
Steel	2×10^{6}	Conductor
Aluminum	3.96×10^{7}	Conductor
Gold	4.1×10^{7}	Conductor
Copper	5.76×10^{7}	Conductor
Silver	6.1×10^{7}	Conductor

Table 10.3 Relative Permeabilities

Material	Relative Permeability (μ_r)	Classification
Silver	0.99998	Diamagnetic
Lead	0.999983	Diamagnetic
Copper	0.999993	Diamagnetic
Free space	1.0	Nonmagnetic
Air	1.0000004	Paramagnetic
Aluminum	1.00002	Paramagnetic
Steel	2,000	Ferromagnetic
Iron	5,000	Ferromagnetic
Purified iron	200,000	Ferromagnetic

wet saturated wood can become somewhat conductive with a value of 2×10^{-4}. This value of conductivity for a tree under wet, rainy conditions may increase if the rain is acidic as is encountered in many parts of the country.

Let us look more closely at conductors. Most conductors utilized in electrical distribution have either a cylindrical shape as in a wire or a rectangular cross section as with a bus bar. When a free charge q_0 is placed inside of a conductor that is produced by a static electric field, the charge density decays exponentially as a function of the relaxation time and is given by

$$q(t) = q_0 e^{-t/t_r} = q_0 e^{-(\sigma/\varepsilon)t} \tag{10.14}$$

The charge migrates to the surface of the conductor so that most of the current is carried along the conductor on its surface. The greater the surface of the conductor, the greater the current carrying capability of the conductor. This phenomenon explains why stranded conductors can carry more current than solid conductors. The many strands in a stranded

conductor have more surface area than the surface of a solid conductor of equal diameter. The relaxation time constant as seen from Equation 10.14 is

$$t_r = \frac{\varepsilon}{\sigma} \tag{10.15}$$

As an example, we may compute the relaxation time constant of gold as compared to Bakelite. From the tables, note that gold has $\varepsilon = \varepsilon_0$, $\sigma = 4.1 \times 10^7$ which yields $t_r = 2.16 \times 10^{-19}$ s. For Bakelite, $\varepsilon = 4.8\ \varepsilon_0$, $\sigma = 10^{-9}$ and yields a value of 0.0425 s.

According to the laws of conservation of charge or sometimes referred to as the conditions for continuity, the current density and the charge density are related by

$$\nabla \cdot \boldsymbol{J} = \frac{\partial q(t)}{\partial t} \tag{10.16}$$

Switch Failure

As an example, we describe the inspection and analysis of a switch that failed. The allegation was that the switch caused a person to be electrically shocked by applying the plunger on the switch. This analysis is consistent with a phenomenon known as arc tracking which is responsible for a variety of electrical failures. This type of failure can occur between insulated wires, or switches, or electrical relays. It is a common phenomenon when the insulating properties of devices degrade. Mechanical degradation, thermal degradation, corrosive degradation, or environmental pollutants such as water are mainly responsible. Sometimes the age of the device produces the effect.

January 17, 1995 commence tests @ 4:22 pm

Preliminary tests on a representative switch

Identifying marks

P.N. 55899 R.S.P.C.
½ H.P. 15A 125/250 vac
10015-80
9340

Description of device

Push button momentary contact switch
Single pole single throw

Housing made of clear plastic material, cast aluminum front plate and button shank, plastic button, plastic plunger, spring loaded. Terminals and reed leaf appear to be copper or copper alloy. Figure 10.3 shows a diagram of a switch that supposedly failed and produces an electrical shock to an individual.

In order for the aluminum to become energized, a conductive path must be established from either terminal through the plastic housing or from the reed leaf to the plastic button through the plunger. This phenomenon is known as arc tracking or treeing in insulation. Please refer to the reference for a complete explanation of the phenomenon.

When large commercial or industrial electrical switchgear equipment fails, there is a potential for an arc flash event to occur. The short circuit current that is produced will

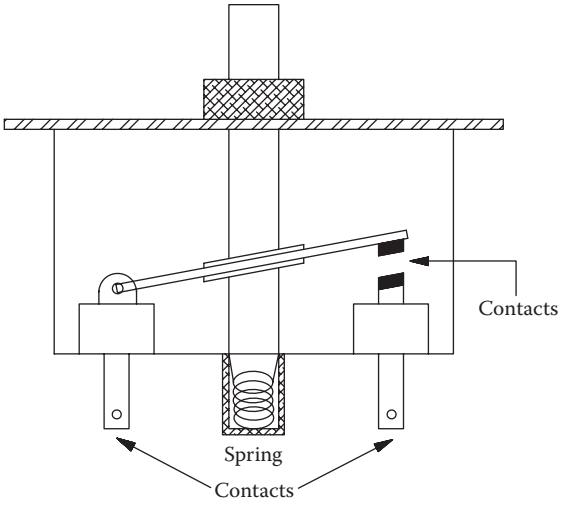

Figure 10.3 Switch diagram.

induce arc temperatures of approximately 10,000° C. The radiant heat generated combined with the expansion of the air is capable of vaporizing the insulating materials and the conductors. The explosive effect of an arc flash event causes damage to equipment and poses a significant danger to personnel. NFPA 70 E provides the requirements for the evaluation of the hazards posed by arc flashes. This type of event is generally restricted to voltages in excess of 600 V encountered in medium voltage applications as described in this chapter. However, arc flashes may also occur in electrical panel boxes at 240 V where the insulation degrades or a worker produces a short circuit in the conductors. The next two sections define the flow of current in typical conductors found in switchgear and electrical panels. These conductors have either circular or rectangular cross sections.

Current in a Bus Bar

This development outlines the flow of current in a bus bar. A bus bar, unlike a solid conductor such as a wire, behaves much like a waveguide where the surface effect of current increases gradually with respect to distance from the center of the bar.

The mathematical development, along with appropriate graphs, is included in this section. A software package called "MathCad" was used to solve for the current "*i*." This development shows that the maximum currents will appear at the surfaces of the bus bar. Consequently, overcurrents in the bus bar will be characterized by dark regions at or near the surface. These overcurrents are also sometimes characterized by beading and melting. The vector notations have been dropped for simplicity.

Defining Basic Equations:

$$\nabla \times E = -\frac{dB}{dt} \quad E = -\frac{dA}{dt} \tag{10.17}$$

where

A is the magnetic vector potential

τ is the resistivity $E = \rho i$

So

$$\rho(\nabla \times i) = -\frac{\partial B}{\partial t}, \quad \rho i = -\frac{dA}{dt} \tag{10.18}$$

Given that μ = permeability

$$\nabla \times B = \mu i, \quad \nabla^2 A = -\mu i \tag{10.19}$$

Now

$$\frac{d}{dt}(\nabla \times B) = \nabla \times \frac{dB}{dt} = \nabla \times (-\nabla \times E) = -(\nabla \times (\nabla \times E)) = -\rho(\nabla \times (\nabla \times i)) = \frac{d\mu i}{dt}$$

Or

$$= -(\nabla \times (\nabla \times i)) = \frac{\mu}{\rho}\frac{di}{dt} \tag{10.20}$$

Vector Identity:

$$-(\nabla \times (\nabla \times i)) = \nabla^2 i - \nabla(\nabla \cdot i)$$

$$\frac{\mu}{\rho}\frac{di}{dt} = \nabla^2 i \tag{10.21}$$

For rectangular coordinates, at 60 Hz, the previous equation becomes

$$\nabla^2 i = j\sigma i \quad \text{where} \quad \sigma = \frac{w\mu}{\rho} \tag{10.22}$$

For copper, σ equals approximately 2.8×10^4 $(\text{ms})^2$

i is a function of X and Y and is defined by

$$i = X(x)Y(y)$$

Now

$$\nabla^2 i = \frac{\partial^2 XY}{\partial x^2} + \frac{\partial^2 XY}{\partial y^2} = j\sigma XY = \frac{1}{X}\frac{\partial^2 X}{\partial x^2} + \frac{1}{Y}\frac{\partial^2 Y}{\partial y^2} = j\sigma \tag{10.23}$$

Let

$$\frac{1}{Y}\frac{d^2 Y}{dy^2} = a^2 \tag{10.24}$$

Then

$$\frac{d^2Y}{dy^2} - a^2Y = 0 \tag{10.25}$$

So

$$Y(y) = A_1e^{ay} + A_2e^{-ay} \tag{10.26}$$

Now solving for X

$$\frac{1}{X}\frac{d^2X}{dx^2} + a^2 = j\sigma \tag{10.27}$$

$$\frac{d^2X}{dx^2} + X(a^2 - j\sigma) = 0 \tag{10.28}$$

Let

$$b^2 = (a^2 - j\sigma) \tag{10.29}$$

Then

$$\frac{d^2X}{dx^2} + b^2X = 0 \tag{10.30}$$

So

$$X(x) = B_1e^{jbx} + B_2e^{-jbx} \tag{10.31}$$

By applying boundary conditions, we may solve for the current distribution.

At the origin, the current is 0 and at the X and Y boundaries, the current is maximum, which for our purposes, shall be defined as 1.

Applying the boundary conditions and solving

$$Y(0) = A_1 + A_2 = 0$$

$$A_1 = -A_2 = A$$

$$Y\left(\frac{h}{2}\right) = A_1e^{ah/2} + A_2e^{-ah/2} = 1$$

$$1 = \frac{-A(e^{-ah/2} - e^{ah/2})2}{2}$$

$$A = \frac{-1}{2\sin h(ah/2)}$$

and a = the distance or $h/2$.

Now solving the X equation

$$X(0) = B_1 + B_2 = 0 \quad B_1 = -B_2 \tag{10.32}$$

$$X\left(\frac{w}{2}\right) = B_1 e^{\frac{jbw}{2}} + B_2 e^{\frac{-jbw}{2}} = 1 \tag{10.33}$$

$$1 = B\left(e^{\frac{jbw}{2}} - e^{\frac{-jbw}{2}}\right)\frac{2j}{2j} \tag{10.34}$$

$$B = \frac{1}{2j\sin\left(\frac{bw}{2}\right)} = -\frac{j}{2\sin\left(\frac{bw}{2}\right)} \tag{10.35}$$

and

$$b^2 = a^2 - j\sigma \tag{10.36}$$

$$|b^2| = (a^4 + \sigma^2)^{1/2} \tag{10.37}$$

$$b = (a^4 + \sigma^2)^{1/4} \tag{10.38}$$

Thus,

$$i = X(x)Y(y) = \frac{j\left(e^{\frac{jwx}{2}} + e^{\frac{-jwx}{2}}\right)\left(e^{\frac{hy}{2}} + e^{\frac{-hy}{2}}\right)}{4\sin\left(\frac{w^2}{4}\right)\sin h\left(\frac{h^2}{4}\right)} \tag{10.39}$$

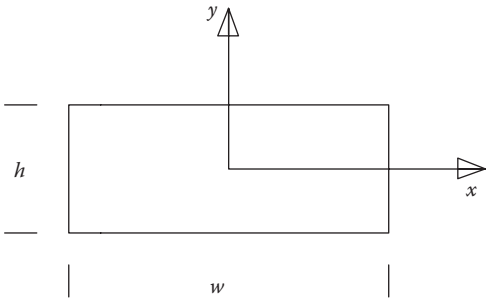

Figure 10.4 Bus bar cross section.

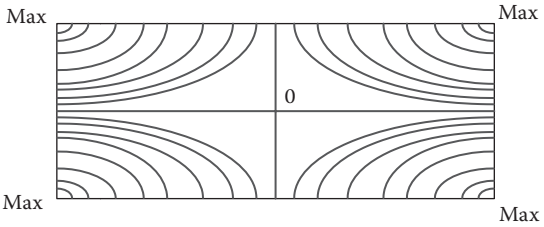

Figure 10.5 Normalized bus bar current distribution.

And breaking it down further

$$i = \frac{\sin h\left(\frac{hy}{2}\right)\sin\left(\frac{wx}{2}\right)}{\sin\left(\frac{w^2}{4}\right)\sin h\left(\frac{h^2}{4}\right)} \tag{10.40}$$

where

$$y = \pm\frac{2}{h}, \quad x = \pm\frac{2}{w} \tag{10.41}$$

Figure 10.4 shows the bus bar cross section. Figure 10.5 shows the magnitude of the normalized current distribution over the cross-section of the bus bar. The maximum current flows at the corners.

Current in a Solid Wire Conductor

When electrical malfunctions occur in circuitry, they are in general due to short circuits between conducting wires or are produced by short circuits between a conductor and ground. Short circuits to ground are generally but not always protected by fuses or circuit breakers. The severity of the short circuit will heat the copper wires to varying degrees. The more severe the short circuit, the more current will flow through the wires. As current increases, the heat buildup will cause arcing and eventually separate

the conductor. This overcurrent phenomenon is characterized by beading of the conductor ends, discoloration of the surface of the wire, and brittleness of the wire near the location of the short circuit.

The beading, due to excessive current in the wire, is produced because current tends to be a surface effect along the outer surface of the wire. In some instances, the evidence of beading, discoloration, and brittleness is lost because the fire, due to external influences, produces temperatures in excess of 1980°F, the melting temperature of copper. Other times, the conductors almost reach melting temperatures and begin the breakdown process but do not fully reach breakdown conditions. A typical scenario for such conditions exists when wires touch each other intermittently causing transient voltages along the transmission path. This section outlines the mathematical development of current distributions across the face of solid cylindrical conductors. The solution for the current in the conductor is best calculated using computer software such as MathCad.

Excessive current in a wire will break down the crystalline structure of the copper near the edges and will be characterized by dark regions. This evidence is more conclusive than beading because it shows the internal failure of the copper conductor. Wires that are not subjected to overcurrents will not exhibit this effect, and their cross-sectional end view will be clear of any breakdown of the crystalline structure of the copper.

In contrast, when electrical wires are subjected to excessive heat from an outside source, no evidence of the earlier phenomenon will be found. These wires will not show any beading of the ends, discoloration of the surface, brittleness of the wires or dark regions near the edges of the cross-sectional area. They will show melting of the copper and the effects of gravity. To solve for the current distribution, we proceed as follows:

i_z = current
E = electric field intensity
A = magnetic vector potential
B = magnetic flux density
μ = permeability
ω = angular frequency
τ = resistivity

$$\nabla \times E = -\frac{dB}{dt} \quad E = \frac{dA}{dt} \tag{10.42}$$

By Ohm's law, $E = \tau i$.

So

$$\tau(\nabla \times i) = -\frac{\delta B}{\delta t} \quad \tau i = -\frac{dA}{dt} \tag{10.43}$$

Given that μ = permeability,

$$\nabla \times B = \mu i \quad \nabla^2 A = -\mu i \tag{10.44}$$

Now

$$\frac{d}{dt}(\nabla \times B) = \nabla \times \frac{dB}{dt} = \nabla \times (-\nabla \times E) = -(\nabla \times (\nabla \times E))$$

$$= -\tau(\nabla \times (\nabla \times i)) = \frac{d}{dt}\mu i \tag{10.45}$$

$$-(\nabla \times (\nabla \times i)) = \frac{\mu}{\tau}\frac{di}{dt} \tag{10.46}$$

Vector Identity:

$$-(\nabla \times (\nabla \times i)) = \nabla^2 i - \nabla(\nabla \cdot i) = \nabla^2 i \tag{10.47a}$$

So

$$\frac{\mu}{\tau}\frac{di}{dt} = \nabla^2 i \tag{10.47b}$$

Figure 10.6 represents a circular conductor.

For $j\omega$ dependence and in cylindrical coordinates, Equation 10.47 becomes

$$j\omega = \frac{\mu}{\tau} i_z = jpi_z = \frac{\delta^2 i_z}{\delta \rho^2} + \frac{1}{\rho}\frac{\delta i_z}{\delta \rho} \tag{10.48}$$

where $p = \omega\mu/\tau$ for copper, $p = 2.8 \times 10^4$ $(\text{ms})^{-2}$. Letting $v = (jp)^{1/2}\rho$, then

$$\frac{\delta i_z}{\delta v^2} + \frac{1}{v}\frac{\delta i_z}{\delta v} i_z = 0 \tag{10.49}$$

This is a modified Bessel's equation of order zero and complex argument whose solutions are

$$i_z = CI_o(v) + DK_o(v) = CI_o[(jp)^{1/2}\rho] + DK_o[(jp)^{1/2}\rho] \tag{10.50}$$

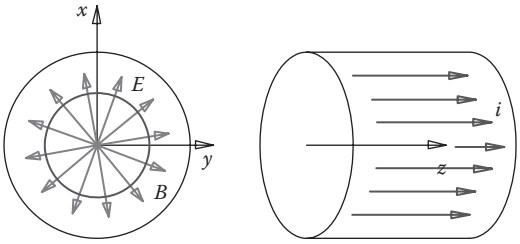

Figure 10.6 Circular conductor.

For a solid conductor, $D = 0$. So $i_z = CI_o(\nu)$ and external radii = a. Applying boundary conditions at

$\rho = 0$, $B = 0$,

$$(\nabla \times i)_{\rho=0}, \quad \frac{\delta i_z}{\delta \rho}\Big|_{\rho=0} = 0 \tag{10.51}$$

at

$$\rho = a, \quad i_z\big|_{\rho=a} = i_0$$

$$i_o = CI_o(v) \Rightarrow C = \frac{i_o}{I_o(v)\big|_{\rho=a}} \tag{10.52}$$

then

$$i_z = \frac{I_o(v)\big|_{i_o}}{I_o(v)\big|_a} = \frac{I_o[(jp)^{1/2}\rho]}{I_o[(jp)^{1/2}a]} i_o \tag{10.53}$$

For numerical computation, since I_o is complex, it must be broken down into its real and imaginary parts, so for argument x,

$$I_o[(j)^{1/2}x] = ber_o(x) + jbei_o(x) \tag{10.54}$$

Using *ber* and *bei* functions and multiplying by $e^{j\omega t}$ and taking the real part, the current density in a solid wire of radius "a" and $i_B = 1$ is

$$i_z = \left(\frac{ber_o^2(p^{1/2}\rho) + bei_o^2(p^{1/2}\rho)}{ber_o^2(p^{1/2}a) + bei_o^2(p^{1/2}\rho)}\right)^{1/2} \cos(\omega t + \alpha) \tag{10.55}$$

$$\alpha = \tan^{-1}\left(\frac{ber_o(p^{1/2}a)bei_o(p^{1/2}\rho) - ber_o(p^{1/2}\rho)bei_o(p^{1/2}a)}{ber_o(p^{1/2}a)ber_o(p^{1/2}\rho) + bei_o(p^{1/2}\rho)bei_o(p^{1/2}a)}\right) \tag{10.56}$$

Subscript "o" denotes the order of I, namely, I_o:

$$ber_o(x) = berx = \sum_{k=0}^{\infty} \frac{(-1)^k x^{4k}}{2^{4k}[(2k)!]^2} \tag{10.57}$$

For simplicity,

$$bei_o[x] = beix = \sum_{k=0}^{\infty} \frac{(-1)^k x^{4k+2}}{2^{4k+2}[(2k+1)!]^2} \tag{10.58}$$

$x = (p^{1/2}\rho)$ and $x = (p^{1/2}a)$ at the surface.

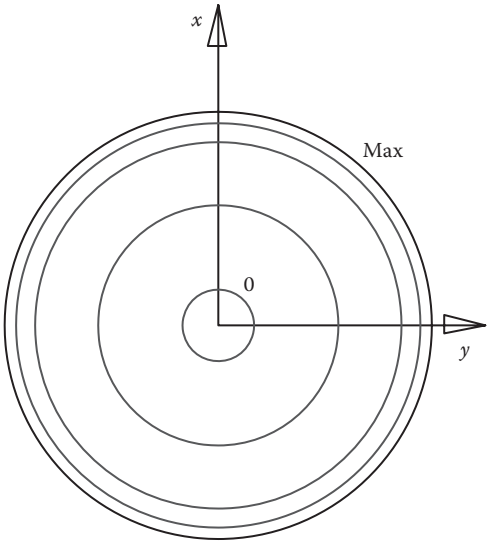

Figure 10.7 Current in a circular conductor.

The magnitude of i_z at $\cos(\omega t + \alpha) = 1$

$$|i_z| = \left(\frac{ber^2(p^{1/2}\rho) + bei^2(p^{1/2}\rho)}{ber^2(p^{1/2}a) + bei^2(p^{1/2}a)} \right)^{1/2} \tag{10.59}$$

at $\rho = 0$, $ber\,(0) = 1$ and $bei\,(0) = 0$ and $|i_z| = 0$ minimum value
at $\rho = a$, $|i_z|$ = maximum value.

Figure 10.7 shows the normalized current distribution.

Testing of Transistors and Electrical Components

In many instances, power transistors can be damaged as a result of electrical faults or overvoltages. The overvoltages may be caused by a variety of factors such as short circuits in different parts of a circuit, by switching transients, or by lightning. Transistors are three-terminal devices that are used in switching or amplifying applications. Discrete transistors have three terminals; the base, the collector, and the emitter. Figure 10.8 shows the two types of discrete transistors and the types of resistances that are expected when taking measurements.

Since the base-to-emitter and collector-to-base junctions of a transistor are pn junctions, these can be checked and identified by resistance measurements with an ordinary ohmmeter. Resistance measured between the collector and emitter should be moderately high, but not necessarily equal, regardless of the direction of the ohmmeter polarity in which it is measured.

Keep in mind that the high- and low-resistance measurements referred to are strictly relative. There is a large variation in the values obtained depending on the power rating and the application of the intended use of the transistor. In general, the ratio of reverse to

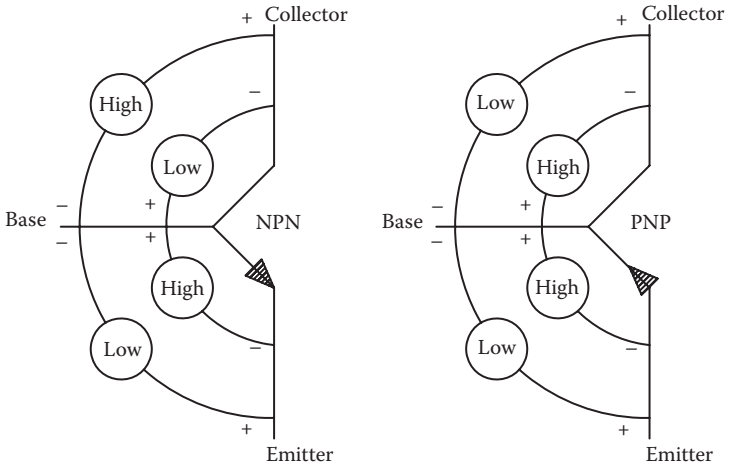

Figure 10.8 Transistor testing.

forward resistance should be at least 30 to one. Since a diode is made from a pn junction, it is the same as the junctions between a base and an emitter or base and a collector in a transistor. Consequently, when forward biased, the transistor has a low resistance and when reverse biased, it has a high resistance.

Integrated circuits pose a different type of problem because of their miniaturization. These circuits perform a variety of functions and operate at reduced voltages in the range of 3–5 V. Discrete devices generally require larger voltages to operate properly. Both discrete and integrated circuits are mounted complex circuit boards so that the evidence that one looks for in the case of a failure is burned or heat damaged components. As a general rule, when investigating failures in electronic circuits, the first place to look is at the power supply. Power supplies always have a transformer so that testing of the transformer is paramount and can also be accomplished with an ohmmeter as described in Figure 10.9.

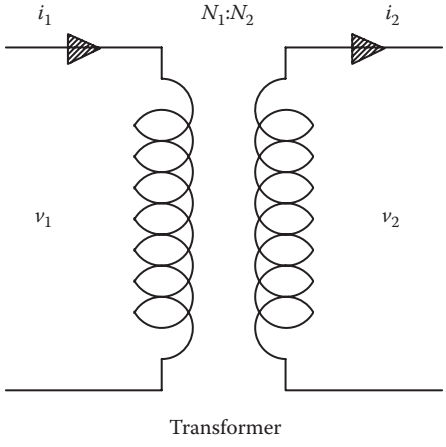

Figure 10.9 Transformer.

Transformers are essentially inductors with a common core. Typically, the core is made of iron to aid in the coupling between the primary and the secondary of the transformer. The basic equation for a transformer is given by

$$L = \frac{\mu N^2 A}{l} \text{henries} \tag{10.60}$$

where

μ is the permeability of the core
N is the number of turns of the windings
A is the cross section of the core
l is the length of the core windings

Since the windings are made of copper wire and the resistance of a copper wire is given by

$$R = \frac{l}{\sigma A_w} \text{ohms} \tag{10.61}$$

where

l is the length of the wire
σ is the conductivity of copper
A_w is the cross-sectional area of the wire

The more windings that are present, the longer the wire of the coils of the inductor, and then the resistance of the coil increases as the windings increase. Therefore, the turns ratio of the transformer may be approximated by simply measuring the resistance of the primary and secondary windings.

For an ideal transformer, the following relationships hold true:

$$\frac{v_1}{v_2} = \frac{N_1}{N_2} \tag{10.62}$$

$$\frac{i_1}{i_2} = \frac{N_2}{N_1} \tag{10.63}$$

Resistance measurements on the primary and secondary windings of the transformer can tell if the device has failed. A partial failure of the insulation of the windings can be determined by the use of a Megger or HighPot tester.

Lightning

Power systems are often subjected to overvoltages whose origins are in atmospheric discharges, in which case they are called external or lightning overvoltages. The magnitude of the external or lightning overvoltages remains essentially independent of the

systems design. Up to approximately 30 kV, the systems insulation has to be designed to withstand lightning surges. High-voltage transmission lines above this value are insulated by distance and generally do not have an insulated covering.

Physical manifestations of lightning have been noted since ancient times, but most of the knowledge concerning the lightning phenomenon has been obtained over the last 50 years. Fundamentally, lightning is a manifestation of a very large electric spark. In an active thunder cloud the larger particles usually possess negative charge and the smaller carriers are positive. Thus, the base of a thunder cloud generally carries a negative charge and the upper part is positive, with the whole being electrically neutral. Typically, the negative charge center may be located anywhere between 500 and 10,000 m aboveground. Lightning discharge is usually initiated at the fringe of a negative charge center. A bolt of negatively induced lightning may readily carry currents in the range of 30–50 kA. This value of current transfers charge in the range of 5 C and may dissipate approximately 500 MJ of energy. Negative lightning strokes last for 10–50 μs. However, as explained in the next section, there may be multiple strokes of negatively induced lightning discharges. In contrast, a positively induced lightning discharge can carry currents of 300–500 kA and transfer charge up to 300 C with a potential difference of 1 GV. Positively induced lightning discharges from the top of the cloud are generally single events that last for hundreds of milliseconds. These positive discharges are much hotter than negative discharges and are capable of greater destruction.

To the eye, a lightning discharge appears as a single luminous discharge although at times branches of variable intensity may be observed which terminate in midair, while the luminous main channel continues in a zigzag path to earth. High-speed photographic techniques reveal that most lightning strokes are followed by multiple strokes that travel along the path established by the first stroke. The stroke is initiated in the region of the negative charge center where the local field intensity approaches ionization (≈30 kV/cm in atmospheric air, or ≈ 10 kV/cm in the presence of water droplets).

During the first stage, the leader discharge, known as the *stepped leader*, moves rapidly downward in steps of 50–100 m and pauses after each step for a few tenths of a microsecond. From the tip of the discharge, a *pilot streamer* having low luminosity and a current of a few amperes propagates into the virgin air with a velocity of about 10^5 m/s. The pilot streamer is followed by the stepped leader with an average velocity of about 5×10^5 m/s and a current of approximately 100 A. A stepped leader from a cloud 3 km aboveground takes about 60 ms to reach the ground. As the leader approaches ground, the potential difference induces a charge in the earth. This charge is augmented by point discharges from earth objects such as tall buildings, trees, etc. At some point, the charge concentration at the earthbound object is high enough to initiate an upward positive streamer. At the instance when the two leaders meet, the *main* or *return* stroke starts from ground to cloud, traveling much faster, approximately 50×10^6 m/s along the previously established ionized channel. The current in the return stroke may approach 250 kA and the temperature within the channel ranges from 15,000°C to 20,000°C and is responsible for the destructive effects of lightning. This effect produces high luminosity and explosive air expansion. The air essentially becomes ionized.

The return stroke is followed by several strokes at 10–300 ms intervals. The leader of the second and subsequent strokes is known as the "dart leader" because of its dart-like appearance. The dart leader follows the path of the first stepped leader with a velocity of about 10 times faster than the stepped leader. The path is usually not branched and is brightly illuminated.

Often, the destructive effect of the return stroke is induced onto the power distribution system of a building. The high currents produce lightning overvoltages in the neighborhood of a million volts. These overvoltages distribute the damage to a building's electrical system in a pattern following terminations and junctures. This damage is usually hidden but may be found through careful observation. When testing electrical systems that are suspected of having been compromised by lightning, the most useful instrument is the HighPot tester. This device will determine the relative dielectric strength of the insulation in the system.

Impulse Voltages

Disturbances of electric power transmission and distribution systems are frequently caused by two kinds of transient voltages whose amplitude may greatly exceed the peak values of the normal a.c. operating voltage. The first kind is lightning overvoltage, originated by lightning strikes hitting the phase wires of overhead lines. The second kind is caused by switching phenomena. Switching phenomena can be created by the actual switching operations in the activations or deactivation of systems or by intermittent touching of conductors when a break in a current carrying line occurs.

A break in a low voltage distribution system (less than 750 V) can create switching transient impulse voltages whose amplitude is related to the operating voltage, and the shape is influenced by the impedance of the system as well as the switching conditions. Although the rate of voltage rise of switching transients is slower than lightning induced transients, these waveforms can be very dangerous to different insulation systems. These switching transients can reach amplitudes of several Kilovolts.

Impulse voltages are defined as unidirectional signals, which rise more or less rapidly to a peak value and then decay relatively slowly to zero. Figure 10.10 illustrates the general

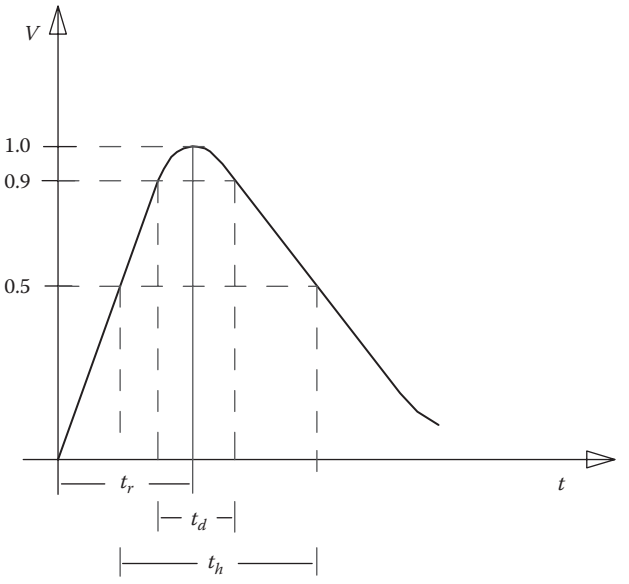

Figure 10.10 Impulse waveform.

shape of a switching induced impulse voltage. Impulse voltage waveforms approximate a unit impulse, commonly known as a Dirac delta function.

The rise time of the waveform t_r including its tolerance is defined as

$$t_r = 250\,\mu s \pm 20\%$$

while the time at 90% of crest value t_d has no exact definition. However, the virtual time to half value t_h is defined as

$$t_h = 2500\,\mu s \pm 60\%$$

According to these definitions, the waveform is described as a 250/2500 impulse. Since these waveforms vary substantially in shape, a general constraint on switching impulses allows them to vary between 100/2500 and 500/2500.

At this juncture it is important to recall the Dirac delta function from mathematics. This function is extremely powerful in analysis and in digital systems. The unit impulse function is defined as a pulse of infinite height and infinitesimal width so that its area is unity. It is represented symbolically in Figure 10.11.

The properties of the unit impulse are summarized as

$$\int_{t_0}^{t_0+1/\varepsilon} \delta(t - t_0)dt = 1 \tag{10.64}$$

For example, for an impulse switching voltage that lasts for 250 μs, according to the definition of the impulse function, its amplitude would be 4000 V. Although the amplitude is not infinite, if this voltage is impressed on the electrical system of a home or office, it can produce significant damage to systems that operate between 120 and 240 V.

When impulse voltages stress the insulation between the conductors, heat is generated within the dielectric. This heat is produced by conduction currents and dielectric losses due to polarization. In general, the conductivity (σ) increases with temperature, and conditions of instability may be reached. This instability is characterized when the rate of heating exceeds the rate of cooling, and the dielectric insulation may undergo thermal breakdown. The situation is illustrated graphically in Figure 10.12, in which the cooling of a dielectric is represented by the straight line and the heating at various voltage levels is represented by the curve.

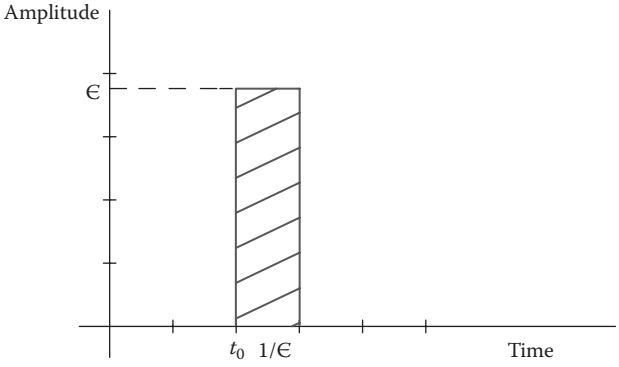

Figure 10.11 Dirac delta function.

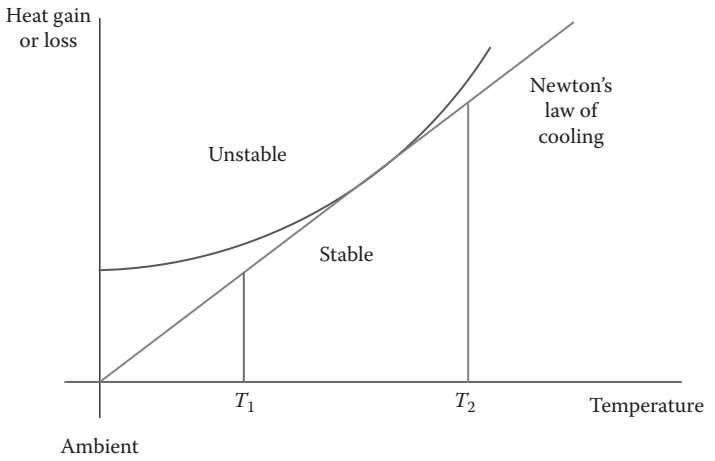

Figure 10.12 Dielectric thermal stability.

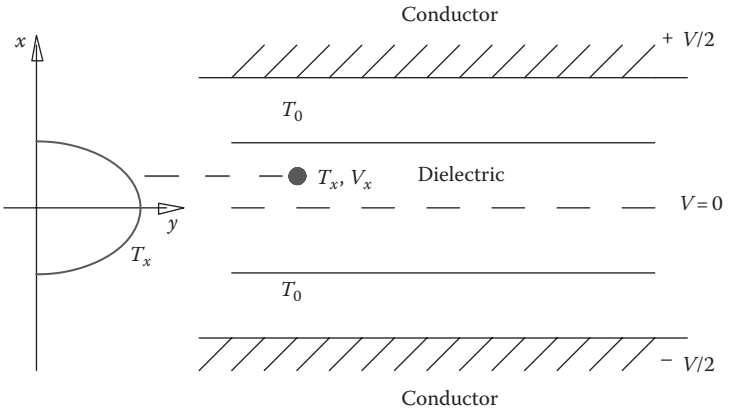

Figure 10.13 Dielectric breakdown.

To obtain equations for thermal breakdown, let us consider a dielectric between two electrodes as shown in Figure 10.13. Conservation of energy requires that heat input must equal heat conducted away plus heat used to raise the temperature T of the dielectric. To calculate the voltage that produces thermal breakdown, consider a point inside the dielectric a distance x from the center. The voltage and temperature are V_x and T_x, respectively. Assuming that all the heat is carried away through the dielectric, Newton's law of cooling states that

$$\sigma E^2 = \frac{d}{dx}\left(K\frac{dT}{dx}\right) \tag{10.65}$$

Using the relations $\sigma E = J$ and $E = -\partial v/\partial x$, we obtain

$$-J\frac{\partial v}{\partial x} = \frac{d}{dx}\left(K\frac{dT}{dx}\right) \tag{10.66}$$

where

K is the thermal conductivity
T is the temperature

$$-J\int_0^{v_x} dv = \int_0^{x} \frac{d}{dx}\left(K\frac{dT}{dx}\right) \tag{10.67}$$

v is the voltage
J is the current density
Integrating to an arbitrary point x in the dielectric

$$-Jv_x = K\frac{dT}{dx} \tag{10.68}$$

Or

$$v_x\sigma\frac{dv}{dx} = K\frac{dT}{dx} \tag{10.69}$$

substituting for $\sigma = \sigma_o\varepsilon^{(-u/kT)}$ and integrating from the center of the dielectric to the electrode

$$\int_0^{\frac{V_c}{2}} v_x dv = \frac{K}{\sigma_o}\int_{T_o}^{T_c} \varepsilon^{\frac{\mu}{kT}} dT \tag{10.70}$$

Or

$$v_c = \sqrt{\frac{8K}{\sigma_o}\int_{T_o}^{T_c} \varepsilon^{\frac{\mu}{kT}} dT} \tag{10.71}$$

Equation 10.71 gives the critical thermal breakdown voltage v_c where

T_o is the ambient temperature
T_c is the critical temperature at which dielectric decomposes
K is the thermal conductivity of the dielectric
σ_o, μ are empirical constants of the dielectric
k is the Boltzmann's constant

The thermal breakdown strength is lower for alternating fields and decreases with increasing frequency. For typical dielectrics, the maximum thermal voltage is between 1 and 5 μV/cm.

Electrocutions 11

Introduction

Electrical energy imposes a very serious hazard to the general public and to workers. For the most part the general public is unaware of the danger posed by electrical energy. Around the home or the office people simply assume that the electrical circuitry including outlets, switches, and light fixtures are safe. In some respects this is true, but in many other instances it is not the case. The National Electrical Code (NEC, NFPA 70) addresses electrical safety regulations for the installation of conductors and equipment in public and private structures. NFPA 70 establishes the provisions for building codes in the United States. In the work environment the Occupational Safety and Health Administration (OSHA) addresses electrical safety in industry. The Code of Federal Regulations (29 CFR) establishes the rules for OSHA.

Most people associate electrocutions with high voltages. However, most electrocutions occur at low voltages between 120 and 240 V. A significant number of electrocutions occur at medium voltages between 600 and 35,000 V. The majority of these electrocutions or injuries occur when humans come into contact with the residential distribution of electricity between the substation and the transformer that provides the service drop to the home or office. Depending on the configuration of the electrical distribution system, these voltages can vary roughly between 2,000 and 13,000 V. These medium-voltage electrocutions and injuries occur when people use ladders or conductive poles. Consequently, the National Electrical Safety Code requires that these distribution lines be at least 22 ft above ground. Insulation of these conductors is provided by a separation of the conductors from normal contact with the public. Workers for the electrical utility, for cable companies, and for telephone companies are susceptible to electrocution from medium voltages because they come in close proximity to the conductors through the course of their work. Most new service drops have insulated conductors into the meter base and therefore do not pose a danger unless the insulation has been degraded. In such an event, the electrocution would be classified as low voltage because the voltage value would not be above 600 V. High-voltage electrocutions with long-distance conductors normally occur with high-voltage workers for the electrical utility. These workers are highly trained and perform their duties under live wire conditions. These conditions require that the worker does not come into contact with a path to ground. Essentially, since no path to ground is established, current does not flow and the worker is protected even though he comes into contact with high voltages. Note that birds often perch on electrified lines at medium and high voltages without consequence. They are protected from injury or electrocution because there is no path to ground and so no current flows through their bodies.

Table 11.1 Effects of Current on Humans

Effect	Men (mA)	Women (mA)
No sensation	0.4	0.3
Perception threshold	1.1	0.7
Mild shock sensation	1.8	1.2
Painful shock	9	6
Let-go threshold	16	10.5
Painful and severe shock	23	15

Electrocution is generally defined as the loss of life resulting from an electrical current passing through the body of a human. In contrast, an electrical shock does not result in death although it may produce extreme damage to human tissue. Microshock refers to cardiac arrhythmia produced by low-intensity current passing through the heart. These low-intensity currents may be produced by higher levels of current produced in an electrocution. Depending on the contact points, electrocutions may distribute the current through different paths. Some of these paths generally pass through the vascular or nervous system because these systems exhibit a lower impedance to electrical current. The term macroshock refers to all other shocks. Moderate 60 Hz current passing through the arms, legs, and chest muscles can produce strong muscle contractions. Current passing through the thorax may contract the respiratory muscles preventing breathing. Current passing through the chest often causes ventricular fibrillation where cardiac output falls to zero. Higher levels of current will produce heating and burns. In electrical accidents where current passes through the body resulting from skin surface contacts, there generally will be some thermal energy injury on the skin contact points. These thermal lesions are produced by arcing at the contact points.

In 1956, Dalziel introduced the term "let-go current" to describe the ability of a human subject to release himself from tetanic muscle contraction produced by alternating current. For 60 Hz current, Dalziel found the average values of let-go current to be 15.87 mA for men and 10.5 mA for women. Table 11.1 illustrates the range of alternating currents at 60 Hz that men and women exhibit according to Dalziel's studies.

The impedance of the human body varies widely between the accepted values of 500 and 5000 Ω. When excited by 120 V, the value of current passing through the body of a human can therefore vary between 24 and 240 mA. These values of current are above the let-go threshold of current as reported by Dalziel and sufficient to cause electrocution. These values of current are also far below most ratings of circuit breakers in 120/240 V systems and will therefore not generally trip a circuit breaker but will produce an electrocution.

Low-Voltage Electrocutions

Low-voltage electrocutions are restricted to voltages less than 600 V that are encountered in residential structures and offices where the current demand is low. Voltages below 50 V RMS are not considered a danger to humans. Home voltages are either 120 or 240 V RMS depending on whether they supply the service to various appliances. What do we mean

when we describe a voltage, or in fact, any value as its RMS equivalent? The voltage in the home is a sinusoidal waveform with a peak value of 170 V at a frequency of 60 Hz or cycles per second. The equation for this voltage waveform is,

$$e(t) = E_p \sin(wt) = 170\sin(2\pi ft) = 170\sin(2\pi 60t) = 170\sin(377t) \tag{11.1}$$

where E_p = 170 is the peak value of the voltage and the frequency is f = 60 Hz. The RMS value of the voltage is defined as the root mean square value and given by the equation

$$E_{RMS} = \sqrt{\frac{1}{T}\int e(t)^2\,dt} = \frac{E_p}{\sqrt{2}} = 120\,\text{V} \tag{11.2}$$

where the period T is the inverse of the frequency f.

If the electrical contact of a low voltage with a human lasts long enough, the current will dissipate throughout the body via the least resistive path. This path is through the aqueous and electrical structures of the human body. These structures are the nervous system and the circulatory system, which of course are connected to the heart. The induced currents produce fibrillation of the heart. This fibrillation is responsible for stopping the heart and producing death unless normal heart rhythms can be reattained. External evidence of the electrocution is generally not found in these instances. There is generally no evidence of burned skin or entry and exit wounds from low-voltage electrocutions.

Swimming Pool Electrocutions

From 1990 to 2004, the U.S. Consumer Product Safety Commission (CPSC) recorded 60 deaths and 50 electrical shock incidents in or around swimming pools owing to defective or improperly installed electrical equipment. In most of these cases, GFCI (ground fault circuit interrupter) devices were not included, and the predominating offending electrical appliances were 120 V AC pool lighting fixtures.

In either the home or industrial environment, the presence of water clearly serves to augment electrical shock and electrocution risk. The risk is produced by the reduction in human contact resistance brought about by improved contact coupling between the victim and the electrical source via the water. The National Institute for Occupational Safety and Health (NIOSH) observes that the presence of moisture from environmental conditions such as standing water, wet clothing, high humidity, or perspiration, increases the possibility of a low-voltage electrocution. However, despite a large amount of literature and research describing shock risk and the water environment, there is still much misconception among electrical engineers regarding the mechanics of shock in damp or water-wet environments.

Typically, the water used in swimming pools, hot tubs, or spas is not ionic fluid and is thus considered a poor conductor. As such, it is not expected to see a substantial current flow between two poles immersed in pool water as the water provides a relatively high-resistance path.

Mathematically, the field produced by a live 120 V AC conductor immersed in a swimming pool is a boundary value problem and is best described through Poisson's equation.

The boundary value problem solution describes the field conditions. This equation is derived from Maxwell's divergence equation. Maxwell's divergence equation in point form is derived by the application of Gauss' law to an infinitesimal volume and is stated as

$$\nabla \cdot \boldsymbol{D} = \rho \tag{11.3}$$

where

$\boldsymbol{D}$ is the flux density (C/m^2)
ρ is the charge density (C/m^3)

Substituting into Equation 11.3 for the electric field intensity $\vec{E}$ and electric potential V, we obtain Poisson's equation:

$$\nabla^2 V = -\frac{\rho}{\varepsilon} \tag{11.4}$$

where ε is the permittivity of the medium (F/m).

In free space, $\rho = 0$ so that Equation 11.4 reduces to Laplaces' equation. The nature of the flow of current through a material determines whether the material is a dielectric, conductor, or semiconductor. In liquids, both positive and negative charges are free to migrate. Generally, the conductivity of a liquid is given by

$$\sigma = \rho_- \mu_- + \rho_+ \mu_+ \, (\Omega/\text{m}) \tag{11.5}$$

where

ρ_- is the density of negatively charged particles (C/m^3)
μ_- is the mobility of negatively charged particles ($m^2/v \cdot s$)
$+$ is the positively charged density and mobility

The first term represents the contribution to the conductivity from negatively charged particles moving opposite to the $\vec{E}$ field and the second term represents the contribution from positively charged particles moving with the $\vec{E}$ field. According to Kraus, water has the following conductivities:

Distilled Water	$\sigma \approx 10^{-4}\,\Omega/\text{m}$	Insulator
Fresh Water	$\sigma \approx 10^{-2}\,\Omega/\text{m}$	Poor Conductor
Sea Water	$\sigma \approx 4\,\Omega/\text{m}$	Conductor

The conductivity of a liquid electrolyte is represented in the Figure 11.1 and explains the movement of charges and the relative direction of the fields with respect to the movements of the charges.

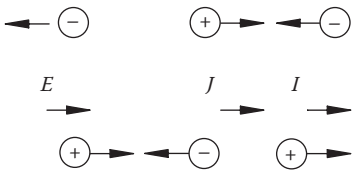

Figure 11.1 Movement of charges.

Swimming pool water has few electrolytes and is therefore at best an insulator or a poor insulator. Measurements of current flow through pool water should not indicate appreciable amounts. GFCIs have a threshold current of 5 mA. Currents above this value are recognized to pose a danger to humans in that they may produce a disruptive effect on the equivalent electric dipole of the heart. This effect can produce death.

The field configuration produced by a live conductor in a swimming pool is dependent on its boundaries. This type of problem may be solved by the application of Poisson's equation, graphically, experimentally, or with an analog or digital computer. Experimental tests were conducted by the authors in a 20 ft by 25 ft swimming pool standardized at neutral pH, requisite chlorine level, and room temperature. A voltage source was supplied by immersion of a two-conductor energized extension cord near the surface at a location near the submersible pool light fixture to simulate a failed and hazardous fixture. A 5 ft by 5 ft rectangular coordinate grid was formed. The grid provides voltages and current measurement distance targets to help explain a field map of the energy distribution in the x–y plane of the pool. A human model was simulated in accordance with IEC 479 and UL data to approximate a nominal human surface area. The model, constructed from a 24-gauge galvanized steel sheet, buoyancy foam, insulators and resistors, was positioned at the various grid nodes while voltage and current measurements were recorded. The findings of the test show that for a substantive shock risk and injury to occur to an immersed human subject, certain physical contact must be made with an energized conductor, regardless of conductor immersion, conductor surface area, or water chemistry, and the water container must present a definite ground.

The voltage measurements along the pool grid were essentially insignificant until the probe was very near the source. Similarly, current measurements were in the microampere range under these conditions. Essentially in this case, the tests indicate that physical contact with the source and grounding of the individual is necessary to produce an electrical shock incident. The electric field produced in a water environment is dependent on the energized surface area, the water chemistry, and the characteristics of the ground. The mathematical development that follows was compared to the physical testing in order to correlate the results.

Theoretical Solution of Poisson's Equation on a Rectangle

$$\nabla^2 V = \frac{\partial^2 V}{\partial x^2} + \frac{\partial^2 V}{\partial y^2} = -K \tag{11.6}$$

The surface of the pool is analyzed as the rectangle in x–y coordinates

V is the voltage on pool surface (V/m)

$$K = \frac{\rho}{\varepsilon} \tag{11.7}$$

ρ is the charge density = 10^{-12} C/m^3 for freshwater

ε is the permittivity of the medium = $80 \times 8.85 \times 10^{-12}$ F/m for freshwater

The charge density can be described as such:

$$\rho = \frac{\sigma}{\mu} \tag{11.8}$$

μ is the mobility of charged particles
σ is the conductivity = 0.01 V/m

Conduction can be varied to depict various sources for freshwater.

Therefore, $K = 0.014$ V/m^2 for freshwater.

Poisson's equation is a nonhomogeneous partial differential equation (PDE) with nonhomogeneous boundary conditions. Therefore, we separate it into

1. Steady-state PDE ($K = 0$) with nonhomogeneous boundary conditions
2. The given PDE ($\nabla^2 V = -K$) with homogenous boundary conditions steady-state PDE

$$\nabla^2 U = \frac{\partial^2 U}{\partial x^2} + \frac{\partial^2 U}{\partial y^2} = 0 \tag{11.9}$$

Boundary conditions:

$$U(x,0) = f(x), \quad U(x,L) = g(x)$$

$$U(0,y) = h(y), \quad U(M,y) = j(y)$$

Figure 11.2 is a 2D diagram of the swimming pool.

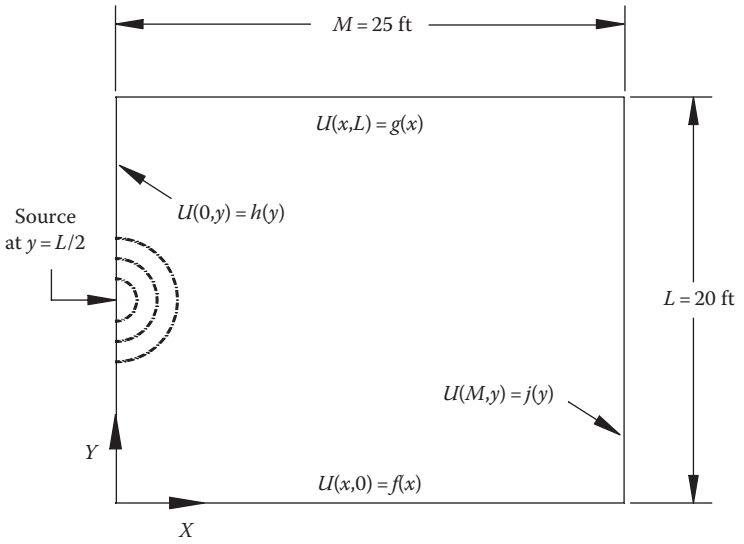

Figure 11.2 Swimming pool.

In this application, the source is along the left boundary ($x = 0$). Therefore, the remaining boundary conditions are set at zero:

$$U(x,0) = 0, \quad U(x,L) = 0$$

$$U(0,y) = h(y), \quad U(M,y) = 0$$

The function $h(y)$ is modeled as a Heaviside, or step, function. ($h(y)$ = 120 V) The width of this function can be varied to depict various sources. By separation of variables and Fourier analysis, the steady-state solution is

$$U(x,y) = \sum \left(\left[c_n \sin h\left(\frac{n\pi x}{L} \right) + d_n \sin h\left(\frac{n\pi(M-x)}{L} \right) \right] \sin\left(\frac{n\pi y}{L} \right) \right) \tag{11.10}$$

The coefficients c_n and d_n are determined by the boundary conditions $h(y)$ and $j(y)$, respectively. The given PDE

$$\nabla^2 W = \frac{\partial^2 W}{\partial x^2} + \frac{\partial^2 W}{\partial y^2} = -K \tag{11.11}$$

Homogeneous boundary conditions:

$$W(x,0) = 0, \quad W(x,L) = 0$$

$$W(0,y) = 0, \quad W(M,y) = 0$$

The "K" value can be considered as a constant across the boundary or as a slowly decaying exponential

$$K = k\left(1 - e^{-\alpha x}\right)\left(1 - e^{-\alpha(M-x)}\right) \tag{11.12}$$

k is a constant (0.014 for freshwater)
α is a constant (10 to ensure no discernable decay)

By separation of variables, the solution $W(x,y)$ is seen as the product of $X(x)$ and $Y(y)$. The functions are determined to satisfy the given PDE and homogeneous boundary conditions. The solution is as follows:

$$W(x,y) = k\left[\frac{1}{\alpha^2}\left(e^{(-\alpha x)} + e^{(-\alpha(M-x))} \right) - \left(1 + e^{(-\alpha M)}\right)\left(\frac{x^2}{2} - \frac{Mx}{2} + \frac{1}{\alpha^2} \right) \right] \tag{11.13}$$

By the principle of superposition, the final solution to Poisson's equation is

$$V(x,y) = U(x,y) + W(x,y) \tag{11.14}$$

This problem was solved in Maple for varying source widths and conductivities. The Maple program and graphical output are as follows: Tables 11.2 through 11.9 outline the theoretical voltages along a line emanating from the source: $V(x, L/2)$. These values represent the maximum estimated voltages and voltage drops across the pool surface.

Table 11.2 Predicted Voltages in the Pool

Coordinate (ft) X	Voltage (V) $V(x, L/2)$	Voltage Drop (V) ΔV
0	3.25	2.85 between 0 and 1 ft
1/4	1.39	
1/2	0.79	
3/4	0.59	
1	0.40	
2	0.23	0.26 between 1 and 5 ft
3	0.17	
4	0.15	
5	0.14	
10	0.12	0.02
15	0.11	0.01
20	0.07	0.04
25	0	0.07

Voltage distribution across center of pool: Conductivity of freshwater ($\sigma = 0.01$ V/m); Width of source, $W = 1/8''$.

Table 11.3 Predicted Voltages in the Pool

Coordinate (ft) X	Voltage (V) $V(x, L/2)$	Voltage Drop (V) ΔV
0	3.25	2.85 between 0 and 1 ft
1/4	1.43	
1/2	0.86	
3/4	0.65	
1	0.40	
2	0.49	−0.32 between 1 and 5 ft
3	0.56	
4	0.64	
5	0.72	
10	1.00	−0.28
15	0.99	0.01
20	0.65	0.34
25	0	0.65

Voltage distribution across center of pool: Conductivity of pool water ($\sigma = 0.1$ V/m); Width of source, $W = 1/8''$.

Table 11.4 Predicted Voltages in the Pool

Coordinate (ft) X	Voltage (V) $V(x, L/2)$	Voltage Drop (V) ΔV
0	25.83	22.66 between 0 and 1 ft
1/4	11.04	
1/2	6.25	
3/4	4.23	
1	3.17	
2	1.60	2.53 between 1 and 5 ft
3	1.07	
4	0.80	
5	0.64	
10	0.31	0.33
15	0.19	0.12
20	0.10	0.09
25	0	0.10

Voltage distribution across center of pool: Conductivity of freshwater ($\sigma = 0.01$ V/m); Width of source, $W = 1''$.

Table 11.5 Predicted Voltages in the Pool

Coordinate (ft) x	Voltage (V) $V(x, L/2)$	Voltage Drop (V) ΔV
0	25.83	
		22.66 between 0 and 1 ft
1/4	11.08	
1/2	6.32	
3/4	4.34	
1	3.17	
2	1.86	1.94 between 1 and 5 ft
3	1.45	
4	1.29	
5	1.23	
10	1.19	0.04
15	1.07	0.08
20	0.68	0.39
25	0	0.68

Voltage distribution across center of pool: Conductivity of pool water ($\sigma = 0.1$ V/m); Width of source, $W = 1''$.

Table 11.6 Predicted Voltages in the Pool

Coordinate (ft) x	Voltage (V) $V(x, L/2)$	Voltage Drop (V) ΔV
0	124.08	105.44 between 0 and 1 ft
1/4	58.76	
1/2	35.23	
3/4	24.52	
1	18.64	
2	9.37	15.13 between 1 and 5 ft
3	6.16	
4	4.52	
5	3.51	
10	1.39	2.12
15	0.65	0.74
20	0.27	0.38
25	0	0.27

Voltage distribution across center of pool: Conductivity of freshwater ($\sigma = 0.01$ V/m); Width of source, $W = 6''$.

Table 11.7 Predicted Voltages in the Pool

Coordinate (ft) x	Voltage (V) $V(x, L/2)$	Voltage Drop (V) ΔV
0	124.08	105.45 between 0 and 1 ft
1/4	58.79	
1/2	35.31	
3/4	24.62	
1	18.63	
2	9.64	14.53 between 1 and 5 ft
3	6.55	
4	5.01	
5	4.10	
10	2.27	1.83
15	1.52	0.75
20	0.86	0.66
25	0	0.86

Voltage distribution across center of pool: Conductivity of pool water ($\sigma = 0.1$ V/m); Width of source, $W = 6''$.

Animal Testing

For obvious reasons, most of the electrical testing performed on biological materials has been conducted on animals. Some studies have been conducted on human tissues. Animal tissues are complex structures made up of many parts. These parts include skin, fat, muscle, bone, tendons and ligaments, blood vessels, organs, fluids, and the nervous system pathways. As with any structure subject to electrical stimulation, the current will flow through

Table 11.8 Predicted Voltages in the Pool

Coordinate (ft) x	Voltage (V) $V(x, L/2)$	Voltage Drop (V) ΔV
0	122.08	18.86 between 0 and 1 ft
1/4	116.03	
1/2	111.58	
3/4	107.37	
1	103.22	
2	87.60	57.03 between 1 and 5 ft
3	73.79	
4	62.03	
5	52.19	
10	22.68	29.51
15	9.93	12.75
20	3.77	6.16
25	0	3.77

Voltage distribution across center of pool: Conductivity of freshwater ($\sigma = 0.01$ V/m); Width of source, $W = 10'$.

Table 11.9 Predicted Voltages in the Pool

Coordinate (ft) x	Voltage (V) $V(x, L/2)$	Voltage Drop (V) ΔV
0	122.08	18.86 between 0 and 1 ft
1/4	116.07	
1/2	111.65	
3/4	107.47	
1	103.22	
2	87.86	50.45 between 1 and 5 ft
3	74.18	
4	62.52	
5	52.77	
10	23.56	29.21
15	10.81	12.75
20	4.35	6.46
25	0	4.35

Voltage distribution across center of pool: Conductivity of pool water ($\sigma = 0.1$ V/m); Width of source, $W = 10'$.

the path of least resistance. The resistance offered by a particular segment of animal tissue is a function of several factors. Some of these factors include the shape and size of the tissue, the temperature, the salinity, and the frequency and strength of the electric field passing though. The many tests that have been conducted by a variety of investigators include resistivity or conductivity values at a variety of frequencies from direct current to microwave frequencies. Table 11.10 is a compilation of average values for the resistivity of various animal structures including humans. These values are over the range of frequencies so that when current calculations are carried out, an appropriate range of values must be included.

Table 11.10 Animal Resistivities

Component	Resistivity (Ω-cm)	Average Resistivity	% of Body Weight
Fluids	30–720	375	7
Muscle	240–1800	1020	40
Organs	100–2100	1100	20
Fat	1100–3500	2300	20
Bone	1800–5000	3400	13

Previously, in this chapter, we stated that human resistance varied from 500 to 5000 Ω. This wide range is generally used because of the difference in the makeup of humans and the path that the current takes when introduced to the human body. In other words, it matters whether the current flows from one hand to the other, from the hand to the foot, or from the head to the chest, as an example. Notice that the resistivity of various components of animals, which includes humans, also varies widely. For a particular human we might approximate the resistance by determining the average value based on Table 11.10. For example,

Bone	Fat	Muscle	Organs	Fluids	Total
(0.13)(3400)	+ (0.2)(2300)	+ (0.4)(1020)	+ (0.2)(1100)	+ (0.07)(375)	= 1556

Other investigators have conducted tests on the resistivity of various human body segments. Some of these segments include the arm, the hand or fingers, the trunk, and the head. All of these resistivities were conducted under direct current conditions. The values obtained ranged from 160 to 840 Ω-cm. In addition, the Commission Electrotechnique International produced a report on the impedance of the human body between different contact areas based as a percentage of the impedance from hand to hand. The impedance values were found to be essentially resistive with a small capacitive reactive component, which can be disregarded for resistance calculations in electrocution cases. Table 11.11 summarizes the percentage impedance from body part to body part.

Table 11.11 Impedances of the Body

Body Part	% Impedance	% Impedance with Both Hands Joined
Hand to hand	100	
Hand to forearm	75	
Hand to biceps	60	
Hand to head	50	30
Hand to neck	40	20
Hand to chest	45	23
Hand to stomach	50	25
Hand to thigh	60	35
Hand to knee	70	45
Hand to calf	75	50
Hand to foot	100	75

Medium-Voltage Electrocutions

In contrast to low-voltage electrocutions or incidents, where there is normally no evidence of entry and exit wounds or burns, medium-voltage incidents are characterized by some physical damage to the skin or the clothing. Additionally, electrical contact with voltages above 600 V may be characterized by strong shock waves that cause the person to be violently thrown. This effect is especially true when contact is made with electrical distribution lines nearing 13,800 V. In low-voltage incidents, the person often is unable to let go of the offending circuitry causing current to pass through the body for extended periods of time. The strength duration time of current passing through the body determines the amount of energy that is expended. Consequently, the longer the duration of the current excitation, the more energy that is expended, and the more damage that is caused.

At higher voltages, the current entering the skin tends to ionize the tissue. Interestingly, it has been reported that the exit wounds are more severe than the entry wounds. In many instances shoes may be blown off the feet as the current pulse exits the body. Many of the victims do not die but are subjected to internal damage to their torsos and organs. In low-voltage electrocutions, the primary cause of death appears to be ventricular fibrillation. In contrast, defibrillation of the heart occurs at much higher voltages in the range of 500–700 V. Medium-voltage incidents tend to damage the musculature, circulatory and nervous systems, as well as the digestive systems of these individuals if they survive.

High-Voltage Electrocutions

Electrical incidents with very high-voltage lines are generally restricted to workers who perform maintenance on these lines. In some rare instances, people have climbed the towers that are used to support these systems and consequently have made contact. The methods employed in this type of work are referred to as live wire because the systems are energized while the work is being performed. According to the National Institute for Occupational Safety and Heath (NIOSH) between 1982 and 1994 approximately 76% of higher voltage incidents involved distribution voltages between 7,200 and 13,800 V. The remaining incidents, approximately 24%, occurred in transmission voltages above 13,800 V. The industry breakdown of the number of the most electrocutions was led by construction, followed by manufacturing, transportation, communications, public utilities, and public administration.

Between 1980 and 1992, worker deaths by electrocution decreased by 23%. The number of electrocution deaths for all people decreased by more than 50%. This difference in the death rate between workers and nonworkers may be attributed to safer devices in the home where most electrocutions occur.

Human Conductivity

The flow of an electrical current through the human body is a complex phenomenon. Electricity flows through the path of least resistance so that in a human body, this path flows through the nervous and circulatory systems. Various studies have been conducted

Table 11.12 Human Conductivity

Conductivity Typical of Human Beings		
Animal fat	Poor insulator	$4 \times 10^{-2}\ \Omega/m$
Animal muscle	Poor conductor	$0.4\ \Omega/m$
Animal blood	Poor conductor	$0.7\ \Omega/m$
Animal body (average)	Poor conductor	$0.2\ \Omega/m$

to determine the conductivity of animals and humans, and the values given in Table 11.12 represent such studies.

The human body is basically cylindrical in shape so that we may determine the resistance path from the equation

$$R = \frac{\ell}{\sigma a}(\text{ohms}) \tag{11.15}$$

where

ℓ is the length of body section (m)
σ is the conductivity of the medium in (Ω/m)
a is the cross-sectional area of body section (m^2)
A typical human arm section is shown in Figure 11.3.

An average human adult has a wrist circumference of 7 in. so that the wrist radius is

$$r = \frac{7\text{ in.}}{2\pi} = 1.114\text{ in.} \tag{11.16}$$

Assuming a variability for the radius of the wrist from

$$1\text{ in.} < r < 1.2\text{ in.} \tag{11.17}$$

We can express this variability of the wrist radius in meters as

$$0.025\text{ m} < r < 0.03\text{ m} \tag{11.18}$$

We can now compute the maximum and minimum area as follows:

$$a_{\min} = \pi r_{\min}^2 = (3.14)(0.025)^2 = 0.00196\text{ m}^2 \tag{11.19}$$

$$a_{\max} = \pi r_{\max}^2 = (3.14)(0.03\text{ m})^2 = 0.00283\text{ m}^2 \tag{11.20}$$

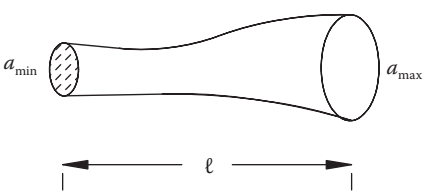

Figure 11.3 Human arm section.

Table 11.13 Body Resistance

R_1 = 2685 ohm
R_2 = 3222 ohm
R_3 = 3877 ohm
R_4 = 4653 ohm

Arm length from the palm of one hand through the torso to the other palm normally varies in humans from 5 to 6 ft. This variation in length in meters is given by

$$1.52\ \text{m} < \ell < 1.824\ \text{m} \tag{11.21}$$

We can now calculate the variation in human resistance by substituting into Equation 11.15 the variabilities in Equations 11.5 through 11.7 and obtain the values as plotted in Table 11.13.

Normal body resistance, therefore, varies as follows for this example:

$$2685\ \Omega < R < 4653\ \Omega \tag{11.22}$$

Using Ohms law and assuming that the supply voltage is 117 V RMS, the current is given by

$$I = \frac{V}{R} \tag{11.23}$$

so that the minimum current is

$$I_{\text{min}} = \frac{117}{4653} = 25\ \text{mA}$$

and the maximum current is

$$I_{\text{max}} = \frac{117}{2685} = 43\,\text{mA}$$

or the variation in the current passing from arm to arm in a typical human when subject to a 117 V shock is

$$25\ \text{mA} < I < 43\ \text{mA} \tag{11.24}$$

These values of the current may be sufficient to cause serious injury or death.

Response of Human Tissue to Electrical Stimulation

In the early 1900's, two researchers described the fundamental law of electrical stimulation to living tissue. Weiss and Lapicque determined that the shorter the duration of the current pulse, the higher current is required to stimulate living tissue. In essence, stimulation is dependent upon the area of the current curve. Figure 11.4 represents the strength duration curve for excitable tissue according to Blair.

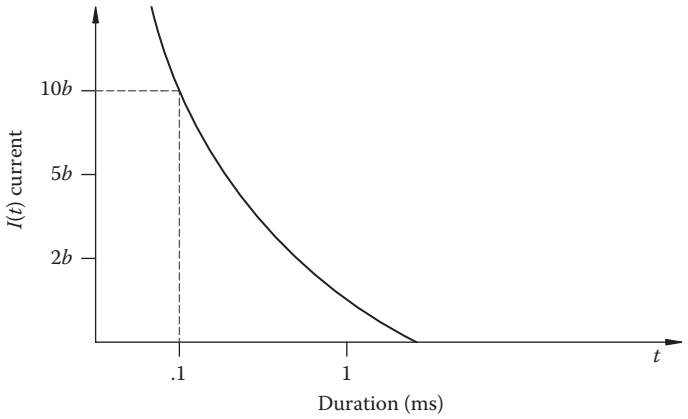

Figure 11.4 Strength duration curve.

Table 11.14 Human Membrane Time Constants

Tissue Type	Time Constant	Temperature (°C)
Motor nerve	0.015	Body
Skin receptors	1.0	Body
Glans penis	0.28	Body
Skin	0.33	Body
Sensory nerve	0.12–0.36	Body
Skeletal muscle	2.0	Body

Based on the resistance and capacitance of cell membranes, the current according to the Blair curve is expressed as

$$I(t) = \frac{b}{1 - e^{-\frac{t}{\tau}}} \tag{11.25}$$

where τ is the membrane time constant. The time constant for different human tissue is shown in Table 11.14.

All excitable cells are surrounded by an ion-permeable membrane, which results in a high concentration of potassium (K^+) ions in the cell and a high concentration of sodium (Na^+) ions outside the cell. The net effect is a transmembrane potential as shown in Figure 11.5.

Dalziel reported the first studies on the threshold for perception to sinusoidal current. Figure 11.6 represents the combined results for the threshold of sensation for various portions of the human body.

Generally, the threshold of sensation is considered to be 5.0 mA for humans. When discussing skin sensation threshold, it is important to note that current density (mA/cm^2) stimulates and that the current threshold will differ for the size of the electrodes. Additionally, different skin sites will have different thresholds. Another important current level as measured by Dalziel is referred to as "let-go" current. Dalziel found that let-go current for men was approximately 15 mA and 10 mA for women. The let-go current is defined as that which a person can tolerate and still release the conductor.

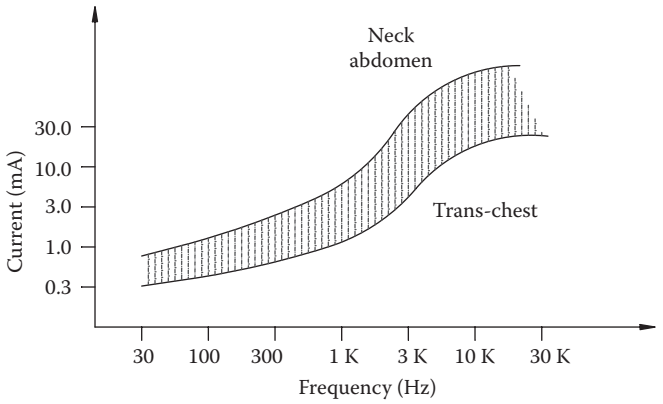

Figure 11.5 Transmembrane potential.

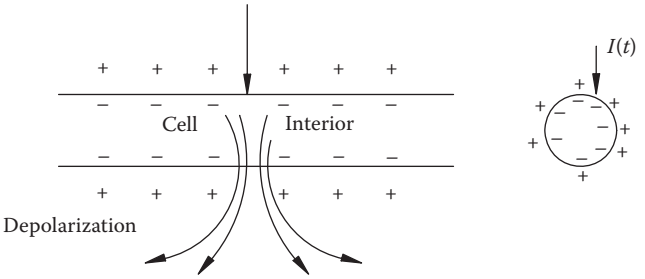

Figure 11.6 Threshold of sensation.

Another important factor in determining the response of human tissue to electrical stimulation is the impedance of the human body. At low commercial frequencies, the body impedance is essentially resistive while at higher frequencies, a capacitive component introduces a nonlinear effect. Dry skin may have a resistance of 100–300 KΩ per square centimeter. When wet, skin may have but 1% of its dry resistance. A value of 500 Ω is commonly used as the minimum resistance of the human body between major extremities. A value of 1500 Ω is used as an average value of human resistance as determined from the examples we have provided.

Electrical Modeling of the Human Body

The various studies that have been performed on humans and animals over the past 100 years have given considerable insight into the response of biological materials to electrical stimuli. It is generally recognized that approximately 50 V is required to produce lasting injury or death to humans. The range of voltages present and available for dissipation throughout the human body ranges from millivolts to near megavolts. Many electronic circuits produce small voltages that are not dangerous to humans. For example, the typical voltages encountered in electronic circuits are approximately 3 V in complementary metal oxide semiconductor (CMOS) circuits and 5 V in transistor–transistor logic (TTL) circuits. Traditional telephone circuits are approximately a few volts and residential doorbell circuits operate at 24 V. There are no reported cases of electrocutions or serious injury at this level

of voltages. Keep in mind that the power supplies to these circuits are normally energized with household circuits at either 120 or 240 V RMS so that the feeders and transformers for the power supplies do pose a significant danger.

The greatest danger posed to humans is at the residential or commercial office level of 120–240 V because of the abundance of circuits at this level of voltages to which humans are exposed. The next level of danger occurs at the industrial level with voltages in the range of 480 V and at the residential distribution level of 1300 V. The least danger and propensity for injury and death occur at higher voltages and most generally involves workers who come into contact with power lines or equipment involved in the transmission and distribution of electrical service.

In all of these cases, it is imperative to quantify the energy available for the injury potential to humans by proper modeling the human body. In many electrical contact cases, the injuries are disputed. The argument made is that the injured person does not show any outward evidence of injury although the electrical contact is not disputed. Sometimes the electrical contact is disputed. Such is the case when a piece of equipment such as a refrigerator is reported to have shocked the individual. Testing of the equipment is imperative in such cases to prove or disprove whether the equipment was faulty. Modeling the human places values of the current that passed though and created the injuries.

Fires 12

Introduction

There are several excellent sources of information relative to the investigation of fires. Most of these sources are associated with the investigation and the determination of the origin and the cause of the fire. DeHann has written *Kirk's Fire Investigations* and is probably one of the best known and most quoted books on fires. Lentini has also written on the subject as well as others. In this chapter we do not attempt to duplicate the investigative techniques that are available in the literature. Rather the focus of this chapter on fires is from a thermodynamic standpoint and the calculations that a forensic engineer may conduct. The first part of the discussion on fires deals with the combustion of the materials in a fire, their decomposition, and the propagation of the fire through the appropriate thermodynamic process.

According to Hilado, the burning process on a microscale can be divided into five separate and distinct stages: (1) heating, (2) transition, (3) degradation, (4) decomposition, and (5) oxidation. The microscale burning process deals with the reactions within a specific polymer and not with the entire material being consumed in a fire. The material being burned is generally made up of different materials that comprise the compound so that the burning process of the material is effectively a macroscale phenomenon. At the macroscale level, the burning process is divided into another set of five stages of combustion. These are (1) heating, (2) decomposition, (3) ignition, (4) combustion, and (5) propagation.

A term often used in the fire sciences is pyrolysis, which is defined as the chemical decomposition of a substance by heat. Pyrolysis is most often referenced when the ignition temperature of a material is lowered as a result of heat. For example, when wood is subject to aging, dryness, and normal ambient heating, it is said that the wood has become pyrolyzed so that its ignition temperature is lowered. The first four stages of the burning process on a microscale can then be considered as pyrolysis. The last stage of oxidation is then the actual burning process. The active principle of burning, characterized by the heat and light of combustion, is defined as the fire. At the macroscale, the heating and decomposition of the material would be considered due to pyrolytic action leading to ignition. Once the material is ignited, combustion takes place. Combustion can only take place if favorable conditions exist to maintain the burning process. Ignition and burning, in a continuous manner, lead to the propagation stage of the fire. The propagation of the fire is exemplified by the transfer and release of heat and light.

Hilado also defines the burning process on a mass scale in terms of five stages. The mass scale of a fire process may involve a piece of equipment, a vehicle, a room or a house, or a large industrial complex. The five stages are (1) initial fire, (2) fire buildup, (3) flashover, (4) fully developed fire, and (5) fire propagation. In this chapter we will not be concerned with the determination of a fire with respect to the different stages in such an extensive classification. Rather we will be concerned with whether the fire had a competent ignition

source, and what the characteristics of the propagation of the fire were, which will be accomplished by analyzing the thermodynamic properties and laws.

In the forensic engineering investigation of fires on a mass scale the initial fire determination is made by calculations as to the probability of a competent ignition source. For example, it is well known that an electrical arc produces sufficient temperatures to ignite some common materials. However, initial ignition of the material may not result in a fire that evolves unless there is sufficient oxygen to continue the burning process. Similarly, as an extreme opposite example, the hot water line in a residence does not produce adequate temperatures to ignite a surrounding wood member. The fire buildup stage is determined by the materials present, their ignition temperatures, their flammability propensity, and their burning properties including the production of smoke. Smoke is important because the constitutive elements of the smoke are themselves flammable and contribute to flashover.

Flashover is restricted to enclosed systems such as a room in a dwelling or a building. Flashover occurs when most of the materials within the compartment reach their ignition temperature at about the same time. This event is characterized by a sudden and sometimes violent engulfment of flames throughout the room. As the initial fire begins to burn, it will generate smoke and other by-products of combustion. As the smoke layer begins to descend and the temperature in the room rises, with sufficient oxygen concentrations, the entire smoke layer can ignite along with the other combustible materials in the room. Flashover can occur in any enclosed compartment including the interior passenger compartment of a vehicle. NFPA 921 defines flashover as

> A transition phase in the development of a compartment fire in which surfaces exposed to thermal radiation reach ignition temperature more or less simultaneously and fire spreads rapidly throughout the space, resulting in full room involvement or total involvement of the compartment or enclosed space.

Extensive testing in room fires has determined that, on average, when a room reaches a temperature of approximately 1200°F, all the items in the room will ignite and flashover will occur.

The final stage of mass burning deals with the propagation of the fire to the fully developed stage where other adjacent or surrounding structures or systems become affected. For example, building codes require that garage spaces in a residence be provided with a 2 hour fire wall. In a basement garage of a house where the exterior walls are made of cementitious block, the ceiling is required to be lined with double inch drywall in order to provide the 2 hour fire wall requirement. In a case where the ceiling in such a garage was lined with one sheet of 5/8 in. drywall, and the fire started in that area and then progressed to the living spaces causing death or loss of property, a case can certainly be made with respect to the adherence of building codes and the failure to follow them. Several parties may be involved including the designer of the home, the builder, and possibly the inspecting agency that approved the construction.

The astute reader will note that there is no mention of outdoor woodland type fires in the introductory discussion of fires in this chapter. We do not mean to discount the importance of woodland, grassland, or forest fires. These fires are extremely destructive and most generally are produced by nature in the form of lightning, or through human intervention whether intentionally or accidentally set. We do not discuss woodland fires because calculations are difficult if not impossible to make for these type of fires in a thermodynamic context. In terms of a forensic engineering context, the spread of the woodland fire can

only be analyzed in general, broad terms with respect to wind, and direction of fire travel. Detailed calculations of heat release may be impossible.

Before we begin the discussion of the thermodynamic properties of fires, it is necessary to introduce a few other definitions relative to fires as found in NFPA 921.

Heat release rate (HRR): The rate at which heat energy is generated by burning. The HRR has the effect and influence on the ambient temperature and the rate at which the fire progresses.

Ignition temperature: *Minimum temperature a substance should attain in order to ignite under specific test conditions.*

The ignition temperature is a measure of the ignitability of the material that is ignited and is produced at the onset of combustion. This ignition temperature for different materials is generally described at atmospheric conditions of pressure and temperature. The conditions at the time of the fire should be determined in order to investigate the appropriate ignition temperature.

Autoignition temperature: The lowest temperature at which a combustible material ignites in air without a spark or flame.

Clearly, from this definition, if the temperature is raised to this point, the material will ignite.

As an example, consider a fire produced by a breach of a refrigerant line in a recreational vehicle (RV). Large class A RVs are often constructed on bus frames that are powered by powerful diesel engines. The exhaust manifolds on diesel engines at engine operating temperatures may reach 900°F–1000°F. A refrigerant for the air-conditioning system for the RV is usually tetrafluoroethane, commonly known as HFC-134A.The Material Safety Data Sheet (MSDS) for this DuPont compound lists the autoignition temperature as 1369°F and states that the material is not flammable in air at temperatures up to 212°F at atmospheric pressures. It further states that mixtures of this refrigerant with high concentrations of air at elevated pressure and/or temperature can become combustible in the presence of an ignition source. The air-conditioning system in vehicles utilizes a compressor mounted on the engine and is usually driven by a belt in order to compress the refrigerant gas back to liquid. The entire system is pressurized where the low-pressure side may be at approximately 50–70 psi and the high-pressure side at approximately 250–300 psi. Recall that atmospheric pressure is approximately 15 psi at sea level so that both the low- and the high-pressure sides of the refrigerant lines are pressurized beyond atmospheric pressure. A calculation or a graph of pressure versus temperature for the refrigerant should be able to answer the question of whether a breach in a refrigerant line striking a 1000° exhaust manifold would ignite and produce a fire. This type of calculation is relatively simple in a thermodynamic context but may not be able to be answered by a fire investigator without engineering training.

Thermodynamic Principles

We begin this discussion with Newton's second law which states that

$$F = ma \tag{12.1}$$

For thermodynamic calculations we usually perform the calculations in the MKS system of units so that the unit of force is the *Newton*, or kg-m/s^2. The unit of energy (work) is

thus the Newton-meter, which is the same as *a joule* or a *watt-second*. However, certain calculations are carried out using units in the English system. The density ρ of a material or substance is its mass (not weight) per unit volume, or

$$\rho = \frac{m}{V}\left(\frac{\text{lb}}{\text{ft}^3}\right)\left(\frac{\text{slugs}}{\text{ft}^3}\right) \tag{12.2}$$

If the mass w is measured in pounds and the volume V in cubic feet, the average density is

$$\rho = \frac{w}{V}\left(\frac{\text{lb}}{\text{ft}^3}\right) \tag{12.3}$$

The specific volume v is the volume of a unit of mass and is the reciprocal of the density, or

$$v = \frac{V}{w} = \frac{1}{\rho}\left(\frac{\text{ft}^3}{\text{lb}}\right) \tag{12.4}$$

The specific weight γ of a substance is the force of gravity on the unit volume usually measured in lb/ft^3. On the surface of the earth the density is equal to the specific weight so that

$$\gamma = \rho \tag{12.5}$$

If gravitational effects are taken into consideration when determining the specific weight relative to the density, then the relationship of Equation 11.5 must be modified to

$$\rho = \left(\frac{g_o}{g}\right)\gamma \quad g_o = \text{standard acceleration of gravity} \tag{12.6}$$

When considering fluid pressure, it may be necessary to take into account the effects of gravity on the fluid. Figure 12.1 represents the analysis of the effects of gravity on pressure for a fluid.

If we sum forces on the element for equilibrium conditions we obtain,

$$(p + dp)A - pA - dF_g = 0 \tag{12.7}$$

$$dp = -\gamma\, dz \tag{12.8}$$

If we know the pressure at h say p_h, which would normally correspond to atmospheric pressure or any other pressure, then integrating Equation 12.8 yields

$$p = p_h + \gamma(h - z) \tag{12.9}$$

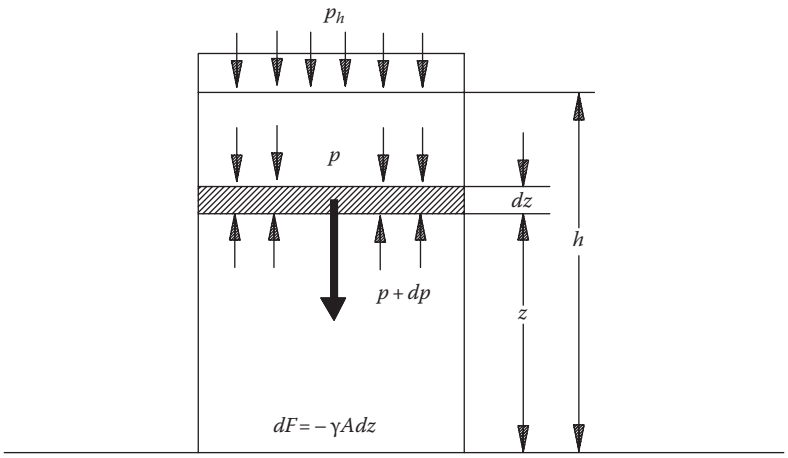

Figure 12.1 Pressure.

In the earlier equations, A represents the area. Normally γ is in units of lb/in.^{3} so that the units of pressure are lb/in.^{2} or psi. A pressure gage determines the pressure of the system above or below atmospheric. Equation 12.9 determines absolute pressure in terms of atmospheric pressure and gage pressure. In the case of a vacuum the plus sign changes to a minus sign. Equation 12.9 also leads to the principle of Archimedes concerning buoyancy. The principle states that an "object, partially or wholly submerged in a fluid, is buoyed by a force equal to the weight of the displaced fluid by the object."

From the earlier discussion, we see that pressure is the force per unit area and it is produced by the rate of change in momentum of the molecules striking the container boundaries of the gas. For a liquid, the effects of gravity must be included. Absolute pressure is defined in terms of atmospheric pressure and the measured pressure of a gage as

$$\text{Absolute Pressure (psia)} = \text{Atmospheric Pressure} \pm \text{Gage Pressure (psig)}$$

The minus sign is used under vacuum conditions. Atmospheric pressure as a standard is 760 mmHg or 29.92 in. Hg at 32°F or 14.696 psia. Temperature is a measure of the average translational kinetic energy of the molecules of the system. As you recall, the temperature of a system may be expressed in terms of various scales. For thermodynamic calculations the absolute temperature scales are used where

$$T°R = t°F + 459.69$$

On the Fahrenheit scale, degrees Rankine (°R) is used, and on the Centigrade scale, Kelvin (°K) is used so that

$$T°K = t°C + 273.16$$

Temperature may be measured in a variety of ways, including a change in volume as with a mercury thermometer, a change in pressure, a change in electrical resistivity, a change

in the electrical potential as with a thermocouple, or optical changes as with an infrared thermometer. For remote measurements, the thermocouple and the infrared systems are the preferred means to measure temperatures especially when testing is conducted.

Systems and Processes

The earlier definitions give the properties of a system. These are the volume, pressure, and temperature. If any of the properties of the system change, we state that the system has undergone a process. If the pressure of a system does not change, the system is *isobaric*. If the volume of the system does not change, the system is *isometric*. If the temperature of the system remains constant, it is an *isothermal* system. Obviously, when dealing with fires we are not concerned with systems that are isothermal but they may be isometric or isobaric. If a system undergoes a series of processes and then returns to its original state, the system has undergone a cycle. In the study of fires, the system, the items being burned, does not return to its original state and thereby does not undergo cycles. However, except in thermonuclear processes, mass is conserved. Thus, in a fire, the chemical reactions taking place stipulate that the mass of the products must be the same as the mass of the reactants. This concept is often utilized when electrical arcing is investigated. Under electrical arcing conditions it is useful to measure the amount of electrical conductive material that has been produced. Calculations can then be performed to determine if the arcing conditions were sufficient to ignite surrounding material and ensure that the fire would progress.

$$\text{Mass In} = \text{Change of Mass of the System} + \text{Mass Out}$$

In equation form, we may state

$$w_i = \Delta w + w_{out} \tag{12.10}$$

If the density and the velocity of a system are approximately the same at all points in a cross section of a system, these conditions may not apply where there exists an abrupt transition such as in an orifice. The abrupt transition generally produces turbulence leading to chaotic behavior of the system. If the system does not undergo a change in mass, then the steady flow continuity equation with $\Delta w = 0$ may be expressed as

$$\frac{dw_i}{dt} = \frac{dw_{out}}{dt} = \rho_1 A_1 v_1 = \rho_2 A_2 v_2 \tag{12.11}$$

Zeroth Law of Thermodynamics

The laws of thermodynamics are observational and based on experience. It has always been observed that a warm body that is brought into contact with a cold body in an isolated environment produces changes in the properties of the two bodies. That is to say

that the volume, pressure, temperature, etc. of the two bodies will change. After sufficient time, these properties will reach an equilibrium state or a steady-state condition. When the steady-state conditions are reached, the bodies are said to be in *thermal equilibrium*. The zeroth law states that "when two bodies are in thermal equilibrium with a third body, they are in thermal equilibrium with each other." It should be noted that thermal equilibrium does not imply chemical equilibrium as with a piece of iron that is corroding so that a chemical reaction is taking place.

Enthalpy

Enthalpy is the measure of the energy content of a system per unit mass. The enthalpy of a medium is the sum of its internal energy per unit weight and the product of its pressure and specific volume, or

$$h = u + \frac{pv}{J} \text{ Btu/lb}$$

This composite property is applicable to all fluids where

h is the enthalpy
p is the pressure
v is the volume
u is the internal energy
J is the Joule's constant = 778.16 ft-lb/Btu

In a combustion reaction such as a fire, heat flows out (exothermic) and the amount of heat is called the heating value or enthalpy of combustion. The heating value of some common fuels is given in the Table 12.1. The values in the table are not exact and for comparative purposes.

Table 12.1 Enthalpy of Combustion

Fuel	Formula	Mol. Weight (Approximate)	Heating Value, h (Btu/lb)	State
Coals			13,100–13,600	Solid
Oak			8,000	Solid
Fuel oil			18,500–19,700	Liquid
Gasoline			18,800–20,200	Liquid
Kerosene			18,500–19,900	Liquid
Methyl alcohol	CH_4O	32	9,000–10,200	Liquid
Ethyl alcohol	C_2H_6O	46	11,900–13,100	Liquid
Acetylene	C_2H_2	26	20,700–21,500	Gas
Hydrogen	H_2	2	51,500–61,000	Gas
Methane	CH_4	16	21,500–23,800	Gas
Natural gas			20,500–23,000	Gas
Propane	C_3H_8	44	19,700–21,600	Gas

Combustion

The burning process involves the combustion of the materials. We may define combustion as the chemical reaction between oxygen and a fuel. Generally combustion is a fast process but the time line can vary widely. As previously explained, the corrosion of a metal in the presence of oxygenated air is a form of a slow combustion. A form of a rapid combustion process is an explosion or a deflagration. In order to gain insight into the combustion processes encountered in fires, some properties of the ideal gas will be discussed.

Boyle's law states that the pressure of a gas expanding at a constant temperature is inversely proportional to the volume. A modification of Equation 12.11 for a constant area yields Boyle's law as

$$p_1 v_1 = p_2 v_2 = \text{constant} \tag{12.12}$$

Charles' law states that the pressure of a gas varies directly with the temperature at a constant volume, and the volume varies directly with the temperature at a constant pressure. In equation form, we state Charles' law as

$$\frac{v_1}{v_2} = \frac{T_1}{T_2} = \frac{p_1}{p_2} \tag{12.13}$$

By combining Boyle's and Charles' laws, we obtain the ideal gas equation of state expressed as

$$pV = nR_o T \tag{12.14}$$

In Equation 12.14, n is the number of pound moles (lb mol) and R_o is the universal gas constant. The quantity of gas expressed in pound mole units is a quantity of gas equivalent to the molecular weight of the gas expressed in pounds. The value of the universal gas constant may be expressed in several units as

$$R_o = 1554.32\,(\text{ft-lb})/(\text{mol-}^\circ\text{R}) = 1.9859\,\text{Btu}/(\text{mol-}^\circ\text{R}) = 2094.73\,\text{J}/(\text{mol-}^\circ\text{R})$$

$$= 8.314 \times 10^7\ \text{ergs}/(\text{gmol-K})$$

Avogadro's law states that equal volumes of all ideal gases at a particular pressure and temperature contain the same number of molecules. The number of molecules in a gmol is 6.0238×10^{23} and is called *Avogadro's number*, N_o.

If we divide, on the molecular level, the gas constant by the number of molecules N_o per mole, we obtain *Boltzmann's constant* k_o:

$$k_o = \frac{R_o}{N_o} = \frac{8.314 \times 10^7}{6.0238 \times 10^{23}} = 1.381 \times 10^{-16}\ \frac{\text{ergs}}{^\circ\text{K-molecule}} \tag{12.15}$$

Table 12.2 gives the values of the gas constant and the molecular weight for some common gases.

Table 12.2 Gas Constants and Molecular Weights of Gases

Gas	Symbol	Molecular Weight, M (lb/mol)	Gas Constant, R (ft-lb)/(lb-°R)
Hydrogen	H_2	2.016	766.54
Helium	He	4.003	386.04
Methane	CH_4	16.042	96.33
Ammonia	NH_3	17.032	90.73
Steam	H_2O	18.016	85.81
Acetylene	C_2H_2	26.036	59.35
Carbon monoxide	CO	28.010	55.170
Nitrogen	N_2	28.016	55.158
Ethylene	C_2H_4	28.052	55.09
Air		28.970	53.342
Ethane	C_2H_6	30.068	51.39
Oxygen	O_2	32.0	48.291
Sulfur	S	32.064	48.194
Argon	A	39.95	38.68
Carbon dioxide	CO_2	44.010	35.117
Propane	C_3H_8	44.094	35.05
n-Butane	C_4H_{10}	58.120	26.59
Sulfur dioxide	SO_2	64.07	24.12
n-Octane	C_8H_{18}	114.224	13.53

Chemical Equations for Combustion

At this point we wish to introduce some basic chemical equations describing the complete combustion of some basic materials. For example, the combustion reaction between 1 mole of solid carbon and 1 mole of oxygen produces 1 mole of carbon dioxide gas and is given by

$$C(s) + O_2(g) \rightarrow CO_2(g) \tag{12.16}$$

One mole of carbon monoxide and 1/2 mole of oxygen produces 1 mole of carbon dioxide:

$$CO(g) + \tfrac{1}{2} O_2(g) \rightarrow CO_2(g) \tag{12.17}$$

One mole of hydrogen and 1/2 mole of oxygen produces 1 mole of water.

$$H_2(g) + \tfrac{1}{2} O_2(g) \rightarrow H_2O(g) \tag{12.18}$$

One mole of sulfur and 1 mole of oxygen combine to produce 1 mole of sulfur dioxide:

$$S(s) + O_2(g) \rightarrow SO_2(g) \tag{12.19}$$

The combustion for the more complex fuels is obtained by combining the four equations shown earlier as will be seen in the examples that follow.

Hydrocarbons

Hydrogen and carbon form hundreds of different compounds. Some of the most important in a forensic engineering investigation of a fire or an explosion include natural gas, gasoline, kerosene, lubricating oils, paraffin, methane, ethylene, and acetylene. Some of the most common hydrocarbons belong to the methane series. Methane constitutes between 90% and 95% of natural gas. Table 12.3 shows some of the most common hydrocarbons in this series. Gasoline is one of the most common accelerants used in incendiary fires. Gasoline is a complex combination of hydrocarbons plus sulfur and other lesser constituents. In order to solve the chemical equation for the combustion of gasoline, the mid-range of hydrocarbons is assumed to be octane. Sulfur and the other constituents are disregarded in the combustion equation which is given by

$$2C_8H_{18} + 25O_2 \rightarrow 18H_2O + 16CO_2 \tag{12.20}$$

Of course, air is the most common source of the oxygen in the majority of fires. In certain fires, oxygen may be a concentrated source as with a cylinder of oxygen in a hospital or a welding facility. The approximate composition of air is as follows:

N_2 = nitrogen = 78.1%
O_2 = oxygen = 20.9%
Argon, carbon dioxide, neon, methane, helium + others = 1%

The power generated in a fire is a measure of the HRR. For a confined space such as a room fire, the HRR is given by

$$\text{HRR(kW)} = 750\, A_o \sqrt{h_o} \tag{12.21}$$

$$\text{HRR(Btu/s)} = 36.5\, A_o \sqrt{h_o} \tag{12.22}$$

Appropriately, the units of Equation 12.21 are meters for h_o and meters squared for A_o. Equation 12.22 is in ft and ft^2. In the earlier equations, A_o represents the ventilation opening and h_o represents the ventilation height. The earlier equations are useful in calculations where fires are determined to be oxygen starved or fuel rich. In both of these cases, fires tend to not produce complete combustion and the fires may die out. These calculations

Table 12.3 Hydrocarbons

Name	Symbol	Boiling Point (°F)
Methane	CH_4	−161.4
Ethane	C_2H_6	−88.3
Propane	C_3H_8	−45.5
Butane	C_4H_{10}	+0.6
Pentane	C_5H_{12}	+36.2
Hexane	C_6H_{14}	+69.0
Heptane	C_7H_{16}	+98.4
Octane	C_8H_{18}	+124.6

are also useful when fire tests are conducted so that the test fires are allowed to proceed to flashover and beyond.

Example 12.1

Enclosures have definite effects on a fire growth. The fire growth rate in the enclosure is determined by the fuel load, the size of the ventilation opening, the volume of the enclosure, the ceiling height, and the location of the fire with respect to the walls and corners. The minimum size of a fire that can cause flashover in a given enclosure is determined by the ventilation provided through the openings. The minimum size fire that causes flashover in a compartment is given by

$$\text{HRR}_{fo}(\text{kW}) = 750\, A_o \sqrt{h_o}$$

where
A_o is the area of opening (m^2)
h_o is the height of the opening (m)

For this fire, there are two openings, the door and the cold air return grill, so that Equation 12.1 must be modified to

$$\text{HRR}_{fo}(\text{kW}) = 750\left(A_g \sqrt{h_g} + A_d \sqrt{h_D}\right)$$

From measurements

$$A_g = .56\ \text{m}^2 \quad h_g = .75\ \text{m}$$

$$A_d = 1.5\ \text{m}^2 \quad h_d = 2\ \text{m}$$

$$\text{HRR}_{fo} = 750\left(.56\sqrt{.75} + 1.5\sqrt{2}\right)$$

$$\boxed{\text{HRR}_{fo} = 1955\,\text{kW}}$$

The fuel load inside the closet is not sufficient to produce flashover unless accelerants are used. The HRR in the closet without accelerants is approximated to be less than 1000 kW. However, a 5 ft^2 pool of gasoline or kerosene (the size of the hole in the floor) would add another 1000 kW of HRR, enabling flashover conditions to exist as was the case in this fire.

Example 12.2

Enclosures have definite effects on a fire growth. The fire growth rate in the enclosure is determined by the fuel load, the size of the ventilation opening, the volume of the enclosure, the ceiling height, and the location of the fire with respect to the walls and corners. The minimum size of fire that can cause flashover in a given enclosure is determined by the ventilation provided through the openings. The minimum size fire that causes flashover in a compartment is given by

$$\text{HRR}_{fo}(\text{kW}) = 750 A_o \sqrt{h_o}$$

where
A_o is the area of opening (m^2)
h_o is the height of the opening (m)

For this fire, there are two openings, the garage door and a window, so that the equation must be modified to

$$\text{HRR}_{fo}(\text{kW}) = 750\left(A_w\sqrt{h_w} + A_d\sqrt{h_d}\right)$$

From measurements

$$A_g = .75\,\text{m}^2 \quad h_g = 2\,\text{m}$$

$$A_d = 6\,\text{m}^2 \quad h_d = 2\,\text{m}$$

$$\text{HRR}_{fo} = 750\left(0.75\sqrt{2} + 6\sqrt{2}\right)$$

$$\boxed{\text{HRR}_{fo} = 7158\,\text{kW}}$$

The fuel load inside the garage is sufficient to produce flashover, consistent with the burning of gasoline.

Table 12.4 is a partial portion of the periodic table of the elements including some of the most common elements and their possible relation encountered in fires. Alkali metals are very active chemically and easily combine with oxygen to readily rust. They react with water with explosive violence and burn vigorously in a chlorine atmosphere. Earth metals also combine with oxygen and chlorine but less violently. As an example we may wish to compute the reaction equation for the combustion equation of 1 mole of ethane C_2H_6. We proceed by multiplying Equation 12.16 by two and Equation 12.18 by three and then adding both equations to obtain

$$C_2H_6 + \frac{7}{2}O_2(g) \rightarrow 2CO_2(g) + 3H_2O(g) \tag{12.23}$$

Table 12.4 Portion of the Periodic Table of Elements

I	II	III	IV	V	VI	VII	O
Hydrogen (1)							Helium (2)
Lithium (7)	Beryllium (9)	Boron (11)	Carbon (12)	Nitrogen (14)	Oxygen (16)	Fluorine (19)	Neon (20)
Metal Alkali	Earth Metal						
Sodium (23)	Magnesium (24)	Aluminum (27)	Silicon (28)	Phosphorus (31)	Sulfur (32)	Chlorine (35)	Argon (40)
Metal Alkali	Earth Metal					*	
Potassium (39)	Calcium (40)						
Metal Alkali	Earth Metal						

In a fire, the oxygen for the combustion reaction comes from the air so that is represented in molar form as

$$O_2 + 3.78N_2 = 4.78Air \tag{12.24}$$

In terms of pounds, we may say

$$1\,\text{lb}\,O_2 + 3.32\,\text{lb}\,N_2 = 4.32\,\text{lb}\,Air \tag{12.25}$$

When performing the theoretical analysis of the products of combustion in a fire, Equation 12.16 should be modified to include the nitrogen in the air. The form of Equation 12.16 is then modified to be

$$C(s) + O_2(g) + 3.78N_2 \rightarrow CO_2(g) + 3.78N_2(g) \tag{12.26}$$

In terms of pounds, we may say

$$1\,\text{lb}\,C(s) + 2.67\,\text{lb}\,O_2(g) + 8.87\,\text{lb}\,N_2(g) \rightarrow 3.67\,\text{lb}\,CO_2(g) + 8.87\,\text{lb}\,N_2(g) \tag{12.27}$$

It should be noted that the nitrogen in Equations 12.26 or 12.27 does not combine chemically.

As another example, let us assume that an incendiary fire is set in a room and we are to determine the weight of the air required for complete combustion. The evidence suggests that approximately 1 lb of gasoline was used and the gasoline was mainly octane. We also wish to determine the volumetric analysis of the products of combustion.

Since octane is C_8H_{18} we see that for 1 lb moles of fuel there are 8 moles of carbon and 9 moles of hydrogen. So we can modify Equations 12.16 and 12.18 as follows,

$$8(C + O_2 \rightarrow CO_2) = 8C + 8O_2 \rightarrow 8CO_2 \tag{12.28}$$

$$9\left(H_2 + \tfrac{1}{2}O_2 \rightarrow H_2O\right) = 9H_2 + 4\tfrac{1}{2}O_2 \rightarrow 9H_2O \tag{12.29}$$

Adding Equations 12.28 and 12.29, we obtain

$$C_8H_{18} + 12\tfrac{1}{2}O_2 \rightarrow 8CO_2 + 9H_2O \tag{12.30}$$

The quantity of air required is obtained from Equation 12.24, so

$$12\tfrac{1}{2}(1\text{ mol }O_2 + 3.78\text{ mol }N_2 = 4.78\text{ mol }air) \tag{12.31}$$

$$12\tfrac{1}{2}\text{ mol }O_2 + 47.25\text{ mol }N_2 = 59.75\,\text{mol }air \tag{12.32}$$

59.75 moles of air are required per mole of octane. The molecular weight of the octane is 114.28 and that of air is 28.97 lb/lb-mole. Then the weight of air required is,

$$\frac{59.75\,\text{mol}\,air}{1\,\text{mol}\,fuel} \times \frac{28.97\,\text{lb/(lb-mol)}}{114\,\text{lb/(lb-mol)}} = 15.18(\text{lb-}air)/(\text{lb-}fuel)$$

The complete reaction is given by

$$C_8H_{18} + 12\,½\,O_2 + 47.25N_2 \rightarrow 8CO_2 + 9H_2O + 47.25N_2 \tag{12.33}$$

At standard atmospheric conditions and temperature, 1 ft^3 of air weighs approximately 0.0807 lb. Therefore, the volume of air required for complete combustion of the fuel is 195.79 ft^3. Assuming that the gasoline was poured in a sealed closet of dimensions $4' \times 4' \times 8'$ or 128 ft^3, the atmosphere in the closet would be fuel rich and would probably extinguish itself for lack of oxygen. Calculations like the one mentioned earlier can determine the amount of air, dependent on the volume of the structure, and whether the fire will proceed or not. For this reason experienced arsonists provide for adequate ventilation of a fire although they may not know the exact science.

Diesel is a common fuel in the automotive industry and sometimes preferred as an accelerant. Diesel consists of approximately 75% saturated and 25% aromatic hydrocarbons that range between $C_{10}H_{20}$ and $C_{15}H_{28}$ with a central value of $C_{12}H_{23}$. The equation for complete combustion of diesel is

$$4C_{12}H_{23} + 71O_2 \rightarrow 48CO_2 + 46H_2O \tag{12.34}$$

Explosive Limits

Explosions are produced when the volume of a gas changes drastically as a result of a chemical reaction or the ignition of the gas within its explosive limits. The greater the volume changes and the more rapidly it does so, the more violent the explosion. When two volumes of hydrogen and one volume of oxygen are mixed to produce two volumes of water vapor, the change in the volume is not very great. However, if we account for the heat evolved, the equation is given by

$$2H_2O + O_2 \rightarrow 2H_2O\,(vapor) + 2 \times 58{,}700\,\text{cal}. \tag{12.35}$$

Charles' law gives the gas expansion of the gas mixture. Even though the specific heats of the gases may be small, the heat of reaction can lead to a considerable expansion of the volume. The equation of the reaction does not indicate whether the explosion will occur. The gas mixture must fall between the explosive limits. Outside the explosive limits, the combination of the gases is too gradual for the explosion to take place. For example, methane will not produce an explosion unless the volume percentage of the methane mixture with air is between 5.5% and 14.5%. Table 12.5 summarizes the lower explosive limits (LELs) and upper explosive limits (UELs) for some common gases as well as other properties.

Flash Points

When fluids evaporate, they may form a sufficient concentration of gas to allow for a combustible mixture. The *flash point* of a liquid chemical is the lowest temperature at which combustion can occur. Table 12.6 shows the flash point and the autoignition temperature for some common compounds.

Table 12.5 Explosive Limits

Gas	LEL% Volume	UEL% Volume	Specific Gravity	Formula	Molecular Weight	Density lbm/ft^3
Air			1.0000		28.9700	0.0807
Alcohols	2.00	36.00	0.7890			
Acetylene	2.50	81.00	0.9000	C_2H_2	26.000	0.0682
Ammonia	15.00	28.00	0.5900	NH_3	17.031	0.0448
Benzene	1.35	6.65	2.6960	C_6H_6	78.110	0.2064
Butane	1.86	8.41	2.0061	C_4H_{10}	58.100	0.1554
Butylene	1.98	9.65	1.9400	C_4H_8	56.110	0.1480[a]
Carbon monoxide	12.00	75.00	0.9667	CO	28.010	0.0727
Ethane	3.00	12.40	1.0378	C_2H_6	30.070	0.0789
Ethylene	2.75	28.6	0.9683	C_2H_4	28.030	0.7860[a]
Fuel oil #1	0.70	5.00	0.8850			
Gasoline	1.40	7.60	0.7200			
Hydrogen	4.00	75.00	0.0696	H_2	2.016	0.0056[a]
Methane	5.00	15.00	0.5537	CH_4	16.043	0.0417
Propane	2.10	10.10	1.5219	C_3H_8	44.090	0.1175
Propylene	2.00	11.10	1.4523	C_3H_6	42.100	0.1091
Toluene	1.27	6.75	3.1082	C_7H_8	92.141	0.2435

[a] At standard temperature and pressure. All other values at normal temperature and pressure.

Table 12.6 Flash Point

Compound	Autoignition Temp. (°F)	Flash Point (°F)
Acetone	869	0
Benzene	1040	12
Ethyl alcohol	689	55
Fuel oils	210–505	100–336
Gasoline	536	−45
Kerosene	563	100–162
Methyl alcohol	725	52
Propane	842	−156
Styrene	914	90
Toluene	849	40
Xylene	867	63
Wood	572	

Transfer of Heat

Heat is the transfer of energy to or from a system by virtue of the temperature difference between the system and its surroundings. In a fire, the main energy that is transferred is in the form of heat. It should be noted that energy in the form of kinetic and potential energy is also transferred by virtue of the disintegration of the surrounding materials. For most fires there is insufficient information to account for those types of energies. Therefore, the most quantifiable form of energy calculation in a fire is that of the heat energy as designated

by the HRR. Heat is positive when it enters a system and negative when it leaves the system. By the work energy principle, in thermodynamic terms, work and heat are the methods of energy transfer in a fire.

The transfer of heat in a fire and the associated work that is developed over the release of the energy constitute the change of energy in the system of a fire. This energy in transition represents the internal energy of the constituents that burned as a result of the fire. We may think of this energy transition in terms of the first law of thermodynamics. A more detailed analysis of the transfer of heat is explained in the section on Thermal Conductivity, Convectivity, and Radiation. For a system such as a fire, the heat that is transferred is mainly by conduction, radiation, or both. Convection simply means the movement of energy from one location to another. In a fire, hot gases are convected to other regions where they may ignite materials. In fact, this process is partially responsible for flashover. Another example of convection is a furnace system in a house where the furnace receives hot air by conduction and radiation. This hot air is then circulated throughout the house releasing the energy again by conduction and radiation. Sometimes, fire investigators mistakenly assume that a fire is produced by warm air from a furnace that ignites material somewhere down the line. Sometimes, they assume that a clothes dryer is capable of producing sufficient heat in the vent to ignite materials. Simple thermodynamic calculations reveal that such events are not possible. Testing of furnaces and clothes dryers validate that such appliances are incapable of producing fires by convection.

First Law of Thermodynamics

Experimental observation reveals that in a system undergoing a cyclic process, the work input and output are proportional to the heat supplied and rejected during the cycle. In equation form we say

$$J\oint \Delta Q = \oint \Delta W \tag{12.36}$$

where

ΔQ represents the change in the heat
ΔW represents the change in the work
the closed integral sign is used to represent the cyclic system
J is Joule's constant and is equal to 778.26 ft-lb/Btu

As a consequence of the first law, for a noncyclic process such as a fire, internal energy exists so that Equation 12.36 is expressed as

$$\int dU = \int dQ - \int dW \tag{12.37}$$

A noncyclic process is also an irreversible process. To further expand on this topic, we introduce another concept of thermodynamics referred to as the second law.

Second Law of Thermodynamics: Entropy

Thermodynamically speaking, we are only concerned with quantities that are measurable. The most common types of measurement of a process are the heat and the work of the process. Again, let us emphasize that fires are irreversible processes. Once combustion takes place, the constituents of the fire release heat and do work. The first law only requires that the energy released in the form of work will equal the difference between the absorbed and rejected energies in the form of heat. The second law is completely independent of the first law and allows us to quantify the amount of energy absorbed as heat and then converted to mechanical work. The second law differentiates between internal energy and mechanical energy. Internal energy deals with the random molecular motion of the system, while the mechanical energy deals with the ordered molecular motion of the irreversible process, which for our purposes is the fire. The second law simply states that no process will result in the absorption of heat, which is converted to mechanical work. The difference between the first and second laws is as follows: The first law does not allow for the creation or destruction of energy, and the second law does not allow for the utilization of energy in a particular manner. Thus, work may be dissipated into heat but heat cannot be entirely converted to work. This observational fact that all natural processes proceed in a one directional manner describes the concept of entropy. The second law of thermodynamics is the law of entropy. Every process in the known universe must follow the law of energy (the first law) and the law of entropy (the second law).

For an irreversible system as shown in Figure 12.2, the temperature versus entropy diagram represents a fire. The heat is Q, the work is W, and T is the temperature.

In accordance with the second law, the entropy may be defined as

$$dS = \frac{dQ}{T} \tag{12.38}$$

The change in entropy is

$$\Delta S = \int \frac{dQ}{T} + \Delta S_p \tag{12.39}$$

where ΔS_p is the entropy production, growth, or irreversibility. The integral in the equation evaluates only the entropy change due to the heat dQ transferred at temperature T.

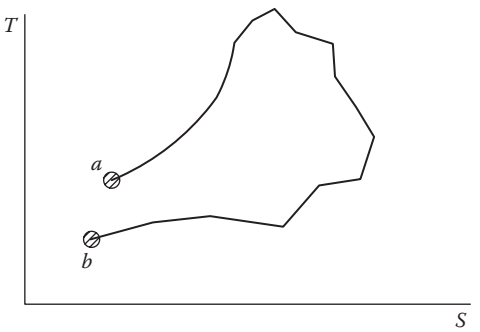

Figure 12.2 Irreversible process.

If we define T_s as the sink temperature of the atmosphere and Q_r as the rejected heat of the system, then E_u is the unavailable energy to do work in the system. Thus,

$$E_u = T_0 \int \frac{dQ}{T} = T_0 \Delta S = T_0 \left(\int \frac{dQ}{T} + \Delta S_p \right) \tag{12.40}$$

The available portion of the heat E_a to do work is then

$$E_a = Q - E_u = Q - T_0 \Delta S \tag{12.41}$$

In an irreversible process, there is an increase in entropy so that we may write

$$\Delta S_{system} + \Delta S_{surroundings} > 0 \tag{12.42}$$

The entropy production S_p is then

$$\Delta S_p = \Delta S_{system} + \Delta S_{source} + \Delta S_{sink} \left(\frac{\text{Btu}}{^\circ\text{R-min}} \right) \tag{12.43}$$

The change in entropy in a fire is due to the flux of heat and the internal irreversibilities of the constituents. The change in entropy is a measure of the amount of energy that becomes unavailable.

Heat Flow

In this section we introduce the notion of heat flow from a mathematical standpoint. Heat may flow via conduction, convection, and radiation. The conduction of heat requires a competent source to allow the transfer of the heat. Generally, a solid object such as a metal will readily conduct heat. Convection of heat requires the transfer of the medium such as in a furnace where air is heated and then moved to another region. This movement is produced by a device such as a blower in the furnace system. Radiant heat is transferred by the emission of the energy from the hot object to its surroundings by electromagnetic waves.

We first begin by discussing the simple one dimensional conduction of heat as shown in Figure 12.3. We assume that one end of the conductor is at a higher temperature than the other end. As the heat is applied, the temperature gradient will proceed to the steady-state condition.

The heat flow per unit time or heat current H is related to the heat flow per unit time as

$$H = \frac{dQ}{d\tau} \tag{12.44}$$

If we know the thermal conductivity of the material k, the heat current may be expressed as

$$H = -kA \frac{dt}{dx} \tag{12.45}$$

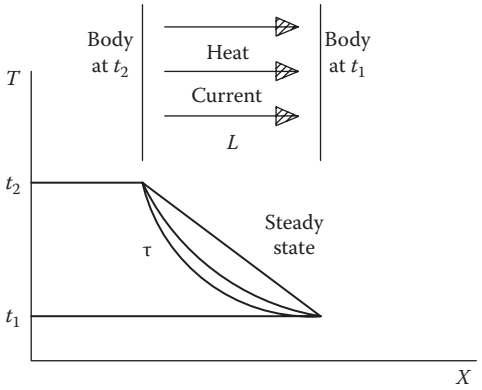

Figure 12.3 Temperature distribution.

where A is the cross-sectional area of the heat flow. Table 12.7 contains the thermal conductivities of common building materials that may be associated with fires. As an example, we wish to determine the propensity of an improperly constructed fireplace to ignite the surrounding wood structure. Figure 12.4 represents the construction of the base of the fireplace. The subbase was constructed with plywood. Over the plywood, cementitious board

Table 12.7 Thermal Conductivities

Material	k Btu/(ft-h°F)
Air	0.01387
Aluminum	144
Asbestos sheet	0.09593
Asphalt	0.4334
Brick/work	0.39875–0.75705
Clay	0.08668–1.444
Concrete	0.2427–0.98243
Copper	231
Cork	0.02543
Cotton wool	0.016759
Earth	0.8668
Fiberglass insulation	0.02774
Fire brick	0.80906
Glass window	0.55478
Granite	0.9824–2.3116
Gypsum board	0.09824
Hardwoods	0.09246
Insulating materials	0.02022–0.09246
Iron	32–46
Marble	1/202–1.699
Plaster	0.1618–0.2774
Plywood	0.07513
Polyurethane foam	0.01558
Rock	1.1558–4.0453
Softwoods	0.06934
Steels	9.24–24.85

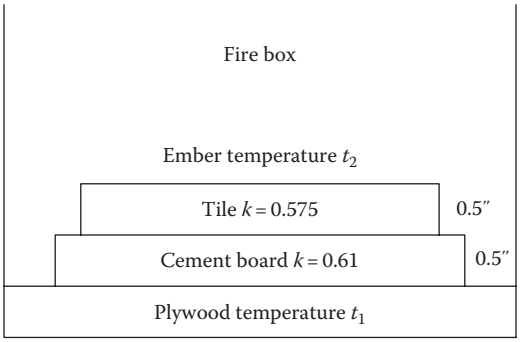

Figure 12.4 Fire box.

was placed so that ceramic tile was used as the base lining of the fire box. This fireplace burned wood on a grill and wood embers would fall upon the base. An inspection of the fire scene revealed that the plywood subbase charred and ignited in the basement below the fireplace. The autoignition temperature of wood is approximately 572°F. Hardwood embers can easily exceed 1000°F. A review of the thermal conductivities in Table 12.7 reveals that cement board has thermal conductivities ranging from 0.24 to 0.98. The median value is 0.61. Similarly, tile, or brickwork has thermal conductivities varying from 0.4 to 0.75 with a median value of 0.575. The basic calculation will be carried out with the median values of thermal conductivities.

Equation 12.45 can be modified to solve for the heat currents through the tile and the cement board as follows:

$$H_1 = \frac{k_1 A(t_2 - t_x)}{L_1} = H_2 = \frac{k_2 A(t_x - t_1)}{L_2} \tag{12.46}$$

Substituting and solving for t_x, we obtain a value of 786°F, which is consistent with the transmission of the heat at the interface between the tile and the cement board. If the fire box had been constructed properly according to code requirements, the lining should have been made of fire brick over the cement board. Fire brick is 2 in. thick instead of tile, which is at most 0.5 in. thick as in the example, and its thermal coefficient is 0.809.

We next turn our attention to heat flow through convection. The transfer of heat through convection requires the motion of the material. In a fire, the convective process is produced by the movement of the surrounding air and the by-products of combustion. The convective process results from the effects of gravity and the temperature gradients that are produced by the fire. These materials along with the heated air will increase the temperature of the surrounding walls, ceilings, floors, and contents of the enclosure. As previously mentioned, when the surroundings reach the critical temperature of approximately 1200°F, flashover occurs. At that temperature most of the materials reach their autoignition temperature and do not require direct flame impingement to burn. The heat transferred through convection per unit area is described by Newton's law of cooling and is given by

$$\frac{dT}{dt} = -k(T - T_a) \tag{12.47}$$

where
T is the temperature
T_a is the ambient temperature
t is the time
k is the convective heat transfer coefficient

We may then say

$$\frac{dT}{(T-T_a)} = -kdt \tag{12.48}$$

Integrating, we obtain

$$\ln(T-T_a) = -kt + C \tag{12.49}$$

To evaluate the constant C, we ascribe T_0 as the temperature at time $t = 0$ so that

$$T = T_a + (T_0 - T_a)\varepsilon^{-kt} \tag{12.50}$$

For air k = 1.0–1.4 Btu/(ft²-h°F).

Explosive Characteristics

Finely divided solid material (dusts and fines), when dispersed in air, can fuel particularly violent and destructive explosions. Dust explosions occur in a variety of materials such as grain dusts and sawdust, coal and charcoal, and a variety of chemicals. Since the combustion reaction takes place at the surface of the dust particle, the rates of pressure rise generated by combustion are largely dependent on the surface area of the dispersed dust particles. For a given mass of dust material, the total surface area, and consequently the violence of the explosion, increase as particle size decreases. In general, an explosion hazard concentration of combustible dusts can exist when the particles are 420 microns or less in diameter. As with ignitable vapors and gases, there are minimum explosive concentrations of specific dusts required for a propagating combustion reaction to occur. Minimum concentrations can vary from 0.015 to 2.0 oz/ft³ with the most common concentrations being less than 1.0 oz/ft³.

Turbulence within the dust air mixture greatly increases the rate of combustion. The shape and size of the confining vessel can have a profound effect on the severity of the explosion by affecting the nature of the turbulence. Generally, increasing the moisture content of the dust particles increases the minimum energy required for ignition. Above the limiting values of moisture, suspensions of the dust will not ignite. Dust explosions have been ignited by open flames, smoking materials, light bulb filaments, welding and cutting, electric arcs, static electric discharges, friction sparks, heated surfaces, and spontaneous heating. Ignition temperatures for most materials range

from 600°F to 1100°F. Layered dusts generally have lower ignition temperatures than the same dusts suspended in air.

Dust explosions are chemical combustion explosions that are labeled propagation reactions because they occur progressively throughout the reactant (fuel) with a definable flame front separating the reacted and unreacted fuel. Dust explosions are generally characterized as low order and are not seated. In general, explosive velocities must exceed the speed of sound (detonations) to produce seated explosions. Nonseated explosions occur most often when the fuels are dispersed or diffused at the time of the explosion because the rates of pressure rise are moderate and the explosive velocities are subsonic (deflagrations).

The nature of the vessel within which the deflagration occurs has a significant effect on its characteristics. The geometry of large length (L) to diameter (D) ratios promotes rapid acceleration of flames. Turbulence producing devices such as valves, elbows, and other obstacles create turbulence that may generate sudden flame acceleration and a consequent rapid increase in pressure. Ignition of a combustible mixture such as dust in a vessel to which a pipe or duct is attached results in a flame front that generates considerable turbulence ahead of itself and precompresses the gas in the pipe or duct. When the flame front reaches the pipe or duct, it is fully developed and turbulent. The result is a flame front that propagates into the pipe or duct with much greater initial violence than that which would result from spark ignition in the pipe or duct, itself.

An explosion is a physical reaction characterized by a high-pressure gas, which is confined or restricted in pressure. The pressure is then released so that damage to the confining structure occurs. The effects of the explosion produce a blast pressure wave effect characterized by two distinct phases. The positive pressure phase is developed as the expanding gases are moving away from the epicenter. This phase is generally more powerful and is responsible for the majority of the pressure damage. The negative pressure phase is created because the expanding wavefront displaces, compresses, and heats the surrounding air, creating a low air pressure area near the epicenter. When this positive pressure wavefront dissipates, the surrounding air mass returns toward the epicenter to reinstate air pressure equilibrium.

Combustion explosions release heat and gases that may ignite nearby combustible materials. Nonseated explosions occur most often when the fuels are dispersed or diffused at the time of the explosion because the rates of pressure rise are moderate, and the explosive velocities are subsonic. The damage caused by the blast pressure wave is dependent on the energy generated and the rate of pressure rise. Low rates of pressure produce pushing or bulging damage effects seen in low-pressure explosions.

Low-order explosions are the result of slow rates of pressure rise and are characterized by relatively large pieces of debris thrown for short distances. Explosions that occur in mixtures at or near the LEL or UEL of a gas or vapor produce low-order explosions. Explosions of mixtures near the LEL do not tend to produce large quantities of postexplosion fire, as nearly all the available fuel is consumed. In contrast, explosions of mixtures near the UEL tend to produce postexplosion fires because of the rich fuel mixture. The delayed combustion of the remaining fuel produces the postexplosion fire. Often a mixture that is near the UEL has fuel that does not burn until it is mixed with air during the explosion's negative pressure phase, thereby producing the characteristic following fire.

The liquid propane (LP) gas mixture in this case was 50% propane and 50% butane. The combustion properties of these fuels are given in the following table:

Fuel	Btu/ft³	LEL%	UEL%	Specific Gravity	Air Needed to Burn 1 ft³	Ignition Temp (°F)
Propane	2516	2.15	9.6	1.52	24.0	920–1120
Butane	3300	1.90	8.5	2.00	31.0	900–1000

The dimensions of the well house were 12 × 12 × 8 so that its volume was 1152 ft³. The damage to the structure and the subsequent fire that ensued indicate that this low-order explosion occurred near the UEL.

This combination LP gas then has an average explosive limit of

$$\mathrm{UEL}_{av} = \frac{9.6 + 8.5}{2} = 9.05\%\ \text{by volume of air}$$

The air needed to burn 1 ft³ of gas averages

$$Vaa = \frac{24 + 31}{2} = 27.5\,\mathrm{ft}^3$$

The gas mixture at the UEL by volume is

$$(9.05\%)(1152\,\mathrm{ft}^3) = 104.2\,\mathrm{ft}^3$$

However, the actual concentration of fuel to air mixture for the given volumetric conditions is

$$\frac{Vaa}{1152} = \frac{27.5}{1152} = 2.38\%$$

which is above the LEL average of 2.025.

The average energy release is then

$$E_{av} = \left(\frac{2516 + 3300}{2}\right)(27.5) = 79{,}970\,\mathrm{BTU}$$

The HRR per second is therefore

$$\mathrm{HRR} = (79{,}970\,\mathrm{BTU})(37.2) = 2975\,\mathrm{kW}$$

$$\mathrm{HRR} \approx 3\,\mathrm{MW}$$

$$v_2 \approx v_1 = \frac{RT_1}{P_1} \tag{12.51}$$

Heavier than air gas explosions are nearly always characterized by low-order explosions and often by postexplosion fires.

In conclusion, this explosion is characterized as

1. Nonseated
2. Low order
3. Combustion
4. Caused by a heavier than air gas mixture
5. Resulted in a fire

Flow of Gas through a Pipe

The flow of a gas or a compressible fluid presents greater difficulty in analyzing than an incompressible fluid. The flow through a reduction in pipe sizes creates the Venturi effect, which can be analyzed as follows:

$$V_2 = \left[\frac{2gRT_1}{1 - \left(\frac{D_2}{D_1} \right)^4} \left(\frac{P_1 - P_2}{P_1} \right) \right]^{1/2} \tag{12.52}$$

Here, V_2 is the velocity of flow through the pipe reduction (or nozzle). The specific volume of a gas is determined by rearranging the ideal gas law.

These equations will be used to determine the validity of claims associated with a natural gas explosion. In this example, we wish to compute the amount of free-flowing gas discharged into a room through an open valve. This scenario involves a garage apartment being renovated by its owner. In the process of its renovation, a new gas meter was being installed. The employee of the gas company was installing the meter outside of the home. As such, the gas company employee was responsible for ensuring that there would be no accidental discharge of gas into the home. As such, it was his duty to close off all valves and ensure that no gas appliances were activated inside the home. This action is verified by pressure testing the system in order to ensure that the system holds pressure (no leaks occur) for a specified time according to the National Gas Code.

When the meter was installed, natural gas was introduced into the pipes within the home. At some later point in time, the owner walked from the meter location to the garage apartment. Inside a bedroom closet, a valve was mounted near the ceiling. The gas company employee had failed to ensure that this valve was closed prior to introducing gas into the system. Upon entering the bedroom, the owner turned on the light switch, which produced an arc. Due to the accumulation of gas within the apartment, this arc ignited the gas, resulting in an explosion.

Representatives of the gas company argued that the owner turned on the main valve at the gas meter, and was thus responsible for causing the explosion. An analysis utilizing these equations disproves this claim. For this example, various assumptions are made, which are outlined in the following.

Assumptions:

1. Outside line diameter, $D_1 = 1.5$ in.
2. Inside line diameter, $D_2 = 0.5$ in.
3. Regulator pressure = 7 oz ÷ 16 oz/lb = 0.4375 psig
4. Room temperature, $T_a = 70°F = 530°R$
5. Barometric pressure = 30.05 in. Hg = 14.74 psia
6. Temperature of gas flowing through the pipe, $T_1 = 60°F = 520°R$
7. When the pressure drop is small, the coefficient of discharge of the orifice is approximately unity. Assume $R_d = 0.98$.
8. Pressure drop caused by pipes: Venturi effect = $P_1 - P_2 = 11.4$ in. Hg.
9. Gas constant, $R = 53.3$ ft-lb/lb-°R

Problem statement

Calculate the amount of free-flowing gas into the room, measured in cubic feet per minute (cfm).

Solution

The atmospheric pressure is known to be 14.74 psia, or roughly 408 in. H_2O. The absolute pressure is given by the summation of the atmospheric (or barometric) and gauge pressures:

$$P_1 = P_a - P_g = 14.74 + 0.4375 = 15.1775 \text{ psia}$$

For small pressure drops, the flow through the specific volume is as follows:

$$v_2 \approx v_1 = \frac{RT_1}{P_1} = \frac{(53.3)(520)}{(15.1775)(144)} = 12.68 \frac{\text{ft}^3}{\text{lb}}$$

As stated in our assumptions, the pressure difference $(P_1 - P_2)$ is assumed to be 11.4 in. Hg, or approximately 0.411 psi. Thus, the velocity of gas through the orifice is given by

$$V_2 = \left[\frac{2gRT_1}{1 - \left(\frac{D_2}{D_1} \right)^4} \left(\frac{P_1 - P_2}{P_1} \right) \right]^{1/2} = \left[\frac{(2)(32.2)(53.3)(520)(0.411)}{\left[1 - \left(\frac{0.5}{1.5} \right)^4 \right] (15.1775)} \right]^{1/2} = 221 \frac{\text{ft}}{\text{s}}$$

Having computed the speed (V_2) at the throat, with corrections for initial speed, the mass flow (ω') can be determined from the following:

$$\omega' = n_d \omega = \frac{n_d A_2 V_2}{v_2} \left[\frac{\text{lb}}{\text{s}} \right] \tag{12.53}$$

Given our prior calculations of specific volume and flow speed, as well as assumptions of discharge coefficient and pipe diameter, the mass flow is computed to be

$$\omega' = \frac{(0.98)(\pi/4)(0.5^2)(221)}{(144)(12.68)} = 0.0233 \text{ lb/s}$$

The volumetric flow rate of gas is therefore

$$V_g' = \frac{\omega' R T_a}{P_1} = \frac{(0.0233)(60)(53.3)(530)}{(15.1775)(144)} = 18 \text{ cfm}$$

In other words, 18 ft^3 of gas would be released each minute.

The median walking speed of humans is around 4.0 ft/s, or about 240 ft/min. The distance traveled from the meter base to the bedroom was approximately 240 ft. Thus, it would have taken the owner approximately 1 min to travel to the bedroom.

Once the main valve was turned on, the new service line from the meter to the house would have been full of air. This air must be displaced before any gas is released into the room. We will assume that the service line is approximately 100 ft in length at an inside diameter of 1.5 in. The volume of that service line is thus

$$V_s = \frac{\pi D_2^2 L}{4} = \frac{\pi(1.5)^2(100)}{(4)(144)} = 1.23 \text{ CF}$$

Given the flow rate of gas discharging through the nozzle, the time to discharge the air in the service line is

$$t_d = \frac{V_S}{V_g'} = \frac{(1.23)(60)}{18} = 4 \text{ s}$$

Under this scenario, if we assume that the attic access hole in the closet is open, the escaping gas reaches the explosive range in the attic between 2.5 and 5 s. In order to reach the explosive limit where the wall switch was located, again assuming that the attic access is open, it would take about twice as long. Thus, 5–10 s would have had to have elapsed between the time the gas company employee turned on the main valve at the meter to the time the owner turned on the light switch in the bedroom closet.

Thermal Conductivity, Convectivity, and Radiation

As previously noted, heat may flow via three modes: conduction, convection, and radiation. In this section we wish to describe the governing equations and concepts for these three modes of thermal heat flux. This section discusses in mathematical terms the modes by which heat is transferred. We have already seen an introduction to conduction in planar flow of heat. Here we will expand on conduction and introduce convection and radiation

for typical geometries. Fourier's equation relates the conduction of heat in terms of planar unidirectional flow from observation as

$$Q_c = -kA\frac{dt}{dL} \tag{12.54}$$

where

Q_c is the rate of heat conduction normal to the surface in Btu/h
A is the surface area in ft^2
dL is the wall thickness in ft
dt is the temperature drop in °F
k is the thermal conductivity in [Btu/(ft-h°F)]

This equation may also be applied to the transfer of heat from fluid to fluid as when the fire inside a room produces the heating effect on an adjacent room through the walls. The astute reader will realize the analogy between heat flow and current flow in an electrical system.

The three common geometries encountered in the flow of heat are rectangular as in buildings, cylindrical as in pipes, and spherical as in heat expansion in free space. Each of these geometries will be addressed independently. First consider a rectangular geometry as shown in Figure 12.5. This geometry may represent the conduction of heat through a wall. We neglect the heat flow in the y-direction. This type of analysis would be suitable for conductive heat flow through wall, floors, ceilings, or roofs in a building. Solving Equation 12.54, we obtain in general terms for the heat flow through medium a

$$Q\int_0^a dL = -k_a A\int_{t_a}^{t_b} dt \tag{12.55}$$

or

$$Q = \frac{k_a A(t_a - t_b)}{a} \tag{12.56}$$

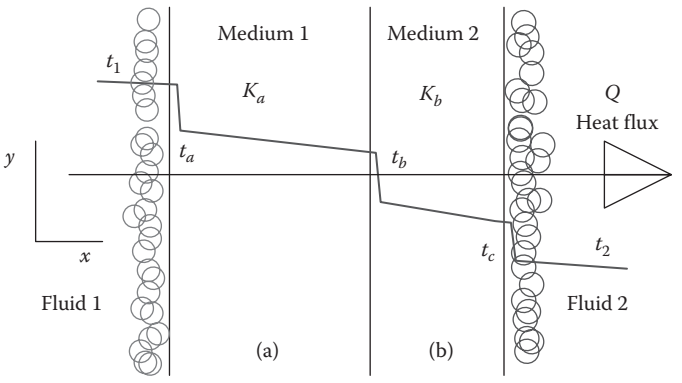

Figure 12.5 Planar conductive heat flow

Since the heat must pass through all the layers, in medium b we have

$$Q = \frac{k_b A(t_b - t_c)}{b} \tag{12.57}$$

Solving for the temperatures and adding, we obtain

$$Q = \frac{A(t_a - t_c)}{a/k_a + b/k_b} \tag{12.58}$$

Equation 12.59 takes into account only the heat flow within the mediums a and b. We also need to consider the boundaries at fluid 1 and 2. Let us begin this discussion by an analysis of Equation 12.56, which may be expressed as

$$Q = \frac{k_a}{a} A\Delta T = hA\Delta T \tag{12.59}$$

In Equation 12.59, h is referred to as the surface conductance. Thus, at the boundary of mediums 1 and 2, we may express the heat flow as

$$Q = h_1 A(t_1 - t_a); \quad Q = h_2 A(t_c - t_2) \tag{12.60}$$

The steady-state heat flow equation is then

$$Q = \frac{A(t_1 - t_2)}{1/h_1 + 1/h_2 + a/k_a + b/k_b} \tag{12.61}$$

As an example, we wish to calculate the heat flow through a wall from a room that is on fire through conduction to the exterior wall. The wall thickness is 8 in., made up of 1/2 in. gypsum board, 3 1/2 in. fiberglass insulation, and 4 in. brick facing. The surface conductance at the interior of the wall can be assumed to be equivalent to a 20 mph wind with a surface conductance of 7.0 Btu/(ft^2-h°F). The exterior surface conductance is assumed to be 1.5 Btu/(ft^2-h°F). Assume the brick thermal conductivity to be 0.5 Btu/(ft-h°F). The other thermal conductivities are obtained from Table 12.7. Note the units of conductance relative to the units of thermal conductivity. Also keep in mind that the inch units must be converted to feet. From Equation 12.61, we may compute the steady-state heat flow per unit area for a temperature differential of 1200°F as follows:

$$Q/A = \frac{1200}{\frac{1}{1.5} + \frac{1}{7} + \frac{0.00416}{0.9824} + \frac{0.291}{0.0274} + \frac{0.333}{0.5}} = 99.3\,\text{Btu/h}$$

Single-walled flue pipes pose a fire danger if the hot gases conducting through the surface of the pipe come into contact with combustible materials. Many fireplaces have been installed with vent pipes. Commonly double- or triple-walled vent pipes are used in these

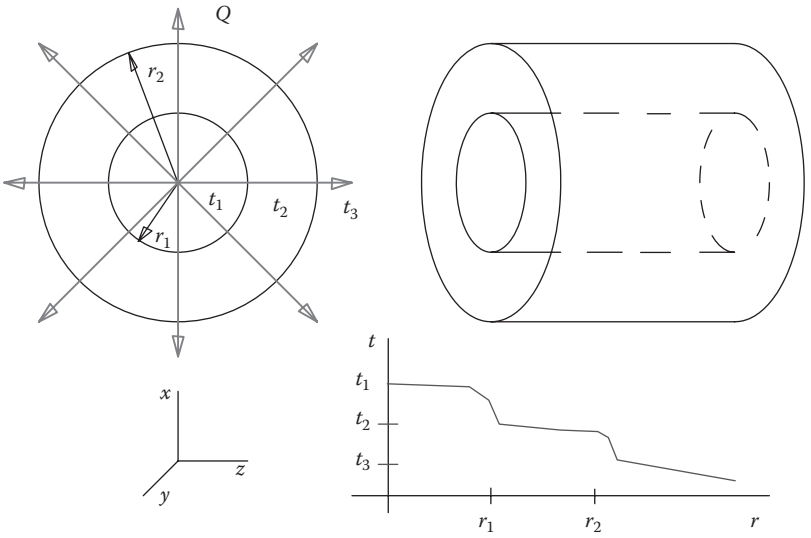

Figure 12.6 Cylindrical conductive heat flow.

applications. Figure 12.6 represents the geometry of a double-walled pipe. The thermal conductivity of the inner pipe is k_1 and that of the outer pipe k_2. Applying Equation 12.54 for the cylindrical geometry, we obtain

$$Q\int_{r_1}^{r_2}\frac{dr}{r} = -2\pi zk\int_{t_1}^{t_2} dt \tag{12.62}$$

$$Q = \frac{2\pi zk(t_1 - t_2)}{\ln(r_2/r_1)} \tag{12.63}$$

Extending the concept as we did for the rectangular geometry and including the film resistances, we may generalize the heat flow equation as

$$Q = \frac{(t_1 - t_2)}{\dfrac{1}{A_1h_1} + \dfrac{1}{A_2h_2} + \dfrac{\ln(r_2/r_1)}{2\pi zk_1} + \dfrac{\ln(r_3/r_2)}{2\pi zk_2}} \tag{12.64}$$

Equation 12.64 may be readily extended to include a triple-walled pipe. It should be noted that A_1 and A_2 represent the areas of the inner and outer cylinders respectively, h_1 and h_2 are the respective surface conductances, and the logarithmic terms represent the respective resistances.

As an example, consider a single-wall pipe used as the flue for a fireplace. The fireplace flue is thin metal and surrounded by cellulose. The outer diameter of the pipe is 1 ft and the inner diameter is 0.95 ft. Assume that the surface conductance at the pipe is 2000 Btu/(h-ft^2) at 600°F. The flue exhaust gases are measured to be 600°F. The conductivity of the steel is 312 (Btu-in.)/(h-ft^2-°F). We wish to determine the heat conduction and the potential for ignition of the cellulose insulation surrounding the flue pipe. These calculations are from an actual case.

The pipe resistance is calculated from

$$R_p = \frac{\ln(r_o/r_i)}{2\pi z k_s} = \frac{\ln(1.0/0.95)}{2\pi(312/12)} = 3.1398\times10^{-4}\ \text{h}^\circ\text{F/Btu}$$

Note that k_s has been divided by 12 to ensure that the units are dimensionally correct.

The film resistance is

$$R_f = \frac{1}{Ah_f} = \frac{1}{2\pi r(2000)} = 0.79577\times10^{-4}\ \text{h°F/Btu}$$

Note that the pipe resistance is determined per foot so that z is unity and the film resistance area is at a radius r of 1 ft. The heat conduction is then

$$Q = \frac{(t_1 - t_2)}{R_{total}} = \frac{600}{3.9455\times10^{-4}} = 1.52\times10^6\ \text{Btu/h per ft}$$

We now want to determine the temperature on the outside of the pipe, which is in contact with the celluloid insulation, so

$$t_1 - t_2 = 600 - t_c$$

and

$$1.52\times10^6 = \frac{600 - t_c}{k_f} \Rightarrow t_c = 479°\text{F}$$

This temperature is certainly sufficient to ignite cellulose insulation. In this actual case, the home owner had constructed the fireplace and exhaust chimney in this manner and when he built a fire, the cellulose insulation ignited and burned his house down.

The conductive heat transfer may also be evaluated in spherical coordinates. This type of analysis lends itself to the evolution of a fire in a room. Of course, the simplification is that convection currents and radiation are disregarded. Figure 12.7 represents the heat conduction for this geometry.

For this geometry, Fourier's equation becomes

$$Q = -kA\frac{dt}{dr} = -k(r^2\sin\theta d\theta d\varphi)\frac{dt}{dr} \tag{12.65}$$

Integrating over the limits

$$Q\int_{r_1}^{r_2}\frac{dr}{r_2} = \int_0^{\pi}\sin\theta d\theta\int_0^{2\pi}d\varphi\int_{t_1}^{t_2}dt \tag{12.66}$$

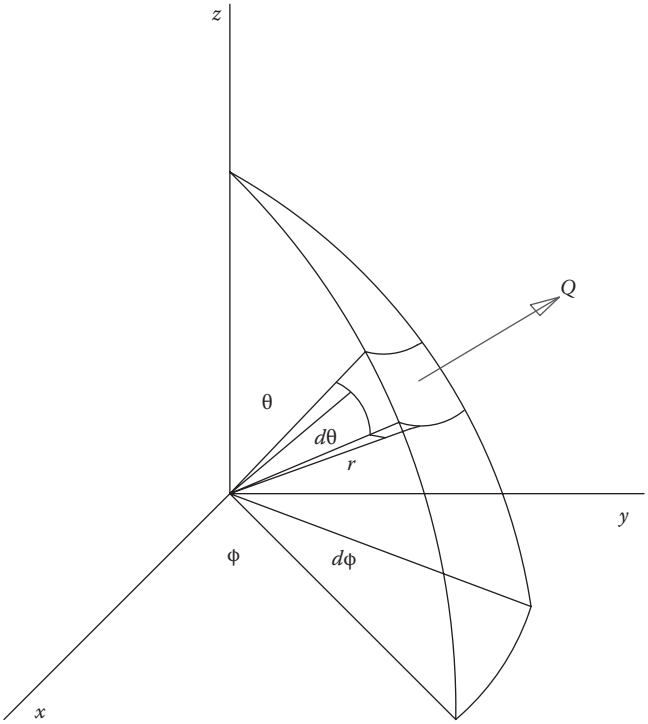

Figure 12.7 Spherical geometry.

or

$$Q = \frac{(t_1 - t_2)}{\dfrac{(r_2 - r_1)}{4\pi k r_1 r_2}} = \frac{\Delta t}{R} \tag{12.67}$$

The preceding equations will allow for the solution of most problems encountered by the forensic engineer with respect to the solution of the transfer of heat through conduction. We now turn our attention to thermal radiation.

Thermal radiation is produced by a differential in temperature. Thermal radiation is continuously produced over a wide range of frequencies. Generally when investigating fires, we are only interested in the frequencies near the visible range. Figure 12.8 shows a part of the electromagnetic spectrum. The abundance of the radiated heat in a fire is in the infrared region with some extending into the visible region.

For an electromagnetic field, the energy per unit area per unit time is given by the Poynting vector as defined in Chapter 10 and is given by

$$\boldsymbol{P} = \boldsymbol{E} \times \boldsymbol{H} \tag{12.68}$$

The time average energy density for the field may be shown to be given by

$$U = \tfrac{1}{2}\left[\varepsilon_0 |\boldsymbol{E}|^2 + \mu_0 |\boldsymbol{H}|^2\right] \tag{12.69}$$

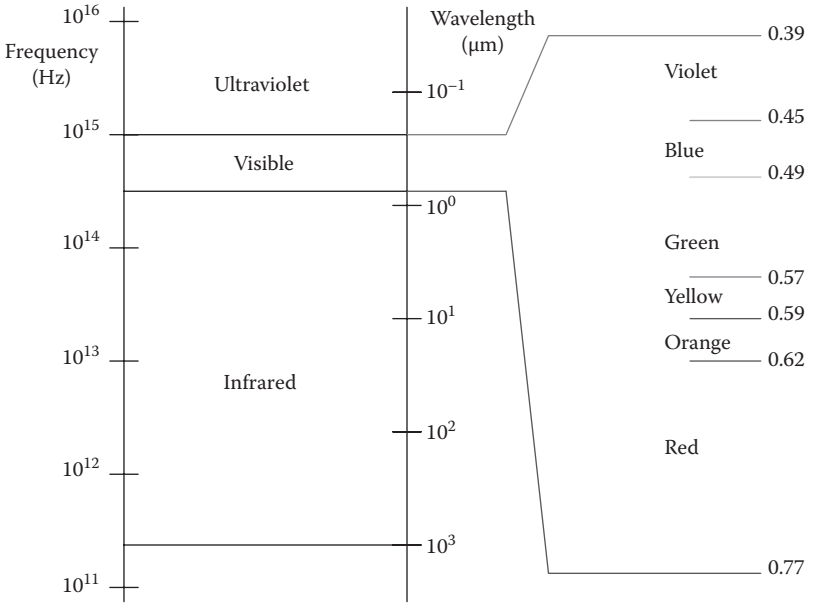

Figure 12.8 Electromagnetic spectrum.

The radiant energy is related to the radiant energy density by

$$\boldsymbol{U} = \frac{\partial \boldsymbol{Q}}{\partial \boldsymbol{V}} \tag{12.70}$$

where

$\boldsymbol{U}$ is the radiant energy density (J/m^3)
$\boldsymbol{Q}$ is the radiant energy (J)
$\boldsymbol{V}$ is volume (m^3)
J = 9.48 × 10^{-4} Btu

The radiant flux is the time rate of change of the radiant energy, or

$$\Phi = \frac{\partial \boldsymbol{Q}}{\partial t} \text{W} \tag{12.71}$$

where

Φ is the radiant flux
t is time
J = 2.778 × 10^{-4} W-h

The radiant flux is also related to the Poynting vector by

$$\Phi = \oint \boldsymbol{P} \circ d\boldsymbol{A} \tag{12.72}$$

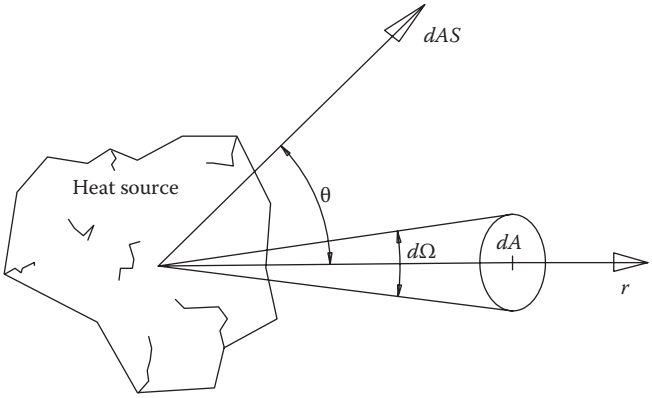

Figure 12.9 Radiant intensity.

The radiant intensity is defined in terms of the radiant flux per unit solid angle and is described by Figure 12.9. In equation form, the radiant intensity is given by

$$I = \frac{\partial \Phi}{\partial \Omega} = \frac{\partial^2 Q}{\partial t \partial \Omega} \text{ W/sr} \tag{12.73}$$

where sr represents the steradian solid angle.

The differential angular dependence of the radial flux density is the radiance. The radiance at a given point and at a given direction is defined as the radiant flux per unit solid angle per unit projected area perpendicular to the propagation direction. In equation form we have

$$R = \frac{\partial \Phi}{\cos\theta \partial \Omega \, \partial A_S} (\text{W/m}^2\text{-sr}) \tag{12.74}$$

Similar to the radiant intensity, the irradiance is defined as the total flux per unit area and given by

$$\boldsymbol{I_R} = \frac{\partial \Phi}{\partial \boldsymbol{A}} \text{ W/m}^2 \tag{12.75}$$

An ideal radiator is called a black body radiator that emits radiation over all ranges of frequencies. Sometimes this ideal radiator is called an isotropic source. The radiance is a function of temperature. Actual sources are not ideal but may be referred to as gray body radiators. The frequency dependence of an actual radiator may contain abrupt changes over its frequency range. Figure 12.10 shows representative curves for different radiators.

The irradiance or emissive power, which is sometimes called the radiant flux density, is defined as the area under the curve of Figure 12.10 or

$$R = \frac{2\pi hc^2}{\lambda^5 (\varepsilon^{hc/k\lambda T} - 1)} \text{ J/(s-m}^3\text{)} \tag{12.76}$$

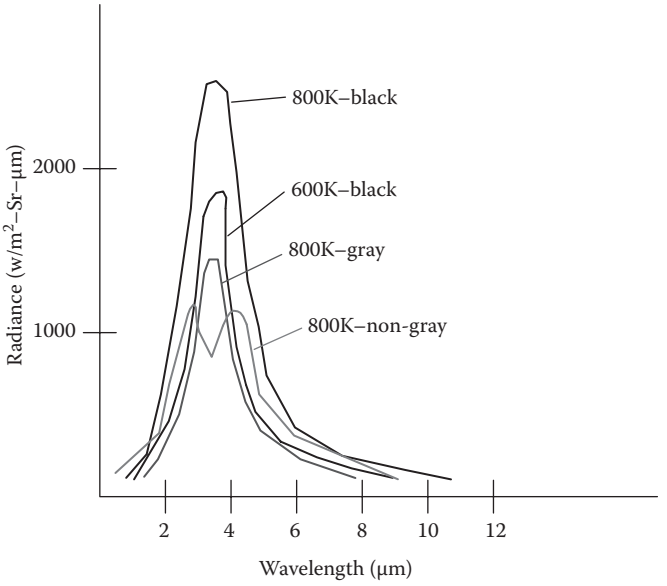

Figure 12.10 Radiance.

and is known as Planck's radiation law. A review of the electromagnetic spectrum and the radiance curves indicates that most of the heat produced in a fire is in the infrared region at wavelengths between 1 and 10 microns. This concept allows us to place limits on the energy density that is produced in a fire over a certain temperature range. For this analysis, we begin by defining some of the basic parameters encountered in Equation 12.76. These are

h is the Planck's constant = 6.62×10^{-27} erg-s = 6.62×10^{-34} J-s
c is the speed of light = 3×10^{8} m/s
k is the Boltzmann's constant = 1.38×10^{-16} ergs/K = 1.38×10^{-23} J/K

To gain a sense of Equation 12.76, we wish to examine the nature of the exponent over the frequency and temperature range in a typical fire. Let

$$x = \frac{hc}{k\lambda T} = \frac{a}{\Delta\lambda\Delta T} = \frac{0.0144\,^{\circ}\text{K-m}}{\Delta\lambda\Delta T} \tag{12.77}$$

Now the curve of Figure 12.10 indicates a range of wavelengths of 9 microns. For a temperature range of 500 K, the exponent x becomes approximately 3.2. Now recall that

$$\frac{1}{\varepsilon^{x}-1} = \varepsilon^{-x} + \varepsilon^{-2x} + \varepsilon^{-3x} + \cdots = \varepsilon^{-x}[1 + \varepsilon^{-x} + \varepsilon^{-2x} + \cdots] \tag{12.78}$$

For the range of values of the exponent in a typical fire, we may disregard the higher order terms so that Equation 12.76 may be approximated as

$$R = \frac{2\pi hc^{2}}{\lambda^{5}\varepsilon^{x}} \tag{12.79}$$

The emissive power for this example would then be

$$R = \frac{2(3.14)(6.62\times10^{-34})(3\times10^{8})^{2}}{(9\times10^{-6})^{5}(24.48)} = 2.58\times10^{8}\ \text{J/(s-m}^{3}\text{)}$$

or approximately 2.58×10^5 kW/m^3 or 7.3 MW/ft^3.

The total time-dependent radiance may be determined by integrating over the wavelength as

$$R_T = 2\pi hc\int_0^{\infty}\frac{d\lambda}{\lambda^5(\varepsilon^{hc/k\lambda T}-1)} \tag{12.80}$$

If we let $x = hc/k\lambda T$, the integral becomes

$$R_T = \frac{2\pi k^4T^4}{h^3c^2}\int_0^{\infty}\frac{x^3}{\varepsilon^x-1}dx \tag{12.81}$$

which can be shown to be

$$R_T = 6.4938\frac{k^4}{h^3c^2}T^4 = \sigma T^4 \tag{12.82}$$

where $\sigma = 5.67032 \times 10^{-8}$ W/m^2-K^4. Equation 12.82 is known as the Stefan–Boltzmann law and does not include the emissivity dependence on the wavelength. Two forms of the integral of Equation 12.81 are possible depending on the argument x. These are

$$\int\frac{x^3}{\varepsilon^x-1}dx = 3x^2Li_2(\varepsilon^x)-6xLi_3(\varepsilon^x)+6Li_4(\varepsilon^x)-\frac{x^4}{4}+x^3Log(1-\varepsilon^x) \tag{12.83}$$

where

$$Li_n(\varepsilon^x) = \sum_{k=1}^{\infty}\frac{(\varepsilon^x)^k}{k^n}/;\quad |\varepsilon^x|<1 \tag{12.84}$$

and

$$\int\frac{x^3}{\varepsilon^x}dx = -\frac{(x^3+3x^2+6x+6)}{\varepsilon^x} \tag{12.85}$$

In either case, these integrals are complex to evaluate so that the approach of Equation 12.79 may be used to gain insight into the emissive power of a fire.

The dynamics of a fire make it virtually impossible to determine the effects of combustion upon the release and transfer of heat in a fire. The analysis of convection is generally restricted to HVAC systems where the capabilities of the forced air system are known and readily determined from manufacturers' specifications. The analysis of fire dynamics can be undertaken through sophisticated computer modeling programs that are discussed in the last section of the book.

Gas Can Burn

Often, gasoline cans or containers are involved in fires. In an accidental fire, when a gasoline can is surrounded by fire, its plastic vent cap may be melted allowing gasoline fumes to escape and ignite. Sometimes, when arson is involved, the arsonist may attempt to explain the release of the fuel with respect to a given time line and indicate that the fuel was not poured but rather escaped and burned through the ventilation opening. Such a scenario was presented to the authors in an arson prosecution. The time involved in the scenario presented by the arsonist was approximately 10 min and involved a 5 gal Eagle Kerosene container filled with 5 gal of gasoline. Preliminary tests conducted by the fire department using an identical can with 2 1/2 gal of gasoline produced a violent flame escaping from the ventilation opening when surrounded by a fire. The time measured by the fire department was approximately 40 min. According to the fire department's reasoning, it would take approximately 80 min to burn off the fuel if the can was filled to capacity, that is, 5 gal.

We may model this process by determining how long it takes a given quantity of gasoline in a container to burn off its fuel if it is surrounded by heat. Let us assume that the container has the dimensions and ventilation opening as shown in Figure 12.11:

A_o = ventilation opening	D_o = ventilation diameter
$A_o = (\pi/4)\ D_o^2 = 1.36\times10^{-3}$ ft^2	D_o = 0.5 in. = 0.04167 ft
$A_o = 1.36 \times 10^{-3}$ ft^2	H_o = ventilation height = 1.5 ft

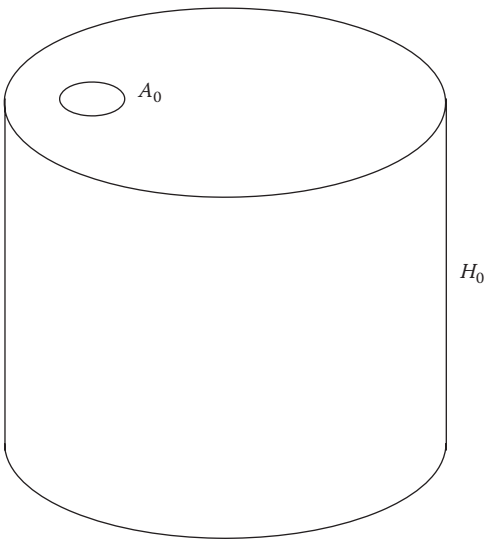

Figure 12.11 Gas can.

The HRR for a ventilation opening A_o at a ventilation height H_o is given by

$$\text{HRR (BTU/s)} = 36.5A_o\sqrt{H_o} \tag{12.86}$$

For the given dimensions,

$$\text{HRR(BTU/s)} = (36.5)(1.36\times10^{-3})(1.5)^{1/2}$$

$$\boxed{\text{HRR} = 6.08\times10^{-2}\ \text{BTU/s}}$$

The heat of combustion for petroleum fuels varies between 10,000 and 16,000 Btu/gal at a constant volume. The accepted heat of combustion for gasoline is 12,000 Btu/gal. For a 5-gal container, the total heat of combustion is

$$H_{ct} = (5\,\text{gal})(12{,}000\,\text{BTU/gal}) = 60{,}000\,\text{BTU}$$

$$\boxed{H_{ct} = 60{,}000\,\text{BTU}}$$

In order to properly model this process, we must understand the composition of gasoline and how its pressure is affected by temperature. We begin with a discussion of petroleum. Many useful products are obtained from petroleum; among them are various kinds of naphthas, kerosene, lubricating oils, petroleum jelly, and paraffin. These products are not single compounds but are mixtures of hydrocarbons boiling between certain limits. A hydrocarbon is defined as a compound consisting of carbon and hydrogen. Under ordinary conditions, some of the hydrocarbons are gases, others liquids, and still others are solids. Certain hydrocarbons mixed in varying proportions are natural gas, gasoline, kerosene, and lubricating oils. All of these petroleum hydrocarbons are combustible. One of the most important classes of hydrocarbons is the methane series under which gasoline falls. Table 12.8 gives the names, chemical formulas, and boiling points of some of the methane series of hydrocarbons.

The hydrocarbons are insoluble in water and are not readily acted upon by other compounds; even strong acids and bases have little or no effect upon them. The lower members of the series from methane to butane are gases at standard temperatures and pressures,

Table 12.8 Methane Series of Hydrocarbons

Name	Chemical Formula	Boiling Point (°F)
Methane	CH_4	−161.4
Ethane	C_2H_6	−88.3
Propane	C_3H_8	−44.5
Butane	C_4H_{10}	+0.6
Pentane	C_5H_{12p}	+36.2
Hexane	C_6H_{14}	+69.0
Heptane	C_7H_{16}	+98.4
Octane	C_8H_{18}	+124.6

while those containing from 5 to 16 carbon atoms are liquids. Those containing more than 16 carbon atoms are solids.

The refining of petroleum normally consists of three stages. First, the crude oil is subjected to fractional distillation. In this first stage, the temperature increases as the distillation proceeds. The product that distills between 200°F and 300°F is called refined oil distillate and belongs to the class of kerosenes. The next distillation is the fraction known as gas oil. The final distillation includes the lubricating oils and paraffin. The second stage involves the purification of the distillates by the agitation of these products with sulfuric acid and washing of the remaining oils. Finally, the different products after treatment with acid and alkali are subjected to redistillation. Various grades of naphthas are produced and used for different purposes, but a great use is as gasoline fuel for internal combustion engines. A principal component of gasoline is octane (Table 12.9).

This temperature versus pressure curve for octane is plotted in Figure 12.12:

$$\Delta P = (10-1)(14.7\,\text{lb/in.}^2) = 132.2\,\text{lb/in.}^2$$

$$\Delta T = (456.4-258)^\circ\text{F} = 198.4^\circ\text{F}$$

$$\Delta P_1 = 73.5 \quad \Delta T_1 = 127.2$$

For a constant volume, Charles' law states that the pressure varies directly as the temperature. In equation form we express this relationship as

$$\frac{P_1}{P_2} = \frac{T_1}{T_2} \tag{12.87}$$

Table 12.9 Temperature of Octane at Various Pressures

Name	Formula	1 ATM	2 ATM	5 ATM	10 ATM
Octane	C_8H_{18}	125.6°C 258°F	152.7°C 306.8°F	196.2°C 385.2°F	235.8°C 456.4°F

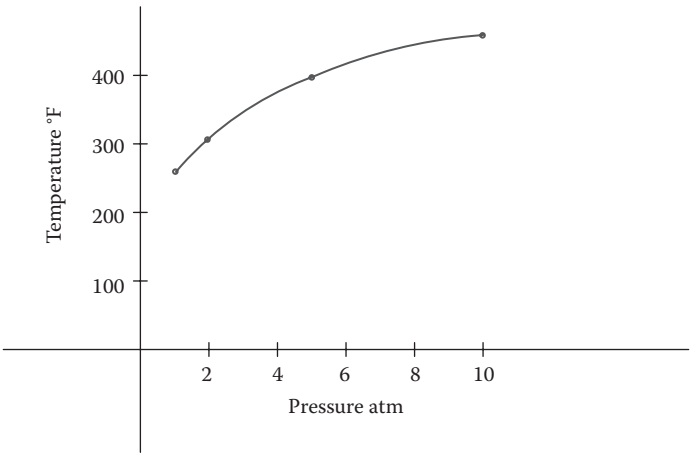

Figure 12.12 *T–P* curve for gasoline.

Defining $\Delta P = P_2 - P_1$ and $\Delta T = T_2 - T_1$, Equation 12.2 becomes

$$P_1 = \left(\frac{\Delta P}{\Delta T}\right) T_1 \tag{12.88}$$

over the linear range of the curve

$$\frac{\Delta P}{\Delta T} = \frac{73.5}{127.2} = 0.5778 \quad \text{so} \quad P_1 = 0.5778T - 1 \tag{12.89}$$

As the temperature rises above ambient, the pressure also rises and causes the fuel to escape more rapidly. A linear approximation for the time required to liberate the heat from a gasoline can surrounded by a fire can be modeled using

$$t_c = \frac{H_c}{\text{HRP}(0.5778T)} \tag{12.90}$$

For a temperature differential of $T = 325°\text{F}$

$$t_c = \frac{60{,}000\,\text{BTU}}{(6.08 \times 10^{-2}\,\text{BTU/s})(187.78)} = 5255\,\text{s}$$

or

$$t_c \approx 88\,\text{min}$$

The pressure of a vapor in equilibrium with the liquid at any temperature is called the "vapor pressure." For water at 212°F, this pressure is 14.7 lb/in.^{2} or 760 mmHg or 1 atm. The vapor pressure of a substance is a function of temperature only, not of volume. Thus, in a vessel containing the liquid and vapor in equilibrium at a fixed temperature, the pressure does not depend on the relative amounts of liquid and vapor present. If the volume is decreased, some of the vapor condenses and vice versa. But, if the temperature is kept constant by removing or adding heat, the pressure does not change.

Several factors influence this time. The most important is, of course, the temperature surrounding the container. As this temperature increases or decreases, the pressure within the vessel will increase or decrease accordingly and will affect the HRR. Additionally, the heat of combustion of the gasoline may vary as well as the vapor pressure calculated in this analysis. However, this time frame analysis is consistent with reported gasoline can fires by various fire departments. The student is encouraged to calculate the time of combustion (t_c) as the specific gravity of the fuel (S_g) varies along with the ventilation height (H_o), the heat of combustion (H), the amount of fuel (G), and the change in temperature (dT). For all of these variable conditions, the analysis reveals that the time of combustion varies between 45 and 110 min. This analysis is left as an exercise at the end of the chapter.

Live Burns

One of the most significant ways in which a forensic engineer differentiates himself from investigators who conduct origin and cause investigations is in testing, measurement and calculations. Recorded live tests of controlled burns are a significant form of verifying or dispelling theories of how structures burn. In this section we detail some characteristics of controlled burns for mobile homes, house fires and vehicle burns.

Mobile Homes

Two almost identical mobile homes were burned. A significant distinction, however, was that one mobile home was accelerated while the other was not. Furnishings and combustible materials within the burn areas of the two mobile homes were also similar so that the significant difference in the fuel load was produced by the accelerant pour in one of the homes. Ventilation openings for both mobile homes were the same and adjusted to ensure that flashover occurred. HRRs and temperature graphs were calculated, measured, and plotted in order to compare the accelerated and nonaccelerated fires. A significant temperature versus time graph differentiates the two burns. The heat inversion phenomenon in mobile homes, reported by other investigators, was also noted in the nonaccelerated fire.

Over the past 50 years, it has been generally agreed upon by experts in the fire sciences that mobile home fires are significantly different from standard construction home fires with respect to a variety of factors including temperature, HRRs, flashover, fire development, fire spread, time of involvement, and burn patterns to name only a few. It is safe to say that at the beginning of the mobile home manufacturing history, there was a significant difference between conventional homes and mobile home construction. Typical mobile homes were much smaller than today, there were no double wides, roof lines were flat, structural walls were constructed of 2 × 2 studs, interior walls were generally paneled, and many were electrically wired with aluminum. Today, the differences between the two types of homes are not as great because mobile home manufacturers have upgraded the wiring standards to copper, walls are generally constructed of 2 × 4 studs, interior wall surfaces now include significant amounts of "sheet rock," and roofs are no longer always flat. Where traditionally, the outer skin, including the roof, of mobile homes has been metal, shingled roofs are found in many double wide homes. Unfortunately, it is still true that four major problems are endemic to mobile homes: materials of construction, metallic sidewalls, rectangular shape, and low ceiling height.

Previously recorded temperatures in mobile home fires have shown that floor level temperatures may exceed the ceiling temperatures by more than 300°F–450°F at flashover and for a period of 30 s to 1 min after flashover. These recorded results are sometimes attributed to flashover or radiation to explain the temperature inversion effects. Generally, fires travel upward and outward, and it is commonly thought that higher temperatures would normally be recorded at higher elevations within a room—a conclusion that may not always hold true for a variety of reasons. Heat is transported by three mechanisms, conduction, convection, and radiation. Although conduction may play a role in heat transfer of the metallic elements, the frame and the skin, as the fire progresses, it is probably not a significant factor until after flashover. Its main effect probably occurs after the fire has penetrated through the roof.

It is, however, true that the fire spread in a mobile home is much more rapid after flashover because of the low ceiling, the tubular construction, and the lack of fire stops and headers above hallway openings. In this context, it is important to understand what is meant by the term flashover. According to NFPA 921, flashover is defined as a stage in the development of a contained fire in which all exposed surfaces reach ignition temperature more or less simultaneously and fire spreads rapidly throughout the space. During the early stages of development of a fire, convection is the major transport vehicle for the spread of the hot gases. As this process continues, radiation begins to increase its effect so that at and after flashover, both radiation and convection are the prime movers for the development of the fire. Some investigators report temperatures exceeding 1800°F during the development of fires after the point of flashover and for some time afterward. Higher temperatures recorded at floor level than at ceiling level are also attributed to the inversion phenomenon. Some of these results may be due to other factors than radiation, convection, and flashover. For example, a couch or stuffed chair will develop a flame when it ignites. The height of this flame may reach the ceiling level, but the highest flame temperature may be at a lower height than the ceiling. This fact alone helps to explain why higher temperatures may be recorded at mid-room or floor level in a fire. Flame temperatures approaching 2400°F have been measured over polyurethane mattresses. In comparison, the flame temperature of gasoline is approximately 1500°F or 810°C. Polyurethane is a common material used in stuffed chairs, couches, carpet padding, and mattresses so that recorded temperatures at floor level may in fact be 400°F or 500°F higher than at ceiling level if these materials are present within the fire evolution and in particular adjacent to or under a thermocouple used to record the temperature. This discussion illustrates the need to meticulously detail the experiment and include the location of the pertinent fuel loads within the fire area with respect to the building dimension and the measurement locations. Filming of the burn in time sequence with the recording of temperatures can help to explain unexpected results and should always be included as part of a scientific live burn exercise.

If the thermocouples used to measure temperatures at various levels within a room are appropriately placed, they will measure the average temperature at that level. One method of ensuring this average temperature measurement is to use a long shielded cable thermocouple that reaches across most of the room where the fire will occur. This method will also tend to avoid any hot spots produced by the ignition of the room contents (such as a couch) and their flame development. NFPA 921 denotes the flashover phenomenon when the surface temperature of combustibles rises so that the upper layer temperature reaches approximately 1100°C and pyrolysis gases from the combustible contents ignite along with the bottom of the ceiling layer. At flashover, the best release rate can reach 10 MW.

The accelerated fire reached the flashover point in approximately 6 min after ignition with the highest recorded temperature of 1090°F at ceiling level. At this point, the mid-room temperature was 900°F while the floor temperature reached 490°F. The temperatures at floor, mid-room, and ceiling level all peaked at the same time. In comparison, the non-accelerated fire reached flashover at about the 14 min mark. At this time, the ceiling temperature reached 1230°F while the floor level temperature was at 1100°F. From this point on, the ceiling temperature began to fall while the floor temperature continued to rise to a value of 1270°F at the 15.5 min mark. By this time, the ceiling temperature had dropped to 900°F, thereby verifying the inversion phenomenon. Flashover was reached in both fires at temperatures consistent with those defined by NFPA 921 (1100°).

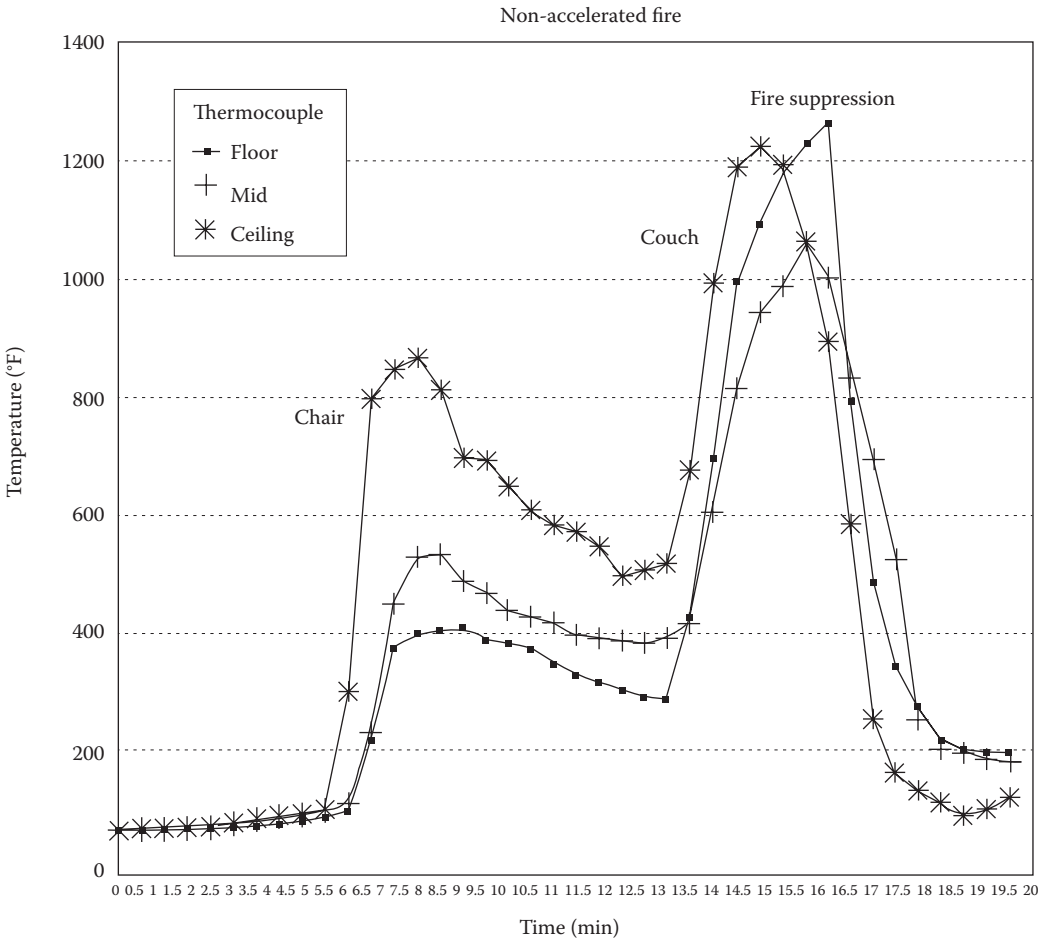

Graph 12.1 Temperature vs. time.

In the accelerated fire, the inversion phenomenon was not noted. Two possible reasons for this fact may be (1) suppression occurred too soon for the inversion phenomenon to occur and/or (2) accelerated fires may not necessarily exhibit the same type of inversion phenomenon or any inversion of temperatures at all. In order to answer this question, it would be necessary to allow an accelerated fire to progress beyond the point of our tests. The graphs shown in Graphs 12.1 and 12.2 show the difference in the two mobile home fires.

House Fires

Fire investigators seldom take into account the fuel load in a confined fire. Sometimes they correctly attribute a rapidly developing high heat fire to the ignition and consumption of a couch. Other times they may attribute the rapid fire development to the use of an accelerant. The addition of an accelerant may often mislead the investigator and cause an inadequate or erroneous determination of the cause of the fire. It is well known that fires involving foam insulation or padding as used in furniture can liberate considerable energy,

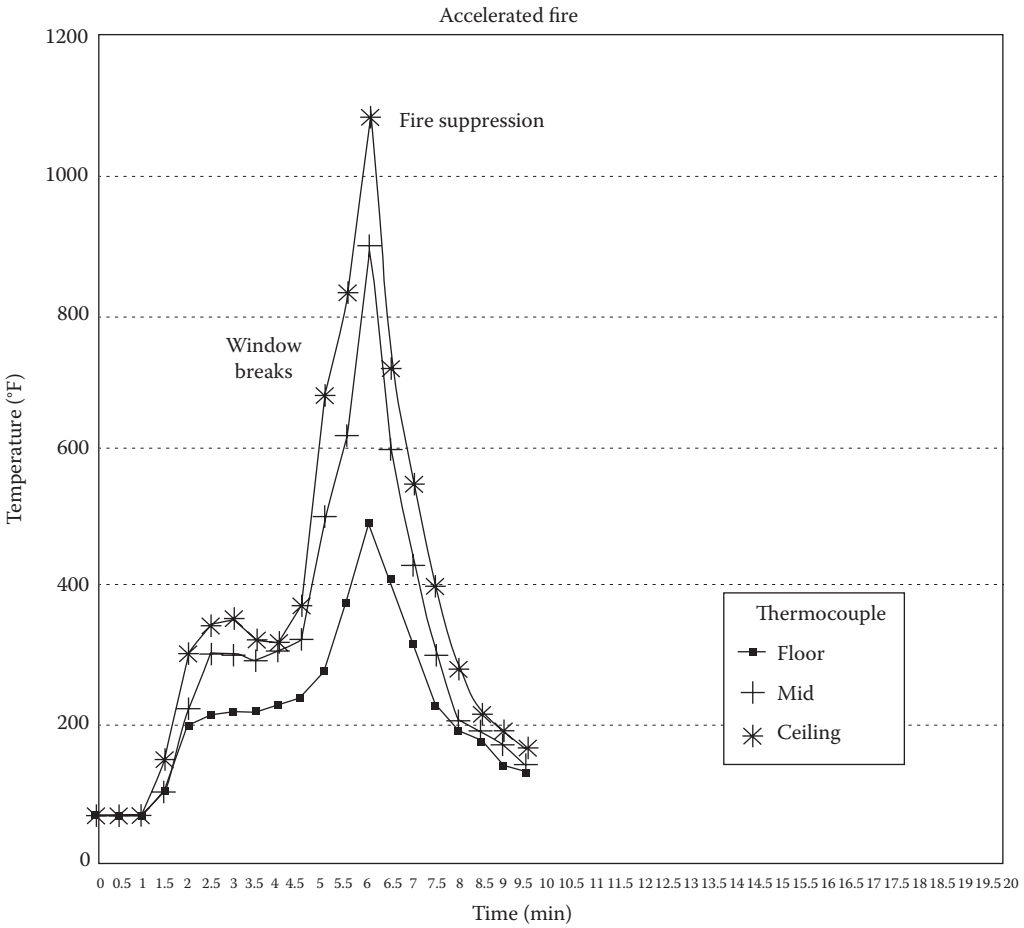

Graph 12.2 Temperature vs. time.

resulting from the fuel load contained within the foam padding and other plastics contained in the furniture. Similarly, present-day vehicles contain an abundance of plastics, which rapidly allow for a well-ventilated fire to develop in a short duration of time. The rapid evolvement of fires in vehicles does not necessarily mean that the vehicle was accelerated as will be seen in the next section.

Through careful analysis of the fuel load present, in conjunction with live fire testing for comparative purposes, the forensic engineer may be able to discern the true nature of the fire. Fire testing indicates that the distinction between accelerated and nonaccelerated fires is often very difficult to distinguish. Extensive testing by the authors indicates that the fuel load from household furnishings plays a greater role in the fire development than the addition of accelerants up to approximately 1 gal. The authors have not conducted tests of accelerated fires with sizable quantities of fuel because of the significant danger associated with such fires. The next two graphs show two fires, one accelerated and the other not. The accelerated kitchen fire, Graph 12.3, took approximately 23 min to develop, while the nonaccelerated living room fire, Graph 12.4, fully developed in 7 min. The contents of the kitchen consisted of a stove, kitchen cabinets, a trash can, a table, and four chairs. The fire was set on top of the stove in a pan with 3/4 gal of kerosene. The living room fire consisted of a couch, a television, a sofa, and a coffee table. Newspapers were ignited on the floor near the couch to simulate an

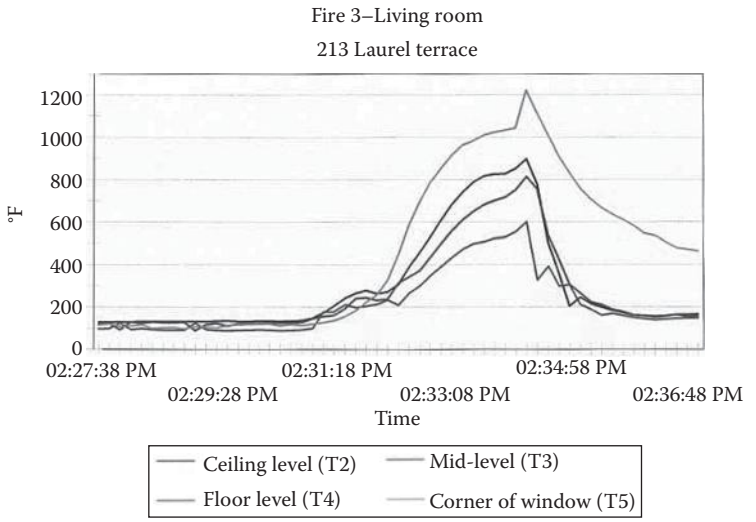

Graph 12.3 Temperature vs. time.

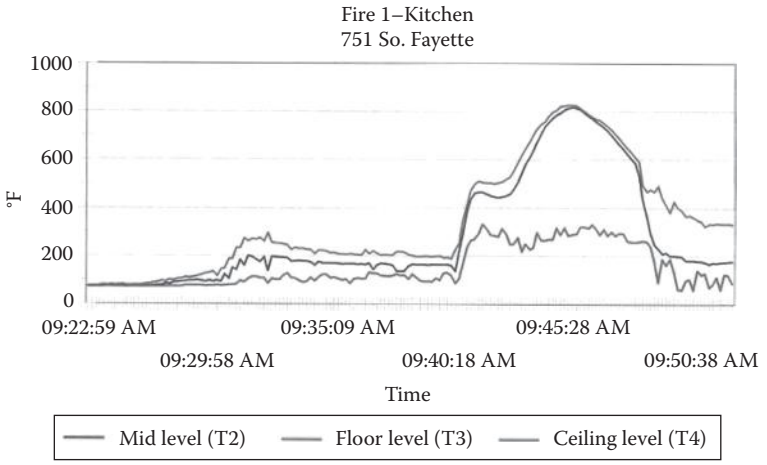

Graph 12.4 Temperature vs. time.

accidental fire. Both rooms measured 11 by 11 ft and the ceilings were 7.5 ft. Both rooms had a ventilation opening of 2 ft^2. Although accelerated fires generally evolve faster than nonaccelerated fires, the time element only varies by a few minutes. From a lay person's point of view, a few minutes difference in the evolution of a fire is insignificant, which may mislead the investigator. Note the significant dichotomy in the graphs we present with respect to a determination of cause by relying on the time element of the evolution of the fires.

Car Fires

Vehicle fires are greatly affected by the ventilation opening that allows air to feed the flames. The location of where the fire starts also has an effect on the development of the fire. For comparative purposes, two almost identical vehicles were burned and the temperatures

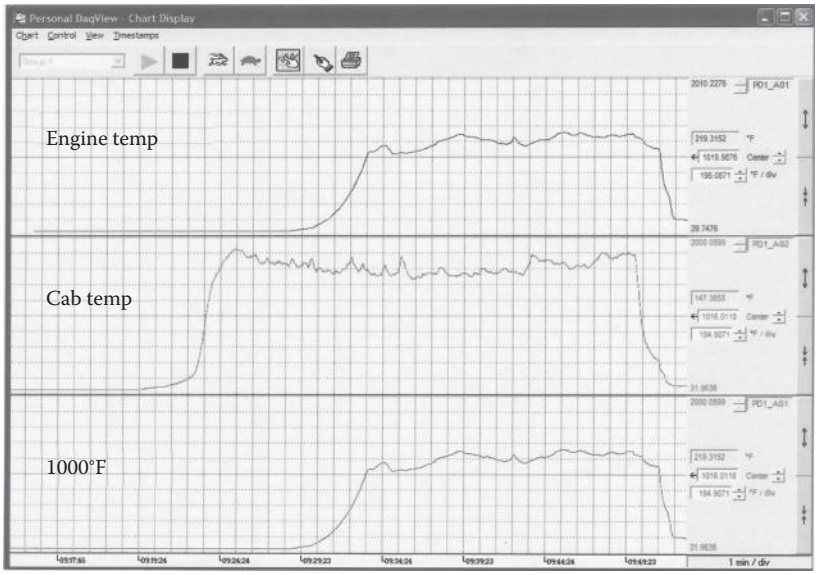

Graph 12.5 Temperature vs. time.

were recorded. The first vehicle was a Mercury Mystique. Thermocouples were placed in the engine compartment (top graph), front passenger's compartment on the dashboard (middle graph), and at the rear passenger's compartment on the left rear window ledge (bottom graph) (see Graph 12.5). This fire was conducted to the point where the entire vehicle was burned, and the flames were self-extinguished. The fire was set by igniting newspapers, motor oil, and charcoal starter in the glove box of the vehicle. The fire lasted approximately 32 min. Note that the temperatures in any location did not significantly exceed 1800°F. Figure 12.13 shows the Mercury at the conclusion of the burn.

Graph 12.6 represents the temperatures taken during the burn of a Ford Contour. This vehicle is almost identical to the Mercury. The thermocouples were again placed at the same locations as the previous burn. The thermocouple in the front passenger's compartment failed in this test and did not record the temperatures as seen in Graph 12.6. This fire was

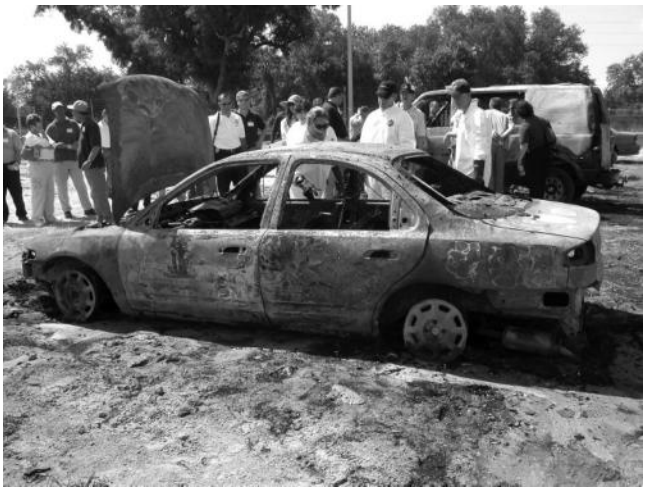

Figure 12.13 Mercury.

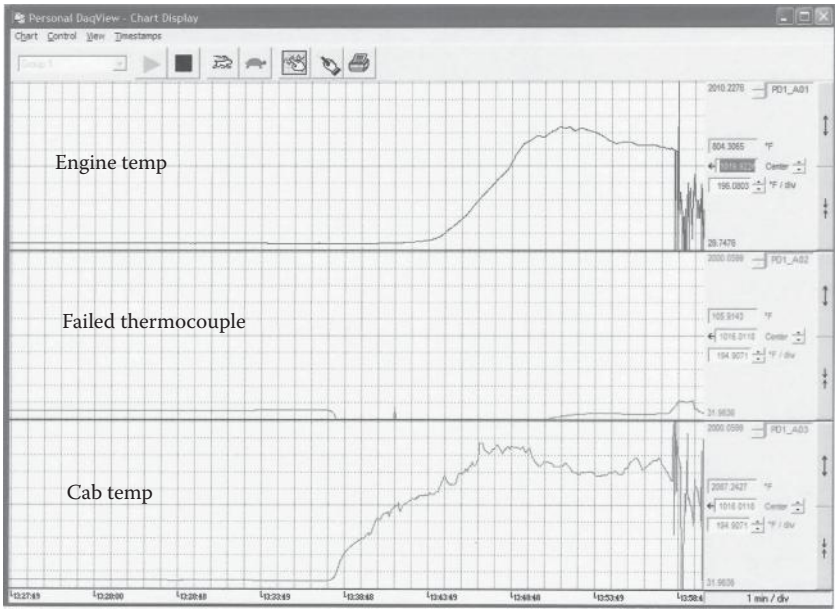

Graph 12.6 Temperature vs. time.

Figure 12.14 Ford.

started on the floor of the passenger's side at the rear. Newspapers and olive oil were ignited. This fire also lasted approximately 31 min. Figure 12.14 shows the Ford after the burn. The vertical grid in the graphs represents approximately 200°. The horizontal grid represents 1 min intervals. Figure 12.15 shows the Mercury as it was being burned in the test.

Fire Dynamics Modeling

The last decade has seen significant inroads into the prediction of the development of fires through the simulation of the dynamics of a fire. The National Institute of Standards and Technology (NIST) though its Building and Fire Research Laboratory has developed a

Figure 12.15 **(See color insert.)** Mercury.

computational fluid dynamics (CFD) computer model for the purpose of predicting the transfer of mass and heat as a consequence of a fire. The Fire Dynamics Simulator (FDS) is a complex computer program made available for free by NIST and can be downloaded simply by visiting their web site. Accompanying the FDS program is a tool that allows for the visualization of the simulation data through Smokeview. Smokeview and FDS are used concurrently to visualize the data obtained by the program results. Fire dynamics modeling presumes a significant level of sophistication by the user in the areas of thermodynamics, CFD, heat flow, mass transfer, and engineering principles. Furthermore, a concise understanding and use of engineering graphics programs facilitate in the simulation. The robustness of FDS allows for "what if" scenarios to be developed, which aid in the determination and progression of a fire. Windows versions of the programs are obtained from http://fire.nist.gov/fds and http://fire.nist.gov/smokeview.

CFD is a special branch of continuum mechanics dating back to the time of Newton. Both Euler and Lagrange formulated concise descriptions in the 1700s. The equations in the continuum are those of motion via a system of partial differential equations (PDEs). The PDEs describe how in the continuum, whether a solid, liquid, or a gas, the equations of motion affect the movement and deformation in space subject to the internal and external forces.

The description according to Euler leads to the Navier–Stokes equations given by the following:

Mass conservation

$$\frac{\partial \rho}{\partial t} + \nabla \circ \rho \boldsymbol{v} = 0 \tag{12.91}$$

Newton's second law

$$\frac{\partial (\rho \boldsymbol{v})}{\partial t} + \nabla \circ \rho \boldsymbol{v}\boldsymbol{v} = \rho \boldsymbol{F} - \nabla p + \nabla \circ \tau_{ij} \tag{12.92}$$

First law of thermodynamics

$$\frac{\partial(\rho h)}{\partial t} + \nabla \circ \rho h \boldsymbol{v} = \frac{Dp}{Dt} + q^{\circ}/// - \nabla \circ q + \Phi \tag{12.93}$$

Perfect gas equation

$$p = \frac{\rho RT}{M} \tag{12.94}$$

where

- ρ is the mass density function
- p is the pressure
- T is the temperature
- $\boldsymbol{v}$ is the 3D velocity
- h is the enthalpy
- t is time
- $\boldsymbol{\tau}_{ij}$ is the stress tensor
- $q^{\circ}///$ is the Huggett's relationship for the HRR per unit volume for a chemical reaction
- Φ is the dissipation function
- $\boldsymbol{q}$ is the HRR

These equations are very complex, and the basic explanation offered earlier is only by way of an introduction. For a complete understanding of fire dynamics simulation, we refer the reader to NIST Special Publication 1018*^.

Miscellaneous Losses 13

Introduction

Often the forensic engineer is asked to investigate some losses that are not of the general type, although most often they are associated with a larger loss such as a vehicular collision. A couple of examples of such a loss are the examinations of lightbulbs and the condition of certain fluids in a vehicle such as the oil, the transmission fluid, and the coolant system fluid. The examination of lightbulbs in a vehicle is pertinent in cases where visibility is an issue. Fog, rain, snow, and nighttime visibility issues often arise in crash investigations. In such cases the examination of the remains of lightbulbs should be carried out in a proper laboratory setting ensuring that the evidence has been properly collected, catalogued, and the chain of custody is intact.

Certain vehicular collisions or losses are attributed to a variety of causes. Sometimes, when a collision occurs, the brake system or the steering system may come into question. Sometimes a motor failure is attributed to driving the vehicle through water. In such cases, laboratory analysis of the motor fluids can assist the investigator in making a determination as to the cause of the failure. Vehicle interrogation tools such as CDR and Scan Tools are invaluable when vehicle failures are alleged or determined.

Some fires or health effects on humans may be attributed to natural gas leaks or carbon monoxide poisoning. These cases involve testing of components and equipment as well as coordinating such activities with medical personnel or coroners. Sometimes the fire suppression system may need to be investigated in order to determine its adequacy and design features. Fire suppression systems are also involved in water-related losses where the system may rupture as a result of cold weather. Knowledge of pertinent NFPA Codes is imperative when assessing such losses.

Sometimes vehicles are reported stolen and recovered in remote areas. The vehicle may have been burned or sunk in a body of water. Issues relative to the condition of the door locks and the ignition may arise that need to be addressed forensically. A knowledge of locks and ignitions along with a good rapport with local automobile dealers helps in these investigations. All of these types of investigations are part of a forensic engineering practice. This chapter covers some of the more common types of miscellaneous losses.

Carbon Monoxide

The inhalation of carbon monoxide poses a considerable threat to life and safety. Carbon monoxide is a by-product of incomplete combustion of a fuel. When fuels are burned, many by-products are released—some as a result of combustion while others as a result of the inefficiency of the equipment or engine producing the combustion process. The two main culprits in carbon monoxide incidents are the internal combustion engine and gas fired appliances in the home. Fires also produce an abundance of carbon monoxide. In a fire, carbon monoxide

forms and is the leading cause of death. The maximum concentration of carbon monoxide for survival is approximately 1.28%. Internal combustion engines are found in mowers, tillers, generators, motorcycles, cars, tractors, and trucks. The equipment generally burns a fuel such as gasoline, or diesel fuel. The gas-fed appliances may burn natural gas or propane and include grills, stoves, furnaces, heaters, and water tanks. The next two tables summarize the effects of carbon monoxide on humans. All concentrations are measured in parts per million (ppm).

Human Response to Carbon Monoxide and Carboxyhemoglobin

The human response to concentration levels of carbon monoxide ranging between 100 and 12,800 ppm is listed in the following table:

Concentration (ppm)	Symptoms
100	No poisoning symptoms even for long periods of time, allowable for several hours
200	Headache after 2–3 h, collapse after 4–5 h
300	Headache after 1.5 h, distinct poisoning after 2–3 h, collapse after 3 h
400	Distinct poisoning, frontal headache, and nausea after 1–2 h, collapse after 2 h, death after 3–4 h
500	Hallucinations felt after 30–120 min
800	Collapse after 1 h, death after 2 h
1,000	Difficulty in ambulation, death after 2 h
1,500	Death after 1 h
2,000	Death after 45 min
3,000	Death after 30 min
8,000	Death by suffocation
12,800	Unconsciousness after 2–3 breaths, death in 1–3 min

The human response to various concentration levels of carboxyhemoglobin is listed in the following table:

Concentration, %	Symptoms
0–10	No signs or symptoms
10–20	Tightness across forehead, possible slight headache, dilation of cutaneous blood vessels
20–30	Headache, throbbing in temples
30–40	Severe headache, weakness, dizziness, dimness of vision, nausea, vomiting, collapse
40–50	Same as above, increase in pulse and breathing rate, greater possibility of collapse, asphyxiation
50–60	Same as above, coma, intermittent convulsions, and Cheyne–Stokes respiration
60–70	Coma, intermittent convulsions, depressed heart action and respiratory rate, possible death
70–80	Weak pulse, slowing of respiration leading to death with hours
80–90	Death in less than 1 h
90–100	Death in a few minutes

When carbon monoxide combines with hemoglobin in the blood, oxygen in the blood is displaced and carboxyhemoglobin is formed. The displacement of the oxygen produces anoxia, which is the total deprivation of oxygen.

In order to determine whether a particular appliance or engine is suspected in a carbon monoxide incident, laboratory tests should be undertaken. These tests should be accomplished under controlled conditions as near to the event as possible. That condition may require that the culprit is tested in situ or in a mockup of the event. Commercially available test equipment to detect carbon monoxide includes multigas analyzers, combustion gasses, and manometers. There is a variety of instrumentation to detect leaks for refrigeration systems.

It should be noted that carbon dioxide in great quantities can be lethal. Air normally has a concentration of 250–350 ppm. At concentrations above 30,000 ppm, the effect on humans is slightly narcotic. At levels of 80,000 ppm, dizziness and possible unconsciousness occurs. At levels of 120,000 ppm, death occurs in minutes.

Chains and Hooks

There are two types of chains. One is a roller chain as used in the drive mechanism of a bicycle, and the other is a link chain that is made from round stock, which is shaped and welded to make the link. In this discussion we will only be dealing with link chain. When used properly, chains and hooks do not fail. That is because these devices have a high factor of safety. Generally the factor of safety is 3 or 4 to one. At first thought one would think that the strength of the link chain is twice the strength of the round stock from which it is made. That is not the case for a couple of reasons. One reason is the strength of the weld and the other is the fact that the stock has been shaped. In order to produce the link, the stock has to be heated to form the link and then the stock is quenched to temper it. Additionally, the tensile properties on the rounded portion are somewhat degraded by the shaping on the link. The strength of the chain is approximately 1.63 times the strength of the rod from which it is made. Figure 13.1 shows a typical chain link.

Tables for chains can be quite misleading because the material used in the links and the grade of the chain may not be specified. For example, Table 13.1 obtained from *The English and American Mechanic* has the following values for the breaking strain of chain.

Table 13.1 gives no information relative to the dimensions of the chain with respect to Figure 13.1 nor to the materials used in the chain or the application for which the chain is intended. There are a variety of grades of chain including stainless steel, passing link chain, coil chain, machine chain, grade 30 proof coil chain, grade 43 high test chain, grade 70 transport chain, grade 80 alloy chain, and grade 100 alloy chain according to the National

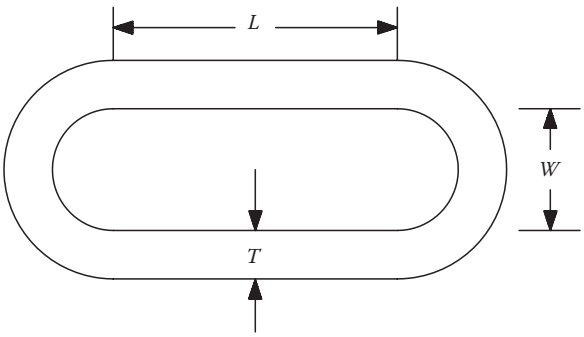

Figure 13.1 Chain link.

Table 13.1 Breaking Strain of Chain

Diameter (in.)	Strain (lb)	Weight of Chain/ft (lb)
3/16	1,731	0.325
1/2	3,069	0.579
7/16	4,794	0.904
3/8	6,922	1.3
7/16	9,408	1.78
1/2	12,820	2.31
9/16	15,590	2.93
5/8	19,219	3.62
11/16	23,274	4.38
3/4	27,687	5.21

Table 13.2 NACM Values

Nominal Chain Size (in.)	Material Diameter (in.)	Working Load Grade100 (lb)	Breaking Force Grade 100 (lb)	Working Load Grade 43 (lb)	Breaking Force Grade 43 (lb)	Working Load Grade 30 (lb)	Breaking Force Grade 30 (lb)
3/8	0.394	8,800	35,200	5,400	16,200	2,650	10,600
1/2	0.512	15,000	60,000	9,200	27,600	4,500	18,000
5/8	0.630	22,600	90,400	13,600	39,000	6,900	27,600
7/8	0.866	42,700	170,800	24,500	73,500	12,800	51,200

Association of Chain Manufacturers (NACM) who promulgate chain specifications. Only alloy chains are to be used for overhead lifting. Table 13.2 gives values for different sizes and grades of chains according to NACM.

Materials for Crane Chains

The best material for crane and hoisting chains is a good grade of wrought iron, in which the percentage of phosphorus, sulfur, silicon, and other impurities is low. The tensile strength of the best grades of wrought iron does not exceed 46,000 lb/in.^{2}, whereas mild steel with about 0.15% carbon has a tensile strength nearly double this amount. The ductility and toughness of wrought iron, however, are greater than that of ordinary commercial steel. For this reason it is preferable for chains subject to heavy intermittent trains be made of wrought iron because wrought iron will always give warning by bending or stretching before breaking. Another important reason for using wrought iron in preference to steel is that a perfect weld can be affected more easily.

Strength of Chains

When calculating the strength of chains, it should be observed that the strength of a link subjected to tensile stresses is not equal to twice the strength of an iron bar of the same diameter as the link stock, but is a certain amount less, owing to the bending action caused

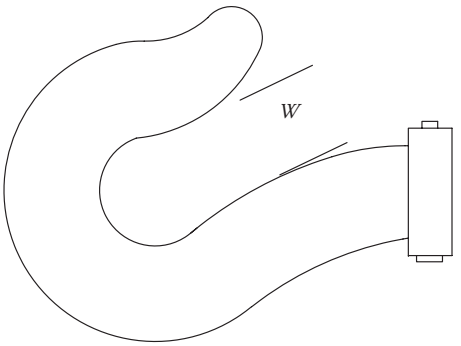

Figure 13.2 Chain hook.

by the manner in which the load is applied to the link. The strength is also reduced somewhat by the weld. The following empirical formula is commonly used for calculating the breaking load, in pounds, of wrought iron crane chains:

$$B_l = 54{,}000\,D^2 \tag{13.1}$$

where

B_l is the breaking load (lb)
D is the diameter of bar from which links are made (in.)

The working load for chains should not exceed one third the value of W, the weight being pulled or lifted, and in many cases it should be less. When chain is wound around a casting and severe bending stresses are introduced, a greater factor of safety should be used.

According to Equation 13.1, the breaking load for 3/8 in. chain would be somewhat above 8383 lb, which would correspond to grade 30 chain. Using a safety factor of 3 as a minimum, the safe load in pounds would be 2794, which is fairly close to the listed value of 2650 lb in Table 13.2. It is imperative to investigate the grade and application of the chain that failed. Based on these factors, the forces applied may be computed to determine why the chain failed. Chains are seldom used alone; they are most often used in combination with a hook as detailed in Figure 13.2.

Figure 13.2 represents a plain hook with pertinent dimensions. Hooks of this type are designed to slip over the chain links and press against the next link. Accordingly, the dimension D should be greater than the chain size of T inches but less than the chain dimension W inches. If the mouth opening of the hook D is larger than the chain inside width W, then the hook may slip over the chain and become ineffective.

Examination of Vehicle Lightbulbs and Filaments

The examination of lightbulbs in vehicles that are involved in accidents to determine whether the bulbs were turned ON is not an exact science. However, depending on the conditions of the remains of the lights, it is sometimes possible to conclusively determine

the ON/OFF status of the bulb. Under ideal conditions, the lamp should be examined immediately after the accident. But in reality, this is seldom possible because investigators are called upon to make a determination days, or weeks after the accident. Under these conditions, the evidence is often lost, damaged, or confused. Special attention should be taken to correctly identify the bulbs closest to the point of impact and the type of filament associated with each bulb. However, even under ideal conditions, undisturbed bulbs and filaments give inconclusive results.

We may categorize this analysis by first determining whether the glass bulb is broken or not, whether the filament is broken or not, and whether the bulb is a single or double filament bulb. Within these categories there are degrees of certainty, which must be taken into consideration before reaching a conclusion:

1. Unbroken glass
   a. If a single filament bulb is unchanged in shape, then it was probably OFF.
   b. If a single filament is stretched and misshapen, then it may have been ON.
   c. If one filament of a double filament light is slightly stretched, then the other filament may have been ON.
   d. If one end of a filament of a double filament bulb has turned purple and the other end is bright silver, then the other filament was ON.
2. Broken glass
   a. The color of a tungsten filament changes when the glass is broken if the filament is hot and therefore ON. Thus, if the filament has turned black, then the filament was ON.
   b. Tungsten oxide deposits a white powder on glass or metal parts of the interior of the bulb. Thus, if white powder remnants are found inside the remains of a broken bulb, then the filament was ON.
   c. If broken filament ends are rounded or beaded, then the filament was probably ON. However, if the broken ends of the filament are ragged, then the filament was probably OFF.
   d. If the bulb contains two filaments, one with a white oxide deposit, then the other filament was ON.
   e. If molten glass fragments are found on the filament or the brass portion of the light base, then the filament was ON.
3. Degrees of certainty
   a. If a filament is black, white oxide covers the inside of the broken bulb glass, part of the filament is melted onto the glass, molten glass remains are found on the filament or the brass portion of the base, or the remaining filament length is stretched and the broken ends of the filament have large beads of molten metal; then the filament was ON when the bulb broke.
   b. If the bulb has double filaments with the above conditions met and the second filament is purple at one end and silver at the other end; then the first filament was ON.
   c. If the glass is unbroken and one filament of a double filament bulb is slightly stretched, then there is a chance that the first filament was ON.
4. Cautions
   a. If the glass fractures while the light is OFF as a consequence of the wreck and someone turns the light ON after the crash; then the filament will burn out.

Under these conditions, it is imperative to find the glass remnants and to look for the white deposit on the inside of the bulb pieces. Care should be taken to find broken filaments in order to determine whether the bulb was ON prior to or after the accident.

b. If glass fusion with or without molten filament pieces is present, then the filament was ON when the bulb broke. If there are tiny blobs of molten glass, then the filament was ON when it fractured.
c. If the filament fracture is clean and ragged, then the filament was cold at the time of the break and was OFF.
d. If in doubt, err on the side of caution and conclude the condition of the light status as undetermined.

Figure 13.3 shows a lightbulb filament where the filament has turned black. Figure 13.4 shows a close-up of this filament and the white tungsten oxide deposited because the bulb was on. Figure 13.5 shows a glass bead that has adhered to a filament also indicating the bulb was on at the time that it broke.

Figure 13.3 **(See color insert.)** Lightbulb filament.

Figure 13.4 **(See color insert.)** Tungsten oxide.

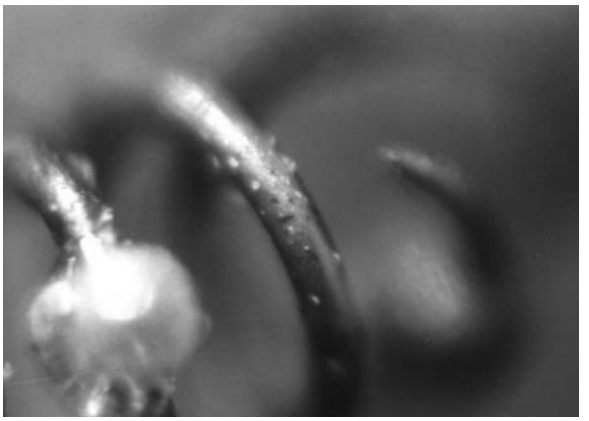

Figure 13.5 (See color insert.) Glass bead.

Defeating Locks

In order to steal a car, the perpetrator needs to have some basic tools. Let us assume that the car is locked and the ignition key is not available. Let us also assume that the ignition key is not resistive, magnetic, or infrared. Some newer cars use more complex locking mechanisms although the basic ignition sequence remains the same. Newer vehicles with more sophisticated locking mechanisms are difficult to overcome and steal. These systems can be overridden with diagnostic tools or by direct starting the engine once the computer systems are defeated. The main reason for vehicles being reported stolen is essentially to have the insurance company pay for the vehicle when the insured is no longer willing or able to afford the payment. These vehicles are often reported stolen and are recovered underwater or burned.

Basic tools

- Slim Jims, slide hammers, coat hangers, screw drivers (short, average Phillips, and flathead), small pry bars or large flat heads, electrical tape, channel locks, punches
- Chilton or Haynes Manual: provides diagrams of ignition and door locks
- Vehicle dealerships are often helpful in providing schematic diagrams or exemplar components

Process

- Defeat door locks using Slim Jims, coat hangers, or slide hammers
- Unscrew steering column cover
- Use a punch to pop the upper ignition
- Use channel locks and screw drivers to separate upper from lower ignition which are connected by a metal rod or similar mechanism
- Insert flat head screwdriver into key hole to unlock steering wheel
- Flat screwdriver in ignition key hole in lower ignition turned clockwise starts the car

Figure 13.6 Typical ignitions.

What to look for

- Tool marks on upper and lower ignitions
- Tool marks on door locks or rods
- Tool marks on connecting spindle—connecting rod between upper and lower ignitions
- Lower ignition bypass of wires, cut insulation, etc.
- Remnants of key in ignition
- Damaged pins and wafers in tumbler cylinder

Figure 13.6 shows three typical vehicle ignitions and Figure 13.7 shows the wafers inside of the tumblers that are activated by the insertion of the key. These components must be defeated in order to start the ignition without a key.

Vehicle Computer Interrogation

Modern passenger vehicles and commercial vehicles have complex electrical circuits and components that monitor and control the performance. These include engine control, ride control, braking action, and air bag status and deployment. The systems monitor parameters that may be of interest in a reconstruction. Virtually all vehicles over the last 10 years have a "black box" recorder or more properly called electronic control units that are monitored by the air bag module. At the present time, the three major American manufacturers of automobiles make the interrogation of many of their vehicles available to investigators. Of the foreign manufacturers of automobiles, Toyota and Lexus make interrogation of the air bag module for a large portion of their vehicles available to be investigated by noncompany representatives. Additionally, commercial tractors' engine control modules may be interrogated with the proper equipment from the manufacturer. Other foreign manufacturers provide this service for a limited segment of their vehicles.

Figure 13.7 Ignition wafers.

If an electrical malfunction is suspected as having caused a collision or a vehicle failure, the status of the electronic systems can be evaluated through the use of a diagnostic interrogation tool. There are many of these tools available from a variety of manufacturers. These tools vary in complexity and some of them access only domestic vehicles. Some vehicles have proprietary tools while others do not allow their interrogation except by trained factory representatives.

Figure 13.8 shows a typical interrogation tool used to troubleshoot passenger vehicles. Similar tools are available to troubleshoot commercial vehicles such as tractors and trailers. For the past two or three decades, all vehicles come with a check engine light. For vehicles

Figure 13.8 Interrogation tool.

manufactured between 1981 and 1995, onboard diagnostics (OBD1) was designed to monitor manufacturer specific systems. In 1996 OBD2 was developed for all cars and light trucks sold in the United States. The vehicle diagnostics are accessed though the data link connector (DLC) generally found under the steering column, behind the ash tray, or under the left corner of the dash. These systems allow for the access to the vehicle's onboard computer system to detect failures in a wide range of vehicles' systems. These tools provide diagnostic trouble codes (DTCs) that specify specific trouble areas such as fuel, ignition, emissions, transmission, and engine control.

A standard volt-ohm-meter whether digital or analog can also be used to trace circuits in a vehicle if it is suspected that an electrical malfunction caused a collision or a problem with the vehicle.

One of the measurements that can be taken on certain vehicles is the interrogation of the air bag module. Air bag modules should be properly interrogated in situ if possible. If the air bag module is removed, it must be properly disconnected and never have its wiring harness cut. Cutting of the air bag module wiring harness can introduce fault signals between the data cables. The preferred method of interrogation is through the DLC generally found under the steering column. A power source from the battery or external is necessary for this procedure and the wiring harnesses in the vehicle need to be intact and not damaged from the collision. If these conditions are not met, then the air bag module should be retrieved and interrogated in the laboratory. Care should be taken not to jostle the module so that the accelerometers in the module are not disturbed.

Figure 13.9 shows the retrieval of the crash data from the air bag module of a vehicle. The accompanying graph of the data is shown in Figure 13.10, and the crush on the vehicle is depicted in Figure 13.11. A standard for the interrogation of the crash information has been developed by ASTM (ASTM E2493-07), which should be followed when these data are retrieved. Please refer to Chapter 15 for the standard.

Figure 13.9 Crash data retrieval.

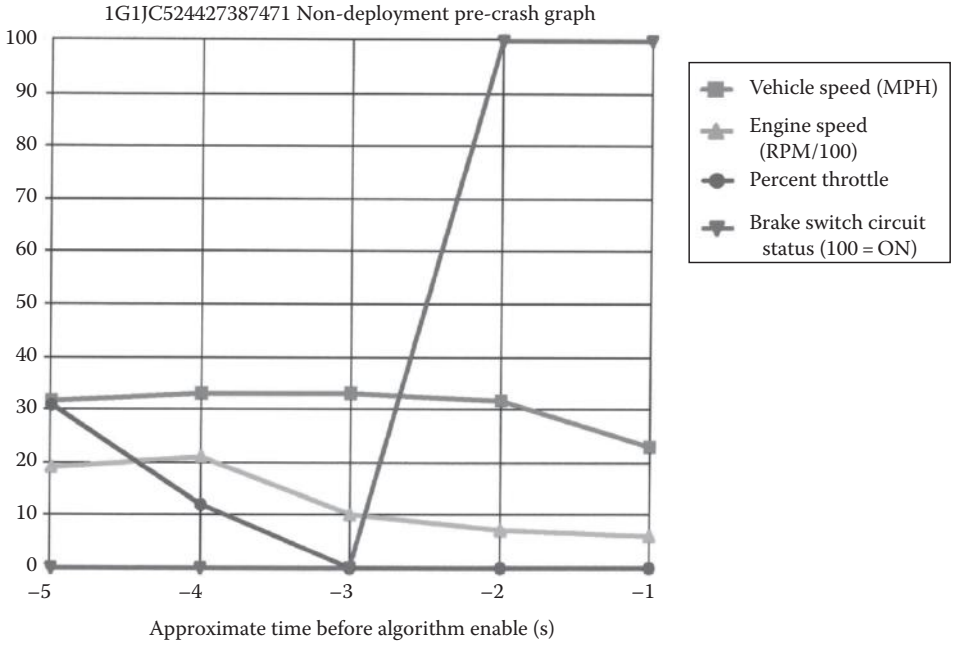

Figure 13.10 CDR graph.

Figure 13.11 Crush on vehicle.

Engine Wear

Many times a vehicle is reported to have been stolen, caught on fire, wrecked by some perpetrator, or submerged in water. The investigating agency, whether governmental such as the police, or private such as the insurance company, may wish to perform some tests on the components of the vehicle. They may need to know whether the door locks were defeated, whether the ignition was compromised, and whether there was excessive wear on the engine

Table 13.3 Engine Wear Indicators

Element	Engine Wear Indication
Aluminum	Pistons, bearings, spacers, shims, washers
Boron	Coolant leaks
Chromium	Rings, valves, or coolant leaks
Copper	Bearings, bushings, valve guides, injector shields, connecting rods, piston pins, coolant from copper radiators
Iron	Engine shafts, cylinder walls, engine block, rings, wrist pins, oil pump
Lead	Lead additive in gear oil, seals, solder, paint, bearing metal, fuel blowby. Bearing wear in diesel engines
Magnesium	Gear box housing and oil pump
Molybdenum	Oil coolers and bearing alloys
Nickel	Bearings, turbo blades, shafts, gears
Silicon	Dirt in air cleaner systems, casting sand in new engines, grinding compound
Silver	Puddle pumps, piping with silver solder joints, bearing cages
Sodium	Coolant leak or oil additive
Tin	Rod and piston coatings, bushing thrust metal and bearings
Titanium	Turbine blades, compressor disks, bearing hub wear

or gear train. The analysis of whether the door locks were defeated is found in this chapter as is the interrogation of the vehicle computer. Simple analysis of the fluids in the engine can also yield valuable information with respect to the condition of the engine at the time of the loss. Excessive engine and drive train wear can indicate that a vehicle was somehow alleged to have been stolen, burned, wrecked, or inundated. For example, it may be claimed that a vehicle was driven through a flooded street and water was ingested into the cylinders through the air intake system. However, inspection of the cylinder heads may reveal that the head gasket was blown allowing coolant to enter a cylinder. Visual inspection and disassembly will reveal the actual mode of failure. Additionally, laboratory analysis of the oil may reveal the presence of antifreeze, which would support the physical evidence of a blown head gasket. Table 13.3 shows a list of the elements found in transmission and engine fluids and what they represent.

Figure 13.12 shows the cylinder head in an engine block where the head gasket had failed between the center and the right cylinders. When the oil was sampled, the oil contained copious amounts of coolant, which verified the leaking head gasket as seen in Figure 13.13. In this case, it was alleged that the vehicle was driven through a flooded street and that water was ingested into the engine through the air intake. The air intake for the engine sits atop the engine so that the water level on the street would have to have entered the cab of the vehicle for such an occurrence to have taken place. No water was found inside the cab. Additionally, water would have entered all the cylinders and not only one cylinder. No water was found in the oil of the engine, only coolant.

Fire Suppression Systems

Fire enunciation and suppression systems are subject to failure as with any other piece of equipment. Enunciation refers to the ability of a system to announce that a fire danger is imminent. In fire suppression systems, enunciation occurs by the detection of either

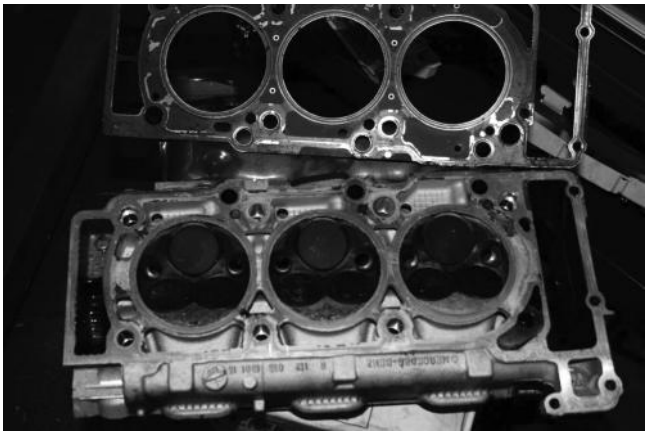

Figure 13.12 Cylinder head.

Figure 13.13 Coolant and oil samples.

smoke and/or temperature. Typically both types of detectors will be present in large building systems.

For residential areas, the fire codes only require the use of smoke detectors. In some cases of residential fires, smoke alarms are not installed, improperly installed, or contain no battery or a dead battery. These conditions make fire response virtually nonexistent until it is too late. The forensic engineer may be called upon to investigate such cases. Knowledge of the applicable codes is of utmost importance with respect to the investigation of these cases. Testing of the remnants and the installation location of smoke alarms is pertinent in such cases. Incorrect location of the smoke alarm in a residence may not allow the occupants sufficient time to escape. The means of egress for the occupants is crucial in such events. The Fire Dynamics Simulation described in the previous chapter is a powerful tool to investigate the smoke and fire evolution. Such analysis may be invaluable in litigation.

Commercial office spaces have more restrictive code requirements. For example, a small office complex may not require a sprinkler system but will require smoke alarms, fire extinguishers, emergency lighting, and lighted exit signs. As a general rule, larger commercial complexes require sprinkler systems of which there are many types depending on

the application. The code requirements vary widely depending on the type of commercial or industrial facility. The two basic types of sprinkler suppression systems are wet and dry. Wet systems contain water throughout all the pipes up to the individual sprinkler heads. Dry systems only have water up to the stand pipe. The stand pipe is the large pipe that enters the building to the pump. The area where the stand pipe is located must be heated because most dry systems are in locations where freezing conditions may occur. One example of a dry system would be in an unheated attic space in a health care facility. The majority of these systems are computer controlled although some older systems are still in use that were installed before the advent of the microprocessor.

The type of fire suppression system is determined from the classification of the occupancy. These classifications fall under the categories of light hazard, ordinary hazard, extra hazard, and special occupancy hazard. Additional types of systems other than wet pipe or dry pipe include preaction systems, deluge systems, combined dry pipe and preaction, multicycle, and antifreeze systems.

Consequently, fire suppression systems may fail in two ways, either the system malfunctioned during a fire, or it malfunctioned without an imminent fire event. A typical case involves a dry system that collects water in the pipes as a result of improper installation and/or condensation. The water freezes, the pipes burst, and cause water damage. Another case may involve sprinklers that do not operate during a fire resulting in a significant fire loss. Obviously there are many other ways in which these systems may fail. The most important codes for such systems are NFPA 13 Standard for the Installation of Sprinkler Systems, as well as NFPA 101, The Life and Safety Code. Many other pertinent codes are listed in Chapter 15.

Probability, Sensitivity, and Uncertainty

14

Introduction

Once a forensic investigation has been performed given the best available data, there is always a measure of uncertainty of some of the parameters. For example, the coefficient of friction in an accident reconstruction is never exactly known, but rather it is estimated. It may be important to know how sensitive some of the parameters are to change, which may affect the equations that are used in the reconstruction. As an example, it is known that T-bone collisions are not very sensitive to preimpact angles and that collinear collisions are quite sensitive to these angles. Parametric analysis, the variation of a parameter from a known or estimated central value, allows for the sensitivity and uncertainty to be quantified. It is always important to perform these calculations because all of the parameters are not exactly known, and the models used in the reconstruction cannot be entirely accurate. From a theoretical standpoint, we will define sensitivity and uncertainty in this chapter and see how they apply in forensic engineering.

Sensitivity and Uncertainty

Let us assume that an equation is a function of several variables. For example, for the stopping distance equation

$$v = \sqrt{2g\mu D} \tag{14.1}$$

The speed v is a function of two variables, namely, μ and D. Thus, we may write

$$v = f(\mu, D) \tag{14.2}$$

Thus, any equation dependent on n variables can be expressed as

$$P = f(x_1, x_2, \ldots, x_n) \tag{14.3}$$

First, let us consider the case where an equation is a function of only one variable, $P = f(x)$.

The sensitivity of P to the variable x is defined as

$$S_x^P = \lim_{\Delta x \to 0} \frac{\dfrac{\Delta P}{P}}{\dfrac{\Delta x}{x}} = \frac{x}{P} \lim_{\Delta x \to 0} \frac{\Delta P}{\Delta x} = \frac{x}{P} \frac{\partial P}{\partial x} = \frac{\partial (\ln P)}{\partial (\ln x)} \tag{14.4}$$

Applying the basic definition of sensitivity, the following relationships may be developed:

$$S_x^{cx} = 1; \quad c = \text{constant} \tag{14.5}$$

$$S_x^P = -S_x^{1/P} \tag{14.6}$$

$$S_x^P = -S_{1/x}^P \tag{14.7}$$

$$S_x^{P_1 P_2} = s_x^{P_1} + S_x^{P_2} \tag{14.8}$$

$$S_x^{P_1/P_2} = S_x^{P_1} - S_x^{P_2} \tag{14.9}$$

$$S_{x^n}^P = \frac{1}{n} S_x^P \tag{14.10}$$

$$S_x^{P_1+P_2} = \frac{P_1 S_x^{P_1} + P_2 S_x^{P_2}}{P_1 + P_2} \tag{14.11}$$

Since most functions are in terms of various parameters, it is important to determine the multiparameter deviations. To do so we begin with the basic definition as expressed in Equation 14.4 so that for small deviations in x we can determine the change in the function due to one element as

$$\Delta P \cong S_x^P \frac{\Delta x}{x} P \tag{14.12}$$

For multiple elements we may expand Equation 14.11 in a Taylor Series to obtain

$$\Delta P \cong \frac{\partial P}{\partial x_1} \Delta x_1 + \frac{\partial P}{\partial x_2} \Delta x_2 + \cdots + \frac{\partial P}{\partial x_m} \Delta x_m + \text{higher order terms} \tag{14.13}$$

For small variations in Δx_j we neglect the higher order terms so that

$$\Delta P \cong \sum_{x_j}^{m} \frac{\partial P}{\partial x_j} \Delta x_j = \sum_{x_j}^{m} \left(\frac{\partial P}{\partial x_j} \frac{x_j}{P} \right) \left(\frac{\Delta x_j}{x_j} \right) P = \sum_{x_j}^{m} S_{x_j}^P V_{x_j} P \tag{14.14}$$

where $V_{x_j} = \Delta x_j / x_j$ = per unit change in the parameter x and is known as the variability of x.

For Equation 14.1 we may determine, as an example, the sensitivity of the parameters μ and D by applying Equation 14.9. The sensitivity for these parameters is ½ for each. This result may also be verified by the application of the basic definition of sensitivity. Applying Equation 14.13, we can determine the per unit variation of the velocity with respect to the parameters μ and D:

$$\frac{\Delta v}{v} = \frac{1}{2}\left(\frac{\Delta \mu}{\mu} + \frac{\Delta D}{D}\right) \tag{14.15}$$

In terms of the root mean square variation, Equation 14.15 becomes

$$\frac{\Delta v}{v}\Big|_{rms} = \frac{1}{2}\sqrt{\left(\frac{\Delta \mu}{\mu}\right)^2 + \left(\frac{\Delta D}{D}\right)^2} \tag{14.16}$$

Equations 14.14 and 14.15 give a measure of the uncertainty of the calculations.

This type of analysis can be used to determine the sensitivity of the momentum equations. Recall that the equations of linear momentum for the postimpact velocities are given by

$$V_{1i} = \frac{V_{1f}\sin(A_{2i} - A_{1f}) + R_{2vl}V_{2f}\sin(A_{2i} - A_{2f})}{\sin(A_{2i} - A_{1i})} = \frac{V_{1f}\sin\varphi_1 + RV_{2f}\sin\varphi_2}{\sin\varphi_5} \tag{14.17}$$

$$V_{2i} = \frac{V_{1f}\sin(A_{1i} - A_{1f}) + R_{2v1}V_{2f}\sin(A_{1i} - A_{2f})}{R_{2v1}\sin(A_{2i} - A_{1i})} = \frac{V_{1f}\sin\varphi_3 + RV_{2f}\sin\varphi_4}{R\sin\varphi_5} \tag{14.18}$$

For Equation 14.17 the sensitivity to φ_5 is

$$S_{\varphi_5}^{V_{1i}} = \frac{-\varphi_5}{\tan\varphi_5} = \underset{\varphi_5 \to 0}{Lim}\frac{d/d\varphi_5(\varphi_5)}{d/d\varphi_5(\tan\varphi_5)} = -1 \tag{14.19}$$

Thus, when the approach angles are nearly equal or opposite, the momentum equations are very sensitive to the angles and are difficult to solve unless parametric studies are undertaken. Parametric studies lend themselves to be solved by spreadsheets or computer programs where several parameters can be varied and their effect studied. It is generally found that some parameters do not affect the results from a particular equation as much as others. Therefore, we always encourage the use of parametric analysis in a reconstruction. When parametric analysis is performed, the uncertainty can be quantified and the effects observed. Again, for Equation 14.17 we may determine the sensitivity to the other parameters as

$$S_{\varphi_1}^{V_{1i}} = \frac{\varphi_1 V_{1f}\cos\varphi_1}{V_{1f}\sin\varphi_1 + RV_{2f}\sin\varphi_2} \tag{14.20}$$

$$S_{\varphi_2}^{V_{1i}} = \frac{\varphi_2 V_{2f} \cos\varphi_2}{V_{1f} \sin\varphi_1 + R V_{2f} \sin\varphi_2} \tag{14.21}$$

$$S_R^{V_{1i}} = \sin\varphi_5 \tag{14.22}$$

$$S_{V_{1f}}^{V_{1i}} = S_{V_{2f}}^{V_{1i}} = 1 \tag{14.23}$$

We see that the initial velocity of vehicle 1 is directly proportional to the final velocities of vehicles 1 and 2 and that the sensitivity as a function of the ratio of the weights R is related to the sine of the difference between the preimpact angles.

Probability and Statistics

In many forensic investigations it becomes necessary to perform some statistical computations. These computations are based on some central measures that are defined in this section. We assume that the range of events is from 1 to n so that with every value x_i there is a descriptive term $f_i \geq 0$. This descriptive term may be the frequency, the mass, the probability, or the reliability of the occurrence of the event. The total weight is

$$N = \sum f_i \tag{14.24}$$

The arithmetic mean is

$$x_{am} = \sum f_i x_i / N \tag{14.25}$$

The geometric mean is

$$x_{gm} = [\Pi x_i^{f_i}]^{1/N} \tag{14.26}$$

The mode M_o for unweighted items $(x_1,\ldots,x_n)$ is the value about which x_i most densely clusters. The median M_e for unweighted items is the value equaled or exceeded by exactly half of the values x_i.

The root mean square is given by

$$RMS = \sqrt{\sum f_i x_i^2 / N} \tag{14.27}$$

The standard deviation is

$$sd = \sqrt{\frac{\sum (x_i - x_{am})^2}{N}} \tag{14.28}$$

The variance is

$$v = (sd)^2 \tag{14.29}$$

The probability that an event E will occur is given by the equation

$$P(E) = \frac{m}{n} \tag{14.30}$$

where

E is the event
$P(E)$ is the probability that the event will occur
m is the corresponds to the event
n is the number of ways possible

Considering events A and B, then the following relations hold true:

$P(A)$ = probability of event A
$P(B)$ = probability of event B
$P(A')$ = probability that event A does not occur
$P(A/B)$ = conditional probability of event B, given event A
$P(A \cup B)$ = probability that event A and/or event B occurs. Union
$P(A \cap B)$ = probability that event A and event B both occur. Intersection

$$P(A \cap B) = P(A)P(B) \tag{14.31}$$

For example, the probability of being in a car accident is 1 in 100 according to national statistics in a given year. Let us say that a given individual is involved in eight accidents in a particular year. Many of the accidents are suspicious so that the insurance company decides to take action. To determine the probability that these eight car accidents occurred, we can use a modification of Equation 14.31 to determine the probability as

$$P(1 \cap 2 \cap 3 \cap 4 \cap 5 \cap 6 \cap 7 \cap 8)$$

$$= (1/100)(1/100)(1/100)(1/100)(1/100)(1/100)(1/100)(1/100) = 10^{-10}$$

It is obvious from this simple calculation that this unfortunate individual could not have experienced eight car accidents in 1 year.

There are approximately 105 million residential households in this country and approximately 350,000 residential fires significant enough to call the fire department so that the probability of a household fire is approximately 1 in 300. For a case in which a homeowner has incurred multiple fires in a year, a similar analysis could be used to determine if these fires were accidental.

Standards 15

Introduction

During the years that the authors have been practicing forensic engineering, it has become evident that there is a great need for standardization. The field of forensic engineering is not well represented by a concise and exhaustive list of standards. Most of the standards that are available to the practicing forensic engineering are from technical societies associated with engineering disciplines, the federal government, and various private testing facilities. Fortunately, in most areas of forensic engineering there is a wealth of information and standards that have been developed over the years. The main thrust of these standards is the same as that in engineering, to protect life and property.

In this book, the authors make no statement with regard to qualifications, experience, or determination as to the suitability of the experts. Simply, that is not the purview of the engineer. Engineers are not the gatekeepers of the system. It is not ethical for an engineer to assess the suitability of another professional. The gatekeeper of the system is the judicial system. The court systems in this country have recognized experts in forensics from many backgrounds. The adversarial nature of the criminal and civil system is designed to challenge experts as to their suitability to offer opinions on such matters. Judges and juries determine the qualifications and competency of the experts. It should be recognized that the level of expertise required for these investigations varies with the complexity of the case. Many forensic investigations require only minimal mathematical skills and a rudimentary knowledge of the physical principles involved. It is recognized that many experts may be very well qualified by their experience and training although their traditional academic training may not be comparable. Some forms of analysis may require significant training in the physical sciences and mathematics that may be beyond the capabilities of some individuals including people with engineering degrees. This book is mainly geared toward the student in a forensic sciences or forensic engineering curriculum and illustrates the common methods in forensic failure analysis.

The forensic engineering student and practitioner should welcome standards and protocols because as humans we make mistakes. Standards and protocols keep us focused and on track. Protocols minimize mistakes and standards put us on solid footings. Applying recognized standards to a forensic investigation makes our work and conclusions much easier and less subject to challenge. It is the method of science and should be embraced by all practitioners.

Protocol for Forensic Investigations

This section should not be construed to apply under all circumstances. Some of the material in this section is covered under NFPA, CFR, ASCE, AIChE, ASME, ASE, ASM, SAE, ANSI, and ASTM standards and guidelines and may be considered repetitive. The list of the standards in this chapter is not exhaustive as it would fill an entire volume. The listings are some of the more common standards encountered in a forensic engineering practice. Most standards are now cross-referenced with the American National Standards Institute (ANSI). For example, the listing may say (ANSI/ASCE) to denote a cross-reference with the American Society of Civil Engineers. Please refer to the applicable standards in this chapter for more detailed explanations of procedural guidelines. Most forensic engineering investigations require at least a fundamental knowledge of the applicable standards.

Standard Guide for Forensic Engineering Inspections and Investigations

Scope

This guide is for individuals who are investigating the events relating to incidents involving persons, vehicles, roadways, structures, equipment, or sites where a loss of property, injury, or a loss of life has occurred. The purpose of this guide is to provide a compendium of information and practices, but not to establish a standard practice or recommend a specific course of action. The guide is intended to increase the awareness of information and approach in this area. The guide covers methodologies and practices for the recognition, documentation, reporting, collection, and preservation of potentially relevant physical items and information pertaining to a forensic incident.

This guide is intended to serve as a reference rather than as a definitive standard. As such, a forensic practitioner may use other relevant standards and protocols to supplement the information in this guide. The guide outlines many courses of action so that the investigator may choose the appropriate course of action relative to the investigation. The nature of the incident and the employer's requirements will also generally dictate the scope of work and practices required. For example, in some instances, the employer may require the investigator to work from existing evidence rather than collecting the evidence. Realizing that such restrictions tend to limit the scope and possibly the accuracy of the work, significant analysis can still be performed. Sometimes, the sites, buildings, structures, vehicles, or equipment may no longer be available or the site may have been altered. Under such circumstances, photographs, databases, simulations, and exemplars may be used to perform the analysis. Computer techniques may also be used to create a virtual scene based on measurements and photogrammetry.

Significance and Use

Every year, injuries, property damage, and business interruptions occur as a result of a variety of incidents. The recording of information, physical data, and evidence following an incident is important if the origins and causes of an incident are to be determined. This document can help convey forensic findings to both technical and nontechnical third parties. The documentary data, including reports and statements, are used to corroborate the findings.

Because the evidence at the scene of an incident is time sensitive, forensic investigations conducted as soon as possible after the incident often collect the most useful information.

In most instances, the forensic practitioners are not afforded the privilege of investigating the incidents soon after they occur. Police or regulatory authorities investigate most incidents within minutes or hours. Police, fire departments, and other responding Authorities Having Jurisdiction (AHJs) are required to document the incident scenes and often perform some of the most immediate site analysis and evidence collection. However, these authorities often have primary statutory responsibilities to protect life and property. Therefore, it is recognized that the reports generated by these agencies, while important, may not include all relevant data. It is in following up that private forensic practitioners play a vital role as they often have greater collection resources and more time to spend on the investigation than the responding AHJ's.

Proper collection of incident details may allow for the replication or reconstruction of an incident. The reconstruction or replication of the incident may take many perfectly valid forms. The reconstruction of the incident, if warranted, can be performed by the application of basic physical laws. The reconstruction may be based on available data or on actual tests with exemplar structures or equipment. The reconstruction may be based on computer simulations and models. A combination of methods may be used to validate the results of the investigation and reconstruction. Wherever practical, it is suggested that more than one method of analysis be used to reach the conclusion of the forensic practitioner.

Equipment

Useful equipment for incident investigations and reconstructions include but are not limited to the following:

1. Measuring devices, total stations, transits, rolling tapes, measuring tapes, micrometers, calipers, dial indicators, feeler gauges, scales, pressure gauges, crush jigs, etc.
2. Diagnostic tools, crash data retrieval tools, volt-ohm meters, oscilloscopes, vacuum gauges, timing lights, calculators, and computers, x-ray machines, MRIs, hardness testers
3. SAE standard and metric wrenches and tools, jacks, stands, and equipment lifts
4. Mirrors, boroscopes, thermal imaging devices, microscopes, x-ray equipment, etc.
5. Cameras with micro and macro capabilities, video and audio recorders
6. Maps, global positioning systems, aerial and satellite images
7. Incident reconstruction and simulation software, equipment specification databases, test data, drawing software

Procedure

The procedure outlined here is not to be construed as a sequence of events that are to be followed in order of appearance. It is realized that these procedures will generally overlap, intersect, and follow in a random sequence:

1. Historical and background data
   Police reports, emergency responders reports, fire department reports, equipment repair estimates, police photographs, news coverage reports, photographs or video, adjuster photographs, injury or medical reports, witness statements, examinations under oath, depositions, maintenance records or repair records, weather and sun or moon position records, illumination records.

2. On-site activities
   Proper documentation of the site with measurements; photographs or video; the use of exemplar equipment, actors, or vehicles to demonstrate particular characteristics concerning the events of the incident; and studies relative to perception, visibility, illumination, and conspicuity.
3. Machinery and equipment inspections
   Establish protocols for the joint inspection of machines or equipment or the retrieval of data from event recorders. Measurements with appropriate equipment along with photographs and video recordings should document the activities. Disassembly of components should be systematically documented. Destructive testing may be agreed upon.
4. Postsite and postequipment inspection activities
   Interviews with police, EMS, and fire department personnel; repair or maintenance facilities; request for production of documents or evidence; aerial or satellite imagery; literature search; policies, codes, and standards; training records.
5. Exemplars and testing
   Useful information may be obtained from destructive and nondestructive testing of exemplar equipment or machinery. Such tests are often undertaken to determine the potential for or mode of failure or safety issues that may arise.
6. Standard analysis
   Basic physical laws, Newtonian mechanics, time motion analysis, damage analysis, mathematical modeling of events, photogrammetry, machinery or equipment performance characteristics, site or structure characteristics.
7. Simulations and computer models
   2D and 3D models and simulations utilizing commercial software.
8. Research activities

Reports

Over the course of a forensic incident investigation and reconstruction, the forensic practitioner may be required to prepare multiple reports in various formats including but not limited to

1. Verbal reports
2. Status reports
3. Preliminary reports
4. Draft reports
5. Interim reports
6. Final reports
7. Amendments to reports

The client may require the forensic investigation report to include where applicable the following information:

1. Signature and professional licensing or certification stamps
2. Credit given to any additional contributors
3. Sources of data relied on and list of references and appendices
4. Other reports, statements, or depositions used or referenced
5. Drawings and calculations
6. Opinions on origins and causes of the incident

ASTM Standards

The following is a list of the American Society of Testing and Materials (ASTM) standards and guides that may be applicable to forensic investigations and reconstructions:

ASTM E 620 Standard practice for reporting opinions of technical experts
ASTM E 678 Standard practice for evaluation of technical data
ASTM E 860 Standard practice for examining and testing items that are or may become involved in litigation
ASTM E 1020 Standard practice for reporting incidents
ASTM 1188 Standard practice for collection and preservation of information and physical items by a technical investigator
ASTM E 2292 Standard practice for investigation of carbon monoxide poisoning incidents
ASTM E 2332 Standard practice for investigation and analysis of physical component failures
ASTM E 2345 Standard practice for investigating electrical incidents
ASTM E 2493 Standard guide for the collection of non-volatile memory data in evidentiary vehicle electronic control units

FMV Standards

The Code of Federal Regulations (CFR) includes sections applicable to forensic investigations and reconstructions. These are

Title 16 Commercial practices
Part 1118 Investigations, inspections and inquiries under the consumer product safety act
Part 1201 Safety standard for architectural glazing materials
Part 1203 Safety standard for bicycle helmets
Part 1205 Safety standard for walk-behind power lawn mowers
Part 1207 Safety standard for swimming pool slides
Part 1406 Coal and wood burning appliances
Part 1407 Portable generators
Part 1420 Requirements for all terrain vehicles

Title 23 Highways
Part 470 Highway systems
Part 625 Design standards for highways
Part 635 Construction and maintenance
Part 646 Railroads
Part 650 Bridges, structures, and hydraulics
Part 652 Pedestrian and bicycle accommodations and projects
Part 655 Traffic operations
Part 657 Certification of size and weight enforcement
Part 658 Truck size and weight, route destinations—length, width and weight limitations
Part 1235 Uniform system for parking for persons with disabilities

Title 29 Labor
Part 1910 Occupational safety and health standard

Title 30 Mineral resources

Title 49 Transportation
- Part 213 Track safety standards
- Part 214 Railroad workplace safety
- Part 215 Railroad freight car safety standards
- Part 217 Railroad operating rules
- Part 218 Railroad operating practices
- Part 221 Rear end marking devices—passenger, commuter and freight trains
- Part 222 Use of locomotive horns at public highway-rail grade crossings
- Part 224 Reflectorization of rail freight rolling stock
- Part 225 Railroad accidents/incidents: Reports classification, and investigations
- Part 228 Hours of service of railroad employees
- Part 229 Railroad locomotive standards
- Part 232 Brake system safety standards
- Part 233 Signal systems reporting requirements
- Part 234 Grade crossing signal system safety
- Part 390 Federal motor carrier safety regulations
- Part 392 Driving of commercial motor vehicles
- Part 393 Parts and accessories necessary for safe operation
- Part 395 Hours of service of drivers
- Part 396 Inspection, repair, and maintenance
- Part 563 Event data recorders
- Part 569 Regrooved tires
- Part 570 Vehicle in use inspection standards
- Part 571 Federal motor vehicle safety standards
- Part 574 Tire identification and recordkeeping
- Part 581 Bumper standard
- Part 605 School bus operations

SAE Standards

The Society of Automotive Engineers have also developed standards or recommended practices applicable to the forensic investigation of accidents as follows:

- SAE J 98 Personnel protection for general purpose industrial machines
- SAE J 224 Collision deformation classification
- SAE J 231 Minimum performance criteria for falling object protective structures (FOPS)
- SAE J 232 Industrial rotary mowers
- SAE J 276 Steering frame lock articulated loaders and tractors
- SAE J 386 Operator restraint systems for off-road work machines
- SAE J 819 Engine cooling system field test
- SAE J 850 Fixed rigid barrier collision tests
- SAE J 972 Moving rigid barrier collision tests
- SAE J 1001 Industrial flail mowers and power rakes
- SAE J 1040 Performance criteria for rollover protective structures (ROPS) for construction
- SAE J 1042 Operator protection for general purpose industrial machines

SAE J 1301 Truck deformation classification
SAE J 1308 Fan guard for off-road machines
SAE J 1388 Personnel protection—Steer skid loaders
SAE J 1674 Early acquisition and preservation of information in a motor vehicle accident
SAE J 2314 Ethics for accident investigation and reconstruction
SAE J 2426 Occupant restraint system evaluation-lateral rollover system-level heavy trucks
SAE J 2505 Measurement of vehicle-roadway frictional drag
SAE J 2808 Road/lane departure warning systems
SAE CRP 9, 12, 13 Heavy truck crashworthiness

Relevant Construction Standards

The list that follows represents some of the more common standards relative to structures:

American Institute of Steel Construction (AISC) Manual of Steel Construction: Load and Resistance Factor Design (LRFD)—Volume I (Structural Members, Specifications, Codes), Volume II (Connections American Forest & Paper Association/American Wood Council—National Design Specifications (NDS) for Wood Construction (ANSI/AF&PA)
Steel Joist Institute (SJI): Standard Specifications—Load Tables and Weight Tables for Steel Joists and Joist Girders
American Concrete Institute (ACI) Building Code Requirements for Structural Concrete (ACI 318) and Commentary (ACI 318R)
National Concrete Masonry Association (NCMA): Design Manual for Segmental Retaining Walls
American Society of Civil Engineers (ASCE) and Structural Engineering Institute (SEI): Minimum Design Loads for Buildings and Other Structures (ASCE 7)
Accessible and Usable Buildings and Facilities (ICC/ANSI 117.1)
Truss Plate Institute (TPI) National Design Standards for Metal-Plate Connected Wood Truss Construction (TPI 1)

NFPA Standards

The National Fire Protection Administration (NFPA) promulgates a plethora of codes related to the prevention and protection of facilities and equipment that may be subject to the dangers posed by fire. The following list includes some of the most important codes although many others may apply:

12A Halon 1301 Fire extinguishing systems
13 Installation of sprinkler systems
Standpipe hose systems
30 Flammable and combustible liquids code
54 National fuel gas code
58 Liquefied petroleum gas code
59A Liquefied natural gas
70 National electrical code

70A Electrical code for one- and two-family dwellings and mobile homes
70B Electrical equipment maintenance
70E Electrical safety in the workplace
72 National fire alarm code
73 Electrical inspection code for existing dwellings
75 Electronic computer/data processing equipment
79 Electrical standard for electrical machinery
90A Air conditioning and ventilation systems
97 Chimneys, vents, and heat producing appliances
101 Life safety code
110 Energy and standby power systems
120 Self propelled and mobile surface mining equipment
211 Chimneys, fireplaces, vents and solid fuel burning appliances
303 Marinas and boatyards
501 Manufactured housing
921 Fire and explosion investigations
1192 Recreational vehicles
5000 Building code

International Standards

Many jurisdictions have made an effort to incorporate International codes promulgated by the International Code Council (ICC) since this effort was initiated in 1997. The member organizations include representatives from the Building Officials and Code Administrators (BOCA), the International Conference of Building Officials (ICBO), and the Southern Building Code Congress International (SBCCI). These codes are updated every 3 years. The codes are an outgrowth and consistent with existing codes:

International Building Code
International Fire Code
International Mechanical Code
International Plumbing Code
International Residential Code

APPENDIX A: Values of Fundamental Constants (MKS Units)

Quantity	Symbol	Value
Absolute zero temperature	0 K	−273.15°C
Acceleration due to gravity	g	9.78 m/s^2
Velocity of light in a vacuum	c	2.9979×10^8 m/s
Electron charge	q_e	-1.602×10^{-19} C
Electron rest mass	m_e	9.109×10^{-31} kg
Planck's constant	h	6.625×10^{-23} J-s
Boltzmann's constant	k	1.380×10^{-23} J/°K
Avogadro's number	N_0	6.025×10^{23} molecules/mole
Universal gas constant	R_0	8.314 J/(mole-°K)
Atmospheric pressure	1 atm	1.013×10^5 N/m^2
Ideal gas volume, 1 atm, 0°C	V_0	22.415 L/mole
Absolute zero	0 K	−273.15°C

APPENDIX B: Acronyms

AAFS	American Academy of Forensic Science
AASHTO	American Association of State Highway and Transportation Officials
ACI	American Concrete Institute
AF&PA	American Forest & Paper Association
AHJ	Authority Having Jurisdiction
AISC	American Institute of Steel Construction
ANSI	American National Standards Institute
API	American Petroleum Institute
ASCE	American Society of Civil Engineers
ASChE	American Society of Chemical Engineers
ASM	American Society of Metals
ASME	American Society of Mechanical Engineers
ASTM	American Society of Testing and Materials
AWS	American Welding Society
BOCA	Building Officials and Code Administrators
CFR	Code of Federal Regulations
CGA	Compressed Gas Association
CMAA	Crane Manufacturers Association of America
CS	Commercial Standard
GREEN BOOK	A Policy on Geometric Design of Highways and Streets
IBC	International Building Code
ICC	International Code Council
IEEE	Institute of Electrical and Electronic Engineers
IMC	International Mechanical Code
IPC	International Plumbing Code
IRC	International Residential Code
MUTCD	Manual on Uniform Traffic Control Devices
NAFE	National Academy of Forensic Engineers
NCMA	National Concrete Masonry Association
NEMA	National Electrical Manufacturers Association
NFPA	National Fire Protection Administration
SJI	Steel Joist Institute
TPI	Truss Plate Institute
UL	Underwriters Laboratory

APPENDIX C: Conversion Factors

Length
- 1 in. = 2.54 cm
- 1 ft = 30.48 cm

Area
- 1 cm^2 = 0.155 $in.^2$
- 1 m^2 = 10.76 ft^2

Volume
- 1 ft^3 = 0.0283 m^3
- 1 L = 1000 cm^3 = 0.2462 gal
- 1 $in.^3$ = 16.39 cm^3 = 7.5 gal

Velocity
- 1 ft/s = 0.6818 mile/h

Acceleration
- 1 m/s^2 = 3.281 ft/s^2

Force
- 1 lb = 4.448 N = 4.448×10^5 dynes

Mass
- 1 g = 6.85×10^{-5} slug = 10^{-3} kgm
- 1 slug = 32.17 lb

Pressure
- 1 atm = 14.7 psi = 1.013×10^6 dynes/cm^2
- 1 atm = 29.92 in. mercury at 0°C

Energy
- 1 J = 10^7 ergs = 0.239 cal
- 1 J = 9.480×10^{-4} Btu
- 1 J = 0.7376 ft-lb
- 1 J = 2.778×10^{-4} W-h
- 1 N-m = 0.7376 ft-lb
- 1 erg = 7.367×10^{-8} ft-lb

Power

1 hp = 745.7 W
1 hp = 550 ft-lb/s
1 W = 3.4129 Btu/h
1 hp = 42.44 Btu/min

Miscellaneous

1 lx = 0.0929 ft-cd
1 ft-cd = 1 lm/ft^2
1 lm = 0.001496 W
1 Np = 8.686 dB

Bibliography

Allen, J.R. 1970. *Physical Processes of Sedimentation*. London, U.K.: Allen & Unwin Ltd.

Allen, M.E. et al. 1994. Acceleration perturbations of daily living. A comparison to whiplash. *SPINE* 19(11): 1285–1290.

American Institute of Steel Construction (AISC). 1994. *Manual of Steel Construction: Volume One*, 2nd edn. Chicago, IL: American Institute of Steel Construction.

American Society of Civil Engineers. Soil Mechanics and Foundations Division. 1969. *Stability and Performance of Slopes and Embankments*. Berkeley, CA: ASCE.

American Society of Testing and Materials (ASTM) E 2493-07. *Standard Guide for the Collection of Non-Volatile Memory Data in Evidentiary Vehicle Control Units*. West Conshohocken, PA: American Society of Testing and Materials (ASTM).

Armstrong, B.R. and William, K. 1984. *Snowy Torrents*, 3rd edn. Jackson, WY: Teton Bookshop Publishing Co.

Armstrong, B.R. and William, K. 1986. *The Avalanche Book*. Golden, CO: Fulcrum, Inc.

ASHRAE Handbook. 2005. *HVAC Applications*. Atlanta, GA: American Society of Heating, Refrigeration and Air Conditioning Engineers, Inc.

Athanasiou, K.A. et al. 1991. Interspecies comparisons of in situ intrinsic mechanical properties of distal femoral cartilage. *J Orthop Res* 9: 330–340.

Babbitt, H.E. and Doland, J.J. 1955. *Water Supply Engineering*, 5th edn. New York: McGraw Hill.

Balanis, C.A. 1989. *Advanced Engineering Electromagnetics*. Hoboken, NJ: John Wiley & Sons.

Barker, D. 1986. The investigation of mobile home fires. South Beloit, IL: Barker and Hebert Laboratories, Burn Test, November 22, 1986.

Beer, F. and Johnston, E.R., Jr. 1962. *Vector Mechanics for Engineers: Statics & Dynamics*. New York: McGraw-Hill.

Benedek, G.B. and Villars, F.M. 2000. *Physics with Illustrative Examples from Medicine and Biology*, 2nd edn. New York: Springer-Verlag.

Berner, R.A. 1971. *Principles of Chemical Sedimentology*. New York: McGraw-Hill.

Betounes, D. 1998. *Partial Differential Equations for Computational Science*. New York: Springer-Verlag.

Blair, H.A. 1932. On the intensity-time relations for stimulation by electric currents. *J Gen Physiol* 15: 177–185, 709–729, 731–755.

Blatt, H., Middleton, G., and Murray, R. 1972. *Origin of Sedimentary Rocks*. Englewood Cliffs, NJ: Prentice Hall.

Brach, R.M. 2005. *Vehicle Accident Analysis and Reconstruction*. Warrendale, PA: SAE International, pp. 168–177.

Bureau of Labor Statistics. Fatal workplace injuries in 1992. Bureau of Labor Statistics, Washington, DC.

CFR30 Mine Safety and Health Administration (MSHA). Washington, DC: MSHA.

CFR49 *Code of Federal Regulations*. Part 1910 Occupational Safety and Health Standards, Washington, DC.

Chapman, A.E. 2008. *Biomechanical Analysis of Fundamental Human Movements*. Champaign, IL: Human Kinetics.

Concrete Manual. 1955. 6th edn. Washington, DC: U.S. Department of the Interior, Bureau of Reclamation.

Cooper, G.R. and McGillem, C.D. 1986. *Probabilistic Methods of Signal and System Analysis*, 2nd edn. McAllen, TX: Holt Reinhart and Winston.

Craig, M. Jaw loading response of current ATD's. Head injury biomechanics. *SAE International* 1: 37.

CRC Handbook of Chemistry and Physics, 71st edn., 1990–1991. Boston, MA: CRC Press.

Crozier, M.J. 1986. *Landslides: Causes, Consequences and Environment*. London, U.K.: Croomhelm.
Dalziel, C.F. 1956a. Effects of electric shock on man. *IEEE Trans Biomed Eng* 5: 44–62.
Damask, A.C. and J. Damask. 1990. *Injury Causation Analysis: Case Studies and Data Sources*. Charlottesville, VA: The Michie Company.
Daryanani, G. 1976. *Principles of Active Network Synthesis and Design*. Murray Hill, NJ: Bell Laboratories, pp. 148–149.
Das, B.M. 1998. *Principles of Geotechnical Engineering*, 4th edn. Boston, MA: PWS Publishing Co.
DeHann, J.D. 1991. *Kirk's Fire Investigation*, 3rd edn. Englewood Cliffs, NJ: Prentice Hall.
DeHann, J.D. and Icove, D.J. 2007. *Kirk's Fire Investigation*, 7th edn. Englewood Cliffs, NJ: Prentice Hall.
Den Hartog, J.P. 1952. *Advanced Strength of Materials*. Mineola, NY: Dover Publications, Inc.
Donders, F.C. 1868. On the speed of mental processes. *Acta Psychol* 30: 412–431.
Dorf, R.C. 1980. *Modern Control Systems*, 3rd edn. Reading, MA: Addison-Wesley.
Douglas, J.D. and Burden, R. 2003. *Numerical Methods*, 3rd edn. Pacific Grove, CA: Thomson Brooks/Cole.
Drucker, D.C. 1967. *Introduction to Mechanics of Deformable Solids*. New York: McGraw Hill.
Failure Analysis and Prevention. 2008. Materials Park, OH: ASM International.
Faires, V.M. 1967. *Thermodynamics*. New York: The MacMillan Co.
FMUSS 105. *Federal Motor Vehicle Safety Standard 105*. Washington, DC: U.S. Department of Transportation.
FMUSS 121 *Federal Motor Vehicle Safety Standard 121*. Washington, DC: U.S. Department of Transportation.
Frederickson, R. 2007. Influence of impact speed on head and brain injury outcome in vulnerable road user impacts on the car hood. *Stapp Car Crash J* 51: 235.
Garber, N.J. and Hoel, L.A. 1996. *Traffic and Highway Engineering*, 2nd edn. Boston, MA: PWS Publishing.
Geddes, L.A. (Ed.) 1995. *Electrical Hazards and Accidents*. Boca Raton, FL: CRC Press.
Giles, R.V. 1962. *Fluid Mechanics and Hydraulics*, 2nd edn. New York: Schaum's Outline Series.
Gillespie, T.D. 1992. *Fundamentals of Vehicle Dynamics*. Warrendale, PA: Society of Automotive Engineers.
Handbook of Case Histories in Failure Analysis. 1999. Materials Park, OH: ASM International.
Handbook of Case Histories in Failure Analysis. 2002. Materials Park, OH: ASM International.
Hariri, E., Gedalia, I., Simkin, A., and Robin, G. January 1974. Breaking strength of fluoride-treated dentin. *J Dental Res* 53: 149.
Harvey, P.D. (Ed.) 2002. *Engineering Properties of Steel*. Metal Parks, OH: ASM.
Hatch, J.E. (Ed.) 1984. *Aluminum Properties and Physical Metallurgy*. Metal Parks, OH: ASM.
Hicks, W.E. 1952. On the rate of gain of information. *Q J Exp Psychol* 4: 11–26.
Higdon, A. et al. 1968. *Mechanics of Materials*. New York: John Wiley & Sons.
Hoffman, J.D. 2001. *Numerical Methods for Engineers and Scientists*, 2nd edn. New York: McGraw Hill.
Human Tolerance to Impact Conditions as Related to Motor Vehicle Design. April 1980. Warrendale, PA: Society of Automotive Engineers J885.
Hure, H. 2006. NHTSA Study. Motorcycle accident cause factors and identification countermeasures. University of Southern California, Los Angeles, CA.
Industrial Hydraulics Manual, 1st edn. 1970. Troy, MI: Vickers Inc.
International Fire Code. 2006. Country Club Hills, IL: International Code Council.
Johanson, G. and Rumer, K. 1971. Driver's brake reaction times. Santa Monica, CA: Human Factors, Vol.
Jones, I.S. October 1983. The effect of impact type and vehicle velocity on vehicle crush characteristics. In *27th Proceedings*, San Antonio, TX. Morton Grove, IL: American Association for Automotive Medicine.
Kazarian, L.E. et al. 1970. Biomechanics of vertebral columns and organ response to seated spinal impact on rhesus monkeys. In *Proceedings of the 14th STAPP Car Crash Conference*, Ann Arbor, MI. Warrendale, PA: Society of Automotive Engineers.

Kehew, A.E. 1995. *Geology for Engineers and Environmental Scientists*, 2nd edn. Englewood Cliffs, NJ: Prentice Hill.
Kosinski, R.J. 2006. *A Literature Review of Reaction Time*. Clemson, SC: Clemson University.
Kosmata, S.H. and Panarese, W.C. 1988. *Design and Control of Concrete Mixtures*, 13th edn. Skokie, IL: Portland Cement Association.
Kraus, J.D. 1984 *Electromagnetics*, 3rd edn. New York: McGraw Hill.
Krim, J. 1996. Friction at the atomic scale. *Sci Am* 275: 74–80.
Kuffel, E. and Zaengl, W.S. 1984. *High Voltage Engineering*. New York: Pergamon Press.
Laming, D.R.J. 1968. *Information Theory of Choice-Reaction Times*. London, U.K.: Academic Press.
Lapicque, L. 1909. Definition experimental de L'excitation. *C.R. Hebd Seances Acad Sci* 67(2): 280–283.
Lentini, J. 2006. *Scientific Protocols for Fire Investigation*. Boca Raton, FL: CRC Press.
Les Renardiers Group. 1977. Positive discharges in long air gaps at Les Renardiers. *Electra* (53): 31.
Lewis, P.R. et al. 2004. *Forensic Materials Engineering—Case Studies*. Boca Raton, FL: CRC Press.
Limpert, R. May/June 1990. Car-pedestrian accidents. *Accid Reconstr J* 2(3): 16–18.
Limpert, R. 1992. *Brake Design and Safety*. Warrendale, PA: Society of Automotive Engineers, pp. 255–258.
Lissner, H.R., Lebow, M., and Evans, F.G. 1960. Experimental studies on the relation between acceleration and intracranial pressure changes in man. *Surg Gyn Obstet* 3: 329.
Loumet, J.R. and Jungbaure, W. 1994. *Train Accident Reconstruction and FELA and Railroad Litigation*. Tucson, AZ: Lawyers & Judges Publishing.
MacGregor, J.G. 1997. *Reinforced Concrete—Mechanics and Design*, 3rd edn. Englewood Cliffs, NJ: Prentice Hall.
Machinery's Handbook, 5th edn. 1917. New York: The Industrial Press.
Manual of Steel Construction, 7th edn. 1975. New York: American Institute of Steel Construction, Inc.
Manual of Steel Construction: Volume One, 2nd edn. 1994. New York: American Institute of Steel Construction (AISC).
Manual on Uniform Traffic Control Devices for Streets and Highways. 2003. Washington, DC: U.S Department of Transportation Federal Highway Administration.
Manual on Uniform Traffic Control Devices for Streets and Highways. 2004. Washington, DC: U.S. Department of Transportation Federal Highway Administration.
McConnell, W.E. et al. March 1993. Analysis of human test subject kinematic responses to low velocity rear impacts. SAE Paper 930889. Warrendale, PA: Society of Automotive Engineers.
Mertz, H.J. and Patrick, L.M. 1967. Investigation of the kinematics and kinetics of whiplash. SAE Paper 670919. Warrendale, PA: Society of Automotive Engineers.
Mertz, H.J and Patrick, L.M. 1971. Strength and response of the human neck. SAE Paper 710855. Warrendale, PA: Society of Automotive Engineers.
Morgan, J.R. and Ivey, D.L. 1987. Analysis of utility pole impacts. SAE Paper 370607. Warrendale, PA: Society of Automotive Engineers.
Murray, E.A. et al. 1994. Acceleration perturbations of daily living, a comparison to whiplash. *SPINE* 19(11): 1285–1290.
Nahum, A.M. and Smith, R. 1977. Intracranial pressure dynamics during head impact. In *Proceedings 21st STAPP Car Crash Conference*, New Orleans, LA. Warrendale, PA: Society of Automotive Engineers.
Nash, W.A. 1957. *Strength of Materials*. New York: Schaum Publishing Co.
National Highway Traffic Safety Administration (NHTSA). Crash tests.
National Institute for Occupational Safety and Health (NIOSH). Washington, DC: Department of Health and Human Services.
Neale, M.J. (Ed.) 1955. *Component Failures*. Warrendale, PA: Society of Automotive Engineers Inc.
New York City DOT. August 1991. Traffic fatalities data in New York City. New York: New York City DOT.
New York State DMV. 2004. Summary of pedestrian/motor vehicle accidents. New York: New York State DMV.

NFPA 921 *Fire and Explosion Investigations*, 1992 edition. Quincy, MA: National Fire Protection Association.
NFPA. 2008a. *Fire Protection Handbook*, Vol. 1. Quincy, MA: National Fire Protection Association.
NFPA. 2008b. *Fire Protection Handbook*. Vol. 2. Quincy, MA: National Fire Protection Association.
Noon, R. 1992. *Introduction to Forensic Engineering*. Boca Raton, FL: CRC Press.
Norman, C.A. 1930. *Principles of Machine Design*. New York: MacMillan Co.
Nystrom, G.A. and Kost, G. 1992. Application of NHTSA crash test data to pole input predictions. SAE Paper 920605. Warrendale, PA: Society of Automotive Engineers.
Occupational Safety and Health Administration (OSHA). Washington, DC: U.S. Department of Labor. Incident Summaries.
Ogan, J.S., Alcorn, T.L., and Scott, J.D. May/June 1993. Acceleration levels and occupant kinematics associated with vehicle to curb impacts. *Accid Reconstr J* 5: 22–26.
Peck, R.B. et al. 1964. *Foundation Engineering*. Hoboken, NJ: John Wiley & Sons.
Pennsylvania Crash Facts and Statistics Report. 2005. Harrisburg, PA: Department of Transportation, Bureau of Highway Safety and Traffic Engineering.
Penrose, R. 2004. *The Road to Reality*. New York: Afred A. Knopf.
Perry, R.H. and Green, D. (Eds.) 1984. *Perry's Chemical Engineers' Handbook*, 6th edn. New York: McGraw-Hill.
Pettijohn, F.J. 1975. *Sedimentary Rocks*, 3rd edn. New York: Harper & Row.
Pike, JA. 1990. Injuries, anatomy, biomechanics and federal regulations seminar. Warrendale, PA: Society of Automotive Engineers.
A Policy on Geometric Design of Highways and Streets. 2001. Washington, DC: American Association of State Highway and Transportation Officials.
A Policy on Geometric Design of Highways and Streets. 2004. Washington, DC: American Association of State Highway and Transportation Officials.
Potiket, N., Chiche, G., and Finger, I.M. November 2004. In vitro fracture strength of teeth restored with different all-ceramic crown systems. *J Prosthet Dent* 92(1): 491–495.
Prasad, A.K. 1990. Energy dissipated in vehicle crush—A study using the repeated test technique. SAE 900412. East Liberty, OH: Transportation Research Center of Ohio, Inc.
Regional Training Seminar Handout. 1994. Mobile home fire investigation, Charleston, WV, November 17–19, 1994.
Reinforced Concrete Design Handbook, 2nd edn. 1955. Detroit, MI: American Concrete Institute.
Roadside Design Guide. 2006. Washington, DC: American Association of State Highway and Transportation Officials.
Rosenbluth, W. 2001. *Investigation and Interpretation of Black Box Data in Automobiles*. West Conshohocken, PA: ASTM.
Sears, F. and Zemansky, M. 1964. *University Physics*. Reading, MA: Addison-Wesley Publishing Company, Inc.
Seelye, E.E. 1955. *Design*, 2nd edn. New York: John Wiley & Sons, Inc.
Shedd, T.C. et al. 1960. *Theory of Simple Structures*, 2nd edn. Hoboken, NJ: John Wiley & Sons.
Smith, G.C., James, M.B., Perl, T.R., and Struble, D.E. December 1987. *Frontal Crush Energy and Impulse Analysis of Narrow Object Impact*. Boston, MA: ASME Paper 87-WA/SAF-5.
Smythe, W.R. 1989. *Static and Dynamic Electricity*, 3rd edn. New York: Hemisphere Publishing Corporation.
Socie, D. and Marquis, G.B. 2000. *Mulliaxial Fatigue*. Warrendale, PA: Society of Automotive Engineers.
Sowers, G.F. 1979. *Introductory Soil Mechanics and Foundations: Geotechnical Engineering*. New York: Macmillan Publishing.
Stalnaker, R.L., Melvin, J.W., Nusholtz, G.S., Alem, N.M., and Benson, J.B. 1977. Head impact response. In *Proceedings of the 21st Stapp Car Crash Conference*, New Orleans, LA. Warrendale, PA: Society of Automotive Engineers.
Standard Mathematical Tables. 1965. Cleveland, OH: The Chemical Rubber Co.

Steidel, R.F., Jr. 1989. *An Introduction to Mechanical Vibrations*, 3rd edn. New York: John Wiley & Sons.
Stout-Wiegard, N. 1987. Characteristics of work-related injuries involving forklifts. *J Saf Res* Winter: 179–190.
Sutphen, R.F. and Varner, R.W. 2003. *Commercial Vehicle Accident Reconstruction and Investigation*. Tucson, AZ: Lawyers and Judges Publishing.
Sutton, J. and Watson, J.V. (Eds.) 1970. *Physical Processes of Sedimentation*. New York: American Elsevier Publishing Company, Inc.
Szaho, T.J. et al. 1994. Human occupant kinematic response to low speed rear end impacts. SAE 940532. Warrendale, PA: Society of Automotive Engineers.
Treschel, H.R. (Ed.) 1984. *Moisture Control in Buildings*. ASTM Manual Series MNL 18. Philadelphia, PA: ASTM.
Triggs, T.J. and Harris, W.S. 1982. Reaction time of drivers to road stimuli. Human Factors Report No. HFR-12. Victoria, Australia: Accident Research Centre, Monesh University.
Urquhart, L.C. (Ed.) 1940. *Civil Engineering Handbook*. New York: McGraw Hill.
U.S. Department of Agriculture. 1993. Economic Research Service. Washington, DC: U.S. Department of Agriculture.
U.S. Department of Health and Human Services, Public Health Service, Centers for Disease and Prevention, National Institute for Occupational Safety and Health (NIOSH). 1998. *Worker Deaths by Electrocution—A Summary of NIOSH Surveillance and Investigative Findings*. Washington, DC: NIOSH, p. 7.
U.S. Department of Transportation, Federal Highway Administration. 1972. Hydraulic engineering circular no. 13. Washington, DC: U.S. Department of Transportation.
Van Cleve, B.F. 1874. *The English and American Mechanic*. Philadelphia, PA: B. Frank Van Cleve.
Veder, C. and Hilbert, F. 1981. *Landslides and Their Stabilization*. New York: Springer-Verlag.
Vehicle Dynamics Terminology, 1976. SAE Technical Report J670e. Warrendale, PA: Society of Automotive Engineers.
Versace, J. 1971. A review of the severity index. In *Proceedings 15th Stapp Car Crash Conference*. Warrendale, PA: Society of Automotive Engineers.
Ward, C., Chan, M., and Nahum, A., 1980. Intercranial pressure—A brain injury criterion. In *Proceedings of the 24th Stapp Car Crash Conference*, Detroit, MI. Warrendale, PA: Society of Automotive Engineers.
Warner, C.F. 1960. *Thermodynamic Fundamentals*. Totowa, NJ: Littlefield, Adams & Co.
Weiss, G.G. 1901. Sur la Possibilité de Rendre Comparables entre eux les Appareils a L'excitation. *Arch Ital Biol* 35: 413–446.
West, D.H., Gough, J.P., and Harper, G.T.K. May/June 1993. Low speed rear end collisions testing using human subjects. *Accid Reconstr J* 5: 22–26.
Whiting, W.C. and Zernicke, R.F. 2008. *Biomechanics of Musculoskeletal Injury*, 2nd edn. Champaign, IL: Human Kinetics, Vol. 6, pp. 177–178.
Wolf, P.R. and Dewith, B.A. 2000. *Elements of Photogrammetry*, 3rd edn. Boston, MA: McGraw-Hill.
www.bts.gov/Bureau of Transportation Statistics. U.S. Department of Transportation. (October 12, 2011.)
www.nacm.info, National Association of Chain Manufacturers. (January 12, 2012.)
www.nsc.org, National Safety Council. (September 17, 2011.)
www.tramac.com, Tramac Worldwide. (November 22, 2011.)
Wylie, C.R. 1966. *Advanced Engineering Mathematics*, 3rd edn. New York: McGraw-Hill.
Yamada, H. 1970. *The Strength of Biological Materials*. Philadelphia, PA: Williams & Wilkins.
Yearance, R.A. February 1992. Arc tracking or treeing in insulation. Appendix G of Ground Fault-Circuit-Interrupter (GFCI) Technical Report by Albert Biss, P.E. Washington, DC: U.S. Consumer Product Safety Commission.
Zaruba, Q. and Mencl, V. 1982. *Landslides and Their Control*, 2nd edn. Maryland Heights, MO: Elsevier Scientific Publishing.

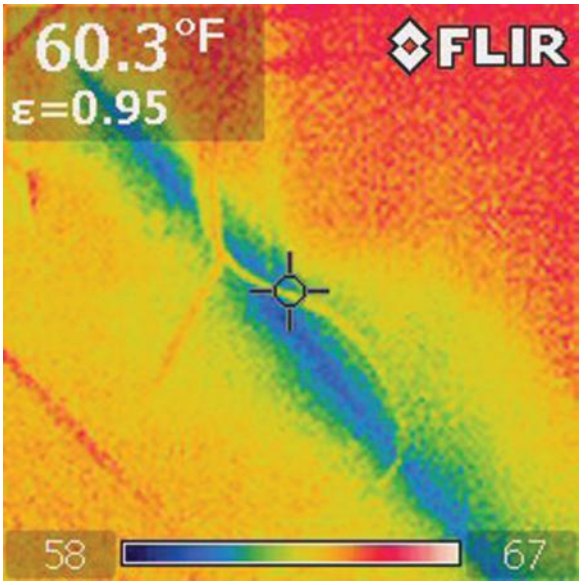

Figure 4.4 Infrared image.

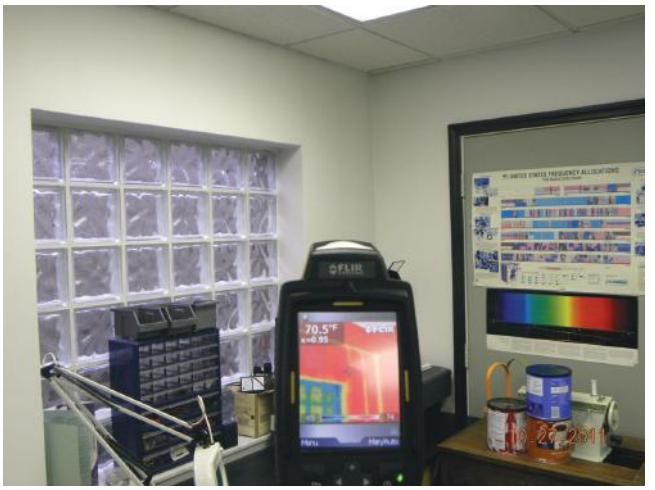

Figure 4.6 Infrared camera.

Figure 6.2 Gas appliance.

Figure 6.3 Electric stove.

Figure 6.8 Absorption refrigerator fire.

Figure 6.9 Pressure testing.

Figure 6.15 Arced conductors.

Figure 6.20 Air conditioner fire.

Figure 6.22 Failed water heater.

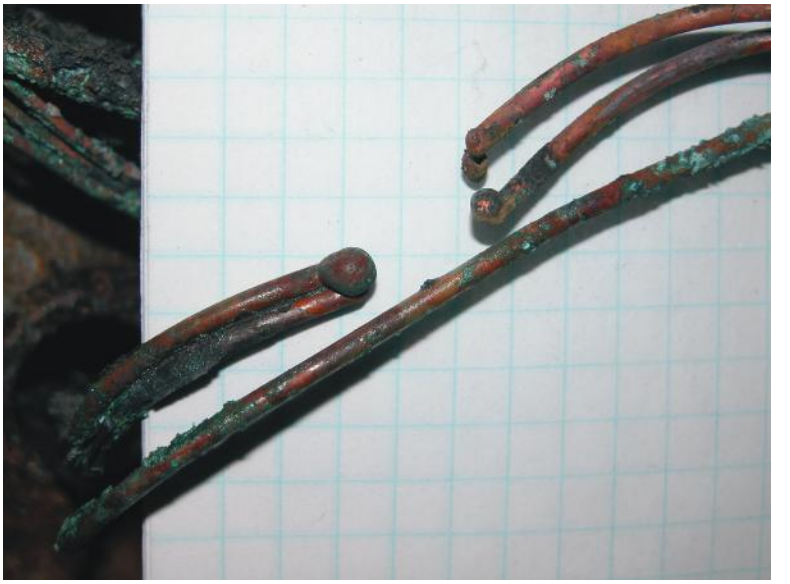

Figure 6.40 Arced solid conductors—beads.

Figure 6.41 Arced solid conductors—saddle.

Figure 6.42 Arced stranded conductors—beads.

Figure 12.15 Mercury.

Figure 13.3 Lightbulb filament.

Figure 13.4 Tungsten oxide.

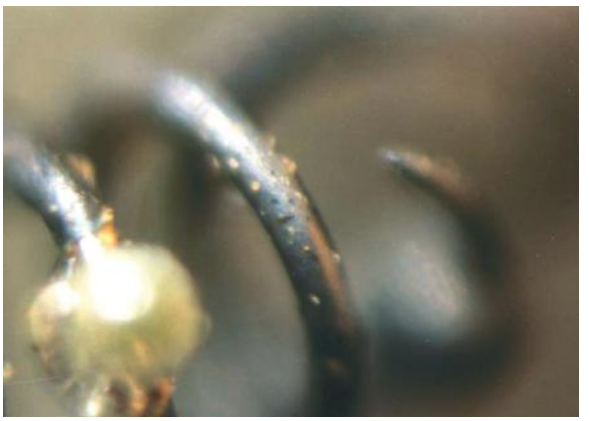

Figure 13.5 Glass bead.

FORENSICS AND CRIMINAL JUSTICE

Forensic Engineering Fundamentals

Forensic engineers often specialize in a particular area such as structures, fires, or accident reconstruction. However, the nature of the work often requires broad knowledge in the interrelated areas of physics, chemistry, biomechanics, and engineering. Covering cases as varied as assessment of workplace accidents to the investigation of Halliburton in the BP oil spill, ***Forensic Engineering Fundamentals*** is a comprehensive introduction to the many diverse facets of the field that forensic engineers must be familiar with in their practice.

Topics include

- The role of the forensic engineer
- Structures, structural distress, and the importance of standards and codes
- The failure of appliances—the cause of many water- or fire-related losses
- Slips, trips, and falls of pedestrians and the accessibility of walking surfaces
- Industrial incidents involving loss of equipment, injury and loss of life, as well as OSHA and MSHA regulations
- Standard accident reconstruction involving vehicles
- Electrical incidents and lightning and the effect of electrical energy on the human body
- Analysis of fires with an emphasis on thermodynamics, testing, and simulation
- Carbon monoxide incidents and common fire suppression and warning systems, as well as the various NFPA codes
- Probability and uncertainty, with some basic calculations available to the forensic engineer
- Applicable standards and protocols that have been developed over the years to protect life and property

Offering readers real-world examples drawn from the authors' 25 years of experience, this volume assists newcomers to the field in understanding the engineering basics underlying the cases they will encounter in their practice. It also serves as a reliable reference for those confronted with issues outside their area of expertise.

K13659

ISBN: 978-1-4398-7839-2
90000
9 781439 878392

CRC Press
Taylor & Francis Group
an **informa** business
www.taylorandfrancisgroup.com

6000 Broken Sound Parkway, NW
Suite 300, Boca Raton, FL 33487
711 Third Avenue
New York, NY 10017
2 Park Square, Milton Park
Abingdon, Oxon OX14 4RN, UK

www.crcpress.com